THE IMMUNOLOGY OF ADVERSE DRUG REACTIONS

EDITED BY: Patricia Illing, Michael R. Ardern-Jones, Nicole Andrea Mifsud and Jason Trubiano

PUBLISHED IN: Frontiers in Immunology and Frontiers in Genetics

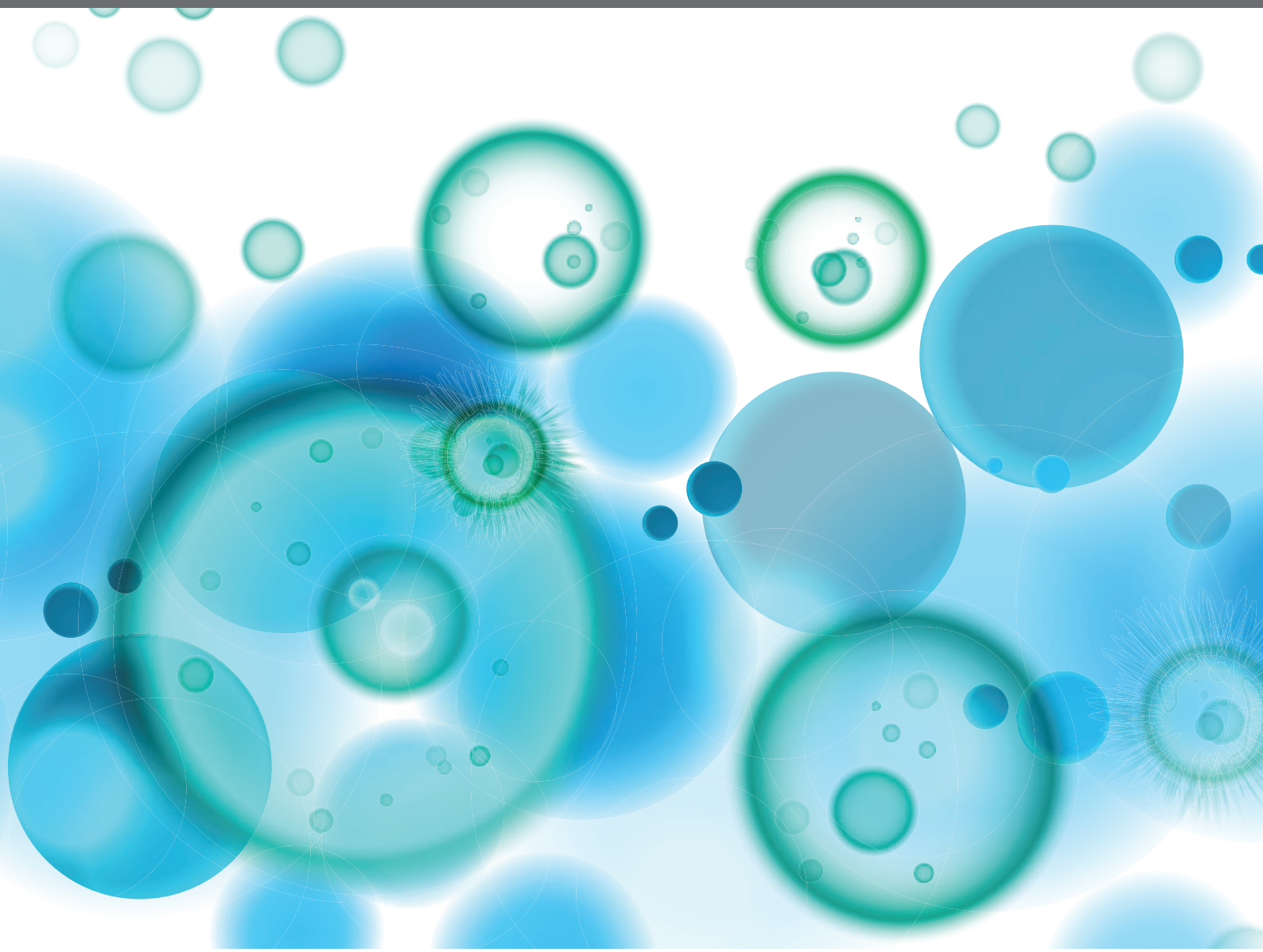

frontiers Research Topics

frontiers

ISSN 1664-8714
ISBN 978-2-88974-669-9
DOI 10.3389/978-2-88974-669-9

About Frontiers

Frontiers is more than just an open-access publisher of scholarly articles: it is a pioneering approach to the world of academia, radically improving the way scholarly research is managed. The grand vision of Frontiers is a world where all people have an equal opportunity to seek, share and generate knowledge. Frontiers provides immediate and permanent online open access to all its publications, but this alone is not enough to realize our grand goals.

Frontiers Journal Series

The Frontiers Journal Series is a multi-tier and interdisciplinary set of open-access, online journals, promising a paradigm shift from the current review, selection and dissemination processes in academic publishing. All Frontiers journals are driven by researchers for researchers; therefore, they constitute a service to the scholarly community. At the same time, the Frontiers Journal Series operates on a revolutionary invention, the tiered publishing system, initially addressing specific communities of scholars, and gradually climbing up to broader public understanding, thus serving the interests of the lay society, too.

Dedication to Quality

Each Frontiers article is a landmark of the highest quality, thanks to genuinely collaborative interactions between authors and review editors, who include some of the world's best academicians. Research must be certified by peers before entering a stream of knowledge that may eventually reach the public - and shape society; therefore, Frontiers only applies the most rigorous and unbiased reviews.
Frontiers revolutionizes research publishing by freely delivering the most outstanding research, evaluated with no bias from both the academic and social point of view. By applying the most advanced information technologies, Frontiers is catapulting scholarly publishing into a new generation.

What are Frontiers Research Topics?

Frontiers Research Topics are very popular trademarks of the Frontiers Journals Series: they are collections of at least ten articles, all centered on a particular subject. With their unique mix of varied contributions from Original Research to Review Articles, Frontiers Research Topics unify the most influential researchers, the latest key findings and historical advances in a hot research area! Find out more on how to host your own Frontiers Research Topic or contribute to one as an author by contacting the Frontiers Editorial Office: frontiersin.org/about/contact

THE IMMUNOLOGY OF ADVERSE DRUG REACTIONS

Topic Editors:
Patricia Illing, Monash University, Australia
Michael R. Ardern-Jones, University of Southampton, United Kingdom
Nicole Andrea Mifsud, Monash University, Australia
Jason Trubiano, University of Melbourne, Australia

Citation: Illing, P., Ardern-Jones, M. R., Mifsud, N. A., Trubiano, J., eds. (2022). The Immunology of Adverse Drug Reactions. Lausanne: Frontiers Media SA.
doi: 10.3389/978-2-88974-669-9

Table of Contents

frontiers in Immunology

EDITORIAL
published: 18 February 2022
doi: 10.3389/fimmu.2022.863414

Editorial: The Immunology of Adverse Drug Reactions

Patricia T. Illing[1]*, *Nicole A. Mifsud*[1], *Michael R. Ardern-Jones*[2,3] and *Jason Trubiano*[4]

[1] Infection and Immunity Program, Monash Biomedicine Discovery Institute and Department of Biochemistry and Molecular Biology, Monash University, Clayton, VIC, Australia, [2] Clinical Experimental Sciences, Faculty of Medicine, University of Southampton, Southampton, United Kingdom, [3] Department of Dermatology, University Hospitals Southampton NHS Foundation Trust, Southampton, United Kingdom, [4] Centre for Antibiotic Allergy and Research, Department of Infectious Diseases, Austin Health, Heidelberg, VIC, Australia

Keywords: adverse drug reaction, T cells, human leukocyte antigen, MRGPRX2, drug allergy, drug hypersensitivity

Editorial on the Research Topic

The Immunology of Adverse Drug Reactions

INTRODUCTION

The immune system has evolved for both breadth and specificity of recognition to protect the body against a wide array of infectious and oncogenic challenges. Unfortunately, this recognition can also extend to certain therapeutic drugs causing drug hypersensitivity in affected individuals. These unwanted responses range in both severity and pathways of immune activation, eliciting deleterious, and in some cases potentially fatal, immune responses. Such adverse events place significant strain on health care systems and prevent use (in susceptible individuals) of key medications that are well tolerated by most patients at therapeutic doses. Here, we bring together experts in the field of adverse drug reactions, incorporating both clinical and laboratory-based researchers, addressing critical areas of prediction, diagnosis and mechanistic understanding of these reactions.

OPEN ACCESS

Edited and reviewed by:
Antoine Toubert, Université Paris Diderot, France

***Correspondence:**
Patricia T. Illing
patricia.illing@monash.edu

Specialty section:
This article was submitted to Alloimmunity and Transplantation, a section of the journal Frontiers in Immunology

Received: *27 January 2022*
Accepted: *31 January 2022*
Published: *18 February 2022*

Citation:
Illing PT, Mifsud NA, Ardern-Jones MR and Trubiano J (2022) Editorial: The Immunology of Adverse Drug Reactions. Front. Immunol. 13:863414. doi: 10.3389/fimmu.2022.863414

T CELL-MEDIATED DRUG HYPERSENSITIVITY

10 articles within this collection focus primarily on T cell-mediated drug hypersensitivity reactions (DHRs), also termed delayed-type drug hypersensitivity or type IV drug hypersensitivity (under the Gell and Coombs classification) (1). T cell-mediated DHRs involve Human Leukocyte Antigen (HLA)-dependent activation of T cells induced by the culprit drug and/or a metabolite *via* a range of mechanisms including: i) generation and presentation of covalently drug modified peptides (*i.e.* hapten/prohapten model) (2, 3), ii) labile interaction of the drug/metabolite with the HLA and/or TCR to trigger T cell activation (*i.e.* p.i. concept) (4) and iii) interaction of the drug within the HLA peptide-binding cleft to change the array and conformation of HLA-bound peptides (*i.e.* altered peptide repertoire) (5, 6). Furthermore, many of these reactions are associated with distinct HLA alleles, suggesting specific interactions and that HLA screening could be used as a predictive tool to prevent prescription to individuals carrying risk alleles. However, as discussed by Li et al., this is not an effective solution for many HLA-associated adverse reactions due to negative predictive values less than 100% and low positive predictive values, necessitating large numbers of individuals to be tested in order to prevent a single adverse event. In light of this, Li et al. explore the evidence for further risk modifiers

within the HLA peptide presentation (Endoplasmic Reticulum aminopeptidase 1 [ERAP1] polymorphism) and recognition (T cell receptors [TCRs] and Killer-cell Immunoglobulin-like Receptors [KIRs]) pathways. Furthermore, they examine the concept of "dynamic risk" engendered by epigenetic changes, infection, and medications such as checkpoint inhibitors.

Original research articles by Pratoomwun et al., Puig et al., Mifsud et al., and Illing et al. focus on defining the molecular mechanisms of HLA-associated adverse reactions to co-trimoxazole, flucloxacillin, carbamazepine and abacavir, respectively. The study by Pratoomwun et al. explores T cell responses in two HLA-B*13:01$^+$ co-trimoxazole (combination sulfamethoxazole [SMX] and trimethoprim) hypersensitive patients. Surprisingly, HLA-B*13:01-restricted CD8$^+$ T cells were not identified, instead the metabolite (nitroso-SMX) and SMX responsive T cell clones were CD4$^+$ and HLA class II restricted, suggesting HLA-B*13:01 was not directly involved in presentation of the immunogenic antigens. Aligned with previous studies (7, 8), there were multiple modes of presentation observed, consistent with covalent modification of presented peptides by nitroso-SMX (in either antigen processing dependent or independent manners) and recognition of soluble SMX. To precisely examine the presented peptides at the cell surface, Puig et al., Mifsud et al., and Illing et al. combine immunopeptidomics with functional analyses to define immune activation *via* the presentation of covalently drug-modified peptides (Puig et al.; HLA-B*57:01-mediated presentation of flucloxacillin modified peptides), labile drug interaction (Mifsud et al.; HLA-B*15:02 and carbamazepine) and an altered peptide repertoire (Illing et al.; HLA-B*57:01 and abacavir) to extend previous mechanistic studies of these reactions (5, 6, 9–11).

In line with the review by Li et al., these studies each demonstrate the influence of antigen processing and presentation including the HLA-TCR/KIR axis. In addition to the identification of covalently modified peptides capable of eliciting T cell responses in transgenic HLA-B*57:01$^+$ mice, Puig et al. speculated that broader changes in the immunopeptidome were due to altered peptide processing, and that the location of identified modifications could alter KIR recognition. Mifsud et al. explored highly focused, private TCR responses to carbamazepine in severe DHRs, and Illing et al. assessed the influence of tapasin and abacavir on peptide loading onto (and dissociation from) HLA-B*57:01, highlighting the potential for antigen processing and presentation machinery to shape the drug-induced immunopeptidome.

Moving beyond the mechanisms for T cell activation, reviews by Schunkert et al. and Bechara et al. focus on the nature of the T cells responding to drug/chemical stimulation. Bechara et al. discuss the role of the naïve T cell repertoire in the recognition of drugs and chemicals and the persisting unknowns of the drug-responsive naïve T cell repertoire such as frequency, public vs private TCRs and origin during thymic selection. Schunkert et al. review the evidence for a role for skin resident memory T cells (T_{RM}) in delayed type hypersensitivity reactions, speculating on the mechanisms by which drug-responsive T_{RM} may be generated and become lodged in the skin. They highlight important challenges in phenotypic analysis which hinder understanding of T_{RM} in delayed type hypersensitivity and posit that novel mouse models of delayed type hypersensitivity [*e.g.* (12)] provide a road forward for dissecting the contribution of T_{RM} by enabling exploration of rechallenge.

DHRs often clinically present as complex immunopathologies. To address this, Thompson et al., Hammond et al., and Hertzman et al. focus on tools and workflows for accurate diagnosis, prediction and multi-omic analysis of DHRs. Through a series of case studies, Thompson et al. present a diagnostic workflow (incorporating patch and intradermal testing) for the assessment of β-lactam cross-reactivity or co-reactivity in non-Stevens-Johnson Syndrome/toxic epidermal necrolysis (SJS/TEN) severe cutaneous adverse reactions to determine whether broad β-lactam avoidance is necessary or careful testing of alternative β-lactams may be tolerated. Hammond et al. explore the utility of different *in vitro* diagnostic assays for the identification of culprit drugs in T cell-mediated drug hypersensitivity as well as preclinical assays to predict immunogenicity. Finally, Hertzman et al. present a tool for the analysis and visualisation of single cell TCR-seq, RNA-seq and Cellular Indexing of Transcriptomes and Epitopes by Sequencing (CITE)-seq data to enable researchers to take advantage of the exciting capacities of these technologies to reveal signatures of distinct cell subsets involved in the pathogenesis and prevention of different adverse reactions.

MAS-RELATED G PROTEIN-COUPLED RECEPTOR X2

Two review articles (Mackay et al. and McNeil) focus on the emerging role for Mas-related G protein-coupled receptor X2 (MRGPRX2) mediated mast cell activation in antibody-independent immediate hypersensitivity reactions. With a focus on anaphylaxis, Mackay et al. discuss strategies to pinpoint the role of MRGPRX2 and isolate biomarkers, further considering roles for MRGPRX2 agonists and antagonists in therapeutic applications. Moreover, McNeil interrogates the relationship between peak serum concentrations, as well as localised areas of increased concentration in specific tissues/locations, and the EC_{50} of known MRGPRX2 agonists in mild-moderate immediate hypersensitivity reactions. Both studies highlight the need for further investigation to understand the role of MRGPRX2 in adverse events and to provide clear diagnostic criteria.

CONCLUDING REMARKS

Collectively these articles highlight that, as for many fields, phenotypic, diagnostic, predictive and mechanistic studies traversing the clinic to the laboratory bench (and computer) and back are critical to understanding the complex biological interactions that characterise drug hypersensitivity. Future genetic and mechanistic analyses will build upon clinical observations, with the capacity to identify new biomarkers and signatures of disease that feedback to improve diagnosis, prediction, and prevention.

AUTHOR CONTRIBUTIONS

PTI drafted the manuscript. All authors edited and approved the manuscript.

REFERENCES

1. Gell PGH, Coombs RRA. *Clinical Aspects of Immunology*. Philadelphia: Davis (1963).
2. Pichler W, Yawalkar N, Schmid S, Helbling A. Pathogenesis of Drug-Induced Exanthems. *Allergy* (2002) 57:884–93. doi: 10.1034/j.1398-9995.2002.02161.x
3. Pohl LR, Satoh H, Christ DD, Kenna JG. The Immunologic and Metabolic Basis of Drug Hypersensitivities. *Annu Rev Pharmacol Toxicol* (1988) 28:367–87. doi: 10.1146/annurev.pa.28.040188.002055
4. Pichler WJ, Beeler A, Keller M, Lerch M, Posadas S, Schmid D, et al. Pharmacological Interaction of Drugs With Immune Receptors: The P-I Concept. *Allergol Int* (2006) 55:17–25. doi: 10.2332/allergolint.55.17
5. Ostrov DA, Grant BJ, Pompeu YA, Sidney J, Harndahl M, Southwood S, et al. Drug Hypersensitivity Caused by Alteration of the MHC-Presented Self-Peptide Repertoire. *Proc Natl Acad Sci USA* (2012) 109:9959–64. doi: 10.1073/pnas.1207934109
6. Illing PT, Vivian JP, Dudek NL, Kostenko L, Chen Z, Bharadwaj M, et al. Immune Self-Reactivity Triggered by Drug-Modified HLA-Peptide Repertoire. *Nature* (2012) 486:554–8. doi: 10.1038/nature11147
7. Ogese MO, Saide K, Faulkner L, Whitaker P, Peckham D, Alfirevic A, et al. HLA-DQ Allele-Restricted Activation of Nitroso Sulfamethoxazole-Specific CD4-Positive T Lymphocytes From Patients With Cystic Fibrosis. *Clin Exp Allergy* (2015) 45:1305–16. doi: 10.1111/cea.12546
8. Schnyder B, Burkhart C, Schnyder-Frutig K, von Greyerz S, Naisbitt DJ, Pirmohamed M, et al. Recognition of Sulfamethoxazole and its Reactive Metabolites by Drug-Specific CD4(+) T Cells From Allergic Individuals. *J Immunol* (2000) 164:6647–54. doi: 10.4049/jimmunol.164.12.6647
9. Waddington JC, Meng X, Illing PT, Tailor A, Adair K, Whitaker P, et al. Identification of Flucloxacillin-Haptenated HLA-B*57:01 Ligands: Evidence of Antigen Processing and Presentation. *Toxicol Sci* (2020) 177:454–65. doi: 10.1093/toxsci/kfaa124
10. Pan RY, Chu MT, Wang CW, Lee YS, Lemonnier F, Michels AW, et al. Identification of Drug-Specific Public TCR Driving Severe Cutaneous Adverse Reactions. *Nat Commun* (2019) 10:3569. doi: 10.1038/s41467-019-11396-2
11. Norcross MA, Luo S, Lu L, Boyne MT, Gomarteli M, Rennels AD, et al. Abacavir Induces Loading of Novel Self-Peptides Into HLA-B*57: 01: An Autoimmune Model for HLA-Associated Drug Hypersensitivity. *AIDS* (2012) 26:F21–9. doi: 10.1097/QAD.0b013e328355fe8f
12. Cardone M, Garcia K, Tilahun ME, Boyd LF, Gebreyohannes S, Yano M, et al. A Transgenic Mouse Model for HLA-B*57:01-Linked Abacavir Drug Tolerance and Reactivity. *J Clin Invest* (2018) 128:2819–32. doi: 10.1172/JCI99321

Conflict of Interest: PTI and NAM were authors of two papers within the collection (Illing et al. and Mifsud et al.).

The remaining authors declare that the research was conducted in the absence of any commercial or financial relationships that could be construed as a potential conflict of interest.

Publisher's Note: All claims expressed in this article are solely those of the authors and do not necessarily represent those of their affiliated organizations, or those of the publisher, the editors and the reviewers. Any product that may be evaluated in this article, or claim that may be made by its manufacturer, is not guaranteed or endorsed by the publisher.

frontiers in Immunology

ORIGINAL RESEARCH
published: 09 February 2021
doi: 10.3389/fimmu.2020.629399

Alterations in the HLA-B*57:01 Immunopeptidome by Flucloxacillin and Immunogenicity of Drug-Haptenated Peptides

Montserrat Puig[1], Suryatheja Ananthula[1], Ramesh Venna[1], Swamy Kumar Polumuri[1], Elliot Mattson[1], Lacey M. Walker[2], Marco Cardone[1], Mayumi Takahashi[3], Shan Su[1], Lisa F. Boyd[4], Kannan Natarajan[4], Galina Abdoulaeva[5], Wells W. Wu[5], Gregory Roderiquez[1], William H. Hildebrand[6], Serge L. Beaucage[3], Zhihua Li[2], David H. Margulies[4] and Michael A. Norcross[1]**

[1] Laboratory of Immunology, Office of Biotechnology Products, Center for Drugs Evaluation and Research, Food and Drug Administration, Silver Spring, MD, United States, [2] Division of Applied Regulatory Science, Office of Translational Science, Center for Drugs Evaluation and Research, Food and Drug Administration, Silver Spring, MD, United States, [3] Laboratory of Biological Chemistry, Office of Biotechnology Products, Center for Drugs Evaluation and Research, Food and Drug Administration, Silver Spring, MD, United States, [4] Molecular Biology Section, Laboratory of Immune System Biology, National Institute of Allergy and Infectious Diseases, National Institutes of Health, Bethesda, MD, United States, [5] Facility for Biotechnology Resources, Center for Biologics Evaluation and Research, Food and Drug Administration, Silver Spring, MD, United States, [6] Department of Microbiology and Immunology, School of Medicine, University of Oklahoma Health Sciences Center, Oklahoma City, OK, United States

OPEN ACCESS

Edited by:
Jason Trubiano,
University of Melbourne, Australia

Reviewed by:
Ian Nicholson,
Victorian Transplantation and Immunogenetics Service, Australia
Jakob Nilsson,
University Hospital Zürich, Switzerland

***Correspondence:**
Montserrat Puig
Montserrat.puig@fda.hhs.gov
Michael A. Norcross
Michael.norcross@fda.hhs.gov

Specialty section:
This article was submitted to Alloimmunity and Transplantation, a section of the journal Frontiers in Immunology

Received: 14 November 2020
Accepted: 23 December 2020
Published: 09 February 2021

Citation:
Puig M, Ananthula S, Venna R, Kumar Polumuri S, Mattson E, Walker LM, Cardone M, Takahashi M, Su S, Boyd LF, Natarajan K, Abdoulaeva G, Wu WW, Roderiquez G, Hildebrand WH, Beaucage SL, Li Z, Margulies DH and Norcross MA (2021) Alterations in the HLA-B*57:01 Immunopeptidome by Flucloxacillin and Immunogenicity of Drug-Haptenated Peptides. Front. Immunol. 11:629399. doi: 10.3389/fimmu.2020.629399

Neoantigen formation due to the interaction of drug molecules with human leukocyte antigen (HLA)-peptide complexes can lead to severe hypersensitivity reactions. Flucloxacillin (FLX), a β-lactam antibiotic for narrow-spectrum gram-positive bacterial infections, has been associated with severe immune-mediated drug-induced liver injury caused by an influx of T-lymphocytes targeting liver cells potentially recognizing drug-haptenated peptides in the context of HLA-B*57:01. To identify immunopeptidome changes that could lead to drug-driven immunogenicity, we used mass spectrometry to characterize the proteome and immunopeptidome of B-lymphoblastoid cells solely expressing HLA-B*57:01 as MHC-I molecules. Selected drug-conjugated peptides identified in these cells were synthesized and tested for their immunogenicity in HLA-B*57:01-transgenic mice. T cell responses were evaluated *in vitro* by immune assays. The immunopeptidome of FLX-treated cells was more diverse than that of untreated cells, enriched with peptides containing carboxy-terminal tryptophan and FLX-haptenated lysine residues on peptides. Selected FLX-modified peptides with drug on P4 and P6 induced drug-specific $CD8^+$ T cells *in vivo*. FLX was also found directly linked to the HLA K146 that could interfere with KIR-3DL or peptide interactions. These studies identify a novel effect of antibiotics to alter anchor residue frequencies in HLA-presented peptides which may impact drug-induced inflammation. Covalent FLX-modified lysines on peptides mapped drug-specific immunogenicity primarily at P4 and P6 suggesting these peptide sites as drivers of off-target adverse reactions mediated by FLX. FLX

modifications on HLA-B*57:01-exposed lysines may also impact interactions with KIR or TCR and subsequent NK and T cell function.

Keywords: flucloxacillin, HLA-B*57:01, drug hypersensitivity, hapten, immunogenicity, transgenic mice

INTRODUCTION

Idiosyncratic drug-induced liver injury (DILI) is a rare but potentially fatal adverse drug reaction and a major obstacle in the development of pharmaceuticals. Understanding the biochemistry and immune pathways that mediate severe adverse drug reactions is critical for identifying treatment and prevention strategies to minimize unwanted off-target drug effects. Although liver injury can result from expected toxicities based on the chemical nature of a drug, idiosyncratic reactions may also manifest in susceptible patients. These reactions are complex and many are considered to be immune-mediated based on (i) the presence of mononuclear cells, including effector $CD8^+$ T cells, in liver biopsies of patients experiencing DILI (1, 2), and (ii) the reactivity of these patients' T cells to drug stimulation *in vitro*, often observed to be dependent on the expression of specific HLA Class-I and II alleles (3–5). Genome-wide association studies in patients with FLX-induced DILI found this adverse reaction to be significantly associated with the expression of HLA-B*57:01 (6) and HLA-B*57:03 (7), allelomorphs that differ by only two amino acid residues. T cell reactivity to FLX was demonstrated *in vitro* to be elicited by both soluble drug and drug-pulsed presenting cells, the latter suggested to be mediated by covalently-linked FLX on protein epitopes (4, 5, 8). FLX-stimulated peripheral blood $CD8^+$ and $CD4^+$ T cells from HLA-B*57:01$^+$ DILI patients primarily in an antigen-processing dependent manner (4). However, T cells from HLA-B*57:01$^+$ drug-naïve healthy individuals required soluble FLX in the cultures and rarely responded to drug-pulsed targets (5, 8). Of note, T cell clones from the HLA-B*57:01$^+$ patients responded to soluble FLX presented by non-B*57:01 HLA alleles (8).

While there is an accepted association between the immune system and drug-mediated liver injury, the mechanisms by which drugs cause immune cell activation are still poorly understood. Proposed molecular mechanisms to explain drug hypersensitivity are based on drug-peptide interactions. T cell responses to non-covalent drug-peptide complexes are known as the pharmaceutical interaction mechanism, while antigen processing-dependent responses are thought to be driven by drug covalently linked to peptides presented by HLA molecules (9–12). In addition, we and others have described a non-covalent mechanism by which abacavir facilitates the loading of novel self-peptides with changes in the consensus C-terminal anchor residues into HLA-B*57:01, inducing autoimmune-like reactions to the drug-altered antigens (13–15). In this report, using immunoproteomics, we show that FLX treatment of antigen presenting cells expressing HLA-B*57:01 effects changes in the immunoproteome by mechanisms different from those of abacavir. Instead, without affecting the cellular proteome, FLX increased the diversity of the peptide repertoire of sampled proteins favoring the presence of tryptophan in the F-pocket anchor motif. We also identified several peptides on the HLA-B*57:01 immunopeptidome pool with FLX-conjugated in lysine residues (FLX-peptides). These were subsequently characterized by mass spectrometry and chemically synthesized for immunogenicity evaluation in an HLA-B*57:01$^+$ transgenic mouse. The immunogenic potential of the FLX-peptides was found to depend on both the peptide sequence as well as the position at which FLX was conjugated.

METHODS

Reagents

Flucloxacillin (FLX) was obtained from Apotex, UK or Sigma-Aldrich, USA. FLX-conjugated lysine residues were prepared according to the method of Scornet et al. (16) (**Figure S1** and **Supplementary Methods**) and used to synthesize FLX-modified peptides by solid-phase Fmoc chemistry.

B-Lymphoblastoid Cell Lines

The HLA-B*57:01 full-length sequence for membrane bound HLA (mHLA) was transduced using a lentiviral expression system. From here on, HLA-B*57:01-expressing cells are referred as B721-5701. The expression of soluble HLA-B*57:01 (sHLA) in the HLA class I-negative EBV-transformed B-lymphoblastoid 721.221 cell line was described elsewhere (14).

Proteomics and LC-MS/MS Analysis

Proteomic characterization of B721-5701 cells is presented in **Supplementary Methods**. Cells were grown in the absence or presence of FLX for 5 days in duplicate cultures. Cells were harvested and proteins extracted and trypsinized. After ion exchange fractionation, peptides were analyzed by LC-MS on a Q-Exactive MS with nano-LC. Data was processed with the PEAKS 8.5 software using Uniprot non-redundant human database (https://www.uniprot.org).

Generation, Isolation, and Identification of HLA-Bound Peptides

B721.5701 cells expressing mHLA were grown without antibiotics in G-Rex 6-Well Plates to high density for 5 days with or without 150 μg/ml FLX as described in **Supplementary Methods**. Cell lysates were immune-affinity purified using anti-HLA class-I antibody W6/32. Acid-eluted peptides were analyzed using nano-LC-MS/MS with a ThermoFisher Ultimate LC and Fusion Orbitrap MS. Soluble HLA from untreated or FLX-treated cultures was collected from continuous cultures as described in **Supplementary Methods**.

Peptides were purified from sHLA/peptide complexes by immuno-affinity purification followed by acid elution and filtration. Peptide identity was determined as detailed in **Supplementary Methods**.

Peptide Docking Modeling

Details of the protocols applied to modeling peptide interactions with drug, HLA and TCR are described in **Supplementary Methods**. Images were generated using PyMOL (The PyMOL Molecular Graphics System, Version 2.0 Schrödinger, LLC).

Treatment of Mice

HLA-B*57:01 transgenic/H2-K^bD^b knockout (Tg/KO) mice were generated by backcrossing HLA-B*57:01/H2-D^d Tg (17) to *H2-K^bD^b* KO C57BL/6 (B6.129P2-*H2-Kb^{tm1}H2-Db^{tm1}* N12) mice (18) (Taconic Biosciences, Hudson, NY). Tg/KO mice were immunized with 100 μg of FLX-haptenated peptide (FLX-peptide) containing immune adjuvants as detailed in **Supplementary Methods**. At day 14, spleens were processed for *in vitro* testing.

Cell Culture

Splenocytes from Tg/KO mice were cultured for 5 days in complete RPMI supplemented with 0.5% heat-inactivated, normal mouse serum (days 0-2) and 10% fetal bovine serum (days 3-5) in the absence or presence of 10 μg/ml of FLX-peptides or unmodified peptide. Secretion of IFN-γ was measured in cell culture supernatants by ELISA.

Flow Cytometry

Flow cytometry was used for mouse phenotyping (**Figure S2**) and to analyze immune cell subsets by intracellular and/or surface marker staining as detailed in the **Supplementary Methods**.

RESULTS

Effect of FLX Treatment on the Proteome and Immunopeptidome of B721-5701 Cells

We hypothesized that FLX-driven changes in the protein content of the cell could impact the quality and quantity of antigen processing and presentation, including FLX-haptenated epitopes. B721-5701 cells were treated with subtoxic concentrations of FLX for 5 days (**Figure S3**). On average, 3,401 proteins were identified per sample by LC-MS/MS (**Figure 1A** and **Table S1**). A high Spearman correlation (>0.943) was obtained for all samples, independent of the

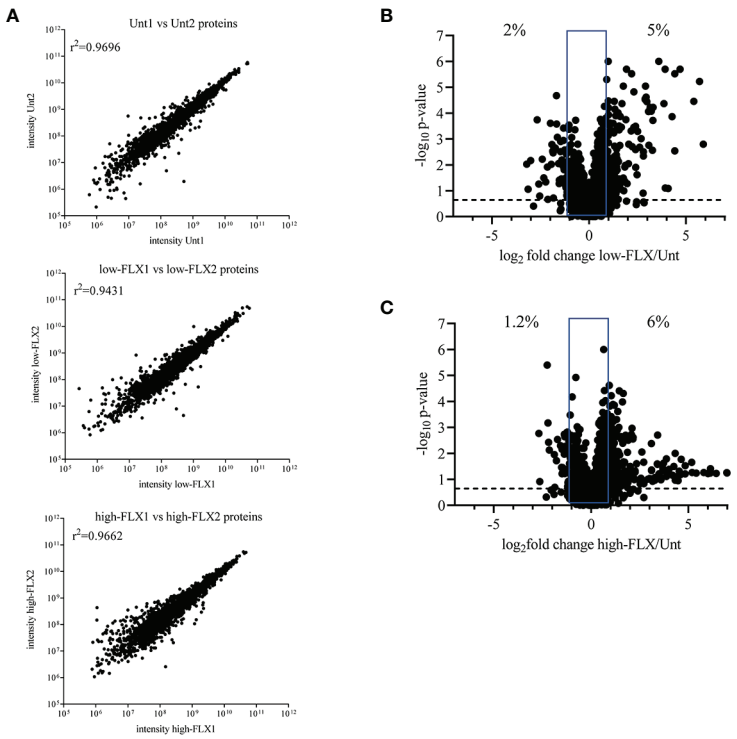

FIGURE 1 | Flucloxacillin (FLX) does not significantly alter the B721-5701 cell proteome. Protein lysates were obtained from ten million B721-5701 cells treated with FLX at 150 μg/ml (low) or 453 μg/ml (high) for 5 days, or from untreated cultures (Unt), in duplicate. Samples were processed by LC-MS/MS and analyzed by Peaks 8.5 software. **(A)** Correlation among biological replicates. Protein abundance is represented in arbitrary units of intensity. **(B, C)** Increased (log_2 fold change ≥ 1) and decreased (log_2 fold change ≤ -1) abundance of proteins in the proteome of cells treated with low-FLX **(B)** or high-FLX concentration **(C)** compared to Unt, considering the average abundance of the two biological replicates per treatment. Percent values indicate divergence in abundance. Statistical differences were calculated by Spearman correlation. Proteome datasets are included in **Table S1**.

treatment, indicating that overall, FLX treatment did not change the proteome of the cell. Changes in the relative counts (intensity) of <7% of proteins of the proteome of cells treated with drug vs untreated cells (**Figures 1B, C**) were not associated with any particular pathway when assessed by ingenuity pathway analysis (data not shown).

In parallel, cells were treated with FLX at 150 μg/ml for 5 days (FLX-cells) or left untreated (Unt-cells) in two biological replicates for immunopeptidome analysis. Among all four samples, LC-MS/MS analysis identified a total of 3,610 peptides of 8–15 amino acids in length, from which 1142 were detected only in FLX-cells and 226 peptides were only found in Unt-cells. The remaining 1121 peptides were common in both treatment groups (**Figure 2A** and **Tables S2A, B**). The peptide length distribution within each one of these subgroups was similar (**Figures 2B, C**), with dominance of sequences of 9–11 amino acids (89 ± 4%), from which 50% were 9-mers. Approximately 12% of the peptides in both datasets presented PTMs (**Figures 2D, E**). Cysteinylated peptides were twice as abundant in the FLX-cells as compared to the Unt-cells.

A total of 1,603 different protein sequences represented by the identified 3,610 peptides (**Tables S2A, B**). Of those, 874 proteins were identified in both treatment conditions, represented by 1238 peptides of the Unt-cells and 1511 peptides of FLX-cells peptide repertoire. The remaining protein sequences were unique to each treatment (**Figure 2F**). Overall, most of the proteins were represented by a single peptide (75.7% in Unt-cells and 70.8% in FLX-cells). Only 16.5% and 18% of the proteins were represented by two peptides (Unt-cells and FLX-cells, respectively), while 7.5% and 10% were proteins with three to five peptides (Unt-cells and FLX-cells, respectively) (**Figure 2G**). Of note, FLX-cells had a larger number of proteins with higher peptide representation than the Unt-cells.

In agreement with others (19, 20), only a fraction of the identified proteins in the proteome were represented in the HLA peptidome of Unt-cells (13%) and FLX-cells (21.8%),

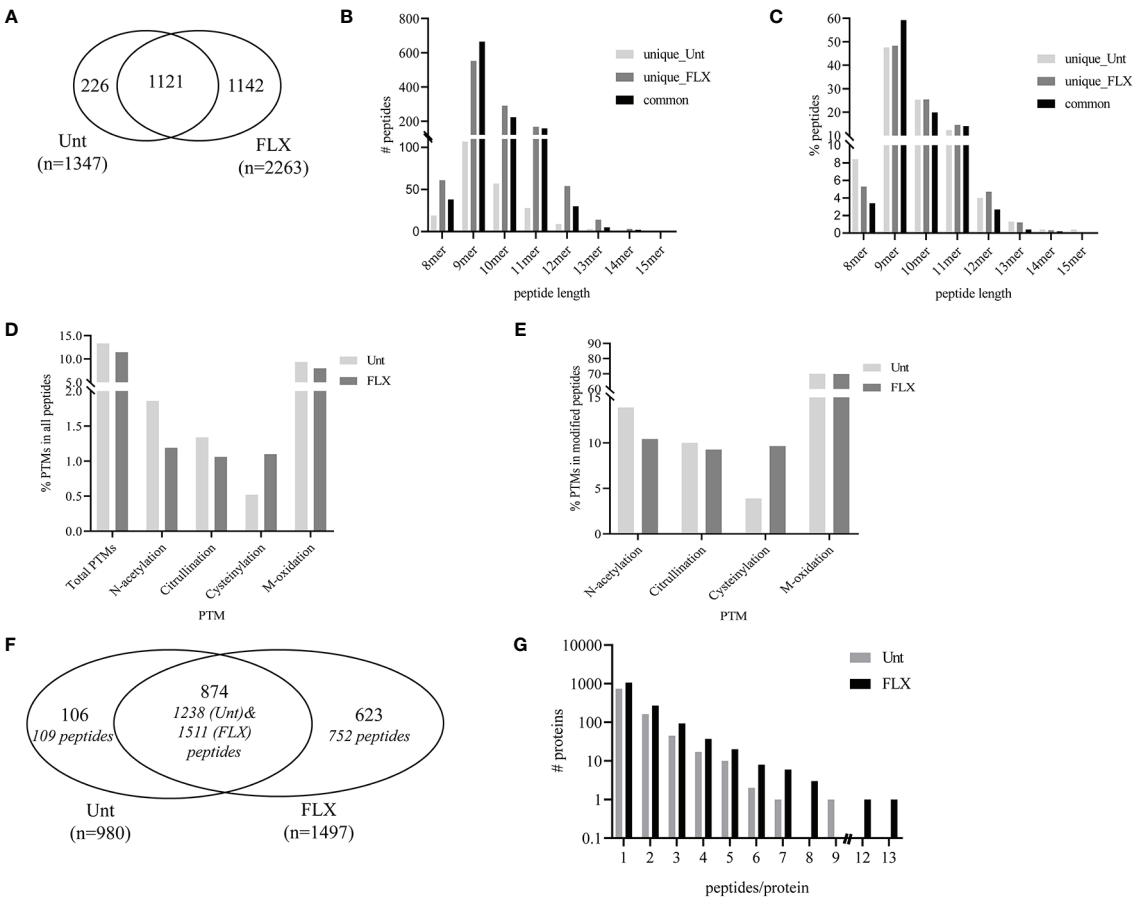

FIGURE 2 | Flucloxacillin (FLX) treatment induces diversity in the peptide repertoire of B721-5701 cells. Common and unique peptides eluted from human leukocyte antigen (HLA)/peptide complexes obtained from two independent cultures of untreated B721-5701 cells (Unt) and of cells treated with 150 μg/ml of FLX (FLX) for 5 days were combined for the analysis **(A)**. Absolute counts **(B)** or frequency **(C)** of 8–15 amino acid peptides. Frequency of peptides with post-translational modification (PTM) within the peptide repertoire **(D)** or among modified peptides **(E)**. Common and unique proteins represented by immunopeptidome-contained sequences (in **Figure 2A**) **(F)**. Protein distribution showing the number of peptides per protein **(G)**. Data analysis was performed using Peaks 8.5 and X software. The datasets of peptides in the B721-5701 peptidomes are provided in **Table S2A, B**.

corresponding to a total of 435 and 699 proteins, respectively. As expected, longer or more abundant proteins contributed to more peptides in the immunopeptidome (**Figures 3A, B**), although the peptide number/protein was significantly higher in both sampled unique and common proteins of FLX-cells (**Figure S4** and **Table S3**). We then calculated the HLA class-I sampling density (D) as described previously (19, 20), a normalization score that takes into account the number of observed HLA peptides of a given protein as a function of its length, and used D to identify proteins that were presented at a higher rate than what was expected for their abundance (represented by D'). Most of the proteins with high over-presentation scores (D/D'>3) had roles in transcription, translation or mitochondrial-related pathways (**Table S3**). Ribosomal subunits had the highest scores (D/D'>5) in both treatment conditions. Interestingly, β_2-microglobulin epitopes were found in the FLX-cell immunopeptidome but not in the Unt-cell (D/D'>6). In general, the FLX-cell proteome had more over-presented proteins (D/D'>2) than the Unt-cell proteome (86 vs 47, respectively) (**Figure 3C** and **Table S3**). This trend did not correlate with protein abundance (r^2<0.00230 and 0.00196 for the control and FLX-treated group, respectively) (**Figure 3C**). These results suggest a qualitative and quantitative impact of the drug in the cell immunopeptidome, which is not associated with a change of the cellular proteome but most likely to an effect on antigen processing and presentation.

FLX Treatment Increases HLA-B*57:01-Presented Peptides Containing Tryptophan in the PΩ Position

The peptide repertoire presented by HLA-B*57:01 molecules is determined by the presence of specific amino acids in the anchor positions of its binding motif. Unlike peptides identified from abacavir-treated cells (13–15), 9-mers in the immunopeptidome of FLX-cells exhibit consensus amino acids for the HLA-B*57:01 peptide anchor motif at position P2 and P9 (**Figure 4A**). However, FLX-cells presented a higher frequency of peptides with tryptophan at PΩ than those untreated, mainly in unique peptides (3.7% in Unt *vs* 79.8% in FLX) (**Tables S2A, B** and **Figure 4A** for 9-mers). Common peptides with C-terminal tryptophan were also more abundant in the FLX-cells (**Figure 4B**). This phenomenon was also observed in two additional independent experiments (**Figure S5**). Interestingly, peptides with C-terminal tryptophan had the highest predicted HLA-binding affinity (<50 nM). Although arginine was dominant at P7 [a secondary anchor residue (21)] of high-affinity peptides, glutamic acid was significantly increased in peptides of FLX-cells (**Figure 4C** and **Tables S2A, B**). These findings suggest that, in contrast to the ability of abacavir to alter the anchor motif of the neoepitopes from phenylalanine, tryptophan or tyrosine to leucine or isoleucine at PΩ, FLX increases the presentation of self-epitopes with predominantly tryptophan at the C-terminal position.

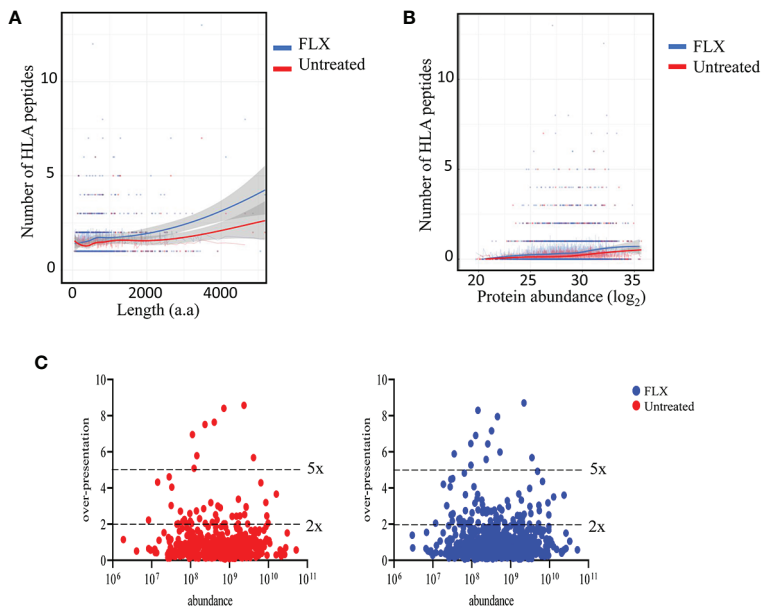

FIGURE 3 | Flucloxacillin (FLX) treatment promotes a higher peptide sampling rate of proteins, independently of the length and abundance of the polypeptide. Abundance of human leukocyte antigen (HLA) peptides from 435 and 699 proteins in the proteome of B721-5701 cells untreated or FLX-treated, respectively, as a function of the protein amino acid length **(A)** or abundance (log_2) **(B)**. Individual proteins and trendlines are represented in the graphs. **(C)** Protein fold over-presentation was calculated based on the ratio between observed (D) and expected (D') peptide density, and represented as function of protein abundance. The dataset of the represented proteins is provided in **Table S3**.

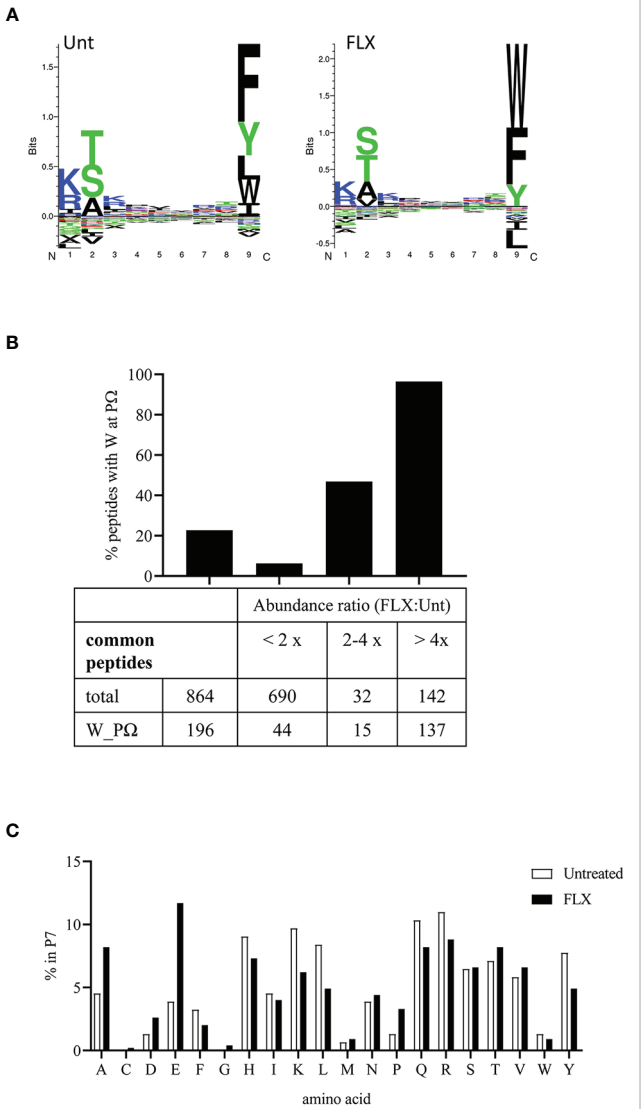

		Abundance ratio (FLX:Unt)		
common peptides		< 2 x	2-4 x	> 4x
total	864	690	32	142
W_PΩ	196	44	15	137

FIGURE 4 | Flucloxacillin (FLX) treatment does not alter consensus peptide binding motif of HLA-B*57:01 peptides but favors peptides with tryptophan in P9/PΩ. **(A)** Unsupervised analysis of the sequence motif from 9-mer sequences in the immunopeptidome of B721-5701 cells, untreated (Unt) or treated with FLX for 5 days (FLX), using Gibbs Cluster 2.0 software (peptide sequence details provided in Table S2A-B). Peptides with PTMs were excluded from this analysis. **(B)** Ratio of the abundance of the common peptides in the FLX vs Unt immunopeptidome samples, including total and C-terminal tryptophan (W) peptides. Ratios are represented as FLX : Unt lower than two-fold, between two- and four-fold or higher than four-fold. Abundance values were calculated using Quant analysis of common peptide quantifiable IDs (<1% FDR). **(C)** Frequency of the different amino acid residues at P7 of 9-mers with predicted binding affinity <50 nM (by NetMHC 4.0 software).

Identification of FLX-Haptenated Self-Peptides Derived From sHLA in B721-5701 Cells

Drug conjugation to self-peptides has been proposed as a molecular mechansim by which FLX leads to the generation of neoepitopes and T cell reactivity (4, 5, 12). Thus, we focused on identifying FLX-haptenated peptides (FLX-peptides) in our peptide dataset. Initial experiments with small scale cultures did not identify FLX-peptides, suggesting that haptenated peptides were in low concentration. In an attempt to increase the amount of HLA and thus the frequency of FLX-sequences, we cultured B721-5701 producing a soluble form of HLA (sHLA) in high density biopharms as described previously (14). We identified several peptides containing FLX on lysines (K) as well as the corresponding unmodified sequences: TAAQITQRKW (TAA) from HLA, KAAKLKEKY (KAA) from the high mobility group HMGB-1 protein and RTKKVGIVGKY (RTKK) from a 60S ribosomal protein. The latter two peptides revealed multiple possible lysine-drug conjugation sites (**Table 1**). Collision-induced dissociation MS2 resulted in complex spectra with peptide fragments along with drug ions +160, +295, and +454 as labelled on the TAA peptide spectrum in **Figure 5A**, even though intact drug was not found on fragmented sequences. However, drug-modified peptides did retain diagnostic fragments containing K+294 FLX, the residual portion of FLX covalently linked to the peptides as illustrated in **Figure 5A**. We identified b4-K+294 in FLX-RTKK_K4 and FLX-KAA-K4, and y2-K+294 in FLX-TAA_K9. Interestingly, the modified lysine in TAA corresponded to K146 of the HLA, an interaction site with KIR-3DL immuno-regulatory receptor of NK cells. Peptides were further validated by chemical syntheses using FLX-coupled Fmoc lysines as described in Methods (**Figure S6A**). In addition, we synthesized two KAA peptides with FLX in lysine 6 or 8 (FLX-KAA_K6 and FLX-KAA_K8) and RTKK with drug in the lysine in position 10 (FLX-RTKK_K10), as controls for immunogenicity studies, although these were not identified in the peptide repertoire. Quality control runs of the synthesized FLX-peptides surprisingly showed RP-HPLC chromatograms with two peaks by retention time (RT) each with the same mass by LC-MS (**Figures S6B, C**). FLX-RTKK_K4 isomeric forms differing in RT were later confirmed in the B721-5701 immunopeptidome (**Figure 5B**). We hypothesized that the difference in RP-HPLC RT was secondary to conformational differences between the FLX adducts. For these reasons, the two RP-HPLC peaks of the FLX-RTKK peptides were purified separately and tested independently in *in vivo* experiments.

The Immunogenic Potential of FLX-Peptides Depends on the Peptide Sequence and the Drug-Conjugated Amino Acid Position

To evaluate the immunogenicity potential of the FLX-peptides, we immunized Tg mice expressing only the chimeric HLA-B*57:01/H2-D^{d}(α3) and not classical mouse MHC-class I (H2-K^{b} and H2-D^{b}) molecules (Tg/KO). Peptide-specific T cell responses were observed in animals treated with several FLX-peptides upon splenocyte *in vitro* restimulation (**Figures 6A, B**). FLX-RTKK_K4 induced higher levels of IFN-γ secretion than FLX-RTKK_K10 in cells of animals immunized with the same peptides, and did not cross-react with either the parent, unlike cells from some of the FLX-RTKK_K10-immunized mice, or the

TABLE 1 | Unmodified and flucloxacillin (FLX)-modified peptides found in B721-5701_HLA cell preparations.

Peptide	FLX-conjugated residue in the protein	Peptide Length	Mass	m/z	z	Protein Accession	Protein Description
KAAKLKEKY	na	9	1,077.6545	539.8342	2	P09429|HMGB1_HUMAN	High mobility group protein B1
KAAK(+453.06)LKEKY	K150	9	1,530.7102	511.2447	3		
RTKKVGIVGKY	na	11	1,247.7714	624.897	2	P61513|RL37A_HUMAN	60S ribosomal protein L37a
RTKK(+453.06)VGIVGKY	K7	11	1,700.8269	567.9514	3		
TAAQITQRKW	na	10	1,201.6524	602.34	2	P18465|1B57_HUMAN	HLA class I histocompatibility antigen B-57 alpha chain
TAAQITQRK(+453.06)W	K145	10	1,654.7124	828.3697	2		

na, not applicable.

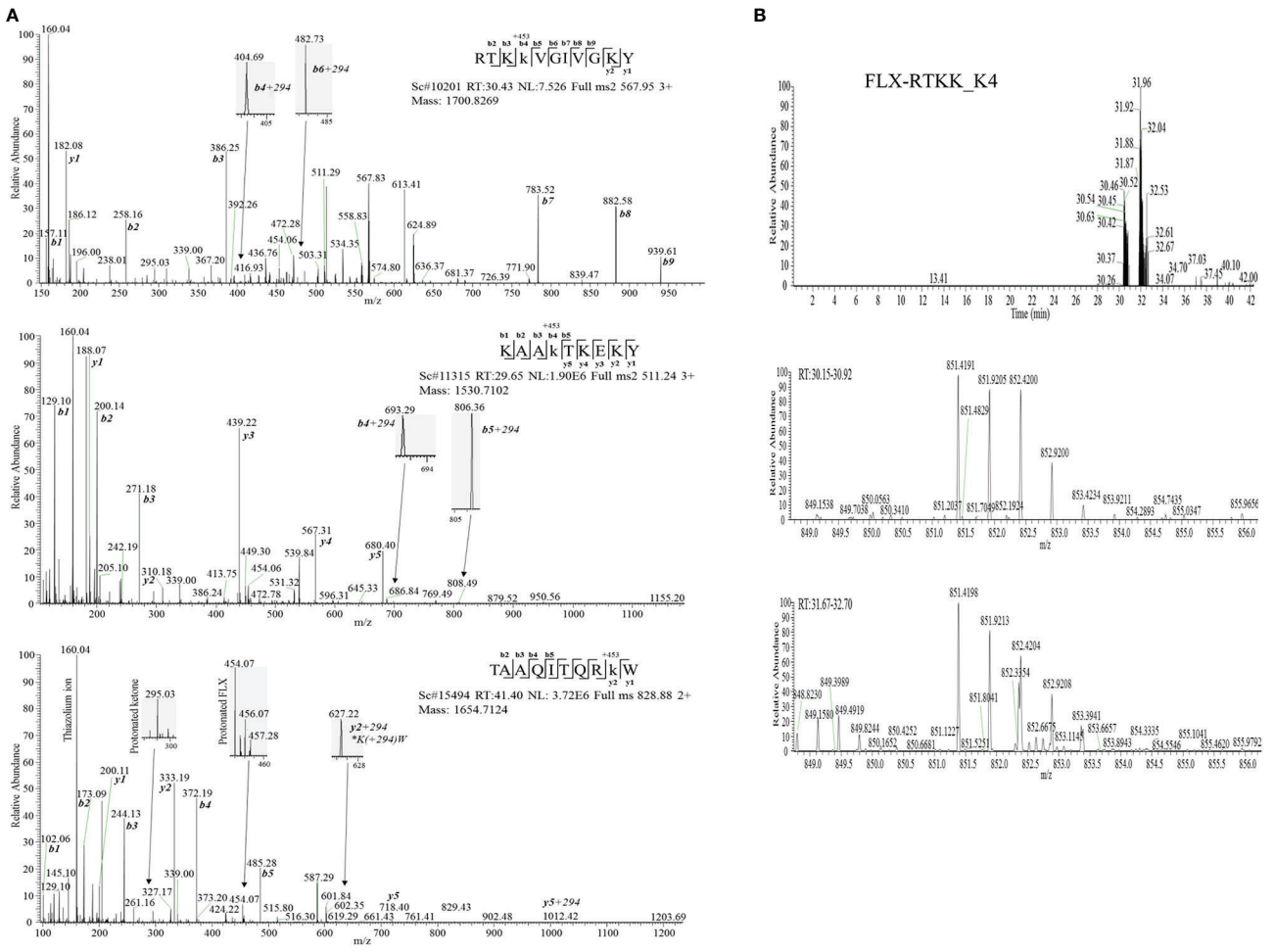

FIGURE 5 | Flucloxacillin modified peptides identified from drug treated HLA-B*57:01 expressing cells. **(A)** MS/MS spectra of parent ions with characteristic b and y ions, drug fragments (160.04, 295.03, 454.06/07) and diagnostic b+294 fragments identified: RTKK(FLX)VGIVGKY (FLX-RTKK_K4, top panel), KAAK(FLX)LKEKY (FLX-KAA_K4, middle panel), and FLX-modified TAAQITQRK(FLX)W (FLX-TAA_K9, bottom panel). **(B)** Two FLX-RTKK_K4 isoforms, with different retention time by RP-HPLC (peaks at minute 30.46 and 31.92) (top chromatogram) but identical mass (m/z=851.4191/2+, m/z=567.85/3+ (data not shown)) (mid and low LC-MS1 spectra). All peptides were identified using PEAKS analysis and verified manually.

other modified counterpart. (**Figures 6A, C**). Both FLX-RTKK peptide isomers showed similar specificity and immunogenic potential (**Figure 6C**). The IFN-γ response was driven by $CD8^+$ but not $CD4^+$ T cells (**Figure 6D**). Importantly, the recognition of FLX-peptides by $CD8^+$ T cells was dependent on the HLA-B*57:01 expression, as evidenced by the effect of an anti-HLA antibody on IFN-γ secretion (**Figure 6A**). Immunizations with FLX-KAA_K4 and _K6 also generated antigen-specific and

HLA-dependent T cell responses but at lower magnitude than the FLX-RTKK_K4. Control FLX-KAA_K8 showed no T cell reactivity (**Figure 6B**). FLX-TAA_K9 also failed to induce an immune response (**Figures 6A, D**). These results suggest that peptides bearing modified lysines in specific positions are more immunogenic than others depending on their exposure to solvent and accessibility to TCR.

To visualize the spatial position of the drug on the peptide, we used computational modeling. This was achieved by docking the peptide into the HLA cleft using FlexPepDock software (22, 23), followed by addition of the drug to the appropriate lysine and energy minimization of the structure using OpenBabel (24). Differences in the location of the drug on the HLA/peptide complex were evident between the immunogenic and not immunogenic peptides (**Figure 7** and **Figure S7**). FLX in lysines at P4 (i.e. FLX-RTKK_K4 in **Figures 7B, E**) or P6 (FLX-KAA_K6 in **Figures S7C, G**) occupies a central location on the HLA cleft, resembling the bulge of a longer peptide, whereas when conjugated in PΩ-1, (i.e. FLX-RTKK_K10 in **Figures 7C, F**) it occupies a position on the outer border of the HLA-bound peptide. Although we do not have FLX-specific T cell receptors (TCR) to model this interaction, we superposed a TCR from the HIV KAF TCR (2YPL) on FLX-RTKK_K4 and _K10 (**Figure S8**). The TCR footprint is consistent with FLX-peptide recognition at K4 interacting with the TCR V-alpha CDR3 (**Figure S8A**). This contrasts with peptide conjugated FLX at PΩ-1 that is oriented more towards TCR V-beta CDR3 (**Figure S8B**).

Althogether, these data indicate that FLX-peptides are immunogenic in association with HLA-B*57:01 and the

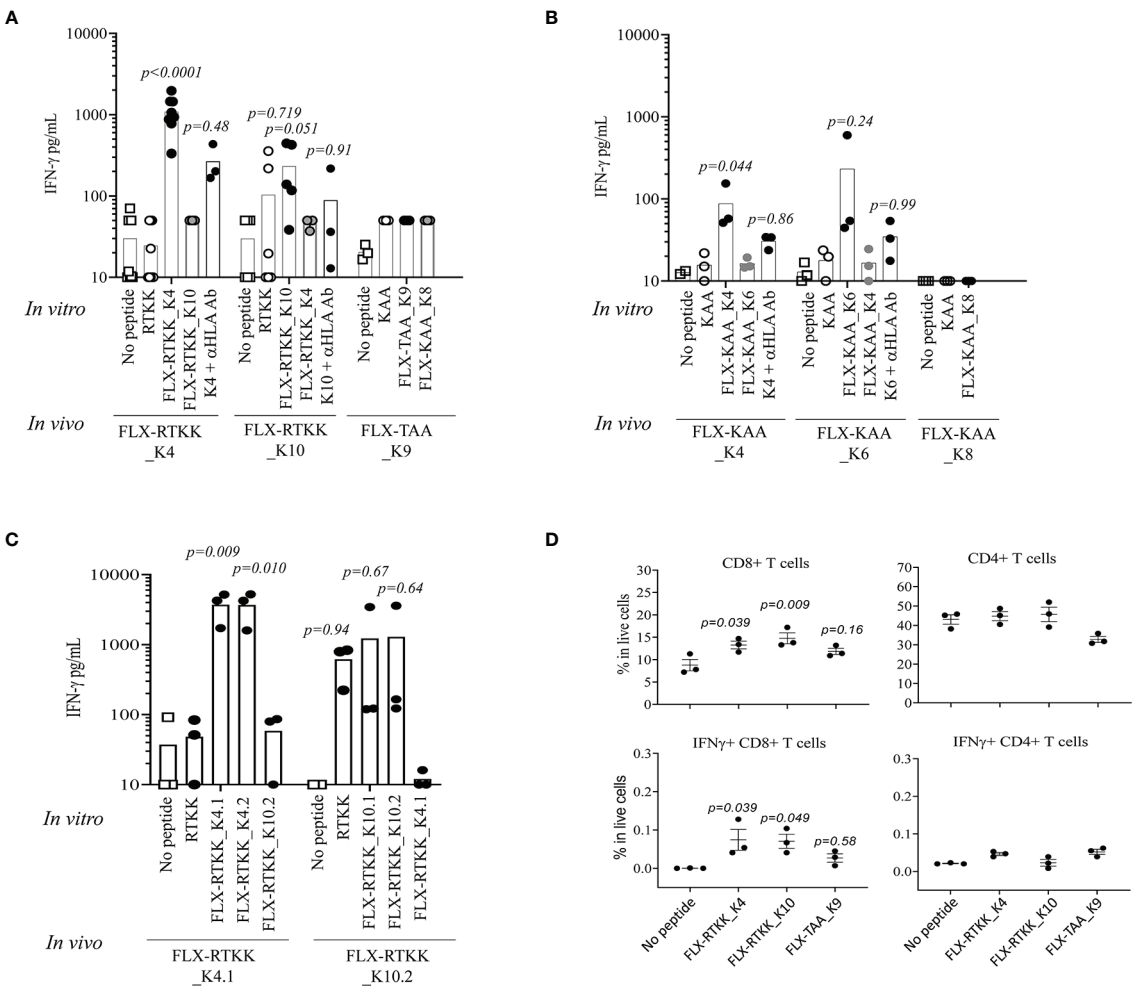

FIGURE 6 | Immunogenicity potential of flucloxacillin (FLX)-haptenated peptide is dependent on the peptide sequence, the position of the lysine to which drug is conjugated and the expression of human leukocyte antigen (HLA). **(A, B)** Tg/KO mice (n=3–9) were immunized by 2 s.c. doses of 100 μg of FLX-peptides together with 150 μg of $HBV_{128-140}$ $CD4^+$ T helper peptide with IFA. Splenocytes were subsequently stimulated *in vitro* with 10 μg/ml peptides (as indicated) for 5 days. IFN-γ was measured in the supernatant of the cultures by ELISA. *In vitro* responses to the *in vivo* immunogen were blocked by anti-HLA B/C antibody. **(C)** Immunizations and cultures were set up similarly to that described in A but with peptide isoforms of the FLX-RTKK peptides. **(D)** IFN-γ intracellular staining of day 5 splenic cell cultures from animals treated with FLX-peptides and stimulated *in vitro* with the same peptide. Graphs show results gated in $CD8^+$ or $CD4^+$ T cell populations (one representative of two experiments). Statistical analysis by one-way ANOVA using the no peptide condition as baseline. *p-values* are only shown if <0.999.

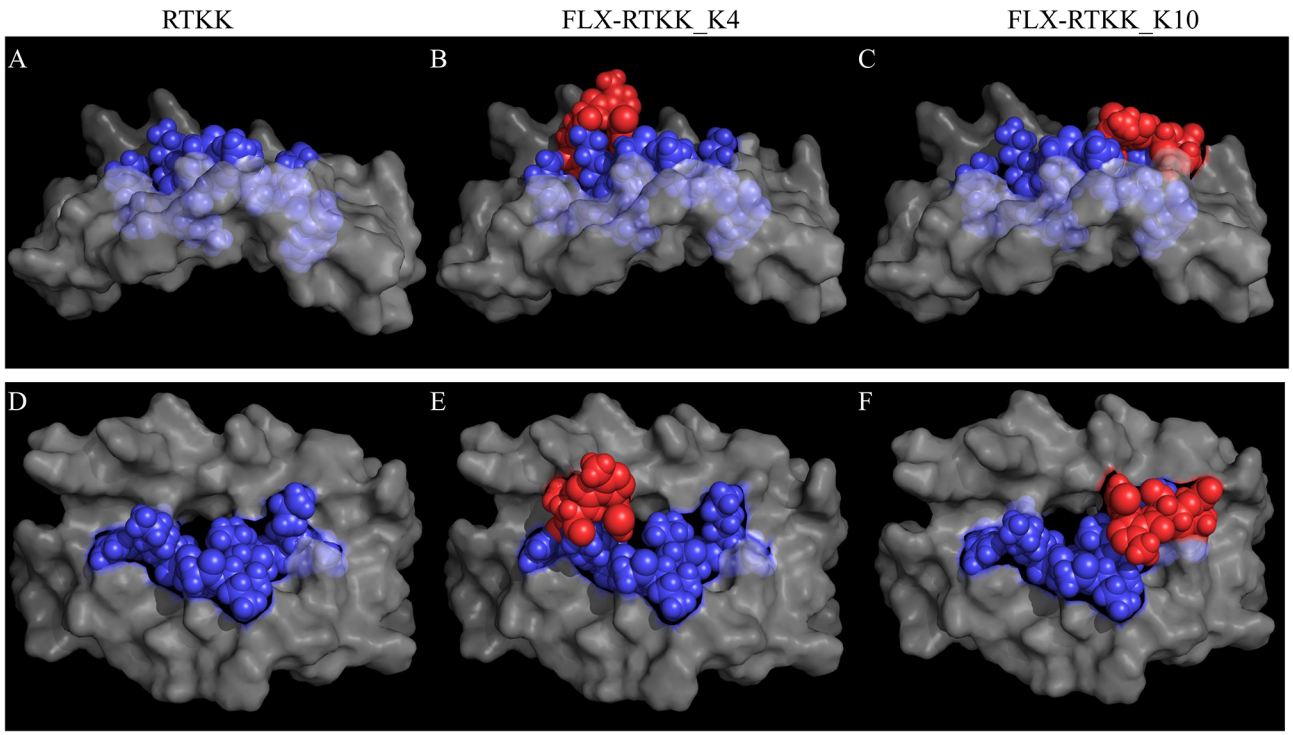

FIGURE 7 | *In silico* prediction of the interactions of parent and flucloxacillin (FLX)-RTKK peptides with HLA-B*57:01 cleft. KAF11 peptide residues (PDB ID: 2YPK) were replaced with those of the RTKK peptide. Docking the peptide into the HLA cleft was performed using FlexPepDock and addition of the drug to the appropriate lysine and energy minimization of the structure using OpenBable (v3.0.0) software. Structures were visualized in PyMOL (v2.3.4). Lateral **(A–C)** and top **(D–F)** views of the human leukocyte antigen (HLA) complex with the unmodified parent sequence of RTKK **(A, D)**, FLX-RTKK_K4 **(B, E)** and FLX-RTKK_K10 **(C, F)**. Peptide sequences are represented in blue spheres, drug is represented by red spheres and $\alpha1\alpha2$ domains of the HLA are depicted in gray color.

potential of FLX to activate a CD8+ T cell response is dependent on the position of the lysine residue in the peptide sequence.

DISCUSSION

Idiosyncratic FLX hypersensitivity reactions driven by immune cells occur at low frequency (2, 25, 26). Expression of HLA-B*57:01 and HLA-B*57:03 alleles was recognized as genetic risk factors for FLX-induced liver injury (6, 7), and thus attention has been paid to understand the molecular mechanisms by which drug can generate neoepitopes that are presented by HLA to activate T cells. To examine these mechanisms, we characterized the effect of FLX on the cell proteome and immunoproteome looking for gobal changes as well as appearance of drug-haptenated peptides.

Alterations of the B721-5701 cellular protein pathways by FLX could impact the abundance of self-epitopes and PTMs as well as the generation of neoepitopes, using these potential mechanisms to boost protein immunogenicity. Although no significant changes were observed in the total protein content of the cells when incubated with FLX, drug treatment induced a higher diversity in the peptide repertoire presented by the HLA which could impact antigen presentation. Increased abundance and diversitiy of sequences of particular proteins in MHC complexes can be due to an enhanced processing rate of such proteins (19). Consistent with this hypothesis, we observed a larger number of proteins represented in the FLX-immunopeptidome with peptide presentation rate above those predicted considering the protein length. Alteration of the peptide processing (immunoproteasome *vs* proteasome) or the peptide loading (e.g. tapasin-dependent or -independent mechanisms) machineries could explain qualitative and quantitative changes on the cell immunopeptidome. Penicillinase-resistant antibiotics, including FLX can induce endoplasmic reticulum stress, which can lead to misfolding of proteins, oxidative stress and caspase-3 activation (27). Although the drug concentrations used in our study were lower than in those studies (0.3-1 mM *vs* >16mM) and the cells tested were different (B cells *vs* hepatocytes), we found that caspase-3 protein expression was elevated in our 1mM-treated FLX-cells, and thus, could indicate the occurrence of non-cytotoxic changes impacting protein processing. However, the mechanisms by which FLX may impact proteosome processing and/or peptide loading and presentation without changing the global protein content of the cell requires further study (see further discussion below).

The generation of neoepitopes by drugs inducing immune-mediated hypersensitivity reactions is believed to occur by covalent adduct formation, pharmacological interaction of the

drug with the peptide, and non-covalent interaction leading to alteration of the peptide repertoire (28) which most likely coexist *in vivo* (29). In our study, no changes were observed in the consensus anchor residues of peptides isolated from FLX-cells, either at the P2 or PΩ positions, consistently with other reports (13–15, 30, 31) A lower frequency of tryptophan at P9 was observed in some of our untreated preparations (**Figure S5**) contrasting with what others reported on HLA-B*57:01 peptide repertoires (21, 31). This variation could be attributed to differences in culture conditions such as absence of other β-lactam antibiotics in the media other than FLX or the use of different cell lines. Nevertheless, and unlike abacavir that increases the presentation of epitopes with unconventional isoleucine or leucine residues in PΩ (13–15), FLX promoted an enrichment of tryptophan at PΩ, in agreement with a trend observed in a recent report (31). We established that the overall net higher frequency of peptides with tryptophan at PΩ in the FLX-cells included both unique sequences (qualitative) and higher abundance in common peptides (quantitative). Because of its greater size, it seems unlikely that FLX can fit directly into the HLA F-pocket in a manner similar to that of abacavir. Therefore, we hypothesize that changes in the peptide repertoire may result from an effect on the peptide processing machinery. Catalytic shifts in proteasomic subunits induced by pathogenic infections but also by oxidative stress (32) increase the immunoproteosome activity of the cell resulting in an enrichment of peptides with higher content of hydrophobic amino acids at the C-terminus promoted by the chymotrypsin activity of LMP2 (33), perhaps favoring tryptophan (34). Whether this occurs indirectly or by direct interaction of FLX with one of the immunoproteasome complex subunits, such as LMP2 or LMP7, has not been addressed in our study. In our studies, peptides with tryptophan in the C-terminus have higher predicted binding affinity to HLA-B*57 (**Tables S2A, B**), consistent with other findings (21). Loading of high-affinity peptides by tapasin-dependent mechanisms could impact self-tolerance, possibly contributing to drug hypersensitivity such as in cases where tissue damage continues even after discontinuation of drug administration.

T-cell recognition of FLX by cells of healthy individuals carrying HLA-B*57:01 can involve processing dependent and independent pathways (4, 5, 8). However, the activation of $CD8^+$ T cells from HLA-B*57:01$^+$ DILI patients by FLX is peptide processing dependent and restricted to the expression of B*57:01 allele (4, 8) possibly explaining the low frequency of FLX-associated DILI and why only the expression of the HLA-B*57:01 or B*57:03 alleles has been linked to FLX-induced liver injury. Processing dependent T cell activation suggests that covalent modifications of protein epitopes generate neoantigen drug targets. To study the immunogenic potential of FLX-conjugated peptides, we used mass spectrometry analysis of HLA purified peptides and identified three FLX-peptide sequences in the B721-5701 immunopeptidome of drug-treated cells. One peptide FLX-TAA_K9 was from HLA itself suggesting that lysines on the HLA surface may also be targets for direct drug modification (31), analogous to FLX modifications of lysines on albumin (12). The other two peptides had multiple lysine residues and were from internal proteins, KAA from a nuclear HMGB-1 DNA binding protein and RTKK from the 60S ribosomal protein, both of which are in high abundance in the cell. Both peptides were modifed on the P4 lysines, suggesting a preference at this position on presented peptides. Generation of haptenated peptides could occur either on the intact protein or on free peptide after proteosome cleavage, as suggested in a recent report by Waddington et al. (31) who also identified FLX modifications on TAA and RTKK, among other peptides. In their study, the position of the modified amino acid in peptides such RTKK was ambiguous and not verified by synthetic chemistry.

Using FLX-lysine Fmoc synthetic conjugates, we synthesized both FLX-peptides identified in the cell immunopeptidome as well as other analogs with FLX on other lysine residues to confirm the identity of the sequences, the position of the drug, and to assess their immunogenic potential Interestingly, RP-HPLC profiles of the synthesized FLX-peptides as well as FLX-RTKK_4 isolated from the cells showed two peaks with distinct retention times but with exact mass, unlike those of the unmodified sequences. We believe that these differences represented two conformational states of the open β-lactam ring of the antibiotic, since two different peaks were also observed for the Fmoc FLX-lysine conjugate after deprotection but not for the FLX-lysine with the intact β-lactam ring (data not shown). Further structural work is required on FLX-peptide conjugates to define these properties and to study further its relation to peptide immunogenicity.

To estimate the immunogenicity potential of FLX-epitope sequences, we immunized HLA-B*57:01 mice lacking the expression of the murine MHC-I molecules H-$2K^b$ and H-$2D^b$ with the selected FLX-peptides. Different levels of immunogenicity were observed depending on the peptide sequence and the position at which the drug was conjugated. Cells from animals primed with FLX-RTKK_K4 or FLX-KAA_K4 sequences, unlike modified TAA peptide, were quickly activated *in vitro* to produce IFN-γ in an antigen-specific and HLA-dependent manner. Interstingly, peptides not detected in the immunopepditome like FLX-KAA_K6 and FLX-RTKK-K10 showed increased immunogenicity (the latter with less specificity), while FLX-KAA_K8 did not activate T cells. For FLX-RTKK peptides, the presumably isomeric sequences were recognized similarly by primed T cells. Failure to identify weak immunogenic peptides in the cell immunopeptidome could be explained by a disadvantage of certain lysine residues to be modified by the drug or interference in peptide loading. Both the physicochemical properties of the peptide (35) and the contact potential among TCR and peptide (36) have been postulated as critical parameters in the prediction of epitope immunogenicity. Notably, FLX conjugates were not found in anchor residues (P2 or PΩ) and the lysine side-chains of FLX-peptides were oriented exposed to solvent away from the HLA cleft. Interestingly, 3 out of the 4 immunogenic peptides tested had drug in lysines in position P4 or P6, positions that are considered critical for contact specificity and generation of

immunogenicity (35). Structural models presented here for P4 and P6 suggest that drug modifications in these positions could be seen by T cells in a manner similar to large peptides that contain bulges in central regions. Using the HLA-B*57:01 restricted HIV-KAF TCR as a model, we showed that the lysine at P4 is at a site that overlaps with the hypothetical footprint of TCR V-alpha CDR3 while lysines at PΩ-1 are not, suggesting that TCR chains could be differentially selected specifically based on the amino acid position of the drug linkage. FLX at PΩ-1 may be outside the footprint of the CDR3 chains or have difficulty in peptide processing/loading to HLA.

As mentioned above, FLX-TAA_K9 is derived from HLA-B*57:01 itself. Direct modification of lysines on HLA has intriguing implications in addition to being target epitopes for T cells after antigen processing. HLA-K146, corresponding to the FLX-modified lysine in FLX-TAA_K9, is positioned near the HLA F-pocket where the peptide C-terminus will interact and is highly conserved among HLA molecules. K-146 is critical for HLA binding to the inhibitory KIR-3DL1 protein on NK cells (37, 38). Direct modification of HLA-K146 by FLX as modeled in **Figure S9** could interfere with the KIR-3DL1-binding and possibly lead to NK activation. Similarly, FLX modification on lysines positioned at PΩ-1 such as on FLX-TAA_K9 could also interfere with the KIR3DL1-binding site and impact KIR function as KIR3DL1 binding was reported to depend on the nature of the amino acid at the PΩ-1 (P8 in Vivian et al. (37)). Activation of NK in addition to $CD8^+$ T cells have been reported in PBMCs isolated from patients with drug hypersensitivity reactions (39) as well as in fluid of skin blisters of patients with Stevens-Johnson syndrom (40), although the exact molecular mechanism involved in such activation is yet to be determined. Further studies are required to elucidate whether K146 or other FLX-modified lysines on HLA can interfere with KIR or T cell receptor binding.

In summary, factors leading to idiosyncratic drug hypersensitivity might involve non-covalent and covalent interactions between drug and peptide. In our study, we showed that FLX treatment of B721-5701 cells can alter the presentation of self-peptides by enriching the peptide repertoire of the cell with sequences containing tryptophan at the C-terminus, a preferred amino acid for immunoproteasome processing and which confers a higher predicted binding affinity to the sequence. We also identified drug-haptenated peptides with immunogenicity potential depending on the lysine at which FLX gets conjugated. Direct modifications of the HLA by FLX at lysines that are believed to play immunoregulatory roles could also participate in the activation of innate immune pathways, contributing inflammatory events to the initiation of immune-mediated drug adverse reactions. Further animal studies will allow us to characterize the generated immune responses in more detail and whether the reactive cells can infiltrate hepatic tissue and lead to DILI. Understanding the mechanisms behind these modifications and their impact on breaking T cell tolerance, individually or as a whole, is critical to drug development and amelioration of adverse side effects.

DATA AVAILABILITY STATEMENT

The raw data supporting the conclusions of this article will be made available by the authors, without undue reservation.

ETHICS STATEMENT

The animal study was reviewed and approved by Institutional Animal Care and Use Committee at FDA.

AUTHOR CONTRIBUTIONS

MP and MN conceived, planned, and supervised the experiments. MP, SA, RV, SP, EM, MC, SS, and GR performed the experiments. MT, SB, and GA chemically synthesized the peptides. WW performed mass spectrometry analysis. LW and ZL performed proteomics data analysis. WH generated large-scale HLA preparations. LB, KN, and DM generated the HLA-B57*01 Tg/KO mice. MP, DM, and MN edited and reviewed the manuscript. All authors contributed to the article and approved the submitted version.

FUNDING

This work was supported by the FDA Intramural Research Program, and in part by a Senior Postgraduate Research Fellowship Award to S.P., E.M. and S.S. from the Oak Ridge Institute for Science and Education (ORISE) through an interagency agreement between the U.S. Department of Energy and the U.S. Food and Drug Administration. DHM's group is supported by the Intramural Research program of the NIAID, NIH.

ACKNOWLEDGMENTS

We thank Janet Woodcock, Director of the Center for Drug Evaluation and Research (CDER, FDA) for her continued support of this project. We wish to thank Sintayehu Gebreyohannes for phenotyping the mice and technical support, and the personnel of the animal facility of the US FDA's Division of Veterinary Medicine for care of the mice. We appreciate Weiming Ouyang and Joao Pedras Vasconcelos's comments on the manuscript.

SUPPLEMENTARY MATERIAL

The Supplementary Material for this article can be found online at: https://www.frontiersin.org/articles/10.3389/fimmu.2020.629399/full#supplementary-material

REFERENCES

1. Olsson R, Wiholm BE, Sand C, Zettergren L, Hultcrantz R, Myrhed M. Liver damage from flucloxacillin, cloxacillin and dicloxacillin. *J Hepatol* (1992) 15 (1):154–61. doi: 10.1016/0168-8278(92)90029-O
2. Wuillemin N, Terracciano L, Beltraminelli H, Schlapbach C, Fontana S, Krähenbühl S, et al. T Cells infiltrate the liver and kill hepatocytes in HLA-B∗57:01-associated floxacillin-induced liver injury. *Am J Pathol* (2014) 184 (6):1677–82. doi: 10.1016/j.ajpath.2014.02.018
3. Bharadwaj M, Illing P, Theodossis A, Purcell AW, Rossjohn J, McCluskey J. Drug hypersensitivity and human leukocyte antigens of the major histocompatibility complex. *Annu Rev Pharmacol Toxicol* (2012) 52:401–31. doi: 10.1146/annurev-pharmtox-010611-134701
4. Monshi MM, Faulkner L, Gibson A, Jenkins RE, Farrell J, Earnshaw CJ, et al. Human leukocyte antigen (HLA)-B*57:01-restricted activation of drug-specific T cells provides the immunological basis for flucloxacillin-induced liver injury. *Hepatology* (2013) 57(2):727–39. doi: 10.1002/hep.26077
5. Wuillemin N, Adam J, Fontana S, Krahenbuhl S, Pichler WJ, Yerly D. HLA haplotype determines hapten or p-i T cell reactivity to flucloxacillin. *J Immunol* (2013) 190(10):4956–64. doi: 10.4049/jimmunol.1202949
6. Daly AK, Donaldson PT, Bhatnagar P, Shen Y, Pe'er I, Floratos A, et al. HLA-B*5701 genotype is a major determinant of drug-induced liver injury due to flucloxacillin. *Nat Genet* (2009) 41(7):816–9. doi: 10.1038/ng.379
7. Nicoletti P, Aithal GP, Chamberlain TC, Coulthard S, Alshabeeb M, Grove JI, et al. Drug-Induced Liver Injury due to Flucloxacillin: Relevance of Multiple Human Leukocyte Antigen Alleles. *Clin Pharmacol Ther* (2019) 106(1):245–53. doi: 10.1002/cpt.1375
8. Yaseen FS, Saide K, Kim SH, Monshi M, Tailor A, Wood S, et al. Promiscuous T-cell responses to drugs and drug-haptens. *J Allergy Clin Immunol* (2015) 136(2):474–6.e8. doi: 10.1016/j.jaci.2015.02.036
9. Ariza A, Garzon D, Abanades DR, de los Rios V, Vistoli G, Torres MJ, et al. Protein haptenation by amoxicillin: high resolution mass spectrometry analysis and identification of target proteins in serum. *J Proteomics* (2012) 77:504–20. doi: 10.1016/j.jprot.2012.09.030
10. Faulkner L, Meng XL, Park BK, Naisbitt DJ. The importance of hapten - protein complex formation in the development of drug allergy. *Curr Opin Allergy Clin Immunol* (2014) 14(4):293–300. doi: 10.1097/ACI.0000000000000078
11. Meng X, Al-Attar Z, Yaseen FS, Jenkins R, Earnshaw C, Whitaker P, et al. Definition of the nature and hapten threshold of the β-Lactam antigen required for T Cell activation in vitro and in patients. *J Immunol* (2017) 198(11):4217. doi: 10.4049/jimmunol.1700209
12. Jenkins RE, Meng X, Elliott VL, Kitteringham NR, Pirmohamed M, Park BK. Characterisation of flucloxacillin and 5-hydroxymethyl flucloxacillin haptenated HSA in vitro and in vivo. *Proteomics Clin Appl* (2009) 3(6):720–9. doi: 10.1002/prca.200800222
13. Ostrov DA, Grant BJ, Pompeu YA, Sidney J, Harndahl M, Southwood S, et al. Drug hypersensitivity caused by alteration of the MHC-presented self-peptide repertoire. *Proc Natl Acad Sci U S A* (2012) 109(25):9959–64. doi: 10.1073/pnas.1207934109
14. Norcross MA, Luo S, Lu L, Boyne MT, Gomarteli M, Rennels AD, et al. Abacavir induces loading of novel self-peptides into HLA-B*57: 01: an autoimmune model for HLA-associated drug hypersensitivity. *Aids* (2012) 26(11):F21–9. doi: 10.1097/QAD.0b013e328355fe8f
15. Illing PT, Vivian JP, Dudek NL, Kostenko L, Chen Z, Bharadwaj M, et al. Immune self-reactivity triggered by drug-modified HLA-peptide repertoire. *Nature* (2012) 486(7404):554–8. doi: 10.1038/nature11147
16. Scornet N, Delarue-Cochin S, Azoury ME, Le Mignon M, Chemelle J-A, Nony E, et al. Bioinspired design and oriented synthesis of immunogenic site-specifically penicilloylated peptides. *Bioconj Chem* (2016) 27(11):2629–45. doi: 10.1021/acs.bioconjchem.6b00393
17. Cardone M, Garcia K, Tilahun ME, Boyd LF, Gebreyohannes S, Yano M, et al. A transgenic mouse model for HLA-B*57:01–linked abacavir drug tolerance and reactivity. *J Clin Invest* (2018) 128(7):2819–32. doi: 10.1172/JCI99321
18. Pérarnau B, Saron MF, Reina San Martin B, Bervas N, Ong H, Soloski MJ, et al. Single H2Kb, H2Db and double H2KbDb knockout mice: peripheral CD8+ T cell repertoire and anti-lymphocytic choriomeningitis virus cytolytic responses. *Eur J Immunol* (1999) 29(4):1243–52. doi: 10.1002/(SICI)1521-4141(199904)29:04<1243::AID-IMMU1243>3.0.CO;2-A
19. Bassani-Sternberg M, Pletscher-Frankild S, Jensen LJ, Mann M. Mass spectrometry of human leukocyte antigen Class I peptidomes reveals strong effects of protein abundance and turnover on antigen presentation. *Mol Cell Proteomics* (2015) 14(3):658–73. doi: 10.1074/mcp.M114.042812
20. Hoof I, van Baarle D, Hildebrand WH, Keşmir C. Proteome sampling by the HLA Class I antigen processing pathway. *PloS Comput Biol* (2012) 8(5): e1002517. doi: 10.1371/journal.pcbi.1002517
21. Illing PT, Pymm P, Croft NP, Hilton HG, Jojic V, Han AS, et al. HLA-B57 micropolymorphism defines the sequence and conformational breadth of the immunopeptidome. *Nat Commun* (2018) 9(1):4693. doi: 10.1038/s41467-018-07109-w
22. Raveh B, London N, Schueler-Furman O. Sub-angstrom modeling of complexes between flexible peptides and globular proteins. *Proteins* (2010) 78(9):2029–40. doi: 10.1002/prot.22716
23. London N, Raveh B, Cohen E, Fathi G, Schueler-Furman O. Rosetta FlexPepDock web server–high resolution modeling of peptide-protein interactions. *Nucleic Acids Res* (2011) 39(Web Server issue):W249–53. doi: 10.1093/nar/gkr431
24. O'Boyle NM, Banck M, James CA, Morley C, Vandermeersch T, Hutchison GR. Open Babel: An open chemical toolbox. *J Cheminform* (2011) 3:33. doi: 10.1186/1758-2946-3-33
25. Rive CM, Bourke J, Phillips EJ. Testing for drug hypersensitivity syndromes. *Clin Biochem Rev* (2013) 34(1):15–38.
26. Uetrecht J, Naisbitt DJ. Idiosyncratic adverse drug reactions: current concepts. *Pharmacol Rev* (2013) 65(2):779–808. doi: 10.1124/pr.113.007450
27. Burban A, Sharanek A, Guguen-Guillouzo C, Guillouzo A. Endoplasmic reticulum stress precedes oxidative stress in antibiotic-induced cholestasis and cytotoxicity in human hepatocytes. *Free Radical Biol Med* (2018) 115:166–78. doi: 10.1016/j.freeradbiomed.2017.11.017
28. White KD, Chung W-H, Hung S-I, Mallal S, Phillips EJ. Evolving models of the immunopathogenesis of T cell–mediated drug allergy: The role of host, pathogens, and drug response. *J Allergy Clin Immunol* (2015) 136(2):219–34. doi: 10.1016/j.jaci.2015.05.050
29. Pirmohamed M, Ostrov DA, Park BK. New genetic findings lead the way to a better understanding of fundamental mechanisms of drug hypersensitivity. *J Allergy Clin Immunol* (2015) 136(2):236–44. doi: 10.1016/j.jaci.2015.06.022
30. Abelin JG, Keskin DB, Sarkizova S, Hartigan CR, Zhang W, Sidney J, et al. Mass spectrometry profiling of HLA-associated peptidomes in mono-allelic cells enables more accurate epitope prediction. *Immunity* (2017) 46(2):315–26. doi: 10.1016/j.immuni.2017.02.007
31. Waddington JC, Meng X, Illing PT, Tailor A, Adair K, Whitaker P, et al. Identification of flucloxacillin-haptenated HLA-B*57:01 ligands: evidence of antigen processing and presentation. *Toxicol Sci* (2020) 177(2):454–65. doi: 10.1093/toxsci/kfaa124
32. Eskandari SK, Seelen MAJ, Lin G, Azzi JR. The immunoproteasome: An old player with a novel and emerging role in alloimmunity. *Am J Transplant* (2017) 17(12):3033–9. doi: 10.1111/ajt.14435
33. Gaczynska M, Rock KL, Goldberg AL. γ-Interferon and expression of MHC genes regulate peptide hydrolysis by proteasomes. *Nature* (1993) 365 (6443):264–7. doi: 10.1038/365264a0
34. Winter MB, La Greca F, Arastu-Kapur S, Caiazza F, Cimermancic P, Buchholz TJ, et al. Immunoproteasome functions explained by divergence in cleavage specificity and regulation. *Elife* (2017) 6:e27364. doi: 10.7554/eLife.27364
35. Calis JJA, Maybeno M, Greenbaum JA, Weiskopf D, De Silva AD, Sette A, et al. Properties of MHC class I presented peptides that enhance immunogenicity. *PloS Comput Biol* (2013) 9(10):e1003266–e. doi: 10.1371/journal.pcbi.1003266
36. Ogishi M, Yotsuyanagi H. Quantitative Prediction of the Landscape of T Cell Epitope Immunogenicity in Sequence Space. *Front Immunol* (2019) 10:827. doi: 10.3389/fimmu.2019.00827
37. Vivian JP, Duncan RC, Berry R, O'Connor GM, Reid HH, Beddoe T, et al. Killer cell immunoglobulin-like receptor 3DL1-mediated recognition of human leukocyte antigen B. *Nature* (2011) 479(7373):401–5. doi: 10.1038/nature10517
38. Saunders PM, Vivian JP, Baschuk N, Beddoe T, Widjaja J, O'Connor GM, et al. The interaction of KIR3DL1*001 with HLA class I molecules is dependent upon molecular microarchitecture within the Bw4 epitope. *J Immunol* (2015) 194(2):781–9. doi: 10.4049/jimmunol.1402542
39. Zawodniak A, Lochmatter P, Yerly D, Kawabata T, Lerch M, Yawalkar N, et al. In vitro detection of cytotoxic T and NK cells in peripheral blood of patients with various drug-induced skin diseases. *Allergy* (2010) 65(3):376–84. doi: 10.1111/j.1398-9995.2009.02180.x.19793058

40. Chung WH, Hung SI, Yang JY, Su SC, Huang SP, Wei CY, et al. Granulysin is a key mediator for disseminated keratinocyte death in Stevens-Johnson syndrome and toxic epidermal necrolysis. *Nat Med* (2008) 14(12):1343–50. doi: 10.1038/nm.1884

Conflict of Interest: The authors declare that the research was conducted in the absence of any commercial or financial relationships that could be construed as a potential conflict of interest.

frontiers in Immunology

ORIGINAL RESEARCH
published: 25 February 2021
doi: 10.3389/fimmu.2021.601954

Cross With Caution: Antibiotic Cross-Reactivity and Co-Reactivity Patterns in Severe Cutaneous Adverse Reactions

Grace Thompson[1], *Andrew McLean-Tooke*[1] *and Michaela Lucas*[1,2*]

[1] Queen Elizabeth II Medical Centre, Department of Clinical Immunology, Sir Charles Gairdner Hospital, Pathwest, Nedlands, WA, Australia, [2] Medical School, University of Western Australia, Nedlands, WA, Australia

Current understanding of cross-reactivity in severe cutaneous adverse reactions to beta-lactam antibiotics is limited, thereby making recommendations for future prescribing difficult. The underlying immunopathogenesis of these reactions is not completely understood but involves interactions between small molecule drugs, T cells and HLA molecules. Historically, these reactions were considered to be specific to the inciting antibiotic and therefore likely to have minimal cross-reactivity. We assessed patients presenting with non-SJS/TEN severe cutaneous adverse reactions to a tertiary hospital drug allergy clinic. In our case series cross-reactivity or co-reactivity commonly occurred among the beta-lactam antibiotic class, however further research is required to investigate and understand patterns of cross-reactivity. Based on our experience we provide clinicians with a practical algorithm for testing for cross-reactivity in non-SJS/TEN severe cutaneous adverse reactions.

Keywords: severe cutaneous adverse drug reactions, antibiotic cross-reactivity, antibiotic co-reactivity, beta-lactam, antibiotics

OPEN ACCESS

Edited by:
Jason Trubiano,
University of Melbourne, Australia

Reviewed by:
Nicole Andrea Mifsud,
Monash University, Australia
Ana Copaescu,
McGill University Health Centre, Canada

***Correspondence:**
Michaela Lucas
Michaela.lucas@health.wa.gov.au

Specialty section:
This article was submitted to Alloimmunity and Transplantation, a section of the journal Frontiers in Immunology

Received: *02 September 2020*
Accepted: *12 January 2021*
Published: *25 February 2021*

Citation:
Thompson G, McLean-Tooke A and Lucas M (2021) Cross With Caution: Antibiotic Cross-Reactivity and Co-Reactivity Patterns in Severe Cutaneous Adverse Reactions. Front. Immunol. 12:601954. doi: 10.3389/fimmu.2021.601954

INTRODUCTION

Severe cutaneous adverse reactions (SCAR's) are a heterogeneous group of delayed T cell mediated hypersensitivity reactions, which include Stevens-Johnson syndrome (SJS), toxic epidermal necrolysis (TEN), drug reaction with eosinophilia and systemic symptoms (DRESS) and acute generalized exanthematous pustulosis (AGEP) (1). Symmetrical drug-related intertriginous and flexural exanthema (SDRIFE) is another delayed cutaneous exanthema which can be severe. Medications are the most common cause of SCAR's causing >85% of cases of SCAR's in adults, of which beta-lactams are frequently implicated (2, 3). Although these conditions are rare, they carry significant morbidity and mortality, particularly if the offending drug is not withdrawn (1). Mortality rates of up to 67% in TEN, 40% in SJS and 10% in DRESS have been reported (4).

Interactions between the culprit drug, human leukocyte antigen (HLA) class I molecules and T cell receptors (TCR) in addition to other factors such as elevated plasma concentrations of the offending drug and viral infectious triggers are all thought to contribute to the immunopathogenesis of all types of SCAR's (1, 5). The interactions between the TCR, HLA molecule and the offending drug are thought to occur in three possible ways. Firstly, in the hapten/prohapten model a drug binds to a

protein that then undergoes antigen processing to generate haptenated-peptides which are recognized as neo-antigens by T cells. Beta-lactam antibiotics have been shown to behave in this manner, as drug modified human serum albumin has been isolated from individuals utilizing piperacillin, penicillin-G and flucloxacillin (6). Furthermore, the sites where drug modification occurs have been mapped using mass spectrometry and synthetic penicilloyl-adduct peptides have been shown to be more potent stimulators of T cells in patients with penicillin hypersensitivity (6). Secondly, the p-i model proposes that small molecule drugs may bind non-covalently to HLA or T cell receptors and directly stimulate T cells (5). Flucloxacillin -mediated delayed hypersensitivity reactions may also act *via* this mechanism, as some flucloxacillin-reacting T cell clones react immediately to flucloxacillin in the presence of antigen presenting cells, which is too rapid for the hapten/prohapten mechanism to occur (7). Lastly, the altered peptide model suggests small molecule drugs can bind non-covalently to the binding cleft of HLA and alter its conformation resulting in presentation of novel peptide ligands which then elicit an immune response (5). To date there is no current evidence for this occurring in beta-lactam hypersensitivity reactions (8).

The resultant characteristic clinical manifestations are then defined by the various effector cells involved. SJS and TEN are considered a continuum of the same disorder, in which CD8+ cytotoxic T cells and NK cells targeting skin keratinocytes can lead to a severe, life threatening exfoliative dermatitis and as a result they are often considered separately from the other SCAR's. In DRESS syndrome drug specific T cells are thought to mediate perforin/granzyme B and Fas/Fas ligand related cell death leading to the characteristic clinical features of widespread rash, eosinophilia, fever and internal organ involvement, most commonly liver injury (1, 9). Histopathology shows an interface dermatitis with spongiosis and expansion of T regulatory cells and eosinophils in the skin (9). Other factors such as mutations in drug metabolizing enzymes, HLA type as well as herpes viral reactivation likely contribute to T cell expansion and cytokine production (9). The exact role of herpes virus reactivation, particularly HHV6 reactivation in DRESS is controversial. Reactivation can be found in 43%–100% of DRESS cases and therefore it is likely that such reactivation is not essential for the development of DRESS but may be an aggravating factor potentially resulting in perpetuation of the inflammatory response. The mechanisms through which reactivation occurs are not entirely clear but may relate to a relative immunocompromised status which occurs early in DRESS or due to the direct effect of drugs or drug metabolites on HHV-6 replication (9). Viral reactivation may contribute to DRESS through further stimulating T cell expansion and cytokine production and may lead to T cell generation through heterologous immunity. Heterologous immunity may lead to the generation of drug-specific T cells through activation of cross-reactive HHV6 specific effector memory T cells (5). In AGEP drug specific T cells and NK cells are activated in the skin inducing apoptosis of keratinocytes *via* Fas/Fas ligand interactions. Production of cytokines and chemokines such as IL17 and CXCL8 leads to neutrophilic inflammation and formation of pustules which is the clinical hallmark of this condition. Histopathological features include spongiform subcorneal and/or intradermal pustules with oedema of the papillary dermis and a polymorphic perivascular infiltrate can be seen (1). Genetic variants in IL36 receptor antagonist gene have also been identified as a potential susceptibility factor (10). The precise pathophysiology of SDRIFE is unknown although it is thought to involve a type IV delayed-hypersensitivity immune response, as it occurs within a few hours to days following drug exposure. There is evidence of a T cell mediated reaction, with patch testing being positive in up to 50% of patients and delayed intradermal testing being positive in up to 70% of patients (11). While strong pharmacogenomic HLA associations have emerged for certain SCAR syndromes and medications, such as carbamazepine-induced SJS/TEN and HLA-B15:02, there is a lack of information regarding known HLA-associations with beta-lactam-induced SCAR's (1, 8)

Cross-reactivity can occur between structurally similar medications and is well described in aromatic anti-convulsant related SCAR's. However, evidence surrounding cross-reactivity in beta-lactam SCAR's is limited (12). Cross-reactivity in both immediate, IgE-mediated, and benign delayed beta-lactam antibiotic hypersensitivity may be due to either reactivity against the beta-lactam ring or more commonly due to shared identical or similar side chains, most commonly the R1 side chain, and has been reported in up to 31.2% of non-SCAR delayed T cell mediated penicillin allergy (13). Mechanistically T cell mediated reactions were thought to be more specific to an individual drug than IgE-mediated reactions as T cell receptors recognize small peptide fragments, although specific evidence supporting this is sparse (1, 14). El-Ghaiesh *et al.* demonstrated that piperacillin-specific CD4 and CD8 T cell clones from patients with delayed piperacillin hypersensitivity did not proliferate with other beta-lactam antibiotics even those with similar side chains (14) but, it is important to note that none of these clones were isolated from patients with SCAR's. In a retrospective review of SJS/TEN cases, two patients were inadvertently given the same or class-related antibiotic post-discharge without reported reaction (12).

Understanding cross-reactivity patterns has important clinical implications as currently recommendations for future antibiotic prescribing must involve a careful balance between the risk of precipitating another severe reaction versus restriction of therapeutic options. In this context we sought to determine if cross-reactivity among the beta-lactam class could be demonstrated in a cohort of non-SJS/TEN beta-lactam SCAR's and if patterns could be elucidated.

MATERIALS AND METHODS

All patients presenting to the Sir Charles Gairdner Hospital and Perth Children's Hospital Immunology clinic with a diagnosis of a beta-lactam antibiotic related non-SJS/TEN SCAR between March 2016 and June 2020 underwent standardized assessment. We receive on average 550–650 adult and 250–300 pediatric drug

allergy referrals per year. The majority are for presumed IgE mediated and non-SCAR non-immediate reactions, not all relate to beta lactam antibiotics. As SCAR reactions are also managed by Dermatology, we cannot exclude that we have not been referred all cases. Patients were included if they were deemed to have a clinical diagnosis of a non-SJS/TEN SCAR as made by a specialist immunologist and had either a positive patch or intradermal test to the suspected culprit antibiotic. Patients were excluded if they did not complete assessment. During this period 11 patients were identified with a non-SJS/TEN SCAR secondary to a beta-lactam antibiotic. One patient was excluded as they did not complete testing and one patient was excluded as they were negative on both patch and intradermal testing to all beta-lactam antibiotics.

Our standardized assessment consisted initially of patch testing to the culprit antibiotics. Patch test were applied to the patients back and left in place for 48 h. Results were read using a semi-quantitative score from no reaction, to +, ++, +++ depending on the degree of skin reaction at 48 h, 72 h and 1 week post initial application. Concentrations were based on non-irritating concentrations for patch testing reported in the literature (15, 16). Concentrations used for patch testing included: benzylpencillin 5% and 10%; penicillin VK 1%, 5%, 10%; amoxicillin 5%, 10%, and 25%; ampicillin 5%; flucloxacillin 1%, 5%, and 10%; cephalexin 5% and 10%; ceftriaxone 5% and 10%; cefepime 5%; cephazolin 5%; tazocin 5% and meropenem 5%.

Patients then went on to have intradermal testing (IDT) with delayed readings to beta-lactam antibiotics: if they had a positive patch test to the culprit antibiotic, this antibiotic alone was *typically* excluded on the IDT. Beta-lactam antibiotics included in this panel were: benzylpenicillin 6 mg/ml, Diater® PPL (major determinant) neat, Diater® MDM (minor determinant) neat, amoxicillin 20 mg/ml, ampicillin 20 mg/ml, amoxicillin/clavulanic acid 20 mg/ml, flucloxacillin 2 mg/ml, piperacillin-tazobactam 4.5 mg/ml, cephazolin 1 mg/ml, ceftriaxone 1 mg/ml, cefepime 1 mg/ml, aztreonam 1 mg/ml, and meropenem 2.5 mg/ml (16, 17). Delayed readings were performed at 48 h, 72 h and 1 week (**Figure 2**). The study was approved for conduct by Sir Charles Gairdner Hospital quality improvement committee (GEKO 28972) and Perth Children's Hospital quality improvement committee (GEKO 26921).

RESULTS

Nine patients were seen with a confirmed diagnosis of a non-SJS/TEN, beta-lactam related SCAR of which 7 (78%) had evidence of cross-reactivity on our testing. The majority of the patients had DRESS syndrome (7/9) with one patient having AGEP and the other having SDRIFE. The average age was 66 years (11–81 years) with a male to female ratio of 4:5. The average time to testing, taken from first onset of symptoms, was 8 months (1-18 months).

Case 1

Thirty-four-year-old male developed AGEP following his second dose of amoxicillin for an upper respiratory tract infection. He developed widespread pustulosis, neutrophilia ($10.29x10^9$/L), mild eosinophilia ($0.97x10^9$/L) and hepatitis (ALT 104U/L). The rash improved following antibiotic cessation and topical corticosteroids. He had a history of rash to an unknown antibiotic in childhood but had no other exposure to antibiotics since. He had no other significant past medical history. Allergy testing was performed 7 months after his initial reaction. Patch testing to amoxicillin was positive. IDT with delayed readings were positive to benzylpenicillin, flucloxacillin, piperacillin-tazobactam, and ampicillin (**Tables 1** and **2**, **Figure 1**).

Case 2

Fifty-six-year-old female developed DRESS following 24 h of flucloxacillin for cellulitis. She developed vomiting, diarrhea, and acute kidney injury (creatinine 440 Ummol/L). Antibiotics were changed to cephazolin and clindamycin during which time she developed a widespread erythematous exanthema and eosinophilia ($1.2x10^9$/L). She was treated with oral prednisolone 50 mg for 1 week followed by 25 mg for a further week in conjunction with oral antihistamines and topical corticosteroids. She had a background history of obesity, hypertension, osteoarthritis and possible anaphylaxis to contrast. Allergy testing was performed 10 months following her initial reaction. Patch testing was positive to penicillin VK and flucloxacillin. IDT with delayed readings were positive to amoxicillin and ampicillin (**Tables 1** and **2**, **Figure 1**).

Case 3

Forty-one-year-old male developed SDRIFE following 24 h of benzylpenicillin and azithromycin for treatment of pneumonia. He developed severe erythema with skin erosion in his flexures, hepatitis (ALT 105 U/L), and eosinophilia ($1.47x10^9$/L). He was treated with corticosteroids. He had no significant past medical history. Allergy testing was performed one month following his initial reaction. Patch testing was positive to penicillin VK and benzylpenicillin but negative to azithromycin. IDT with delayed readings were positive to benzylpenicillin and ampicillin (**Tables 1** and **2**, **Figure 1**). An outpatient supervised oral challenge was planned to azithromycin but unfortunately the patient did not attend.

Case 4

Thirty-one-year-old male developed DRESS on day six of phenoxymethylpenicillin for treatment of tonsillitis. He developed a diffuse maculopapular rash, fever, arthritis and eosinophilia ($0.8x10^9$/L). He was treated with oral corticosteroids. He had a background history of atopic disease with anaphylaxis to sunflower seeds, allergic rhinitis, and mild eczema. Allergy testing was performed 6 months after his initial reaction. Patch testing was positive to phenoxymethylpenicillin. IDT with delayed readings was positive to benzylpenicillin, amoxicillin, ampicillin, amoxicillin/clavulanic acid, flucloxacillin and equivocal to piperacillin-tazobactam (**Tables 1** and **2**, **Figure 1**).

Case 5

Eleven-year-old female developed DRESS on day 15 of intravenous piperacillin/tazobactam for an infective exacerbation of cystic

TABLE 1 | Clinical details of cases.

	1	2	3	4	5	6	7	8	9
Age	34	56	41	31	11	41	63	78	39
Sex	M	F	M	M	F	M	M	F	F
Cormorbidities	Nil	Obesity, HTN, OA	Nil	AR, eczema, food allergy	CF	Nil	BKA	HTN, hyperchol, OA, TIA	AIH
Beta lactam antibiotic implicated	Amx	Flx	Ben Pen	PmPen	Taz	Multiple	Mero	Cef	Taz, Mero
Indication for antibiotic	URTI	Cellulitis	Pneumonia	Tonsilitis	CF	Septic Arthritis	Cellulitis	PJI	Cholangitis
SCAR syndrome	AGEP	DRESS	SDRIFE	DRESS	DRESS	DRESS	DRESS	DRESS	DRESS
Probability score	Naranjo score 6	Regi-SCAR 5	Naranjo score 6	Regi-SCAR 3	Regi-SCAR 3	RegiSCAR 5	Regi-SCAR 5	RegiSCAR 7	RegiSCAR 6
Clinical manifestation	Pustular rash, neutrophilia, hepatitis	Rash, eosin, vomiting/ diarrhea, AKI	Erosive flexural rash, hepatitis, eosin	Rash, fever, arthritis, eosin	Rash, fevers, facial swelling eosin, hepatitis	Rash, fevers, LN, eosin, lymphocytosis	Rash, fevers, facial oedema hepatitis eosin	Rash, fevers, eosin, pulmonary infiltrates	Rash, eosin, fevers
Treatment	Top cst	Cst	Cst	Cst	Cst	Cst	Cst	Cst	Cst

HTN, hypertension, OA, osteoarthritis; AR, allergic rhinitis, CF, cystic fibrosis; BKA, bellow knee amputation; hyperchol, hypercholesterolaemia; TIA, transient ischemic attack; URTI, upper respiratory tract infection; PJI, prosthetic joint infection; AKI, acute kidney injury; Amx, Amoxycillin; Flx, flucloxacillin; ben pen, benxylpenicillin; PmPen, phenoxymethylpenicillin; Taz, Piperacillin/tazobactam; Mero, Meropenem; Cef, ceftriaxone; eosin, eosinophilia; LN, lymphadenopathy; top cst, topical corticosteroids; Cst, systemic corticosteroids.

fibrosis. She developed fevers, maculopapular rash, facial swelling, eosinophilia ($0.81x10^9$/L) and hepatitis (ALT 234 U/L). She was inadvertently subsequently prescribed amoxicillin/clavulanate and cephalexin which she tolerated without reaction. Allergy testing was performed 16 months following the initial reaction. Patch testing to piperacillin/tazobactam was positive. IDT with delayed readings was positive to aztreonam but not performed against piperacillin/tazobactam (**Tables 1** and **2**).

Case 6

Fourty-one-year-old male developed DRESS in the setting of multiple antibiotics including cefepime, meropenem, ciprofloxacin, vancomycin, rifampicin, clindamycin, flucloxacillin and cephalexin given for treatment of left knee septic arthritis following an elective arthroscopy and meniscal repair. He developed fevers, rash, lymphadenopathy, eosinophilia (1.0 x 10^9/L) and lymphocytosis (10.7 x 10^9/L). He required a prolonged course of oral corticosteroids initially 75 mg for 4 days, then 50 mg, followed by a weaning course down to 15 mg over 6 weeks, however on reduction of steroids bellow 15 mg he had recurrence of rash, requiring a slower steroid taper over the subsequent 4 months. While still on 1mg of prednisolone he was treated with cephalexin for a finger laceration and within 3 days of therapy developed fevers and rash. He was treated with a single dose of IV hydrocortisone 200mg and his symptoms resolved. Patch testing 6 months later revealed positive results to ceftriaxone, cefepime, meropenem and ciprofloxacin at 48 h (**Tables 1** and **2**, **Figure 1**).

Case 7

Sixty-three-year-old male with a background of traumatic below knee amputation developed DRESS syndrome characterized by periorbital oedema, maculopapular rash, eosinophilia ($0.69 x10^9$/L) and hepatitis (ALT 347 U/ml) 1 week after commencement of meropenem and vancomycin for treatment of cellulitis. This is on a background of a likely SCAR occurring in 1976 characterized by fevers, erythrodermic skin rash with desquamation and collapse six weeks into antibiotic therapy with a sulphonamide and an unknown penicillin antibiotic. Because of concerns about his historical reaction potentially being SJS/TEN we undertook patch testing to a broad panel of beta-lactam antibiotics, 6 months after the most recent reaction and did not perform IDT with delayed readings. This was positive to benzylpenicillin, penicillin VK, amoxicillin, amipicillin, flucloxacillin, cephalexin, ceftriaxone, cephazolin, meropenem, vancomycin and sulfamethoxazole/trimethoprim at 48 h (**Tables 1** and **2**, **Figure 1**).

Case 8

Seventy-eight-year-old female developed DRESS syndrome characterized by rash, fevers, eosinophilia (peak $5.9x10^9$/L) four weeks into a course of ceftriaxone and ciprofloxacin for a prosthetic hip joint infection. She also reported dyspnoea with pulmonary infiltrates detected on a CT chest. Her BNP was mildly elevated at 250 and an echocardiogram was normal. She initially responded well to oral corticosteroids but had recurrence of symptoms on multiple attempts at steroid weaning requiring addition of mycophenolate. She had a past medical history of hypertension, hypercholesterolaemia, osteoarthritis and a transient ischaemic attack. Patch testing 18 months later was positive to ceftriaxone. The patient subsequently tolerated amoxicillin with clavulanic acid and piperacillin/tazobactam as well as a ciprofloxacin challenge (**Tables 1** and **2**).

Case 9

Thirty-nine-year-old female with a background of autoimmune liver disease developed DRESS characterized by rash, fevers and

TABLE 2 | Patch and intradermal testing results for cases.

Case	Syndrome	Culprit	Time to testing (months)	Beta-lactam antibiotics tolerated post reaction	Patch test to culprit	Delayed intradermal results										
						PPL	MDM	BP	AMX	AMP	AMC	FLU	TZP	CFZ	CRO	FEP	MEM	ATM
1	AGEP	Amoxycillin	7		+[b]	–	–	+[a]	NP	+[a]	NP	+[a]	+[a]	–	–	–	–	–
2	DRESS	Flucloxacillin	10		+[b]	–	–	–	+[a]	+[a]	NP	NP	–	–	–	–	NP	NP
3	SDRIFE	Benzylpenicillin	1		+[b]	–	–	+[a]	–	+[a]	NP	–	–	–	–	–	NP	NP
4	DRESS	Phenoxymethyl penicillin	6		+[b]	–	–	+[a]	+[a]	+[a]	+[a]	+[a]	E[a]	–	–	–	NP	NP
5	DRESS	Piperacillin/tazobactam	16	Amoxycillin with clavulanic acid Cephalexin	+[c]	–	–	–	–	–	NP	–	NP	–	–	–	–	+[a]
6	DRESS	Unknown	15		*[b]	–	–	–	–	–	–	–	–	–	NP	NP	NP	–
7	DRESS	(1)Unknown penicillin (2) Meropenem	6		*[b]	NP	NP	NP	NP	NP	NP	NP	NP	NP	NP	NP	NP	NP
8	DRESS	Ceftriaxone	18	Amoxycillin with clavulanic acid Piperacillin/tazobactam	+[b]	–	–	–	NP	–	–	–	–	NP	NP	–	–	–
9	DRESS	Meropenem	3	Amoxycillin Piperacillin/tazobactam	+[b]	–	–	–	–	–	NP	–	–	–	–	–	NP	–

*Patient 6: Positive to ceftriaxone, cefepime, meropenem, ciprofloxacin. Patient 7: Positive to benzylpenicillin, penicillin VK, amoxicillin, amipicillin, flucloxacillin, cephalexin, ceftriaxone, cephazolin, meropenem, vancomycin and sulfamethoxazole/trimethoprim.

+= Positive, – = Negative, NP = not performed, E = equivocal.

AGEP, acute generalized erythematous pustulosis; DRESS, drug reaction with eosinophilia and systemic symptoms; SDRIFE, symmetrical drug related intreginous flexural exanthema; PPL, Diater PPL; MDM, Diater MDM; BP, benzylpenicillin; AMX, Amoxycillin; AMP, Ampicillin; FLU, flucloxacillin; TZP, piperacillin-tazobactam; CFZ, cephazolin; CRO, ceftriaxone; FEP, cefepime; MEM, meropenem; ATM, aztreonam.

Time to positivity [a]24 h, [b]48 h and [c]72 h.

eosinophilia ($3.2x10^9$/L) after treatment with multiple antibiotics including tazocin (piperacillin/tazobactam), ciprofloxacin, vancomycin and meropenem for cholangitis. She had been on treatment with azathioprine but this was ceased during this same admission as it was deemed to be ineffective due to progressive liver disease. She responded to treatment with oral prednisolone 50mg which was tapered and ceased over 2 months. Patch testing 3 months later was positive to meropenem. IDT with delayed readings was negative to other penicillin and cephalosporin antibiotics and she subsequently tolerated oral challenges to amoxicillin and ciprofloxacin and a course of piperacillin/tazobactam (**Tables 1** and **2**).

DISCUSSION

We describe a cohort of nine patients with non-SJS/TEN SCAR in which we found evidence of cross-reactivity in 75% in which the patterns of cross-reactivity seen were not predictable based on reactivity to the beta-lactam ring or the R1 side chain. The mechanisms of cross-reactivity in beta-lactam allergies include reactivity to the common beta-lactam ring, which is rare in IgE mediated allergy and absent in those with T cell mediated allergy (18) or more commonly due to structural similarities between side chain structures, most frequently the R1 side chain. Cross-reactivity between penicillins and cephalosporins in low-risk delayed T cell mediated reactions has been found to occur in 2.8–31.2% of patients (13, 19), most commonly among the aminocephalosporins, but there is limited literature addressing cross-reactivity in beta-lactam SCAR's specifically. Cross reactivity between penicillins and carbapenems is less than 1% and has is thought to be absent with aztreonam (18).

Our cross-reactivity rate of 75% is higher than what has been described to date in the literature. Romano et al. described a cohort of 214 patients with non-immediate reactions to aminopenicillins, which included eight patients with a SCAR, 5 with TEN and 3 with AGEP. Of those with a non-SJS/TEN SCAR 66.6% (2/3) were found to have either a positive patch or delayed IDT to at least one aminocephalosporin (13). More recently Berot et al. described 56 patients with delayed beta-lactam allergies including 26 patients with non-SJS/TEN SCAR's. Of these patients, 30% (1/3 DRESS cases; 8/23 AGEP cases) had evidence of cross reactivity on patch testing (20).

In our patients with evidence of cross-reactivity on testing, four patients were positive to multiple penicillins without positivity to cephalosporins, two patients were positive to multiple penicillin and cephalosporin antibiotics as well as meropenem and non-beta-lactam antibiotics and one patient was unusually positive only to Tazocin and aztreonam and had tolerated other beta-lactam antibiotics.

Cases 1–4 had positive testing against multiple penicillins without associated positivity to cephalosporins, suggesting a penicillin class effect. This has been described in the literature before, including in beta-lactam SCAR's. Watts et al. described a patient with benzylpenicillin DRESS who had evidence of cross-

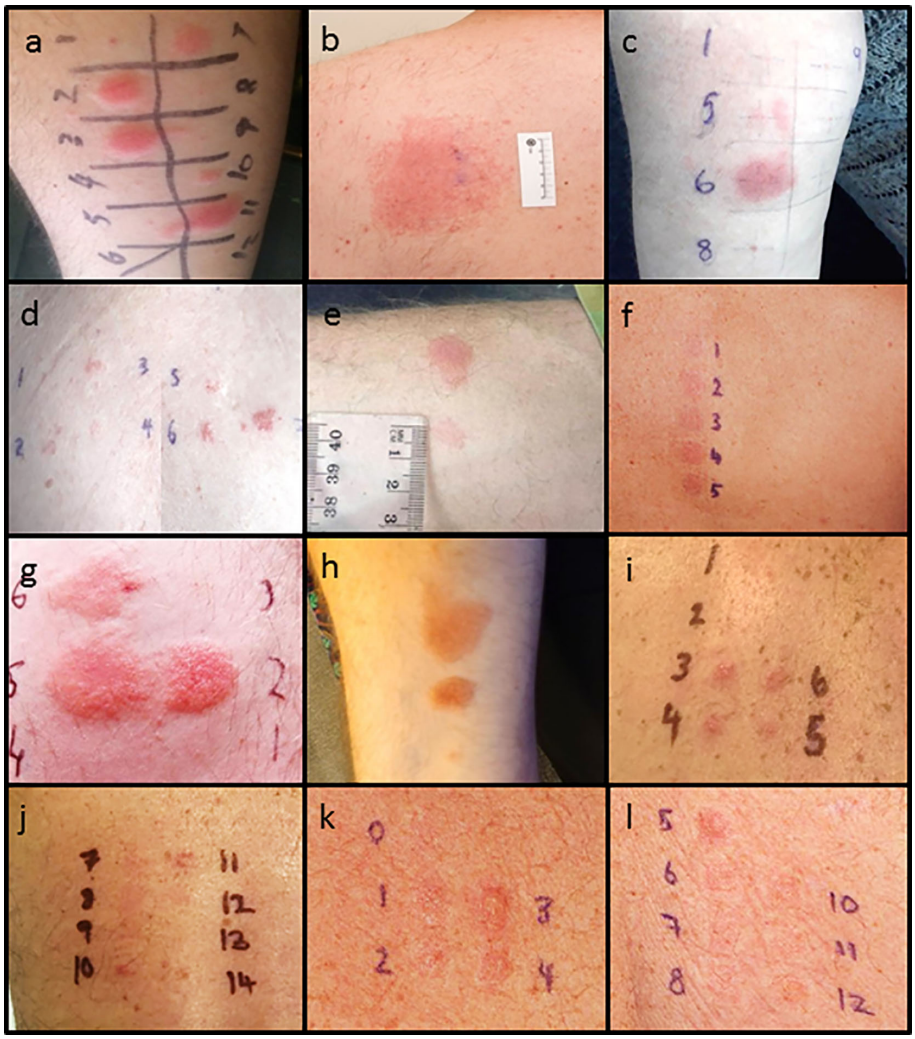

FIGURE 1 | Delayed intradermal and patch test results for cases. **(A)** Case 1 positive delayed intradermal to benzylpenicillin 6 mg/ml (2, 3), flucloxacillin 2 mg/ml (7), piperacillin-tazobactam 4.5 mg/ml (10) and ampicillin 20 mg/ml (11) at 8 h **(B)** Case 1 positive patch test to amoxycillin 10% and 25%s. **(C)** Case 2 positive amoxicillin 20 mg/ml (5) and ampicillin 20 mg/ml (6) **(D)** Case 2 positive patch test to penicillin VK 1%, 5%, 10% (2, 3, 4) and flucloxacillin 1%, 5% and 10% (5, 6, and 7). **(E)** Case 3 positive intradermal test to benzylpenicillin 6 mg/ml (upper) and ampicillin 20 mg/ml (lower). **(F)** Case 3 patch test positive to penicillin VK 10% (2) and benzylpencillin 10,000 IU/g (4). **(G)** Case 4: Positive intradermal test to benzylpenicillin 6 mg/ml (2), ampicillin 20 mg/ml (5), and amoxycillin 20 mg/ml (6) at 72 h. **(H)** Case 4: Positive intradermal test to amoxycillin-clavulanic acid 20 mg/ml (upper), flucloxacillin 2 mg/ml (middle) and equivocal piperacillin-tazobactam 4.5 mg/ml (lower). **(I)** Case 6: Positive patch test to ceftriaxone 10% (3), cefepime 5 and 10% (4, 5), meropenem 5% (6). **(J)** Case 6: Positive patch test to ciprofloxacin 10 and 20% (10, 11). **(K)** Case 7: Positive patch test to benzylpenicillin 10% (1), penicillin VK 10% (2), amoxycillin 10% (3), ampicillin 10% (4). **(L)** Case 7: positive patch test to flucloxacillin 10% (5), cephalexin 10% (6), vancomycin 10% (7), bactrim 10% (8), ceftriaxone 5%(10), cephazolin 5% (11), meropenem 5%(12). Patch test concentrations: benzylpencillin 5% and 10%; penicillin VK 1%, 5%, 10%; amoxicillin 5%, 10%, and 25%; ampicillin 5%; flucloxacillin 1%, 5%, and 10%; cephalexin 5% and 10%; ceftriaxone 5% and 10%; cefepime 5%; cephazolin 5%; tazocin 5% and meropenem 5%. Intradermal test concentrations: Benzylpenicillin 6 mg/ml, Diater® PPL (major determinant) neat, Diater® MDM (minor determinant) neat, amoxicillin 20 mg/ml, ampicillin 20 mg/ml, amoxicillin/clavulanic acid 20 mg/ml, flucloxacillin 2 mg/ml, piperacillin-tazobactam 4.5 mg/ml, cephazolin 1 mg/ml, ceftriaxone 1 mg/ml, cefepime 1 mg/ml, meropenem 2.5 mg/ml, and aztreonam 1 mg/ml.

reactivity to amoxicillin on patch and delayed IDT but tolerated cephalexin (21). The mechanism responsible for this pattern of cross-reactivity among the penicillin class is not understood, but may be due to more complex antigen structures following molecular processing, and protein folding during antigen presentation or may be due to coexisting sensitivities to different beta-lactam antibiotics (22). The majority of non-SJS/TEN SCAR patients with cross-reactivity in the Berot et al. study had initially reacted to amoxicillin and then had positive penicillin M and Penicillin G/V patch tests (20). In the Romano et al. cohort the cross-reactivity patterns in the two non-SJS/TEN and two TEN SCAR patients appeared to occur exclusively to aminopenicillins and therefore could be explained by the shared R1 side chain (13). Interestingly based on our testing, none of our cases of cross-reactivity appeared to be due to the R1 side chain.

Case 5 in our study had demonstrable positivity to aztreonam following DRESS secondary to piperacillin/tazobactam, despite the patient subsequently tolerating other beta-lactams including amoxicillin with clavulanic acid and cephalexin. It is unknown whether this result represents a true allergy to aztreonam or a false positive intradermal test as reactivity to aztreonam in patients with delayed penicillin allergy has been thought to be close to zero, although this has only been examined *via* patch and skin testing in eight patients with beta-lactam SCAR's (13, 22). Another unrelated co-existing sensitisation to aztreonam may be an alternative explanation for this finding.

Multiple drug reactivity (MDR) or co-sensitisation/reactivity is another possible explanation for our findings. MDR is described in DRESS syndrome where multiple positive patch tests are detected to chemically unrelated drugs (23). This phenomenon is very uncommon in other types of cutaneous adverse drug reactions (0.3%) but can occur in up to 18% of DRESS cases (23). This may best explain the results in case 6, in which positivity was found to both a 3rd and a 4th generation cephalosporin, meropenem and ciprofloxacin and in case 7 in which positivity was found to multiple penicillins, 1st and 3rd generation cephalosporins and meropenem as well as vancomycin and sulfamethoxazole/trimethoprim. The underlying pathogenesis of MDR is unknown but a potential explanation is that the enhanced stimulation of the immune response from co-stimulation by viral reactivation and/or the initial drug stimulation could lead to generation of an immune response to another drug-protein conjugate (23).

Diagnostic testing for drug causality and cross-reactivity is difficult in SCAR's due to the low sensitivity of testing, the multitude of drugs often implicated and the risk of precipitating a reaction (1). Testing options include a combination of patch and IDT with delayed readings (24). Our approach to testing involves patch testing against the culprit antibiotics in all SCAR's. In non-SJS/TEN beta-lactam SCAR's this is followed by IDT with delayed readings at 48 h, 72 h and 1 week, to a broad panel of beta-lactam antibiotics. If the culprit antibiotic is positive on patch testing this is then omitted from the IDT panel. If there is evidence of cross-reactivity on skin testing then avoidance of the whole beta-lactam class is justified. In those cases without evidence of cross-reactivity a graded challenge to an alternative, clinically relevant, oral beta-lactam antibiotic can be considered (**Figure 2**). We typically give 100th of a standard dose, followed by a 10th of a standard dose and then a full dose at one weekly intervals. Locally this approach has been applied at two of the three tertiary hospitals in Western Australia that offer drug allergy testing and we have found this approach to be safe, with all of our cases tolerating skin testing and oral challenges when performed. This is in keeping with the literature that IDT with delayed readings is safe and increases diagnostic sensitivity when patch testing is negative in non-SJS/TEN beta-lactam SCARs (2, 23). This particular algorithm has not been published previously in the literature but is in line with the current European Academy of Allergy and Clinical Immunology (EAACI) guidelines which recommend patch testing as the first line of testing in patients with SCAR's and proceeding to IDT if PT is negative (22).

Furthermore, we were able to identify a high rate of cross-reactivity to a range of beta-lactam antibiotics on intradermal

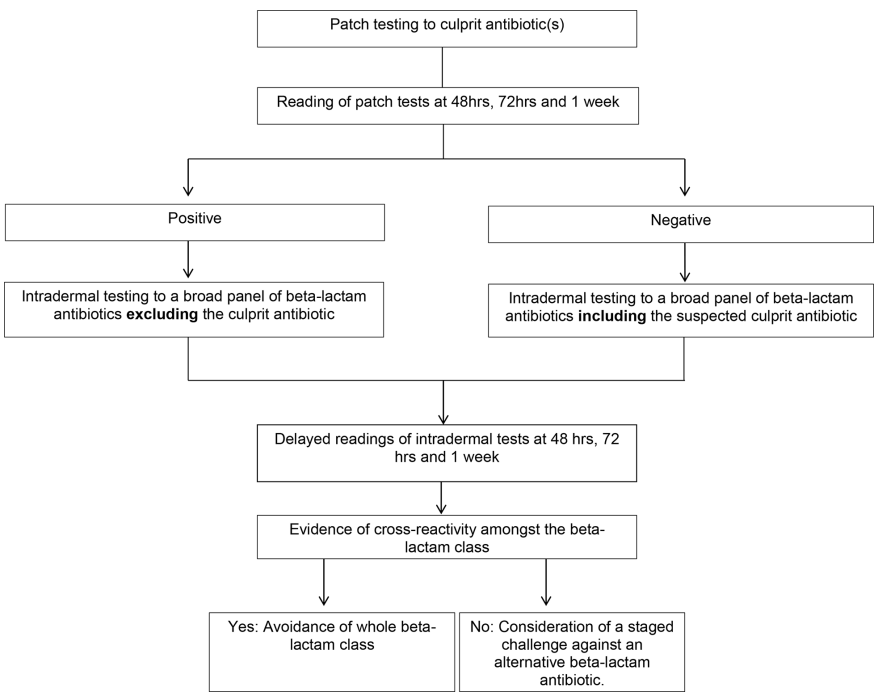

FIGURE 2 | Algorithm for skin testing in non- Stevens-Johnson syndrome (SJS)/toxic epidermal necrolysis (TEN) beta-lactam severe cutaneous adverse reactions (SCAR's).

testing. Our cases highlight that the patterns of cross-reactivity seen in beta-lactam SCAR's are not always predictable based on reactivity to the beta-lactam ring or to a side chain, and therefore we believe a standardized approach to testing against a wide variety of beta-lactam antibiotics including aztreonam is justified. This approach differs to that of Berot et al. in which patch testing was performed against a panel of penicillin and cephalosporin antibiotics and IDT was only performed if the patch test was negative. As a result this study did not find IDT with delayed readings to be of added diagnostic value (20).

Our study included patients with SCAR's to a range of beta-lactam antibiotics which is in contrast to Romano's and Berot's studies in which 97% and 82.1% of the patients included had previously reacted to an aminopenicillin (13, 20). Finally, in these previous cohort studies they were comprised predominantly of benign delayed drug reactions with a small number of SCAR patients included, making it difficult to assess results on the SCAR patients separately.

There are several limitations to our study. Firstly, none of our cases with evidence of cross-reactivity on skin testing underwent oral challenges, as it is contraindicated, and therefore the true clinical cross-reactivity remains unconfirmed by provocation. Secondly, we are reporting on findings from a small case series which is a direct result of the rarity of these conditions. Finally, we had a relative predominance of DRESS cases in our case series; this is in keeping with the known prevalence of DRESS compared with other SCAR's in the literature, but may have influenced our results.

Despite these limitations our case series highlights that cross-reactivity or co-reactivity does occur among non-SJS/TEN beta-lactam SCAR's and potentially may occur more commonly than previously described. Furthermore, the patterns of cross-reactivity we observed were most commonly that of multiple penicillins being positive without cephalosporins or that of multiple drug reactivity or co-reactivity. Interestingly we did not observe cross-reactivity due to the R1 side chain in our cohort which is thought to be the most common cause of cross-reactivity in both IgE and T cell mediated allergy (22). Given the current lack of evidence and understanding around cross-reactivity patterns in beta-lactam SCAR's a standardized approach to assessment is required. Further research in larger cohorts to better understand the underlying pathophysiology of beta-lactam SCAR's is also critical to determining cross-reactivity patterns to allow for safe but avoiding unnecessarily restrictive prescribing.

DATA AVAILABILITY STATEMENT

The raw data supporting the conclusions of this article will be made available by the authors, without undue reservation.

ETHICS STATEMENT

The study was approved for conduct by Sir Charles Gairdner Hospital quality improvement committee (GEKO 28972) and Perth Childrens Hospital quality improvement committee (GEKO 26921). Written informed was obtained from the individual(s) for the publication of any potentially identifiable images in this article.

AUTHOR CONTRIBUTIONS

GT - data collection and analysis, wrote paper. AM-T - data contribution and paper review. ML - study design and conception, data contribution and paper review. All authors contributed to the article and approved the submitted version.

REFERENCES

1. Adler N AA, Ergen E, Trubiano J, Goh M, Philips E. Recent advances in the understanding of severe cutaneous adverse reactions. *Br J Dermatol* (2017) 177:1234–47. doi: 10.1111/bjd.15423
2. Trubiano J DA, Goh M, Slavin M, Philips E. The safety of antibiotic skin testing in severe T cell-mediated hypersensitivity of immunocompetent and immunocompromised hosts. *J Allergy Clin Immunol Pract* (2018) 7 (4):1341–3.
3. Sassolas B, Haddad C, Mockenhaupt M, Dunant A, Liss Y, Bork K, et al. ALDEN, an algorithm for assessment of drug causality in Stevens–Johnson syndrome and toxic epidermal necrolysis: comparison with case–control analysis. *Clin Pharmacol Ther* (2010) 88(1):60–8. doi: 10.1038/clpt.2009.252
4. Lin YF, Yang CH, Sindy H, Lin JY, Rosaline Hui CY, Tsai YC, et al. Severe cutaneous adverse reactions related to systemic antibiotics. *Clin Infect Dis* (2014) 58(10):1377–85. doi: 10.1093/cid/ciu126
5. White KD, Chung WH, Hung SI, Mallal S, Phillips EJ, et al. Evolving models of the immunopathogenesis of T cell–mediated drug allergy: The role of host, pathogens, and drug response. *J Allergy Clin Immunol* (2015) 136(2):219–34. doi: 10.1016/j.jaci.2015.05.050
6. Illing PT, Mifsud NA, Purcell AW. Allotype specific interactions of drugs and HLA molecules in hypersensitivity reactions. *Curr Opin Immunol* (2016) 42:31–40. doi: 10.1016/j.coi.2016.05.003
7. Pichler WJ, Adam J, Watkins S, Wuillemin N, Yun J, Yerly D, et al. Drug hypersensitivity: how drugs stimulate T cells via pharmacological interaction with immune receptors. *Int Arch Allergy Immunol* (2015) 168(1):13–24. doi: 10.1159/000441280
8. Goh SJR, Tuomisto JEE, Purcell AW, Mifsud NA, Illing PT. The complexity of T cell-mediated penicillin hypersensitivity reactions. *Allergy* (2020) 76 (1):150–67. doi: 10.1111/all.14355
9. Cho Y-T, Yang C-W, Chu C-Y. Drug reaction with eosinophilia and systemic symptoms (DRESS): an interplay among drugs, viruses, and immune system. *Int J Mol Sci* (2017) 18(6):1243. doi: 10.3390/ijms18061243
10. Feldmeyer L, Heidemeyer K, Yawalkar N. Acute generalized exanthematous pustulosis: pathogenesis, genetic background, clinical variants and therapy. *Int J Mol Sci* (2016) 17(8):1214. doi: 10.3390/ijms17081214
11. de Risi-Pugliese T, Barailler H, Hamelin A, Amsler E, Gaouar H, Kurihara F, et al. Symmetrical drug-related intertriginous and flexural exanthema: A little-known drug allergy. *J Allergy Clin Immunol: In Pract* (2020) 8(9):3185–3189. e4. doi: 10.1016/j.jaip.2020.04.052
12. Goldblatt C KS, Booth J, Urbancic K, Grayson M, Trubiano J. Poor reporting and documentation in drug-associated Stevens Johnson Syndrome and toxic epidermal necrolysis- lessons for medication safety. *Br J Pharmacol* (2016) 83:224–6. doi: 10.1111/bcp.13103
13. Romano A GF, Valluzzi R, Maggioletti M, Caruso C, Quaratino D. Cross-reactvitiy and tolerability of aztreonam and cephalosporins in subjects with a

T cell-mediated hypersensitivityto penicillins. *J Allergy Clin Immunol* (2016) 138(1):179–86. doi: 10.1016/j.jaci.2016.01.025
14. El-Ghaiesh S MM, Whitaker P, Jenkins R, Meng X, et al. Characterisation of the antigen specificity of T-cell clones from piperacillin-hypersensitive patients with cystic fibrosis. *J Pharmacol Exp Ther* (2012) 341(3):597–610. doi: 10.1124/jpet.111.190900
15. Gonçalo M, Bruynzeel DP. Patch testing in adverse drug reactions. *Contact Dermatitis* (2020) p:1–21. doi: 10.1007/978-3-319-72451-5_26-1
16. Brockow K, Garvey LH, Aberer W, Atanaskovic-Markovic M, Barbaud A, Bilo MB, et al. Skin test concentrations for systemically administered drugs–an ENDA/EAACI Drug Allergy Interest Group position paper. *Allergy* (2013) 68 (6):702–12. doi: 10.1111/all.12142
17. Torres MJ, Blanca M, Fernandez J, Romano A, Weck A, Aberer W, et al. Diagnosis of immediate allergic reactions to beta-lactam antibiotics. *Allergy* (2003) 58(10):961–72. doi: 10.1034/j.1398-9995.2003.00280.x
18. Romano A, Gaeta F, Arribas Poves MF, Valluzzi RL. Cross-reactivity among beta-lactams. *Curr Allergy Asthma Rep* (2016) 16(3):24. doi: 10.1007/s11882-016-0594-9
19. Phillips E, Knowles SR, Weber EA, Blackburn D. Cephalexin tolerated despite delayed aminopenicillin reactions. *Allergy* (2001) 56(8):790–0. doi: 10.1034/j.1398-9995.2001.056008790.x
20. Bérot V, Gener G, Ingen-Housz-Oro S, Gaudin O, Paul M, Chosidow O, et al. Cross-reactivity in beta-lactams after a non-immediate cutaneous adverse reaction: experience of a reference centre for toxic bullous diseases and severe cutaneous adverse reactions. *J Eur Acad Dermatol Venereol* (2019) 34(4):787–94. doi: 10.1111/jdv.15986
21. Watts T LP, Haque R. DRESS syndrome due to benzylpenicillin with cross-reactivity to amoxycillin. *J Allergy Clin Immunol Pract* (2018) 6(5):1766–8.. doi: 10.1016/j.jaip.2018.01.011
22. Romano A, Atanaskovic-Markovic M, Barbaud A, Bircher AJ, Brockow K, Caubet JC, et al. Towards a more precise diagnosis of hypersensitivity to beta-lactams—an EAACI position paper. *Allergy* (2020) 75(6):1300–15. doi: 10.1111/all.14122
23. Barbaud A CE, Milpied B, Assier H, Staumont D, Avenel-Audran M, et al. A multicentre study to determine the value and safety of drug patch tests for the three main classes of severe cutaneous adverse drug reactions. *Br J Dermatol* (2013) 168:555–62. doi: 10.1111/bjd.12125
24. Romano A VR, Caruso C, Maggioletti M, Gaeta F. Non-immediate cutaneous reactions to beta-lactams: approach to diagnosis. *Curr Allergy Asthma Rep* (2017) 17(23). doi: 10.1007/s11882-017-0691-4

Conflict of Interest: The authors declare that the research was conducted in the absence of any commercial or financial relationships that could be construed as a potential conflict of interest.

frontiers in Immunology

ORIGINAL RESEARCH
published: 12 April 2021
doi: 10.3389/fimmu.2021.653710

Carbamazepine Induces Focused T Cell Responses in Resolved Stevens-Johnson Syndrome and Toxic Epidermal Necrolysis Cases But Does Not Perturb the Immunopeptidome for T Cell Recognition

Nicole A. Mifsud[1†], Patricia T. Illing[1†], Jeffrey W. Lai[1], Heidi Fettke[1], Luca Hensen[2], Ziyi Huang[1], Jamie Rossjohn[1,3,4], Julian P. Vivian[1,3], Patrick Kwan[5,6,7] and Anthony W. Purcell[1]*

[1] Infection and Immunity Program, Department of Biochemistry and Molecular Biology, Biomedicine Discovery Institute, Monash University, Clayton, VIC, Australia, [2] Department of Microbiology and Immunology, Peter Doherty Institute for Infection and Immunity, University of Melbourne, Parkville, VIC, Australia, [3] Australian Research Council Centre of Excellence for Advanced Molecular Imaging, Monash University, Clayton, VIC, Australia, [4] Institute of Infection and Immunity, Cardiff University School of Medicine, Cardiff, United Kingdom, [5] Department of Neuroscience, Central Clinical School, Alfred Hospital, Monash University, Melbourne, VIC, Australia, [6] Departments of Medicine and Neurology, Royal Melbourne Hospital, University of Melbourne, Parkville, VIC, Australia, [7] Department of Medicine and Therapeutics, Prince of Wales Hospital, Chinese University of Hong Kong, Hong Kong, Hong Kong

Antiseizure medications (ASMs) are frequently implicated in T cell-mediated drug hypersensitivity reactions and cause skin tropic pathologies that range in severity from mild rashes to life-threatening systemic syndromes. During the acute stages of the more severe manifestations of these reactions, drug responsive proinflammatory $CD8^+$ T cells display classical features of Th1 cytokine production (*e.g.* IFNγ) and cytolysis (*e.g.* granzyme B, perforin). These T cells may be found locally at the site of pathology (*e.g.* blister cells/fluid), as well as systemically (*e.g.* blood, organs). What is less understood are the long-lived immunological effects of the memory T cell pool following T cell-mediated drug hypersensitivity reactions. In this study, we examine the ASM carbamazepine (CBZ) and the CBZ-reactive memory T cell pool in patients who have a history of either Stevens-Johnson syndrome (SJS) or toxic epidermal necrolysis (TEN) from 3-to-20 years following their initial adverse reaction. We show that *in vitro* drug restimulation of CBZ-reactive $CD8^+$ T cells results in a proinflammatory profile and produces a mainly focused, yet private, T cell receptor (TCR) usage amongst human leukocyte antigen (HLA)-B*15:02-positive SJS or TEN patients. Additionally, we show that expression of these CBZ-reactive TCRs in a reporter cell line, lacking endogenous αβTCR, recapitulates the features of TCR activation reported for ASM-treated T cell lines/clones, providing a useful tool for further functional validations. Finally, we conduct a comprehensive evaluation of the HLA-B*15:02

OPEN ACCESS

Edited by:
Ilan Bank,
Sheba Medical Center, Israel

Reviewed by:
Simon Mallal,
Vanderbilt University Medical Center, United States
Teresa Bellon,
University Hospital La Paz Research Institute (IdiPAZ), Spain

***Correspondence:**
Anthony W. Purcell
Anthony.Purcell@monash.edu

[†]These authors have contributed equally to this work and share first authorship

Specialty section:
This article was submitted to T Cell Biology, a section of the journal Frontiers in Immunology

Received: *15 January 2021*
Accepted: *22 March 2021*
Published: *12 April 2021*

Citation:
Mifsud NA, Illing PT, Lai JW, Fettke H, Hensen L, Huang Z, Rossjohn J, Vivian JP, Kwan P and Purcell AW (2021) Carbamazepine Induces Focused T Cell Responses in Resolved Stevens-Johnson Syndrome and Toxic Epidermal Necrolysis Cases But Does Not Perturb the Immunopeptidome for T Cell Recognition. Front. Immunol. 12:653710. doi: 10.3389/fimmu.2021.653710

immunopeptidome following ASM (or a metabolite) treatment of a HLA-B*15:02-positive B-lymphoblastoid cell line (C1R.B*15:02) and minor perturbation of the peptide repertoire. Collectively, this study shows that the CBZ-reactive T cells characterized require both the drug and HLA-B*15:02 for activation and that reactivation of memory T cells from blood results in a focused *private* TCR profile in patients with resolved disease.

Keywords: T cells, SJS, Stevens-Johnson syndrome, carbamazepine, drug hypersensitivity, immunopeptidomics, T cell receptor

INTRODUCTION

Antiseizure medications (ASMs) are routinely used to treat epilepsy and other neuropsychiatric conditions, such as neuropathic pain and bipolar affective disorder. Commonly prescribed ASMs, including carbamazepine (CBZ) and phenytoin (PHT), have been implicated in life-threatening drug hypersensitivity reactions (DHRs) that predominantly target the skin (1). These drug reactions typically occur in the first 2-3 months of drug administration and span a range of clinical pathologies, including mild rash [*e.g.* maculopapular exanthema (MPE)], systemic symptoms [*e.g.* drug reaction with eosinophilia and systemic symptoms (DRESS)], as well as more severe bullous reactions involving rapid development of blisters and lesions accompanied by skin detachment [*e.g.* Stevens-Johnson syndrome (SJS) and toxic epidermal necrolysis (TEN)] (2–5). Whilst early drug withdrawal can ameliorate symptoms in milder cases, the more severe cutaneous reactions require specific clinical treatments and hospitalization for disease resolution.

ASMs can be segregated into two main groups, aromatic and non-aromatic compounds. Reports have shown that aromatic compounds [*e.g.* CBZ, oxcarbazepine (OXC; a structural derivative of CBZ), PHT, lamotrigine, phenobarbital] are highly associated with cutaneous DHRs (1) in individuals of particular ethnicities driven by their human leukocyte antigen (HLA) genetic profile. In contrast, the non-aromatic ASMs (*e.g.* valproic acid, gabapentin) are considerably less associated with DHRs [extensively reviewed in (6)]. The greatest risk association reported for CBZ-induced SJS/TEN is expression of HLA-B*15:02 in individuals of Han Chinese descent (Odds Ratio 895) (7), as well as other Asian ethnicities including Thai, Malaysian and Indian (8–10). Indeed, carriers of the broad HLA-B75 serotype (includes B*15:02, B*15:08, B*15:11, B*15:21) are also adversely affected by CBZ treatment (8, 10–14). HLA-A allotype risk associations for HLA-A*31:01, -A*24:02 and -B*57:01 have also been reported for CBZ-induced SJS/TEN, DRESS and MPE across different ethnicities (Han Chinese, Korean, European, Japanese) (13, 15–20), with lower risk associations.

Small molecule drugs, such as ASMs, can promote immune reactions *via* T cell activation. ASM-induced T cell activation is proposed to occur *via* non-covalent and labile interactions between the drug, or a metabolite of the parent drug, and the HLA/peptide complex and T cell receptor (TCR) (21). Additionally, whilst peptide occupancy of the HLA molecule is necessary, there is no requirement for *de novo* peptide/HLA complex formation (21) and the drug does not markedly alter the anchor residue preference of HLA-B*15:02 suggesting it is not binding within the primary anchor pockets during peptide loading (22). Contesting the latter, a recent report has suggested that the CBZ metabolite, carbamazepine-10,11-epoxide (ECBZ), is capable of altering the HLA-B*15:02 immunopeptidome and anchor residue prevalence (23). To date there is no published structure of the interaction of CBZ and the peptide/HLA and/or TCR, although diverse *in silico* models have been generated ranging from our previous proposal of occupation of the antigen-binding cleft, to more surface exposed positions, or, with the additional inclusion of identified drug-reactive TCRs, the HLA-TCR interface (21, 22, 24).

In contrast to the antiretroviral drug abacavir, which drastically alters the immunopeptidome and facilitates a diverse and polyclonal T cell response (25–27), examination of CBZ-induced T cells revealed a much more focused TCR usage associated with SJS/TEN (28). A recent study utilized next generation sequencing to examine the blister cells of CBZ-induced SJS/TEN patients identifying a public HLA-B*15:02-restricted αβTCR [complementarity determining region (CDR)3 sequence; TCRα VFDNTDKLI and TCRβ ASSLAGELF] that also recognized structural analogs of CBZ (24). These TCR signatures contrast with an early report demonstrating the expansion of VA-22 and VB-11-ISGSY dominant clonotypes derived from the blister fluid of SJS/TEN patients recruited in Taiwan expressing HLA-B*15:02 (28). These TCRs were identified using traditional Sanger sequencing and were confounded by *in vitro* T cell co-culture with antigen presenting cells (APCs), which has been suggested to bias the outgrown T cell repertoire (29). Another study examining the *ex vivo* TCRβ repertoire in peripheral blood mononuclear cells (PBMCs) isolated from CBZ-induced SJS (n=5) or TEN (n=1) patients showed that diversity was directly linked to disease severity, with the TEN patient having a significantly decreased TCRβ repertoire compared to SJS patients (30).

What is less understood are the long-lived immunological features of the CBZ-responsive memory T cell pool in patients

Abbreviations: APC, antigen presenting cell; ASM, antiseizure medication; CBZ, carbamazepine; DRESS, drug reaction with eosinophilia and systemic symptoms; DHR, drug hypersensitivity reaction; HLA, human leukocyte antigen; MPE, maculopapular exanthema; TCR, T cell receptor; PBMC, peripheral blood mononuclear cell; SJS, Stevens-Johnson syndrome; TEN, toxic epidermal necrolysis.

with resolved disease. Do these patients exhibit similar immunological profiles to those reported during active disease, such as effector functions including Th1 cytokine production (*e.g.* IFNγ) (28) and cytolytic molecules (*e.g.* granzyme B, perforin) (31), TCR repertoire clonality, mode of drug recognition and cross-reactivity towards other ASMs? This study shows that the *in vitro* drug expanded TCR repertoire of resolved CBZ-induced SJS or TEN patients remains relatively clonal years after acute disease. These T cells respond to HLA-B15-positive APCs in the presence of CBZ, as well as related compounds, a finding that is recapitulated by expression of these cloned TCRs in a reporter cell line. Here, the responses required the continuous presence of soluble drug and HLA-B15 expression, without the need for *de novo* generation of the peptide/HLA complex. No marked drug-induced alteration in peptide anchor preference of HLA-B*15:02 was induced by any of CBZ, the metabolite ECBZ, or the structurally related ASM OXC. Together these data support the presence of a long-lived memory pool of CBZ responsive T cells in SJS or TEN patients, which are activated by structurally related ASMs in the absence of marked alteration of the immunopeptidome.

MATERIALS AND METHODS

Study Cohort

Eight patients were recruited from Hong Kong, with six HLA-B*15:02-positive patients experiencing CBZ-induced SJS or TEN, one HLA-B*15:02-negative patient with CBZ-induced SJS and one CBZ-tolerant (**Table 1**, **Supplementary Table 1**). As described in our previous studies (32, 33) the diagnosis of SJS or TEN was based on the criteria by Roujeau and Stern (2) defined by skin detachment in two or more mucosal sites, and was confirmed by dermatologists. Healthy HLA-B*15:02$^+$ individual controls (AP numbers; n=7; **Table 1**) were also recruited from both Monash University and the Australian Bone Marrow Donor Registry. All study participants provided written consent, with ethics approval granted by the Joint Chinese University of Hong Kong-New Territories East Cluster Clinical Research Ethics Committee (Hong Kong; CRE-2006.203 for patients), Monash University (Victoria, Australia; HREC-4717 for healthy individuals) and the Australian Bone Marrow Donor Registry (New South Wales, Australia; 2013/04 for healthy individuals).

Cell Preparation and *In Vitro* Expansion of Drug-Induced T Cells

Blood samples were collected from study participants, with PBMCs isolated using Ficoll-Paque (GE Healthcare, Uppsala, Sweden) density gradient centrifugation and either used immediately or cryopreserved in fetal calf serum (FCS) containing 10% DMSO (Sigma-Aldrich, MO, USA) at -196°C until required. Before use for T cell stimulation, PBMCs were quickly thawed in 37°C and washed twice in RPMI 1640 (Gibco, Life Technologies, NY, USA) and resuspended in Complete Medium [RPMI 1640 supplemented with 2 mM MEM nonessential amino acid solution (Gibco), 100 mM HEPES (Gibco), 2 mM L-glutamine (Gibco), Penicillin/Streptomycin (Gibco), 50 μM 2-mercaptoethanol (Sigma-Aldrich) and 10% heat inactivated human blood group AB serum (Sigma-Aldrich)].

Drug-induced T cells were *in vitro* expanded following PBMC stimulation at a density of 5 million per 2 mL of Complete Medium in a 24-well plate with 25 μg/mL of either CBZ (Sigma) or the metabolite ECBZ (Sigma or SYNthesis med chem, Australia). On days 4 to 14, T cell cultures were supplemented with 50 U/mL of recombinant human IL-2 (Peprotech, NJ, USA) and subcultured as required to ensure optimal outgrowth.

Antigen Presenting Cells and HLA Expression

C1R.B*15:01, C1R.B*15:02, C1R.B*15:21, C1R.B*15:25 and C1R.B*08:01 transfectants and transductants were generated from the HLA class I-reduced C1R B-lymphoblastoid cell line, which has minimal HLA-B*35:03 and normal levels of HLA-C*04:01 cell surface expression (34, 35). All APCs were cultured

TABLE 1 | Study participants: cases and healthy donors.

Participant	ID	Gender	CBZ exposure	Reaction	HLA-B*15:02	Post-reaction sample collection (months)
Cases	T00016	Female	Yes	SJS	Positive	49
	T00024	Female	Yes	SJS	Positive	39
	E10056	Female	Yes	TEN	Positive	129
	E10076	Male	Yes	SJS	Positive	58
	E10314	Male	Yes	SJS	Negative	166
	E10367	Female	Yes	SJS	Positive	144
	E10630	Female	Yes	SJS	Positive	246
	E10493	Female	Yes	Tolerant	Negative	N/A
Healthy donors	AP005	Unknown	No	N/A	Positive	N/A
	AP017	Unknown	No	N/A	Positive	N/A
	AP022	Unknown	No	N/A	Positive	N/A
	AP026	Unknown	No	N/A	Positive	N/A
	AP027	Unknown	No	N/A	Positive	N/A
	AP029	Unknown	No	N/A	Positive	N/A
	AP102	Female	No	N/A	Positive	N/A

N/A, not applicable; SJS, Stevens-Johnson syndrome; TEN, toxic epidermal necrolysis.

in RF10 [same constituents as Complete Medium except 10% heat inactivated FCS (Sigma-Aldrich)]. Maintenance of transfected HLA expression (except green fluorescent protein (GFP) tagged C1R.B*15:21 and C1R.B*15:25) during long-term culture was facilitated by selection antibiotics [Geneticin G418 (0.5 mg/ml; Roche Diagnostics, Mannheim, Germany) or hygromycin B (0.3 mg/ml; Life Technologies, Carlsbad, CA)] as required. GFP expression is used as a reporter of HLA expression facilitating flow cytometric sorting. Increased HLA-I expression (compared to C1R Parental) was confirmed *via* flow cytometry by indirect staining with appropriate antibodies; anti-human pan HLA-I (W6/32 hybridoma; **Supplementary Figure 1A**), anti-human HLA-Bw6 (HB152 hybridoma; **Supplementary Figure 1B**) and a secondary goat anti-mouse IgG phycoerythrin (PE) (1:200 dilution; Southern Biotech, Birmingham, AL). All hybridomas were produced in-house. Stained cells were acquired on LSRII flow cytometer [Becton Dickinson (BD), San Jose, CA]. Flow cytometry data was analyzed using FlowJo software (version 10, BD).

Drug-Pulsed APCs and T Cell Stimulation

Functionality of the drug-induced T cells, including cross-reactivity, was assessed using intracellular cytokine staining (ICS) for production of either IFNγ and/or TNF (36). Briefly, day 14 T cells ($2x10^5$) were restimulated with Dynabeads® Human T-Activator CD3/CD28 beads (positive control; Life Technologies), drug alone (25 μg/mL), APC alone ($1x10^5$; APC) or APC in the presence of drug ($1x10^5$; APC+25 μg/mL drug) for a total of six hours. Brefeldin A (10 μg/mL; Sigma-Aldrich) was added for the last 4 hours of co-culture. Cells were then surface labeled with LIVE/DEAD® fixable Aqua stain (Life Technologies), CD4 PE (clone RPA-T4), CD8 PerCP-Cy5.5 (clone SK1), fixed in 1% paraformaldehyde (ProSciTech, Queensland, Australia) in phosphate buffered saline (PBS) and then permeabilized with 0.3% Saponin (Sigma-Aldrich) containing IFNγ PE-Cy7 (clone B27) and TNFα V450 (clone MAb11) before acquisition on a LSRII flow cytometer [Becton Dickinson (BD), San Jose, CA, USA] (**Supplementary Figure 2A**). All monoclonal antibodies were purchased from BD and titrated for optimal staining efficiency. A maximum of 50,000 lymphocytes were acquired on a BD LSRII flow cytometer utilizing BD FACSDIVA™ software (FlowCore, Monash University) and analyzed using FlowJo software (version 10, BD). Representative gating strategy is shown in **Supplementary Figure 2B**.

Paired αβTCR Analysis of Drug-Induced T Cells

A single-cell sort was performed to characterize the αβTCR signature of drug-induced T cells using the IFNγ Secretion Assay–Detection Kit (allophycocyanin; Miltenyi Biotec, CA, USA). Cryopreserved T cell lines were thawed and rested overnight in Complete Medium. T cell lines (maximum of $5x10^6$ cells) were incubated with either C1R.B*15:02 alone or C1R.B*15:02 + drug (25 μg/mL) target cells (2:1 ratio) in RH5 media (same constituents as Complete Medium, except 5% heat inactivated human blood group AB serum) for 4 hours at 37°C, 5% CO_2. Cells were washed in cold Wash Buffer (0.5% FCS, 2 mM EDTA pH 8.0 in PBS), centrifuged (285 ×*g*, 5 min, 4°C) and supernatant aspirated before addition of IFNγ catch reagent antibody according to manufacturer's instructions. Cells were incubated on ice for 5 min and topped up to 10 mL with warm RH5 media, and drug (25 μg/mL) was re-added. Cells were incubated for 45 min at 37°C, 5% CO_2 with rotation. Cells were washed in cold Wash Buffer, centrifuged and supernatant aspirated prior to co-staining with IFNγ allophycocyanin detection reagent and CD8 FITC (clone HIT8a). Cells were incubated on ice for 20 min, washed in cold Wash Buffer, centrifuged and resuspended in 300 μL cold Wash Buffer (**Supplementary Figure 2C**).

Single cells were sorted on a BD Influx flow cytometer (FlowCore, Monash University) directly into 96-well PCR plates (Bio-Rad, Hercules, CA, USA) based on $CD8^+IFN\gamma^-$ for drug-unresponsive T cells (negative control) and $CD8^+IFN\gamma^+$ for drug-induced T cells (**Supplementary Figure 2C**). Sorted plates were immediately stored at -80°C until required. Analysis of paired TCRα and β genes was carried out by multiplex nested RT-PCR and sequencing of α and β products as described previously (37). Both external and internal rounds of PCR included 40 TRAV and 27 TRBV forward primers, and a TRAC and TRBC reverse primer, as detailed elsewhere (37). Sequences were analyzed according to the ImMunoGeneTics/V-QUEry and STandardization web-based tool (38). All TCR nomenclature was according to Folch et al. (39). CDR3 amino acid sequences described within the text start from CDR3-position 3, which is equivalent to amino acid position 107 of the TRAV and TRBV segments, and end at TRAJ-position 10 or TRBJ-position 6.

Generation of SKW3.TCR Cell Lines

Full-length human TCRα and TCRβ cDNA was cloned into pMIG vector separated by a self-cleaving 2A peptide as described previously (40, 41). A pMIG vector, with IRES-linked GFP expression, containing a specific TCR for AP026/CBZ, E10056/CBZ, or E10630/CBZ (4 μg) was retrovirally transduced into SKW3.hCD8αβ cells (kindly provided by Dr. Zhenjun Chen, Peter Doherty Institute for Infection and Immunity, University of Melbourne; hereafter referred to as SKW3), which is negative for endogenous TCRαβ but contains CD3 and its signaling components, using HEK293T packaging cells, pEQ-pam3(-E) (4 μg) and pVSV-G (2 μg) packaging vectors and Lipofectamine 3000 as previously described (41). The original SKW3 parental cell line was kindly provided by Dr. Klaus Steube, Leibniz Institute DSMZ-German Collection of Microorganisms and Cell Cultures (Braunschweig, Germany). The HLA typing of SKW3 cells is HLA-A*11:01, 30:01; B*35:01, 44:02; C*04:01, 05:01; DRB1*01:03, 04:01; DQB1*03:01; DPB1*04:01, 04:02. A non-specific control, SKW3.LC13 cell line, specific for an EBV epitope FLRGRAYGL ($EBNA3A_{325-333}$) restricted to HLA-B*08:01 was generated in our previous study (41). The SKW3.TCR cell lines were maintained in RF10 media (**Supplementary Figure 1C**).

Functional T Cell Assays

Activation of SKW3.TCR cells ($1x10^5$) was assessed using cell-surface CD69 upregulation after 17-20 hours incubation with either C1R Parental, C1R.B*15:01, C1R.B*15:02, C1R.B*15:21, C1R.B*15:25 or C1R.B*08:01 targets (1:1 ratio) under different sets of conditions, including either direct drug addition (25 µg/mL) or by drug-pulsing APC (25 µg/mL) overnight then thorough washing in RPMI before SKW3.TCR co-incubation. SKW3.TCR cells were co-stained with CD3 PE-Cy7 (clone SK7), CD8 PerCP-Cy5.5 (clone SK1), CD69 APC (clone L78), LIVE/DEAD® fixable Aqua stain. For all experiments, stimulation with Dynabeads® Human T-Activator CD3/CD28 beads (Life Technologies) served as a positive control, and SKW3.TCR cells alone as a negative control. Flow cytometry data were acquired and analyzed as described previously (41). The CD69 expression profiles were measured as geometric mean fluorescence intensity (MFI) to provide more meaningful evaluation of changes in the relative amounts of expressed protein per cell. A maximum of 50,000 lymphocytes were acquired on a BD LSRII flow cytometer utilizing BD FACSDIVA™ software (FlowCore, Monash University) and analyzed using FlowJo software (version 10, BD).

Immunopeptidome Analysis

The C1R.B*15:02 cell line was *in vitro* expanded in RF10, and treatment of cells with either CBZ (Sigma), ECBZ (Sigma or SYNthesis med chem, Australia) or OXC (SYNthesis med chem) for peptide elutions was performed at 25 µg/mL for 48 hours in roller bottles prior to harvesting. Cells ($0.9\text{-}1.1 \times 10^9$) were pelleted, washed twice in PBS and snap-frozen in liquid nitrogen. Cells were lysed, and the HLA class I isolated by immunoaffinity purification using solid-phase bound pan HLA class I antibody W6/32 as described previously (42). Peptides were dissociated using 10% acetic acid and separated from the HLA heavy and light (beta-2 microglobulin; β_2m) chains by Reversed Phase HPLC (RP-HPLC) as described (43), monitoring elution by 215nm absorbance and collecting 500 µL fractions. The retention times of CBZ, ECBZ and OXC were determined through subjecting each molecule to the same RP-HPLC protocol. Peptide containing fractions, avoiding regions containing β_2m and heavy chain, were vacuum concentrated and concatenated to generate 13 pools, including 3 pools aligned with the retention times of CBZ (pool 10), ECBZ (pool 12) and OXC (pool 13). Pools were vacuum concentrated to remove residual acetonitrile (ACN) and reconstituted in 15 µL 2% ACN, 0.1% formic acid (FA), spiked with 250 fmol iRT peptides (44).

Pools were analyzed by liquid chromatography-tandem mass spectrometry (LC-MS/MS) using a data dependent acquisition (DDA) strategy on a Q-Exactive Plus Hybrid Quadrupole Orbitrap (Thermo Fisher Scientific) utilizing a Dionex UltiMate 3000 RSLCnano system (Thermo Fisher Scientific). 5-6 µL of concentrated material was loaded onto an Acclaim PepMap 100 (100 µm x 2 cm, nanoViper, C18, 5 µm, 100Å; Thermo Scientific) in 2% ACN, 0.1% FA at a flow rate of 15 µL/min. Peptides were separated over an Acclaim PepMap RSLC (75 µm x 50 cm, nanoViper, C18, 2 µm, 100Å; Thermo Scientific) at 250 nL/min using a gradient of Buffer A (0.1% FA) and Buffer B (80% ACN, 0.1% FA) as follows: 2.5-7.5% B in 1 min, 7.5-32.5% B in 55 min, 32.5-40% B in 5 min, 40-99% B in 5 min, 99% B for 6 minutes, and 99-2.5% B in 1 min, prior to re-equilibration at 2.5% B for 20 min. Data were collected in positive mode: MS1 resolution 70,000, scan range 375-2000 m/z; MS2 resolution 17500, scan range 200-2000 m/z. The top 12 ions of +2 to +5 charge per cycle were chosen for MS/MS with a dynamic exclusion of 15 seconds.

Peptide sequences were assigned using PEAKS X+ (Bioinformatics Solutions Inc.) *via* a database search against the reviewed human proteome (UniProt/Swiss-Prot, accessed October 2018), and a database of common contaminants. The following settings were employed: Instrument – OrbiTrap (Orbi-Orbi), Fragment – HCD, Acquisition - DDA, Parent Mass Error Tolerance - 20.0 ppm, Fragment Mass Error Tolerance - 0.02 Da, Precursor Mass Search Type - monoisotopic, Enzyme - None, Variable Modifications - Oxidation (M) 15.99, Deamidation (NQ) 0.98, and Cysteinylation: 119.00, Max Variable PTM Per Peptide - 3. Peptides assigned at a 5% peptide false discovery rate (FDR) were utilized in downstream analyses. DDA data from previous analyses of the immunopeptidome of endogenous HLA I and II of C1R cells (43) were searched separately *via* the same pipeline as control datasets.

To characterize the HLA-B*15:02 binding motif, peptide sequences identified at a 5% peptide FDR in control data sets representing the endogenous HLA class I and II of C1R cells were removed. So too were peptides assigned without a protein accession or mapping exclusively to proteins in the contaminant database. For peptide counts, motif and length distribution analysis, only 7-20mer peptides were considered and peptides sequences containing deamidations or cysteinylations were treated as distinct from the native sequence. Figures were generated using Prism 9.0, GraphPad software (San Diego, CA). The mass spectrometry proteomics data have been deposited to the ProteomeXchange Consortium *via* the PRIDE (45) partner repository with the dataset identifier PXD023545 and 10.6019/PXD023545.

Identification of Co-Purified Drugs/Metabolites

Drugs/metabolites were detected using a targeted LC-multiple reaction monitoring-MS (LC-MRM-MS) approach on a SCIEX QTRAP® 6500 plus mass spectrometer, coupled to an Ekspert™ nanoLC 415. For pools aligned with the RP-HPLC retention time of CBZ (pool 10), ECBZ (pool 12) and OXC (pool 13), residual sample post-peptide analysis was diluted by a factor of ~2. 6 µL diluted sample was loaded onto a NanoLC Trap ChromXP C18 column (350 µm x 0.5 mm, 3 µm particle size, 120 Å pore size) in 2% ACN, 0.1% FA at a flow rate of 5 µL/min for 5 minutes, prior to separation over a ChromXP nanoLC C18 column (75 µm x 15 cm, 3 µm particle size, 120 Å pore size) at 300 nL/min using an increasing gradient of Buffer B (80% ACN, 0.1% FA): 0–1 min 2% B, 1-2 min 2–12% B, 2–30 min 12–35% B, 30–50 min 35–80% B, 50–54 min hold at 80% B, 54-55 min 80-2% B, 55-65 min re-equilibration at 2% B. The QTRAP® 6500 was operated in

positive mode, MRM scan type, in unit resolution for Q1 and Q3. For detection of CBZ three transitions were set with a Q1 mass of 237.102, and Q3 masses of 192.082 [Collision Energy (CE) 30], 194.097 (CE 25) and 220.077 (CE 15). For ECBZ and OXC, five transitions were set with a Q1 mass of 253.097, and Q3 masses of 180.082 (CE 30), 182.096 (CE 25), 208.076 (CE 30), 210.092 (CE 25) and 236.071 (CE 25). CE values were optimized based on injection of solubilized drug/metabolite. Three transitions for each iRT peptide were also monitored. Drug peaks areas are the sum peak areas of the monitored transitions. Drug peak areas were normalized to the sum peak areas of iRT peptides B-G (GAGSSEPVTGLDAK, VEATFGVDESNAK, YILAGVENSK, TPVISGGPYEYR, TPVITGAPYEYR, DGLDAASYYAPVR). Figures were generated using Prism 9.0, GraphPad software.

Statistical Analysis

All data were reported as mean ± standard error of the mean (SEM), unless stated otherwise. Statistical significance was determined by nonparametric one-way ANOVA with post-hoc Tukey's multiple comparison test, Mann-Whitney test or multiple comparisons using Holm-Sidak method (Prism 8.0, GraphPad software) with *p<0.05, **p<0.005 and ****p<0.0001. Standard error of the difference between mean amino acid prevalence was calculated using the Welch t-test (Prism 9.0, GraphPad software).

RESULTS

Drug-Induced Recall Responses Are Restricted to CD8$^+$ T Cells in Recovered SJS or TEN Patients

We examined the immune reactivity profiles of convalescent SJS or TEN patients (7 cases and one drug-tolerant case) to determine whether they maintain a memory pool of T cells specific to the culprit drug that can be reactivated following subsequent drug exposures (**Table 1**). PBMCs treated with 25 μg/mL CBZ were expanded *in vitro* for 14 days. Outgrown CBZ-induced T cell lines were then restimulated in a 6-hour ICS assay with either no drug (untreated), CBZ (25 μg/mL), or with HLA-B*15:02$^+$ APCs C1R.B*15:02 or C1R.B*15:02+CBZ (25 μg/mL) to measure activation *via* production of Th1 cytokines (IFNγ and TNF). Group data of the recovered patients showed that the CBZ-reactive T cell response, where activation was observed following CBZ and APC+CBZ stimulation, was primarily restricted to CD8$^+$ T cells. However, the CD4$^+$ T cells did show immune recognition of CBZ alone, likely *via* the mechanism of self-T cell presentation (*i.e.* T-T presentation). Here, 6 out of 7 patients expressing HLA-B*15:02 demonstrated non-specific CD4$^+$ T cell responses towards the APCs most likely due to HLA class II mismatches expressed by the C1R.B*15:02 transfectant (**Figure 1A**). Optimization experiments, using healthy donors, showed similar CD4$^+$ T cell immune responses (*i.e.* production of Th1 cytokines IFNγ and TNFα) to both the C1R parental and C1R.B*15:02 APC in either the presence or absence of CBZ (data not shown). Dissection of the individual CD8$^+$ T cell responses profiled either by single or dual expression of IFNγ and TNF demonstrated significantly higher responses were driven by IFNγ production (p-value <0.05; Mann-Whitney test; **Figure 1B**). As expected, the drug-tolerant case did not respond to CBZ (red dot; **Figure 1B**).

Priming of Drug-Naïve HLA-B*15:02$^+$ Individuals Required Multiple Rounds of Drug Exposure

To demonstrate both the kinetics and magnitude of T cell activation following drug exposure we *in vitro* stimulated HLA-B*15:02$^+$ drug-naïve PBMCs (n=7; **Table 1**) with either CBZ or its metabolite ECBZ at 25 μg/mL. On days 13 and 27, outgrown T cells were restimulated with drug (as per day 0) for continued *in vitro* expansion. Drug-induced T cell lines were tested prior to each restimulation and at day 40 (3 intervals total: day 13, 27 and 40) in a 6-hour ICS assay with either no drug (untreated), drug (CBZ or ECBZ; 25 μg/mL), or using C1R.B*15:02 or C1R.B*15:02+drug (CBZ or ECBZ; 25 μg/mL) as APC with activation quantitated by either IFNγ and/or TNF production. For CBZ-induced T cells, we observed similar findings to resolved cases (**Figure 1**) but with delayed kinetics as drug-specificity predominantly mediated by CD8$^+$ T cells that was more pronounced by day 40 (**Figure 2A**). For ECBZ-induced T cells, the greatest magnitude of immune recognition was 2.7-fold lower than the CBZ parent drug on day 40 for IFNγ producing cells (C1R.B*15:02+drug; mean ± SEM: 14.28% ± 4.6 for CBZ and 5.16% ± 1.1 for ECBZ; p=0.0029 multiple comparisons using Holm-Sidak method) (**Figure 2B**). Although not all healthy donors demonstrated ECBZ-reactive CD8$^+$ T cell responses. No drug-induced immunogenicity was shown by CD4$^+$ T cells, with T-T presentation of CBZ or ECBZ resulting in minor responses (**Figures 2A, B**). Examination of individual data for CBZ-induced CD8$^+$ IFNγ$^+$ T cells showed strong responsiveness for both AP026 (21.5%) and AP029 (33.7%) on day 27 that equated to a 41.4-fold and 48.1-fold increase, respectively, over the APC background control (*i.e.* C1R.B*15:02 vs C1R.B*15:02+CBZ). This net effect was also demonstrated on day 40 for AP022 (25.4%), AP026 (34.2%) and AP029 (19.5%) with 14.1-fold, 72.9-fold and 17.3-fold increases, respectively (**Figure 2C**). Interestingly, the same level of *in vitro* expansion was not observed with the ECBZ metabolite, with only moderate CD8$^+$IFNγ$^+$ T cell responses measured (5-10% of total CD8$^+$ T cells) on days 27 and 40, with high APC control background on day 40 being observed across all individuals (**Figure 2D**).

CBZ-Reactive T Cell Cross-Reactivity Towards Tricyclic Aromatics

A previous study examining active cases of HLA-B*15:02-positive SJS (and one SJS/TEN) and CBZ-tolerant controls showed CBZ-induced CD8$^+$ T cell cross-reactivity towards other tricyclic aromatic compounds (21). We wanted to determine whether T cell cross-reactivity can be achieved following reactivation of drug-induced T cells in our cohort of resolved HLA-B*15:02-positive SJS or TEN patients and a

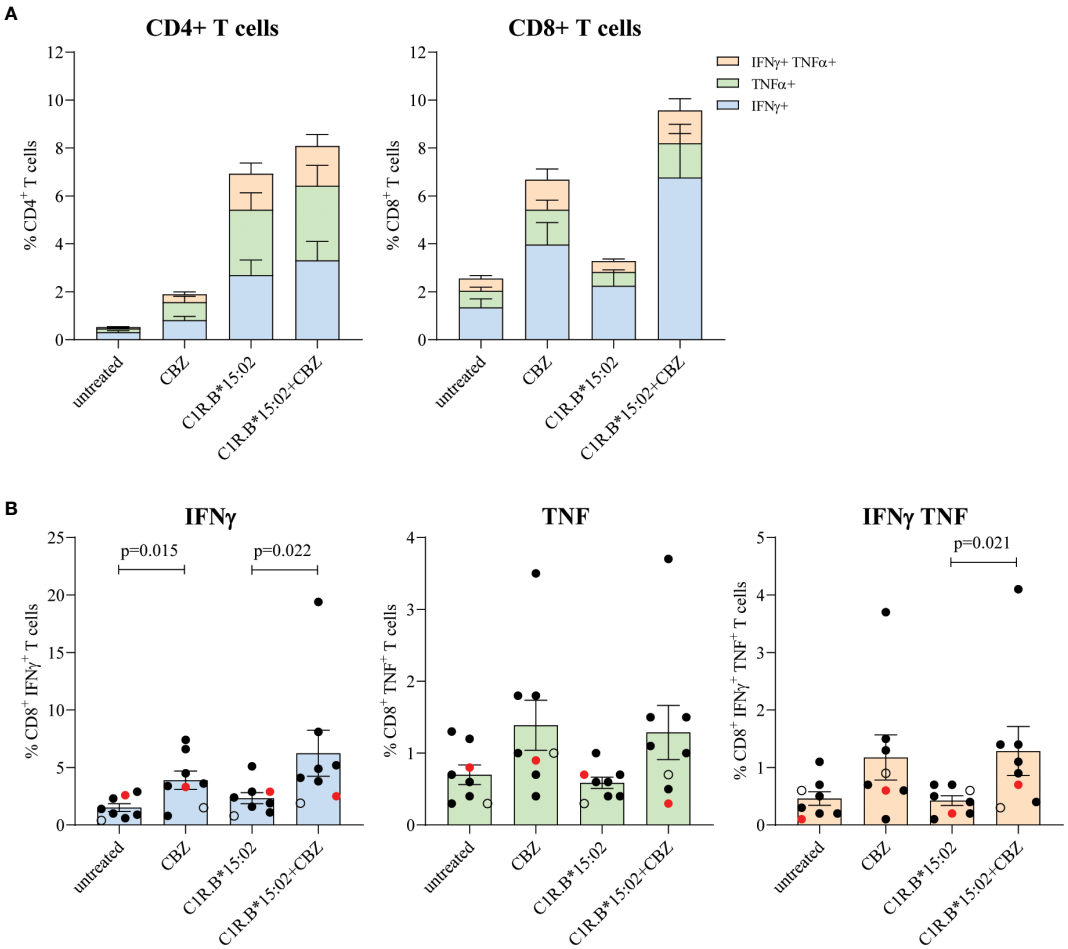

FIGURE 1 | Restimulation of drug-reactive memory cells in recovered CBZ-induced SJS and TEN patients is restricted to $CD8^+$ T cells. PBMCs were co-cultured in the presence of 25 μg/mL CBZ for 14 days. T cell subset phenotype ($CD4^+$ or $CD8^+$) and activation status (production of either IFNγ and/or TNFα) were measured following a 6-hour restimulation with either no drug (untreated), CBZ (25 μg/mL), C1R.B*15:02 or C1R.B*15:02+CBZ (25 μg/mL). Data was acquired on LSRII flow cytometer (BD) and analyzed using FlowJo software (version 10, BD). All data is expressed as mean ± SEM. **(A)** Grouped data demonstrated a drug-reactive response in $CD8^+$ T cells expressing the different combinations of proinflammatory cytokines, but this was not observed for $CD4^+$ T cells (n=7, single data). **(B)** Individual data (B*15:02 positive SJS or TEN ([n=6, solid black dots] and Tolerant [n=1, red dot], B*15:02 negative SJS [n=1, open black dot], single data) showed that activated $CD8^+$ T cell produced significantly more IFNγ than TNFα (p-value <0.05; Mann-Whitney test; **B**).

drug-tolerant control, where PBMCs were collected between 3-to-20 years post-reaction (**Table 1**). Here, *in vitro* expanded CBZ-induced T cell lines (generated for **Figure 1**) were restimulated in a 6-hour ICS assay with media alone (untreated), CBZ (25 μg/mL) or C1R.B*15:02 APCs in the absence or presence of drug (CBZ, ECBZ, OXC, PHT; 25 μg/mL) and T cell activation measured *via* IFNγ production, with statistical significance only observed between untreated and C1R.B*15:02+CBZ (p=0.111, one-way ANOVA with post-hoc Tukey's multiple comparison test). We show that $CD8^+$ T cells primed against the parent drug CBZ can cross-react towards other ASMs following restimulation with C1R.B*15:02+drug. As expected, restimulation in the presence of CBZ+APC generated the highest reactivity (mean ± SEM; 6.771 ± 2.220), followed by cross-reactivity towards OXC (3.014 ± 0.831) and ECBZ (2.943 ± 0.496) (**Figures 3A, B**). Whilst, minimal $CD8^+$ T cell cross-reactivity was observed towards the aromatic drug PHT (1.657 ± 0.561), reflecting the more chemically diverse structure of PHT compared to the other more closely related compounds to CBZ (**Figure 3C**).

$CD8^+$ T Cells That Respond to CBZ Exhibit a High Degree of TCR Clonality

To evaluate whether the TCR repertoire of activated $CD8^+$ T cells was remodeled following CBZ culture, we analyzed *in vitro* expanded HLA-B*15:02-positive PBMCs from two drug-naïve donors (AP022, AP026), five CBZ-induced SJS cases (T00016, T00024, E10076, E10314, E10630) and one CBZ-induced TEN case (E10056) (**Table 1**). CBZ-reactive T cell lines established from each individual were restimulated for 4-hours with

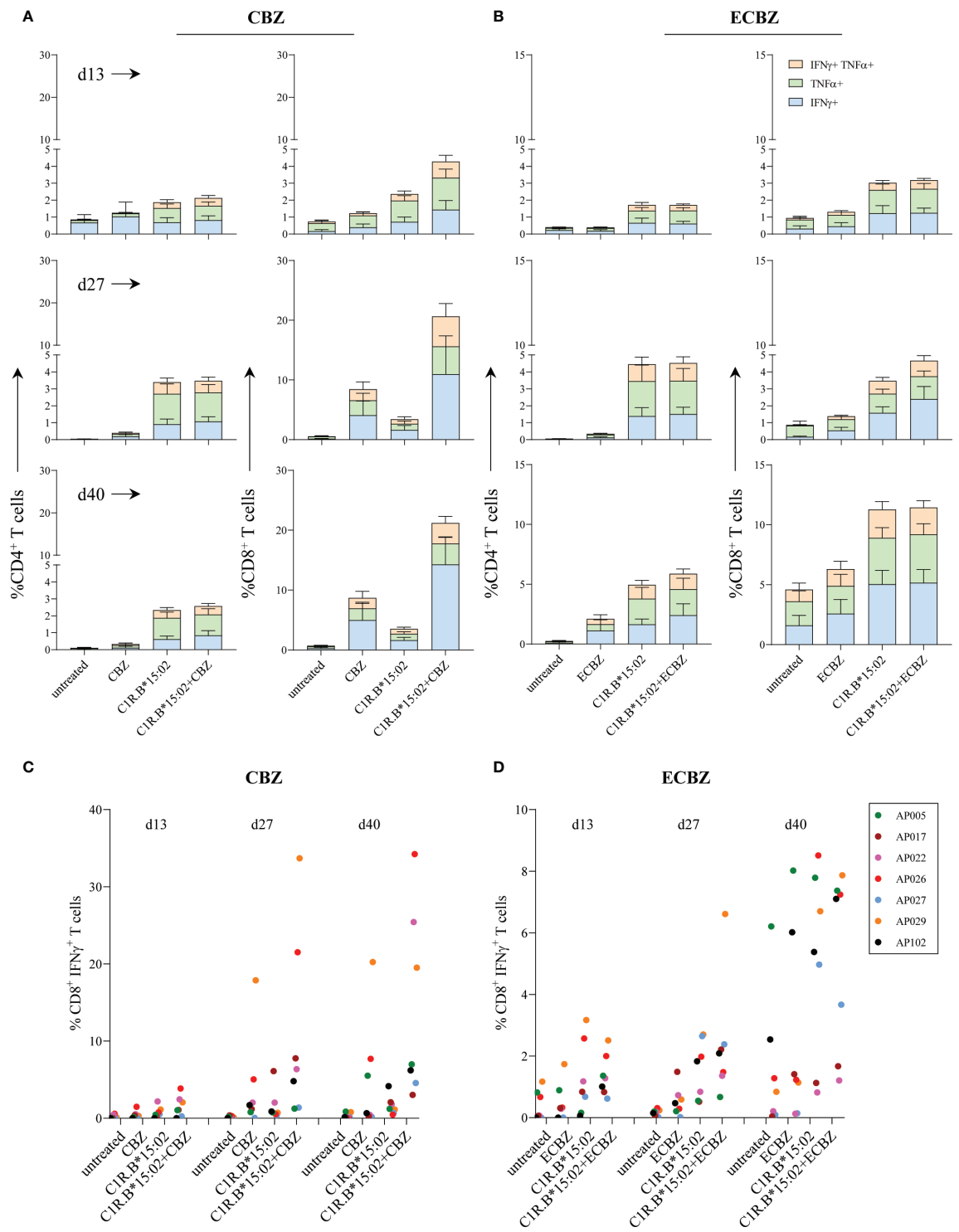

FIGURE 2 | Time course of *in vitro* priming of drug-naïve HLA-B*15:02+ individuals. PBMCs derived from drug-naïve individuals were co-cultured in the presence of either 25 μg/mL CBZ or ECBZ for 13 to 40 days, with drug restimulation on days 13 and 27. T cell subset phenotype ($CD4^+$ or $CD8^+$) and activation status (production of either IFNγ and/or TNFα) were measured following a 6-hour restimulation with either no drug (untreated), drug (25 μg/mL; CBZ or ECBZ), C1R.B*15:02 or C1R.B*15:02+drug (25 μg/mL; CBZ or ECBZ). Data was acquired on LSRII flow cytometer (BD) and analyzed using FlowJo software (version 10, BD). All data is expressed as mean ± SEM. Grouped data demonstrated drug-reactive responses were restricted to $CD8^+$ T cells expressing the different combinations of proinflammatory cytokines when primed with either **(A)** CBZ or **(B)** ECBZ (n=7, single data). Individual data tracking of immune reactivity to drugs demonstrated that multiple rounds of exposure with either **(C)** CBZ or **(D)** ECBZ were required for activation of $CD8^+$ $IFN\gamma^+$ T cells.

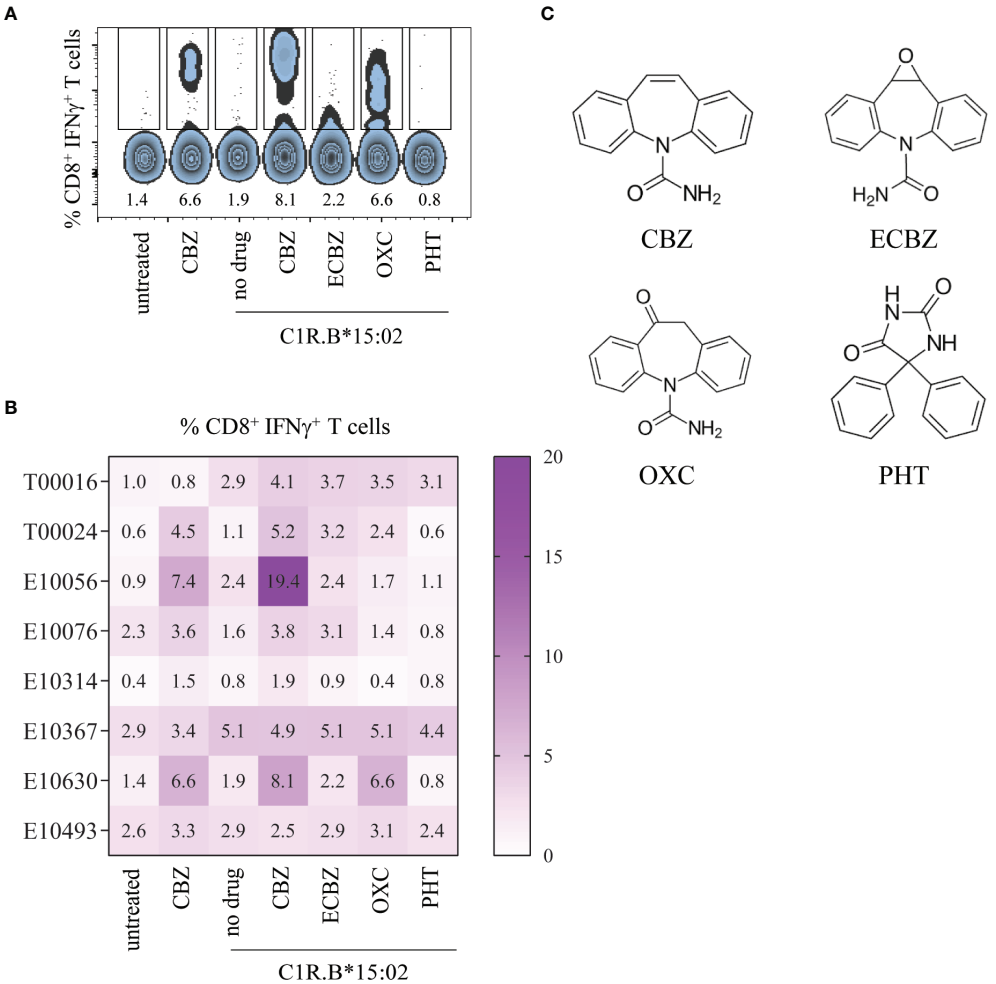

FIGURE 3 | CBZ-reactive T cell cross-reactivity towards structures comprising a tricyclic ring. Day 14 CBZ-induced T cell lines derived from SJS and TEN patients (from **Figure 1**) were restimulated in a 6-hour ICS assay with media alone (untreated), CBZ (25 μg/mL) or C1R.B*15:02 APCs in the absence or presence of drug (25 μg/mL; CBZ, ECBZ, OXC, PHT) to measure $CD8^+$ T cell activation *via* IFNγ production. Data was acquired on LSRII flow cytometer (BD) and analyzed using FlowJo software (version 10, BD). **(A)** Representative flow cytometric data for SJS patient E10630. **(B)** Matrix of CBZ-reactive T cell cross-reactivity towards ASMs with either bicyclic or tricyclic rings in CBZ-reactive patients (single data). **(C)** Chemical structures of ASMs and the ECBZ metabolite.

C1R.B*15:02 APCs either in the absence (untreated) or presence of CBZ (treated, 25 μg/mL), with activated T cells detected by IFNγ secretion. T cells were segregated based on phenotype and activation status (non-activated: $CD8^+IFN\gamma^-$ or activated: $CD8^+IFN\gamma^+$), then single cell sorted for subsequent αβTCR repertoire analysis (**Supplementary Figure 2C**). Profiling of the activated CBZ-reactive $CD8^+$ TCRs revealed a single major clonotype observed for the majority of individuals; AP022 (TRAV12-3/TRBV5-5; n=9/23 pairs), AP026 (TRAV26-1/TRBV27; 16/16), T00024 (TRAV4/TRBV3-1or3-2; 6/23), E10056 (TRAV21/TRBV30; 8/12) and E10630 (TRAV1-2/TRBV27; 18/24). Interestingly, AP026 and E10630 share the same TRBV27 usage (**Figure 4**, **Table 2**). Whilst, two major clonotypes were detected for T00016 (TRAV1-1/TRBV14; 4/23 and TRAV8-2 or 8-4/TRBV15; 4/23) and no clonality was demonstrated for E10076 or E10314 (HLA-B*15:02-negative donor). All TCR sequencing information is listed in **Supplementary Table 2**. We selected three CBZ-reactive $CD8^+$ TCRs for further functional validation to understand antigen processing requirements for T cell stimulation (**Figure 4**, **Table 2**).

Clonotypic TCRs Exhibit Cross-Reactivity Towards CBZ Metabolites and Related ASMs

Retroviral transduction of selected CBZ-reactive $CD8^+$ TCRs into the SKW3 reporter cell line enabled us to conduct cellular investigations of TCR recognition to confirm drug specificity without confounding background T-T presentation (SKW3 reporter cell lines are HLA-B15-negative). Here, TCR activation was determined by cell surface upregulation of CD69, with the shift in geometric MFI being measured by flow cytometry (**Figure 5A**). We next explored whether HLA

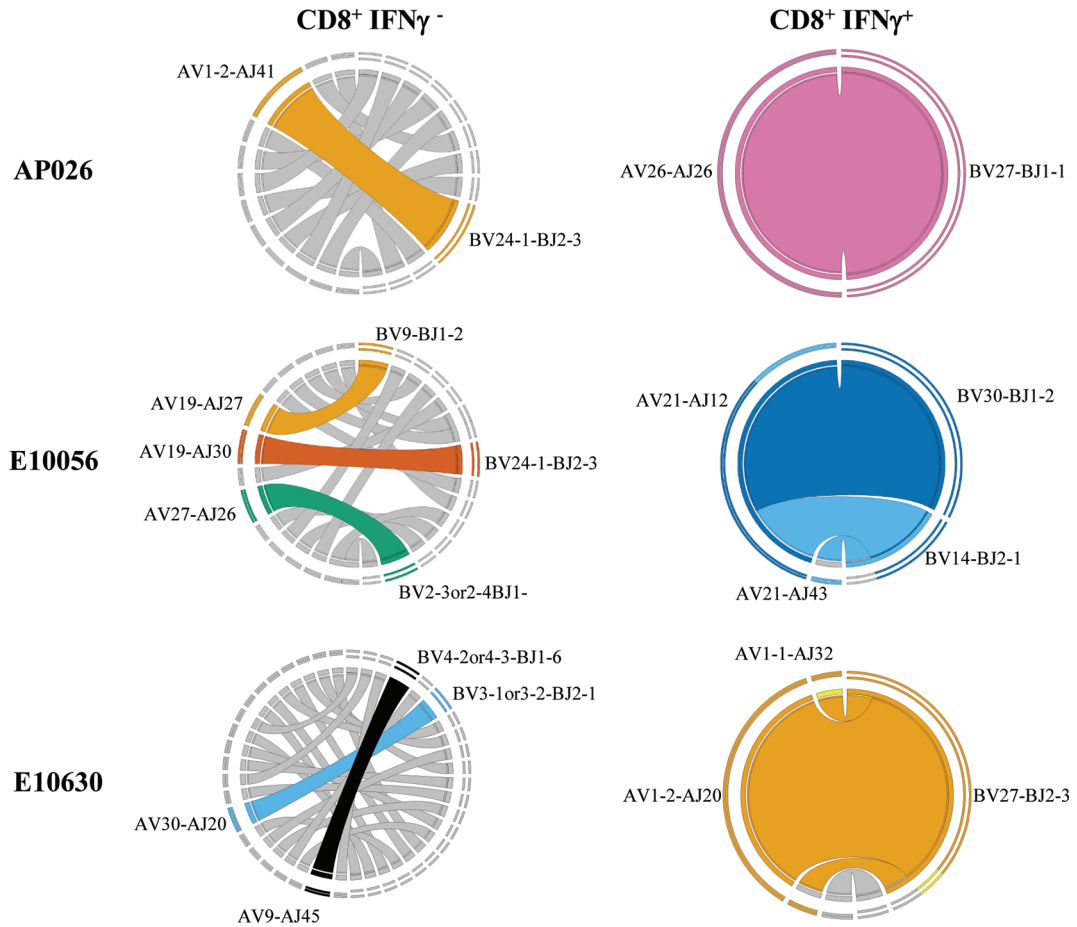

FIGURE 4 | CBZ exposure drives TCR clonality. Representative Circos plots for drug-naïve individual (AP026) and resolved SJS (E10630) and TEN (E10056) patients showing dominant αβTCR clonotype pairings for both $CD8^+$ $IFN\gamma^-$ and $CD8^+$ $IFN\gamma^+$ T cell subsets. Circos plots were generated using an on-line feature based on concatenated pairings of TCRAVJ-CDR3A and TCRBVJ-CDR3B (46). Complete TCR sequencing is shown in **Supplementary Table 2**.

TABLE 2 | αβTCR profiling of CBZ-reactive $CD8^+$ T cells.

ID	Drug Reaction	TRAV	TRAJ	CDR3α	TRBV	TRBJ	CDR3β	Pair frequency (n)
AP026	Naïve	26-1	26	CIVRSLRDNYGQNFVF	27	1-1	CASRAGGNTEAFF	16/16
E10056	TEN	21	12	CAAKDGMDSSYKLIF	30	1-2	CAWLGAGKVDGYTF	8/12
E10630	SJS	1-2	20	CAAFGDYKLSF	27	2-3	CASSSLSGGWPDTQYF	18/24

allotypes associated with SJS/TEN risk (HLA-B*15:02, B*15:21; members of B75 serological subgroup) or non-risk (B*15:01, B*15:25; members of B62 serological subgroup) were able to stimulate CBZ-reactive TCRs in the presence of drug. A control APC presenting an irrelevant viral peptide (C1R.B*08:01/FLR) was also included. For SKW3.AP026, the greatest responses were observed for CBZ, ECBZ and OXC in the presence of C1R.B*15:02-positive cells. However, there does appear to be evidence of non-specific TCR drug-induced responsiveness across all HLA-B15 allotypes, as well as the HLA-B*08:01 control (**Figure 5B**, top panel). For SKW3.E10056, TCR recognition was highly restricted to HLA risk allotypes B*15:02 and B*15:21 and almost exclusively directed against the CBZ parent drug, with a small response shown for ECBZ in the presence of C1R.B*15:02 cells. Whilst for SKW3.E10630, the patterns observed for TCR recognition indicate a high degree of promiscuity towards risk and non-risk HLA-B15 allotypes across all drugs. Additionally, the hierarchy of drug recognition was altered by the presenting allotype, with risk allotype (HLA-B*15:02/B*15:21) mediated responses being highest for

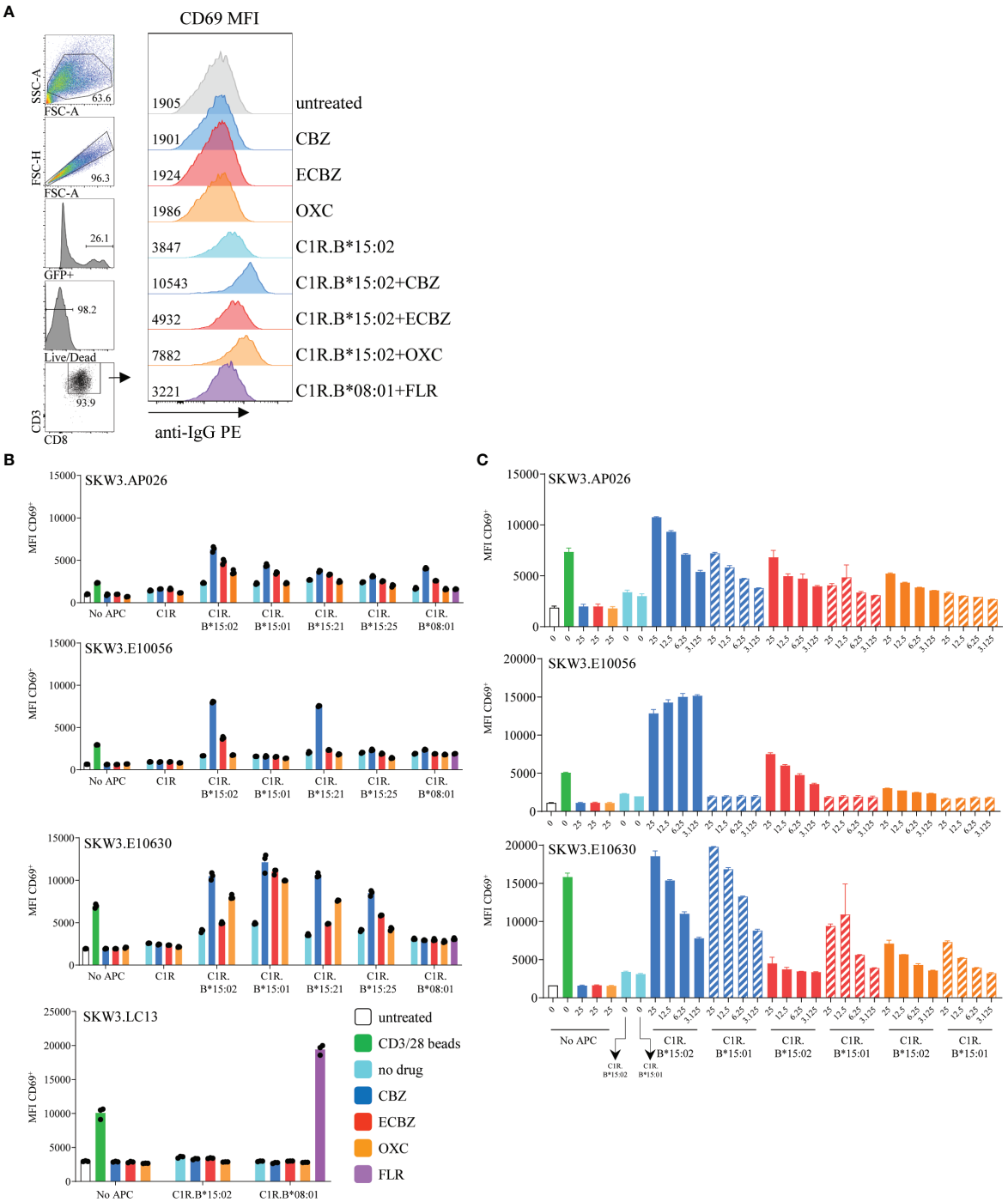

FIGURE 5 | HLA-B*15:02-restricted CBZ-reactive TCRs recognize other drug-exposed HLA-B15 allomorphs. **(A)** CD69 upregulation assay and flow cytometric gating strategy to measure activated SKW3.TCR transfectants. Representative data shown from SKW3.E10630, with cell surface CD69 measured as geometric mean fluorescence intensity (MFI). **(B)** CBZ-reactive TCR lines (SKW3.AP026, SKW3.E10056, SKW3.E10630) and an EBV-specific irrelevant control (SKW3.LC13) were stimulated with APCs expressing different HLA-B15 allomorphs in the presence of tricyclic aromatic compounds, and the control C1R.B*08:01 presenting an irrelevant viral peptide (C1R.B*08:01+FLR) for 17-20 hours. Cells were then stained and data was acquired by flow cytometry (triplicate data, mean ± SEM). **(C)** Drug dose response titrations (3.125 to 25 µg/mL) were performed for each HLA-B15 allomorph prior to stimulation of CBZ-reactive TCR lines (SKW3.AP026, SKW3.E10056, SKW3.E10630) (duplicate data, mean ± SEM).

CBZ>OXC>ECBZ, whilst non-risk allotype (HLA-B*15:01/B*15:25) mediated responses showed an alternate hierarchy of CBZ>ECBZ>OXC. As expected, no SKW3.E10056 and SKW3.E10630 TCR activation towards the irrelevant control (C1R.B*08:01/FLR) was observed (**Figure 5B**, middle panels). Notably, none of the TCRs examined displayed responses to any of the drugs in the presence of the parental C1R cell line, which lacks HLA-A and -B expression. An irrelevant TCR control, SKW3.LC13, was also examined to demonstrate TCR specific recognition of C1R.B*08:01/FLR and non-activation by drug in the presence of C1R.B*08:01 or C1R.B*15:02 APCs (**Figure 5B**, lower panel).

To determine whether TCR recognition of the non-risk HLA allotype B*15:01 was drug dose dependent, the drug was titrated 4-fold from 25 μg/mL down to 3.125 μg/mL in the presence of APCs. For both SKW3.AP026 and SKW3.E10630, as anticipated TCR activation reduced in accordance with decreasing concentrations of drug. However, this effect was comparable in both the risk and non-risk HLA allotypes, B*15:02 and B*15:01, respectively. Whilst SKW3.E0056 showed remarkable specificity and sensitivity towards CBZ and decreasing responses towards the less immunogenic ECBZ, but only when presented by B*15:02-expressing APC (**Figure 5C**).

SKW3.TCR Reporter Cells Are Activated *via* a Non-Covalent Drug Interaction

We explored whether the SKW3.TCR cells were activated by the same non-covalent drug interactions as observed for *in vitro* expanded CBZ-induced T cell lines. Here, we tested the TCR transduced reporter cells capacity for activation when both C1R.B*15:02 and drug were present throughout the assay (drug addition), as well as when C1R.B*15:02 was pulsed overnight with drug and then washed prior to co-incubation. Both SKW3.AP026 (drug-naïve healthy control) and SKW3.E10630 (SJS patient) cell lines showed a significant decrease in TCR activation for C1R.B*15:02 drug-pulsed, compared to C1R.B*15:02 drug addition, across all three drugs tested (CBZ, ECBZ, OXC; $p<0.0001$ ANOVA with Tukey correction) (**Figure 6A**). These observations mirrored T cell line data (**Figures 1B**, **2A**) demonstrating a labile drug-HLA-B*15 interaction in keeping with non-covalent binding.

SKW3.TCR Reporter Cells Do Not Require Intracellular Antigen Processing for Activation

We measured whether active antigen processing in APCs for *de novo* generation of peptide/HLA complexes was required for SKW3.TCR activation. Following fixation of C1R.B*15:02 with 1% paraformaldehyde, TCR activation was significantly reduced, compared to non-fixed C1R.B*15:02, but a notable drug-specific response was still observed for all three SKW3.TCR cell lines (**Figure 6B**, $p<0.0001$ ANOVA with Tukey correction). These data align with the nature of interaction between TCR/drug/HLA molecule not requiring active antigen processing pathways. Finally, we investigated whether the drug itself binds stably to the TCR. Here SKW3.E10056 and SKW3.E10630 cells were either untreated or pulsed with drug (and washed to remove unbound drug) prior to stimulation with C1R.B*15:02 in either the absence or presence of drug. Here, maximal TCR activation was only observed when TCR/drug/C1R.B*15:02 were present throughout the assay. Thus, potential TCR/drug interactions alone were assumed to lack the stability to be maintained without either maintenance of the drug in solution or stabilization by the HLA present on APC (**Figure 6C**, $p<0.0001$ and $p<0.005$ ANOVA with Tukey correction).

Minimal Impact of CBZ/ECBZ/OXC on Peptide Binding Specificity of HLA-B*15:02

Previous analyses of the ligandome of HLA-B*15:02 from CBZ treated cells have observed co-purification of CBZ (22, 47). Furthermore, we previously described a minor alteration of the immunopeptidome reflected in conservation of anchor residue biases (P2, P9) of co-purified peptides, and modulation of residues across non-anchor positions. This earlier observation led us to postulate drug binding at a central position in the antigen-binding cleft (22). In contrast the metabolite ECBZ has been suggested to alter peptide binding to soluble HLA-B*15:02, through interaction in the region of the F-pocket (23). Given the responses of CBZ-reactive T cells to CBZ, ECBZ and OXC we sought to determine whether we could define common changes in peptide binding induced by these three small molecules that might shed light on the interaction. As previously, we utilized the C1R.B*15:02 cell line due to its demonstrated ability to present these molecules in an immunogenic fashion (**Figures 5**, **6**). Membrane-bound HLA molecules were extracted from 0.9-1.1 x 10^9 cells through non-denaturing lysis and immunoaffinity purification, prior to acid elution of peptides, fractionation by RP-HPLC and LC-MS/MS analysis. Experiments were performed in duplicate for each of untreated and CBZ treated (25 μg/mL) cells, whilst single experiments for ECBZ and OXC treatment (25 μg/mL) conditions were performed to determine if ECBZ and OXC recapitulated observations for CBZ treatment.

As CBZ, ECBZ and OXC were observed to have distinct chromatographic retention times during RP-HPLC, aligned with fraction pools 10 (CBZ), 12 (ECBZ) and 13 (OXC), these specific pools were also analyzed by multiple reaction monitoring (MRM) to determine whether drug had co-purified with the HLA-B*15:02 during immunoaffinity purification. As anticipated, clear signal for CBZ was observed in pool 10 for CBZ treated samples at 36 minutes, for ECBZ in pool 12 of ECBZ treated samples at 28 minutes, and for OXC in pool 13 for OXC treated samples at 30 minutes (**Supplementary Figure 3**). Despite identical masses and monitored transitions, OXC and ECBZ are distinguished by distinct retention times and transition hierarchies (**Supplementary Figure 3B** *vs* **3C**). In the ECBZ sample, a second peak was also observed at 21 minutes (**Supplementary Figure 3B**). Evolution of this second, earlier, peak was also seen over increased time in the autosampler for ECBZ prepared as a comparator. Subsequent analysis suggested that ECBZ is unstable over time in the loading conditions used for LC-MS analysis (2% ACN, 0.1% FA), with an increase in signal for a mass consistent with the hydrolysis product (10,11-dihydroxycarbamazepine, m/z = 271.1+) co-eluting with the earlier peak (data not shown). It is therefore hypothesized that

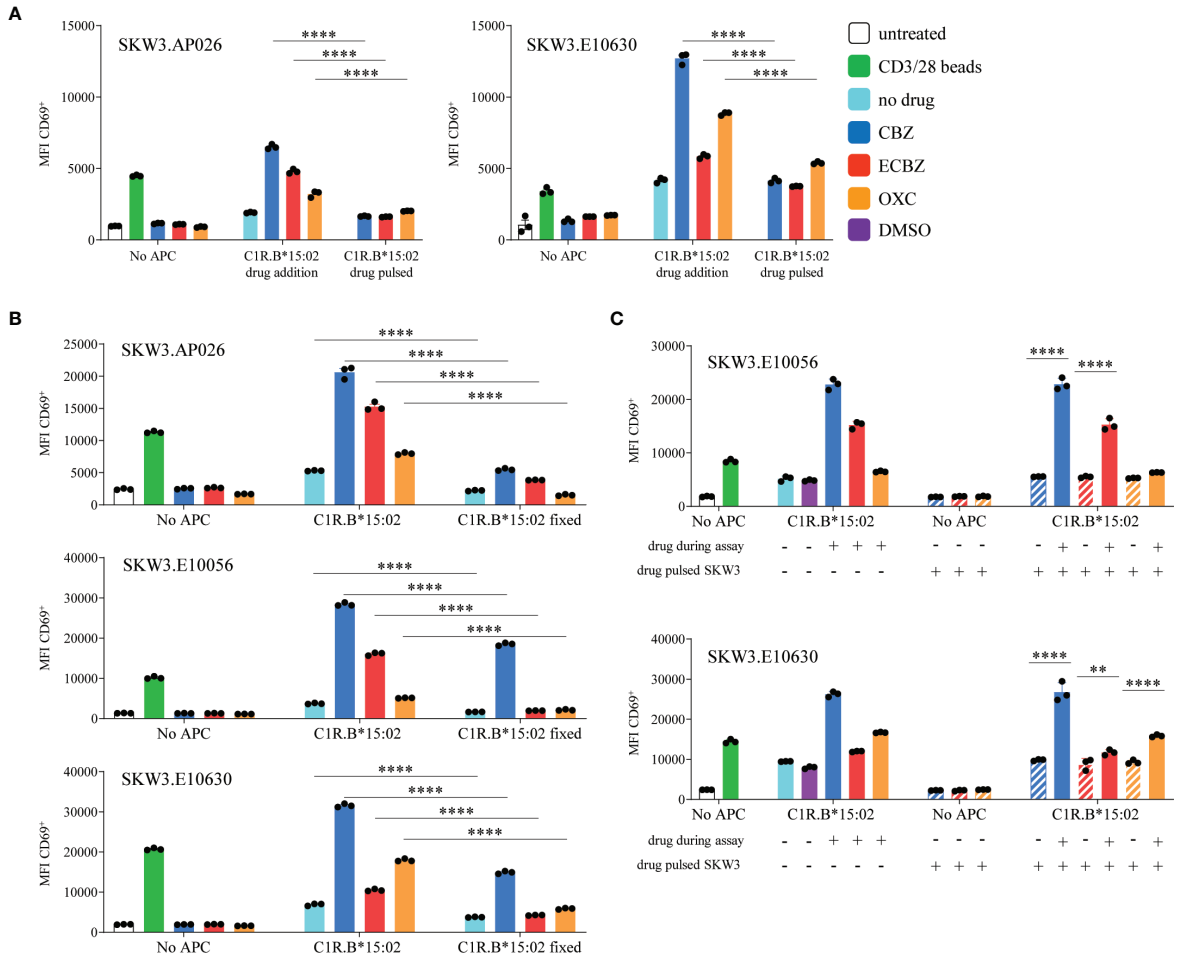

FIGURE 6 | Features of SKW3.TCR activation. **(A)** CBZ-reactive TCR lines (SKW3.AP026, SKW3.E10630) were stimulated for 17-20 hours with C1R.B*15:02 either in the presence of drug throughout the assay (drug addition) or drug-pulsed overnight and then washed. Cells were then stained and data was acquired by flow cytometry (triplicate data, mean ± SEM). A significant decrease was observed when SKW3.TCR cells were stimulated with drug-pulsed C1R.B*15:02 (****p<0.0001; ANOVA with Tukey correction). **(B)** SKW3.TCR cells (AP026, E10056, E10630) were stimulated with either untreated or fixed C1R.B*15:02 for 17-20 hours. Cells were then stained and data was acquired by flow cytometry (triplicate data, mean ± SEM). Whilst a significant reduction in TCR activation was shown, a drug-reactive response was still observed (****p<0.0001; ANOVA with Tukey correction). **(C)** SKW3.E10056 and SKW3.E10630 cells were either untreated or pulsed with drug prior to stimulation with C1R.B*15:02 ± drug. TCR/drug interactions alone were unable to induce CD69 upregulation (****p<0.0001 and **p<0.005; ANOVA with Tukey correction).

the earlier peak is 10,11-dihydroxycarbamazepine, some of which undergoes dehydration during electrospray ionization to regenerate ECBZ.

Analysis of the eluted peptides identified more than 9900 peptides of 7-20 residues per data set (**Figure 7A**) as described in the Materials and Methods. Over 24,000 peptides were identified in total, with more than 7,000 peptides identified in all treatments (**Figure 7B**). Peptides were predominantly 9 amino acids in length, which were heavily biased towards Leu (~30%)>Val (~16%)>Gln (~14%) at position 2 of the peptide, and Tyr (~48%)>Phe (~24%)>Met (~15%)>Leu (~10%) at position 9 (**Figure 7C**). Proline was observed at P4 and P5 in approximately 12% and 10% of peptides respectively, whilst Ser, Thr and Val were often seen in positions 5-8 of the peptide (**Figure 7C**). Only minor differences in amino acid prevalence were observed between individual treatments and the untreated control, and no common perturbation of residue preference was noted for the three molecules when considering the global immunopeptidome as might be expected from their cross-reactivity (**Supplementary Figure 4**). Due to previous reports of increased prevalence of deamidated peptides bound to HLA-B*15:02 after treatment with ECBZ, particularly at P4 (23), we considered deamidated Asn and Gln separately from their native form in motif analysis. However, deamidated peptides were observed to be rare in our analysis (**Supplementary Figure 5**). We previously observed minor perturbations of non-anchor residues when considering peptides uniquely identified in HLA-I purifications of CBZ treated C1R.B*15:02 as compared to untreated cells, in analyses based on a smaller dataset (<2000 peptides/condition) (22). The current analysis incorporates more

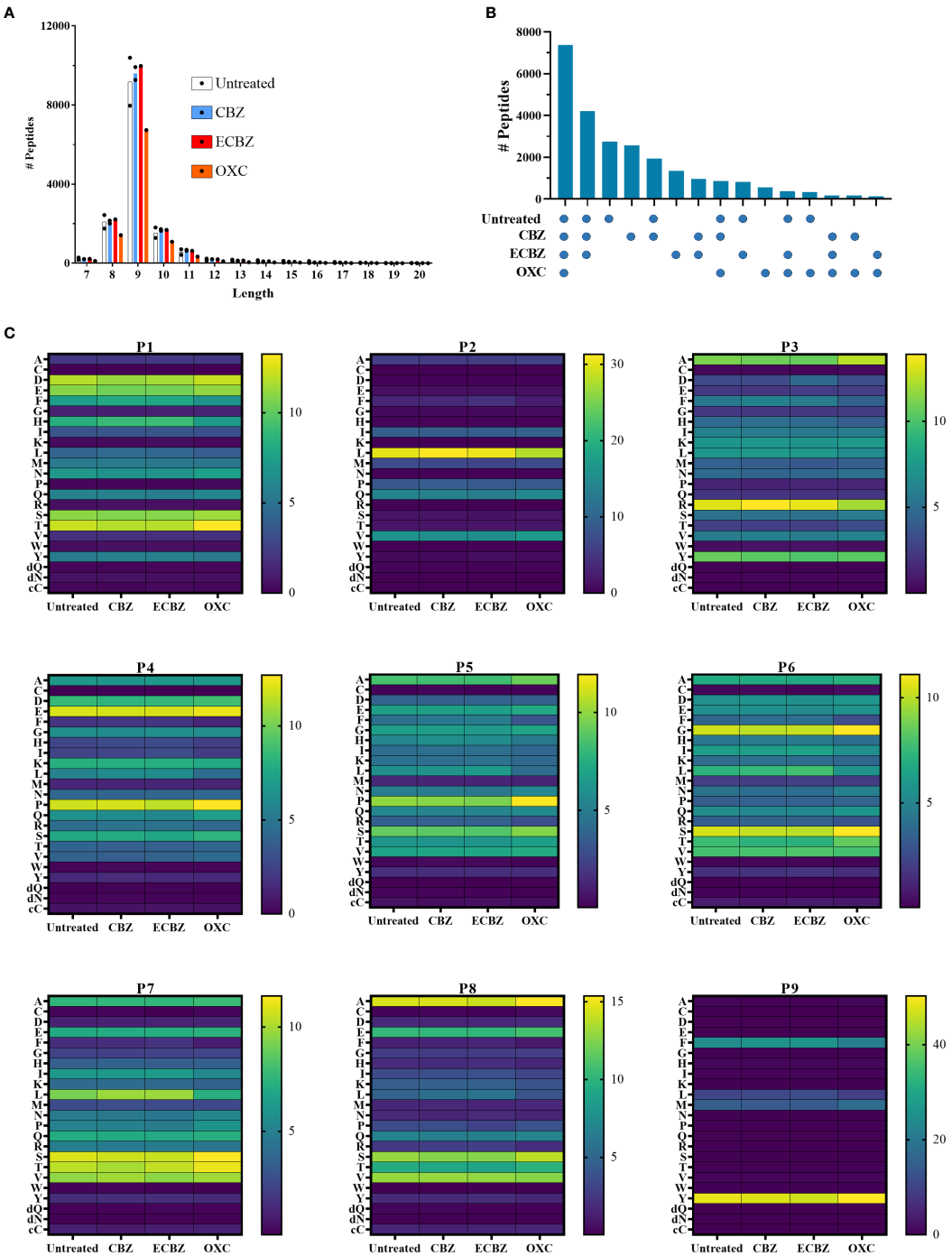

FIGURE 7 | Binding specificity of HLA-B*15:02 is not overtly perturbed by CBZ, ECBZ or OXC. C1R.B*15:02 were cultured for 48 hours in the presence of 25 μg/mL CBZ, ECBZ or OXC, or without drug. HLA class I molecules were isolated by immunoaffinity purification and the bound peptides/drugs eluted and analyzed by LC-MS/MS to characterize the HLA-B*15:02 immunopeptidome under these conditions. Experiments were performed in duplicate for untreated and CBZ treatment conditions, and single experiments were performed for ECBZ and OXC treatment conditions. **(A)** Shows the length distribution of peptides identified in each condition with points representing the number of peptides in individual data sets, and bars representing the mean number of the peptides from duplicate experiments. **(B)** To identify the similarity between the conditions, peptides identified in duplicate experiments were combined and the number of peptides overlapping between the conditions depicted as an upset plot. Points below the graph depict the conditions to which the peptides are common. **(C)** The proportion of 9mers in each condition (mean for duplicate experiments) possessing a given amino acid at P1-P9 are depicted as heat maps. Individual scale bars are provided per position. Amino acids are shown using the single letter code, with the addition of dQ and dN [representing deamidated Gln(Q) and Asn(N)], and cC (representing Cysteinylation at Cys).

than 9900 peptides (>6000 nonameric peptides) per experiment, and more than 18,000 peptides (>11,000 nonamers) per untreated and CBZ treated conditions when replicates are combined. We therefore again determined the peptides that were common (identified in at least 1 replicate of each condition) and unique (identified in at least 1 replicate of the condition, but never in the compared condition). We identified more than 14,000 peptides (>9000 nonamers) common to untreated and CBZ treatment conditions, with 4246 (2126 nonamers) and 3871 (2129 nonamers) peptides identified in untreated only (untreated unique) and CBZ treatment only (CBZ unique), respectively. Focusing on the nonamer peptides, as anticipated we saw similar anchor preferences to the whole data set analysis. As observed previously, there were some variations across the backbone of the peptide (**Supplementary Figures 6**), but few were recapitulated in similar analyses of ECBZ and OXC compared to untreated cells (**Supplementary Figures 7**, **8**), and overall only 2738 (1211 nonamers) were only identified in the untreated condition (when compared to all drug treatment conditions) (**Figure 7B**). It is therefore difficult to discern a compelling common drug induced motif across the three treatments, although a slight reduction in acidic residues at P1 and tyrosine at P3 were commonly observed (**Supplementary Figures 6**–**8**), as noted previously for CBZ (22). A subtle increase in Pro at P2 was also observed in peptides uniquely identified in drug treatments, although Leu remained the dominant anchor residue.

DISCUSSION

Adaptive immune recognition of a foreign entity by T cells relies on two signals; (1) interaction between an immunogenic antigen/HLA complex and the TCR and (2) co-stimulation provided by engagement of B7 (*i.e.* CD80/CD86) on APCs and CD28 expressed on T cells. The ensuing response drives expansion and proliferation of T cells containing an armory of effector functions, including pro-inflammatory cytokine production and release of cytotoxic molecules, that eliminate pathogen-infected or neoplastic cells. Once the elimination process is completed, attrition of effector T cells leads to the establishment of a memory T cell pool to combat secondary encounters with the same immunogenic antigen/HLA complex which lacks the necessity for signal 2 to allow rapid deployment. Whilst T cell-mediated immune responses are critical in controlling initial and subsequent challenges, responses against innocuous stimuli sometimes occur and are associated with autoimmunity and allergy, including DHRs.

The impacts of ASM-induced T cell-mediated DHRs have been well reported [comprehensively reviewed (6, 48)]. Key insights have been drawn from investigation of three main cohorts; ASM-induced DHRs [spanning mild (MPE), moderate (DRESS) and severe (SJS and/or TEN) cases], drug tolerant patients and drug-naïve healthy donors. Comparison between these cohorts has provided critical information regarding the culprit ASM (*e.g.* CBZ, OXC, PHT, lamotrigine) as well as the association of HLA allotype (*e.g.* B*15:02, A*31:01) and ethnicity (*e.g.* Han Chinese ancestry) on DHR outcomes. Importantly, immunopathological examinations during the active phase of the hypersensitivity reaction has demonstrated a dominant role for $CD8^+$ T cells and the involvement of key cytolytic (*e.g.* granulysin, perforin, granzyme) and proinflammatory cytokines (*e.g.* IFNγ, macrophage inflammatory protein-1α) (21, 28, 31, 49–52).

In this study, we examined long-lived T cell reactivity profiles of resolved CBZ-induced SJS (and one TEN) patients, ranging from 3 to 20 years post-active disease. In particular, we were interested in determining whether CBZ-reactive memory T cells activated upon re-exposure to drug showed similar profiles to those reported in active disease, considering effector functions, TCR repertoire clonality, mode of drug recognition and cross-reactivity towards other ASMs.

CBZ-reactive T cells derived from SJS or TEN patient PBMCs were expanded for 2 weeks *in vitro* following a single round of CBZ exposure. The outgrown bulk T cell culture was then restimulated with drug either in the absence or presence of an HLA-B*15:02-expressing APC, and immunophenotypic properties of CBZ-reactive effector T cells measured by flow cytometry. We showed that these restimulated T cells were primarily restricted to the $CD8^+$ T cell lineage and were capable of Th1 pro-inflammatory cytokine production (IFNγ > TNF), aligning with reported studies of SJS/TEN patients during active disease (21, 28). For drug-naïve healthy donors, 2-3 rounds of drug exposure (CBZ or ECBZ) were required for *in vitro* priming and expansion of drug-reactive T cells. Whilst, CBZ- and ECBZ-reactive $CD8^+$ T cells were observed by day 40 in all individuals, the ECBZ metabolite had lower levels of immune responsiveness (with IFNγ > TNF) compared to the parent drug, CBZ.

A common complication of prescribed ASMs is that individuals who have experienced a DHR are at higher risk of developing the same, if not, a more severe form of DHR with an alternate ASM. Indeed, structural similarities exhibited by aromatic ASMs (*i.e.* CBZ, OXC, PHT, lamotrigine) provide a framework for cross-reactive T cell recognition that perpetuates secondary reactions in between 13-80% of DHR patients (53–56). This observation is supported by cellular investigations in SJS/TEN patients with CBZ-induced T cells (generated following 4-5 rounds of *in vitro* culture) exhibiting cross-reactivity towards other aromatic compounds such as ECBZ, OXC, lamotrigine and eslicarbazepine (21). Whilst, non-aromatic ASMs (*i.e.* valproic acid and gabapentin) are not generally associated with DHRs (57). In this study, we demonstrated that CBZ-reactive T cells (generated following a single *in vitro* drug exposure) cross-react with HLA-B*15:02$^+$ APCs in the presence of aromatic ASMs ECBZ and OXC. The majority of patients showed higher levels of cross-reactivity towards the ECBZ metabolite, albeit one individual (E10630) demonstrated greater reactivity towards OXC. These data suggest an immune hierarchy of T cell cross-reactivity towards ASMs is likely driven by the common tricyclic ring structure between CBZ, ECBZ and OXC, but modulated by different side groups. These observations demonstrate that

resolved SJS and TEN patients, many years post-DHR, can still vigorously respond to alternate aromatic ASMs, and that T cell immune monitoring should be undertaken when considering different treatment options.

We next examined the HLA-B*15:02-restricted TCR repertoire of CBZ-reactive $CD8^+$ T cells in two drug-naïve individuals and six SJS or TEN patients. In most cases, a single major TCR clonotype was observed, which supports previous findings of focused TCR usage in SJS/TEN patients (28). However, most of these TCR repertoires showcased private specificities, with only two individuals (AP026 and E10630) sharing the same TRBV27 usage, but lacking common CDR3 regions. These findings diverge from previous reports of a more public TCR usage within the HLA-B*15:02-restricted CBZ-induced TCR repertoire in SJS and/or TEN patients; that exhibited dominant Vα and Vβ clonotypes (28) and a public αβTCR CDR3 sequence (24). Differences in TCR repertoire may also be attributed to either the site of origin for CBZ-reactive T cells [*i.e.* blister fluid/cells vs PBMCs [this study)] and/or collection of biospecimens during active or resolved (this study) disease states. It is also important to acknowledge reported biases associated with the *in vitro* expansion of T cell lines (29, 58), with the likelihood of different TCR clonotypes being expressed by drug-naïve and drug-experienced individuals, as well as their localization at different sites of pathology (i.e. blister fluid vs PBMCs). In particular, the study by Pan et al. (24) could not recapitulate TCR clonotype findings reported by Ko et al. (28) in the PBMC and blister fluid of SJS/TEN patients. Although, we have previously shown in anti-viral TCRs that a bias was not induced between *ex vivo* PBMCs and day 14 *in vitro* T cell cultures (59).

Limited patient biospecimen availability makes it difficult to conduct a multitude of cellular assays, even with *in vitro* expansion of T cell lines and clones. Here we take advantage of a known reporter system utilizing αβTCR deficient SKW3 cells (41, 60) to examine drug-induced HLA-restricted T cell promiscuity and the mode of drug presentation. Single major TCR clonotypes, for one drug-naïve individual (AP026) and two patients (E10056, E10630), were cloned into the SKW3 reporter cell line. Firstly, we investigated whether these TCRs demonstrated HLA-B15 specificity towards SJS or TEN risk (B75 subgroup) and non-risk (B62 subgroup) allotypes (21). Interestingly, we observed highly restricted TCR recognition for E10056 towards B75 subgroup members B*15:02 and B*15:21, whilst both AP026 and E10630 showed high degree of cross-reactivity towards risk and non-risk HLA-B*15 allotypes. This observation was apparent for all HLA-B15 APCs in the presence of CBZ, ECBZ or OXC in a dose dependent fashion. Furthermore, no responses were observed in the presence of HLA-B-negative C1R cells. These observations suggest that non-risk HLA-B15 molecules may also support the ligation of certain CBZ-reactive TCRs, implying the association of SJS or TEN with HLA-B*15:02, but not HLA-B*15:01, is not as simple as the ability of the drug to uniquely interact with one HLA allomorph but not another.

Secondly, we examined whether ASMs stimulated SKW3.TCR reporter cells using the same mechanisms required for T cell lines. As observed by others (21, 49, 52), we found it was essential to maintain soluble drug continuously within the assay for TCR activation, consistent with a non-covalent and labile interaction between the drug and peptide/HLA and/or TCR complex. Additionally, we showed that fixation of APCs did not abrogate drug-induced TCR activation, which aligns with the interaction occurring with pre-existing peptide/HLA complexes, hence not requiring additional antigen processing. Finally, we showed that TCR/drug interactions were not maintained on washing of the reporter cells at physiological pH suggesting any interactions lack sufficient stability to be maintained in the absence of the peptide/HLA complex. Whilst it has been suggested that binding can occur directly with a public CBZ-specific αβTCR in the absence of the peptide/HLA complex (24), we only observed reporter cell activation in the presence of drug treated HLA-B*15-positive APCs. Hence, the presence of peptide/HLA, and TCR are necessary for maximal functional coordination of the drug interaction. Collectively, these data validate the use of SKW3.TCR reporter cells as an immunological tool for DHR cellular investigations and confirm that non-covalent and labile drug/TCR/peptide/HLA interactions in the absence of new peptide/HLA generation underpin CBZ-induced DHRs.

In line with the inability of drug pulsed C1R.B*15:02 to stimulate reporter cell responses, modulation of the immunopeptidome by CBZ and its derivatives was subtle. This is distinct from the interaction of abacavir and HLA-B*57:01, where stable, non-covalent binding within the antigen binding cleft causes a perturbation of self-peptide presentation, initiated predominantly in the ER, and alteration of the PΩ anchor preference of abacavir occupied HLA-B*57:01 molecules (22, 26, 27). We previously observed subtle modulation of non-anchor residues of peptides bound to HLA-B*15:02 through comparison of a smaller dataset of HLA-B*15:02 ligands (<2000 peptides per condition). With the current larger dataset (>9900 peptides per condition) and comparison to cross-reactive molecules ECBZ and OXC not all changes were recapitulated, although a subtle reduction in acidic amino acids at P1 and tyrosine at P3 were consistent for peptides unique to drug treatments (22). This is not to say there are not HLA/peptide/drug complexes formed but the mechanism for their formation clearly follows a different trajectory to that of HLA-B*57:01/abacavir/peptide complexes. Interestingly, our data contrasted a recent report that ECBZ alters peptide presentation by soluble HLA-B*15:02 (23). Whether this is due to differences between soluble and membrane-bound HLA such as reduced interaction with the peptide loading complex, or the workflow used (*e.g.* the necessity for use of detergents to extract membrane-bound HLA, peptide elution conditions), which might impact complex stability, remains to be clarified.

As described previously, CBZ and ECBZ were detected in eluates from affinity purified HLA class I molecules of drug treated cells (22, 23, 47), an observation that was extended to OXC. This residual drug is maintained despite washing of the source cells, as well as the immunoaffinity purified HLA class I molecules, at physiological pH, a process shown to abrogate APC

immunogenicity in functional experiments. Given the rapid titration of responses to CBZ, ECBZ and OXC, it is possible that whilst washing reduces the number of peptide/HLA/drug complexes below the threshold for activation, some level of binding is maintained. Regardless, failure to identify a distinct peptide motif in drug treated cells and the inability of either the peptide/HLA or TCR alone to maintain sufficient drug interaction for immunogenicity on removal of soluble drug, collectively suggest that CBZ and related compounds form a tripartite interaction with peptide/HLA/TCR. Furthermore, differences in recognition hierarchies of CBZ, ECBZ and OXC by the three TCRs investigated suggest the epoxide (ECBZ) and ketone (OXC) more prominently impact TCR ligation as opposed to interaction with the HLA, thus may be oriented towards the TCR.

In conclusion, this study confirms the presence of long-lived immunological effects in resolved CBZ-induced SJS and TEN patients, which are characterized by a highly clonal drug-reactive $CD8^+$ TCR repertoire. Furthermore, using a combination of the definition of the functional requirements for TCR engagement using transduced reporter cell lines and detailed study of the impact of CBZ, ECBZ and OXC on HLA-B*15:02 peptide presentation, our work supports the hypothesis that peptide/HLA and TCR are required for drug interactions able to elicit TCR activation.

DATA AVAILABILITY STATEMENT

The datasets presented in this study can be found in online repositories. The names of the repository/repositories and accession number(s) can be found below: https://www.ebi.ac.uk/pride/archive/, PXD023545.

ETHICS STATEMENT

The studies involving human participants were reviewed and approved by Joint Chinese University of Hong Kong-New Territories East Cluster Clinical Research Ethics Committee (Hong Kong; CRE-2006.203 for patients), Monash University (Victoria, Australia; HREC-4717 for healthy individuals), and the Australian Bone Marrow Donor Registry (New South Wales, Australia; 2013/04 for healthy individuals). The patients/participants provided their written informed consent to participate in this study.

AUTHOR CONTRIBUTIONS

NM, PI, JR, JV, and AP designed experiments. NM, PI, JL, HF, and ZH performed experiments. LH, PK, and AP provided reagents and/or patient samples. NM, PI, JL, and AP analyzed data. NM, PI, and AP wrote the manuscript. All authors contributed to the article and approved the submitted version.

FUNDING

PI was supported by a National Health and Medical Research Council of Australia (NHMRC) Early Career Fellowship (1072159, 2014-2017) and a Monash University Faculty of Medicine, Nursing and Health Sciences Senior Postdoctoral Fellowship (2020). LH was recipient of Melbourne International Research Scholarship and Melbourne International Fee Remission Scholarship. JR is supported by Australian Research Council Australia Laureate Fellowship. PK is supported by a Medical Research Future Fund Fellowship (MRF1136427). AP is supported by a NHMRC Principal Research Fellowship (1137739). We acknowledge funding support from a NHMRC Project grants 1103979 (to PK) and 1122099 (to AP and JV).

ACKNOWLEDGMENTS

The authors acknowledge the Monash University FlowCore Facility for flow cytometry instrumentation and technical support, the services and facilities of Micromon Genomics at Monash University, and the Monash Proteomics & Metabolomics Facility for the provision of mass spectrometry instrumentation, training and technical support. Micromon Computational resources were supported by the R@CMon/Monash Node of the NeCTAR Research Cloud, an initiative of the Australian Government's Super Science Scheme and the Education Investment Fund.

SUPPLEMENTARY MATERIAL

The Supplementary Material for this article can be found online at: https://www.frontiersin.org/articles/10.3389/fimmu.2021.653710/full#supplementary-material

Supplementary Figure 1 | HLA staining of Antigen Presenting Cells and SKW3.TCR expression. C1R Parental and transfected cells expressing different HLA-B15 allotypes were stained with primary antibodies **(A)** anti-human pan HLA-I (W6/32 hybridoma) and **(B)** anti-human HLA-Bw6 (HB152 hybridoma) followed by a goat anti-mouse IgG PE secondary antibody. A secondary (2°) antibody alone control was used for background staining. **(C)** All four SKW3 cell lines were periodically tested for TCR cell surface expression. A total of 30,000 cells were acquired on LSRII flow cytometer (BD) and data was analyzed using FlowJo software (version 10, BD).

Supplementary Figure 2 | *In vitro* expansion of CBZ-reactive T cells and cell sorting for αβTCR repertoire analysis. **(A)** Drug-reactive T cells were outgrown following 14 days of PBMC stimulation with 25 μg/mL CBZ. Day 14 T cells were restimulated for 6 hours with C1R cells expressing different HLA-B15 allotypes in the presence or absence of 25 μg/mL CBZ. T cell phenotype and activation was then measured by flow cytometry. **(B)** Gating strategy shown is representative data from SJS patient E10630. A maximum of 50,000 lymphocytes were acquired on LSRII flow cytometer (BD) and data was analyzed using FlowJo software (version 10, BD). **(C)** Day 14 CBZ-reactive T cells were restimulated with C1R.B*15:02 in either the absence (negative control) or presence of 25 μg/mL CBZ for 4 hours. Activated CD8+ T cells were detected using an IFNγ secretion assay. Single cell sorting of both $CD8^+$ $IFN\gamma^-$ and $CD8^+$ $IFN\gamma^+$ T cell subsets for TCR repertoire analysis were performed using an Influx flow cytometer (BD).

Supplementary Figure 3 | Drug molecules co-purify with HLA-B*15:02. **(A-C)** Show raw intensities for transitions monitoring **(A)** CBZ in pool 10 of CBZ replicate 1, **(B)** ECBZ in pool 12 of ECBZ, **(C)** OXC in pool 13 of OXC. **(D-F)** summarize the normalized signal for CBZ **(D)**, ECBZ (separated into the signal at 21 minutes (RT 21) and 28 minutes (RT 28) **(E)** and OXC **(F)** in pools 10, 12 and 13, respectively.

Supplementary Figure 4 | Deviations in amino acid prevalence observed between treatments are minimal. Points represent differences between the amino acid prevalence at each position for drug/metabolite treatments as compared to the untreated control (mean of duplicate experiments). For CBZ, points are the difference of the mean of duplicate data sets with error bars showing standard error of the difference (calculated using Welch t-test).

Supplementary Figure 5 | No major alteration of the contribution of deamidated peptides to the HLA-B*15:02 immunopeptidome by drug treatment. Graphs show the percentage of 9mer peptides annotated as containing native Glutamine (top left), native Asparagine (top right), deamidated Glutamine (bottom left) and deamidated asparagine (bottom right) at each position of the peptide. For untreated and CBZ treatment, values are the mean of two replicate experiments, error bars show the standard deviation. ECBZ and OXC treatment are singlet values.

Supplementary Figure 6 | Amino acid prevalence for 9mer peptides unique to CBZ treatment when compared to control conditions. Combined lists of peptides identified in at least 1 replicate of the control condition (untreated) and CBZ treatment were generated and compared to generate 3 categories; untreated unique – identified in at least one replicate of the untreated control, but not in either replicate of CBZ treatment, common – identified in at least one replicate of the untreated control and at least one replicate of the CBZ treatment, and CBZ unique – identified in neither replicate of the untreated control, but in at least one replicate of CBZ treatment. Bar graphs show the percentage of 9mer peptides possessing a given amino acid at each position of the peptide per category. n is the number of 9mer peptides in the category. Arrows indicate residues discussed in the text.

Supplementary Figure 7 | Amino acid prevalence for 9mer peptides unique to ECBZ treatment when compared to control conditions. A combined list of peptides identified in at least 1 replicate of the control condition (untreated) was generated and compared to the ECBZ treatment data set to generate 3 categories; untreated unique – identified in at least one replicate of the untreated control, but not in ECBZ treatment, common – identified in at least one replicate of the untreated control and in the ECBZ treatment, and ECBZ unique – identified in neither replicate of the untreated control, but in ECBZ treatment. Bar graphs show the percentage of 9mer peptides possessing a given amino acid at each position of the peptide per category. n is the number of 9mer peptides in the category. Arrows indicate residues discussed in the text.

Supplementary Figure 8 | Amino acid prevalence for 9mer peptides unique to OXC treatment when compared to control conditions. A combined list of peptides identified in at least 1 replicate of the control condition (untreated) was generated and compared to the OXC treatment data set to generate 3 categories; untreated unique – identified in at least one replicate of the untreated control, but not in OXC treatment, common – identified in at least one replicate of the untreated control and in the OXC treatment, and OXC unique – identified in neither replicate of the untreated control, but in OXC treatment. Bar graphs show the percentage of 9mer peptides possessing a given amino acid at each position of the peptide per category. n is the number of 9mer peptides in the category. Arrows indicate residues discussed in the text.

REFERENCES

1. Micheletti RG, Chiesa-Fuxench Z, Noe MH, Stephen S, Aleshin M, Agarwal A, et al. Stevens-Johnson Syndrome/Toxic Epidermal Necrolysis: A Multicenter Retrospective Study of 377 Adult Patients from the United States. *J Invest Dermatol* (2018) 138(11):2315–21. doi: 10.1016/j.jid.2018.04.027
2. Roujeau JC, Stern RS. Severe Adverse Cutaneous Reactions to Drugs. *New Engl J Med* (1994) 331(19):1272–85. doi: 10.1056/NEJM199411103311906
3. De A, Rajagopalan M, Sarda A, Das S, Biswas P. Drug Reaction with Eosinophilia and Systemic Symptoms: An Update and Review of Recent Literature. *Indian J Dermatol* (2018) 63(1):30–40. doi: 10.4103/ijd.IJD_582_17
4. Marson AG, Al-Kharusi AM, Alwaidh M, Appleton R, Baker GA, Chadwick DW, et al. The SANAD study of effectiveness of carbamazepine, gabapentin, lamotrigine, oxcarbazepine, or topiramate for treatment of partial epilepsy: an unblinded randomised controlled trial. *Lancet* (2007) 369(9566):1000–15. doi: 10.1016/S0140-6736(07)60460-7
5. Mockenhaupt M, Messenheimer J, Tennis P, Schlingmann J. Risk of Stevens-Johnson syndrome and toxic epidermal necrolysis in new users of antiepileptics. *Neurology* (2005) 64(7):1134–8. doi: 10.1212/01.WNL.0000156354.20227.F0
6. Mullan KA, Anderson A, Illing PT, Kwan P, Purcell AW, Mifsud NA. HLA-associated antiepileptic drug-induced cutaneous adverse reactions. *HLA* (2019) 93(6):417–35. doi: 10.1111/tan.13530
7. Chung WH, Hung SI, Hong HS, Hsih MS, Yang LC, Ho HC, et al. Medical genetics: a marker for Stevens-Johnson syndrome. *Nature* (2004) 428 (6982):486. doi: 10.1038/428486a
8. Mehta TY, Prajapati LM, Mittal B, Joshi CG, Sheth JJ, Patel DB, et al. Association of HLA-B*1502 allele and carbamazepine-induced Stevens-Johnson syndrome among Indians. *Indian J Dermatol Venereol Leprol* (2009) 75(6):579–82. doi: 10.4103/0378-6323.57718
9. Tangamornsuksan W, Chaiyakunapruk N, Somkrua R, Lohitnavy M, Tassaneeyakul W. Relationship between the HLA-B*1502 allele and carbamazepine-induced Stevens-Johnson syndrome and toxic epidermal necrolysis: a systematic review and meta-analysis. *JAMA Dermatol* (2013) 149(9):1025–32. doi: 10.1001/jamadermatol.2013.4114
10. Tassaneeyakul W, Tiamkao S, Jantararoungtong T, Chen P, Lin SY, Chen WH, et al. Association between HLA-B*1502 and carbamazepine-induced severe cutaneous adverse drug reactions in a Thai population. *Epilepsia* (2010) 51(5):926–30. doi: 10.1111/j.1528-1167.2010.02533.x
11. Ikeda H, Takahashi Y, Yamazaki E, Fujiwara T, Kaniwa N, Saito Y, et al. HLA class I markers in Japanese patients with carbamazepine-induced cutaneous adverse reactions. *Epilepsia* (2010) 51(2):297–300. doi: 10.1111/j.1528-1167.2009.02269.x
12. Kaniwa N, Saito Y, Aihara M, Matsunaga K, Tohkin M, Kurose K, et al. HLA-B*1511 is a risk factor for carbamazepine-induced Stevens-Johnson syndrome and toxic epidermal necrolysis in Japanese patients. *Epilepsia* (2010) 51 (12):2461–5. doi: 10.1111/j.1528-1167.2010.02766.x
13. Kim SH, Lee KW, Song WJ, Kim SH, Jee YK, Lee SM, et al. Carbamazepine-induced severe cutaneous adverse reactions and HLA genotypes in Koreans. *Epilepsy Res* (2011) 97(1-2):190–7. doi: 10.1016/j.eplepsyres.2011.08.010
14. Shi YW, Min FL, Qin B, Zou X, Liu XR, Gao MM, et al. Association between HLA and Stevens-Johnson syndrome induced by carbamazepine in Southern Han Chinese: genetic markers besides B*1502? *Basic Clin Pharmacol Toxicol* (2012) 111(1):58–64. doi: 10.1111/j.1742-7843.2012.00868.x
15. Genin E, Chen DP, Hung SI, Sekula P, Schumacher M, Chang PY, et al. HLA-A*31:01 and different types of carbamazepine-induced severe cutaneous adverse reactions: an international study and meta-analysis. *Pharmacogenom J* (2014) 14(3):281–8. doi: 10.1038/tpj.2013.40
16. Hsiao YH, Hui RC, Wu T, Chang WC, Hsih MS, Yang CH, et al. Genotype-phenotype association between HLA and carbamazepine-induced hypersensitivity reactions: strength and clinical correlations. *J Dermatol Sci* (2014) 73(2):101–9. doi: 10.1016/j.jdermsci.2013.10.003
17. Hung SI, Chung WH, Jee SH, Chen WC, Chang YT, Lee WR, et al. Genetic susceptibility to carbamazepine-induced cutaneous adverse drug reactions. *Pharmacogenet Genomics* (2006) 16(4):297–306. doi: 10.1097/01.fpc.0000199500.46842.4a
18. McCormack M, Alfirevic A, Bourgeois S, Farrell JJ, Kasperaviciute D, Carrington M, et al. HLA-A*3101 and carbamazepine-induced hypersensitivity reactions in Europeans. *N Engl J Med* (2011) 364(12):1134–43. doi: 10.1056/NEJMoa1013297
19. Ozeki T, Mushiroda T, Yowang A, Takahashi A, Kubo M, Shirakata Y, et al. Genome-wide association study identifies HLA-A*3101 allele as a genetic risk factor for carbamazepine-induced cutaneous adverse drug reactions in Japanese population. *Hum Mol Genet* (2011) 20(5):1034–41. doi: 10.1093/hmg/ddq537

20. Mockenhaupt M, Wang CW, Hung SI, Sekula P, Schmidt AH, Pan RY, et al. HLA-B*57:01 confers genetic susceptibility to carbamazepine-induced SJS/TEN in Europeans. *Allergy* (2019) 74(11):2227–30. doi: 10.1111/all.13821
21. Wei CY, Chung WH, Huang HW, Chen YT, Hung SI. Direct interaction between HLA-B and carbamazepine activates T cells in patients with Stevens-Johnson syndrome. *J Allergy Clin Immunol* (2012) 129(6):1562–9 e5. doi: 10.1016/j.jaci.2011.12.990
22. Illing PT, Vivian JP, Dudek NL, Kostenko L, Chen Z, Bharadwaj M, et al. Immune self-reactivity triggered by drug-modified HLA-peptide repertoire. *Nature* (2012) 486(7404):554–8. doi: 10.1038/nature11147
23. Simper GS, Ho GT, Celik AA, Huyton T, Kuhn J, Kunze-Schumacher H, et al. Carbamazepine-Mediated Adverse Drug Reactions: CBZ-10,11-epoxide but Not Carbamazepine Induces the Alteration of Peptides Presented by HLA-B *15:02. *J Immunol Res* (2018) 2018:5086503. doi: 10.1155/2018/5086503
24. Pan RY, Chu MT, Wang CW, Lee YS, Lemonnier F, Michels AW, et al. Identification of drug-specific public TCR driving severe cutaneous adverse reactions. *Nat Commun* (2019) 10(1):3569. doi: 10.1038/s41467-019-11396-2
25. Illing PT, Mifsud NA, Purcell AW. Allotype specific interactions of drugs and HLA molecules in hypersensitivity reactions. *Curr Opin Immunol* (2016) 42:31–40. doi: 10.1016/j.coi.2016.05.003
26. Ostrov DA, Grant BJ, Pompeu YA, Sidney J, Harndahl M, Southwood S, et al. Drug hypersensitivity caused by alteration of the MHC-presented self-peptide repertoire. *Proc Natl Acad Sci USA* (2012) 109(25):9959–64. doi: 10.1073/pnas.1207934109
27. Norcross MA, Luo S, Lu L, Boyne MT, Gomarteli M, Rennels AD, et al. Abacavir induces loading of novel self-peptides into HLA-B*57: 01: an autoimmune model for HLA-associated drug hypersensitivity. *AIDS* (2012) 26(11):F21–F9. doi: 10.1097/QAD.0b013e328355fe8f
28. Ko TM, Chung WH, Wei CY, Shih HY, Chen JK, Lin CH, et al. Shared and restricted T-cell receptor use is crucial for carbamazepine-induced Stevens-Johnson syndrome. *J Allergy Clin Immunol* (2011) 128(6):1266–76 e11. doi: 10.1016/j.jaci.2011.08.013
29. Koning D, Costa AI, Hasrat R, Grady BP, Spijkers S, Nanlohy N, et al. In vitro expansion of antigen-specific CD8(+) T cells distorts the T-cell repertoire. *J Immunol Methods* (2014) 405:199–203. doi: 10.1016/j.jim.2014.01.013
30. Xiong H, Wang L, Jiang M, Chen S, Yang F, Zhu H, et al. Comprehensive assessment of T cell receptor beta repertoire in Stevens-Johnson syndrome/toxic epidermal necrolysis patients using high-throughput sequencing. *Mol Immunol* (2019) 106:170–7. doi: 10.1016/j.molimm.2019.01.002
31. Lichtenfels M, Farrell J, Ogese MO, Bell CC, Eckle S, McCluskey J, et al. HLA restriction of carbamazepine-specific T-Cell clones from an HLA-A*31:01-positive hypersensitive patient. *Chem Res Toxicol* (2014) 27(2):175–7. doi: 10.1021/tx400460w
32. Cheung YK, Cheng SH, Chan EJ, Lo SV, Ng MH, Kwan P. HLA-B alleles associated with severe cutaneous reactions to antiepileptic drugs in Han Chinese. *Epilepsia* (2013) 54(7):1307–14. doi: 10.1111/epi.12217
33. Shi YW, Min FL, Zhou D, Qin B, Wang J, Hu FY, et al. HLA-A*24:02 as a common risk factor for antiepileptic drug-induced cutaneous adverse reactions. *Neurology* (2017) 88(23):2183–91. doi: 10.1212/WNL.0000000000004008
34. Zemmour J, Little AM, Schendel DJ, Parham P. The HLA-A,B "negative" mutant cell line C1R expresses a novel HLA-B35 allele, which also has a point mutation in the translation initiation codon. *J Immunol* (1992) 148(6):1941–8.
35. Storkus WJ, Howell DN, Salter RD, Dawson JR, Cresswell P. NK susceptibility varies inversely with target cell class I HLA antigen expression. *J Immunol* (1987) 138(6):1657–9.
36. Mifsud NA, Nguyen THO, Tait BD, Kotsimbos TC. Quantitative and functional diversity of cross-reactive EBV-specific CD8+ T cells in a longitudinal study cohort of lung transplant recipients. *Transplantation* (2010) 90(12):1439–49. doi: 10.1097/TP.0b013e3181ff4ff3
37. Wang GC, Dash P, McCullers JA, Doherty PC, Thomas PG. T cell receptor alphabeta diversity inversely correlates with pathogen-specific antibody levels in human cytomegalovirus infection. *Sci Transl Med* (2012) 4(128):128ra42. doi: 10.1126/scitranslmed.3003647
38. Brochet X, Lefranc MP, Giudicelli V. IMGT/V-QUEST: the highly customized and integrated system for IG and TR standardized V-J and V-D-J sequence analysis. *Nucleic Acids Res* (2008) 36(Web Server issue):W503–8. doi: 10.1093/nar/gkn316
39. Folch G, Scaviner D, Contet V, Lefranc MP. Protein displays of the human T cell receptor alpha, beta, gamma and delta variable and joining regions. *Exp Clin Immunogenet* (2000) 17(4):205–15. doi: 10.1159/000019140
40. Szymczak AL, Workman CJ, Wang Y, Vignali KM, Dilioglou S, Vanin EF, et al. Correction of multi-gene deficiency in vivo using a single 'self-cleaving' 2A peptide-based retroviral vector. *Nat Biotechnol* (2004) 22(5):589–94. doi: 10.1038/nbt957
41. Nguyen TH, Rowntree LC, Pellicci DG, Bird NL, Handel A, Kjer-Nielsen L, et al. Recognition of distinct cross-reactive virus-specific CD8+ T cells reveals a unique TCR signature in a clinical setting. *J Immunol* (2014) 192(11):5039–49. doi: 10.4049/jimmunol.1303147
42. Purcell AW, Ramarathinam SH, Ternette N. Mass spectrometry–based identification of MHC-bound peptides for immunopeptidomics. *Nat Protoc* (2019) 14(6):1687–707. doi: 10.1038/s41596-019-0133-y
43. Koutsakos M, Illing PT, Nguyen THO, Mifsud NA, Crawford JC, Rizzetto S, et al. Human CD8+ T cell cross-reactivity across influenza A, B and C viruses. *Nat Immunol* (2019) 20(5):613–25. doi: 10.1038/s41590-019-0320-6
44. Escher C, Reiter L, MacLean B, Ossola R, Herzog F, Chilton J, et al. Using iRT, a normalized retention time for more targeted measurement of peptides. *Proteomics* (2012) 12(8):1111–21. doi: 10.1002/pmic.201100463
45. Perez-Riverol Y, Csordas A, Bai J, Bernal-Llinares M, Hewapathirana S, Kundu DJ, et al. The PRIDE database and related tools and resources in 2019: improving support for quantification data. *Nucleic Acids Res* (2019) 47 (D1):D442–d50. doi: 10.1093/nar/gky1106
46. Krzywinski M, Schein J, Birol I, Connors J, Gascoyne R, Horsman D, et al. Circos: an information aesthetic for comparative genomics. *Genome Res* (2009) 19(9):1639–45. doi: 10.1101/gr.092759.109
47. Yang C-WO, Hung S-I, Juo C-G, Lin Y-P, Fang W-H, Lu IH, et al. HLA-B*1502-bound peptides: implications for the pathogenesis of carbamazepine-induced Stevens-Johnson syndrome. *J Allergy Clin Immunol* (2007) 120 (4):870–7. doi: 10.1016/j.jaci.2007.06.017
48. White KD, Chung WH, Hung SI, Mallal S, Phillips EJ. Evolving models of the immunopathogenesis of T cell-mediated drug allergy: The role of host, pathogens, and drug response. *J Allergy Clin Immunol* (2015) 136(2):219–34; quiz 35. doi: 10.1016/j.jaci.2015.05.050
49. Wu Y, Sanderson JP, Farrell J, Drummond NS, Hanson A, Bowkett E, et al. Activation of T cells by carbamazepine and carbamazepine metabolites. *J Allergy Clin Immunol* (2006) 118(1):233–41. doi: 10.1016/j.jaci.2006.03.005
50. Mauri-Hellweg D, Bettens F, Mauri D, Brander C, Hunziker T, Pichler WJ. Activation of drug-specific CD4+ and CD8+ T cells in individuals allergic to sulfonamides, phenytoin, and carbamazepine. *J Immunol* (1995) 155(1):462–72.
51. Naisbitt DJ, Britschgi M, Wong G, Farrell J, Depta JPH, Chadwick DW, et al. Hypersensitivity reactions to carbamazepine: Characterization of the specificity, phenotype, and cytokine profile of drug-specific T cell clones. *Mol Pharmacol* (2003) 63(3):732–41. doi: 10.1124/mol.63.3.732
52. Naisbitt DJ, Farrell J, Wong G, Depta JP, Dodd CC, Hopkins JE, et al. Characterization of drug-specific T cells in lamotrigine hypersensitivity. *J Allergy Clin Immunol* (2003) 111(6):1393–403. doi: 10.1067/mai.2003.1507
53. Alvestad S, Lydersen S, Brodtkorb E. Cross-reactivity pattern of rash from current aromatic antiepileptic drugs. *Epilepsy Res* (2008) 80(2-3):194–200. doi: 10.1016/j.eplepsyres.2008.04.003
54. Hirsch LJ, Arif H, Nahm EA, Buchsbaum R, Resor SRJr, Bazil CW. Cross-sensitivity of skin rashes with antiepileptic drug use. *Neurology* (2008) 71 (19):1527–34. doi: 10.1212/01.wnl.0000334295.50403.4c
55. Hyson C, Sadler M. Cross sensitivity of skin rashes with antiepileptic drugs. *Can J Neurol Sci* (1997) 24(3):245–9. doi: 10.1017/S0317167100021880
56. Wang XQ, Lang SY, Shi XB, Tian HJ, Wang RF, Yang F. Cross-reactivity of skin rashes with current antiepileptic drugs in Chinese population. *Seizure* (2010) 19(9):562–6. doi: 10.1016/j.seizure.2010.09.003
57. Seitz CS, Pfeuffer P, Raith P, Brocker EB, Trautmann A. Anticonvulsant hypersensitivity syndrome: cross-reactivity with tricyclic antidepressant agents. *Ann Allergy Asthma Immunol* (2006) 97(5):698–702. doi: 10.1016/S1081-1206(10)61103-9
58. Cardone M, Garcia K, Tilahun ME, Boyd LF, Gebreyohannes S, Yano M, et al. A transgenic mouse model for HLA-B*57:01-linked abacavir drug tolerance and reactivity. *J Clin Invest* (2018) 128(7):2819–32. doi: 10.1172/JCI99321
59. Rowntree LC, Nguyen THO, Farenc C, Halim H, Hensen L, Rossjohn J, et al. A Shared TCR Bias toward an Immunogenic EBV Epitope Dominates in HLA-B*07:02-Expressing Individuals. *J Immunol* (2020) 205(6):1524–34. doi: 10.4049/jimmunol.2000249
60. Rowntree LC, van den Heuvel H, Sun J, D'Orsogna LJ, Nguyen THO, Claas FHJ, et al. Preferential HLA-B27 Allorecognition Displayed by

Multiple Cross-Reactive Antiviral CD8(+) T Cell Receptors. *Front Immunol* (2020) 11:248. doi: 10.3389/fimmu.2020.00248

Conflict of Interest: *The authors declare that the research was conducted in the absence of any commercial or financial relationships that could be construed as a potential conflict of interest.*

frontiers in Immunology

REVIEW
published: 13 April 2021
doi: 10.3389/fimmu.2021.630530

In-Vitro Approaches to Predict and Study T-Cell Mediated Hypersensitivity to Drugs

Sean Hammond[1,2*], *Paul Thomson*[1], *Xiaoli Meng*[1] *and Dean Naisbitt*[1*]

[1] MRC Centre for Drug Safety Science, Department of Molecular and Clinical Pharmacology, University of Liverpool, Liverpool, United Kingdom, [2] ApconiX, Alderley Park, Alderley Edge, United Kingdom

Mitigating the risk of drug hypersensitivity reactions is an important facet of a given pharmaceutical, with poor performance in this area of safety often leading to warnings, restrictions and withdrawals. In the last 50 years, efforts to diagnose, manage, and circumvent these obscure, iatrogenic diseases have resulted in the development of assays at all stages of a drugs lifespan. Indeed, this begins with intelligent lead compound selection/design to minimize the existence of deleterious chemical reactivity through exclusion of ominous structural moieties. Preclinical studies then investigate how compounds interact with biological systems, with emphasis placed on modeling immunological/toxicological liabilities. During clinical use, competent and accurate diagnoses are sought to effectively manage patients with such ailments, and pharmacovigilance datasets can be used for stratification of patient populations in order to optimise safety profiles. Herein, an overview of some of the *in-vitro* approaches to predict intrinsic immunogenicity of drugs and diagnose culprit drugs in allergic patients after exposure is detailed, with current perspectives and opportunities provided.

Keywords: drug hypersensitivity, *in-vitro*, preclinical, predictive, T-cell, immunogenicity

OPEN ACCESS

Edited by:
Michael R. Ardern-Jones, University of Southampton, United Kingdom

Reviewed by:
Andrew D. Wells, Children's Hospital of Philadelphia, United States
Grzegorz Porebski, Jagiellonian University Medical College, Poland

***Correspondence:**
Dean Naisbitt
dnes@liverpool.ac.uk
Sean Hammond
Seanhammond033@gmail.com

Specialty section:
This article was submitted to T Cell Biology, a section of the journal Frontiers in Immunology

Received: *17 November 2020*
Accepted: *17 March 2021*
Published: *13 April 2021*

Citation:
Hammond S, Thomson P, Meng X and Naisbitt D (2021) In-Vitro Approaches to Predict and Study T-Cell Mediated Hypersensitivity to Drugs. Front. Immunol. 12:630530. doi: 10.3389/fimmu.2021.630530

INTRODUCTION

Immune-mediated idiosyncratic adverse drug reactions constitute an existential threat to prospective new chemical entities, encumbering the drug development process throughout its progression in an abstruse fashion. Since these iatrogenic reactions are enigmatic and rare, they are seldom encountered in the early stages of drug discovery, and often precipitate upon exposure to wider populations with potentially terminal consequences for both patients and drug. It is therefore astute to screen new therapeutics for the capacity to elicit such reactions, and attempt to eliminate compounds with unacceptable liability for hypersensitivity early in development. Much investment has been made to this end with several approaches developed, each with its advantages and limitations. Non-human *in-vivo* models (1, 2) possess obvious limitations in terms of translational relevance, and the fact that such equivalent models have been rendered obsolete in the field of cosmetics safety perhaps indicates a finite time for their application in drug safety studies.

Despite continued efforts, understanding of hypersensitivity reactions is yet to reach satisfactory resolution. It is therefore not surprising that preclinical screening does not yet provide a blanket barrier

to the progression of compounds that have the capacity to cause these reactions. The central dogma of sensitization and elicitation phases gleaned from the field of contact sensitization fundamentally holds true for drug hypersensitivity reactions (3). Indeed, there is consensus that the majority of these reactions proceed through the basic dogma of T-cell immunology; a T-cell receptor expressed on a T-cell recognizing an antigen presented in the context of human leukocyte antigen (HLA), with drug-induced perturbation of this immunological synapse and the ensuing aberrant deployment of T-cell responses a fundamental feature. Beyond this, the field dramatically diverges, with multiple pathways of antigen derivation gleaned to date; hapten (4), Pi (5), and altered self-repertoire (6), outlined in (**Figure 1**) and reviewed in detail elsewhere (7). Indeed antigen generation has been an important focus of the field for some time, and while understanding is far from complete in this area, there has been excellent progress, with some studies elegantly demonstrating how antigens can be formed in exquisite detail. Unfortunately, antigen generation is not itself the critical determinant of hypersensitivity. Rather, it appears to be a function of antigen perception and density. A simple, but helpful way to consider the induction/precipitation of such reactions is through a vaccine metaphor; broadly characterizing attributes into antigenicity (signal 1) and adjuvant potency (signal 2), with a plethora of drug and patient specific factors contributing to both (**Figure 2**). Where hypersensitivity reactions are particularly challenging is the immunological mechanisms that underpin the initiating adjuvant sequence. This aspect, embodied as the "danger hypothesis" (9, 10) is much less defined; it is heterogeneous, and probably interchangeable, but essential for an antigen perception that favours an aberrant T-cell response (11). It is known that signal 2 can be achieved via cellular stress/damage through damage associated molecular pattern (DAMP) signaling, which can be attributed to a drug by means of direct toxicological properties, or through disease/environmental factors. It can also be determined by pathogen associated molecular pattern (PAMP) signaling, as is seen with infections. Finally, what has become clear in recent times with the unpropitious outcomes seen with concomitant medication usage alongside immune checkpoint inhibitors (12–17), is that the adjuvant component is truly the dynamic and complex setting of immune regulation, and that opposing tolerance mechanisms play a critical role in determination of antigen perception. Advanced discussion on the etiology of hypersensitivity reactions is outside of the scope of this review; for extensive reading on this topic, and the mechanisms by which T-cells elicit cellular damage in the context of drug hypersensitivity the authors refer readers to a number of key reviews (7, 18–21).

These multi-mechanistic pathways of antigenicity and adjuvanticity, overlaid with the variety of tissue specific factors pertaining to localized metabolism, damage/pathogen derived signaling and cellular milieu results in extensive heterogeneity of these reactions. This heterogeneity makes preclinical assays with good coverage challenging to construct. It also translates to the challenges within the clinic in terms of clinical presentation. Indeed, manifestations are diverse, and often lack pathognomonic features

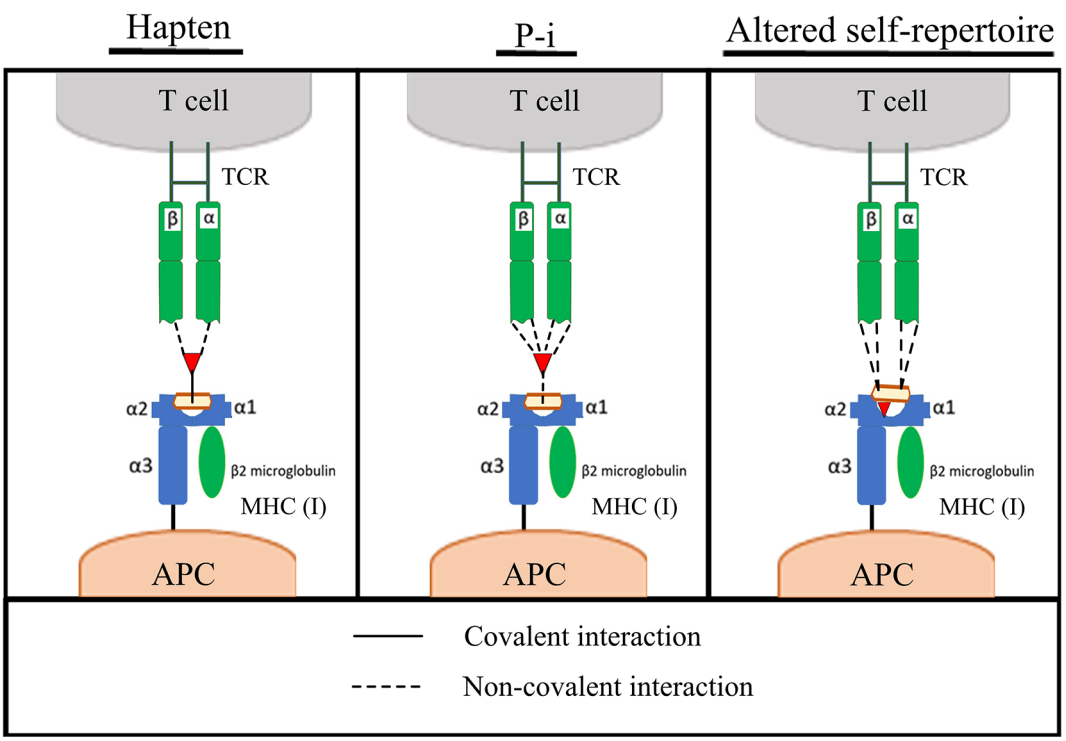

FIGURE 1 | Pathways of T-cell activation by compounds. Left to right; Hapten, pharmacological interact (Pi) and altered self-repertoire hypotheses for the mechanism of antigen presentation in drug hypersensitivity. Adapted from (7, 8).

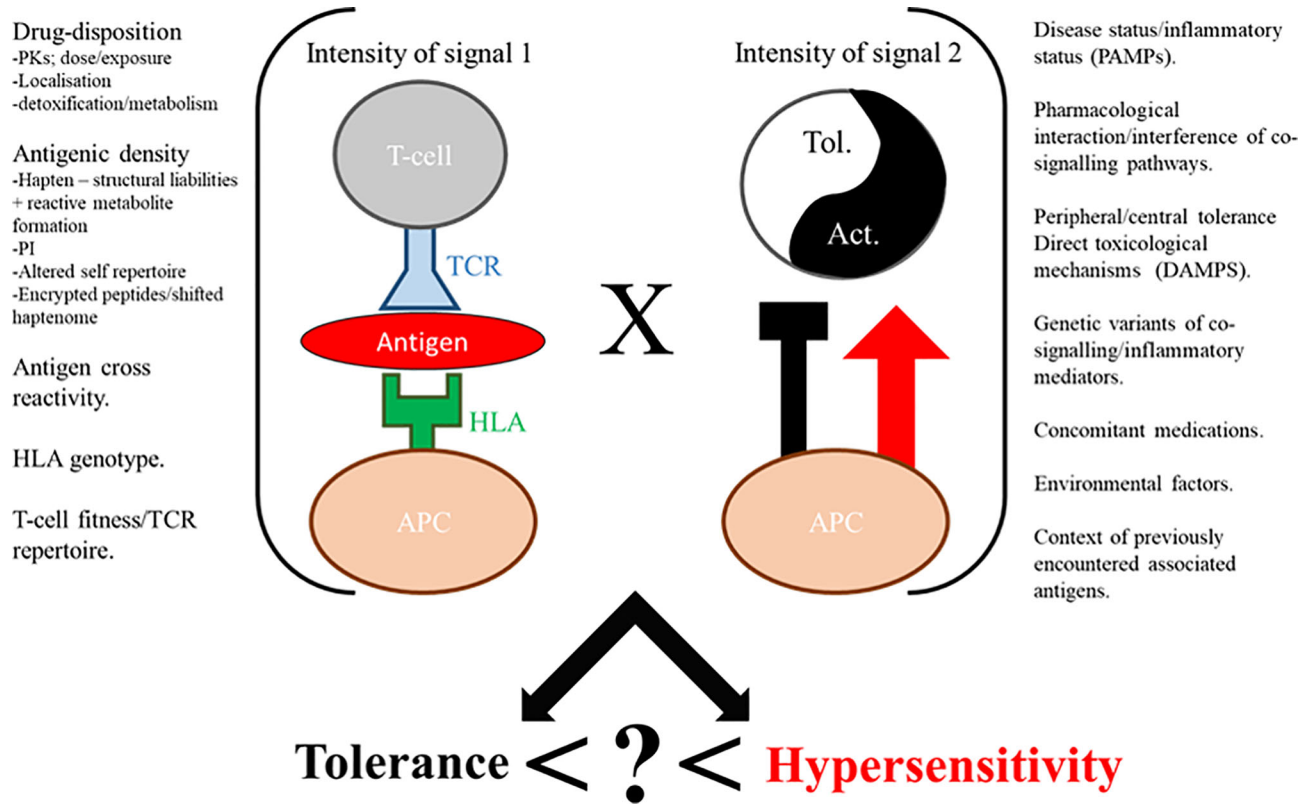

FIGURE 2 | Immunological perception of drugs expressed as a function of signal 1 x signal 2 factors, with an unknown composite (?) yielding hypersensitivity. Tol. = tolerance, Act. = activation.

(22, 23), making diagnostic certainty and effective coverage from methodologies challenging to obtain.

The imperfect classification of compounds yielded by currently available preclinical assays has resulted in the presence of many drugs with such issues within a physician's armamentarium. Therefore, effective and safe diagnosis of hypersensitivity reactions when they do occur is paramount; in order to mitigate the re-administration of offending agents and identify liabilities of compounds in polypharmacy settings. As direct re-exposure of hypersensitive individuals is undesirable due to understandable patient anxiety and the potential for extreme risk, it is transparent that there is demand for the development of *in-vitro* methods in order to aid clinical diagnoses of hypersensitive individuals whilst mitigating re-exposure risk for suspected drugs. Hypothetically though, the ultimate goal should be the development and implementation of efficacious investigative procedures which facilitate the circumvention of hypersensitivity in early product development. Hence, this review predominantly covers the topic of *in-vitro* diagnostic assays, and provides an overview of the established and prospective efforts underway in preclinical development to circumvent the progression of compounds carrying unacceptable hypersensitivity risk profiles.

IN-VIVO DIAGNOSIS/ASSESSMENT

Drug Provocation and Skin Testing

The gold standard for diagnosis of drug hypersensitivity is the recurrence of injury upon rechallenge with the offending compound (24). Although not infallible, positive re-challenges (often following a positive de-challenge; where injury resolves upon drug cessation) provide tangible and clinically relevant evidence for or against hypersensitivity and thus whether continuation with the drug is a viable course of action. A common feature of positive re-challenge events is that the injury recrudesces in a more rapid and severe manner (25). Although beneficial for the positive identification of hypersensitivity, this phenomenon also represents a significant drawback of re-challenge; the risk of serious injury or mortality. This is highlighted by the 51% fatality rate reported for positive re-challenge events concerning the general anaesthetic halothane (26). As a result of this risk, many governing/advisory bodies issue caution when considering re-challenge where drug-induced liver injury or serious idiosyncratic adverse drug reactions are observed. A common, less hazardous approach is that of skin testing; multiple variations of skin testing exist, with the clinically utilised procedures being the skin prick test, intradermal test, patch test and photopatch test. These assays have seen clinical validation and are used

routinely; for those seeking more comprehensive review of their utility, the authors refer readers to several specialist publications (27–34). Despite uptake within clinical practice, all 3 of the described skin tests possess limited sensitivity and specificity, with variable values for each parameter reported in literature (28, 35, 36). Given the limitations of skin testing, and the undesirable crux of patient exposure to a compound they are suspected to be hypersensitive to (37), there has been a longstanding necessity for minimally invasive, *in-vitro* assays that add value in diagnosis of compound hypersensitivity.

HLA Associations and Screening

The incredible capacity for HLA genotype to predict an individual's propensity for hypersensitivity to a selection of pharmaceuticals has brought Pharmacogenetics to the fulcrum of discussion in the field. The exquisite sensitivity of carriage of the HLA-B*57:01 "risk" allele as a determinant of an individual's susceptibility to hypersensitivity with the nucleoside reverse transcriptase inhibitor abacavir (38–42), is the quintessential utility of this approach. Indeed, not only did the discovery of this association warrant the cost-effective and efficacious implementation of preclusive screening of prospective abacavir patients (43–46). It also laid foundations upon which mechanistic studies were able to build, eventually leading to the elucidation of a novel mechanism by which compounds can elicit hypersensitivity (6, 47). HLA screening has also been adopted for circumvention of SJS/TEN hypersensitivity reactions associated with carbamazepine, with HLA-B*15:02 featuring as the implicated allele (48). Application of pharmacogenetics is now a widespread method by which information on hypersensitivity reactions with given compounds is divulged, with a brief investigation of literature yielding no shortage of manuscripts sporting comprehensive lists of such associations. While the aforementioned HLA alleles, among others, possess exploitable odds ratios, many of the cited associations are not of consequence in terms of viable/cost effective mitigating action. The reproducibility of studies utilizing this approach has also been questionable on a number of occasions. Inversely, the fact that positive predictive values even in the most impressive of allelic associations are not 100% [abacavir exhibits only around 55% PPV (40)], alludes to the notion that confounding factors further influence susceptibility. Thus, while HLA alleles occasionally constitute a critical prerequisite, they far from guarantee the manifestation of hypersensitivity reactions (8).

Another, more fundamental issue with HLA screening in prediction of hypersensitivity is the paradoxical juxtaposition between prediction and retrospection of this approach. Crucially, a prerequisite to the delineation of risk alleles is the exposure of (often immensely proportioned) patient populations to a given pharmaceutical. Thus, patient safety is breached at the inception of these studies (an undesirable outcome in any case), therefore, HLA screening is currently confined to being a tool generated from clinical data, which on occasion has proven to powerfully contribute to the iterative process of optimization of drug safety profiles. Nevertheless, elements of this can, and have been incorporated into preclinical prospective platforms, some of which are covered below.

IN-VITRO DIAGNOSTIC/INVESTIGATIVE ASSAYS

LTT

The lymphocyte transformation test (LTT) has been a mainstay in the limited toolkit for *in vitro* diagnosis of hypersensititivity for around half a century, with several technical revisions since its inception (49–52). An LTT entails the culture of PBMC from an individual with suspect compounds for 6-7 days, with the output being a function of lymphoblastic transformation/proliferation. Several variations have evolved since the primitive methods described by Halpern & Amache, 1967 (53), each with benefits and drawbacks. The most prominent of these is tritiated ^{3}H-thymidine incorporation (**Figure 3**). Less hazardous options include ELISA-based 5-bromo-2'-deoxyuridine incorporation method, or carboxyflourescein diacetate succinimidyl ester (CFSE) serial dilution and ki-67 expression as measured by flow cytometry. CFSE/dye dilution-type and ki-67 based assays have an additional advantage in that they can facilitate identification of the effector cell of origin (54). However both come with concerns over technical requirements, and ease of interpretation.

LTT results appear to be highly variable in terms of sensitivity and specificity, with concerns over sensitivity in particular drawing criticism which dates back to its early use (55). Confounding factors include; the clinical manifestation of the reaction (and thus the presentation-specific mechanisms), latency from reaction to test, the culprit compound in question [whether it possesses properties intrinsically inhibitory or stimulatory to T-cell proliferation e.g.; methotrexate (56)], concomitant therapy that may have bearing on the test such as immunosuppressant therapeutics, and (often overlooked) laboratory specific technique.

Clinical manifestations of drug hypersensitivity are, as discussed (8, 22, 53) heterogeneous. This heterogeneity and the delay from reaction to LTT has been posited to be absolutely critical to the validity of the test. Conventionally, a minimal interval of 3 weeks is allowed to elapse before *in vitro* tests begin, allowing elimination of both culprit drugs and immunosuppressant/anti-allergic drugs (57). Presumably this period also correlates with contraction of the adaptive response and the development of a memory component that is stabilized in terms of proliferation (as in the acute phase, highly activated PBMC may generate backgrounds which conceal responses). Further complicating this area is the contrasting time-LTT response relationship seen depending on the manifestation of the hypersensitivity reaction. Findings by Kano et al. (58), indicate that allowing time to elapse following hypersensitivity leads to opposite effects in merit of the test depending on the clinical presentation; patients with SJS/TEN exhibited prominent LTT responses in the acute phase (within 1 week), which substantially diminished upon recovery phase (>5 weeks), whilst the inverse was seen in DIHS/DRESS patients.

The transparency of compound specific variation of LTTs is epitomized by the fact that stimulation index (SI) values (and thus threshold of the definition of positive responses) are not universal. Rather, they are determined through experience with

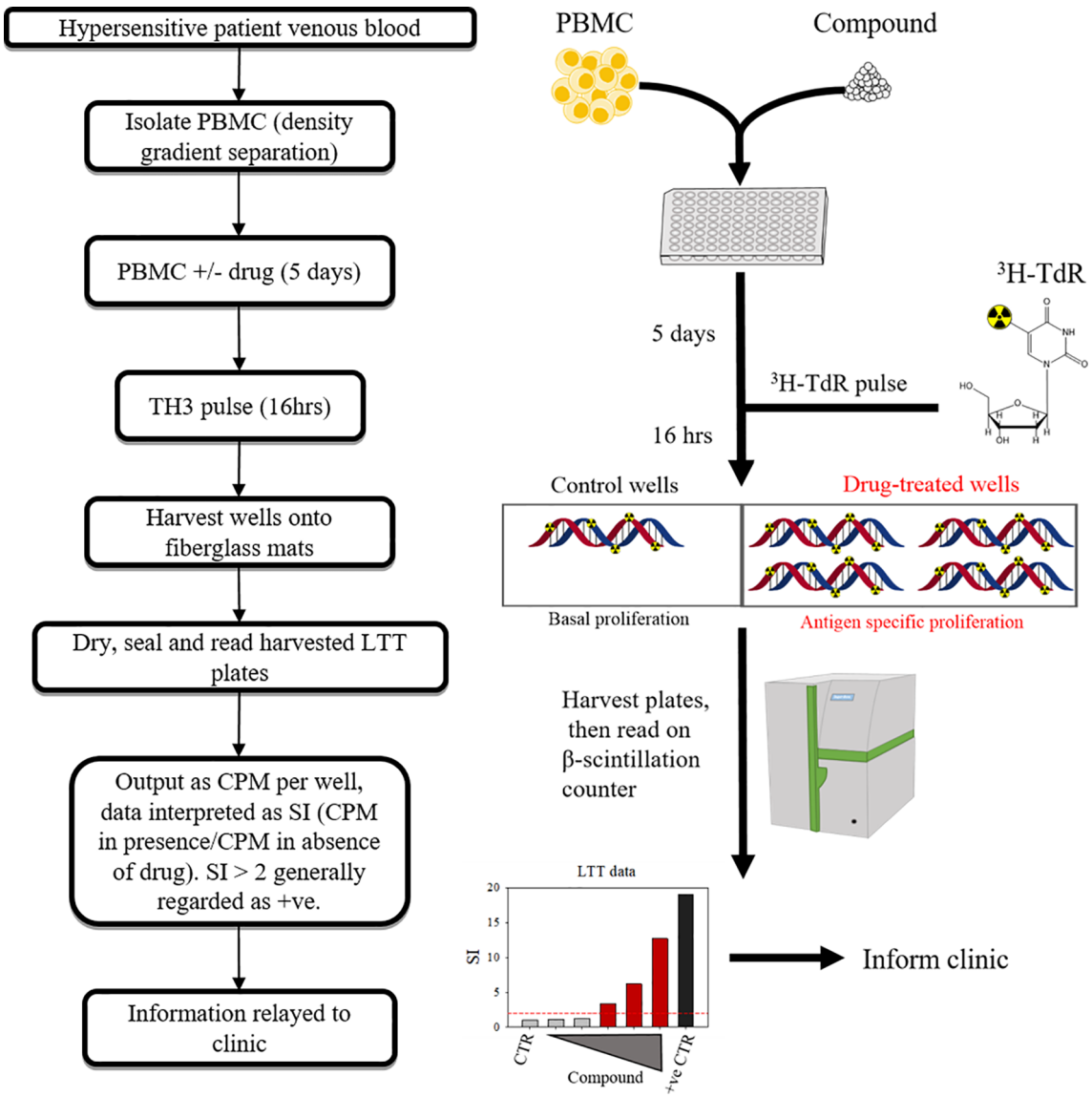

FIGURE 3 | Overview of lymphocyte transformation test methodology.

the compounds themselves, for example; while many drugs are assigned a threshold SI of >2, Beta lactams tend to be assigned a threshold of >3, and some radio contrast media responses must reach SIs >4 to be deemed positive (57). With this comes several issues which the field has failed to address universally, the first of which being inconsistent threshold SI values utilized throughout literature for compounds. For example; SIs of >2 (59), >3 (60) and >4 (57) have been adjudicated as positive responses for radio contrast media. Similarly, there remains inconsistency with Beta lactams, with SI thresholds set at >2 (61), and >3 (57). In light of this, one may be tempted to speculate that the stimulation index (and thus sensitivity and specificity of lymphocyte transformation test) is "optimized" to the data it generates. Therefore, when interpreting the sensitivity and specificity of the test cited throughout literature, this must be considered as a potential caveat. To optimize diagnosis of hypersensitivity, it would be of best interest to the field to universally agree on pre-defined SI thresholds, retrospective analyses of cumulative data from multiple laboratories may be a fruitful avenue in this respect. A second, seemingly less rectifiable issue, is that if SI threshold values may only be set retrospectively, the LTT (although useful as a diagnostic tool for hypersensitive individuals), is inherently flawed for use in determining/diagnosing potential immunogenicity of a prospective therapeutic compound in early clinical development.

Concomitant therapy is common in the aftermath of drug hypersensitivity reactions, not least due to medication taken to alleviate the reaction itself. The nature of these drugs has been suggested to influence the results of LTTs, immunosuppressant drugs such as corticosteroids (e.g.: prednisolone) have been

logically suggested to inhibit proliferation and cytokine responses, patients taking > 0.2 mg/kg of such drugs are often excluded (62). Prostaglandin E2 concentration has also been posited to influence LTT results with high levels (as seen with macrophage overrepresentation in culture) and low levels (sometimes caused by use of non-steroidal anti-inflammatory drugs) reducing and enhancing LTT responses respectively (63).

Attempts to revise the LTT have included enrichment of professional antigen presenting cells within the culture, inclusion of metabolites derived from parent drug, depletion of T regulatory populations, and effector cell identification/evaluation. The enrichment of immature dendritic cells (CD14 +ve) and independent pulsing with antigen prior to co-culture, demonstrated superior LTT responses in patients with amoxicillin induced maculopapular exanthema relative to standard B cells and monocytes. These modifications enhanced sensitivity, while tolerant controls remained negative- thereby maintaining specificity (64). Concordant results were also obtained from patients with heparin hypersensitivity, with the added advantage of prolongation of the sensitive detection period following the ADR (65). Antunez et al. investigated maculopapular exanthema reactions induced by iodine contrast media, finding that the CD14 enriched LTT yielded superior responses in most (but not all) patients (60), with the enrichment attenuating one patients response, and raising the baseline proliferation in at least one control. Prevailing thoughts regarding the mechanisms underpinning the superiority of dendritic cells as antigen-presenting cells (APC) in LTTs include that they are simply more adept at antigen presentation, or that as observed with nickel and DNCB (66) compounds can induce their maturation directly, in a manner that promotes immunological elicitation. The subtype of dendritic cells used to enrich the LTT must also be given consideration, as heterogeneity in response to nickel was detected when comparing Langerhans cells and circulating dendritic cells.

The role of regulatory T cells has also been scrutinized in recent times, with selective depletion of these cells from LTTs being attempted in several assays. One premise being that in some cases, although drug-specific precursors may exist, their response is suppressed by the action of regulatory T cells, hence, in their absence, the sensitivity to compounds would be unveiled. To this end, CD25+ve depletion from the culture has been utilized several times, as regulatory T cells constitutively express high levels (67, 68). In the context of allergic contact dermatitis (69), CD25 +ve depletion encouragingly yielded augmented responses to the contact allergens 2,4,6-trinitrobenzene sulfonic acid, FITC, and a-hexylcinnamaldehyde. However, responses to non-sensitizing compounds such as dimethyl sulfoxide were also augmented (albeit generally to a lesser degree). Additionally, CD25 is not exclusively highly expressed on regulatory T cells, and it is well documented that it is also expressed on B cells, activated effector T cells and certain subsets of memory T cells (68, 70–72). Therefore, the depletion of CD25 expressing cells may have unprecedented effects on the utility of the LTT (especially if PBMC are sampled in the acute phase as recommended in SJS), due to collateral removal of these other cell types, potentially resulting in false negative results through removal of drug-activated T-cells, rather than the unveiling of an otherwise suppressed response. Another modification pertaining to immune-regulation is the incorporation of immune checkpoint inhibitors. Sugita et al. (73) reported that incorporation of CTLA-4 augmented LTT sensitivity. This is an enticing prospect, but a critical question to address here would be the extent to which the enhanced sensitivity observed impacts upon the specificity of the assay. Regulatory T-cell components and regulatory pathways are likely to be critical in determining the hypersensitive status of individuals, and so false positive results would be a possible eventuality with their removal/suppression. A more detailed understanding of utility of such approaches within LTTs (perhaps even considering inter-individual components) is therefore required before it will be appropriate to routinely apply checkpoint inhibitors within such assays.

The inadequacy of the LTT in addressing metabolites derived from the parent drug may contribute to its lack of sensitivity, as some metabolites may be tissue specific. Indeed, the erratic returns from LTTs performed on drug-induced liver injury patients serve as testament to such limitations (74), as does the enhanced diagnostic performance of this assay when relevant drug metabolites are synthesized and included in LTT assessment of compounds known to undergo bio-activation (75). For metabolite coverage, several variations on LTTs have been utilized, but often these models are cumbersome; commonly relying on allogeneic metabolizing systems/cell lines such as rat/human hepatic microsomes, hepG2, hepaRG cell lines or primary hepatocytes to generate reactive metabolites, therefore restricting direct cellular contact and/or coming with the distinct caveat that allogeneic responses may undermine the assay. Nevertheless, some success has been reported with such approaches, though a degree of allogeneic response is duly reported (76, 77). In a research setting, the ultimate goal to overcome such issues would be to incorporate autologous tissues such as keratinocytes or hepatocytes which could possibly be derived through induced pluripotent stem cells, though this is impracticable for routine diagnostics. A utilitarian solution to installment of metabolizing systems within the LTT should be pursued if this assay is to realize its maximal potential in terms of diagnostic value for reactions attributable to metabolites.

Since PBMCs are the cellular input into the LTT, consideration must always be given that the output will reflect this. While use of these circulating lymphocytes is minimally invasive and is relatively practical, it does ultimately mean that translational relevance of any LTT outcome is a function of responses arising from circulating populations of lymphocytes. This equates to surveying only a small percentage of peripheral blood T-cells, which, even in totality, actually only represent around 2-2.5% of the entire T-cell complement populating an individual (78). Thus, tissue resident T-cells and specialized antigen presenting cells will be poorly (if at all) represented, and it remains imperative to consider this limitation when assessing hypersensitive statuses of patients exhibiting tissue specific responses. A similar argument may also be made for

drug-associated antigens derived from tissue specific peptide repertoires. Moreover, LTTs are somewhat limited in sensitivity even if the relevant cells are present within samples. Indeed, signals from T-cells present at only low pre-cursor frequencies can be lost among backgrounds generated by heterogeneous populations within PBMCs, as has been demonstrated through T-cell cloning procedures conducted on bulk cultures from patients negative in LTTs (79–81). This is a limitation of bulk proliferation assays and indicates that there is room for improvement in terms of the threshold at which presence of T-cells actually yields detectable responses in LTTs. Finally, the quality of PBMCs available for such assays has substantial bearing on the validity of the assay; the idealistic scenario is that PBMC isolation and LTT can be performed on fresh blood within hours of phlebotomy. Frozen PBMC is reputed to be less reliable, which may be attributable to differential sensitivity to cryopreservation across cellular components (82), particularly if this significantly alters the composition of the resulting PBMC. Regardless, robust LTT responses have been observed in patient samples that have been isolated and cryopreserved, and shipped internationally to specialist laboratories. Thus, if PBMC are proficiently isolated and cryopreserved, this may represent a more pragmatic option.

Another potential avenue of consideration for the LTT is that entire formulations must be scrutinized- a recently well documented example has been that of clavulanate, which is co-formulated with amoxicillin and ticarcillin to augment antimicrobial efficacy by functioning as "cannon fodder" for bacterial beta-lactamase enzymes, acting as a substrate and thus competitively inhibiting the lactamase action on the primary active ingredient. Unfortunately however, the addition of clavulanic acid to amoxicillin precipitates drug-induced liver injury in a percentage of patients which is not eclipsed with amoxicillin alone (83). Later studies depicted distinct immunogenicity profiles for both compounds, with no cross reactivity, indicating the immunogenicity of clavulanic acid (84). Further expanding investigation of formulation leads to inclusion of excipients for a given therapeutic. Indeed, when pure substance is not available, it is recommended that injectable forms of the drug or crushed pills are used (62), albeit with the caveat of procedural artifacts. On the flipside to this however, is that batch specific immune reactions due to impurities/contamination could perhaps be identified through tablet testing, potentially absolving an active pharmaceutical ingredient of responsibility for a reaction. It is feasible that investigations of this nature could be facilitated by stability samples stored by pharma.

Cytokine Synthesis and Secretion Detection Assays

In-vitro tests targeting the function of the drug specific T-cells; cytokine/cytolytic molecule secretion assays can be both diagnostic of an individual's hypersensitivity status, and informative in relation to pathomechanistic aspects of the reaction (85). Typical procedures used include ELISA, ELISpot (**Figure 4**), flow cytometry (intracellular cytokine staining), PCR and cytokine bead array assays. The detection parameters in such assays ultimately correspond to the synthesis and/or secretion of a given cytokine, which raises the predicament of which cytokines to use. Cytokines including IFN-γ, IL-2, IL-5, IL-13 and various cytolytic molecules such as perforin, granzyme B, and granulysin often feature, each with its merits and disadvantages depending on the clinical presentation and compound in question (57). This lead to the general recommendation that a panel of cytokines be used in order to enhance the highly variable sensitivity reported (86). Advantages of cytokine assays include the mechanistic insight provided and the relatively quick time to result (3 days), while drawbacks are the reported lack of specificity, high expense and specialist technical requirements.

Surface Marker Expression Assays

Cluster of differentiation 69 is a member of the c-type lectin family involved in T-cell proliferation pathways (87). The upregulation of this marker (measured using flow cytometry) has therefore been utilized as an early activation marker of T-cells in delayed drug hypersensitivity and has been compared to the LTT with advantages being the quicker time to result (48 hrs rather than 1 week), the omission of the use of radioactive materials and some drug-specific peculiarities (88, 89). Markers associated with T-cell cytotoxic effector functions have also been interrogated for use in causality assessment. Intracellular granulysin expression in NKp46+ve and CD4+ve cells has been proposed in the problematic assessment of SJS/TEN (90). Similarly, surface expression of the degranulation CD107a (LAMP1) on T and NK cells, has been described for heterogeneous hypersensitivity reactions, and provides comparable mechanistic insight to that provided by ELISpot/ELISA assays (91). Other activation induced surface markers such as CD154, CD25, OX40 and PDL-1 have been used in vaccine development for some time (92, 93), notably for the detection of rare memory T-cell responses (94). Approaches such as these may therefore be of interest as sensitivity of many aforementioned assays is inadequate.

Cytotoxicity

Inter-individual differences in the toxicological profiles of compounds (essentially detected in non-specific toxicity assays) have been linked to the hypersensitivity status of patients in several different settings. Early studies identified augmented cytotoxicity in hypersensitive patient PBMCs when co-cultured with metabolism conferring murine microsomal activating systems (95–97). Despite obvious caveats with these assays; namely the use of a xenoco-culture system, the observation of such toxicity appears to constitute a link between direct toxicity intrinsic to the individual, and the ensuing immunogenicity seen in immune-mediated idiosyncratic adverse drug reactions. Interestingly, the discrepancy in sensitivity exhibited hereditary correlation as parents of hypersensitive individuals expressed intermediate sensitivity (between controls and patients) (95), indicating a discernible role of intrinsic genetic predisposition factors. Several decades later, this approach was reinvented, employing the use of monocyte derived hepatocyte-like cells to form an autologous, metabolically competent model (98).

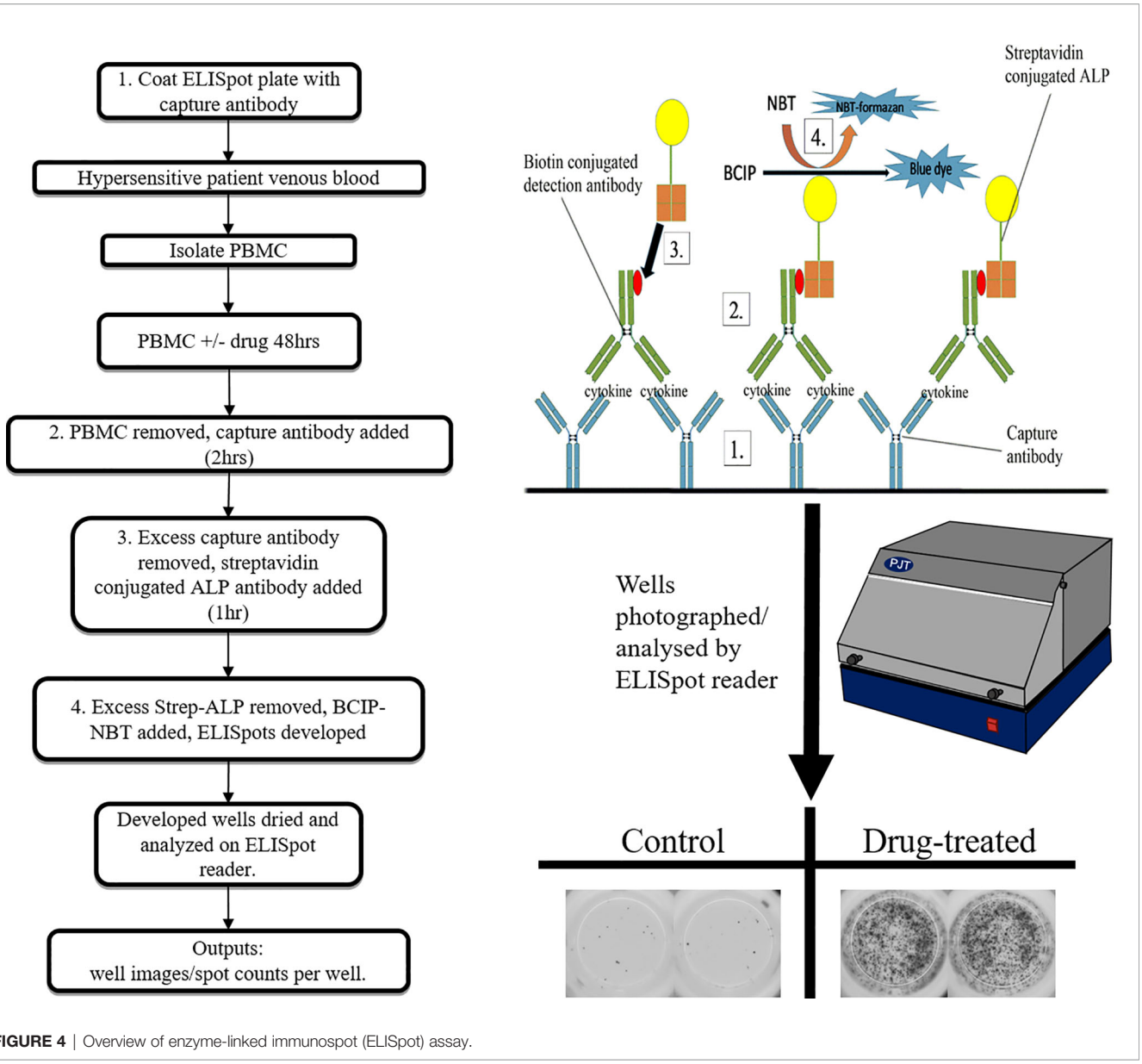

FIGURE 4 | Overview of enzyme-linked immunospot (ELISpot) assay.

Analogous to the results seen in the aforementioned studies, toxicity in monocyte derived hepatocyte-like cells was useful in causality assessment of idiosyncratic drug induced liver injury with comparable accuracy to that of the "gold standard" Roussel Uclaf causality assessment method (99, 100). Although this avenue of hypersensitivity investigation is in its early stages of resurrection, with other groups yet to replicate findings of these studies, it holds much promise both in utility as a diagnostic/predictive tool, and as a probe for understanding of the fundamental pre-disposing factors that influence an individual's propensity for hypersensitivity.

Perspective of Diagnostic Assays

To summarize, a number of diagnostic options can be pursued by a clinician in order to seek confirmation that a pharmaceutical agent should be contraindicated on the grounds of hypersensitivity. A conceptual shift has been underway for some time toward these tests being conducted *ex-vivo*, with the aim of obtaining diagnostic information while eliminating the risk of exposure for the individual in question. Unfortunately however, the battery of available *in-vitro* assays are still at various stages of development and are not yet of adequate maturity (through respective sensitivity/specificity/accessibility/standardization) to be routinely implemented into algorithms currently deployed for clinical diagnoses. It is disappointing that no functional diagnostic assay has achieved validation to date, especially given the length of time some have been studied for. A prime example of this is the LTT, which for nearly half a century has probably been the most established and clinically recognized *in-vitro* diagnostic assay, and therefore best situated for clinical validation. This is attributable to its unreliable sensitivity/specificity, and perhaps more importantly, lack of

standardization. As a result, and due to the antiquated and cumbersome *in-vitro* technologies routinely used, this assay is not likely to see clinical implementation within the next decade. The widespread availability of flow cytometry probably means that any easily implementable assay will arise on this platform. Such an application also provides opportunity to multiplex features of several of the aforementioned parameters, with this type of approach likely to yield a superior, or at least more utilitarian assay. In order to facilitate this, research groups equipped to conduct these assays will need to harmonise protocols and readout thresholds in order to work collaboratively in the establishment of what would be the first legitimized *in-vitro* option for diagnosis of hypersensitivity reactions. Thereafter, efforts can be directed toward the enhancement of its sensitivity and specificity with several promising avenues discussed. As adeptly demonstrated through the peculiar retrospective/predictive properties of HLA genotyping, translational solutions are long-awaited and can be exceptionally effective in this area, but it takes standardized, translational approaches to deliver them.

As aforementioned, an idealistic goal would be to minimize or render obsolete the diagnostic field through the installation of effective preclinical screening assays. This is far from realization, with several compounds reaching clinical phases of development before programme termination in recent times, and numerous drugs in clinical circulation that have less than desirable records in terms of hypersensitivity rates. There has therefore been no shortage of incentive to gauge the intrinsic immunogenicity of prospective pharmaceuticals within preclinical development in order to select optimal lead compounds for progression. The remainder of this review therefore focuses on some of the established strategies employed within industrial settings, and outlines novel assays currently in development that may one day form part of preclinical safety studies.

PROSPECTIVE ASSESSMENT OF IMMUNOGENICITY

Structural Alerts

Around 30 years ago, John Ashby, of imperial chemical industries, identified a codification of chemical structures that possessed genotoxic liabilities; structural alerts (101, 102). This codification was largely constructed from empirical evidence accumulated on chemical moieties responsible for covalent binding to cellular macromolecules (103–108). Since then, this basic dogma of identifying electrophilic structures that react with biological nucleophiles has undergone iterations and refinements for a variety of toxicological applications. Indeed, several *in-silico* models are now available for use as rapid, cheap, guidance tools for prediction of chemical toxicity, with the benefit of application before a compound is even synthesized (109). Understanding of the fundamental mechanisms of electrophilic reaction chemistry is therefore important in order to facilitate this philosophical shift from empirical knowledge, toward more general rules which can help inform design of such predictive tools. On this note, electrophilic reactions with biological nucleophiles have been posited to proceed through 6 basic mechanisms; S_N1, S_N2, S_NAr, acylation, Michael addition and Schiff base formation (110). For each of these, the outline of mechanism, alongside a pertinent example is provided in (**Figures 5** and **6**).

Though compounds can be intrinsically reactive as seen with β-lactam antibiotics (121), the true extent of conjugative chemistry for a given compound is often a function of its capacity to form reactive metabolites. Hence, the term toxicophore can be used interchangeably with structural alert, to refer to a compound which has reactivity imparted *via* metabolism. This has been identified as a mechanism of direct toxicity (122–124), with a direct link to hapten theory, and the propensity of compounds to cause idiosyncratic, immune-mediated reactions (125–127). The ratio of the appearance of structural alerts across drugs withdrawn/issued a black box warning relative to drugs with superior safety profiles demonstrates their unpropitious nature (128). Examples of chemical moieties that commonly feature in drugs that cause idiosyncratic toxicity include p-aminophenols or aromatic amines that can be oxidized to them (quinone reactive metabolites) (128–130), and anilines/anilides (hydroxylamine/nitroso reactive metabolites) (131–133). The logical application of such findings is therefore to design out structural alerts either in early compound design, or in an iterative fashion once the initial compound encounters idiosyncratic safety issues. One straightforward example to illustrate this approach can be found with the non-steroidal anti-inflammatory drugs suprofen and ketoprofen (**Figure 7**, top). Suprofen, which contains a thiophene structural alert, was withdrawn due to renal toxicity (134–136). Toxicological salvation can be achieved *via* replacement of the thiophene moiety present in suprofen with a phenyl ring, resulting in the safer alternative ketoprofen (137). Another example can be found in the evolution of antimalarial 4-aminoquinolones. Clinical utility of amodiaquine has been somewhat vitiated by its capacity to elicit idiosyncratic adverse drug reactions; particularly hepatotoxicity and agranulocytosis (138, 139). Amodiaquine sports an aminophenol structural alert which undergoes enzyme-mediated oxidation to form a reactive quinoneimine species which covalently binds proteins and elicits immunological responses (129, 140–145). To circumvent this deleterious bioactivation, several routes of structural redesign were pursued (**Figure 7**, bottom); including the addition of two electron accepting groups at 3′ and 5′ positions to enhance potency (146) and isomerization of the 4′-hydroxyl group with the 3′-diethylamino side chain or fluorination of the 4′-position to prevent quinonoid bioactivation (147, 148).

Structural alerts represent an anecdotal weight of knowledge through experience and should therefore be used accordingly; as a guide rather than a standard operating procedure. They far from guarantee safety; even if one was to eschew from all leads containing structural alerts, there exists several high profile examples of drugs lacking such motifs that have been withdrawn due to idiosyncratic toxicity (ximelegatran, chlormezanone, isoxicam, and pemoline) (128, 149, 150). Conversely, hit attrition concerns highlight how unsatisfactory such a parochial approach would be, with toxicophores frequently featuring in top pharmaceuticals (128, 151), and

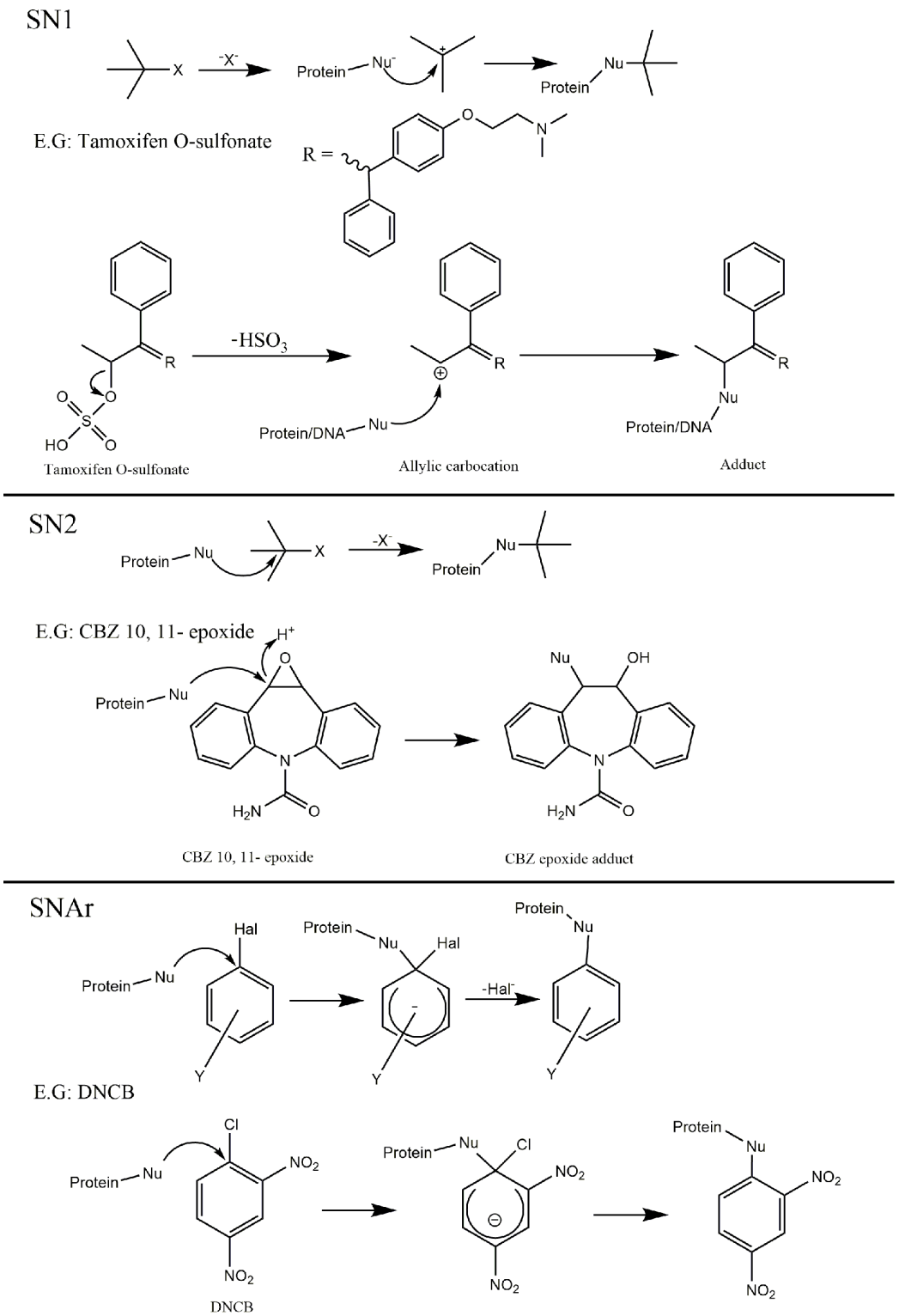

FIGURE 5 | Mechanisms of covalent binding. Outline of the 6 key mechanisms by which electrophiles react with biological nucleophiles with an example compound provided for each. SN1; Tamoxifen O-sulfonate metabolite (derived from sulfonation of a-hydroxytamoxifen) can collapse yielding an allylic carbocation reactive metabolite susceptible to nucleophilic attack, resulting in protein and adducts (111–114). SN2; Carbamazepine (CBZ) 10, 11 - epoxide (reactive metabolites derived from carbamazepine) (115). SNAr; Dinitrochlorobenzene (116).

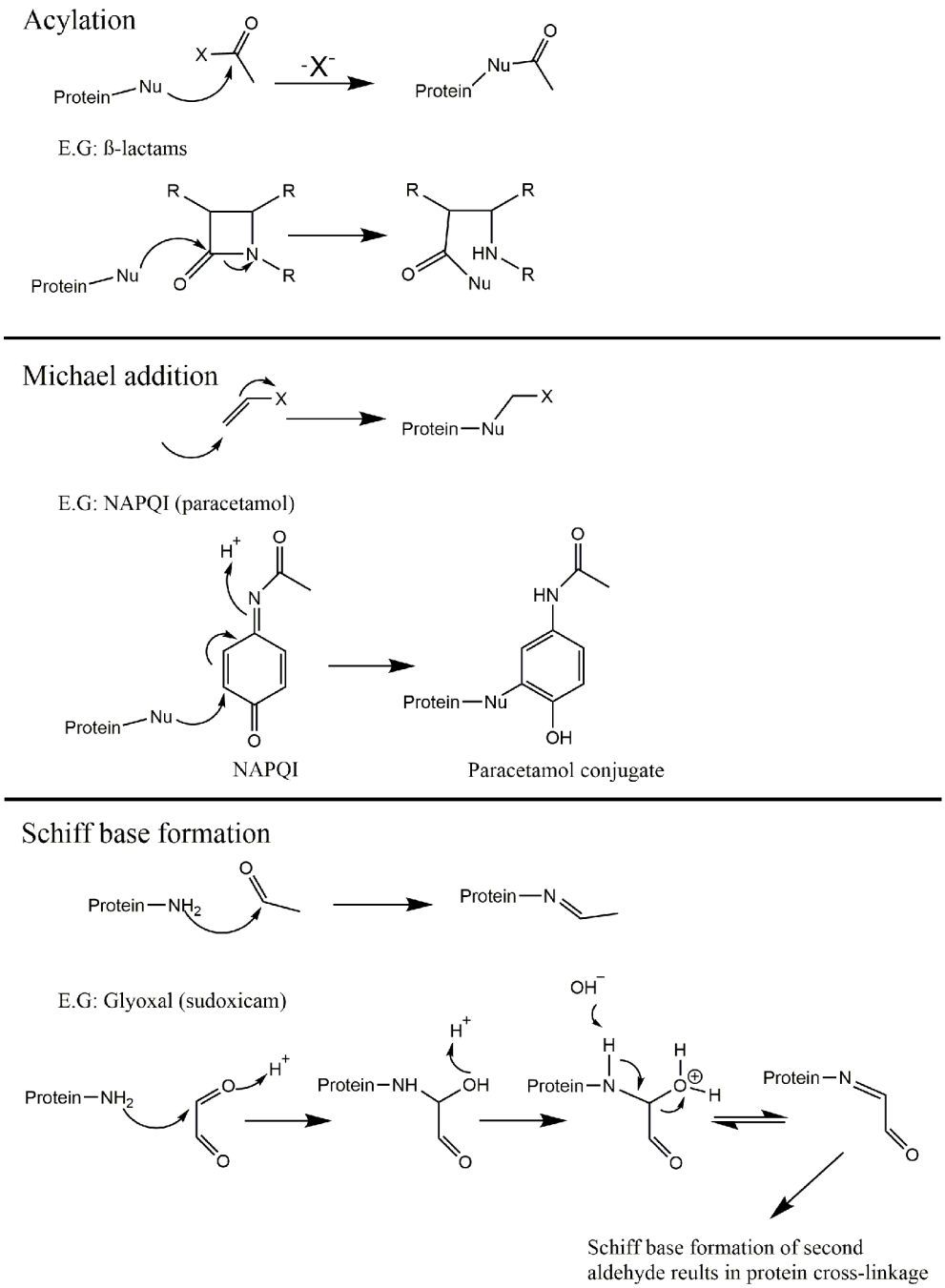

FIGURE 6 | Mechanisms of covalent binding. Outline of the 6 key mechanisms by which electrophiles react with biological nucleophiles with an example compound provided for each (continued). Acylation; B-lactam containing compounds (117). Michael addition; N-acetyl-p-benzo-quinone imine (NAPQI) (reactive metabolite derived from Paracetamol) (118). Schiff base formation; glyoxal (released via bioactivation of sudoxicam) (119, 120).

many drugs dependent on covalent mechanisms of action (128, 149, 151). Furthermore, while structural alerts indicate the possibility of a molecule covalently binding, this does not always translate; compounds containing structural alerts do not always form chemically reactive metabolites, and competing clearance pathways can trivialize the presence of alerts that do undergo bioactivation (128, 149). With regards to hypersensitivity, these examples serve to demonstrate that avoidance of structural alerts is not essential, that total body burden of chemically reactive metabolites (and therefore ensuing antigenic density) can be an important determinant, and that subtle re-design can save a lead compound.

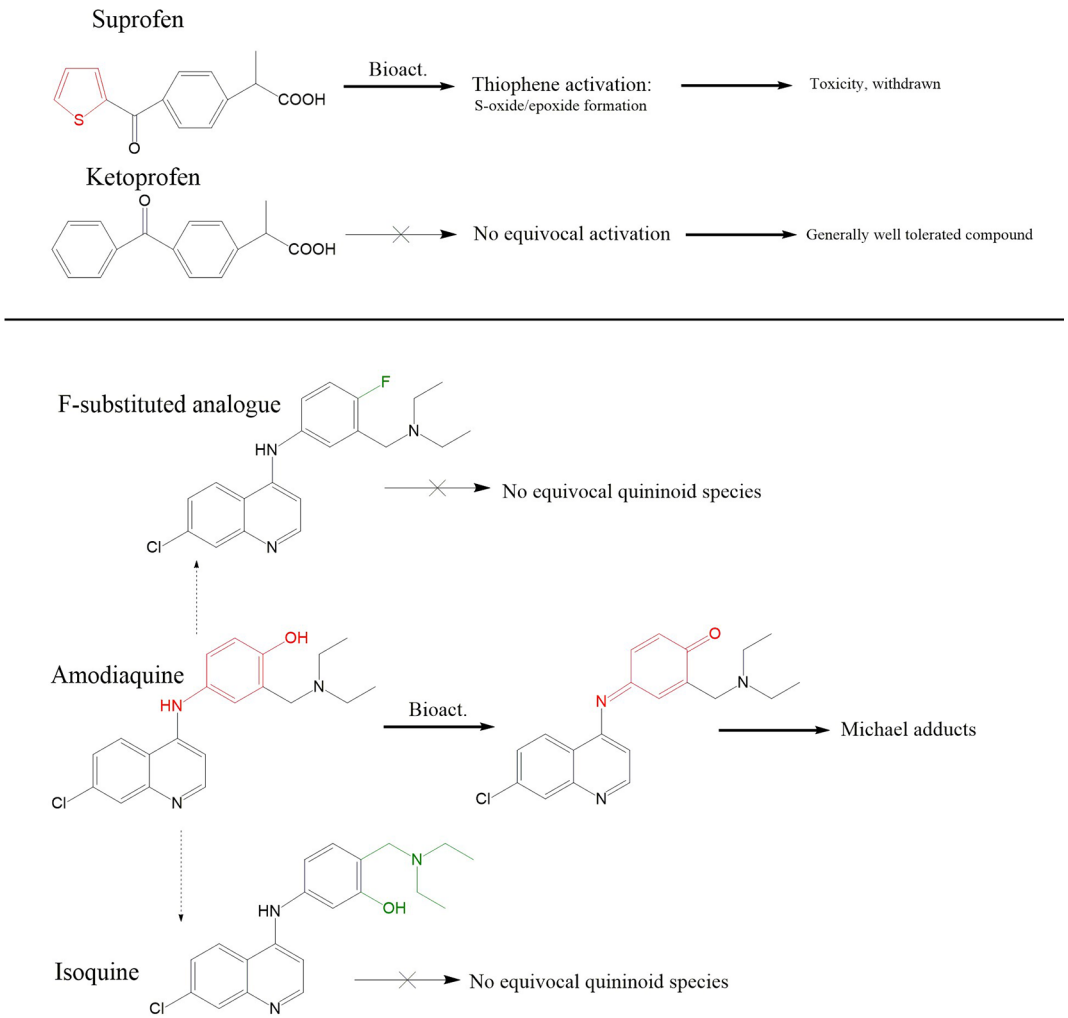

FIGURE 7 | Pharmaceutical application of structural alert chemistry. Top panel; Disparity in metabolic fates of suprofen and related ketoprofen, and their downstream tolerability profiles, are generally attributed to suprofen's possession of the thiophene ring structural alert which is capable of undergoing oxidation to S-oxides/epoxides. Ketoprofen's phenyl ring does not undergo equivalent bio-activation. Middle panel: Iterative synthesis series of amodiaquine in pursuit of a compound with reduced ADR liabilities; Amodiaquine possesses the p-aminophenol structural alert which can be bioactivated to the Michael acceptor ACQI which is reported to be responsible for its idiosyncratic ADR liabilities in a fashion akin to paracetamol and NAPQI. Structural analogues in the form of fluorination at the 4 positions, or isomerization of the hydroxyl and diethylamino side chain leads to compounds impervious to quininoid bioactivation.

For now, due to the emphasis on chemical reactivity with structural alerts, this type of approach currently only has utility for drugs which exert antigenicity *via* hapten/covalent binding related mechanisms. However, as patterns of drug hypersensitivity *via* the various mechanisms continue to emerge, perhaps we will eventually see inclusion of chemical codifications which confer immunogenicity, through each or all of the described antigenicity mechanisms [**Figure 1**, (8)], and/or particularly high affinity interactions for (common) constituents of the immunological synapse. One can envision that a nascent database of such "Immunocophores" could be procured from compounds that have failed at various stages of development due to idiosyncratic, immune-mediated toxicity and used to mitigate risk. Proof-of-concept iterative medicinal chemistry studies in pursuit of an analogue of abacavir devoid of hypersensitivity liabilities with preserved pharmacological action have embodied a promising prototypical approach to disconnect pharma- and immuno-cophores. Cross-disciplinary laboratories operated using *in-silico* docking models alongside functional studies to simultaneously decipher pharmacological (anti-viral) and immunological (T-cell activation) structure-activity-relationships of compound series (152, 153). Digressing from such idealistic goals, many of the following experimental assays have essentially been devised to address various aspects that lie within the void of knowledge between such conventional theoretical chemistry-based wisdom, and pragmatic transition of a compound to clinical use.

Electrophile Trapping Assays

Reactive electrophile species formed through the bioactivation of drug candidates often exhibit insufficient stability to be directly identified through liquid chromatography-mass spectrometric methods. Hence, in order to delineate metabolites that can be derived from a given compound, a metabolically competent *in-vitro* system (cofactor fortified S9 fraction, microsomes, hepatocytes) is employed to generate reactive metabolites, which form adducts with characterised endogenous or exogenous nucleophiles, yielding "smoking gun" conjugates, providing insight into reactive metabolites formed and the mechanism by which they interact with nucleophiles (**Figure 8**). Since endogenous nucleophiles do not lend themselves to high throughput screening methods, in early compound development, small molecule nucleophilic traps are preferred. The armamentarium of these nucleophilic warheads includes the thiol-containing soft nucleophiles (glutathione, cysteine, N-acetylcysteine and 2-mercaptoethanol) for detection of soft electrophiles, and non-thiol hard nucleophiles (cyanide, semicarbazide, methoxylamine, DNA bases) for detection of hard electrophiles (154). These types of assays are mostly qualitative, but a degree of quantitative value can be added through the incorporation of radiolabelled analogues of corresponding nucleophile probes [^{35}S] GSH and [^{14}C] KCN (155).

Electrophile trapping assays are amenable to high throughput screening translation/automation and so feature prominently across drug discovery programmes. Despite their value and widespread utility, limitations to application of trapping in hypersensitivity prediction include: 1. the nucleophiles themselves, as any approach using exogenous nucleophiles is reliant on the assumption that these selected surrogate nucleophiles recapitulate the mechanism of adduct formation on biological macromolecules in a toxicologically/immunologically relevant fashion. 2. The physiological relevance of the somewhat simplistic *in-vitro* cultures (as detoxification pathways are not well accounted for). 3. Reactive compounds missed by such assays such as acyl glucuronides and CoA thioesters (154).

Adductomics

Adductomics denotes a method that studies the magnitude of covalent adducts bound to tissue or blood nucleophiles which can characterise the electrophilic potential of drugs or indeed their bioactivated metabolites. This procedure involves the co-incubation of the drug-metabolite in question with conjugate proteins such as GSTP or HSA in a dose dependent manner (115). The formation of adducts can then be quantified by the use of western blotting or mass spectrometry to identify the bound amino acid residue. Protein adduction studies have been pivotal in the research of a plethora of drugs/metabolites to delineate the mechanism by which they elicit T-cell activation and whether the parent drug or a metabolite thereof exhibits the immunogenic liability (156). Jenkins et al. successfully identified the irreversible binding of flucloxacillin to HSA, in a mechanism involving nucleophilic attack of the β-lactam ring of flucloxacillin to lysine residues present on peptides (157) (**Figure 6**). This procedure has also been used for mechanistic resolution in discrimination between drugs which possess hapten functionalities and those which do not. One rather controversial example in this light is the antibiotic sulfamethoxazole, which is known to activate T-cells through a mechanism which bypasses antigen processing, namely the PI mechanism (5, 158–160) (161). However, sulfamethoxazole undergoes oxidative bioactivation to yield the metabolite nitrososulfamethoxazole. This metabolite exhibits strong reactivity toward cysteine residues, forming covalent bonds and acting as a hapten (131, 162). Accordingly, distinct patterns of T-cell activation between the relatively inert parent drug and a bioactivated metabolite can often be obtained from mechanistic studies on isolated T-cell clones (158).

Despite protein adduction of a compound not converting to a compounds liabilities in terms of capacity to elicit hypersensitivity reactions in a straightforward fashion. Drug-protein adducts have been successfully identified with antibiotics such as piperacillin (163), flucloxacillin and amoxicillin (164, 165) as well as reverse transcriptase inhibitors such as nevirapine (166). This approach has also been utilised to identify a range of peptides susceptible to covalent modification by the drug/hapten in question (121). Successful identification of such a drug-modified protein can then allow for the synthesis of designer peptides which can be integrated into T-cell assays, for analysis of their immunogenic potential (167), in a similar manner to those designed for vaccine use (168). An area of interest which may be important for the future of adductomics (with regards to both investigative and preclinical assays) will be the selected endogenous nucleophiles, and whether there may be some proteins for which covalent binding is poorly immunologically tolerated.

Peptide Elution Studies

Within the human system HLA complexes are essential proteins which are expressed on the surfaces of many cell types which function to present peptides to T-cells. MHC class I, which presents to CD8+ T-cells, is comprised of HLA-A,B and C molecules. Meanwhile, HLA class II serves to present to CD4+ T-cells, and consists of HLA-DP, DQ and DR molecules. Many peptides from the constitutive repertoire of the host are tolerated by T-cells due to prior exposure during thymic development. However, peptides encountered thereafter such as those of viral or bacterial origin can elicit an immune response if accompanied by appropriate co-signaling and the presence of DAMPs or PAMPs (169).

Several approaches can be utilised to isolate HLA-bound peptides from a variety of cell lines. The simplest of which entails acid stripping the surfaces of cells in culture using an acidic buffer (170–172). However, this has been reported to result in high levels of contaminating peptides which can hinder the analysis of the immunopeptidome. A more commonly utilised approach involves the direct separation of solubilised HLA-complexes isolated from cell lines. This approach entails the immunoprecipitation of HLA molecules and the subsequent

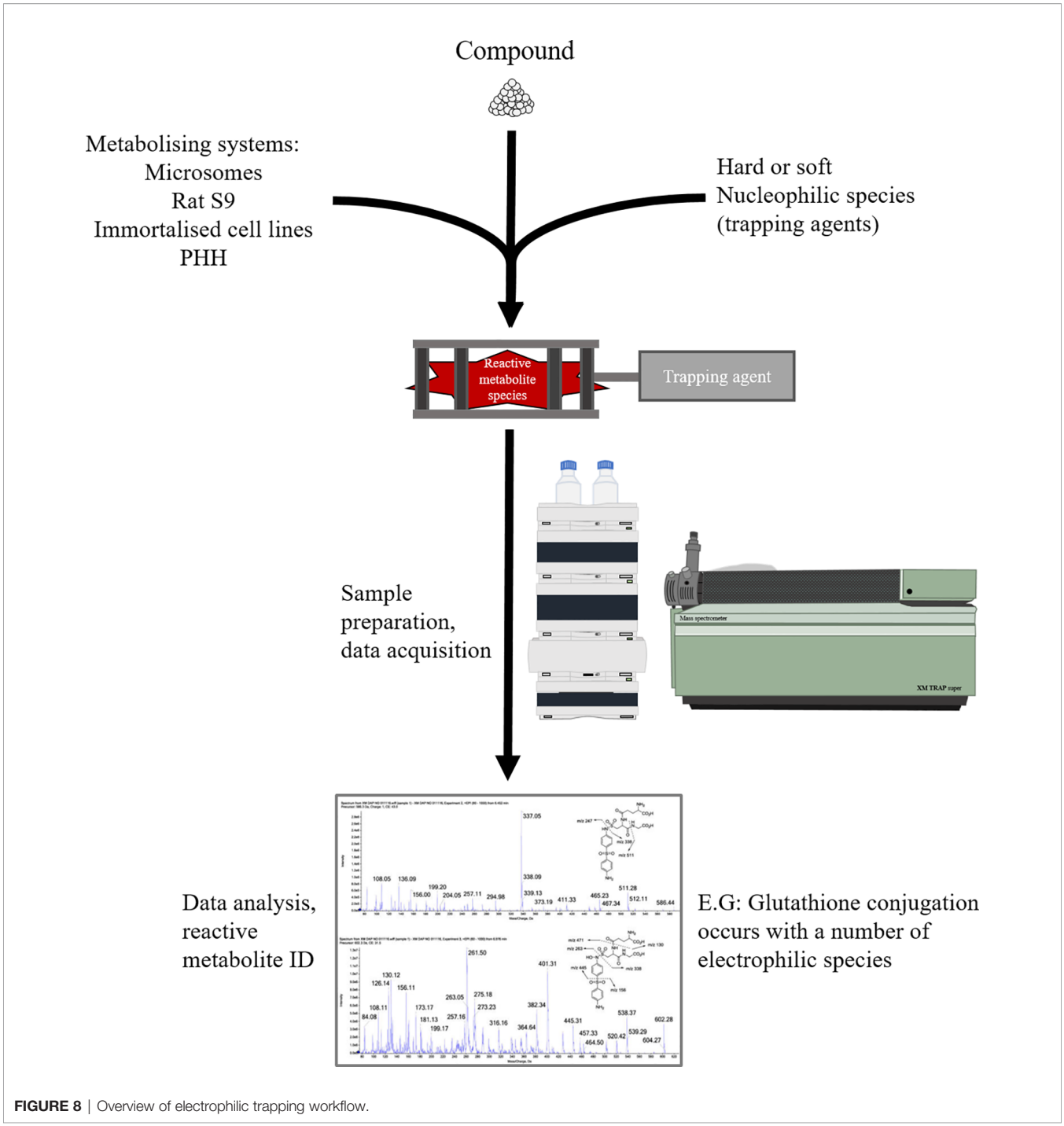

FIGURE 8 | Overview of electrophilic trapping workflow.

dissociation of the HLA-bound peptide complex which can then be analysed *via* m/s [**Figure 9**, (173, 174)].

Mass spectrometric analysis of HLA-peptide complexes has successfully identified thousands of natural MHC peptides presented on the cellular surface. These studies have been successful in the identification of the peptide binding preferences to alleles in a plethora of diseases including type 1 diabetes (175) and cancer (176, 177). Peptide elution studies have also been carried out as a pre-requisite for the study of peptide binding HLA's, and in such cases helped to identify the N-terminal escape of 9-11 mer peptides when HLA bound (178).

It is well known that the induction of hypersensitivity reaction entails the presentation of a drug-related antigen on the surface of MHCs for scrutiny by T-cells. Indeed, this has been an area of considerable interest in recent times, including the

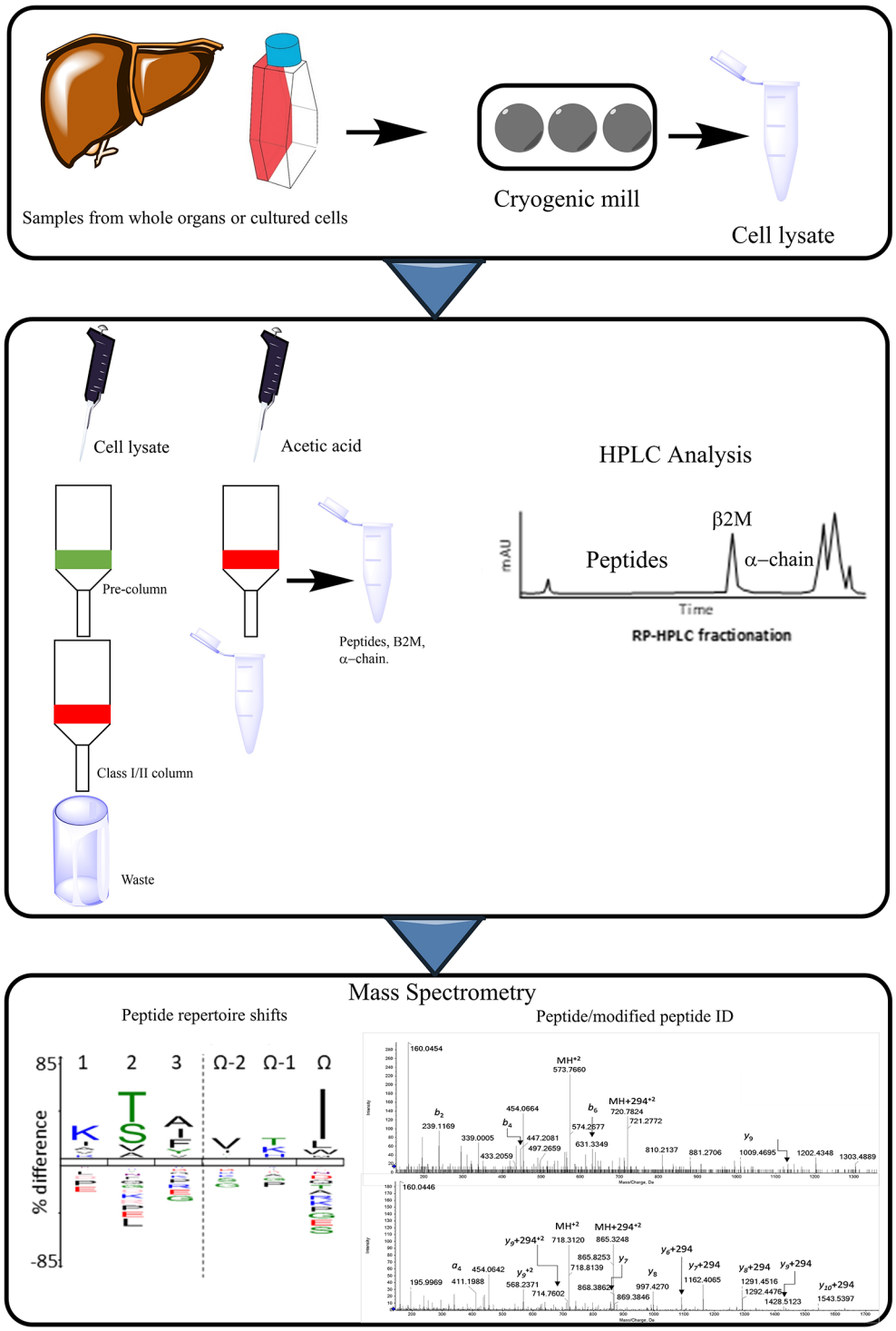

FIGURE 9 | Procedural workflow of peptide elution assays. MHC complexes are purified from the samples, which can comprise of cultured cells (i.e. transfected B-cells expressing HLA allele of interest), or cells deriving from whole organs or biopsies (liver). Cell pellets can be ground using cryogenic mill and are then lysed. Immunoprecipitation takes place from the cell lysate, this occurs through running the sample through columns specific for the MHC in question, as well as a pre-column to remove non-specific binding. HPLC is then conducted to separate the MHC peptides from the larger components such as β_2M and the alpha chain. Pooled fractions can then be analyzed *via* m/s allowing for the identification of modified peptides or an altered repertoire of peptides presented to T-cells.

identification of drug modified peptides or an altered repertoire of peptides on the surface of MHC. Elegant studies conducted by Illing et al. in 2012 utilised peptide elutions to positively identify a skewage toward peptides terminating in small aliphatic amino acids (I, L and V) over the conventional aromatic amino acids (F/W/P) in HLA-B*57:01+ APCs co-incubated with abacavir (179). This was achieved *via* the prolonged incubation of C1R-B*57:01 cells with abacavir followed by peptide elutions from the class I MHC and analysis by mass spectrometry (m/s). This was further reinforced in 2019 when abacavir analogues with a similar T-cell liability were found to perturb the HLA-B*57:01 peptide repertoire in a similar convention to abacavir, while those with no T-cell liability did not (180). This concept was further explored *via* the use of the β-lactam antibiotic flucloxacillin which was identified to covalently haptenate HLA-B*57:01 native peptides which were subsequently processed and presented on the MHC for T-cell recognition. This occurred through multiple mechanisms, namely, through antigen processing and direct haptenation of pre-presented peptides. Indeed, utilization of m/s analysis identified the presence HLA-B*57:01 peptides that were covalently modified with flucloxacillin haptens at lysine and arginine (181).

An obvious drawback of the peptide elution studies is the extent of technical demand; up to $1x10^9$ cells can be required for the incubation in the presence of the drug prior to conducting the elutions, mandating laborious cell culture. In the cases where specific HLA alleles are implicated, transfection of B-cell lines with the relevant alleles is standard procedure, further complicating matters, though a number of such cell lines expressing HLA alleles of interest are now commercially available. There are also procedural challenges pertaining to the translational relevance of peptides that arise through elution of transformed cell lines subject to extended culture, from which peptides are eluted in a process that may not entirely recapitulate peptides actually presented. Of considerable concern on these lines is the reported yield of peptides from such procedures (182). Further issues lie with the analysis softwares used for immunoproteomic profiling, as they exhibit shortcomings in terms of detection, particularly of drug-adducted peptides; expert mass spectrometric/adductomic analysis is therefore necessitated in many studies. Thus, the considerable technical demands, translational limitations and the level of expertise required to process analytical findings have largely confined such methods to specialist investigative studies. Peptide elution studies are therefore at the time of writing very low throughput, expensive assays which are geared toward identification of critical neoantigens (eluted peptides), and thereby the nature of culprit HLA presented T-cell epitopes associated with treatment of APCs, affording valuable insight into the mechanisms of T-cell activation by a given compound. Encouragingly, peptide elution methods feature with increasing frequency in various oncological applications such as peptide vaccination and adoptive cell transfer workflows where the field is now entering a realm of discovery in personalised/tumour personalised therapeutic approaches (183–185).

Covalent Binding Studies

Considered as the "gold standard" and often featuring as a synergistic counterpart to trapping assays are covalent binding studies. Here, radiolabelled analogs of the candidate compound are synthesised to facilitate the measurement of covalent binding in various models. Such studies commonly feature *in-vitro* studies on human and rat liver preparations (microsomes, hepatocytes), to investigate covalent binding and interspecies translatability (154). As well as *in-vivo* models where rodent species are subject to either quantitative whole body autoradiography or radiometric analysis of harvested tissues (coupled with excretion studies) in order to determine disposition of drug-related material (186). These studies are informative in terms of qualitatively and quantitatively scrutinizing covalent binding, thereby offering insight into the extent of and localisation of hapten formation and thus which organs may be most likely targeted. However, information derived from such studies comes with several notable caveats. Firstly, custom radio-synthesis of a compound requires careful selection of radioactive atom placement to avoid metabolism induced loss, and so is an expensive pursuit, not well suited to high throughput screening. Secondly, the limitations of translational relevance of human based *in-vitro* assays as well as utility of rodents within *in-vivo* studies must always be considered. Thirdly, as with failings of electrophilic trapping and adductomics, studies of this type will not be effective in detecting compounds which confer antigenicity through non-covalent mechanisms.

Finally, there is much ambiguity as to the advisable course of action to take upon the discovery of covalent binding, with multiple confounding factors such as the lack of definitive and transparently quantifiable translation to toxicity decisions (187), with projected drug dose, purpose, and mechanism of action complicating the implementation of an isolated, binary decision. These assays are therefore to be interpreted in the context of a weight of knowledge accrued on a given chemical entity, to inform decision making in drug design, and ultimately serve to help direct drug design toward a lead optimization process that mitigates/minimalizes bio-activation.

Enzyme Inactivation

Another avenue by which toxicity can be identified is through detection of mechanism-based inhibition of metabolic enzymes (mainly CYPs) (188). Various applications of this principle and the relevant models are described adeptly in (186). Although not proving the formation of reactive metabolites per-se, findings of enzyme inactivation are often indicative that compounds undergo bioactivation. In terms of liabilities for the culprit compound, enzyme inhibition may result from the alkylation of the enzyme (often by the reactive metabolite the enzyme catalyses the formation of), which may provoke an immunogenic response through neoantigen generation such as that seen with halothane (189) and tienilic acid (190). An important consideration with this type of assay is that it is already integrated into drug development, and may therefore shed light on potential sources of neoantigens responsible for

certain tissue restricted hypersensitivity reactions (particularly idiosyncratic liver injury) and highlight the responsible enzyme for reactive metabolite formation and antigenic generation early in preclinical development.

Antigen Presenting Cell Maturation/ Activation Assays

While the antigenicity of a compound is important in terms of density/affinity/variety of antigens produced, another important component of drugs liabilities for hypersensitivity reactions may well be its capacity to generate signal 2. Indeed, classic studies have elegantly demonstrated a distinction and synergy between a chemical sensitizer and an irritant (191–193), thus, a compound's intrinsic capacity to elicit both signal 1 and 2 contributes to its overall sensitization potential. One can consider this phenomenon in a manner akin to vaccines; while peptide epitopes are the focal point of the resulting T-cell response, co-administered adjuvants are often required to provoke immune elicitation rather than tolerance to the objective epitope.

This theme is evident within T-cell priming assays to compounds, where maturation stimuli cocktails such as LPS/ TNF-α are deployed in order to mature dendritic cells prior to co-culture and facilitate T-cell priming (194, 195). From this foundation a conclusion can be drawn that a compound that possesses both qualities is less desirable than either in isolation, as such a compound is self-propagating in terms of T-cell liabilities. Certainly, assays that concentrate on a compounds capacity to promote APC maturation have proven effective in the realm of contact sensitization, with the human cell line activation test (h-CLAT) a validated and widely accepted assay routinely used for determination of sensitizer potential of prospective compounds (196–199). Intriguingly, such assays can actually distinguish between irritants and sensitizers (200). Some drugs containing structural alerts can indeed elicit direct semi-maturation of dendritic cells directly, as has been demonstrated within h-CLAT assays (196, 201) and in monocyte derived dendritic cells (64) for penicillin G and amoxicillin respectively. However, this rather appeasing correlation is afflicted with the same limitations as structural alerts, in that bioactivation can also generate chemical species capable of APC maturation as seen with nitrososulfamethoxazole (202) thus limiting application of such assays unless competent metabolizing systems are in place. Additional consideration can be given to the contiguity between danger signaling a drug may elicit through direct toxicological mechanisms, and the bearing that this may have on the interpretation of antigens and target tissue for adaptive immune sequelae. Indeed, within contact sensitization studies, response element reporters are used to detect cellular stress in assays such as keratinoSens™ (203), and combinatorial models including these types of assays are being pursued with increasing frequency (204, 205). Comparable response element/gene expression based assays have also been evaluated within hepatic models with some merit (206, 207). Investigation of the hepatic-innate immune interface for liver injury causing drugs in the form of supernatant/ exosomal transfer experiments has yielded meagre returns to date with no overt increase in maturation marker expression of dendritic cells observed, although release of various cytokines was reported (208, 209), as was the basis for a communication pathway between hepatocytes and the innate immune system (210–214). These experimental platforms have paved the way for development of a new series of co-culture models that explore this interface in a fashion that may be amenable to medium throughput screening (215), offering a promising avenue for APC activation based assays to be implemented alongside conventional direct toxicological studies. Ultimately, there does appear to be potential utility for assays that focus on the intrinsic potential for a compound to generate signal 2, and they have proven useful in contact sensitizer classification. However, compounds that cause drug hypersensitivity that do act through such mechanisms appear to do so subtly, thus, current models are of inadequate sensitivity to draw robust verdicts on a compounds liability to cause hypersensitivity. In any case, for these adjuvant/perception type assays to be interpreted effectively they will likely need to be paired with one or more assays that indicate a compounds capacity to generate signal 1. It also needs to be accepted that with hypersensitivity reactions often occurring at extremely low frequencies, coincidental events that provide danger signaling; infections/trauma/co-medications/environmental factors and perception of cross-reactive antigens may play a role in at least some individuals and therefore serve to reduce or even nullify the necessity for a compound to generate an adjuvant signal in order to elicit T-cell responses.

In-Vitro Priming Assays

Competent *in-vitro* assessment of the potential of small molecular weight compounds to elicit *de-novo* T-cell responses has been an aspiration within the field of hypersensitivity for some time, with establishment and validation of such screening assays currently an unmet need in drug development programmes. Early studies to this end consisted of a simple repetitive stimulation of drug-naïve donor PBMC with drug and a 48hr stimulation culture followed by a 16hr ^{3}H-thymidine incorporation period conducted under IL-2 deprived conditions (216). In recent times, efforts have been made to adapt established peptide priming methods (194, 217) into a formulation which facilitates the incorporation of drug-related antigens (195). These assays, repurposed from their original application in the field of contact sensitization (218), entail the co-culture of cytokine-induced dendritic cells derived from monocytes (6 day culture, matured overnight with LPS/TNF-α) with the naïve T-cell component of PBMC in the presence of antigen for 8-14 days, followed by a re-constitution and re-challenge with a fresh batch of dendritic cells and drug antigen (195). Such procedures have been utilized in the exploration of *de-novo* priming to numerous compounds, with varying degrees of priming observed, and encouragingly, some dependency on the expression of HLA risk allele for selected drugs (219, 220). Additionally, the priming assay is sensitive to perturbation of immune-regulation, with the integration of immune checkpoint inhibitors influencing the intensity of priming to compounds (221,

222), a matter that is of increasing translational pertinence (15, 16, 18).

Unfortunately, while the *in-vitro* priming assays consistently yield robust priming responses to the paradigm compound nitrososulfamethoxazole and contact sensitizers such as bandrowski's base, there are instances (as for the parent drug sulfamethoxazole) where they do not even appear as adept as the previously described PBMC methods at detecting drug-specific responses (216, 223). This has been attributed to a lack of sensitivity as signals from T-cells present at low precursor frequencies are lost among the "noise" generated by the bulk T-cell lines produced through T-cell priming assays, as has been demonstrated by limiting dilution and clonal characterization studies (223). Recently, this lack of sensitivity has been addressed through an additional iteration of the priming assay (224), which has resulted in experimental procedures closely aligned with those described for contact sensitization (225), which permits greater numbers of experimental replicates comprised of miniaturized priming cultures. This has facilitated detection of drug-specific responses arising from rare T-cells, albeit at the price of more turbulent baselines relative to the conventional priming assay. Immuno-regulatory aspects of the T-cell multi-well assay (TMWA) have also been evaluated, with evidence for modulation of priming to compounds by checkpoint inhibitors (224).

It is fair to consider T-cell priming assays of each format as in-development. Several limitations of these assays encumber their implementation as potential screening assays within the drug development process. The first is their sensitivity; although the TMWA represents progress in this avenue, it is still limited with many pharmaceuticals, especially compounds that do not categorise as contact sensitizers. Another limitation is that of inputting the "correct", or rather the most immunologically relevant derivative of the drug; as with the diagnostic assays, these assays are comprised of metabolically incompetent cell types (dendritic cells and T-cells). Thus, if a metabolite's formation is dependent on metabolically active cell types is responsible for a drug's immunological liabilities, as is the case for many pharmaceuticals, then it is unlikely that T-cell priming assays in their current format will adequately detect immunogenicity from the input of parent drug. The detection of such responses therefore depends on; 1. The integration of a translationally relevant metabolizing system into such assays, or 2. The identification of metabolites, their synthesis and input into assays. The former of which is impeded by allogenicity/cumbersome nature of such systems, and the latter represents a challenging, expensive and possibly impractical prospect, especially regarding extensively metabolized compounds. Other limitations include the cellular input (PBMCs) as tissue resident T-cells are neglected (as with diagnostic assays), poor representation of certain T-cell responses (e.g., CD4 may predominate), and the possibility of biased effector phenotypes driven by the maturation stimuli utilized.

The weight of risk determinant that HLA allele expression contributes to T-cell responses involved in hypersensitivity is highly variable; with some drugs exhibiting extreme odds ratios to particular alleles (HLA-B*5701 and abacavir) (42) while others have no known associated HLA. An important question is whether the former represent an intractable issue when it comes to preclinical screening; the incorporation of HLA allele variants into such assays would mandate dozens of parallel assays, even to cover the most abundant alleles. Finally, the question of whether these *de-novo* responses actually do translate well to what is seen within patients is poorly defined. Within priming cultures, regulatory (amongst other) constituents of PBMC are removed and extreme inflammatory conditions are used in order to provoke T-cell responses against compounds. Indeed, the question answered from a positive assay result will almost certainly be "can" rather than "would" T-cells be activated by a given compound. Regardless, satisfactory development of T-cell priming assays would likely be a welcome addition to the barrage of available immunotoxicological assays.

In-Silico Approaches

The recent emergence of nascent *in-silico* modelling systems in toxicological prediction of compounds hopefully portends a new era in the field of prediction of idiosyncratic adverse drug reactions. Systems currently available include aforementioned structural alert/chemical characteristic based softwares (109, 226–228), and models that attempt to integrate *in-vitro* findings to a toxicity assessment output (229, 230). DILIsym is perhaps the most prominent of these *in-silico* biological systems (231) and though it currently lacks an adaptive immune component, it has still exhibited utility when investigating/comparing compounds which appear to proceed through adaptive mechanisms (232–234), perhaps due to factors that propagate deployment of such abberant immunological responses. With such powerful *in-silico* methods at the disposal of the field, there are examples where modelling has been utilised even with the more complex assays such as immunopetidomics, with docking models for HLA based risk assessment of prospective compounds a particularly ambitious venture of interest (235). However, a caveat of currently employed docking studies is that they focus on only one component of the immunological synapse; the HLA, and therefore do not reflect interactions dependent on other interchangable components. Exceptionally challenging barriers exist to hinder the successful, universal, transition to prediction of signal 1 for a given compound within *in-silico* docking models through modelling of the focal point of the immunological synapse. The first is the profound polymorphism of HLA itself; to the extent that, coupled with heterozygosity of individuals, HLA genotyping can be utilized for paternal testing (236) and forensic science (237). The allelic variation is mostly restricted to residues that form the peptide binding groove, with important consequences for the respective peptide binding repertoire of each HLA (238). Second is the peptide repertoire that is expressed, which is diverse and will exhibit cell type and status specific profiles (239–241). Third is the vast heterogeneity of T-cell receptors, with clonotypic expression of TCRs shown to be important for hypersensitivity reactions occurring with a select number of drugs in the context of risk HLAs (242, 243). TCRs possess remarkable variation including that of hypervariable

CDR3 region (244), and exhibit high variability in docking topology with the HLA-peptide ligand (245).

Upon successful modeling of those components, topological perturbations induced by drug and any relevant metabolites, *via* each of the known mechanisms by which small molecular weight compounds activate T-cells would need to be investigated; hapten (conjugated peptides presented), Pi (pharmacological interaction with both TCR and MHC-peptides) and altered self-repertoire (topological disruption of the HLA-peptide interaction resulting in alternative TCR specificity). Thus, while the modification of abacavir (as described in *Structural Alerts*) serves as a striking application for *in-silico* modelling, the importance of accompanying functional studies was demonstrated, and the challenges associated with redesign for circumvention of deleterious interaction with even a single HLA allele illustrates the scale of development required for these assays to come to fruition. Moreover, there is no assurance in such studies that the redesign of immunocophore implicated in HLA-B*57:01 associated hypersensitivity does not give rise to a problematic, potentially worse scenario with another HLA allele. In the future, computer systems may be developed that incorporate outputs from many of the aforementioned *in-vitro* assays to yield an estimated risk assessment based on compound performance across the board. It must be noted however, that as discussed, *in-silico* models will likely only be as good as the data provided to them. Hence, further development of existing, and inception of novel assays will likely prove imperative to optimal implementation of such systems.

Perspective of Preclinical Assays

Great strides have been made in the last 50 years to utilise empirical evidence relating chemical structure to direct and immuno-toxicological profiles, and to use this alongside preclinical screening assays in weight of evidence decision making processes. Despite this, the process is far from perfect, and several high profile therapeutics have failed at late stages of development in recent years. The current approach in industrial drug development heavily relies on chemical properties, particularly reactivity. This has substantially contributed to better informed drug design and more effective management of the risk profiles of established compounds with hypersensitivity liabilities. However, as outlined herein, these characteristics do not directly or completely translate to biological response, and much of the focus has been on mitigating direct toxicological properties rather than immunological liabilities per-se, and so there is an unmet requirement for cell-based assays to indicate these potential risks of compounds. The unfortunate truth in the arena of preclinical assays for hypersensitivity (delayed-type hypersensitivity reactions in particular) is that there is not yet an assay with adequate predictive capacity to mitigate such risk. As such, S8 2.7 of the ICH safety guidelines offers little in terms of recommended precautionary action (246). No *in-vitro* preclinical assay exists which possesses overarching applicability across all immune-mediated hypersensitivity reactions, which perhaps reflects the heterogeneity of such reactions. A quixotic, overarching model is unachievable at this time and so a composite of existing and future assays that feed into the two signal model is likely to be key to improvement and further bridging of the gap *in-vitro*. As outlined in (**Figure 2**), there are a plethora of factors that feed into both of these attributes, while drug development workflows can focus on drug-dependent liabilities, many of these factors are drug-independent. Careful due diligence in the form of target safety assessments may shed light on potential challenges with intended populations and pharmacological effects, and help aid with construction of product-tailored models. *In-silico* methods may also be useful in this regard to incorporate population specific parameters for initiating toxicological mechanisms and also to facilitate safety margin approximations. However, it will ultimately be incredibly difficult to build idiosyncratic features into preclinical development models, and so we may need to accept there will always be unknowns in this regard with each development venture. This is where precision medicine is needed, and HLA genotyping has proven how mechanistic insight and astute pharmacovigilance can be critical (to the point of therapeutic resurrection) once a drug encounters such issues within the clinic.

CONCLUSIONS

The prediction of hypersensitivity/idiosyncratic liabilities for a given compound in drug development and diagnosis of individuals with such ailments remain largely intractable issues. Investment required for development of new therapeutics is ascending, thus so too is the cost of attrition due to hypersensitivity. Moreover, in this era of immunological enlightenment, where pharmacological attempts to wield the immune system are becoming ever more frequent, it is becoming apparent that these therapeutics and their associated risks will bring the field to the fore of development toxicology. Better *in-vitro* assays to diagnose and predict immune liabilities of therapeutics are therefore long awaited and needed more now than ever. Half a century of investment and progress in understanding the mechanistic aspects of these reactions has yielded some great returns. As our understanding of hypersensitivity reactions continues to evolve, so too will our progression in modelling, accurate diagnosis and prediction of them in the coming decades. One anticipates that key frontiers in the immediate future will be the modernisation and harmonisation of *in-vitro* diagnostic assays, and the investment in (and composite interpretation of) biological assays that independently encapsulate antigenicity or adjuvanticity of therapeutics.

AUTHOR CONTRIBUTIONS

SH and PT wrote the manuscript and created the figures. XM and DN revised the manuscript. All authors contributed to the article and approved the submitted version.

FUNDING

This manuscript received no direct funding.

SH and PT were funded by grants from Otsuka Pharmaceutical and Merck Pharmaceuticals respectively.

REFERENCES

1. Roth RA, Ganey PE. Animal models of idiosyncratic drug-induced liver injury–current status. *Crit Rev Toxicol* (2011) 41(9):723–39. doi: 10.3109/10408444.2011.575765
2. Uetrecht J. Role of animal models in the study of drug-induced hypersensitivity reactions. *AAPS J* (2005) 7(4):E914–E21. doi: 10.1208/aapsj070489
3. Esser PR, Martin SF. Pathomechanisms of Contact Sensitization. *Curr Allergy Asthma Rep* (2017) 17(12):83. doi: 10.1007/s11882-017-0752-8
4. Landsteiner K, Jacobs J. Studies on the sensitization of animals with simple chemical compounds. *J Exp Med* (1935) 61(5):643–56. doi: 10.1084/jem.61.5.643
5. Zanni MP, von Greyerz S, Schnyder B, Brander KA, Frutig K, Hari Y, et al. HLA-restricted, processing-and metabolism-independent pathway of drug recognition by human alpha beta T lymphocytes. *J Clin Invest* (1998) 102 (8):1591. doi: 10.1172/JCI3544
6. Illing PT, Vivian JP, Dudek NL, Kostenko L, Chen Z, Bharadwaj M, et al. Immune self-reactivity triggered by drug-modified HLA-peptide repertoire. *Nature* (2012) 486(7404):554–8. doi: 10.1038/nature11147
7. Pichler WJ. Immune pathomechanism and classification of drug hypersensitivity. *Allergy* (2019) 74(8):1457–71. doi: 10.1111/all.13765
8. Hammond S, Thomson PJ, Ogese MO, Naisbitt DJ. T-cell activation by low molecular weight drugs and factors that influence susceptibility to drug hypersensitivity. *Chem Res Toxicol* (2019) 33(1):77–94. doi: 10.1021/acs.chemrestox.9b00327
9. Matzinger P. Tolerance, danger, and the extended family. *Annu Rev Immunol* (1994) 12(1):991–1045. doi: 10.1146/annurev.iy.12.040194.005015
10. Matzinger P. The danger model: a renewed sense of self. *Science* (2002) 296 (5566):301–5. doi: 10.1126/science.1071059
11. Chen L, Flies DB. Molecular mechanisms of T cell co-stimulation and co-inhibition. *Nat Rev Immunol* (2013) 13(4):227–42. doi: 10.1038/nri3405
12. Shirali AC, Perazella MA, Gettinger S. Association of acute interstitial nephritis with programmed cell death 1 inhibitor therapy in lung cancer patients. *Am J Kidney Dis* (2016) 68(2):287–91. doi: 10.1053/j.ajkd.2016.02.057
13. Koda R, Watanabe H, Tsuchida M, Iino N, Suzuki K, Hasegawa G, et al. Immune checkpoint inhibitor (nivolumab)-associated kidney injury and the importance of recognizing concomitant medications known to cause acute tubulointerstitial nephritis: A case report. *BMC Nephrol* (2018) 19(1):48. doi: 10.1186/s12882-018-0848-y
14. Kimura H, Hasegawa A, Takei I, Kawai T, Tsuchida Y, Abe Y, et al. Characteristic pathological features of keratinocyte death in a case of Stevens–Johnson syndrome manifested by an immune checkpoint inhibitor. *J Eur Acad Dermatol Venereol* (2020) 35(2):e142–5. doi: 10.1111/jdv.16872
15. Ford M, Sahbudin I, Filer A, Steven N, Fisher BA. High proportion of drug hypersensitivity reactions to sulfasalazine following its use in anti-PD-1-associated inflammatory arthritis. *Rheumatology* (2018) 57(12):2244–6. doi: 10.1093/rheumatology/key234
16. Yamazaki N, Uhara H, Fukushima S, Uchi H, Shibagaki N, Kiyohara Y, et al. Phase II study of the immune-checkpoint inhibitor ipilimumab plus dacarbazine in Japanese patients with previously untreated, unresectable or metastatic melanoma. *Cancer Chemother Pharmacol* (2015) 76(5):969–75. doi: 10.1007/s00280-015-2870-0
17. Uhara H, Kiyohara Y, Tsuda A, Takata M, Yamazaki N. Characteristics of adverse drug reactions in a vemurafenib early post-marketing phase vigilance study in Japan. *Clin Trans Oncol* (2018) 20(2):169–75. doi: 10.1007/s12094-017-1706-2
18. Naisbitt DJ, Olsson-Brown A, Gibson A, Meng X, Ogese MO, Tailor A, et al. Immune dysregulation increases the incidence of delayed-type drug hypersensitivity reactions. *Allergy* (2019) 75(2):781–97. doi: 10.1111/all.14127
19. Li J, Uetrecht JP. The danger hypothesis applied to idiosyncratic drug reactions. *Handb Exp Pharmacol* (2010) 196):493–509. doi: 10.1007/978-3-642-00663-0_18
20. Mayorga C, Fernandez TD, Montañez MI, Moreno E, Torres MJ. Recent developments and highlights in drug hypersensitivity. *Allergy* (2019) 74 (12):2368–81. doi: 10.1111/all.14061
21. White KD, Chung W-H, Hung S-I, Mallal S, Phillips EJ. Evolving models of the immunopathogenesis of T cell–mediated drug allergy: The role of host, pathogens, and drug response. *J Allergy Clin Immunol* (2015) 136(2):219–34. doi: 10.1016/j.jaci.2015.05.050
22. Brockow K, Ardern-Jones MR, Mockenhaupt M, Aberer W, Barbaud A, Caubet JC, et al. EAACI position paper on how to classify cutaneous manifestations of drug hypersensitivity. *Allergy* (2019) 74(1):14–27. doi: 10.1111/all.13562
23. Uetrecht J, Naisbitt DJ. Idiosyncratic adverse drug reactions: current concepts. *Pharmacol Rev* (2013) 65(2):779–808. doi: 10.1124/pr.113.007450
24. Aberer W, Bircher A, Romano A, Blanca M, Campi P, Fernandez J, et al. Drug provocation testing in the diagnosis of drug hypersensitivity reactions: general considerations. *Allergy* (2003) 58(9):854–63. doi: 10.1034/j.1398-9995.2003.00279.x
25. Andrade RJ, Robles M, Lucena MI. Rechallenge in drug-induced liver injury: the attractive hazard. *Expert Opin Drug Saf* (2009) 8(6):709–14. doi: 10.1517/14740330903397378
26. Mushin WW, Rosen M, Jones E. Post-halothane jaundice in relation to previous administration of halothane. *Br Med J* (1971) 3(5765):18–22. doi: 10.1136/bmj.3.5765.18
27. Brockow K, Romano A, Blanca M, Ring J, Pichler W, Demoly P. General considerations for skin test procedures in the diagnosis of drug hypersensitivity. *Allergy* (2002) 57(1):45–51. doi: 10.1046/j.0105-4538.2001.00001.x-i8
28. Romano A, Viola M, Gaeta F, Rumi G, Maggioletti M. Patch testing in non-immediate drug eruptions. *Allergy Asthma Clin Immunol* (2008) 4(2):66–74. doi: 10.1186/1710-1492-4-2-66
29. Brockow K, Romano A. Skin tests in the diagnosis of drug hypersensitivity reactions. *Curr Pharm Des* (2008) 14(27):2778–91. doi: 10.2174/138161208786369821
30. Romano A, Viola M, Mondino C, Pettinato R, Di Fonso M, Papa G, et al. Diagnosing nonimmediate reactions to penicillins by in vivo tests. *Int Arch Allergy Immunol* (2002) 129(2):169–74. doi: 10.1159/000065876
31. Torres MJ, Sanchez-Sabate E, Alvarez J, Mayorga C, Fernandez J, Padial A, et al. Skin test evaluation in nonimmediate allergic reactions to penicillins. *Allergy* (2004) 59(2):219–24. doi: 10.1046/j.1398-9995.2003.00308.x
32. Brockow K, Przybilla B, Aberer W, Bircher AJ, Brehler R, Dickel H, et al. Guideline for the diagnosis of drug hypersensitivity reactions. *Allergo J Int* (2015) 24(3):94–105. doi: 10.1007/s40629-015-0052-6
33. Barbaud A, Weinborn M, Garvey LH, Testi S, Kvedariene V, Bavbek S, et al. Intradermal Tests With Drugs: An Approach to Standardization. *Front Med* (2020) 7:156. doi: 10.3389/fmed.2020.00156
34. Doña I, Romano A, Torres MJ. Algorithm for betalactam allergy diagnosis. *Allergy* (2019) 74(9):1817–9. doi: 10.1111/all.13844
35. Lammintausta K, Kortekangas-Savolainen O. The usefulness of skin tests to prove drug hypersensitivity. *Br J Dermatol* (2005) 152(5):968–74. doi: 10.1111/j.1365-2133.2005.06429.x
36. Padial A, Antunez C, Blanca-Lopez N, Fernandez TD, Cornejo-Garcia JA, Mayorga C, et al. Non-immediate reactions to beta-lactams: diagnostic value of skin testing and drug provocation test. *Clin Exp Allergy* (2008) 38(5):822–8. doi: 10.1111/j.1365-2222.2008.02961.x
37. Schnyder B, Helbling A, Kappeler A, Pichler W. Drug-induced papulovesicular exanthema. *Allergy* (1998) 53(8):817–8. doi: 10.1111/j.1398-9995.1998.tb03985.x
38. Mallal S, Phillips E, Carosi G, Molina J-M, Workman C, Tomažič J, et al. HLA-B* 5701 screening for hypersensitivity to abacavir. *N Engl J Med* (2008) 358(6):568–79. doi: 10.1056/NEJMoa0706135
39. Saag M, Balu R, Phillips E, Brachman P, Martorell C, Burman W, et al. High sensitivity of human leukocyte antigen-b* 5701 as a marker for immunologically confirmed abacavir hypersensitivity in white and black patients. *Clin Infect Dis* (2008) 46(7):1111–8. doi: 10.1086/529382
40. Hetherington S, Hughes AR, Mosteller M, Shortino D, Baker KL, Spreen W, et al. Genetic variations in HLA-B region and hypersensitivity reactions to abacavir. *Lancet* (2002) 359(9312):1121–2. doi: 10.1016/S0140-6736(02)08158-8
41. Young B, Squires K, Patel P, Dejesus E, Bellos N, Berger D, et al. First large, multicenter, open-label study utilizing HLA-B*5701 screening for abacavir

hypersensitivity in North America. *AIDS (London England)* (2008) 22 (13):1673–5. doi: 10.1097/QAD.0b013e32830719aa
42. Mallal S, Nolan D, Witt C, Masel G, Martin AM, Moore C, et al. Association between presence of HLA-B*5701, HLA-DR7, and HLA-DQ3 and hypersensitivity to HIV-1 reverse-transcriptase inhibitor abacavir. *Lancet* (2002) 359(9308):727–32. doi: 10.1016/S0140-6736(02)07873-X
43. Ruiz-Iruela C, Padulles-Zamora N, Podzamczer-Palter D, Alonso-Pastor A, Candas-Estebanez B, Alia-Ramos P, et al. HLA-B*57:01 genotyping in the prevention of hypersensitivity to abacavir: 5 years of experience. *Pharmacogenet Genomics* (2016) 26:390–6. doi: 10.1097/FPC.0000000000000229
44. Hughes DA, Vilar FJ, Ward CC, Alfirevic A, Park BK, Pirmohamed M. Cost-effectiveness analysis of HLA B* 5701 genotyping in preventing abacavir hypersensitivity. *Pharmacogenet Genomics* (2004) 14(6):335–42. doi: 10.1097/00008571-200406000-00002
45. Calatrava DN, de la Calle-Martín Ó, Iribarren-Loyarte JA, Rivero-Román A, García-Bujalance L, Pérez-Escolano I, et al. Cost-effectiveness analysis of HLA-B* 5701 typing in the prevention of hypersensitivity to abacavir in HIV + patients in Spain. *Enferm Infecc Microbiol Clin* (2010) 28(9):590–5. doi: 10.1016/j.eimc.2009.09.010
46. Schackman BR, Scott CA, Walensky RP, Losina E, Freedberg KA, Sax PE. The cost-effectiveness of HLA-B* 5701 genetic screening to guide initial antiretroviral therapy for HIV. *AIDS (London England)* (2008) 22(15):2025. doi: 10.1097/QAD.0b013e3283103ce6
47. Chessman D, Kostenko L, Lethborg T, Purcell AW, Williamson NA, Chen Z, et al. Human leukocyte antigen class I-restricted activation of CD8+ T cells provides the immunogenetic basis of a systemic drug hypersensitivity. *Immunity* (2008) 28(6):822–32. doi: 10.1016/j.immuni.2008.04.020
48. Chung W-H, Hung S-I, Hong H-S, Hsih M-S, Yang L-C, Ho H-C, et al. Medical genetics: a marker for Stevens–Johnson syndrome. *Nature* (2004) 428(6982):486. doi: 10.1038/428486a
49. Halpern B, Amache N. Diagnosis of drug allergy in vitro with the lymphocyte transformation test. *J Allergy* (1967) 40(3):168–81. doi: 10.1016/0021-8707(67)90006-8
50. Holland P, Mauer A. Drug-induced *in-vitro* stimulation of peripheral lymphocytes. *Lancet* (1964) 283(7347):1368–9. doi: 10.1016/S0140-6736(64)92046-X
51. Caron G, Sarkany I, Williams H, Todd A, Gell HC. Radioactive method for the measurement of lymphocyte transformation in vitro. *Lancet* (1965) 286 (7425):1266–8. doi: 10.1016/S0140-6736(65)92282-8
52. Warrington R, Tse K. Lymphocyte transformation studies in drug hypersensitivity. *Can Med Assoc J* (1979) 120(9):1089.
53. Pichler WJ. Delayed drug hypersensitivity reactions. *Ann Internal Med* (2003) 139(8):683–93. doi: 10.7326/0003-4819-139-8-200310210-00012
54. Doña I, Torres MJ, Montañez MI, Fernández TD. In vitro diagnostic testing for antibiotic allergy. *Allergy Asthma Immunol Res* (2017) 9(4):288–98. doi: 10.4168/aair.2017.9.4.288
55. Vischer T. Lymphocyte cultures in drug hypersensitivity. *Lancet* (1966) 288:467–9. doi: 10.1016/S0140-6736(66)92773-5
56. Johnston C, Russell A, Aaron S. The effect of in vivo and in vitro methotrexate on lymphocyte proliferation as measured by the uptake of tritiated thymidine and tritiated guanosine. *Clin Exp Rheumatol* (1988) 6 (4):391–3.
57. Porebski G, Gschwend-Zawodniak A, Pichler WJ. In vitro diagnosis of T cell-mediated drug allergy. *Clin Exp Allergy* (2011) 41(4):461–70. doi: 10.1111/j.1365-2222.2011.03701.x
58. Kano Y, Hirahara K, Mitsuyama Y, Takahashi R, Shiohara T. Utility of the lymphocyte transformation test in the diagnosis of drug sensitivity: dependence on its timing and the type of drug eruption. *Allergy* (2007) 62 (12):1439–44. doi: 10.1111/j.1398-9995.2007.01553.x
59. Torres M, Mayorga C, Cornejo-Garcia J, Lopez S, Chaves P, Rondon C, et al. Monitoring non-immediate allergic reactions to iodine contrast media. *Clin Exp Immunol* (2008) 152(2):233–8. doi: 10.1111/j.1365-2249.2008.03627.x
60. Antunez C, Barbaud A, Gomez E, Audonnet S, Lopez S, Guéant-Rodriguez RM, et al. Recognition of iodixanol by dendritic cells increases the cellular response in delayed allergic reactions to contrast media. *Clin Exp Allergy* (2011) 41(5):657–64. doi: 10.1111/j.1365-2222.2010.03693.x
61. Whitaker P, Meng X, Lavergne SN, El-Ghaiesh S, Monshi M, Earnshaw C, et al. Mass Spectrometric Characterization of Circulating and Functional Antigens Derived from Piperacillin in Patients with Cystic Fibrosis. *J Immunol* (2011) 187(1):200–11. doi: 10.4049/jimmunol.1100647
62. Pichler WJ, Tilch J. The lymphocyte transformation test in the diagnosis of drug hypersensitivity. *Allergy* (2004) 59(8):809–20. doi: 10.1111/j.1398-9995.2004.00547.x
63. Walker C, Kristensen F, Bettens F. Lymphokine regulation of activated (G1) lymphocytes. I. Prostaglandin E2-induced inhibition of interleukin 2 production. *J Immunol* (1983) 130(4):1770–3.
64. Rodriguez-Pena R, Lopez S, Mayorga C, Antunez C, Fernandez TD, Torres MJ, et al. Potential involvement of dendritic cells in delayed-type hypersensitivity reactions to β-lactams. *J Allergy Clin Immunol* (2006) 118 (4):949–56. doi: 10.1016/j.jaci.2006.07.013
65. Lopez S, Torres M, Rodríguez-Pena R, Blanca-Lopez N, Fernandez T, Antunez C, et al. Lymphocyte proliferation response in patients with delayed hypersensitivity reactions to heparins. *Br J Dermatol* (2009) 160 (2):259–65. doi: 10.1111/j.1365-2133.2008.08875.x
66. Aiba S, Terunuma A, Manome H, Tagami H. Dendritic cells differently respond to haptens and irritants by their production of cytokines and expression of co-stimulatory molecules. *Eur J Immunol* (1997) 27 (11):3031–8. doi: 10.1002/eji.1830271141
67. Francisco LM, Salinas VH, Brown KE, Vanguri VK, Freeman GJ, Kuchroo VK, et al. PD-L1 regulates the development, maintenance, and function of induced regulatory T cells. *J Exp Med* (2009) 206(13):3015–29. doi: 10.1084/jem.20090847
68. Fontenot JD, Rasmussen JP, Williams LM, Dooley JL, Farr AG, Rudensky AY. Regulatory T cell lineage specification by the forkhead transcription factor foxp3. *Immunity* (2005) 22(3):329–41. doi: 10.1016/j.immuni.2005.01.016
69. Vocanson M, Cluzel-Tailhardat M, Poyet G, Valeyrie M, Chavagnac C, Levarlet B, et al. Depletion of human peripheral blood lymphocytes in CD25 + cells allows for the sensitive in vitro screening of contact allergens. *J Invest Dermatol* (2008) 128(8):2119. doi: 10.1038/jid.2008.15
70. Triplett TA, Curti BD, Bonafede PR, Miller WL, Walker EB, Weinberg AD. Defining a functionally distinct subset of human memory CD4+ T cells that are CD25POS and FOXP3NEG. *Eur J Immunol* (2012) 42(7):1893–905. doi: 10.1002/eji.201242444
71. Amu S, Strömberg K, Bokarewa M, Tarkowski A, Brisslert M. CD25-expressing B-lymphocytes in rheumatic diseases. *Scand J Immunol* (2007) 65(2):182–91. doi: 10.1111/j.1365-3083.2006.01889.x
72. Herndler-Brandstetter D, Schwaiger S, Veel E, Fehrer C, Cioca DP, Almanzar G, et al. CD25-expressing CD8+ T cells are potent memory cells in old age. *J Immunol (Baltimore Md 1950)* (2005) 175(3):1566–74. doi: 10.4049/jimmunol.175.3.1566
73. Sugita K, Kabashima K, Sawada Y, Haruyama S, Yoshioka M, Mori T, et al. Blocking of CTLA-4 on lymphocytes improves the sensitivity of lymphocyte transformation tests in a patient with nickel allergy. *Eur J Dermatol* (2012) 22(2):268–9. doi: 10.1684/ejd.2012.1641
74. Berg PA, Becker EW. The lymphocyte transformation test-a debated method for the evaluation of drug allergic hepatic injury. *J Hepatol* (1995) 22(1):115–8. doi: 10.1016/0168-8278(95)80270-3
75. Lavergne SN, Park BK, Naisbitt DJ, Whitaker P, Peckham D, Conway S. Drug Metabolite-Specific Lymphocyte Responses in Sulfamethoxazole Allergic Patients with Cystic Fibrosis. *Chem Res In Toxicol* (2010) 23 (6):1009–11.ss. doi: 10.1021/tx100151v
76. Sachs B, Erdmann S, Al-Masaoudi T, Merk H. In vitro drug allergy detection system incorporating human liver microsomes in chlorazepate-induced skin rash: drug-specific proliferation associated with interleukin-5 secretion. *Br J Dermatol* (2001) 144(2):316–20. doi: 10.1046/j.1365-2133.2001.04021.x
77. Hertl M, Jugert F, Merk H. CD8+ dermal T cells from a sulphamethoxazole-induced bullous exanthem proliferate in response to drug-modified liver microsomes. *Br J Dermatol* (1995) 132(2):215–20. doi: 10.1111/j.1365-2133.1995.tb05016.x
78. Ganusov VV, De Boer RJ. Do most lymphocytes in humans really reside in the gut? *Trends Immunol* (2007) 28(12):514–8. doi: 10.1016/j.it.2007.08.009

79. Thomson PJ, Kafu L, Meng X, Snoeys J, De Bondt A, De Maeyer D, et al. Drug-specific T-cell responses in patients with liver injury following treatment with the BACE inhibitor atabecestat. *Allergy* (2020) 1–11. doi: 10.1111/all.14652
80. Gibson A, Hammond S, Jaruthamsophon K, Roth S, Mosedale M, Naisbitt DJ. Tolvaptan-and Tolvaptan-Metabolite-Responsive T Cells in Patients with Drug-Induced Liver Injury. *Chem Res Toxicol* (2020) 33(11):2745–8. doi: 10.1021/acs.chemrestox.0c00328
81. Monshi MM, Faulkner L, Gibson A, Jenkins RE, Farrell J , Earnshaw CJ, et al. Human leukocyte antigen (HLA)-B*57:01-restricted activation of drug-specific T cells provides the immunological basis for flucloxacillin-induced liver injury. *Hepatology* (2013) 57(2):727. doi: 10.1002/hep.26077
82. Baust JG, Gao D, Baust JM. Cryopreservation: An emerging paradigm change. *Organogenesis* (2009) 5(3):90–6. doi: 10.4161/org.5.3.10021
83. De Abajo FJ, Montero D, Madurga M, Rodríguez LAG. Acute and clinically relevant drug-induced liver injury: a population based case-control study. *Br J Clin Pharmacol* (2004) 58(1):71–80. doi: 10.1111/j.1365-2125.2004.02133.x
84. Kim SH, Saide K, Farrell J, Faulkner L, Tailor A, Ogese M, et al. Characterization of amoxicillin-and clavulanic acid-specific T cells in patients with amoxicillin-clavulanate–induced liver injury. *Hepatology* (2015) 62(3):887–99. doi: 10.1002/hep.27912
85. Merk HF. Diagnosis of drug hypersensitivity: lymphocyte transformation test and cytokines. *Toxicology* (2005) 209(2):217–20. doi: 10.1016/j.tox.2004.12.026
86. Mayorga C, Celik G, Rouzaire P, Whitaker P, Bonadonna P, Rodrigues-Cernadas J, et al. In vitro tests for drug hypersensitivity reactions: an ENDA/EAACI Drug Allergy Interest Group position paper. *Allergy* (2016) 71 (8):1103–34. doi: 10.1111/all.12886
87. Ziegler SF, Ramsdell F, Alderson MR. The activation antigen CD69. *Stem Cells (Dayton Ohio)* (1994) 12(5):456–65. doi: 10.1002/stem.5530120502
88. Simms PE, Ellis TM. Utility of flow cytometric detection of CD69 expression as a rapid method for determining poly-and oligoclonal lymphocyte activation. *Clin Diagn Lab Immunol* (1996) 3(3):301–4. doi: 10.1128/CDLI.3.3.301-304.1996
89. Beeler A, Zaccaria L, Kawabata T, Gerber BO, Pichler WJ. CD69 upregulation on T cells as an in vitro marker for delayed-type drug hypersensitivity. *Allergy* (2008) 63(2):181–8. doi: 10.1111/j.1398-9995.2007.01516.x
90. Porebski G, Pecaric-Petkovic T, Groux-Keller M, Bosak M, Kawabata T, Pichler WJ. In vitro drug causality assessment in Stevens–Johnson syndrome–alternatives for lymphocyte transformation test. *Clin Exp Allergy* (2013) 43(9):1027–37. doi: 10.1111/cea.12145
91. Zawodniak A, Lochmatter P, Yerly D, Kawabata T, Lerch M, Yawalkar N, et al. In vitro detection of cytotoxic T and NK cells in peripheral blood of patients with various drug-induced skin diseases. *Allergy* (2010) 65(3):376–84. doi: 10.1111/j.1398-9995.2009.02180.x
92. Thakur A, Pedersen LE, Jungersen G. Immune markers and correlates of protection for vaccine induced immune responses. *Vaccine* (2012) 30 (33):4907–20. doi: 10.1016/j.vaccine.2012.05.049
93. Bolton DL, Roederer M. Flow cytometry and the future of vaccine development. *Expert Rev Vaccines* (2009) 8(6):779–89. doi: 10.1586/erv.09.41
94. Dan JM, Arlehamn CSL, Weiskopf D, da Silva Antunes R, Havenar-Daughton C, Reiss SM, et al. A cytokine-independent approach to identify antigen-specific human germinal center T follicular helper cells and rare antigen-specific CD4+ T cells in blood. *J Immunol* (2016) 197(3):983–93. doi: 10.4049/jimmunol.1600318
95. Shear NH, Spielberg SP, Grant DM, Tang BK, Kalow W. Differences in metabolism of sulfonamides predisposing to idiosyncratic toxicity. *Ann Internal Med* (1986) 105(2):179–84. doi: 10.7326/0003-4819-105-2-179
96. Rieder MJ, Uetrecht J, Shear NH, Cannon M, Miller M, Spielberg SP. Diagnosis of sulfonamide hypersensitivity reactions by *in-vitro* "rechallenge" with hydroxylamine metabolites. *Ann Intern Med* (1989) 110(4):286–9. doi: 10.7326/0003-4819-110-4-286
97. Shear N, Spielberg S. In vitro evaluation of a toxic metabolite of sulfadiazine. *Can J Physiol Pharmacol* (1985) 63(11):1370–2. doi: 10.1139/y85-225
98. Benesic A, Rahm NL, Ernst S, Gerbes AL. Human monocyte-derived cells with individual hepatocyte characteristics: a novel tool for personalized in vitro studies. *Lab Invest* (2012) 92(6):926–36. doi: 10.1038/labinvest.2012.64
99. Benesic A, Rotter I, Dragoi D, Weber S, Buchholtz ML, Gerbes AL. Development and Validation of a Test to Identify Drugs That Cause Idiosyncratic Drug-Induced Liver Injury. *Clin Gastroenterol Hepatol* (2018) 16(9):1488–94.e5. doi: 10.1016/j.cgh.2018.04.049
100. Benesic A, Leitl A, Gerbes AL. Monocyte-derived hepatocyte-like cells for causality assessment of idiosyncratic drug-induced liver injury. *Gut* (2016) 65(9):1555–63. doi: 10.1136/gutjnl-2015-309528
101. Ashby J. Fundamental structural alerts to potential carcinogenicity or noncarcinogenicity. *Environ Mutagen* (1985) 7(6):919–21. doi: 10.1002/em.2860070613
102. Ashby J, Tennant RW. Chemical structure, Salmonella mutagenicity and extent of carcinogenicity as indicators of genotoxic carcinogenesis among 222 chemicals tested in rodents by the US NCI/NTP. *Mutat Res Genet Toxicol* (1988) 204(1):17–115. doi: 10.1016/0165-1218(88)90114-0
103. Ames BN, . Mott prize CS. The detection of environmental mutagens and potential carcinogens. *Cancer* (1984) 53(10):2034–40. doi: 10.1002/1097-0142(19840515)53:10<2034::AID-CNCR2820531005>3.0.CO;2-S
104. Miller EC, Miller JA. The presence and significance of bound aminoazo dyes in the livers of rats fed p-dimethylaminoazobenzene. *Cancer Res* (1947) 7 (7):468–80.
105. Miller EC, Miller JA. Searches for ultimate chemical carcinogens and their reactions with cellular macromolecules. *Cancer* (1981) 47 (10):2327–45. doi: 10.1002/1097-0142(19810515)47:10<2327::AID-CNCR2820471003>3.0.CO;2-Z
106. Zeiger E. Carcinogenicity of mutagens: predictive capability of the Salmonella mutagenesis assay for rodent carcinogenicity. *Cancer Res* (1987) 47(5):1287–96.
107. Brodie BB, Reid WD, Cho AK, Sipes G, Krishna G, Gillette JR. Possible mechanism of liver necrosis caused by aromatic organic compounds. *Proc Natl Acad Sci* (1971) 68(1):160–4. doi: 10.1073/pnas.68.1.160
108. Gillette JR, Mitchell JR, Brodie BB. Biochemical mechanisms of drug toxicity. *Annu Rev Pharmacol* (1974) 14(1):271–88. doi: 10.1146/annurev.pa.14.040174.001415
109. Yang H, Sun L, Li W, Liu G, Tang Y. In Silico Prediction of Chemical Toxicity for Drug Design Using Machine Learning Methods and Structural Alerts. *Front Chem* (2018) 6:30. doi: 10.3389/fchem.2018.00129
110. Plošnik A, Vračko M, Sollner Dolenc M. Mutagenic and carcinogenic structural alerts and their mechanisms of action. *Arh Hig Rada Toksikol* (2016) 67(3):169–82. doi: 10.1515/aiht-2016-67-2801
111. Martin EA, Rich KJ, White IN, Woods KL, Powles TJ, Smith LL. 32P-postlabelled DNA adducts in liver obtained from women treated with tamoxifen. *Carcinogenesis* (1995) 16(7):1651–4. doi: 10.1093/carcin/16.7.1651
112. Boocock DJ, Maggs JL, White IN, Park BK. α-Hydroxytamoxifen, a genotoxic metabolite of tamoxifen in the rat: identification and quantification in vivo and in vitro. *Carcinogenesis* (1999) 20(1):153–60. doi: 10.1093/carcin/20.1.153
113. Shibutani S, Dasaradhi L, Terashima I, Banoglu E, Duffel MW. α-Hydroxytamoxifen is a substrate of hydroxysteroid (alcohol) sulfotransferase, resulting in tamoxifen DNA adducts. *Cancer Res* (1998) 58(4):647–53.
114. Shibutani S, Shaw PM, Suzuki N, Dasaradhi L, Duffel MW, Terashima I. Sulfation of alpha-hydroxytamoxifen catalyzed by human hydroxysteroid sulfotransferase results in tamoxifen-DNA adducts. *Carcinogenesis* (1998) 19 (11):2007–11. doi: 10.1093/carcin/19.11.2007
115. Yip VLM, Meng X, Maggs JL, Jenkins RE, Marlot PT, Marson AG, et al. Mass Spectrometric Characterization of Circulating Covalent Protein Adducts Derived from Epoxide Metabolites of Carbamazepine in Patients. *Chem Res Toxicol* (2017) 30(7):1419–35. doi: 10.1021/acs.chemrestox.7b00063
116. Aleksic M, Pease CK, Basketter DA, Panico M, Morris HR, Dell A. Mass spectrometric identification of covalent adducts of the skin allergen 2, 4-dinitro-1-chlorobenzene and model skin proteins. *Toxicol Vitro* (2008) 22 (5):1169–76. doi: 10.1016/j.tiv.2008.03.006
117. Xiaoli M, Al-Attar Z, Yaseen FS, Jenkins R, Earnshaw C, Whitaker P, et al. Definition of the Nature and Hapten Threshold of the β-Lactam Antigen

Required for T Cell Activation In Vitro and in Patients. *J Immunol* (2017) 198(11):4217–27. doi: 10.4049/jimmunol.1700209
118. Park KB, Dalton-Brown E, Hirst C, Williams DP. Selection of new chemical entities with decreased potential for adverse drug reactions. *Eur J Pharmacol* (2006) 549(1-3):1–8. doi: 10.1016/j.ejphar.2006.08.025
119. Marquié C. Chemical reactions in cottonseed protein cross-linking by formaldehyde, glutaraldehyde, and glyoxal for the formation of protein films with enhanced mechanical properties. *J Agric Food Chem* (2001) 49 (10):4676–81. doi: 10.1021/jf0101152
120. Enoch SJ, Ellison CM, Schultz TW, Cronin MT. A review of the electrophilic reaction chemistry involved in covalent protein binding relevant to toxicity. *Crit Rev Toxicol* (2011) 41(9):783–802. doi: 10.3109/10408444.2011.598141
121. Meng X, Al-Attar Z, Yaseen FS, Jenkins R, Earnshaw C, Whitaker P, et al. Definition of the Nature and Hapten Threshold of the beta-Lactam Antigen Required for T Cell Activation In Vitro and in Patients. *J Immunol (Baltimore Md 1950)* (2017) 198(11):4217–27. doi: 10.4049/jimmunol.1700209
122. Williams DP, Park BK. Idiosyncratic toxicity: the role of toxicophores and bioactivation. *Drug Discov Today* (2003) 8(22):1044–50. doi: 10.1016/S1359-6446(03)02888-5
123. Williams DP, Naisbitt DJ. Toxicophores: groups and metabolic routes associated with increased safety risk. *Curr Opin Drug Discov Devel* (2002) 5(1):104–15.
124. Park K, Williams DP, Naisbitt DJ, Kitteringham NR, Pirmohamed M. Investigation of toxic metabolites during drug development. *Toxicol Appl Pharmacol* (2005) 207(2 Suppl):425–34. doi: 10.1016/j.taap.2005.02.029
125. Sanderson JP, Naisbitt DJ, Park BK. Role of bioactivation in drug-induced hypersensitivity reactions. *AAPS J* (2006) 8(1):E55–64. doi: 10.1208/aapsj080107
126. Lavergne SN, Park BK, Naisbitt DJ. The roles of drug metabolism in the pathogenesis of T-cell-mediated drug hypersensitivity. *Curr Opin Allergy Clin Immunol* (2008) 8(4):299–307. doi: 10.1097/ACI.0b013e3283079c64
127. Naisbitt DJ, Williams DP, Pirmohamed M, Kitteringham NR, Park BK. Reactive metabolites and their role in drug reactions. *Curr Opin Allergy Clin Immunol* (2001) 1(4):317–25. doi: 10.1097/01.all.0000011033.64625.5a
128. Stepan AF, Walker DP, Bauman J, Price DA, Baillie TA, Kalgutkar AS, et al. Structural alert/reactive metabolite concept as applied in medicinal chemistry to mitigate the risk of idiosyncratic drug toxicity: a perspective based on the critical examination of trends in the top 200 drugs marketed in the United States. *Chem Res Toxicol* (2011) 24(9):1345–410. doi: 10.1021/tx200168d
129. Maggs J, Tingle M, Kitteringham N, Park B. Drug-protein conjugates—XIV: mechanisms of formation of protein-arylating intermediates from amodiaquine, a myelotoxin and hepatotoxin in man. *Biochem Pharmacol* (1988) 37(2):303–11. doi: 10.1016/0006-2952(88)90733-2
130. James LP, Mayeux PR, Hinson JA. Acetaminophen-induced hepatotoxicity. *Drug Metab Dispos* (2003) 31(12):1499–506. doi: 10.1124/dmd.31.12.1499
131. Callan HE, Jenkins RE, Maggs JL, Lavergne SN, Clarke SE, Naisbitt DJ, et al. Multiple adduction reactions of nitroso sulfamethoxazole with cysteinyl residues of peptides and proteins: implications for hapten formation. *Chem Res Toxicol* (2009) 22(5):937–48. doi: 10.1021/tx900034r
132. Alzahrani A, Ogese M, Meng X, Waddington JC, Tailor A, Farrell J, et al. Dapsone and Nitroso Dapsone Activation of Naive T-Cells from Healthy Donors. *Chem Res Toxicol* (2017) 30(12):2174–86. doi: 10.1021/acs.chemrestox.7b00263
133. Kalgutkar AS, Gardner I, Obach RS, Shaffer CL, Callegari E, Henne KR, et al. A comprehensive listing of bioactivation pathways of organic functional groups. *Curr Drug Metab* (2005) 6(3):161–225. doi: 10.2174/1389200054021799
134. Bakke OM, Manocchia M, de Abajo F, Kaitin KI, Lasagna L. Drug safety discontinuations in the United Kingdom, the United States, and Spain from 1974 through 1993: a regulatory perspective. *Clin Pharmacol Ther* (1995) 58 (1):108–17. doi: 10.1016/0009-9236(95)90078-0
135. O'Donnell JP, Dalvie DK, Kalgutkar AS, Obach RS. Mechanism-based inactivation of human recombinant P450 2C9 by the nonsteroidal anti-inflammatory drug suprofen. *Drug Metab Dispos* (2003) 31(11):1369–77. doi: 10.1124/dmd.31.11.1369
136. Snyder S,, Teehan BP. Suprofen and renal failure. *Ann Internal Med* (1987) 106(5):776–. doi: 10.7326/0003-4819-106-5-776_1
137. Carbone C, Rende P, Comberiati P, Carnovale D, Mammì M, De Sarro G. The safety of ketoprofen in different ages. *J Pharmacol Pharmacother* (2013) 4(Suppl1):S99. doi: 10.4103/0976-500X.120967
138. Lind D, Levi J, Vincent P. Amodiaquine-induced agranulocytosis: toxic effect of amodiaquine in bone marrow cultures in vitro. *Br Med J* (1973) 1 (5851):458–60. doi: 10.1136/bmj.1.5851.458
139. Neftel KA, Woodtly W, Schmid M, Frick PG, Fehr J. Amodiaquine induced agranulocytosis and liver damage. *Br Med J (Clin Res Ed)* (1986) 292 (6522):721–3. doi: 10.1136/bmj.292.6522.721
140. Harrison AC, Kitteringham NR, Clarke JB, Park BK. The mechanism of bioactivation and antigen formation of amodiaquine in the rat. *Biochem Pharmacol* (1992) 43(7):1421–30. doi: 10.1016/0006-2952(92)90198-R
141. Jewell H, Maggs J, Harrison A, O'neill P, Ruscoe J, Park B. Role of hepatic metabolism in the bioactivation and detoxication of amodiaquine. *Xenobiotica* (1995) 25(2):199–217. doi: 10.3109/00498259509061845
142. Clarke J, Maggs J, Kitteringham N, Park B. Immunogenicity of amodiaquine in the rat. *Int Arch Allergy Immunol* (1990) 91(4):335–42. doi: 10.1159/000235138
143. Shimizu S, Atsumi R, Itokawa K, Iwasaki M, Aoki T, Ono C, et al. Metabolism-dependent hepatotoxicity of amodiaquine in glutathione-depleted mice. *Arch Toxicol* (2009) 83(7):701. doi: 10.1007/s00204-009-0436-9
144. Clarke J, Neftel K, Kitteringham N, Park B. Detection of antidrug IgG antibodies in patients with adverse drug reactions to amodiaquine. *Int Arch Allergy Immunol* (1991) 95(4):369–75. doi: 10.1159/000235475
145. Liu F, Cai P, Metushi I, Li J, Nakayawa T, Vega L, et al. Exploring an animal model of amodiaquine-induced liver injury in rats and mice. *J Immunotoxicol* (2016) 13 (5):694–712. doi: 10.3109/1547691X.2016.1166167
146. Delarue S, Girault S, Maes L, Debreu-Fontaine M-A, Labaeïd M, Grellier P, et al. Synthesis and in vitro and in vivo antimalarial activity of new 4-anilinoquinolines. *J Med Chem* (2001) 44(17):2827–33. doi: 10.1021/jm010842o
147. Purser S, Moore PR, Swallow S, Gouverneur V. Fluorine in medicinal chemistry. *Chem Soc Rev* (2008) 37(2):320–30. doi: 10.1039/B610213C
148. Park BK, Kitteringham NR, O'Neill PM. Metabolism of fluorine-containing drugs. *Annu Rev Pharmacol Toxicol* (2001) 41(1):443–70. doi: 10.1146/annurev.pharmtox.41.1.443
149. Kalgutkar AS, Dalvie D. Predicting toxicities of reactive metabolite-positive drug candidates. *Annu Rev Pharmacol Toxicol* (2015) 55:35–54. doi: 10.1146/annurev-pharmtox-010814-124720
150. Testa L, Bhindi R, Agostoni P, Abbate A, Zoccai GGB, Van Gaal WJ. The direct thrombin inhibitor ximelagatran/melagatran: a systematic review on clinical applications and an evidence based assessment of risk benefit profile. *Expert Opin Drug Saf* (2007) 6(4):397–406. doi: 10.1517/14740338.6.4.397
151. Park BK, Boobis A, Clarke S, Goldring CE, Jones D, Kenna JG, et al. Managing the challenge of chemically reactive metabolites in drug development. *Nat Rev Drug Discov* (2011) 10(4):292–306. doi: 10.1038/nrd3408
152. Thomson PJ, Illing PT, Farrell J, Alhaidari M, Bell CC, Berry N, et al. Modification of the cyclopropyl moiety of abacavir provides insight into the structure activity relationship between HLA-B* 57: 01 binding and T-cell activation. *Allergy* (2020) 75(3):636–47. doi: 10.1111/all.14057
153. Naisbitt DJ, Yang EL, Alhaidari M, Berry NG, Lawrenson AS, Farrell J, et al. Towards depersonalized abacavir therapy: chemical modification eliminates HLA-B∗ 57: 01-restricted CD8+ T-cell activation. *Aids* (2015) 29(18):2385–95. doi: 10.1097/QAD.0000000000000867
154. Kumar S, Mitra K, Kassahun K, Baillie TA. Approaches for minimizing metabolic activation of new drug candidates in drug discovery. *Handb Exp Pharmacol* (2010) 196):511–44. doi: 10.1007/978-3-642-00663-0_19
155. Inoue K, Shibata Y, Takahashi H, Ohe T, Chiba M, Ishii Y. A trapping method for semi-quantitative assessment of reactive metabolite formation using [35S]cysteine and [14C]cyanide. *Drug Metab Pharmacokinet* (2009) 24 (3):245–54. doi: 10.2133/dmpk.24.245
156. Naisbitt DJ, Hough SJ, Gill HJ, Pirmohamed M, Kitteringham NR, Park BK. Cellular disposition of sulphamethoxazole and its metabolites: implications for hypersensitivity. *Br J Pharmacol* (1999) 126(6):1393–407. doi: 10.1038/sj.bjp.0702453
157. Jenkins RE, Meng X, Elliott VL, Kitteringham NR, Pirmohamed M, Park BK. Characterisation of flucloxacillin and 5-hydroxymethyl flucloxacillin

haptenated HSA in vitro and in vivo. *Proteomics Clin Appl* (2009) 3(6):720–9. doi: 10.1002/prca.200800222
158. Schnyder B, Burkhart C, Schnyder-Frutig K, von Greyerz S, Naisbitt DJ, Pirmohamed M, et al. Recognition of sulfamethoxazole and its reactive metabolites by drug-specific CD4+ T cells from allergic individuals. *J Immunol* (2000) 164(12):6647–54. doi: 10.4049/jimmunol.164.12.6647
159. Pichler WJ, Beeler A, Keller M, Lerch M, Posadas S, Schmid D, et al. Pharmacological interaction of drugs with immune receptors: the pi concept. *Allergol Int* (2006) 55(1):17–25. doi: 10.2332/allergolint.55.17
160. Watkins S, Pichler WJ. Activating interactions of sulfanilamides with T cell receptors. *Open J Immunol* (2013) 03(03):139–57. doi: 10.4236/oji.2013.33019
161. Depta JP, Altznauer F, Gamerdinger K, Burkhart C, Weltzien HU, Pichler WJ. Drug interaction with T-cell receptors: T-cell receptor density determines degree of cross-reactivity. *J Allergy Clin Immunol* (2004) 113 (3):519–27. doi: 10.1016/j.jaci.2003.11.030
162. Tailor A, Waddington JC, Hamlett J, Maggs J, Kafu L, Farrell J, et al. Definition of haptens derived from sulfamethoxazole: in vitro and in vivo. *Chem Res Toxicol* (2019) 32(10):2095–106. doi: 10.1021/acs.chemrestox.9b00282
163. Jenkins RE, Yaseen FS, Monshi MM, Whitaker P, Meng X, Farrell J, et al. beta-Lactam antibiotics form distinct haptenic structures on albumin and activate drug-specific T-lymphocyte responses in multiallergic patients with cystic fibrosis. *Chem Res Toxicol* (2013) 26(6):963–75. doi: 10.1021/tx400124m
164. Meng X, Earnshaw CJ, Tailor A, Jenkins RE, Waddington JC, Whitaker P, et al. Amoxicillin and Clavulanate Form Chemically and Immunologically Distinct Multiple Haptenic Structures in Patients. *Chem Res Toxicol* (2016) 29(10):1762–72. doi: 10.1021/acs.chemrestox.6b00253
165. Grujic S, Vasiljevic T, Lausevic M, Ast T. Study on the formation of an amoxicillin adduct with methanol using electrospray ion trap tandem mass spectrometry. *Rapid Commun Mass Spectrom* (2008) 22(1):67–74. doi: 10.1002/rcm.3333
166. Meng X, Howarth A, Earnshaw CJ, Jenkins RE, French NS, Back DJ, et al. Detection of drug bioactivation in vivo: mechanism of nevirapine-albumin conjugate formation in patients. *Chem Res Toxicol* (2013) 26(4):575–83. doi: 10.1021/tx4000107
167. Tailor A, Meng X, Adair K, Farrell J, Waddington J, Daly A, et al. HLA DRB1* 15: 01-DQB1* 06: 02-restricted human CD4+ T-cells are selectively activated with amoxicillin-peptide adducts. *Toxicol Sci* (2020) 178(1):115–26. doi: 10.1093/toxsci/kfaa128
168. Kangueane P, Sakharkar MK. T-Epitope Designer: A HLA-peptide binding prediction server. *Bioinformation* (2005) 1(1):21–4. doi: 10.6026/97320630001021
169. Pirmohamed M, Naisbitt DJ, Gordon F, Park BK. The danger hypothesis–potential role in idiosyncratic drug reactions. *Toxicology* (2002) 181-182:55–63. doi: 10.1016/S0300-483X(02)00255-X
170. Storkus WJ, Zeh HJ,3, Salter RD, Lotze MT. Identification of T-cell epitopes: rapid isolation of class I-presented peptides from viable cells by mild acid elution. *J Immunother Emphasis Tumor Immunol* (1993) 14(2):94–103. doi: 10.1097/00002371-199308000-00003
171. Storkus WJ, Zeh HJ,3, Maeurer MJ, Salter RD, Lotze MT. Identification of human melanoma peptides recognized by class I restricted tumor infiltrating T lymphocytes. *J Immunol* (1993) 151(7):3719–27.
172. Castelli C, Storkus WJ, Maeurer MJ, Martin DM, Huang EC, Pramanik BN, et al. Mass spectrometric identification of a naturally processed melanoma peptide recognized by CD8+ cytotoxic T lymphocytes. *J Exp Med* (1995) 181 (1):363–8. doi: 10.1084/jem.181.1.363
173. Purcell AW, Ramarathinam SH, Ternette N. Mass spectrometry–based identification of MHC-bound peptides for immunopeptidomics. *Nat Protoc* (2019) 14(6):1687–707. doi: 10.1038/s41596-019-0133-y
174. Schittenhelm RB, Dudek NL, Croft NP, Ramarathinam SH, Purcell AW. A comprehensive analysis of constitutive naturally processed and presented HLA-C*04:01 (Cw4) – specific peptides. *Tissue Antigens* (2014) 83(3):174–9. doi: 10.1111/tan.12282
175. Godkin A, Friede T, Davenport M, Stevanovic S, Willis A, Jewell D, et al. Use of eluted peptide sequence data to identify the binding characteristics of peptides to the insulin-dependent diabetes susceptibility allele HLA-DQ8 (DQ 3.2). *Int Immunol* (1997) 9(6):905–11. doi: 10.1093/intimm/9.6.905
176. Rozanov DV, Rozanov ND, Chiotti KE, Reddy A, Wilmarth PA, David LL, et al. MHC class I loaded ligands from breast cancer cell lines: A potential HLA-I-typed antigen collection. *J Proteomics* (2018) 176:13–23. doi: 10.1016/j.jprot.2018.01.004
177. Antwi K, Hanavan PD, Myers CE, Ruiz YW, Thompson EJ, Lake DF. Proteomic identification of an MHC-binding peptidome from pancreas and breast cancer cell lines. *Mol Immunol* (2009) 46(15):2931–7. doi: 10.1016/j.molimm.2009.06.021
178. Pymm P, Illing PT, Ramarathinam SH, O'Connor GM, Hughes VA, Hitchen C, et al. MHC-I peptides get out of the groove and enable a novel mechanism of HIV-1 escape. *Nat Struct Mol Biol* (2017) 24(4):387–94. doi: 10.1038/nsmb.3381
179. Illing PT, Vivian JP, Dudek NL, Kostenko L, Chen Z, Bharadwaj M, et al. Immune self-reactivity triggered by drug-modified HLA-peptide repertoire. *Nature* (2012) 486(7404):554–8. doi: 10.1038/nature11147
180. Thomson PJ, Illing PT, Farrell J, Alhaidari M, Bell CC, Berry N, et al. Modification of the cyclopropyl moiety of abacavir provides insight into the structure activity relationship between HLA-B*57:01 binding and T-cell activation. *Allergy* (2019) 75(3):636–47. doi: 10.1111/all.14057
181. Waddington J, Meng X, Illing P, Tailor A, Adair K, Whitaker P, et al. Identification of flucloxacillin-haptenated HLA-B* 57: 01 ligands: evidence of antigen processing and presentation. *Toxicol Sci* (2020) 177(2):454–65. doi: 10.1093/toxsci/kfaa124
182. Hassan C, Kester MG, Oudgenoeg G, de Ru AH, Janssen GM, Drijfhout JW, et al. Accurate quantitation of MHC-bound peptides by application of isotopically labeled peptide MHC complexes. *J Proteomics* (2014) 109:240–4. doi: 10.1016/j.jprot.2014.07.009
183. Bassani-Sternberg M, Coukos G. Mass spectrometry-based antigen discovery for cancer immunotherapy. *Curr Opin Immunol* (2016) 41:9–17. doi: 10.1016/j.coi.2016.04.005
184. Walz S, Stickel JS, Kowalewski DJ, Schuster H, Weisel K, Backert L, et al. The antigenic landscape of multiple myeloma: mass spectrometry (re) defines targets for T-cell–based immunotherapy. *Blood* (2015) 126(10):1203–13. doi: 10.1182/blood-2015-04-640532
185. Freudenmann LK, Marcu A, Stevanović S. Mapping the tumour human leukocyte antigen (HLA) ligandome by mass spectrometry. *Immunology* (2018) 154(3):331–45. doi: 10.1111/imm.12936
186. Stachulski AV, Baillie TA, Park BK, Obach RS, Dalvie DK, Williams DP, et al. The generation, detection, and effects of reactive drug metabolites. *Med Res Rev* (2013) 33(5):985–1080. doi: 10.1002/med.21273
187. Evans DC, Watt AP, Nicoll-Griffith DA, Baillie TA. Drug– protein adducts: an industry perspective on minimizing the potential for drug bioactivation in drug discovery and development. *Chem Res Toxicol* (2004) 17(1):3–16. doi: 10.1021/tx034170b
188. Ghanbari F, Rowland-Yeo K, Bloomer J, Clarke S, Lennard M, Tucker G, et al. A critical evaluation of the experimental design of studies of mechanism based enzyme inhibition, with implications for in vitro-in vivo extrapolation. *Curr Drug Metab* (2006) 7(3):315–34. doi: 10.2174/138920006776359293
189. Madan A, Parkinson A. Characterization of the NADPH-dependent covalent binding of [14C] halothane to human liver microsomes: a role for cytochrome P4502E1 at low substrate concentrations. *Drug Metab Dispos* (1996) 24(12):1307–13.
190. Lecoeur S, Bonierbale E, Challine D, Gautier J-C, Valadon P, Dansette PM, et al. Specificity of in vitro covalent binding of tienilic acid metabolites to human liver microsomes in relationship to the type of hepatotoxicity: comparison with two directly hepatotoxic drugs. *Chem Res Toxicol* (1994) 7(3):434–42. doi: 10.1021/tx00039a023
191. Kligman AM. The identification of contact allergens by human assay: II. Factors influencing the induction and measurement of allergic contact dermatitis. *J Invest Dermatol* (1966) 47(5):375–92. doi: 10.1038/jid.1966.159
192. Nilzen A, Wikstrom K. The influence of lauryl sulphate on the sensitization of guineapigs to chrome and nickle. *Acta Derm Venereol* (1955) 35(4-5):292.
193. Cumberbatch M, Scott R, Basketter D, Scholes E, Hilton J, Dearman R, et al. Influence of sodium lauryl sulphate on 2, 4-dinitrochlorobenzene-induced lymph node activation. *Toxicology* (1993) 77(1-2):181–91. doi: 10.1016/0300-483X(93)90148-L

194. Moser JM, Sassano ER, Leistritz DC, Eatrides JM, Phogat S, Koff W, et al. Optimization of a dendritic cell-based assay for the in vitro priming of naive human CD4+ T cells. *J Immunol Methods* (2010) 353(1-2):8–19. doi: 10.1016/j.jim.2009.11.006
195. Faulkner L, Martinsson K, Santoyo-Castelazo A, Cederbrant K, Schuppe-Koistinen I, Powell H, et al. The Development of In Vitro Culture Methods to Characterize Primary T-Cell Responses to Drugs. *Toxicol Sci* (2012) 127 (1):150. doi: 10.1093/toxsci/kfs080
196. Nukada Y, Ashikaga T, Miyazawa M, Hirota M, Sakaguchi H, Sasa H, et al. Prediction of skin sensitization potency of chemicals by human Cell Line Activation Test (h-CLAT) and an attempt at classifying skin sensitization potency. *Toxicol Vitro* (2012) 26(7):1150–60. doi: 10.1016/j.tiv.2012.07.001
197. Sakaguchi H, Ashikaga T, Miyazawa M, Kosaka N, Ito Y, Yoneyama K, et al. The relationship between CD86/CD54 expression and THP-1 cell viability in an in vitro skin sensitization test–human cell line activation test (h-CLAT). *Cell Biol Toxicol* (2009) 25(2):109–26. doi: 10.1007/s10565-008-9059-9
198. Ashikaga T, Yoshida Y, Hirota M, Yoneyama K, Itagaki H, Sakaguchi H, et al. Development of an in vitro skin sensitization test using human cell lines: The human Cell Line Activation Test (h-CLAT): I. Optimization of the h-CLAT protocol. *Toxicol Vitro* (2006) 20(5):767–73. doi: 10.1016/j.tiv.2005.10.012
199. Sakaguchi H, Ashikaga T, Miyazawa M, Yoshida Y, Ito Y, Yoneyama K, et al. Development of an in vitro skin sensitization test using human cell lines; human Cell Line Activation Test (h-CLAT) II. An inter-laboratory study of the h-CLAT. *Toxicol Vitro* (2006) 20(5):774–84. doi: 10.1016/j.tiv.2005.10.014
200. dos Santos GG, Reinders J, Ouwehand K, Rustemeyer T, Scheper R, Gibbs S. Progress on the development of human in vitro dendritic cell based assays for assessment of the sensitizing potential of a compound. *Toxicol Appl Pharmacol* (2009) 236(3):372–82. doi: 10.1016/j.taap.2009.02.004
201. Tourkova IL, Yurkovetsky ZR, Shurin MR, Shurin GV. Mechanisms of dendritic cell-induced T cell proliferation in the primary MLR assay. *Immunol Lett* (2001) 78(2):75–82. doi: 10.1016/S0165-2478(01)00235-8
202. Sanderson JP, Naisbitt DJ, Farrell J, Ashby CA, Tucker MJ, Rieder MJ, et al. Sulfamethoxazole and its metabolite nitroso sulfamethoxazole stimulate dendritic cell costimulatory signaling. *J Immunol (Baltimore Md 1950)* (2007) 178(9):5533–42. doi: 10.4049/jimmunol.178.9.5533
203. Natsch A, Ryan CA, Foertsch L, Emter R, Jaworska J, Gerberick F, et al. A dataset on 145 chemicals tested in alternative assays for skin sensitization undergoing prevalidation. *J Appl Toxicol* (2013) 33(11):1337–52. doi: 10.1002/jat.2868
204. Macmillan DS, Chilton ML. A defined approach for predicting skin sensitisation hazard and potency based on the guided integration of in silico, in chemico and in vitro data using exclusion criteria. *Regul Toxicol Pharmacol* (2019) 101:35–47. doi: 10.1016/j.yrtph.2018.11.001
205. Cho SA, Choi M, Park SR, An S, Park JH. Application of Spectro-DPRA, KeratinoSens™ and h-CLAT to estimation of the skin sensitization potential of cosmetics ingredients. *J Appl Toxicol* (2020) 40(2):300–12. doi: 10.1002/jat.3904
206. Oda S, Matsuo K, Nakajima A, Yokoi T. A novel cell-based assay for the evaluation of immune-and inflammatory-related gene expression as biomarkers for the risk assessment of drug-induced liver injury. *Toxicol Lett* (2016) 241:60–70. doi: 10.1016/j.toxlet.2015.10.029
207. Herpers B, Wink S, Fredriksson L, Di Z, Hendriks G, Vrieling H, et al. Activation of the Nrf2 response by intrinsic hepatotoxic drugs correlates with suppression of NF-κB activation and sensitizes toward TNFα-induced cytotoxicity. *Arch Toxicol* (2016) 90(5):1163–79. doi: 10.1007/s00204-015-1536-3
208. Kato R, Uetrecht J. Supernatant from hepatocyte cultures with drugs that cause idiosyncratic liver injury activates macrophage inflammasomes. *Chem Res Toxicol* (2017) 30(6):1327–32. doi: 10.1021/acs.chemrestox.7b00065
209. Ogese MO, Faulkner L, Jenkins RE, French NS, Copple IM, Antoine DJ, et al. Characterization of Drug-Specific Signaling Between Primary Human Hepatocytes and Immune Cells. *Toxicol Sci* (2017) 158(1):76–89. doi: 10.1093/toxsci/kfx069
210. Ogese MO, Jenkins RE, Adair K, Tailor A, Meng X, Faulkner L, et al. Exosomal transport of hepatocyte-derived drug-modified proteins to the immune system. *Hepatology* (2019) 70(5):1732–49. doi: 10.1002/hep.30701
211. Mosedale M, Eaddy JS, Trask OJJr, Holman NS, Wolf KK, LeCluyse E, et al. miR-122 release in exosomes precedes overt tolvaptan-induced necrosis in a primary human hepatocyte micropatterned coculture model. *Toxicol Sci* (2018) 161(1):149–58. doi: 10.1093/toxsci/kfx206
212. McGill MR, Jaeschke H. MicroRNAs as signaling mediators and biomarkers of drug-and chemical-induced liver injury. *J Clin Med* (2015) 4(5):1063–78. doi: 10.3390/jcm4051063
213. Thacker SE, Nautiyal M, Otieno MA, Watkins PB, Mosedale M. Optimized methods to explore the mechanistic and biomarker potential of hepatocyte-derived exosomes in drug-induced liver injury. *Toxicol Sci* (2018) 163(1):92–100. doi: 10.1093/toxsci/kfy015
214. Holman NS, Church RJ, Nautiyal M, Rose KA, Thacker SE, Otieno MA, et al. Hepatocyte-derived exosomes promote liver immune tolerance: Possible implications for idiosyncratic drug-induced liver injury. *Toxicol Sci* (2019) 170(2):499–508. doi: 10.1093/toxsci/kfz112
215. Oda S, Uchida Y, Aleo MD, Koza-Taylor PH, Matsui Y, Hizue M, et al. An in vitro coculture system of human peripheral blood mononuclear cells with hepatocellular carcinoma-derived cells for predicting drug-induced liver injury. *Arch Toxicol* (2020) 95:1–20. doi: 10.1007/s00204-020-02882-4
216. Engler OB, Strasser I, Naisbitt DJ, Cerny A, Pichler WJ. A chemically inert drug can stimulate T cells in vitro by their T cell receptor in non-sensitised individuals. *Toxicology* (2004) 197:47–56. doi: 10.1016/j.tox.2003.12.008
217. Ho WY, Nguyen HN, Wolfl M, Kuball J, Greenberg PD. In vitro methods for generating CD8+ T-cell clones for immunotherapy from the naive repertoire. *J Immunol Methods* (2006) 310(1-2):40–52. doi: 10.1016/j.jim.2005.11.023
218. Martin SF, Esser PR, Schmucker S, Dietz L, Naisbitt DJ, Park BK, et al. T-cell recognition of chemicals, protein allergens and drugs: towards the development of in vitro assays. *Cell Mol Life Sci* (2010) 67(24):4171–84. doi: 10.1007/s00018-010-0495-3
219. Usui T, Faulkner L, Farrell J, French NS, Alfirevic A, Pirmohamed M, et al. Application of in Vitro T Cell Assay Using Human Leukocyte Antigen-Typed Healthy Donors for the Assessment of Drug Immunogenicity. *Chem Res Toxicol* (2018) 31(3):165–7. doi: 10.1021/acs.chemrestox.8b00030
220. Faulkner L, Gibson A, Sullivan A, Tailor A, Usui T, Alfirevic A, et al. Detection of Primary T Cell Responses to Drugs and Chemicals in HLA-Typed Volunteers: Implications for the Prediction of Drug Immunogenicity. *Toxicol Sci* (2016) 154(2):416–29. doi: 10.1093/toxsci/kfw177
221. Gibson A, Faulkner L, Lichtenfels M, Ogese M, Al-Attar Z, Alfirevic A, et al. The Effect of Inhibitory Signals on the Priming of Drug Hapten–Specific T Cells That Express Distinct Vβ Receptors. *J Immunol* (2017) 199(4):1223–37. doi: 10.4049/jimmunol.1602029
222. Gibson A, Ogese M, Sullivan A, Wang E, Saide K, Whitaker P, et al. Negative regulation by PD-L1 during drug-specific priming of IL-22-secreting T cells and the influence of PD-1 on effector T cell function. *J Immunol (Baltimore Md 1950)* (2014) 192(6):2611–21. doi: 10.4049/jimmunol.1302720
223. Gibson A, Faulkner L, Wood S, Park BK, Naisbitt DJ. Identification of drug- and drug-metabolite immune responses originating from both naive and memory T cells. *J Allergy Clin Immunol* (2017) 140(2):578. doi: 10.1016/j.jaci.2016.11.032
224. Ogese MO, Watkinson J, Lister A, Faulkner L, Gibson A, Hillegas A, et al. Development of an Improved T-cell assay to assess the intrinsic immunogenicity of haptenic compounds. *Toxicol Sci* (2020) 175(2):266–78. doi: 10.1093/toxsci/kfaa034
225. Dietz L, Esser PR, Schmucker SS, Goette I, Richter A, Schnölzer M, et al. Tracking human contact allergens: from mass spectrometric identification of peptide-bound reactive small chemicals to chemical-specific naive human T-cell priming. *Toxicol Sci* (2010) 117(2):336–47. doi: 10.1093/toxsci/kfq209
226. Zhang C, Cheng F, Li W, Liu G, Lee PW, Tang Y. In silico prediction of drug induced liver toxicity using substructure pattern recognition method. *Mol Inf* (2016) 35(3-4):136–44. doi: 10.1002/minf.201500055
227. Xu Y, Dai Z, Chen F, Gao S, Pei J, Lai L. Deep learning for drug-induced liver injury. *J Chem Inf Model* (2015) 55(10):2085–93. doi: 10.1021/acs.jcim.5b00238
228. Zhang H, Ding L, Zou Y, Hu S-Q, Huang H-G, Kong W-B, et al. Predicting drug-induced liver injury in human with Naïve Bayes classifier approach. *J Comput Aided Mol Des* (2016) 30(10):889–98. doi: 10.1007/s10822-016-9972-6

229. Chen M, Borlak J, Tong W. A Model to predict severity of drug-induced liver injury in humans. *Hepatology* (2016) 64(3):931–40. doi: 10.1002/hep.28678
230. Muller C, Pekthong D, Alexandre E, Marcou G, Horvath D, Richert L, et al. Prediction of drug induced liver injury using molecular and biological descriptors. *Comb Chem High Throughput Screen* (2015) 18(3):315–22. doi: 10.2174/1386207318666150305144650
231. Watkins PB. The DILI-sim initiative: insights into hepatotoxicity mechanisms and biomarker interpretation. *Clin Trans Sci* (2019) 12 (2):122–9. doi: 10.1111/cts.12629
232. Woodhead JL, Watkins PB, Howell BA, Siler SQ, Shoda LK. The role of quantitative systems pharmacology modeling in the prediction and explanation of idiosyncratic drug-induced liver injury. *Drug Metab Pharmacokinet* (2017) 32(1):40–5. doi: 10.1016/j.dmpk.2016.11.008
233. Woodhead JL, Pellegrini L, Shoda LKM, Howell BA. Comparison of the Hepatotoxic Potential of Two Treatments for Autosomal-Dominant Polycystic Kidney DiseaseUsing Quantitative Systems Toxicology Modeling. *Pharm Res* (2020) 37(2):24. doi: 10.1007/s11095-019-2726-0
234. Woodhead JL, Brock WJ, Roth SE, Shoaf SE, Brouwer KLR, Church R, et al. Application of a Mechanistic Model to Evaluate Putative Mechanisms of Tolvaptan Drug-Induced Liver Injury and Identify Patient Susceptibility Factors. *Toxicol Sci* (2017) 155(1):61–74. doi: 10.1093/toxsci/kfw193
235. Isogai H, Miyadera H, Ueta M, Sotozono C, Kinoshita S, Tokunaga K, et al. In silico risk assessment of HLA-A* 02: 06-associated Stevens-Johnson syndrome and toxic epidermal necrolysis caused by cold medicine ingredients. *J Toxicol* (2013) 2013:1–6. doi: 10.1155/2013/514068
236. Terasaki PI. Resolution by HLA testing of 1000 paternity cases not excluded by ABO testing. *J Fam L* (1977) 16:543.
237. Erlich H. HLA DNA typing: past, present, and future. *Tissue Antigens* (2012) 80(1):1–11. doi: 10.1111/j.1399-0039.2012.01881.x
238. Faridi P, Li C, Ramarathinam SH, Vivian JP, Illing PT, Mifsud NA, et al. A subset of HLA-I peptides are not genomically templated: Evidence for cis- and trans-spliced peptide ligands. *Sci Immunol* (2018) 3(28):eaar3947. doi: 10.1126/sciimmunol.aar3947
239. Vizcaíno JA, Kubiniok P, Kovalchik KA, Ma Q, Duquette JD, Mongrain I, et al. The Human Immunopeptidome Project: A Roadmap to Predict and Treat Immune Diseases. *Mol Cell Proteomics* (2020) 19(1):31–49. doi: 10.1074/mcp.R119.001743
240. Faridi P, Aebersold R, Caron E. A first dataset toward a standardized community-driven global mapping of the human immunopeptidome. *Data Brief* (2016) 7:201–5. doi: 10.1016/j.dib.2016.02.016
241. Schuster H, Shao W, Weiss T, Pedrioli PGA, Roth P, Weller M, et al. A tissue-based draft map of the murine MHC class I immunopeptidome. *Sci Data* (2018) 5:180157. doi: 10.1038/sdata.2018.157
242. Pan R-Y, Chu M-T, Wang C-W, Lee Y-S, Lemonnier F, Michels AW, et al. Identification of drug-specific public TCR driving severe cutaneous adverse reactions. *Nat Commun* (2019) 10(1):1–13. doi: 10.1038/s41467-019-11396-2
243. Ko T-M, Chung W-H, Wei C-Y, Shih H-Y, Chen J-K, Lin C-H, et al. Shared and restricted T-cell receptor use is crucial for carbamazepine-induced Stevens-Johnson syndrome. *J Allergy Clin Immunol* (2011) 128(6):1266–76.e11. doi: 10.1016/j.jaci.2011.08.013
244. Arstila TP, Casrouge A, Baron V, Even J, Kanellopoulos J, Kourilsky P. A direct estimate of the human αβ T cell receptor diversity. *Science* (1999) 286 (5441):958–61. doi: 10.1126/science.286.5441.958
245. Godfrey DI, Rossjohn J, McCluskey J. The fidelity, occasional promiscuity, and versatility of T cell receptor recognition. *Immunity* (2008) 28(3):304–14. doi: 10.1016/j.immuni.2008.02.004
246. The International Council for Harmonisation of Technical Requirements for Pharmaceuticals for Human Use (ICH). *Immunotoxicity studies for human pharmaceuticals (S8:2.7.).* (2005). Available at: https://www.ich.org/page/safety-guidelines, [cited 2021 March 13].

Conflict of Interest: SH was employed by the company ApconiX.

The remaining authors declare that the research was conducted in the absence of any commercial or financial relationships that could be construed as a potential conflict of interest.

frontiers in Genetics

MINI REVIEW
published: 16 April 2021
doi: 10.3389/fgene.2021.641905

Genomic Risk Factors Driving Immune-Mediated Delayed Drug Hypersensitivity Reactions

Yueran Li[1], Pooja Deshpande[1], Rebecca J. Hertzman[1], Amy M. Palubinsky[2], Andrew Gibson[1] and Elizabeth J. Phillips[1,2]*

[1] *Institute for Immunology and Infectious Diseases, Murdoch University, Murdoch, WA, Australia,* [2] *Department of Medicine, Vanderbilt University Medical Centre, Nashville, TN, United States*

Adverse drug reactions (ADRs) remain associated with significant mortality. Delayed hypersensitivity reactions (DHRs) that occur greater than 6 h following drug administration are T-cell mediated with many severe DHRs now associated with human leukocyte antigen (HLA) risk alleles, opening pathways for clinical prediction and prevention. However, incomplete negative predictive value (NPV), low positive predictive value (PPV), and a large number needed to test (NNT) to prevent one case have practically prevented large-scale and cost-effective screening implementation. Additional factors outside of HLA contributing to risk of severe T-cell-mediated DHRs include variation in drug metabolism, T-cell receptor (TCR) specificity, and, most recently, HLA-presented immunopeptidome-processing efficiencies via endoplasmic reticulum aminopeptidase (ERAP). Active research continues toward identification of other highly polymorphic factors likely to impose risk. These include those previously associated with T-cell-mediated HLA-associated infectious or auto-immune disease such as Killer cell immunoglobulin-like receptors (KIR), epistatically linked with HLA class I to regulate NK- and T-cell-mediated cytotoxic degranulation, and co-inhibitory signaling pathways for which therapeutic blockade in cancer immunotherapy is now associated with an increased incidence of DHRs. As such, the field now recognizes that susceptibility is not simply a static product of genetics but that individuals may experience dynamic risk, skewed toward immune activation through therapeutic interventions and epigenetic modifications driven by ecological exposures. This review provides an updated overview of current and proposed genetic factors thought to predispose risk for severe T-cell-mediated DHRs.

Keywords: delayed hypersensitivity, human leukocyte antigen, T-cell receptor, endoplasmic reticulum aminopeptidase, genetic risk, immune checkpoint

OPEN ACCESS

Edited by:
Jason Trubiano, University of Melbourne, Australia

Reviewed by:
Ana Copaescu, McGill University Health Centre, Canada
Ursula Amstutz, University of Bern, Switzerland

****Correspondence:***
Andrew Gibson
a.gibson@iiid.com.au

Specialty section:
This article was submitted to Pharmacogenetics and Pharmacogenomics, a section of the journal Frontiers in Genetics

Received: *15 December 2020*
Accepted: *08 March 2021*
Published: *16 April 2021*

Citation:
Li Y, Deshpande P, Hertzman RJ, Palubinsky AM, Gibson A and Phillips EJ (2021) Genomic Risk Factors Driving Immune-Mediated Delayed Drug Hypersensitivity Reactions. Front. Genet. 12:641905. doi: 10.3389/fgene.2021.641905

INTRODUCTION

Adverse drug reactions (ADRs) are estimated as the fourth to sixth leading cause of death (Dormann et al., 2000; Pouyanne et al., 2000; Miya et al., 2019). While the majority are classified as type A, predictable based on drug pharmacology, the remainder are off-target type B ADRs and inclusive of T-cell-mediated delayed drug hypersensitivity reactions (DHRs). While DHRs

may elicit systemic effects, diverse clinical reactions also target specific organs including drug-induced liver injury (DILI), associated with nausea, fatigue, jaundice, and mortality up to 9.4% (Leise et al., 2014). However, most often they target skin, with presentation from mild rash (fixed drug eruption, maculopapular exanthema) to life-threatening severe cutaneous adverse reactions (SCARs) including Stevens-Johnson Syndrome/Toxic Epidermal Necrolysis (SJS/TEN) and drug reaction with eosinophilia and systemic symptoms (DRESS) (Peter et al., 2017). DRESS has a mortality up to 10% (Kardaun, 2019; Wolfson et al., 2019) and is characterized by widespread skin eruption, lymphadenopathy, fever, and multiple organ involvement (Choudhary et al., 2013; Kardaun, 2019). SJS and TEN are the same disease across a spectrum of severity with the higher end of mortality (TEN) associated with up to 50% death (Patel et al., 2013; Langley et al., 2018). SJS/TEN is characterized by blistering and involvement of at least two mucous membranes (Paulmann and Mockenhaupt, 2015; Miya et al., 2019; Zimmerman and Dang, 2020). Despite clinical distinction, lack of mechanistic delineation has precluded development of disease-specific treatment and prevention strategies (Pavlos et al., 2015; Redwood et al., 2018). In recent years many DHRs have been associated with strong human leukocyte antigen (HLA) class I associations opening pathways to prediction and prevention (**Figure 1**).

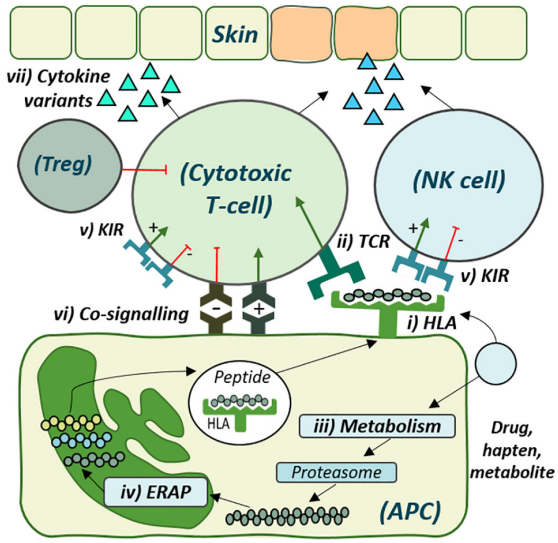

FIGURE 1 | The cellular role of genetic risk factors defined and proposed for development of delayed drug hypersensitivity reactions. Drug antigen may bind directly to (i) specific human leukocyte antigen (HLA) molecules on the surface of antigen-presenting cells (APC) for recognition by corresponding (ii) T-cell receptors (TCRs). Alternatively, drug may undergo (iii) metabolism and cellular processing by (iv) endoplasmic reticulum aminopeptidase (ERAP), with the peptide products then presented by the risk HLA molecule for TCR recognition. (v) Distinct killer-cell immunoglobulin-like receptors (KIR), expressed on both T-cell and Natural Killer (NK) cells, also show specificity for HLA-antigen interaction, which may regulate cytotoxic degranulation. (vi) Co-signaling pathways also regulate T-cell activation, with overall co-inhibition or co-stimulation leading to (vii) cytokine release and respective tolerance with T-regulatory cell (Treg)-induced immunosuppression or inflammation and cytotoxic degranulation, respectively.

THE EVOLVING COMPLEXITY OF DRUG-, REACTION-, AND POPULATION-RESTRICTED HLA RISK

Abacavir Hypersensitivity

The HLA locus is highly polymorphic with >25,000 allelic variants annotated (HLA.alleles.org). In 2002, Mallal demonstrated carriage of HLA-B*57:01 among 78% of HIV patients with abacavir hypersensitivity, which is a well-characterized systemic syndrome, opposed to just 2% of tolerant patients (Mallal et al., 2002). A randomized double blind clinical trial of real-time HLA-B*57:01 screening versus abacavir treatment without real-time screening showed a negative predictive value (NPV) of 100% and a positive predictive value (PPV) of 55% (Mallal et al., 2008), demonstrating that HLA-B*57:01 screening eliminates patch test positive abacavir hypersensitivity. This PREDICT-1 study was the licensing study upon which guideline-based HLA-B*57:01 screening prior to abacavir prescription was established.

Carbamazepine Hypersensitivity

In 2004, association between HLA-B*15:02 and carbamazepine (CBZ)-induced SJS/TEN in Taiwan was reported, which followed the translational roadmap provided by abacavir such that 0/4120 Taiwanese HLA-B*15:02-negative patients developed SJS/TEN after CBZ exposure (Chung et al., 2004). Pre-prescription HLA-B*15:02 screening for CBZ is now active in Hong Kong, Singapore, and Thailand where there is high allelic prevalence (FerrellJr., and McLeod, 2008). However, HLA-B*15:02 is expressed in <1% of patients of European or African ancestry despite global disease burden, restricting universal screening and inferring that different HLA alleles drive reactions in different populations (Karnes et al., 2019). Indeed, multiple alleles are now associated with CBZ-SCAR in distinct populations, with HLA-A*31:01 associated with DRESS in Europeans and Chinese, but not SJS/TEN (McCormack et al., 2011; Genin et al., 2014), highlighting propensity for distinct alleles to define risk for specific reactions. Most recently, Nicoletti reported HLA-A*31:01 as a strong risk factor broadly across CBZ-induced SCAR and DILI in Europeans (Nicoletti et al., 2019) while Mockenhaupt described an HLA-B*57:01 association for CBZ-SJS/TEN in Europeans (Mockenhaupt et al., 2019). These studies demonstrate that HLA restriction may be complex, with influence from multiple alleles restricted to antigen, reaction phenotype, and population (**Table 1**).

HLA AND ITS USE IN CLINICAL PRACTICE

HLA-B*58:01 and Allopurinol-DRESS

Other strong HLA associations have been described with near-complete NPV for WHO essential medicines, the most effective

TABLE 1 | HLA risk alleles associated with delayed type drug hypersensitivity reactions.

Drug	HLA risk allele	Reaction	Ethnic population	PPV (NPV)	References
Abacavir	B*57:01	HSS	African	50 (100)	Saag et al., 2008
			Caucasian	50 (100)	Mallal et al., 2002, 2008
			Hispanic	96 (60)	Sousa-Pinto et al., 2015
Acetazolamide	B*59	SJS/TEN	Korean		Her et al., 2011
Allopurinol	B*58:01	DRESS, SJS/TEN	Caucasian		Jarjour et al., 2015
		DRESS	Caucasian (Portuguese)		Gonçalo et al., 2013
		DRESS, SJS/TEN	Han Chinese	3 (100)	Chiu et al., 2012
		DRESS, SJS/TEN	Korean	2.06 (99.98)	Kang et al., 2011
		DRESS	Thai	8.26 (100)	Sukasem et al., 2016
		MPE, SJS/TEN	Japanese		Kaniwa et al., 2008; Jarjour et al., 2015
		MPE	Thai	5.13 (99.90)	Sukasem et al., 2016
		SJS/TEN	Caucasian		Lonjou et al., 2008; Yu et al., 2017
			Thai	10.48 (100)	Sukasem et al., 2016
	C*03:02	DRESS, SJS/TEN	Korean	1.77 (99.98)	Kang et al., 2011
	A*33:02	DRESS, SJS/TEN	Korean	0.8 (99.96)	Kang et al., 2011
Amoxicillin-clavulanate	DRB1*15:01	DILI	Caucasian		Lucena et al., 2011
Azathioprine	DQA1*02:01	Pancreatitis	Caucasian		Heap et al., 2014
	DRB1*07:01				Heap et al., 2014
Benznidazole	A*11:01	MPE, DRESS	Bolivian	100 (70)	Balas et al., 2020
	A*29:02			100 (70)	
	A*68			48 (84)	
Carbamazepine	A*24:02	SJS/TEN	Han Chinese		Shi et al., 2012
	A*31	DRESS, SJS/TEN, MPE	Japanese		Niihara et al., 2012
	A*31:01	DRESS	Caucasian	0.77 (99.98)	Genin et al., 2014
			Han Chinese	0.67 (99.97)	Genin et al., 2014
		SJS/TEN	Caucasian		McCormack et al., 2011
			Han Chinese		Genin et al., 2014
		DRESS, SJS/TEN	Korean		Kim et al., 2011b
		SCAR, DILI	Caucasian		Nicoletti et al., 2019)
	B*15:02	SJS/TEN	Han Chinese	2.24 (99.94)	Tangamornsuksan et al., 2013; Genin et al., 2014
			Indian		Mehta et al., 2009
			Korean		Tangamornsuksan et al., 2013
			Malaysian		Tangamornsuksan et al., 2013
			Thai		Tangamornsuksan et al., 2013; Sukasem et al., 2018
			Taiwanese	93.6 (100)	Chung et al., 2004
	B*15:11	SJS/TEN	Han Chinese		Shi et al., 2012
			Asian	43.8 (95.1)	Wang et al., 2017
	B*15:21	SJS/TEN	Thai		Sukasem et al., 2018
		SJS/TEN	Filipino	1.03 (87.5)	Capule et al., 2020
	B*51:01	DRESS, MPE	Han Chinese		Wang et al., 2017
	B*57:01	SJS/TEN	Caucasian		Mockenhaupt et al., 2019
	B*58:01	DRESS, MPE	Asian	90.4 (37)	Wang et al., 2017; Sukasem et al., 2018
	DRB1*14:05	MPE	Han Chinese		Li et al., 2013
Co-trimoxazole	B*15:02, C*08:01	SJS/TEN	Thai		Sukasem et al., 2020
	B*13:01	DRESS			
Dapsone	B*13:01	DRESS	Chinese	7.8 (99.8)	Zhang et al., 2013

(Continued)

TABLE 1 | Continued

Drug	HLA risk allele	Reaction	Ethnic population	PPV (NPV)	References
		DRESS, SJS/TEN	Thai		Tempark et al., 2017
		DRESS	Taiwanese		Chen et al., 2018
			Malaysian		
Flucloxacillin	B*57:01	DILI	Caucasian	0.12 (99.99)	Daly et al., 2009
Isoxicam, Piroxicam	A*02	SJS/TEN	Caucasian		Roujeau et al., 1987
	B*12				
Lamotrigine	A*02:07	MPE, DRESS, SJS/TEN	Thai		Koomdee et al., 2017
	A*24:02, C*01:02	MPE	Korean		Moon et al., 2015
	A*30:01		Han Chinese		Li et al., 2013
	B*13:02				
	A*33:03		Thai		Koomdee et al., 2017
	B*44:03				
	A*31:01	DRESS, SJS/TEN	Korean		Kim et al., 2017
	A*68:01	DRESS, SJS/TEN	Caucasian		Kazeem et al., 2009
	B*15:02	SJS/TEN	Han Chinese		Cheung et al., 2013
		DRESS, SJS/TEN, MPE	Thai		Koomdee et al., 2017
		SJS/TEN	Iranian	78.57 (56.41)	Sabourirad et al., 2020
	B*38	SJS/TEN	Caucasian		Lonjou et al., 2008
	B*58:01	DRESS, SJS/TEN	Caucasian		Kazeem et al., 2009
	C*07:18				
	DQB1*06				
	DRB1*13				
Methazolamide	B*59:01	SJS/TEN	Japanese		Nakatani et al., 2019
			Korean		Tangamornsuksan and Lohitnavy, 2019
			Han Chinese	100 (96.8)	Yang et al., 2015; Tangamornsuksan and Lohitnavy, 2019
Minocycline	B*35:02	DILI	Caucasian		(Urban et al., 2017)
Nevirapine	Cw4	DRESS	Han Chinese		Gao et al., 2012
	C*04:01	SJS/TEN	Malawian	2.6 (99.2)	Carr et al., 2013, 2017
	C*08	DRESS	Japanese		Gatanaga et al., 2007
	C*08:02, B*14:02	DRESS	Caucasian (Sardinian)		Littera et al., 2006
	B*35:05	Skin Rash	Thai		Chantarangsu et al., 2009
	DRB1*01:01	DRESS	Caucasian		Martin et al., 2005
Oxcarbazepine	A*03:01	MPE	Uighur Chinese		Zhao et al., 2020
	B*07:02				
	B*15:02	MPE, SJS/TEN	Han Chinese		Hung et al., 2010
	B*38:02	MPE			Lv et al., 2013
Oxicams	B*73	SJS/TEN	Caucasian		Lonjou et al., 2008
Phenobarbital	B*51:01	SJS/TEN	Japanese		Kaniwa et al., 2013
Phenytoin	B*13:01	SJS/TEN	East Asian		Su et al., 2019
	B*15:02	SJS/TEN	East Asian		Su et al., 2019
			Han Chinese		(Cheung et al., 2013
			Malaysian		(Chang et al., 2017
			Thai	33 (100)	Locharernkul et al., 2008
	B*15:13	DRESS, SJS/TEN	Malaysian		Chang et al., 2017
	B*56:02	SJS/TEN	Thai		Tassaneeyakul et al., 2016
		DRESS	Australian Aboriginal		Somogyi et al., 2019
	Cw*08:01	SJS/TEN	Han Chinese		Hung et al., 2010
	DRB1*16:02				
Raltegravir	B*53:01	DRESS	African		Thomas et al., 2017
Strontium Renalate	A*33:03	SJS/TEN	Han Chinese		Lee et al., 2016

(Continued)

TABLE 1 | Continued

Drug	HLA risk allele	Reaction	Ethnic population	PPV (NPV)	References
	B*58:01				
Sulfamethoxazole	A*29	SJS/TEN	Caucasian		Roujeau et al., 1987
	A*30	FDE	Turkish		Özkaya-Bayazit and Akar, 2001
	A*30-B*13-C*06				
	A*11:01	SJS/DRESS	Japanese		Nakamura et al., 2020
	B*13:01	SCAR	Asian	4.05 (99.92)	Wang et al., 2020
		DRESS		3.64 (99.92)	
	B*14:01	DILI	European American		Li et al., 2020
	B*35:01		African American		Li et al., 2020
	B*44 (B12 serotype)	SJS/TEN	Caucasian		Liang et al., 2013
	B*38	SJS/TEN	Caucasian		Lonjou et al., 2008
	DR*07				
Sulfasalazine	B*13:01	DRESS	Han Chinese		Yang et al., 2014
Ticlopidine	A*33:03	DILI	Japanese		Hirata et al., 2008
Terbinafine	A*33:01	DILI	Caucasian		Fontana et al., 2018
Vancomycin	A*32:01	DRESS	Caucasian		Konvinse et al., 2019
Zonisamide	A*02:07	SJS/TEN	Japanese		Kaniwa et al., 2013

References included were studies associated with clinically defined DHR. DILI, drug-induced liver injury; DRESS, drug reaction with eosinophilia and systemic symptoms; FDE, fixed drug eruption; HSS, hypersensitivity syndrome; MPE, maculopapular eruption; NPV, negative predictive value; PPV, positive predictive value; SCAR, severe cutaneous adverse reaction; SJS/TEN, Stevens-Johnson Syndrome/Toxic Epidermal Necrolysis. NPV and PPV are based on case-control studies and require ongoing validation and thus subject to change.

and safe drugs to meet the most important needs, such as allopurinol, dapsone, and vancomycin (WHO, 2021). Allopurinol is used for treatment of gout but is also the most prevalent drug cause of DRESS in the FDA Adverse event reporting system (Bluestein et al., 2021). In 2005, HLA-B*58:01 was associated with allopurinol-induced SCAR with 100% NPV in Southeast Asians (Hung et al., 2005). Subsequent studies confirmed risk in cohorts from Europe (Lonjou et al., 2008), Japan (Kaniwa et al., 2008), Thailand (Yu et al., 2017), South Korea (Kang et al., 2011), and Portugal (Gonçalo et al., 2013), but, as with CBZ, comparative strength of association and allelic frequency is not replicated and is far lower in Europeans (Génin et al., 2011). Currently, where patients are known to be HLA-B*58:01+, the European Medicines Agency advises clinicians to avoid allopurinol and screening is recommended in Korean, Thai, or Han Chinese patients (Ke et al., 2017). However, recent analysis in the UK defined the number needed to test (NNT) as 11,286, leading the panel to advise against routine screening (Plumpton et al., 2017).

HLA-B*13:01 and Dapsone-SCAR

The antibiotic dapsone is predominantly associated with treatment of leprosy (Wolf et al., 2002). In 2013, HLA-B*13:01 was described with 99.8% NPV and 7.8% PPV as a risk factor among Chinese patients for dapsone hypersensitivity (Zhang et al., 2013). While prevalent in Chinese and Indian populations, HLA-B*13:01 is comparatively absent among Europeans and Africans. HLA-B*13:01 risk is now confirmed for dapsone-SCAR in Thailand (Tempark et al., 2017) and research has modeled drug interaction within the HLA binding site (Watanabe et al., 2017). Most recently, Chen expanded HLA-B*13:01 risk to patients from Malaysia and Taiwan (Chen et al., 2018), and Zhao identified dapsone-responsive HLA-B*13:01-restricted $CD8^+$ T-cells in patients (Zhao et al., 2019).

HLA-A*32:01 and Vancomycin-DRESS

Vancomycin, a front-line treatment for beta-lactam-resistant infections (Rybak et al., 2009; Frymoyer et al., 2013; Moore et al., 2020), is the most common antibiotic instigator of DRESS (Wolfson et al., 2019). In 2019, Konvinse published strong association between HLA-A*32:01 and vancomycin-DRESS determining that 20% of HLA-A*32:01+ patients would develop the disease (Konvinse et al., 2019). With a European prevalence of 6.8%, they predicted the NNT as just 75 and have since developed an HLA-A*32:01-specific, cost-effective real-time PCR screen (Rwandamuriye et al., 2019). In 2020, Nakkam described cross-reactivity with an alternate glycopeptide antibiotic, teicoplanin, in 16% of HLA-A*32:01+ vancomycin-DRESS patients predicted by a shared class II HLA haplotype (Nakkam et al., 2020). These data implicate risk alleles with influence not simply to dictate predisposition but with ramifications for ongoing treatment. Importantly, while predictive values defined by limited case-control studies may not be indicative of risk in the underlying population, warranting caution, in vitro assays have functionally confirmed that HLA risk restricted drug-specific T-cell activation for abacavir, CBZ, allopurinol, dapsone, and vancomycin (Chessman et al., 2008; Wei et al., 2012; Yun et al., 2014; Zhao et al., 2019; Nakkam et al., 2020).

RECENTLY REPORTED HLA ASSOCIATIONS (2019-)

Single HLA associations up until 2019 have been extensively reviewed (White et al., 2015; Karnes et al., 2019;

Oussalah et al., 2020). Since then, further advancement in sequencing platforms has been providing increased resolution that has enabled discovery of novel HLA associations (LaHaye et al., 2016; van der Ven et al., 2018; Giannopoulou et al., 2019; Mimori et al., 2019). In 2019, Nakatani reported a Japanese association between SJS/TEN, HLA-A*02:06:01, and cold medicines containing non-steroidal anti-inflammatories (Nakatani et al., 2019). Furthermore, Tangamornsuksan reported an association between methazolamide-induced SJS/TEN and HLA-B*59:01 in Koreans and Han Chinese (Tangamornsuksan and Lohitnavy, 2019). In 2020, within a Thai HIV cohort, Sukasem reported an association between co-trimoxazole-induced DRESS with HLA-B*13:01 and SJS/TEN with HLA-B*15:02 and HLA-C*08:01 (Sukasem et al., 2020). Furthermore, MPE and DRESS resulting from benznidazole was associated with HLA-A*68, A*11:01, and A*29:02 in Bolivian patients with Chagas disease (Balas et al., 2020). Most recently, Zhao reported an association between oxcarbazepine-induced MPE and HLA-A*03:01 and HLA-B*07:02 in patients of Uighur Chinese ethnicity (Zhao et al., 2020). Moreover, HLA associations have also been reported for herbal medicines including green tea (Hoofnagle et al., 2020) and polygonum multiflorum with HLA-B*35:01 (Li et al., 2019). These studies provide a glimpse into the recent progress toward risk prediction specific to populations, yet a significant hurdle remains risk discovery in minority groups for whom access to large cohorts for traditional population studies is nearly impossible. One strategy is to maximize utility of international SCAR registries where careful patient matching for drug, reaction phenotype, and ethnicity may provide means to explore shared risk (Somogyi et al., 2019). Indeed, Somogyi identified three patients of Australian Indigenous ethnicity with phenytoin-DRESS sharing HLA-B*56:02 (Somogyi et al., 2019). Critically, HLA-B*56:02 frequency ranges up to 19% in this population but is absent from the predominant Australian European populace, highlighting utility of detailed biobanking with functional validation of proposed risk alleles (Monshi et al., 2013; Pan et al., 2019). Another possibility is the likelihood that alleles with shared specificities drive response to the same drug, as for nevirapine (Chantarangsu et al., 2009; Carr et al., 2013). Here, association with HLA-C*04 across ethnicities is driven by a unique F pocket motif that determines similar binding specificity for HLA-C*04:01 with HLA-C*05:01 and HLA-C*18:01, dominant in Hispanics and Africans, respectively (Pavlos et al., 2017). The ability to design HLA crystal structures combined with HLA binding algorithms provides a functional bridge to understand whether proposed antigen binds to diverse alleles (Pavlos et al., 2017). Nonetheless, HLA is not the sole requirement for T-cell activation and other parameters are proposed to retain the HLA-restricted "positive predictive gap."

T-CELL RECEPTORS PROVIDE SPECIFICITY FOR RECOGNITION OF RISK HLA-ANTIGEN COMPLEX

Antigenic peptides bound to HLA must contact the T-cell receptor (TCR) to trigger T-cell activation (**Figure 1**). Each individual's TCR repertoire comprises a diverse blend of public and private TCRs, which, through prior antigen exposure, may be uniquely distributed in tissues (Robins et al., 2010). A polyclonal response is well documented for abacavir (Redwood et al., 2019). This is in keeping with the altered peptide repertoire hypothesis suggesting that abacavir binds within the F pocket of the HLA-B*57:01 peptide binding groove altering its peptide specificity and the repertoire of self-peptides recognized as immunogenic (Illing et al., 2012). Polyclonal response is also observed during CDR3 spectratyping after the *in vitro* priming of naïve T-cells to the immunogenic drug metabolite sulfamethoxazole-nitroso (SMX-NO) (Gibson et al., 2017). Here the authors implicate the high protein reactivity of SMX-NO thought to drive formation of multiple haptens, each with potential to produce a diverse array of antigenic peptides. However, early work by Nassif reports predominant expression of Vβ 13.1 and 14 on T-cells in the blister of such patients, suggesting that early response in tissue is driven by more select, dominant clonotypes (Nassif et al., 2002). In 2019, Pan reported dominant single, public "VFDNTDKLI" TCRα CDR3 and "ASSLAGELFF" TCRβ CDR3 in HLA-B*15:02+ patients with CBZ hypersensitivity, rare in blood but dominantly expressed in blister (Pan et al., 2019). The dominant TCR was identified on T-cells expressing granulysin, a key cytotoxic mediator with precedent in eliciting tissue damage (Pan et al., 2019). Furthermore, the complete TCR blueprint provided by single-cell sequencing was synthetically reconstructed and shown to trigger T-cell activation specific to CBZ and HLA-B*15:02. Preferential TCR expansion has also been described in blister during HLA-B*58:01-associated allopurinol-SCAR (Chung et al., 2015). While further studies are warranted, those described begin to elucidate the specificity of a single dominantly expanded TCR to drive early response in the tissue of HLA-predisposed patients.

ERAP VARIANTS SKEW THE HLA-RESTRICTED IMMUNOPEPTIDOME

Although drug-protein conjugates are found at similar levels in allergic and tolerant patients (Park et al., 1998; Sullivan et al., 2015), the downstream impact of N-terminal peptide trimming that shapes the HLA-presented immunopeptidome has remained undefined. This process is performed by endoplasmic reticulum aminopeptidases (ERAPs) 1 and 2 (Serwold et al., 2001; Chang et al., 2005; **Figure 1**) for which polymorphic variants alter susceptibility and outcome to autoimmune disease and viral infections with HLA class I-restricted etiologies (Evans et al., 2011; Guerini et al., 2012; Biasin et al., 2013; Fruci et al., 2014; Reeves and James, 2015; Saulle et al., 2019; Vidal-Castiñeira et al., 2020). Specifically, distinct ERAP1 allotypes skew the HLA-class I-expressed immunopeptidome during infectious disease, where hypoactive allotypes result in longer sub-dominant peptides that impair $CD8^+$ T-cell response (Kemming et al., 2019). Intriguingly, peptides with aromatic or hydrophobic C-terminal amino acids are favored by ERAP1 for efficient N-terminal trimming and treatment of cells with abacavir alters the self-peptide preference toward the same amino acids (Chang et al., 2005; Ostrov et al., 2012). In 2020, Pavlos identified

ERAP1 as a novel predictor of abacavir tolerance among HLA-B*57:01+ patients. Tolerant patients were significantly more likely to express ERAP1 hypoactive allotypes with reduced trimming efficiency compared to hypersensitive patients (Pavlos et al., 2020). While yet to transverse other drugs, the epistatic relationship between HLA and ERAP raises intrigue to the influence of other such genes. One such entity is the highly polymorphic Killer-cell Immunoglobulin-like receptors (KIRs) expressed on T-cells and Natural Killer (NK) cells (Mingari et al., 1997; LeMaoult et al., 2005), with both cell types reporting the predominant infiltrate of in SJS/TEN blister (Chung and Hung, 2010). HLA alleles are the distinct ligands for KIRs that regulate cytotoxic degranulation in a complex interaction with sensitivity to the presented peptide via overlapped TCR binding (Mandelboim et al., 1997; Boyington and Sun, 2002; Thananchai et al., 2007; Fadda et al., 2010; **Figure 1**). Notably, specific KIR have been associated with progression of HLA-restricted infectious disease (Bellón, 2019). Description by Fasbender of the induction of NK-activating ligands on hepatocytes after drug exposure, driving NK-mediated cytotoxicity, spurs interest given that T-cells in the blood of SJS/TEN patients overexpress KIR2DL2 and KIR2DL3 (Morel et al., 2010; Fasbender et al., 2020). With yet unreported genetic or functional assessment, studies are warranted to understand the combined influence of these interactions.

THE LIMITED ROLE OF ALTERED DRUG METABOLISM IN FORMATION OF IMMUNOGENIC MOIETIES

Drugs lacking protein reactivity may directly activate T-cells (Schnyder et al., 1997; Zanni et al., 1997; Naisbitt et al., 2003). However, metabolic detoxification pathways form protein-reactive metabolites, also reported to activate drug-specific T-cells (Naisbitt et al., 2001; Sullivan et al., 2015; **Figure 1**). Metabolism is highly varied due to polymorphic enzymes, with cytochrome P450 (CYP450) enzymes responsible for 90% of drug metabolism (Lynch and Price, 2007) and for which allelic variants are described from poor to ultrarapid metabolisers (Zanger and Schwab, 2013). While metabolic activity of skin is considered limited (Sharma et al., 2019), keratinocytes show capacity to metabolize and present drug-derived antigens (Reilly et al., 2000; Roychowdhury and Svensson, 2005). Several studies now investigate metabolic variants associated with DHR, most notably for phenytoin, predominantly oxidized to an inactive metabolite by CYP2C9 with minor contribution by CYP2C19. Genetic analyses show that CYP2C9*2 and CYP2C9*3 low function variants extend exposure to the immunogenic parent drug (Aynacioglu et al., 1999; Silvado et al., 2018). Specifically, CYP2C9*3 is associated with SJS/TEN in both Han Chinese (Chung et al., 2014) and Thai (Suvichapanich et al., 2015; Tassaneeyakul et al., 2016). In addition, CYP2C19*3 is associated with phenytoin-DRESS in Thai (Yampayon et al., 2017). In 2019, Su et al. (2019) published on the utility of combined risk HLA and CYP2C9*3 genetic testing in Asian populations to prevent phenytoin hypersensitivity. It is now advised that physicians reduce the starting dose by 25% for patients classed as intermediate metabolizers, defined by CYP2C9*1/*3 and CYP2C9*1/*2 carriage (Caudle et al., 2014). Metabolic variation is also associated with DHR driven by nevirapine, hydroxylated by CYP2B6. Loss of functional alleles CYP2B6*6 and CYP2B6*18 are associated with increased susceptibility for nevirapine-SJS/TEN, with the *18 variant only observed in patients of African ancestry (Ciccacci et al., 2013; Carr et al., 2014). A handful of other associations are explored by Pirmohamed and were not significant upon multiple-testing correction (Pirmohamed et al., 2000); thus, most data to date implicate only a minor role for metabolic variation in DHR.

THE INFLUENCE OF INFECTIOUS DISEASE

There are three main aspects to consider for the impact of infectious disease on DHR. The first aspect is the effect of cumulative drug exposure in cohorts where long-term exposures are driven by repeat infection like antibiotic hypersensitivity in patients with cystic fibrosis (CF). Indeed, CF patients are far more likely to develop an allergy to beta-lactams than patients without (Burrows et al., 2007; Wright et al., 2018); thus, it is possible that repeat high dosing and antigen accumulation contributes to risk. Second is the potential for disease-associated immune dysregulation to heighten allergic susceptibility. An example is the reduced DHR incidence in HIV patients following initiation of successful highly active antiretroviral therapy, which controls viral progression, preventing deterioration of immune function (Coopman et al., 1993; Li et al., 1998). Similarly, studies show that CF patients have dysfunctional antiviral T-cell responses (Hubeau et al., 2004). Indeed, toll-like receptor 4, which mediates inflammatory cytokine expression, is reduced in CF airway cell lines (John et al., 2010; Keiser et al., 2015). Interestingly, cytokine variants predispose to DHRs such as liver injury: IL10-592 AA and IL10-819 TT are associated with docetaxel-induced liver injury, and polymorphism-380G/A in TNF−α is associated with hepatitis induced by antituberculosis drugs (Kim et al., 2011a; Liang et al., 2013; **Figure 1**). Evidence suggests that drug antigens may mount response in tissue through pre-existing antiviral T-cells in a heterologous immunity model (Descamps et al., 2003; Mitani et al., 2005). Functional evidence is based on work by Lucas who showed that all drug-naive HLA-B*57:01+ individuals have T-cells responsive to abacavir (Lucas et al., 2015; Gibson et al., 2017). Such reactive promiscuity across all healthy donors implicates cross-reactivity with common broad-exposure pathogens (Smith et al., 2016).

THE INFERRED ROLE OF EPIGENETIC RISK

It is now well established that epigenetic modifications to open or close the transcriptional template of genes impacts immunological processes (North and Ellis, 2011;

Moggs et al., 2012). Epigenetic influence is environmental with documented effects from diet, viral exposures, and pollution driving distinguishable differences in immune status; thus, it may drive not only inter-individual but also intra-individual risk over time, proposing dynamic susceptibility. Indeed, Nadeau describes hypermethylation of the FOXP3 locus affecting Treg function and asthma severity in patients who live in areas with higher air pollution (Nadeau et al., 2010). Evidence now suggests that epigenetic effects may be multi-generational, with lead exposure and subsequent DNA methylation of fetal germ cells in grandparents traced through to grandchildren (Sen et al., 2015). While likely, epigenetic influence has yet to be directly inferred upon susceptibility to DHR, but there is some initial evidence. In 2018, Cheng published that risk of allopurinol-induced SCAR was attributed to variants of HCP5, PSORS1C1, TSHZ2, and NOTCH4. Although distinct polymorphisms and thus genetic variants, intriguingly NOTCH4 and TSHZ2, were included as genes that presented as highly differentially methylated, a form of epigenetic regulation (Cheng et al., 2017). Furthermore, Monroy-Arreola demonstrated upregulation of microRNA-21, -18, and -155 in drug-specific CD4+ T-cells from hypersensitive patients (Monroy-Arreola et al., 2018). While microRNA may regulate post-transcriptional gene expression, others bind to control regulators of epigenetic modification including DNA methyltransferases (Sato et al., 2011).

DYNAMIC DYSREGULATION IMPOSED BY IMMUNE CHECKPOINTS SPANS GENETIC AND THERAPEUTIC RISK

Immune checkpoints regulate T-cell activation to prevent uncontrolled activation. This complex process is the summation of varied co-stimulatory and opposingly co-inhibitory pathways (**Figure 1**). Intriguingly, polymorphic variants of checkpoints are linked to numerous autoimmune diseases including rheumatoid arthritis (Kong et al., 2005), multiple sclerosis (Kroner et al., 2005), and ankylosing spondylitis (Kantarci et al., 2003). While allelic influence is yet to be translated to risk for DHR, mechanistic studies have demonstrated the impact of blocking programmed death-1 (PD-1) or cytotoxic lymphocyte antigen-4 (CTLA4) axes to enhance naive T-cell priming to drug antigens (Gibson et al., 2014, 2017). Checkpoint inhibition is now widely adopted in cancer immunotherapy to re-invigorate anti-tumor T-cell responses, but dysregulation is not antigen-specific and immune-mediated ADR are common (Naidoo et al., 2015; Saw et al., 2017; Lomax et al., 2019). While reactions are varied and typically reported as enhanced immunogenicity to self (Mangan et al., 2020), emerging small cohort studies describe a high incidence of DHR in immune checkpoint inhibitor-treated patients (Imafuku et al., 2017; Ford et al., 2018). These studies remain only clinical observations and distinct checkpoint alleles have not been identified in genome-wide association studies; however, given the influence of multiple, counteracting co-signaling pathways, it may be that single variants have a low individual effect for which the previous studies have been underpowered. Further study is now warranted to define association with a greater risk of drug hypersensitivity reactions.

SUMMARY

Given a lack of a single HLA allele to provide complete PPV, other risk factors must further restrict response and recent advances have detailed (i) application of single-cell sequencing to define the HLA-restricted dominant TCR driving early response in tissue and (ii) the impact of ERAP variants to skew immunodominant peptide presentation. Intriguingly, other proposed risk factors such as checkpoint receptors span genetic and epigenetic risk, with expression subject to environmental or therapeutic pressures, implicating highly dynamic risk. Strategies are now needed to identify risk alleles in minority populations where large clinical cohorts are impossible to obtain. The availability of multi-omic approaches offers opportunity to merge high-resolution genotyping with single-cell phenotyping to tease out more complex risk signatures that may also enable cost-effective patient screening.

AUTHOR CONTRIBUTIONS

YL, PD, RH, and AP contributed writing toward individual sections of the manuscript, led and majority authored by YL. AG and EP provided expert review, direction, and guidance. All authors contributed to the article and approved the submitted version.

FUNDING

EP reports grants from the National Institutes of Health (P50GM115305, R01HG010863, R01AI152183, R21AI139021, and U01AI154659) and from the National Health and Medical Research Council of Australia. EP was Drug Allergy Section Editor and receives royalties from Uptodate and consulting fees from Biocryst, Janssen and Vertex. She is co-director of IIID Pty Ltd. that holds a patent for HLA-B*57:01 testing for abacavir hypersensitivity, and she holds a patent for Detection of Human Leukocyte Antigen-A*32:01 in connection with Diagnosing Drug Reaction with Eosinophilia and Systemic Symptoms without any financial remuneration and not directly related to the submitted work. Funders played no role in any aspect of this Review.

REFERENCES

Aynacioglu, A. S., Brockmöller, J., Bauer, S., Sachse, C., Güzelbey, P., Ongen, Z., et al. (1999). Frequency of cytochrome P450 CYP2C9 variants in a Turkish population and functional relevance for phenytoin. *Br. J. Clin. Pharmacol.* 48, 409–415. doi: 10.1046/j.1365-2125.1999.00012.x

Balas, A., Ramírez, E., Trigo, E., Cabañas, R., Fiandor, A., Arsuaga, M., et al. (2020). HLA-A* 68,-A* 11: 01, and-A* 29: 02 alleles are strongly associated with

benznidazole-induced maculopapular exanthema (MPE)/DRESS. *J. Allergy Clin. Immunol. Pract.* 8, 3198–3200.e3.

Bellón, T. (2019). Mechanisms of severe cutaneous adverse reactions: recent advances. *Drug Saf.* 42, 973–992. doi: 10.1007/s40264-019-00825-2

Biasin, M., Sironi, M., Saulle, I., De Luca, M., La Rosa, F., Cagliani, R., et al. (2013). Endoplasmic reticulum aminopeptidase 2 haplotypes play a role in modulating susceptibility to HIV infection. *AIDS* 27, 1697–1706. doi: 10.1097/qad.0b013e3283601cee

Bluestein, S., Yu, R., Stone, C., and Phillips, E. (2021). A review of drug reaction with eosinophilia and systemic symptoms in the FDA adverse event reporting system (FAERS). *J. Allergy Clin. Immunol.* 147:AB12. doi: 10.1016/j.jaci.2020.12.085

Boyington, J. C., and Sun, P. D. (2002). A structural perspective on MHC class I recognition by killer cell immunoglobulin-like receptors. *Mol. Immunol.* 38, 1007–1021. doi: 10.1016/s0161-5890(02)00030-5

Burrows, J. A., Nissen, L. M., Kirkpatrick, C. M., and Bell, S. C. (2007). Beta-lactam allergy in adults with cystic fibrosis. *J. Cystic Fibrosis* 6, 297–303. doi: 10.1016/j.jcf.2006.11.001

Capule, F., Tragulpiankit, P., Mahasirimongkol, S., Jittikoon, J., Wichukchinda, N., Theresa Alentajan-Aleta, L., et al. (2020). Association of carbamazepine-induced Stevens-Johnson syndrome/toxic epidermal necrolysis with the HLA-B75 serotype or HLA-B*15:21 allele in Filipino patients. *Pharmacogenomics J.* 20, 533–541. doi: 10.1038/s41397-019-0143-8

Carr, D. F., Bourgeois, S., Chaponda, M., Takeshita, L. Y., Morris, A. P., Castro, E. M. C., et al. (2017). Genome-wide association study of nevirapine hypersensitivity in a sub-Saharan African HIV-infected population. *J. Antimicrob. Chemother.* 72, 1152–1162.

Carr, D. F., Chaponda, M., Cornejo Castro, E. M., Jorgensen, A. L., Khoo, S., Van Oosterhout, J. J., et al. (2014). CYP2B6 c.983T>C polymorphism is associated with nevirapine hypersensitivity in Malawian and Ugandan HIV populations. *J. Antimicrob. Chemother.* 69, 3329–3334. doi: 10.1093/jac/dku315

Carr, D. F., Chaponda, M., Jorgensen, A. L., Castro, E. C., van Oosterhout, J. J., Khoo, S. H., et al. (2013). Association of human leukocyte antigen alleles and nevirapine hypersensitivity in a Malawian HIV-infected population. *Clin. Infect. Dis.* 56, 1330–1339. doi: 10.1093/cid/cit021

Caudle, K. E., Rettie, A. E., Whirl-Carrillo, M., Smith, L. H., Mintzer, S., Lee, M. T., et al. (2014). Clinical pharmacogenetics implementation consortium guidelines for CYP2C9 and HLA-B genotypes and phenytoin dosing. *Clin. Pharmacol. Ther.* 96, 542–548. doi: 10.1038/clpt.2014.159

Chang, C. C., Ng, C. C., Too, C. L., Choon, S. E., Lee, C. K., Chung, W. H., et al. (2017). Association of HLA-B*15:13 and HLA-B*15:02 with phenytoin-induced severe cutaneous adverse reactions in a Malay population. *Pharmacogenomics J.* 17, 170–173. doi: 10.1038/tpj.2016.10

Chang, S. C., Momburg, F., Bhutani, N., and Goldberg, A. L. (2005). The ER aminopeptidase, ERAP1, trims precursors to lengths of MHC class I peptides by a "molecular ruler" mechanism. *Proc. Natl. Acad. Sci. U.S.A.* 102, 17107–17112. doi: 10.1073/pnas.0500721102

Chantarangsu, S., Mushiroda, T., Mahasirimongkol, S., Kiertiburanakul, S., Sungkanuparph, S., Manosuthi, W., et al. (2009). HLA-B* 3505 allele is a strong predictor for nevirapine-induced skin adverse drug reactions in HIV-infected Thai patients. *Pharmacogenetics Genomics* 19, 139–146. doi: 10.1097/fpc.0b013e32831d0faf

Chen, W. T., Wang, C. W., Lu, C. W., Chen, C. B., Lee, H. E., Hung, S. I., et al. (2018). The function of HLA-B*13:01 involved in the pathomechanism of dapsone-induced severe cutaneous adverse reactions. *J. Invest. Dermatol.* 138, 1546–1554. doi: 10.1016/j.jid.2018.02.004

Cheng, L., Sun, B., Xiong, Y., Hu, L., Gao, L., Lv, Q., et al. (2017). The minor allele HCP5 rs3099844 A, PSORS1C1 rs3131003 G are associated with allopurinol−induced severe cutaneous adverse reactions in Han Chinese: a multicentre retrospective case−control clinical study. *Br. J. Dermatol.* 178, e191–e193.

Chessman, D., Kostenko, L., Lethborg, T., Purcell, A. W., Williamson, N. A., Chen, Z., et al. (2008). Human leukocyte antigen class I-restricted activation of CD8+ T cells provides the immunogenetic basis of a systemic drug hypersensitivity. *Immunity* 28, 822–832. doi: 10.1016/j.immuni.2008.04.020

Cheung, Y.-K., Cheng, S.-H., Chan, E. J. M., Lo, S. V., Ng, M. H. L., and Kwan, P. (2013). HLA-B alleles associated with severe cutaneous reactions to antiepileptic drugs in Han Chinese. *Epilepsia* 54, 1307–1314. doi: 10.1111/epi.12217

Chiu, M. L. S., Hu, M., Ng, M. H. L., Yeung, C. K., Chan, J. C. Y., Chang, M. M., et al. (2012). Association between HLA−B58:01 allele and severe cutaneous adverse reactions with allopurinol in Han Chinese in Hong Kong. *Br. J. Dermatol.* 167, 44–49. doi: 10.1111/j.1365-2133.2012.10894.x

Choudhary, S., McLeod, M., Torchia, D., and Romanelli, P. (2013). Drug reaction with eosinophilia and systemic symptoms (DRESS) syndrome. *J. Clin. Aesthet. Dermatol.* 6:31.

Chung, W. H., Chang, W. C., Lee, Y. S., Wu, Y. Y., Yang, C. H., Ho, H. C., et al. (2014). Genetic variants associated with phenytoin-related severe cutaneous adverse reactions. *JAMA* 312, 525–534.

Chung, W. H., and Hung, S. I. (2010). Genetic markers and danger signals in stevens-johnson syndrome and toxic epidermal necrolysis. *Allergol. Int.* 59, 325–332. doi: 10.2332/allergolint.10-rai-0261

Chung, W.-H., Hung, S.-I., Hong, H.-S., Hsih, M.-S., Yang, L.-C., Ho, H.-C., et al. (2004). A marker for Stevens–Johnson syndrome. *Nature* 428:486.

Chung, W.-H., Pan, R.-Y., Chu, M.-T., Chin, S.-W., Huang, Y.-L., Wang, W.-C., et al. (2015). Oxypurinol-specific T cells possess preferential TCR clonotypes and express granulysin in allopurinol-induced severe cutaneous adverse reactions. *J. Invest. Dermatol.* 135, 2237–2248. doi: 10.1038/jid.2015.165

Ciccacci, C., Di Fusco, D., Marazzi, M. C., Zimba, I., Erba, F., Novelli, G., et al. (2013). Association between CYP2B6 polymorphisms and Nevirapine-induced SJS/TEN: a pharmacogenetics study. *Eur. J. Clin. Pharmacol.* 69, 1909–1916. doi: 10.1007/s00228-013-1549-x

Coopman, S. A., Johnson, R. A., Platt, R., and Stern, R. S. (1993). Cutaneous disease and drug reactions in HIV infection. *New Engl. J. Med.* 328, 1670–1674. doi: 10.1056/nejm199306103282304

Daly, A. K., Donaldson, P. T., Bhatnagar, P., Shen, Y., Pe'er, I., Floratos, A., et al. (2009). HLA-B5701 genotype is a major determinant of drug-induced liver injury due to flucloxacillin. *Nat. Genet.* 41, 816–819. doi: 10.1038/ng.379

Descamps, V., Mahe, E., Houhou, N., Abramowitz, L., Rozenberg, F., Ranger−Rogez, S., et al. (2003). Drug−induced hypersensitivity syndrome associated with Epstein–Barr virus infection. *Br. J. Dermatol.* 148, 1032–1034. doi: 10.1046/j.1365-2133.2003.05330.x

Dormann, H., Muth-Selbach, U., Krebs, S., Criegee-Rieck, M., Tegeder, I., Schneider, H. T., et al. (2000). Incidence and costs of adverse drug reactions during hospitalisation. *Drug Saf.* 22, 161–168. doi: 10.2165/00002018-200022020-00007

Evans, D. M., Spencer, C. C., Pointon, J. J., Su, Z., Harvey, D., Kochan, G., et al. (2011). Interaction between ERAP1 and HLA-B27 in ankylosing spondylitis implicates peptide handling in the mechanism for HLA-B27 in disease susceptibility. *Nat. Genet.* 43, 761–767.

Fadda, L., Borhis, G., Ahmed, P., Cheent, K., Pageon, S. V., Cazaly, A., et al. (2010). Peptide antagonism as a mechanism for NK cell activation. *Proc. Natl. Acad. Sci. U.S.A.* 107, 10160–10165. doi: 10.1073/pnas.0913745107

Fasbender, F., Obholzer, M., Metzler, S., Stöber, R., Hengstler, J. G., and Watzl, C. (2020). Enhanced activation of human NK cells by drug-exposed hepatocytes. *Arch. Toxicol.* 94, 439–448. doi: 10.1007/s00204-020-02668-8

Ferrell, P. B. Jr., and McLeod, H. L. (2008). Carbamazepine, HLA-B*1502 and risk of Stevens-Johnson syndrome and toxic epidermal necrolysis: US FDA recommendations. *Pharmacogenomics* 9, 1543–1546. doi: 10.2217/14622416.9.10.1543

Fontana, R. J., Cirulli, E. T., Gu, J., Kleiner, D., Ostrov, D., Phillips, E., et al. (2018). The role of HLA-A*33:01 in patients with cholestatic hepatitis attributed to terbinafine. *J. Hepatol.* 69, 1317–1325. doi: 10.1016/j.jhep.2018.08.004

Ford, M., Sahbudin, I., Filer, A., Steven, N., and Fisher, B. A. (2018). High proportion of drug hypersensitivity reactions to sulfasalazine following its use in anti-PD-1-associated inflammatory arthritis. *Rheumatology* 57, 2244–2246. doi: 10.1093/rheumatology/key234

Fruci, D., Romania, P., D'Alicandro, V., and Locatelli, F. (2014). Endoplasmic reticulum aminopeptidase 1 function and its pathogenic role in regulating innate and adaptive immunity in cancer and major histocompatibility complex class I−associated autoimmune diseases. *Tissue Antigens* 84, 177–186. doi: 10.1111/tan.12410

Frymoyer, A., Guglielmo, B. J., and Hersh, A. L. (2013). Desired vancomycin trough serum concentration for treating invasive methicillin-resistant Staphylococcal infections. *Pediatr. Infect. Dis. J.* 32, 1077–1079. doi: 10.1097/inf.0b013e318299f75c

Gao, S., Gui, X.-E., Liang, K., Liu, Z., Hu, J., and Dong, B. (2012). HLA-dependent hypersensitivity reaction to nevirapine in Chinese Han HIV-infected patients. *AIDS Res. Hum. Retroviruses* 28, 540–543. doi: 10.1089/aid.2011.0107

Gatanaga, H., Yazaki, H., Tanuma, J., Honda, M., Genka, I., Teruya, K., et al. (2007). HLA-Cw8 primarily associated with hypersensitivity to nevirapine. *AIDS* 21, 264–265. doi: 10.1097/qad.0b013e32801199d9

Genin, E., Chen, D., Hung, S., Sekula, P., Schumacher, M., Chang, P., et al. (2014). HLA-A* 31: 01 and different types of carbamazepine-induced severe cutaneous adverse reactions: an international study and meta-analysis. *Pharmacogenomics J.* 14, 281–288. doi: 10.1038/tpj.2013.40

Génin, E., Schumacher, M., Roujeau, J.-C., Naldi, L., Liss, Y., Kazma, R., et al. (2011). Genome-wide association study of Stevens-Johnson syndrome and toxic epidermal necrolysis in Europe. *Orphanet J. Rare Dis.* 6:52.

Giannopoulou, E., Katsila, T., Mitropoulou, C., Tsermpini, E. E., and Patrinos, G. P. (2019). Integrating next-generation sequencing in the clinical pharmacogenomics workflow. *Front. Pharmacol.* 10:384. doi: 10.3389/fphar.2019.00384

Gibson, A., Faulkner, L., Lichtenfels, M., Ogese, M., Al-Attar, Z., Alfirevic, A., et al. (2017). The effect of inhibitory signals on the priming of drug hapten-specific T cells that express distinct Vβ receptors. *J. Immunol.* 199, 1223–1237. doi: 10.4049/jimmunol.1602029

Gibson, A., Ogese, M., Sullivan, A., Wang, E., Saide, K., Whitaker, P., et al. (2014). Negative regulation by PD-L1 during drug-specific priming of IL-22-secreting T cells and the influence of PD-1 on effector T cell function. *J. Immunol.* 192, 2611–2621. doi: 10.4049/jimmunol.1302720

Gonçalo, M., Coutinho, I., Teixeira, V., Gameiro, A. R., Brites, M. M., Nunes, R., et al. (2013). HLA-B*58:01 is a risk factor for allopurinol-induced DRESS and Stevens-Johnson syndrome/toxic epidermal necrolysis in a Portuguese population. *Br. J. Dermatol.* 169, 660–665. doi: 10.1111/bjd.12389

Guerini, F. R., Cagliani, R., Forni, D., Agliardi, C., Caputo, D., Cassinotti, A., et al. (2012). A functional variant in ERAP1 predisposes to multiple sclerosis. *PLoS One* 7:e29931. doi: 10.1371/journal.pone.0029931

Heap, G. A., Weedon, M. N., Bewshea, C. M., Singh, A., Chen, M., Satchwell, J. B., et al. (2014). HLA-DQA1–HLA-DRB1 variants confer susceptibility to pancreatitis induced by thiopurine immunosuppressants. *Nat. Genet.* 46, 1131–1134.

Her, Y., Kil, M. S., Park, J. H., Kim, C. W., and Kim, S. S. (2011). Stevens–Johnson syndrome induced by acetazolamide. *J. Dermatol.* 38, 272–275. doi: 10.1111/j.1346-8138.2010.00921.x

Hirata, K., Takagi, H., Yamamoto, M., Matsumoto, T., Nishiya, T., Mori, K., et al. (2008). Ticlopidine-induced hepatotoxicity is associated with specific human leukocyte antigen genomic subtypes in Japanese patients: a preliminary case–control study. *Pharmacogenomics J.* 8, 29–33. doi: 10.1038/sj.tpj.6500442

Hoofnagle, J. H., Bonkovsky, H. L., Phillips, E. J., Li, Y. J., Ahmad, J., Barnhart, H., et al. (2020). HLA−B35:01 and green tea induced liver injury. *Hepatology* doi: 10.1002/hep.31538 [Epub ahead of print],

Hubeau, C., Le Naour, R., Abély, M., Hinnrasky, J., Guenounou, M., Gaillard, D., et al. (2004). Dysregulation of IL-2 and IL-8 production in circulating T lymphocytes from young cystic fibrosis patients. *Clin. Exp. Immunol.* 135, 528–534. doi: 10.1111/j.1365-2249.2003.02385.x

Hung, S.-I., Chung, W.-H., Liou, L.-B., Chu, C.-C., Lin, M., Huang, H.-P., et al. (2005). HLA-B* 5801 allele as a genetic marker for severe cutaneous adverse reactions caused by allopurinol. *Proc. Natl. Acad. Sci. U.S.A.* 102, 4134–4139. doi: 10.1073/pnas.0409500102

Hung, S. I., Chung, W. H., Liu, Z. S., Chen, C. H., Hsih, M. S., Hui, R. C., et al. (2010). Common risk allele in aromatic antiepileptic-drug induced Stevens-Johnson syndrome and toxic epidermal necrolysis in Han Chinese. *Pharmacogenomics* 11, 349–356. doi: 10.2217/pgs.09.162

Illing, P. T., Vivian, J. P., Dudek, N. L., Kostenko, L., Chen, Z., Bharadwaj, M., et al. (2012). Immune self-reactivity triggered by drug-modified HLA-peptide repertoire. *Nature* 486, 554–558. doi: 10.1038/nature11147

Imafuku, K., Yoshino, K., Ymaguchi, K., Tsuboi, S., Ohara, K., and Hata, H. (2017). Nivolumab therapy before vemurafenib administration induces a severe skin rash. *J. Eur. Acad. Dermatol. Venereol.* 31, e169–e171.

Jarjour, S., Barrette, M., Normand, V., Rouleau, J. L., Dubé, M. P., and de Denus, S. (2015). Genetic markers associated with cutaneous adverse drug reactions to allopurinol: a systematic review. *Pharmacogenomics* 16, 755–767. doi: 10.2217/pgs.15.21

John, G., Yildirim, A. O., Rubin, B. K., Gruenert, D. C., and Henke, M. O. (2010). TLR-4–mediated innate immunity is reduced in cystic fibrosis airway cells. *Am. J. Respir. Cell Mol. Biol.* 42, 424–431. doi: 10.1165/rcmb.2008-0408oc

Kang, H.-R., Jee, Y. K., Kim, Y.-S., Lee, C. H., Jung, J.-W., Kim, S. H., et al. (2011). Positive and negative associations of HLA class I alleles with allopurinol-induced SCARs in Koreans. *Pharmacogenet. Genomics* 21, 303–307. doi: 10.1097/fpc.0b013e32834282b8

Kaniwa, N., Saito, Y., Aihara, M., Matsunaga, K., Tohkin, M., Kurose, K., et al. (2008). HLA-B locus in Japanese patients with anti-epileptics and allopurinol-related Stevens-Johnson syndrome and toxic epidermal necrolysis. *Pharmacogenomics* 9, 1617–1622. doi: 10.2217/14622416.9.11.1617

Kaniwa, N., Sugiyama, E., Saito, Y., Kurose, K., Maekawa, K., Hasegawa, R., et al. (2013). Specific HLA types are associated with antiepileptic drug-induced Stevens-Johnson syndrome and toxic epidermal necrolysis in Japanese subjects. *Pharmacogenomics* 14, 1821–1831. doi: 10.2217/pgs.13.180

Kantarci, O. H., Hebrink, D. D., Achenbach, S. J., Atkinson, E. J., Waliszewska, A., Buckle, G., et al. (2003). CTLA4 is associated with susceptibility to multiple sclerosis. *J. Neuroimmunol.* 134, 133–141. doi: 10.1016/s0165-5728(02)00395-8

Kardaun, S. H. (2019). "Drug reaction with eosinophilia and systemic symptoms (DRESS)," in *Advances in Diagnosis and Management of Cutaneous Adverse Drug Reactions*, eds N. H. Shear and R. P. Dodiuk-Gad (Cham: Springer), 87–104.

Karnes, J. H., Miller, M. A., White, K. D., Konvinse, K. C., Pavlos, R. K., Redwood, A. J., et al. (2019). Applications of immunopharmacogenomics: predicting, preventing, and understanding immune-mediated adverse drug reactions. *Annu. Rev. Pharmacol. Toxicol.* 59, 463–486. doi: 10.1146/annurev-pharmtox-010818-021818

Kazeem, G. R., Cox, C., Aponte, J., Messenheimer, J., Brazell, C., Nelsen, A. C., et al. (2009). High-resolution HLA genotyping and severe cutaneous adverse reactions in lamotrigine-treated patients. *Pharmacogenet. Genomics* 19, 661–665. doi: 10.1097/fpc.0b013e32832c347d

Ke, C. H., Chung, W. H., Wen, Y. H., Huang, Y. B., Chuang, H. Y., Tain, Y. L., et al. (2017). Cost-effectiveness analysis for genotyping before allopurinol treatment to prevent severe cutaneous adverse drug reactions. *J. Rheumatol.* 44, 835–843. doi: 10.3899/jrheum.151476

Keiser, N. W., Birket, S. E., Evans, I. A., Tyler, S. R., Crooke, A. K., Sun, X., et al. (2015). Defective innate immunity and hyperinflammation in newborn cystic fibrosis transmembrane conductance regulator–knockout ferret lungs. *Am. J. Respir. Cell Mol. Biol.* 52, 683–694. doi: 10.1165/rcmb.2014-0250oc

Kemming, J., Reeves, E., Nitschke, K., Widmeier, V., Emmerich, F., Hermle, T., et al. (2019). ERAP1 allotypes shape the epitope repertoire of virus-specific CD8+ T cell responses in acute hepatitis C virus infection. *J. Hepatol.* 70, 1072–1081. doi: 10.1016/j.jhep.2019.01.034

Kim, B. K., Jung, J. W., Kim, T. B., Chang, Y. S., Park, H. S., Moon, J., et al. (2017). HLA-A*31:01 and lamotrigine-induced severe cutaneous adverse drug reactions in a Korean population. *Ann. Allergy Asthma Immunol.* 118, 629–630. doi: 10.1016/j.anai.2017.02.011

Kim, S.-H., Kim, S.-H., Yoon, H., Shin, D., Park, S.-S., Kim, Y.-S., et al. (2011a). TNF−α genetic polymorphism -308G/A and antituberculosis drug−induced hepatitis. *Liver Int.* 32, 809–814. doi: 10.1111/j.1478-3231.2011.02697.x

Kim, S.-H., Lee, K. W., Song, W.-J., Kim, S.-H., Jee, Y.-K., Lee, S.-M., et al. (2011b). Carbamazepine-induced severe cutaneous adverse reactions and HLA genotypes in Koreans. *Epilepsy Res.* 97, 190–197. doi: 10.1016/j.eplepsyres.2011.08.010

Kong, E. K., Prokunina-Olsson, L., Wong, W. H., Lau, C. S., Chan, T. M., Alarcón-Riquelme, M., et al. (2005). A new haplotype of PDCD1 is associated with rheumatoid arthritis in Hong Kong Chinese. *Arthritis Rheum.* 52, 1058–1062. doi: 10.1002/art.20966

Konvinse, K. C., Trubiano, J. A., Pavlos, R., James, I., Shaffer, C. M., Bejan, C. A., et al. (2019). HLA-A*32:01 is strongly associated with vancomycin-induced drug reaction with eosinophilia and systemic symptoms. *J. Allergy Clin. Immunol.* 144, 183–192.

Koomdee, N., Pratoomwun, J., Jantararoungtong, T., Theeramoke, V., Tassaneeyakul, W., Klaewsongkram, J., et al. (2017). Association of HLA-A and HLA-B alleles with lamotrigine-induced cutaneous adverse drug reactions in the Thai population. *Front. Pharmacol.* 8:879. doi: 10.3389/fphar.2017.00879

Kroner, A., Mehling, M., Hemmer, B., Rieckmann, P., Toyka, K. V., Mäurer, M., et al. (2005). A PD-1 polymorphism is associated with disease progression in multiple sclerosis. *Ann. Neurol.* 58, 50–57. doi: 10.1002/ana.20514

LaHaye, S., Corsmeier, D., Basu, M., Bowman, J. L., Fitzgerald-Butt, S., Zender, G., et al. (2016). Utilization of whole exome sequencing to identify causative mutations in familial congenital heart disease. *Circulation* 9, 320–329. doi: 10.1161/circgenetics.115.001324

Langley, A., Worley, B., Pardo, J. P., Beecker, J., Ramsay, T., Saavedra, A., et al. (2018). Systemic interventions for treatment of Stevens−Johnson syndrome (SJS), toxic epidermal necrolysis (TEN), and SJS/TEN overlap syndrome. *Cochrane Database Syst. Rev.* 2018:CD013130.

Lee, H. Y., Shen, M. X., Lim, Y. L., Tay, Y. K., Chan, M. M. F., Pang, S. M., et al. (2016). Increased risk of strontium ranelate-related SJS/TEN is associated with HLA. *Osteoporosis Int.* 27, 2577–2583. doi: 10.1007/s00198-016-3568-9

Leise, M. D., Poterucha, J. J., and Talwalkar, J. A. (2014). *Drug-induced Liver Injury. Mayo Clinic Proceedings*. Amsterdam: Elsevier.

LeMaoult, J., Zafaranloo, K., Le Danff, C., and Carosella, E. D. (2005). HLA−G up−regulates ILT2, ILT3, ILT4, and KIR2DL4 in antigen presenting cells, NK cells, and T cells. *FASEB J.* 19, 1–23. doi: 10.1096/fj.04-1617fje

Li, C., Rao, T., Chen, X., Zou, Z., Wei, A., Tang, J., et al. (2019). HLA-B*35:01 allele is a potential biomarker for predicting polygonum multiflorum-induced liver injury in humans. *Hepatology* 70, 346–357.

Li, L.-J., Hu, F.-Y., Wu, X.-T., An, D.-M., Yan, B., and Zhou, D. (2013). Predictive markers for carbamazepine and lamotrigine-induced maculopapular exanthema in Han Chinese. *Epilepsy Res.* 106, 296–300. doi: 10.1016/j.eplepsyres.2013.05.004

Li, T. S., Tubiana, R., Katlama, C., Calvez, V., Mohand, H. A., and Autran, B. (1998). Long-lasting recovery in CD4 T-cell function and viral-load reduction after highly active antiretroviral therapy in advanced HIV-1 disease. *Lancet* 351, 1682–1686. doi: 10.1016/s0140-6736(97)10291-4

Li, Y.-J., Phillips, E., Dellinger, A., Nicoletti, P., Schutte, R., Li, D., et al. (2020). HLA-B14:01 and HLA-B35:01 are associated with trimethoprim-sulfamethoxazole induced liver injury. *Hepatology* 73, 268–281.

Liang, X., Zhang, J., Zhu, Y., Lu, Y., Zhou, X., Wang, Z., et al. (2013). Specific genetic polymorphisms of IL10-592 AA and IL10-819 TT genotypes lead to the key role for inducing docetaxel-induced liver injury in breast cancer patients. *Clin. Transl. Oncol.* 15, 331–334. doi: 10.1007/s12094-012-0936-6

Littera, R., Carcassi, C., Masala, A., Piano, P., Serra, P., Ortu, F., et al. (2006). HLA-dependent hypersensitivity to nevirapine in Sardinian HIV patients. *AIDS* 20, 1621–1626. doi: 10.1097/01.aids.0000238408.82947.09

Locharernkul, C., Loplumlert, J., Limotai, C., Korkij, W., Desudchit, T., Tongkobpetch, S., et al. (2008). Carbamazepine and phenytoin induced Stevens−Johnson syndrome is associated with HLA−B* 1502 allele in Thai population. *Epilepsia* 49, 2087–2091. doi: 10.1111/j.1528-1167.2008.01719.x

Lomax, A. J., McQuillan, P. I. A., Hall, A., and McArthur, G. A. (2019). Acute toxic epidermal necrolysis reaction post single dose pembrolizumab with preceding cephalosporin exposure: successful rechallenge with anti-PD-1 therapy. *Intern. Med. J.* 49, 1051–1053. doi: 10.1111/imj.14388

Lonjou, C., Borot, N., Sekula, P., Ledger, N., Thomas, L., Halevy, S., et al. (2008). A European study of HLA-B in Stevens–Johnson syndrome and toxic epidermal necrolysis related to five high-risk drugs. *Pharmacogenet. Genomics* 18, 99–107. doi: 10.1097/fpc.0b013e3282f3ef9c

Lucas, A., Lucas, M., Strhyn, A., Keane, N. M., McKinnon, E., Pavlos, R., et al. (2015). Abacavir-reactive memory T cells are present in drug naïve individuals. *PLoS One* 10:e0117160. doi: 10.1371/journal.pone.0117160

Lucena, M. I., Molokhia, M., Shen, Y., Urban, T. J., Aithal, G. P., Andrade, R. J., et al. (2011). Susceptibility to Amoxicillin-Clavulanate-Induced Liver Injury Is Influenced by Multiple HLA Class I and II Alleles. *Gastroenterology* 141, 338–347. doi: 10.1053/j.gastro.2011.04.001

Lv, Y.-D., Min, F.-L., Liao, W.-P., He, N., Zeng, T., Ma, D.-H., et al. (2013). The association between oxcarbazepine-induced maculopapular eruption and HLA-B alleles in a Northern Han Chinese population. *BMC Neurol.* 13:75. doi: 10.1186/1471-2377-13-75

Lynch, T., and Price, A. (2007). The effect of cytochrome P450 metabolism on drug response, interactions, and adverse effects. *Am. Fam. Phys.* 76, 391–396.

Mallal, S., Nolan, D., Witt, C., Masel, G., Martin, A., Moore, C., et al. (2002). Association between presence of HLA-B* 5701, HLA-DR7, and HLA-DQ3 and hypersensitivity to HIV-1 reverse-transcriptase inhibitor abacavir. *Lancet* 359, 727–732. doi: 10.1016/s0140-6736(02)07873-x

Mallal, S., Phillips, E., Carosi, G., Molina, J.-M., Workman, C., Tomažič, J., et al. (2008). HLA-B* 5701 screening for hypersensitivity to abacavir. *New Engl. J. Med.* 358, 568–579.

Mandelboim, O., Wilson, S. B., Valés-Gómez, M., Reyburn, H. T., and Strominger, J. L. (1997). Self and viral peptides can initiate lysis by autologous natural killer cells. *Proc. Natl. Acad. Sci. U.S.A.* 94, 4604–4609. doi: 10.1073/pnas.94.9.4604

Mangan, B. L., McAlister, R. K., Balko, J. M., Johnson, D. B., Moslehi, J. J., Gibson, A., et al. (2020). Evolving insights into the mechanisms of toxicity associated with immune checkpoint inhibitor therapy. *Br. J. Clin. Pharmacol.* 86, 1778–1789. doi: 10.1111/bcp.14433

Martin, A. M., Nolan, D., James, I., Cameron, P., Keller, J., Moore, C., et al. (2005). Predisposition to nevirapine hypersensitivity associated with HLA-DRB1*0101 and abrogated by low CD4 T-cell counts. *AIDS* 19, 97–99. doi: 10.1097/00002030-200501030-00014

McCormack, M., Alfirevic, A., Bourgeois, S., Farrell, J. J., Kasperavičiūtė, D., Carrington, M., et al. (2011). HLA-A*3101 and carbamazepine-induced hypersensitivity reactions in Europeans. *N. Engl. J. Med.* 364, 1134–1143.

Mehta, T. Y., Prajapati, L. M., Mittal, B., Joshi, C. G., Sheth, J. J., Patel, D. B., et al. (2009). Association of HLA-B* 1502 allele and carbamazepine-induced Stevens-Johnson syndrome among Indians. *Indian J. Dermatol. Venereol. Leprol.* 75:579.

Mimori, T., Yasuda, J., Kuroki, Y., Shibata, T. F., Katsuoka, F., Saito, S., et al. (2019). Construction of full-length Japanese reference panel of class I HLA genes with single-molecule, real-time sequencing. *Pharmacogenomics J.* 19, 136–146. doi: 10.1038/s41397-017-0010-4

Mingari, M. C., Ponte, M., Cantoni, C., Vitale, C., Schiavetti, F., Bertone, S., et al. (1997). HLA-class I-specific inhibitory receptors in human cytolytic T lymphocytes: molecular characterization, distribution in lymphoid tissues and co-expression by individual T cells. *Int. Immunol.* 9, 485–491. doi: 10.1093/intimm/9.4.485

Mitani, N., Aihara, M., Yamakawa, Y., Yamada, M., Itoh, N., Mizuki, N., et al. (2005). Drug−induced hypersensitivity syndrome due to cyanamide associated with multiple reactivation of human herpesviruses. *J. Med. Virol.* 75, 430–434. doi: 10.1002/jmv.20295

Miya, R., Malpani, A. K., Keri, S., and Panagaon, R. (2019). Drug induced Steven-Johnson syndrome (SJS). *Indian J. Pharm. Pract.* 12:133. doi: 10.5530/ijopp.12.2.28

Mockenhaupt, M., Wang, C. W., Hung, S. I., Sekula, P., Schmidt, A. H., Pan, R. Y., et al. (2019). HLA−B* 57: 01 confers genetic susceptibility to carbamazepine−induced SJS/TEN in Europeans. *Allergy* 74, 2227–2230. doi: 10.1111/all.13821

Moggs, J. G., Terranova, R., Kammüller, M. E., Chibout, S.-D., Chapman, V., Dearman, R. J., et al. (2012). Regulation of allergic responses to chemicals and drugs: possible roles of epigenetic mechanisms. *Toxicol. Sci.* 130, 60–69. doi: 10.1093/toxsci/kfs207

Monroy-Arreola, A., Durán-Figueroa, N. V., Méndez-Flores, S., Domínguez-Cherit, J., Watkinson, J., Badillo-Corona, J. A., et al. (2018). Up-regulation of T-cell activation microRNAs in drug-specific CD4(+) T-cells from hypersensitive patients. *Chem. Res. Toxicol.* 31, 454–461. doi: 10.1021/acs.chemrestox.7b00330

Monshi, M. M., Faulkner, L., Gibson, A., Jenkins, R. E., Farrell, J., Earnshaw, C. J., et al. (2013). Human leukocyte antigen (HLA)−B* 57: 01−restricted activation of drug−specific T cells provides the immunological basis for flucloxacillin−induced liver injury. *Hepatology* 57, 727–739. doi: 10.1002/hep.26077

Moon, J., Park, H. K., Chu, K., Sunwoo, J. S., Byun, J. I., Lim, J. A., et al. (2015). The HLA-A*2402/Cw*0102 haplotype is associated with lamotrigine-induced maculopapular eruption in the Korean population. *Epilepsia* 56, e161–e167.

Moore, J. A., Meakin, M., Earl, M. H., Kummer, T. M., McAleer, J. P., and Long, T. E. (2020). Effects of caspofungin, tolcapone, and other FDA-approved medications on MRSA susceptibility to vancomycin. *J. Glob. Antimicrob. Resist.* 22, 283–289. doi: 10.1016/j.jgar.2020.03.014

Morel, E., Escamochero, S., Cabañas, R., Díaz, R., Fiandor, A., and Bellón, T. (2010). CD94/NKG2C is a killer effector molecule in patients with Stevens-Johnson syndrome and toxic epidermal necrolysis. *J. Allergy Clin. Immunol.* 125, 703–710.e708. doi: 10.1016/j.jaci.2009.10.030

Nadeau, K., McDonald-Hyman, C., Noth, E. M., Pratt, B., Hammond, S. K., Balmes, J., et al. (2010). Ambient air pollution impairs regulatory T-cell function in asthma. *J. Allergy Clin. Immunol.* 126, 845–852.e10.

Naidoo, J., Page, D. B., Li, B. T., Connell, L. C., Schindler, K., Lacouture, M. E., et al. (2015). Toxicities of the anti-PD-1 and anti-PD-L1 immune checkpoint antibodies. *Ann. Oncol.* 26, 2375–2391. doi: 10.1093/annonc/mdv383

Naisbitt, D., Britschgi, M., Wong, G., Farrell, J., Depta, J., Chadwick, D., et al. (2003). Hypersensitivity reactions to carbamazepine: characterization of the specificity, phenotype, and cytokine profile of drug-specific T cell clones. *Mol. Pharmacol.* 63, 732–741. doi: 10.1124/mol.63.3.732

Naisbitt, D. J., Williams, D. P., Pirmohamed, M., Kitteringham, N. R., and Park, B. K. (2001). Reactive metabolites and their role in drug reactions. *Curr. Opin. Allergy Clin. Immunol.* 1, 317–325. doi: 10.1097/01.all.0000011033.64625.5a

Nakamura, R., Ozeki, T., Hirayama, N., Sekine, A., Yamashita, T., Mashimo, Y., et al. (2020). Association of HLA-A*11:01 with sulfonamide-related severe cutaneous adverse reactions in Japanese patients. *J. Invest. Dermatol.* 140, 1659–1662.e6.

Nakatani, K., Ueta, M., Khor, S.-S., Hitomi, Y., Okudaira, Y., Masuya, A., et al. (2019). Identification of HLA-A* 0 2: 06: 01 as the primary disease susceptibility HLA allele in cold medicine-related Stevens-Johnson syndrome with severe ocular complications by high-resolution NGS-based HLA typing. *Sci. Rep.* 9, 1–8.

Nakkam, N., Gibson, A., Mouhtouris, E., Konvinse, K. C., Holmes, N., Chua, K. Y., et al. (2020). Cross-reactivity between vancomycin, teicoplanin, and telavancin in patients with HLA-A*32:01-positive vancomycin-induced DRESS sharing an HLA class II haplotype. *J. Allergy Clin. Immunol.* 147, 403–405. doi: 10.1016/j.jaci.2020.04.056

Nassif, A., Bensussan, A., Bachot, N., Bagot, M., Boumsell, L., Roujeau, J.-C., et al. (2002). Drug specific cytotoxic T-cells in the skin lesions of a patient with toxic epidermal necrolysis. *J. Invest. Dermatol.* 118, 728–733. doi: 10.1046/j.1523-1747.2002.01622.x

Nicoletti, P., Barrett, S., McEvoy, L., Daly, A. K., Aithal, G., Lucena, M. I., et al. (2019). Shared genetic risk factors across carbamazepine-induced hypersensitivity reactions. *Clin. Pharmacol. Ther.* 106, 1028–1036.

Niihara, H., Kakamu, T., Fujita, Y., Kaneko, S., and Morita, E. (2012). HLA−A31 strongly associates with carbamazepine−induced adverse drug reactions but not with carbamazepine−induced lymphocyte proliferation in a Japanese population. *J. Dermatol.* 39, 594–601. doi: 10.1111/j.1346-8138.2011.01457.x

North, M. L., and Ellis, A. K. (2011). The role of epigenetics in the developmental origins of allergic disease. *Ann. Allergy Asthma Immunol.* 106, 355–361; quiz62.

Ostrov, D. A., Grant, B. J., Pompeu, Y. A., Sidney, J., Harndahl, M., Southwood, S., et al. (2012). Drug hypersensitivity caused by alteration of the MHC-presented self-peptide repertoire. *Proc. Natl. Acad. Sci. U.S.A.* 109, 9959–9964. doi: 10.1073/pnas.1207934109

Oussalah, A., Yip, V., Mayorga, C., Blanca, M., Barbaud, A., Nakonechna, A., et al. (2020). Genetic variants associated with T cell-mediated cutaneous adverse drug reactions: a PRISMA-compliant systematic review-An EAACI position paper. *Allergy* 75, 1069–1098. doi: 10.1111/all.14174

Özkaya-Bayazit, E., and Akar, U. (2001). Fixed drug eruption induced by trimethoprim-sulfamethoxazole: evidence for a link to HLA-A30 B13 Cw6 haplotype. *J. Am. Acad. Dermatol.* 45, 712–717. doi: 10.1067/mjd.2001.117854

Pan, R.-Y., Chu, M.-T., Wang, C.-W., Lee, Y.-S., Lemonnier, F., Michels, A. W., et al. (2019). Identification of drug-specific public TCR driving severe cutaneous adverse reactions. *Nat. Commun.* 10, 1–13. doi: 10.1007/978-3-662-58713-3_36-1

Park, B. K., Pirmohamed, M., and Kitteringham, N. R. (1998). Role of drug disposition in drug hypersensitivity: a chemical, molecular, and clinical perspective. *Chem. Res. Toxicol.* 11, 969–988. doi: 10.1021/tx980058f

Patel, T. K., Barvaliya, M. J., Sharma, D., and Tripathi, C. (2013). A systematic review of the drug-induced Stevens-Johnson syndrome and toxic epidermal necrolysis in Indian population. *Indian J. Dermatol. Venereol. Leprol.* 79, 389. doi: 10.4103/0378-6323.110749

Paulmann, M., and Mockenhaupt, M. (2015). Severe drug-induced skin reactions: clinical features, diagnosis, etiology, and therapy. *J. Dtsch. Dermatol. Ges.* 13, 625–645. doi: 10.1111/ddg.12747

Pavlos, R., Deshpande, P., Chopra, A., Leary, S., Strautins, K., Nolan, D., et al. (2020). New genetic predictors for abacavir tolerance in HLA-B* 57: 01 positive individuals. *Hum. Immunol.* 81, 300–304. doi: 10.1016/j.humimm.2020.02.011

Pavlos, R., Mallal, S., Ostrov, D., Buus, S., Metushi, I., Peters, B., et al. (2015). T cell–mediated hypersensitivity reactions to drugs. *Annu. Rev. Med.* 66, 439–454. doi: 10.1146/annurev-med-050913-022745

Pavlos, R., McKinnon, E. J., Ostrov, D. A., Peters, B., Buus, S., Koelle, D., et al. (2017). Shared peptide binding of HLA Class I and II alleles associate with cutaneous nevirapine hypersensitivity and identify novel risk alleles. *Sci. Rep.* 7:8653.

Peter, J. G., Lehloenya, R., Dlamini, S., Risma, K., White, K. D., Konvinse, K. C., et al. (2017). Severe delayed cutaneous and systemic reactions to drugs: a global perspective on the science and art of current practice. *J. Allergy Clin. Immunol. Pract.* 5, 547–563. doi: 10.1016/j.jaip.2017.01.025

Pirmohamed, M., Alfirevic, A., Vilar, J., Stalford, A., Wilkins, E. G., Sim, E., et al. (2000). Association analysis of drug metabolizing enzyme gene polymorphisms in HIV-positive patients with co-trimoxazole hypersensitivity. *Pharmacogenetics* 10, 705–713. doi: 10.1097/00008571-200011000-00005

Plumpton, C. O., Alfirevic, A., Pirmohamed, M., and Hughes, D. A. (2017). Cost effectiveness analysis of HLA-B*58:01 genotyping prior to initiation of allopurinol for gout. *Rheumatology (Oxford)* 56, 1729–1739. doi: 10.1093/rheumatology/kex253

Pouyanne, P., Haramburu, F., Imbs, J. L., and Bégaud, B. (2000). Admissions to hospital caused by adverse drug reactions: cross sectional incidence study. *BMJ* 320:1036. doi: 10.1136/bmj.320.7241.1036

Redwood, A. J., Pavlos, R. K., White, K. D., and Phillips, E. J. (2018). HLAs: Key regulators of T-cell-mediated drug hypersensitivity. *HLA* 91, 3–16. doi: 10.1111/tan.13183

Redwood, A. J., Rwandamuriye, F., Chopra, A., Leary, S., Ram, R., McDonnell, W., et al. (2019). Single-cell transcriptomics reveal polyclonal memory T-cell responses in skin with positive abacavir patch test results. *J. Allergy Clin. Immunol.* 144, 1413–1416.e7.

Reeves, E., and James, E. (2015). The role of endoplasmic reticulum aminopeptidase 1 biology in immune evasion by tumours. *J. Vaccines Immunol.* 1, 28–35.

Reilly, T. P., Lash, L. H., Doll, M. A., Hein, D. W., Woster, P. M., and Svensson, C. K. (2000). A role for bioactivation and covalent binding within epidermal keratinocytes in sulfonamide-induced cutaneous drug reactions. *J. Invest. Dermatol.* 114, 1164–1173. doi: 10.1046/j.1523-1747.2000.00985.x

Robins, H. S., Srivastava, S. K., Campregher, P. V., Turtle, C. J., Andriesen, J., Riddell, S. R., et al. (2010). Overlap and effective size of the human CD8+ T cell receptor repertoire. *Sci. Transl. Med.* 2:47ra64. doi: 10.1126/scitranslmed.3001442

Roujeau, J. C., Huynh, T. N., Bracq, C., Guillaume, J. C., Revuz, J., and Touraine, R. (1987). Genetic susceptibility to toxic epidermal necrolysis. *Arch. Dermatol.* 123, 1171–1173. doi: 10.1001/archderm.123.9.1171

Roychowdhury, S., and Svensson, C. K. (2005). Mechanisms of drug-induced delayed-type hypersensitivity reactions in the skin. *AAPS J.* 7, E834–E846.

Rwandamuriye, F. X., Chopra, A., Konvinse, K. C., Choo, L., Trubiano, J. A., Shaffer, C. M., et al. (2019). A rapid allele-specific assay for HLA-A* 32: 01 to identify patients at risk for vancomycin-induced Drug Reaction with Eosinophilia and systemic symptoms. *J. Mol. Diagn.* 21, 782–789. doi: 10.1016/j.jmoldx.2019.04.006

Rybak, M. J., Lomaestro, B. M., Rotscahfer, J. C., Moellering, R. C. Jr., Craig, W. A., Billeter, M., et al. (2009). Vancomycin therapeutic guidelines: a summary of consensus recommendations from the infectious diseases Society of America, the American society of health-system pharmacists, and the society of infectious diseases pharmacists. *Clin. Infect. Dis.* 49, 325–327. doi: 10.1086/600877

Saag, M., Balu, R., Phillips, E., Brachman, P., Martorell, C., Burman, W., et al. (2008). High sensitivity of human leukocyte antigen-b* 5701 as a marker for immunologically confirmed abacavir hypersensitivity in white and black patients. *Clin. Infect. Dis.* 46, 1111–1118. doi: 10.1086/529382

Sabourirad, S., Mortezaee, R., Mojarad, M., Eslahi, A., Shahrokhi, Y., Kiafar, B., et al. (2020). Investigating the association of Lamotrigine and Phenytoin-induced Stevens-Johnson syndrome/Toxic Epidermal Necrolysis

with HLA-B*1502 in Iranian population. *Exp. Dermatol.* 30, 284–287. doi: 10.1111/exd.14240

Sato, F., Tsuchiya, S., Meltzer, S. J., and Shimizu, K. (2011). MicroRNAs and epigenetics. *FEBS J.* 278, 1598–1609. doi: 10.1111/j.1742-4658.2011.08089.x

Saulle, I., Ibba, S. V., Vittori, C., Fenizia, C., Piancone, F., Minisci, D., et al. (2019). Endoplasmic reticulum associated aminopeptidase 2 (ERAP2) is released in the secretome of activated MDMs and reduces in vitro HIV-1 infection. *Front. Immunol.* 10:1648. doi: 10.3389/fimmu.2019.01648

Saw, S., Lee, H. Y., and Ng, Q. S. (2017). Pembrolizumab-induced Stevens-Johnson syndrome in non-melanoma patients. *Eur. J. Cancer* 81, 237–239. doi: 10.1016/j.ejca.2017.03.026

Schnyder, B., Mauri-Hellweg, D., Zanni, M., Bettens, F., and Pichler, W. J. (1997). Direct, MHC-dependent presentation of the drug sulfamethoxazole to human alphabeta T cell clones. *J. Clin. Invest.* 100, 136–141. doi: 10.1172/jci119505

Sen, A., Heredia, N., Senut, M. C., Land, S., Hollocher, K., Lu, X., et al. (2015). Multigenerational epigenetic inheritance in humans: DNA methylation changes associated with maternal exposure to lead can be transmitted to the grandchildren. *Sci. Rep.* 5:14466.

Serwold, T., Gaw, S., and Shastri, N. (2001). ER aminopeptidases generate a unique pool of peptides for MHC class I molecules. *Nat. Immunol.* 2, 644–651. doi: 10.1038/89800

Sharma, A., Saito, Y., Hung, S.-I., Naisbitt, D., Uetrecht, J., and Bussiere, J. (2019). The skin as a metabolic and immune-competent organ: implications for drug-induced skin rash. *J. Immunotoxicol.* 16, 1–12. doi: 10.1080/1547691x.2018.1514444

Shi, Y.-W., Min, F.-L., Qin, B., Zou, X., Liu, X.-R., Gao, M.-M., et al. (2012). Association between HLA and Stevens–Johnson Syndrome Induced by Carbamazepine in Southern Han Chinese: genetic markers besides B*1502? *Basic Clin. Pharmacol. Toxicol.* 111, 58–64.

Silvado, C. E., Terra, V. C., and Twardowschy, C. A. (2018). CYP2C9 polymorphisms in epilepsy: influence on phenytoin treatment. *Pharmgenomics Pers. Med.* 11, 51–58. doi: 10.2147/pgpm.s108113

Smith, C. J., Quinn, M., and Snyder, C. M. (2016). CMV-specific CD8 T cell differentiation and localization: implications for adoptive therapies. *Front. Immunol.* 7:352. doi: 10.3389/fimmu.2016.00352

Somogyi, A. A., Barratt, D. T., Phillips, E. J., Moore, K., Ilyas, F., and Gabb, G. M. (2019). High and variable population prevalence of HLA—B* 56: 02 in indigenous Australians and relation to phenytoin—associated drug reaction with eosinophilia and systemic symptoms. *Br. J. Clin. Pharmacol.* 85, 2163–2169. doi: 10.1111/bcp.14025

Sousa-Pinto, B., Pinto-Ramos, J., Correia, C., Gonçalves-Costa, G., Gomes, L., Gil-Mata, S., et al. (2015). Pharmacogenetics of abacavir hypersensitivity: a systematic review and meta-analysis of the association with HLA-B*57:01. *J. Allergy Clin. Immunol.* 136, 1092–1094.e3.

Su, S. C., Chen, C. B., Chang, W. C., Wang, C. W., Fan, W. L., Lu, L. Y., et al. (2019). HLA Alleles and CYP2C9*3 as predictors of phenytoin hypersensitivity in East Asians. *Clin. Pharmacol. Ther.* 105, 476–485. doi: 10.1002/cpt.1190

Sukasem, C., Chaichan, C., Nakkrut, T., Satapornpong, P., Jaruthamsophon, K., Jantararoungtong, T., et al. (2018). Association between HLA-B alleles and carbamazepine-induced maculopapular exanthema and severe cutaneous reactions in Thai Patients. *J. Immunol. Res.* 2018, 1–11. doi: 10.1155/2018/2780272

Sukasem, C., Jantararoungtong, T., Kuntawong, P., Puangpetch, A., Koomdee, N., Satapornpong, P., et al. (2016). HLA-B (*) 58:01 for allopurinol-induced cutaneous adverse drug reactions: implication for clinical interpretation in Thailand. *Front. Pharmacol.* 7:186. doi: 10.3389/fphar.2016.00186

Sukasem, C., Pratoomwun, J., Satapornpong, P., Klaewsongkram, J., Rerkpattanapipat, T., Rerknimitr, P., et al. (2020). Genetic association of co-trimoxazole-induced severe cutaneous adverse reactions is phenotype-specific: HLA class I genotypes and haplotypes. *Clin. Pharmacol. Therap.* 108, 1078–1089. doi: 10.1002/cpt.1915

Sullivan, A., Gibson, A., Park, B. K., and Naisbitt, D. J. (2015). Are drug metabolites able to cause T-cell-mediated hypersensitivity reactions? *Expert Opin. Drug Metab. Toxicol.* 11, 357–368. doi: 10.1517/17425255.2015.992780

Suvichapanich, S., Jittikoon, J., Wichukchinda, N., Kamchaisatian, W., Visudtibhan, A., Benjapopitak, S., et al. (2015). Association analysis of CYP2C9*3 and phenytoin-induced severe cutaneous adverse reactions (SCARs) in Thai epilepsy children. *J. Hum. Genet.* 60, 413–417. doi: 10.1038/jhg.2015.47

Tangamornsuksan, W., Chaiyakunapruk, N., Somkrua, R., Lohitnavy, M., and Tassaneeyakul, W. (2013). Relationship between the HLA-B*1502 Allele and Carbamazepine-induced stevens-johnson syndrome and toxic epidermal necrolysis: a systematic review and meta-analysis. *JAMA Dermatol.* 149, 1025–1032. doi: 10.1001/jamadermatol.2013.4114

Tangamornsuksan, W., and Lohitnavy, M. (2019). Association between HLA-B*5901 and methazolamide-induced Stevens-Johnson syndrome/toxic epidermal necrolysis: a systematic review and meta-analysis. *Pharmacogenomics J.* 19, 286–294. doi: 10.1038/s41397-018-0052-2

Tassaneeyakul, W., Prabmeechai, N., Sukasem, C., Kongpan, T., Konyoung, P., Chumworathayi, P., et al. (2016). Associations between HLA class I and cytochrome P450 2C9 genetic polymorphisms and phenytoin-related severe cutaneous adverse reactions in a Thai population. *Pharmacogenet. Genomics* 26, 225–234. doi: 10.1097/fpc.0000000000000211

Tempark, T., Satapornpong, P., Rerknimitr, P., Nakkam, N., Saksit, N., Wattanakrai, P., et al. (2017). Dapsone-induced severe cutaneous adverse drug reactions are strongly linked with HLA-B*13: 01 allele in the Thai population. *Pharmacogenet. Genomics* 27, 429–437. doi: 10.1097/fpc.0000000000000306

Thananchai, H., Gillespie, G., Martin, M. P., Bashirova, A., Yawata, N., Yawata, M., et al. (2007). Cutting Edge: Allele-specific and peptide-dependent interactions between KIR3DL1 and HLA-A and HLA-B. *J. Immunol.* 178, 33–37. doi: 10.4049/jimmunol.178.1.33

Thomas, M., Hopkins, C., Duffy, E., Lee, D., Loulergue, P., Ripamonti, D., et al. (2017). Association of the HLA-B*53:01 Allele with drug reaction with eosinophilia and systemic symptoms (DRESS) syndrome during treatment of HIV infection with raltegravir. *Clin. Infect. Dis.* 64, 1198–1203. doi: 10.1093/cid/cix096

Urban, T. J., Nicoletti, P., Chalasani, N., Serrano, J., Stolz, A., Daly, A. K., et al. (2017). Minocycline hepatotoxicity: clinical characterization and identification of HLA-B*35:02 as a risk factor. *J. Hepatol.* 67, 137–144. doi: 10.1016/j.jhep.2017.03.010

van der Ven, A. T., Connaughton, D. M., Ityel, H., Mann, N., Nakayama, M., Chen, J., et al. (2018). Whole-exome sequencing identifies causative mutations in families with congenital anomalies of the kidney and urinary tract. *J. Am. Soc. Nephrol.* 29, 2348–2361.

Vidal-Castiñeira, J. R., López-Vázquez, A., Diaz-Bulnes, P., Díaz-Coto, S., Márquez-Kisinousky, L., Martínez-Borra, J., et al. (2020). Genetic contribution of endoplasmic reticulum aminopeptidase 1 polymorphisms to liver fibrosis progression in patients with HCV infection. *J. Mol. Med.* 98, 1245–1254. doi: 10.1007/s00109-020-01948-1

Wang, C.-W., Tassaneeyakul, W., Chen, C.-B., Chen, W.-T., Teng, Y.-C., Huang, C.-Y., et al. (2020). Whole genome sequencing identifies genetic variants associated with co-trimoxazole hypersensitivity in Asians. *J. Allergy Clin. Immunol.* [Epub ahead of print].

Wang, Q., Sun, S., Xie, M., Zhao, K., Li, X., and Zhao, Z. (2017). Association between the HLA-B alleles and carbamazepine-induced SJS/TEN: a meta-analysis. *Epilepsy Res.* 135, 19–28. doi: 10.1016/j.eplepsyres.2017.05.015

Watanabe, H., Watanabe, Y., Tashiro, Y., Mushiroda, T., Ozeki, T., Hashizume, H., et al. (2017). A docking model of dapsone bound to HLA-B*13:01 explains the risk of dapsone hypersensitivity syndrome. *J. Dermatol. Sci.* 88, 320–329. doi: 10.1016/j.jdermsci.2017.08.007

Wei, C.-Y., Chung, W.-H., Huang, H.-W., Chen, Y.-T., and Hung, S.-I. (2012). Direct interaction between HLA-B and carbamazepine activates T cells in patients with Stevens-Johnson syndrome. *J. Allergy Clin. Immunol.* 129, 1562–1569.e5.

White, K. D., Chung, W.-H., Hung, S.-I., Mallal, S., and Phillips, E. J. (2015). Evolving models of the immunopathogenesis of T cell-mediated drug allergy: the role of host, pathogens, and drug response. *J. Allergy Clin. Immunol.* 136, 219–235. doi: 10.1016/j.jaci.2015.05.050

WHO (2021). *WHO Model Lists of Essential Medicines*. Geneva: WHO.

Wolf, R., Matz, H., Orion, E., Tuzun, B., and Tuzun, Y. (2002). Dapsone. *Dermatol. Online J.* 8:2.

Wolfson, A. R., Zhou, L., Li, Y., Phadke, N. A., Chow, O. A., and Blumenthal, K. G. (2019). Drug reaction with eosinophilia and systemic symptoms (DRESS) syndrome identified in the electronic health record allergy module. *J. Allergy Clin. Immunol. Pract.* 7, 633–640. doi: 10.1016/j.jaip.2018.08.013

Wright, M. F., Bush, A., and Carr, S. B. (2018). Hypersensitivity reactions to intravenous antibiotics in cystic fibrosis. *Paediatr. Respir. Rev.* 27, 9–12. doi: 10.1016/j.prrv.2018.01.003

Yampayon, K., Sukasem, C., Limwongse, C., Chinvarun, Y., Tempark, T., Rerkpattanapipat, T., et al. (2017). Influence of genetic and non-genetic factors on phenytoin-induced severe cutaneous adverse drug reactions. *Eur. J. Clin. Pharmacol.* 73, 855–865. doi: 10.1007/s00228-017-2250-2

Yang, F., Gu, B., Zhang, L., Xuan, J., Luo, H., Zhou, P., et al. (2014). HLA-B*13:01 is associated with salazosulfapyridine-induced drug rash with eosinophilia and systemic symptoms in Chinese Han population. *Pharmacogenomics* 15, 1461–1469. doi: 10.2217/pgs.14.69

Yang, F., Xuan, J., Chen, J., Zhong, H., Luo, H., Zhou, P., et al. (2015). HLA-B*59:01: a marker for Stevens-Johnson syndrome/toxic epidermal necrolysis caused by methazolamide in Han Chinese. *Pharmacogenomics J.* 16, 83–87. doi: 10.1038/tpj.2015.25

Yu, K. H., Yu, C. Y., and Fang, Y. F. (2017). Diagnostic utility of HLA−B* 5801 screening in severe allopurinol hypersensitivity syndrome: an updated systematic review and meta−analysis. *Int. J. Rheum. Dis.* 20, 1057–1071. doi: 10.1111/1756-185x.13143

Yun, J., Marcaida, M. J., Eriksson, K. K., Jamin, H., Fontana, S., Pichler, W. J., et al. (2014). Oxypurinol directly and immediately activates the drug-specific T cells via the preferential use of HLA-B* 58: 01. *J. Immunol.* 192, 2984–2993. doi: 10.4049/jimmunol.1302306

Zanger, U. M., and Schwab, M. (2013). Cytochrome P450 enzymes in drug metabolism: regulation of gene expression, enzyme activities, and impact of genetic variation. *Pharmacol. Therap.* 138, 103–141. doi: 10.1016/j.pharmthera.2012.12.007

Zanni, M. P., Mauri-Hellweg, D., Brander, C., Wendland, T., Schnyder, B., Frei, E., et al. (1997). Characterization of lidocaine-specific T cells. *J. Immunol.* 158, 1139–1148.

Zhang, F.-R., Liu, H., Irwanto, A., Fu, X.-A., Li, Y., Yu, G.-Q., et al. (2013). HLA-B* 13: 01 and the dapsone hypersensitivity syndrome. *New Engl. J. Med.* 369, 1620–1628.

Zhao, Q., Alhilali, K., Alzahrani, A., Almutairi, M., Amjad, J., Liu, H., et al. (2019). Dapsone−and nitroso dapsone−specific activation of T cells from hypersensitive patients expressing the risk allele HLA−B* 13: 01. *Allergy* 74, 1533–1548.

Zhao, T., Wang, T.-T., Jia, L., Wang, F., Bahatibieke, M., Liu, W-l, et al. (2020). The association between HLA-A*03:01 and HLA-B*07:02 alleles and oxcarbazepine-induced maculopapular eruption in the Uighur Chinese Population. *Seizure* 81, 43–46. doi: 10.1016/j.seizure.2020.05.006

Zimmerman, D., and Dang, N. H. (2020). Stevens–Johnson Syndrome (SJS) and toxic epidermal necrolysis (TEN) immunologic reactions. *Oncol. Crit. Care* 2020, 267–280. doi: 10.1007/978-3-319-74588-6_195

Conflict of Interest: The reviewer AC declared a past co-authorship with the authors AG and EP to the handling editor.

EP was Drug Allergy Section Editor and receives royalties from Uptodate and consulting fees from Biocryst, Janssen and Vertex. She is co-director of IIID Pty Ltd that holds a patent for HLA-B*57:01 testing for abacavir hypersensitivity, and she holds a patent for Detection of Human Leukocyte Antigen-A*32:01 in connection with Diagnosing Drug Reaction with Eosinophilia and Systemic Symptoms without any financial remuneration and not directly related to the submitted work. Funders played no role in any aspect of this Review.

The remaining authors declare that the research was conducted in the absence of any commercial or financial relationships that could be construed as a potential conflict of interest.

frontiers in Immunology

ORIGINAL RESEARCH
published: 29 April 2021
doi: 10.3389/fimmu.2021.658593

Characterization of T-Cell Responses to SMX and SMX-NO in Co-Trimoxazole Hypersensitivity Patients Expressing *HLA-B*13:01*

*Jirawat Pratoomwun[1,2], Paul Thomson[3], Kanoot Jaruthamsophon[4], Rawiporn Tiyasirichokchai[1], Pimonpan Jinda[1], Ticha Rerkpattanapipat[5], Wichittra Tassaneeyakul[6], Nontaya Nakkam[6], Pawinee Rerknimitr[7], Jettanong Klaewsongkram[8], Yuttana Srinoulprasert[9], Munir Pirmohamed[3], Dean J. Naisbitt[3] and Chonlaphat Sukasem[1]**

[1] Division of Pharmacogenomics and Personalized Medicine, Department of Pathology, Faculty of Medicine Ramathibodi Hospital, Mahidol University, Bangkok, Thailand, [2] Department of Clinical Chemistry, Faculty of Medical Technology, Huachiew Chalermprakiet University, Samut Prakan, Thailand, [3] MRC Centre for Drug Safety Science, Department of Molecular and Clinical Pharmacology, University of Liverpool, Liverpool, United Kingdom, [4] Division of Human Genetics, Department of Pathology, Faculty of Medicine, Prince of Songkla University, Hat Yai, Thailand, [5] Division of Allergy Immunology and Rheumatology, Department of Medicine, Faculty of Medicine, Ramathibodi Hospital, Mahidol University, Bangkok, Thailand, [6] Department of Pharmacology, Faculty of Medicine, Khon Kaen University, Khon Kaen, Thailand, [7] Division of Dermatology, Department of Medicine, Faculty of Medicine, Skin and Allergy Research Unit, Chulalongkorn University, Bangkok, Thailand, [8] Skin and Allergy Research Unit, Division of Allergy and Clinical Immunology, Department of Medicine, Faculty of Medicine, Chulalongkorn University, Bangkok, Thailand, [9] Department of Immunology, Faculty of Medicine Siriraj Hospital, Mahidol University, Bangkok, Thailand

OPEN ACCESS

Edited by:
Nicole Andrea Mifsud,
Monash University, Australia

Reviewed by:
Silvana Gaudieri,
University of Western Australia, Australia
Michaela Lucas,
University of Western Australia, Australia

***Correspondence:**
Chonlaphat Sukasem
chonlaphat.suk@mahidol.ac.th

Specialty section:
This article was submitted to T Cell Biology, a section of the journal Frontiers in Immunology

Received: 26 January 2021
Accepted: 07 April 2021
Published: 29 April 2021

Citation:
Pratoomwun J, Thomson P, Jaruthamsophon K, Tiyasirichokchai R, Jinda P, Rerkpattanapipat T, Tassaneeyakul W, Nakkam N, Rerknimitr P, Klaewsongkram J, Srinoulprasert Y, Pirmohamed M, Naisbitt DJ and Sukasem C (2021) Characterization of T-Cell Responses to SMX and SMX-NO in Co-Trimoxazole Hypersensitivity Patients Expressing HLA-B*13:01. Front. Immunol. 12:658593. doi: 10.3389/fimmu.2021.658593

*HLA-B*13:01*-positive patients in Thailand can develop frequent co-trimoxazole hypersensitivity reactions. This study aimed to characterize drug-specific T cells from three co-trimoxazole hypersensitive patients presenting with either Stevens-Johnson syndrome or drug reaction with eosinophilia and systemic symptoms. Two of the patients carried the HLA allele of interest, namely *HLA-B*13:01*. Sulfamethoxazole and nitroso sulfamethoxazole specific T cell clones were generated from T cell lines of co-trimoxazole hypersensitive *HLA-B*13:01*-positive patients. Clones were characterized for antigen specificity and cross-reactivity with structurally related compounds by measuring proliferation and cytokine release. Surface marker expression was characterized *via* flow cytometry. Mechanistic studies were conducted to assess pathways of T cell activation in response to antigen stimulation. Peripheral blood mononuclear cells from all patients were stimulated to proliferate and secrete IFN-γ with nitroso sulfamethoxazole. All sulfamethoxazole and nitroso sulfamethoxazole specific T cell clones expressed the CD4+ phenotype and strongly secreted IL-13 as well as IFN-γ, granzyme B and IL-22. No secretion of IL-17 was observed. A number of nitroso sulfamethoxazole-specific clones cross-reacted with nitroso dapsone but not sulfamethoxazole whereas sulfamethoxazole specific clones cross-reacted with nitroso sulfamethoxazole only. The nitroso sulfamethoxazole specific clones were activated in both antigen processing-dependent and -independent manner, while sulfamethoxazole activated T cell responses *via* direct HLA binding. Furthermore, activation of nitroso sulfamethoxazole-specific,

but not sulfamethoxazole-specific, clones was blocked with glutathione. Sulfamethoxazole and nitroso sulfamethoxazole specific T cell clones from hypersensitive patients were CD4+ which suggests that *HLA-B*13:01* is not directly involved in the iatrogenic disease observed in co-trimoxazole hypersensitivity patients.

Keywords: co-trimoxazole, drug hypersensitivity, human leukocyte antigen, sulfamethoxazole, T cell

INTRODUCTION

Co-trimoxazole (CTX) is a combination drug consisting of trimethoprim (TMP) and sulfamethoxazole (SMX). It is commonly used for treatment of urinary tract infections due to *E. coli*, *Klebsiella* and *Enterobacter* spp. and also suitable for gastrointestinal infections against *E. coli*, *Shigella* spp. and *Salmonella typhi*. It is the drug of choice for the treatment and prophylaxis of *Pneumocystis jirovecii* pneumonia (PCP) in the Human Immunodeficiency Virus (HIV) patients (1). Approximately 1 to 3% of CTX prescribed HIV-uninfected patients develop mild to serious skin reactions including erythema multiforme, Stevens–Johnson syndrome (SJS), toxic epidermal necrolysis (TEN) and drug rash with eosinophilia and systemic symptoms (DRESS), whereas such reactions occurred in about 40 to 80% of HIV-infected patients (2–4).

Several forms of drug hypersensitivity reactions are associated with the carriage of human leukocyte antigens (HLA). Presentation of drug, drug modified or altered peptide sequences (due to drugs binding deep within the peptide binding groove) on the surface of HLA to T cell lymphocytes may stimulate an immune response *via* triggering of the T cell receptor (TCR) (5, 6). Co-trimoxazole-induced SJS/TEN is associated with *HLA-B*15:02*, *HLA-C*06:02*, and *HLA-C*08:01* in Thai population (7) and *HLA-B*38* in Europeans (8). Interestingly, our previous case-control study demonstrated that *HLA-B*13:01* is associated with co-trimoxazole-induced DRESS in Thai population, while co-trimoxazole-induced SJS/TEN was associated with *HLA-B*15:02* (9). This observation on co-trimoxazole-induced SJS/TEN was consistent with previous studies (7). However, not all patients with an *HLA* risk allele developed reactions. As T cells are thought to be involved in the molecular pathogenesis of many forms of severe cutaneous adverse reactions (10–12), a global TCR repertoire analysis in *HLA-B*15:02* positive patients with carbamazepine-induced SJS/TEN was studied and clearly demonstrated that restricted TCR usage of drug-specific T cells participated in the development of a reaction (8). Moreover, the analysis of TCR Vβ repertoire of *HLA-B*57:01* positive patients susceptible to abacavir hypersensitivity illustrated polyclonal TCR usages recognize the drug-HLA complex, then driving the T cell activation (13–15).

T cell activation and the release of effector molecules depends on drug (antigen) recognition by T cell receptors located on the cell surface. The T cell receptor receives signals from the drug, peptide and HLA protein which form a complex and are displayed on the surface of antigen presenting cells. Thus, this study aimed to characterize the T cell responses from Thai patients with co-trimoxazole-induced drug rash with eosinophilia and systemic symptoms. The assessment of specific T cell responses is essential to better understand the nature of the immune response induced and disease progression.

MATERIALS AND METHODS

Study Population

Co-trimoxazole-induced Stevens–Johnson syndrome (SJS) and drug reaction with eosinophilia and systemic symptoms (DRESS) patients were recruited from Ramathibodi Hospital and Srinagarind Hospital between 2018 and 2019. All of the patients studied were HIV negative. Reactions were assessed by two dermatologists or allergists who reviewed photographs, pathological slides, clinical morphology and medical records. SJS is defined as skin detachment of BSA < 10%, the clinical features of DRESS follow criteria from RegiSCAR and is defined as patients presenting with fever, maculopapular rash with internal organ involvement, and hematologic abnormalities. We evaluated co-trimoxazole was the causative drug of SJS or DRESS using Naranjo algorithm (16), the score of the algorithm of drug causality for epidermal necrolysis (ALDEN) (17). The cases defined as possible, probable and definite were recruited in this study. The blood samples were collected after the patients recovered from the reaction between 2-5 years. The lymphocyte transformation test (LTT) and IFN-γ ELISpot was also performed on patient's PBMC to identify the presence of circulating drug responsive T cells.

The study was performed according to the approval by the Ramathibodi Hospital and Srinagarind Hospital ethical review board, and both informed and written consent forms were obtained from all the participants.

DNA Extraction and *HLA* Genotyping

The DNA was extracted from PBMC by DNA extraction automated MagNA Pure Compact (Roche Diagnostics GmbH, Germany). The concentration of genomic DNA for all individuals was assessed by using NanoDrop 2000 for measuring the genomic DNA as well as purity with dynamic range around 220 to 750 nm. Wavelength at 260 nm is suitable for measuring the genomic DNA and at 280 nm was used to evaluate contaminated protein in the sample.

HLA alleles were genotyped using sequence-specific oligonucleotides (PCR-SSOs). In brief, the diluted DNA sample obtained from each patient were amplified polymerase chain reaction (PCR) by GeneAmp®PCR System 9700 (Applied Biosystems, Waltham, USA). The PCR product was then

hybridized against a panel of oligonucleotide probes on coated polystyrene microspheres that had sequences complementary to stretches of polymorphism within the target HLA alleles using the Lifecodes HLA SSO typing kits (Immucor, West Avenue, Stamford, USA). The amplicon-probe complex was then visualized using a colorimetric reaction and fluorescence detection technology by the Luminex®IS 100 systems (Luminex Corporation, Austin, Texas, USA). Analysis of the HLA alleles was performed using MATCH IT DNA software version 3.2.1 (One Lambda, Canoga Park, CA, USA).

Chemicals, Cell Culture, Generation of EBV

Dapsone (DDS), SMX and TMP were purchased from Sigma-Aldrich, (Buchs, Switzerland). EBV-transformed autologous B lymphoblastoid cell lines (B-LCLs) were used as antigen-presenting cells (APCs). PBMCs were isolated from co-trimoxazole induced DRESS carrying *HLA-B*13:01* using Ficoll density gradient centrifugation. For APC generation, the supernatant of B95.8 cells was filtered and added to $5x10^6$ PBMCs, then 1 μg/mL cyclosporin A (CSA) was added. The PBMC were then incubated in 5% CO_2 incubator at 37°C overnight. The mixture was centrifuged at 1500 rpm for 10 minutes, then the cells were re-suspended in 2 mL culture medium with CSA and transferred to a 24 well plate. Culture medium consisted of RPMI 1640, 10% pooled fetal bovine serum (FBS), HEPES buffer (25mM), L-glutamine (2mM), streptomycin (100 μg/mL) and penicillin (100 U/mL). To maintain B cell transformation, medium and CSA were replaced twice a week for 3 weeks. Eventually the transformed B cell lines were maintained with medium in the absence of CSA before being transferred to a flask. These cells were used as a ready supply of immortalized autologous APC.

Generation and Characterization of Drug Specific T Cell Clones

T cell lines were generated by culturing PBMCs with dapsone (DDS, 125 μM), nitroso-dapsone (DDS-NO, 10 μM), sulfamethoxazole (SMX, 1 mM) and nitroso-sulfamethoxazole (SMX-NO, 20 μM) in medium for 14 days (37°C; 5% CO_2) and media containing IL-2 (2 μL/mL) was added to maintain proliferation on day 6 and 9. Culture medium consisted of RPMI 1640, 10% pooled heat inactivated human AB serum, HEPES buffer (25 mM), L-glutamine (2 mM), transferrin (25 μg/mL), streptomycin (100 μg/mL), penicillin (100 U/mL). T cells clones were generated by serial dilution (18). The characterization of T cell clones was conducted in terms of cellular surface marker expression, HLA mismatch assay, HLA restriction assay, antigen presenting cell pulsing and fixation assay, the effect of glutathione and enzyme inhibitor; methimazole (an inhibitor of peroxidases and flavin–mono-oxygenases; Meth) and 1-aminobenzotriazole (a nonselective suicide inhibitor; ABT). Detailed methods are provided as **Supplementary S1** and **Supplementary Figure 1**.

RESULTS

Clinical Manifestation of Patients and *In Vitro* Activation of Patient's Peripheral Blood Mononuclear Cells

Three patients that developed CTX-induced SJS and DRESS were utilized in this study. The causality assessment and *in vitro* test of the patients are shown in **Table 1**. PBMC from all patients were stimulated to proliferate and secrete IFN-γ with SMX-NO. PBMC from one patient were also stimulated with SMX, the parent compound. Additionally, PBMC from all patients secreted IFN-γ once PBMC were cultured with SMX. The proliferation of PMBC from one patient was observed when PBMC were cultured with nitroso-dapsone (DDS-NO), a structurally-related compound (**Supplementary Figure 2**).

Generation and Characterization of Drug Specific T Cell Clones

For BAC-02, two of forty-nine clones and three of sixty-four clones were specific to SMX and SMX-NO, respectively. For BAC-12, eight of thirty-two clones were specific to SMX-NO. No specific clones were generated from BAC-08. Cellular surface marker expression was assayed using flow cytometry. All SMX and SMX-NO specific T cell clones expressed the CD4+ phenotype as shown in **Table 2**.

Twenty five percent of SMX-NO specific clones displayed cross-reactivity with DDS-NO, a structurally-related drug

TABLE 1 | Clinical characteristics, causality assessment and *in vitro* test of the patients with co-trimoxazole-induced SCARs.

Patient ID	Sex	Age	Clinicalmanifestation	Onset of reaction (days)	SCARs	LTT	IFN-γ ELISpot	Naranjo score		Alden score		DRESS score	
								Score	Remark	Score	Remark	Score	Remark
BAC-02	Male	27	Maculopapular rash: face and extremities, abnormal liver function tests	28	DRESS	+	+	6	Probable	N/A	N/A	5	Probable
BAC-08	Female	25	Generalized dusky erythematous patches with some vesicles on neck with nikolsky's sign on neck and upper chest	9	SJS	+	+	5	Probable	4	Probable	N/A	N/A
BAC-12	Female	44	Confluent maculopapular rash on trunk and extremities, abnormal liver function tests	30	DRESS	+	+	6	Probable	N/A	N/A	4	Probable

DRESS, drug reaction with eosinophilia and systemic symptoms; ELISpot, enzyme-linked immunospot; IFN-γ, Interferon gamma; LTT, lymphocyte transformation test; N/A, not available; SCARs, severe cutaneous adverse reactions; SJS, Stevens-Johnson syndrome.

TABLE 2 | Number, cellular phenotype and cross reactivity of drug-specific T cell clones.

Patients	Total number of clones	Number of specific clones	Phenotype (%)	Cross reactivity (%)			
			CD4	SMX	SMX-NO	DDS	DDS-NO
BAC-02							
- SMX	49	2	100	0	50	0	0
- SMX-NO	64	3	100	0	0	0	0
BAC-08							
- SMX	9	0	–	–	–	–	–
- SMX-NO	47	0	–	–	–	–	–
BAC-12							
- SMX	1	0		0	0	0	0
- SMX-NO	32	8	100	0	0	0	25

DDS, dapsone; DDS-NO, nitroso dapsone; SMX, sulfamethoxazole; SMX-NO, nitroso sulfamethoxazole.
-, not done.

metabolite, but not SMX, whereas SMX specific clones cross-reacted with SMX-NO only (**Table 2** and **Supplementary Figure 3**). High levels of IL-13 were detected from all T cell clones, while some T cell clones weakly secreted IFN-γ, granzyme B and IL-22. Interestingly, no T cell clones secreted IL-17 (**Figure 1**).

Activation of CD4+ Clones With SMX and SMX-NO is HLA Class II Restricted

The proliferation of T cell clones to SMX-NO was blocked in the presence of HLA class II blocking antibody (**Figure 2A**), indicating that the proliferative response of CD4+ specific T

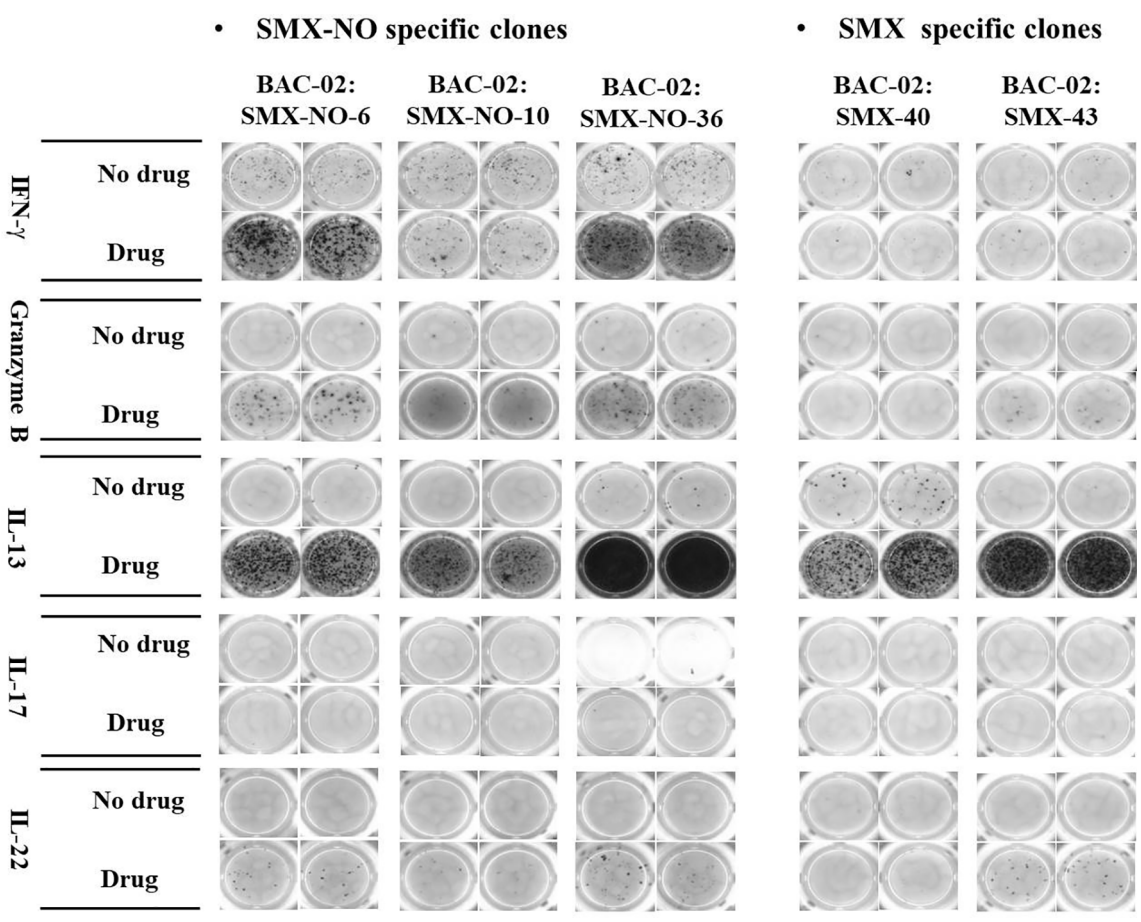

FIGURE 1 | ELISpot images of cytokine secretion by SMX-NO and SMX specific T cell clones. TCCs ($5x10^4$) were cultured with irradiated autologous EBV-transformed B-cells ($1x10^4$) in the presence or absence of SMX-NO (40 μM) or SMX (1 mM) in an ELISpot plate pre-coated for IFN-γ, granzyme B, IL-13, IL-17 and IL-22 for 48h (37°C; 5% CO_2). Following incubation, the plate was developed according to the manufactures instructions visualized by ELISpot AID reader.

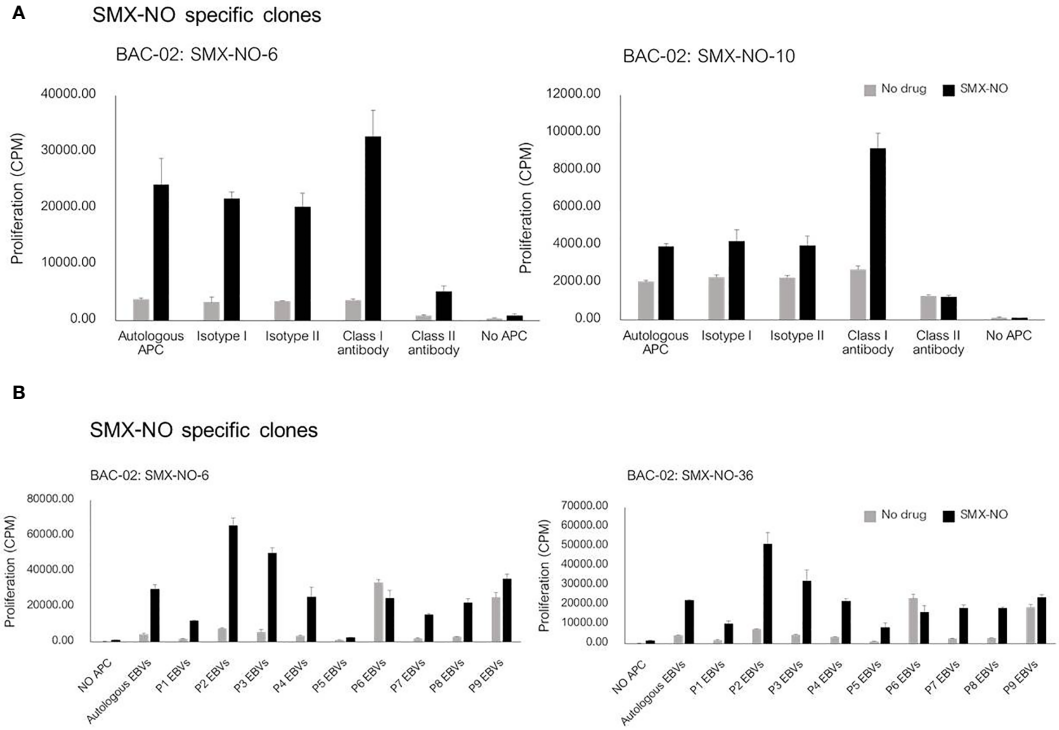

HLA genotype of patients EBVs in HLA mismatch assay

Patients	HLA-A	HLA-B	HLA-C	HLA-DRB1
BAC-02	*11:01/68:01*	*13:01/52:01*	*03:04/12:02*	*15:01/15:01*
BAC-08	*11:01/24:10*	*15:01/46:11*	*04:01/07:01*	*07:01/14:01*
BAC-12	*11:01/33:03*	*13:01/58:01*	*03:02/03:04*	*03:01/16:02*
P1	*11:01/33:03*	*13:01/58:01*	*03:02/03:04*	*03:01/16:02*
P2	*11:01/24:02*	*13:01/15:25*	*03:04/04:03*	*12:02/15:01*
P3	*11:01/11:01*	*13:01/38:02*	*03:04/07:02*	*15:01/15:02*
P4	*01:01/01:01*	*57:01/07:02*	*07:02/06:02*	*01:01/15:01*
P5	*01:01/32:01*	*57:01/57:01*	*06:02/06:02*	*07:01/07:01*
P6	*02:01/03:01*	*57:01/44:02*	*05:01/06:02*	*04:01/07:01*
P7	*01:01/32:01*	*08:01/14:01*	*07:01/08:02*	*04:04/15:01*
P8	*02:01/68:01*	*07:02/35:01*	*04:01/07:02*	*04:04/15:01*
P9	*01:01/02:01*	*07:02/51:01*	*01:02/04:01*	*04:01/15:01*

FIGURE 2 | The proliferative response of SMX-NO specific T cell clones. **(A)** T cell clones ($5x10^4$) were culture with autologous EBV-transformed B-cells ($1x10^4$) and SMX-NO (40 μM) in the presence or absence of HLA class I and class II blocking antibodies for 48 hours (37°C, 5% CO_2). Following incubation, [3H]-thymidine (0.5 μCi) were added to measure proliferative response. **(B)** T cell activation of SMX-NO clones in the response of different HLA-B. T cell clones ($5x10^4$) were cultured with SMX-NO (40 μM) and irradiated EBV-transformed B-cells ($1x10^4$) from 9 different patients carrying *HLA-B*13:01* (P1-3), *-B*57:01* (P4-6) and other *HLA-B* (P7-9).

cells might be HLA class II restricted. Additionally, to investigate the involvement of *HLA-B*13:01* in the co-trimoxazole hypersensitivity reaction, SMX-NO specific T cell clones were cultured with EBV-transformed B cells from three other patients carrying *HLA-B*13:01* (P1-3), three patients EBVs carrying *HLA-B*57:01* (P4-6) and cells from three donors carrying other alleles (not *HLA-B*13:01* or *-B*57:01*, P7-9). **Figure 2B** shows T cell clones were stimulate to proliferate in the presence of SMX-NO and antigen presenting cell expressing a range of HLA class I and II molecules.

SMX-NO Binds Covalently to Antigen Presenting Cells and Activates CD4+ T Cells Through Processing-Dependent and Processing-Independent Manners

Eight SMX-NO specific clones were used to investigate pathways of drug presentation. The proliferative response of four clones was blocked when APC were fixed with glutaraldehyde. In contrast, with the other four clones, T cell proliferative responses were detected when the drug metabolite was

presented by irradiated or fixed APC (**Figure 3**). All clones were stimulated to proliferate when APC pulsed with SMX-NO for 1 or 16 h were added to the assay as a source of antigen (**Figure 3**). The strength of the induced response was similar to that observed with the soluble drug metabolite.

In separate experiments, the SMX-NO specific T cell clones were incubated with autologous APC and SMX-NO in the presence and absence of glutathione (GSH), which functions to reduce SMX-NO protein binding *via* quenching the metabolites reactivity. The proliferative response of SMX-NO specific clones reduced when GSH was cultured with soluble SMX-NO. Furthermore, proliferative responses were inhibited when GSH was included in a 2h APC pulsing experiments (**Figure 4A**). T cell clones abrogated by the 2 h-pulse with GSH (**Figure 4A**). Activation of SMX-NO specific clones was not altered in the presence of enzyme inhibitors ABT and methimazole (**Figure 4B**).

SMX Specific Clones Are Activated Through a Direct HLA Binding Interaction

The SMX specific T cell clone was stimulated to proliferate in the presence of soluble drug, but not with APC pulsed with SMX for 1 or 16h (**Figure 5**). The T cell proliferative response was

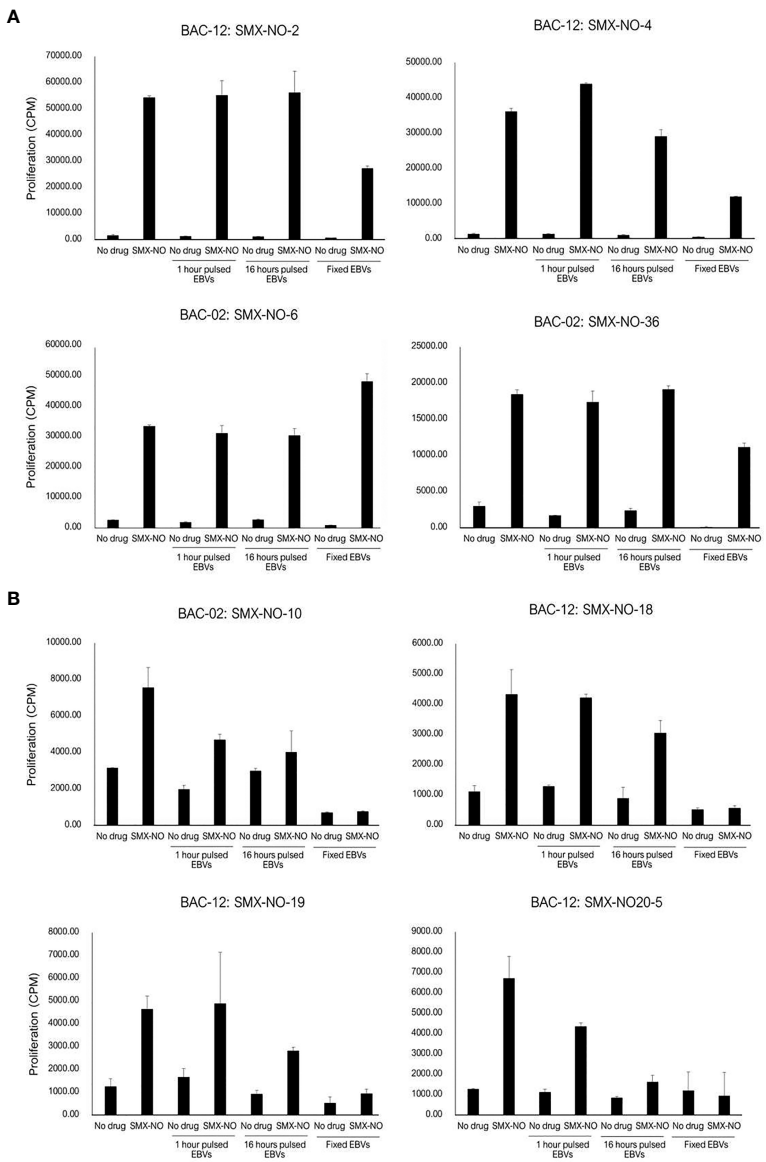

FIGURE 3 | SMX-NO stimulates specific T cell *via* antigen processing-dependent and processing-independent pathways. Autologous EBV-transformed B-cells ($1x10^4$) were incubated with T cell clones ($5x10^4$) in the presence or absence of SMX-NO (40 μM) for 1 and 16 hours. For fixation assay, SMX-NO specific clones ($5x10^4$) were cultured with either irradiated or glutaraldehyde-fixed autologous EBV-transformed B-cell ($1x10^4$) in the presence of SMX-NO (40 μM) for 48 hours (37°C; 5% CO_2). [^{3}H]-thymidine (0.5 μCi) incorporation was used to measure proliferative response. **(A)** SMX-NO T cell clones are stimulated in the presence of glutaraldehyde-fixed APC **(B)** Glutaraldehyde-fixed APC reduced the proliferative response of SMX-NO T cell clones.

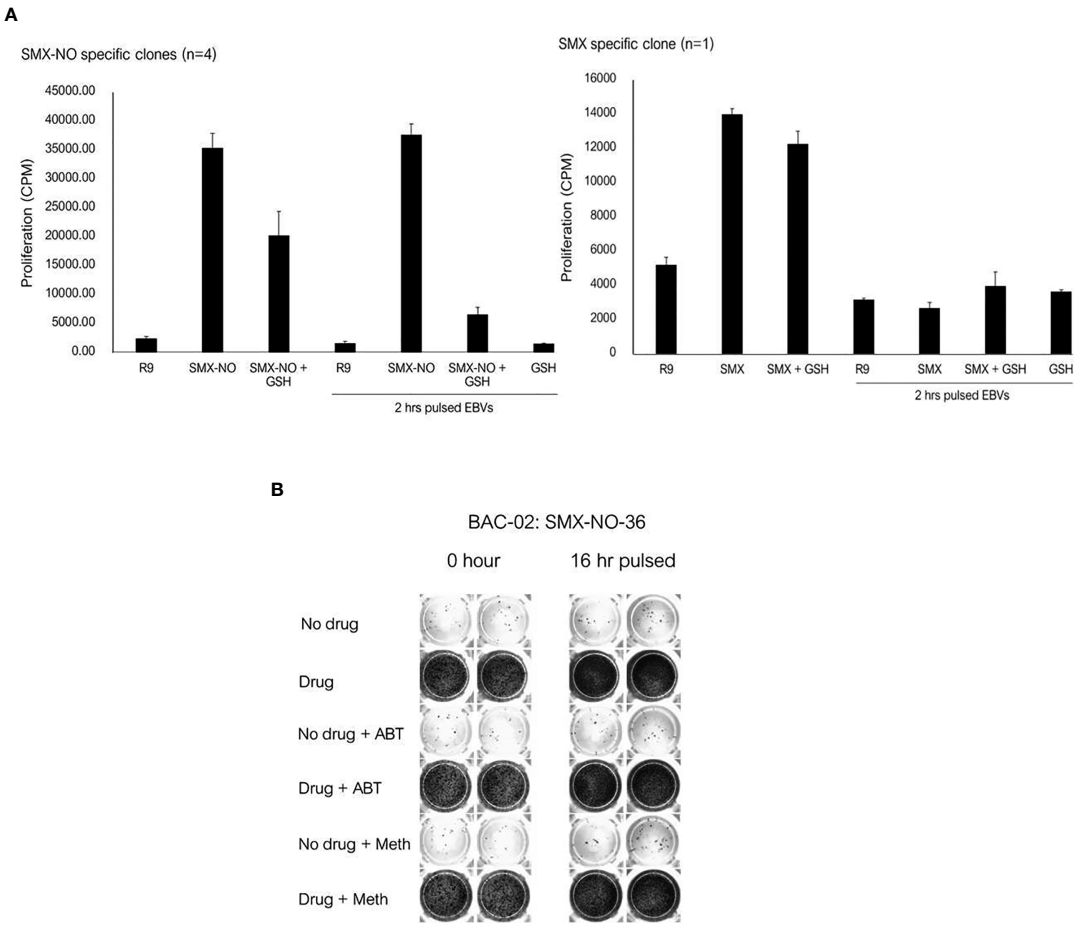

FIGURE 4 | The proliferative response of SMX-NO and SMX specific T cell clones in the presence of glutathione (GSH) and enzyme inhibitors. **(A)** Autologous EBV-transformed B-cells ($1x10^4$) were culture with T cell clones ($5x10^4$) in the presence or absence of GSH (1 mM). For pulsing EBVs, T cell clones ($5x10^4$) were culture with and without 2 h pulsed-antigen presenting cells ($1x10^4$) in the presence or absence of SMX-NO (40 μM) or SMX (1 mM) for 48 hours (37°C; 5% CO_2). After incubation, [3H]-thymidine (0.5 μCi) were added to measure proliferative response. **(B)** 16 h-enzyme inhibitor pulsed EBVs ($1x10^4$) were incubated with T cell clones ($5x10^4$) for 48 hours (5% CO_2 at 37°C). For normal condition, Autologous EBV-transformed B-cells were cultured with T cell clones and enzyme inhibitors for 1 hour (5% CO_2 at 37°C) and 40 μM nitroso sulfamethoxazole. Following incubation, the plate was developed according to the manufactures instructions visualized by ELISpot AID reader. Methimazole; Meth, 1-aminobenzotriazole; ABT.

observed when the clone was cultured with soluble SMX and glutaraldehyde-fixed APC. The presence of GSH and ABT had no effect on activation of the SMX specific T cell clone with soluble drug.

DISCUSSION

Several studies have shown a strong association between expression of a particular HLA allele and an increased susceptibility to drug hypersensitivity reactions. For example, *HLA-B*13:01* is associated with dapsone-induced hypersensitivity reactions among leprosy patients and non-leprosy patients in Chinese and Thai (19–21). Other genetic associations between medication-induced cutaneous adverse reactions and specific *HLA* alleles have been identified in various populations, including *HLA-B*57:01* and abacavir in Western Australian and North American populations (22, 23), *HLA-B*15:02* and carbamazepine in Han Chinese and Thai populations (24–27), *HLA-A*31:01* and carbamazepine and *HLA-A*32:01* and vancomycin in European populations (28, 29) and *HLA-B*58:01* and allopurinol in Han Chinese, Japanese and Thai populations (30–32). However, known associations between expression of an *HLA* risk allele and co-trimoxazole hypersensitivity are limited. Only one study by Kongpan et al. (7) demonstrated that *HLA-B*15:02*, *HLA-C*06:02*, and *HLA-C*08:01* were significantly associated with co-trimoxazole-induced SJS/TEN. Recently, a genetic study showed that the *HLA-B*13:01* allele is associated with co-trimoxazole-induced DRESS in Thai population (9).

In this study, T cells were characterized from co-trimoxazole hypersensitive patients to 1) define the nature of the antigenic determinant that activates T cells, 2) determine pathways of drug-specific T cell activation and 3) explore whether drug *HLA-B*13:01* binding is directly involved in the T cell response. The

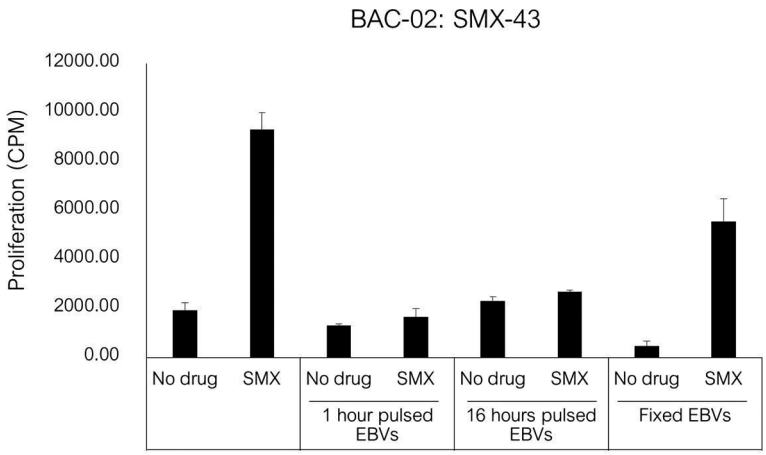

FIGURE 5 | T cell activation in response to antigen stimulation of SMX specific clone. Autologous EBV-transformed B-cells ($1x10^4$) were incubated with SMX (1 mM) for 1 and 16 hours, and then incubated with T cell clones ($5x10^4$) after three washing steps. For fixation assay, SMX specific T cell clones ($1x10^4$) were cultured with either irradiated or glutaraldehyde-fixed autologous EBV-transformed B-cell ($5x10^4$) in the presence of SMX (1 mM) for 48 hours (37°C, 5% CO_2). After incubation, [3H]-thymidine (0.5 μCi) incorporation was used to measure proliferative response.

lymphocyte transformation test is a useful tool to define the causative agent that can be performed during the recovery phase of a hypersensitivity reaction (33, 34). A small cohort of CBZ-hypersensitive patients demonstrated that the lymphocyte transformation test was positive in only the hypersensitive patients (35), while in β-lactam hypersensitive patients with cystic fibrosis, the lymphocyte transformation test had a sensitivity of approximately 75% (36). In this study, three patients' peripheral blood mononuclear cells were found to proliferate in the presence of sulfamethoxazole and/or its reactive nitroso metabolite. IFN-γ PBMC ELISpot was used to confirm the positive result (**Supplementary Figure 2**). Two SMX and eleven SMX-NO specific T cells were generated from T-cell lines generated from two of the hypersensitive patients. Both patients carried *HLA-B*13:01*. The SMX-NO specific clones cross-reacted with the structurally related compound, nitroso dapsone (DDS-NO), which demonstrates the importance of the reactive nitroso functionality in the T cell response. A clinical cross-reactivity rate between co-trimoxazole and dapsone has been estimated to be approximately 22% and this may be due to the cross-reactivity of the metabolite-responsive T cells (37). Dapsone is related to SMX in that it contains an aromatic amine and a sulfone function, but the drugs differ in terms of their side-chains.

All of the SMX and SMX-NO specific T cell clones expressed a CD4+ phenotype which concordant to previous studies (38, 39). Immunohistochemical studies have shown that the cell infiltrate in maculopapular exanthema predominantly consists of CD4+ T cells (40, 41), whereas a predominance of epidermal CD8+ T cells is seen drug-induced bullous exanthem (42). Previous studies have revealed that drug-specific T cells secrete various cytokines including IFN-γ, IL-13, IL-22 (43, 44). The present study showed that both SMX and SMX-NO specific T cells secreted high levels of IL-13 along with lower levels of IL-22, IFN-γ and granzyme B secretion. However, IL-17 secretion from the clones was not observed. Eosinophilia is naturally reported in DRESS. Under inflammatory conditions, IL-13 is excreted by eosinophils which drives inflammatory responses and is typically associated with allergic inflammation (45–47).

Genetic association studies have shown a significant association between *HLA-B*13:01* and co-trimoxazole-induced DRESS in patients with HIV infection (9). These data suggest that the causative drug might interact with the HLA-B*13:01 protein to activate CD8+ T cells in hypersensitive patients. Co-trimoxazole hypersensitivity is observed at a much lower frequency in patients without HIV infection. The reason for this is unclear, but may relate to a redox imbalance in patients with HIV infection, or altered metabolism, that leads to the formation of higher levels of sulfamethoxazole protein adducts (9, 48). A significant higher frequency of the *HLA-B*13:01-C*03:04* haplotype was detected in co-trimoxazole-induced DRESS in the Thai population (9) and this is in linkage disequilibrium (LD) in Chinese (49) and Korean populations (50). Furthermore, these two alleles are also in LD with a HLA class II allele, namely *HLA-DRB1*12:02* (50).

Somewhat surprisingly, the clones identified as drug-responsive in this study were CD4+ and T cell activation was diminished upon the blockade of *HLA* class II. This finding is in agreement with the study of Ogese and colleagues (38), which explored SMX T-cell responses in European patients, with hypersensitivity of mild to moderate severity, that were unlikely to express *HLA-B*13:01*. Ogese et al. demonstrated that the response of SMX-NO specific CD4+ T cells was restricted to the *HLA-DQ* allele, indicating that *HLA* class II plays an important role in the T cell activation in patients presenting with differing reaction phenotypes. In future studies

it will be of interest to identify T cell receptor (TCR) repertoire expressed by drug-responsive T-cell clones and then determine their frequency in hypersensitive and tolerant patient PBMC.

The availability of SMX and SMX-NO responsive T cells allowed us to probe pathways of drug presentation by the HLA class II molecules. The SMX-NO responsive clones were stimulated to proliferate with APC pulsed with the drug metabolite for 1- and 16-hours. These data demonstrate that formation of a stable complex between the drug metabolite and antigen presenting cells is important for T cell activation. These data are concordant with Schnyder et al. which demonstrated the responsive T cell clones from SMX hypersensitive patients recognized covalently bound SMX-NO (39). The proliferative response of 5 out of 9 of the SMX-NO specific T cell clones analyzed was abolished APC were fixed with glutaraldehyde. This indicates that the T cell activation is dependent upon antigen processing and that the T cells are likely activated with drug-modified peptides. On the contrary, fixed antigen presenting cells had little effect on the activation of the remaining 4 clones. These clones are presumably activated when SMX-NO binds directly with surface peptides embedded within the HLA class II proteins. Finally, a SMX specific clone, SMX-43, was subjected to the same experiments. This clone was stimulated to proliferate with soluble drug in the presence of irradiated and fixed APC, while SMX-pulsed APC did not activate the T-cells. Direct interactions of drugs (p-i model) are not stable and washing the cells abolishes reactivity. Previous studies suggest that SMX may interact directly with either HLA-peptide complex (p-i HLA) or T cell receptors (p-i TCR) which can induce T cell activation (51, 52).

The tripeptide glutathione functions to prevent SMX-NO from covalently modifying proteins *via* quenching its reactivity (53, 54). Addition of glutathione to SMX-NO specific T cells blocked the induced proliferative response of the drug metabolite, whereas glutathione had no effect on the activation of clones with SMX (43, 53).

In conclusion, the generation of SMX and SMX-NO specific T-cell clones from co-trimoxazole hypersensitive patients suggests an immune mediated basis for the hypersensitivity reactions observed in individuals expressing *HLA-B*13:01*. The clones were CD4+ and activation was HLA class II-restricted indicating that *HLA-B*13:01* was not directly involved in the disease pathogenesis.

DATA AVAILABILITY STATEMENT

The original contributions presented in the study are included in the article/**Supplementary Material**. Further inquiries can be directed to the corresponding author.

ETHICS STATEMENT

The studies involving human participants were reviewed and approved by Institutional Review Boards in Mahidol University. The patients/participants provided their written informed consent to participate in this study.

AUTHOR CONTRIBUTIONS

TR, WT, NN, PR, JK and YS reviewed and collected the clinical data. CS, DN, and MP designed the research and supervised the project. JP, PT, KJ, RT, and PJ recruited subjects and performed the experiment. JP and PT analyzed the data and drafted the manuscript. CS, DN, and MP revised critical revision of the article and approved the final version to be published. All authors contributed to the article and approved the submitted version.

FUNDING

This study was supported by grants from the (1) the Royal Golden Jubilee Ph.D. (RGJ-PHD) Program (PHD/0153/2559) (2) Newton Fund - PhD Placements for Scholars. (3) Huachiew Chalermprakiet University (4) The International Research Network-The Thailand Research Fund (IRN60W003) (5) Faculty of Medicine Ramathibodi Hospital, Mahidol University (6) Skin and Allergy Research Unit, Chulalongkorn University (7) Thailand Center of Excellence for Life Sciences (grant number TC-12/63) (8) Health System Research Institute under Genomics Thailand Strategic Fund (9) Merck Pharmaceuticals. The funder was not involved in the study design, collection, analysis, interpretation of data, the writing of this article or the decision to submit it for publication.

ACKNOWLEDGMENTS

The authors thank the study participants and staff of the Pharmacogenomics and Personalized Medicine laboratory, Ramathibodi Hospital, MRC Centre for Drug Safety Science, University of Liverpool, Liverpool, UK.

SUPPLEMENTARY MATERIAL

The Supplementary Material for this article can be found online at: https://www.frontiersin.org/articles/10.3389/fimmu.2021.658593/full#supplementary-material

Supplementary Figure 1 | Flow chart of the study.

Supplementary Figure 2 | The proliferative response and IFN-γ ELISPOT of three hypersensitive patients **(A)** hypersensitive patients' PBMCs ($1.5x10^6$) were cultures with SMX (1 and 2 mM), SMX-NO (10 and 20 μM), TMP (10 and 25 μM), DDS (125 and 250 μM) and DDS-NO (5 and 10 μM) for 6 days (37°C, 5% CO_2). Following incubation, [3H]-thymidine (0.5 μCi) were added to measure proliferative response. **(B)** PBMCs ($5x10^6$) were cultured in the presence of SMX (1mM), SMX-NO (20 μM), DDS (125 μM) and DDS-NO (10 μM) for 48 hours (37°C, 5% CO_2). Following incubation, the plate was developed according to the manufactures instructions visualized by ELISpot AID reader.

Supplementary Figure 3 | Cross-reactivity of SMX-NO specific T cell clones. Autologous EBV-transformed B-cells ($1x10^4$) were incubated with SMX-NO specific clones ($5x10^4$) in the presence of various drugs at difference concentration including SMX (1mM), SMX-NO (20 and 40 μM), DDS (62.5 and 125 μM), DDS-NO (5 and 10 μM) and phytohemagglutinin (PHA; 5 μg/mL). The proliferative response was measured using [3H]-thymidine incorporation assay.

REFERENCES

1. Alanazi MQ, Alqahtani FY, Aleanizy FS. An Evaluation of E. Coli in Urinary Tract Infection in Emergency Department At KAMC in Riyadh, Saudi Arabia: Retrospective Study. *Ann Clin Microbiol Antimicrob* (2018) 17:3. doi: 10.1186/s12941-018-0255-z
2. Ho JM, Juurlink DN. Considerations When Prescribing Trimethoprim-Sulfamethoxazole. *Cmaj* (2011) 183:1851–8. doi: 10.1503/cmaj.111152
3. Rueda-Valencia Mde L, Infante S, Campos M, Beléndez C, Lozano JS. Trimethoprim-Sulfamethoxazole-Induced DRESS Syndrome in a 4-Year-Old Child. *Ann Allergy Asthma Immunol* (2016) 116:366–7. doi: 10.1016/j.anai.2015.12.009
4. Taqi SA, Zaki SA, Nilofer AR, Sami LB. Trimethoprim-Sulfamethoxazole-Induced Steven Johnson Syndrome in an HIV-infected Patient. *Indian J Pharmacol* (2012) 44:533–5. doi: 10.4103/0253-7613.99346
5. Rosati E, Dowds CM, Liaskou E, Henriksen EKK, Karlsen TH, Franke A. Overview of Methodologies for T-cell Receptor Repertoire Analysis. *BMC Biotechnol* (2017) 17:1–16. doi: 10.1186/s12896-017-0379-9
6. Hausmann O, Schnyder B, Pichler WJ. Etiology and Pathogenesis of Adverse Drug Reactions. *Chem Immunol Allergy* (2012) 97:32–46. doi: 10.1159/000335614
7. Kongpan T, Mahasirimongkol S, Konyoung P, Kanjanawart S, Chumworathayi P, Wichukchinda N, et al. Candidate HLA Genes for Prediction of Co-Trimoxazole-Induced Severe Cutaneous Reactions. *Pharmacogenet Genomics* (2015) 25:402–11. doi: 10.1097/FPC.0000000000000153
8. Lonjou C, Borot N, Sekula P, Ledger N, Thomas L, Halevy S, et al. A European Study of HLA-B in Stevens-Johnson Syndrome and Toxic Epidermal Necrolysis Related to Five High-Risk Drugs. *Pharmacogenet Genomics* (2008) 18:99–107. doi: 10.1097/FPC.0b013e3282f3ef9c
9. Sukasem C, Pratoomwun J, Satapornpong P, Klaewsongkram J, Rerkpattanapipat T, Rerknimitr P, et al. Genetic Association of Co-Trimoxazole-Induced Severe Cutaneous Adverse Reactions is Phenotype-Specific: Hla Class I Genotypes and Haplotypes. *Clin Pharmacol Ther* (2020) 108:1078–89. doi: 10.1002/cpt.1915
10. Ko TM, Chung WH, Wei CY, Shih HY, Chen JK, Lin CH, et al. Shared and Restricted T-cell Receptor Use is Crucial for Carbamazepine-Induced Stevens-Johnson Syndrome. *J Allergy Clin Immunol* (2011) 128:1266–76.e11. doi: 10.1016/j.jaci.2011.08.013
11. Chung WH, Pan RY, Chu MT, Chin SW, Huang YL, Wang WC, et al. Oxypurinol-Specific T Cells Possess Preferential TCR Clonotypes and Express Granulysin in Allopurinol-Induced Severe Cutaneous Adverse Reactions. *J Invest Dermatol* (2015) 135:2237–48. doi: 10.1038/jid.2015.165
12. Pan RY, Chu MT, Wang CW, Lee YS, Lemonnier F, Michels AW, et al. Identification of Drug-Specific Public TCR Driving Severe Cutaneous Adverse Reactions. *Nat Commun* (2019) 10:3569. doi: 10.1038/s41467-019-11396-2
13. Illing PT, Vivian JP, Dudek NL, Kostenko L, Chen Z, Bharadwaj M, et al. Immune Self-Reactivity Triggered by Drug-Modified HLA-peptide Repertoire. *Nature* (2012) 486:554–8. doi: 10.1038/nature11147
14. Yerly D, Pompeu YA, Schutte R, Eriksson KK, Strhyn A, Bracey AW, et al. Structural Elements Recognized by Abacavir-Induced T Cells. *Int J Mol Sci* (2017) 18:1464. doi: 10.3390/ijms18071464
15. Bell CC, Faulkner L, Martinsson K, Farrell J, Alfirevic A, Tugwood J, et al. T-Cells From HLA-B*57:01+ Human Subjects are Activated With Abacavir Through Two Independent Pathways and Induce Cell Death by Multiple Mechanisms. *Chem Res Toxicol* (2013) 26:759–66. doi: 10.1021/tx400060p
16. Naranjo CA, Busto U, Sellers EM, Sandor P, Ruiz I, Roberts EA, et al. A Method for Estimating the Probability of Adverse Drug Reactions. *Clin Pharmacol Ther* (1981) 30:239–45. doi: 10.1038/clpt.1981.154
17. Sassolas B, Haddad C, Mockenhaupt M, Dunant A, Liss Y, Bork K, et al. ALDEN, an Algorithm for Assessment of Drug Causality in Stevens-Johnson Syndrome and Toxic Epidermal Necrolysis: Comparison With Case-Control Analysis. *Clin Pharmacol Ther* (2010) 88:60–8. doi: 10.1038/clpt.2009.252
18. Zhao Q, Alhilali K, Alzahrani A, Almutairi M, Juwaria A, Liu H, et al. Dapsone- and Nitroso Dapsone-Specific Activation of T Cells From Hypersensitive Patients Expressing the Risk Allele HLA-B*13:01. *Allergy* (2019) 74:1533–48. doi: 10.1111/all.13769
19. Chen WT, Wang CW, Lu CW, Chen CB, Lee HE, Hung SL, et al. The Function of HLA-B*13:01 Involved in the Pathomechanism of Dapsone-Induced Severe Cutaneous Adverse Reactions. *J Invest Dermatol* (2018) 138:1546–54. doi: 10.1016/j.jid.2018.02.004
20. Tempark T, Satapornpong P, Rerknimitr P, Nakkam N, Saksit N, Wattanakrai P, et al. Dapsone-Induced Severe Cutaneous Adverse Drug Reactions are Strongly Linked With HLA-B*13: 01 Allele in the Thai Population. *Pharmacogenet Genomics* (2017) 27:429–37. doi: 10.1097/FPC.0000000000000306
21. Wang H, Yan L, Zhang G, Chen X, Yang J, Li M, et al. Association Between HLA-B*1301 and Dapsone-Induced Hypersensitivity Reactions Among Leprosy Patients in China. *J Invest Dermatol* (2013) 133:2642–44. doi: 10.1038/jid.2013.192
22. Hetherington S, Hughes AR, Mosteller M, Shortino D, Baker KL, Spreen W, et al. Genetic Variations in HLA-B Region and Hypersensitivity Reactions to Abacavir. *Lancet* (2002) 359:1121–2. doi: 10.1016/S0140-6736(02)08158-8
23. Mallal S, Nolan D, Witt C, Masel G, Martin AM, Moore C, et al. Association Between Presence of HLA-B*5701, Hla-DR7, and HLA-DQ3 and Hypersensitivity to HIV-1 Reverse-Transcriptase Inhibitor Abacavir. *Lancet* (2002) 359:727–32. doi: 10.1016/s0140-6736(02)07873-x
24. Locharernkul C, Loplumlert J, Limotai C, Korkij W, Desudchit T, Tongkobpetch S, et al. Carbamazepine and Phenytoin Induced Stevens-Johnson Syndrome is Associated With HLA-B*1502 Allele in Thai Population. *Epilepsia* (2008) 49:2087–91. doi: 10.1111/j.1528-1167.2008.01719.x
25. Tassaneeyakul W, Tiamkao S, Jantararoungtong T, Chen P, Lin SY, Chen WH, et al. Association Between HLA-B*1502 and Carbamazepine-Induced Severe Cutaneous Adverse Drug Reactions in a Thai Population. *Epilepsia* (2010) 51:926–30. doi: 10.1111/j.1528-1167.2010.02533.x
26. Sukasem C, Chaichan C, Nakkrut T, Satapornpong P, Jarutamsophon K, Jantararoungtong T, et al. Association Between HLA-B Alleles and Carbamazepine-Induced Maculopapular Exanthema and Severe Cutaneous Reactions in Thai Patients. *J Immunol Res* (2018) 2018:2780272. doi: 10.1155/2018/2780272
27. Chung WH, Hung SL, Hong HS, Hsih MS, Yang LC, Ho HC, et al. A Marker for Stevens–Johnson Syndrome. *Nature* (2004) 428:486. doi: 10.1038/428486a
28. McCormack M, Alfirevic A, Bourgeois S, Farrell JJ, Kasperavičiūtė D, Carrington M, et al. Hla-A*3101 and Carbamazepine-Induced Hypersensitivity Reactions in Europeans. *N Engl J Med* (2011) 364:1134–43. doi: 10.1056/NEJMoa1013297
29. Konvinse KC, Trubiano JA, Pavlos R, James I, Shaffer CM, Bejan CA, et al. Hla-A*32:01 is Strongly Associated With Vancomycin-Induced Drug Reaction With Eosinophilia and Systemic Symptoms. *J Allergy Clin Immunol* (2019) 144:183–92. doi: 10.1016/j.jaci.2019.01.045
30. Sukasem C, Jantararoungtong T, Kuntawong P, Puangpetch A, Koomdee N, Satapornpong P, et al. Hla-B*58:01 for Allopurinol-Induced Cutaneous Adverse Drug Reactions: Implication for Clinical Interpretation in Thailand. *Front Pharmacol* (2016) 7:186. doi: 10.3389/fphar.2016.00186
31. Hung SI, Chung WH, Liou LB, Chu CC, Lin M, Huang HP, et al. Hla-B*5801 Allele as a Genetic Marker for Severe Cutaneous Adverse Reactions Caused by Allopurinol. *Proc Natl Acad Sci USA* (2005) 102:4134–9. doi: 10.1073/pnas.0409500102
32. Tohkin M, Kaniwa N, Saito Y, Sugiyama E, Kurose K, Nishikawa J, et al. A Whole-Genome Association Study of Major Determinants for Allopurinol-Related Stevens-Johnson Syndrome and Toxic Epidermal Necrolysis in Japanese Patients. *Pharmacogenomics J* (2013) 13:60–9. doi: 10.1038/tpj.2011.41
33. Kano Y, Hirahara K, Mitsuyama Y, Takahashi R, Shiohara T. Utility of the Lymphocyte Transformation Test in the Diagnosis of Drug Sensitivity: Dependence on its Timing and the Type of Drug Eruption. *Allergy* (2007) 62:1439–44. doi: 10.1111/j.1398-9995.2007.01553.x
34. Tang YH, Mockenhaupt M, Henry A, Bounoua M, Naldi L, Gouvello SL, et al. Poor Relevance of a Lymphocyte Proliferation Assay in Lamotrigine-Induced Stevens-Johnson Syndrome or Toxic Epidermal Necrolysis. *Clin Exp Allergy* (2012) 42:248–54. doi: 10.1111/j.1365-2222.2011.03875.x
35. Naisbitt DJ, Britschgi M, Wong G, Farrell J, Depta JPH, Chadwick DW, et al. Hypersensitivity Reactions to Carbamazepine: Characterization of the Specificity, Phenotype, and Cytokine Profile of Drug-Specific T Cell Clones. *Mol Pharmacol* (2003) 63:732–41. doi: 10.1124/mol.63.3.732
36. Whitaker P, Meng X, Lavergne SN, El-Ghaiesh S, Monshi M, Earnshaw C, et al. Mass Spectrometric Characterization of Circulating and Functional Antigens Derived From Piperacillin in Patients With Cystic Fibrosis. *J Immunol* (2011) 187:200–11. doi: 10.4049/jimmunol.1100647

37. Holtzer CD, Flaherty JF Jr, Coleman RL. Cross-Reactivity in HIV-infected Patients Switched From Trimethoprim-Sulfamethoxazole to Dapsone. *Pharmacotherapy* (1998) 18:831–5. doi: 10.1002/j.1875-9114.1998.tb03904.x
38. Ogese MO, Saide K, Faulkner L, Whitaker P, Peckham D, Alfirevic A, et al. Hla-DQ Allele-Restricted Activation of Nitroso Sulfamethoxazole-Specific CD4-Positive T Lymphocytes From Patients With Cystic Fibrosis. *Clin Exp Allergy* (2015) 45:1305–16. doi: 10.1111/cea.12546
39. Schnyder B, Burkhart C, Schnyder-Frutig K, von Greyerz S, Naisbitt DJ, Pirmohamed M, et al. Recognition of Sulfamethoxazole and its Reactive Metabolites by Drug-Specific CD4+ T Cells From Allergic Individuals. *J Immunol* (2000) 164:6647–54. doi: 10.4049/jimmunol.164.12.6647
40. Pichler WJ, Yawalkar N, Britschgi M, Depta J, Strasser I, Schmid S, et al. Cellular and Molecular Pathophysiology of Cutaneous Drug Reactions. *Am J Clin Dermatol* (2002) 3:229–38. doi: 10.2165/00128071-200203040-00001
41. Yawalkar N, Egli F, Hari Y, Nievergelt H, Braathen LR, Pichler WJ. Infiltration of Cytotoxic T Cells in Drug-Induced Cutaneous Eruptions. *Clin Exp Allergy* (2000) 30:847–55. doi: 10.1046/j.1365-2222.2000.00847.x
42. Hertl M, Jugert F, Merk HF. CD8+ Dermal T Cells From a Sulphamethoxazole-Induced Bullous Exanthem Proliferate in Response to Drug-Modified Liver Microsomes. *Br J Dermatol* (1995) 132:215–20. doi: 10.1111/j.1365-2133.1995.tb05016.x
43. Elsheikh A, Castrejon L, Lavergne SN, Whitaker P, Monshi M, Callan H, et al. Enhanced Antigenicity Leads to Altered Immunogenicity in Sulfamethoxazole-Hypersensitive Patients With Cystic Fibrosis. *J Allergy Clin Immunol* (2011) 127:1543–51.e3. doi: 10.1016/j.jaci.2010.12.1119
44. Gibson A, Ogese M, Sullivan A, Wang E, Saide K, Whitaker P, et al. Negative Regulation by PD-L1 During Drug-Specific Priming of IL-22-Secreting T Cells and the Influence of PD-1 on Effector T Cell Function. *J Immunol* (2014) 192:2611–21. doi: 10.4049/jimmunol.1302720
45. Mori F, Caffarelli C, Caimmi S, Bottau P, Liotti L, Franceschini F, et al. Drug Reaction With Eosinophilia and Systemic Symptoms (DRESS) in Children. *Acta BioMed* (2019) 90:66–79. doi: 10.23750/abm.v90i3-S.8167
46. Schmid-Grendelmeier P, Altznauer F, Fischer B, Bizer C, Straumann A, Menz G, et al. Eosinophils Express Functional IL-13 in Eosinophilic Inflammatory Diseases. *J Immunol* (2002) 169:1021–7. doi: 10.4049/jimmunol.169.2.1021
47. Teraki Y, Fukuda T. Skin-Homing Il-13-Producing T Cells Expand in the Circulation of Patients With Drug Rash With Eosinophilia and Systemic Symptoms. *Dermatology* (2017) 233:242–9. doi: 10.1159/000475546
48. Coco-Bassey SB, Asemota EA, Okoroiwu HU, Etura JE, Efiong EE, Inyang IJ. Glutathione, Glutathione Peroxidase and Some Hematological Parameters of HIV-seropositive Subjects Attending Clinic in University of Calabar Teaching Hospital, Calabar, Nigeria. *BMC Infect Dis* (2019) 19:1–10. doi: 10.1186/s12879-019-4562-6
49. Zhang FR, Liu H, Irwanto A, Fu XA, Li Y, Yu GQ, et al. Hla-B*13:01 and the Dapsone Hypersensitivity Syndrome. *N Engl J Med* (2013) 369:1620–8. doi: 10.1056/NEJMoa. 1213096.
50. Park HJ, Park JW, Kim SH, Choi SY, Kim HK, Jung CG, et al. The HLA-B*13:01 and the Dapsone Hypersensitivity Syndrome in Korean and Asian Populations: Genotype- and Meta-Analyses. *Expert Opin Drug Saf* (2020) 19:1349–56. doi: 10.1080/14740338. 2020.1796965.
51. Pacher P, Nivorozhkin A, Szabó C. Therapeutic Effects of Xanthine Oxidase Inhibitors: Renaissance Half a Century After the Discovery of Allopurinol. *Pharmacol Rev* (2006) 58:87–114. doi: 10.1124/pr.58.1.6
52. Watkins S, Pichler W. Activating Interactions of Sulfanilamides With T Cell Receptors. *Open J Immunol* (2013) 3:139–57. doi: 10.4236/oji.2013.33019
53. Burkhart C, von Greyerz S, Depta JP, Naisbitt DJ, Britschgi M, Park KB, et al. Influence of Reduced Glutathione on the Proliferative Response of Sulfamethoxazole-Specific and Sulfamethoxazole-Metabolite-Specific Human CD4+ T-Cells. *Br J Pharmacol* (2001) 132:623–30. doi: 10.1038/sj.bjp.0703845
54. Naisbitt DJ, O'Neill PM, Pirmohamed M, Park BK. Synthesis and Reactions of Nitroso Sulphamethoxazole With Biological Nucleophiles: Implications for Immune Mediated Toxicity. *Bioorganic Med Chem Lett* (1996) 6:1511–6. doi: 10.1016/S0960-894X(96)00260-0

Conflict of Interest: The authors declare that the research was conducted in the absence of any commercial or financial relationships that could be construed as a potential conflict of interest.

frontiers in Immunology

ORIGINAL RESEARCH
published: 19 May 2021
doi: 10.3389/fimmu.2021.672737

Kinetics of Abacavir-Induced Remodelling of the Major Histocompatibility Complex Class I Peptide Repertoire

Patricia T. Illing[1†], Andy van Hateren[2†], Rachel Darley[2], Nathan P. Croft[1], Nicole A. Mifsud[1], Samuel King[2‡], Lyudmila Kostenko[3], Mandvi Bharadwaj[3], James McCluskey[3], Tim Elliott[2,4] and Anthony W. Purcell[1*]*

[1] Infection and Immunity Program, Department of Biochemistry and Molecular Biology, Monash Biomedicine Discovery Institute, Monash University, Clayton, VIC, Australia, [2] Institute for Life Sciences and Centre for Cancer Immunology, Faculty of Medicine, University of Southampton, Southampton, United Kingdom, [3] Department of Microbiology and Immunology, Peter Doherty Institute for Infection and Immunity, University of Melbourne, Parkville, VIC, Australia, [4] Nuffield Department of Medicine, University of Oxford, Oxford, United Kingdom

Abacavir hypersensitivity syndrome can occur in individuals expressing the HLA-B*57:01 major histocompatibility complex class I allotype when utilising the drug abacavir as a part of their anti-retroviral regimen. The drug is known to bind within the HLA-B*57:01 antigen binding cleft, leading to the selection of novel self-peptide ligands, thus provoking life-threatening immune responses. However, the sub-cellular location of abacavir binding and the mechanics of altered peptide selection are not well understood. Here, we probed the impact of abacavir on the assembly of HLA-B*57:01 peptide complexes. We show that whilst abacavir had minimal impact on the maturation or average stability of HLA-B*57:01 molecules, abacavir was able to differentially enhance the formation, selectively decrease the dissociation, and alter tapasin loading dependency of certain HLA-B*57:01-peptide complexes. Our data reveals a spectrum of abacavir mediated effects on the immunopeptidome which reconciles the heterogeneous functional T cell data reported in the literature.

Keywords: MHC I antigen presentation, abacavir, T cells, drug hypersensitivity, immunopeptidome, tapasin, peptide selection

OPEN ACCESS

Edited by:
Thomas Herrmann, Julius Maximilian University of Würzburg, Germany

Reviewed by:
Malini Raghavan, University of Michigan, United States
Werner Pichler, Universität Bern, Switzerland

****Correspondence:***
Tim Elliott
tim.elliott@ndm.ox.ac.uk
Anthony W Purcell
anthony.purcell@monash.edu

[†]These authors have contributed equally to this work

[‡]Present address:
Samuel King, Anaesthetic Department, Plymouth Hospitals NHS Trust, Plymouth, United Kingdom

Specialty section:
This article was submitted to T Cell Biology, a section of the journal Frontiers in Immunology

Received: *26 February 2021*
Accepted: *26 April 2021*
Published: *19 May 2021*

Citation:
Illing PT, van Hateren A, Darley R, Croft NP, Mifsud NA, King S, Kostenko L, Bharadwaj M, McCluskey J, Elliott T and Purcell AW (2021) Kinetics of Abacavir-Induced Remodelling of the Major Histocompatibility Complex Class I Peptide Repertoire. Front. Immunol. 12:672737. doi: 10.3389/fimmu.2021.672737

INTRODUCTION

Major histocompatibility complex class I (MHC I) molecules acquire peptide antigens in the endoplasmic reticulum (ER) and present their peptide cargo at the cell surface for scrutiny by cytotoxic T lymphocytes (CTLs). These peptide antigens are derived from the degradation of intracellular proteins along with other sources, including peptides derived from defective ribosomal

Abbreviations: MHC I, Major histocompatibility complex class I; CTLs, cytotoxic T lymphocytes; HLA, Human Leukocyte Antigen; ER, Endoplasmic reticulum; PBMCs, peripheral blood mononuclear cells; LC-MS/MS, liquid chromatography-tandem mass spectrometry; LC-MRM-MS, liquid chromatography-multiple reaction monitoring-mass spectrometry; β_2m, β_2-microglobulin.

products (DRiPs) produced during aborted protein synthesis (1). Therefore, the peptides presented by MHC I molecules (coined the immunopeptidome) provide an overview of cellular protein production. As such, virus infected or cancerous cells can be detected when novel peptides, such as those derived from the viral proteome or neo-epitopes generated during oncogenesis, are presented on the cell surface. Their recognition by CTLs stimulates cytotoxicity against the antigen presenting cells, facilitating elimination of the infected or transformed cells.

MHC I molecules are noted for their exceptionally high allelic polymorphism and subsequent sequence diversity. The polymorphisms that differentiate MHC I allotypes are generally concentrated within the antigen binding groove. Consequently, each MHC I allotype has a unique peptidome, containing characteristic ligands with positional biases for subsets of amino acid residues at two to four "anchor" positions of the bound peptide. As a result, the peptide repertoire displayed by MHC I molecules at the cell surface is shaped by both the peptides liberated during protein degradation as well as by polymorphisms within the antigen binding groove that dictate ligand selection and further interactions with peptide loading chaperones (2–4).

In humans, classical MHC I molecules are co-dominantly expressed from three gene loci known as Human Leukocyte Antigen (HLA)-*A*, -*B* and -*C*. In addition to expected genetic associations between different HLA-A, B, and C allotypes and susceptibility to various infectious agents (5–10) or autoimmune disorders (11–18), quite profound associations have also been made between these genes and drug hypersensitivity reactions (19). Some of these HLA associations represent the strongest of any HLA-linked responses with odds ratios (>500) for distinct hypersensitivity reactions towards the anti-epileptic carbamazepine and HLA-B*15:02, the anti-hyperuricaemic allopurinol and HLA-B*58:01, and the anti-retroviral abacavir and HLA-B*57:01 (20–22). The molecular interaction underpinning these associations is only known for abacavir, where the drug behaves as a non-peptide ligand of HLA-B*57:01, binding within the peptide-binding groove and partially satiating the unique F pocket of this HLA allotype. This effectively creates a distinct, shallower antigen binding cleft that selects novel co-occupying peptide ligands (23–25). The immunopeptidome perturbation is characterised by a switch in C-terminal anchor residue (PΩ) preference from "canonical" HLA-B*57:01 peptides with aromatic residues (Trp/Phe/Tyr) at their C-terminus to "abacavir-induced" peptides with smaller aliphatic residues (Ile/Leu/Val) at this position. This results in the appearance of a large number of novel HLA–abacavir–peptide complexes at the cell surface and corresponding vigorous CTL responses against drug exposed cells (25, 26). These drug-induced anti-"altered self" responses are the proposed basis of the potentially deadly abacavir hypersensitivity syndrome in HLA-B*57:01$^+$ HIV patients utilising the drug as a part of their anti-retroviral regimen.

The involvement of the conventional MHC I antigen presentation pathway in the generation of abacavir-specific responses (26) suggests that novel HLA-B*57:01–peptide complexes are formed *de novo* in the ER in the presence of the drug (25). Peptide selection and the formation of stable ligand bound complexes is an intrinsic property of MHC I molecules, a process that varies in efficiency between allotypes and is enhanced *via* a macromolecular peptide loading complex (3, 27, 28). Peptide selection is thought to result from an iterative process in the ER in which MHC I molecules progressively replace low affinity peptides with those that bind with higher affinity (29, 30). A key constituent of this loading complex is the MHC I-specific co-factor tapasin, which is chiefly responsible for increasing the rate and extent of peptide loading and enhancing the discrimination that occurs between peptides (31–34). As such, tapasin ensures that MHC I preferentially assembles with high affinity peptides conferring increased expression at the cell surface (3, 35, 36). Although abacavir has a clear impact on the final immunopeptidome, it is unknown how abacavir interacts with this editing process.

Previous studies have indicated that the sensitisation of HLA-B*57:01$^+$ targets for killing by drug responsive T cells is dependent on a functional peptide loading complex and required *de novo* generation of HLA–drug–peptide complexes (25, 26). However, a small subset of drug-responsive CTLs are reported to target HLA-B*57:01$^+$ cells almost immediately upon abacavir exposure, raising the possibility that abacavir might exert a direct effect on HLA-B*57:01 molecules expressed at the cell surface (37). We therefore sought to i) define the kinetics of abacavir-induced changes in the HLA-B*57:01 immunopeptidome and to assess whether this correlates with *de novo* HLA-B*57:01 complex formation and immunogenicity; and ii) characterise the impact of abacavir on the association and dissociation of specific canonical and abacavir induced peptide ligands of HLA-B*57:01 using an *in vitro* peptide loading assay. In doing so, we generated a model in which abacavir allows the introduction of novel self-peptides into the immunopeptidome of HLA-B*57:01 that are not normally selected by HLA-B*57:01, as well as enhancing presentation of a subset of constitutive ligands by augmenting their association to, and reducing their dissociation from, HLA-B*57:01. The diverse effect that abacavir has on the selection of the B*57:01 peptide repertoire likely underpins the heterogeneity in response kinetics of different abacavir-induced T cell clones (37).

MATERIALS AND METHODS

Ethics and Sample Collection

*HLA-B*57:01*$^+$ healthy individuals (n = 3) were recruited for the study. Ethics approval was granted by both Monash University (HREC 4717 & 2297) and the Australian Bone Marrow Donor Registry (2013/04). Informed consent was obtained from all subjects. Peripheral blood samples were collected in heparinised vacutainer tubes and peripheral blood mononuclear cells (PBMCs) isolated by Ficoll–Paque (GE Healthcare) and density gradient centrifugation and cryopreserved until required.

Cell Lines

The C1R.B*57:01 cell line is a HLA-B*57:01 transfectant of the Class I reduced C1R cell line [expresses low levels of endogenous

HLA-A2 and -B35, and normal levels HLA-Cw4 (38, 39)] and has been previously used in studies of interactions between abacavir and HLA-B*57:01 (25, 26). HLA expression was maintained in long-term culture through addition of Geneticin, 0.5 mg/ml (G418; Life Technologies). C1R.B*57:01 were cultured in RF10 [RPMI 1640 (Life Technologies) supplemented with 10% foetal calf serum (FCS; Sigma), 7.5 mM HEPES (MP Biomedicals), 100 U/ml Pen Strep (benzyl–penicillin/streptomycin, Life Technologies), 2 mM L-glutamine (MP Biomedicals), 76 μM β-mercaptoethanolamine (Sigma), and 150 μM non-essential amino acids (Life Technologies)] at 37°C with 5% CO_2. HLA-expression phenotype was confirmed by flow cytometry using W6/32 (pan HLA class I, produced in-house from hybridoma) or 3E12 [HLA-B57 specific (40)] antibodies.

The 721.220 and tapasin transfectant 721.220.tapasin are previously described (3, 27) and were maintained in RPMI (Sigma) with 10% foetal bovine serum (Globepharm), 2 mM L-glutamine (Sigma), and 10 mM HEPES (Lonza) at 37°C with 5% CO_2. HLA-B*57:01 cDNA encoding amino acids −24 to 338 were cloned into pMCFR containing a puromycin selection marker. 721.220 and 721.220.tapasin cells were transfected using Nucleofection, program A-23, solution T (Amaxa) with 2 μg purified plasmid (Qiagen). Stable, polyclonal transfectants were selected with 1.5 μg/ml puromycin (Sigma) and/or 1 mg/ml G418 (Invitrogen) for tapasin expressing cell lines. The HLA-expression phenotype of the cells was confirmed by flow cytometry using W6/32 antibody.

Isolation of HLA Ligands

C1R.B*57:01 cells were grown to high density in RF10 containing 0.5 mg/ml G418 with the addition of 35 μM abacavir (Ziagen® tablets, GlaxoSmithKline) for the final 2, 4, 6, 12, or 16 h of culture, or with abacavir maintained at 35 μM throughout culture, or without abacavir. Cells were harvested by centrifugation (500 g, 5 min, 4°C), washed twice in chilled PBS and pellets of 10^8 cells snap frozen by submersion in liquid nitrogen. All samples were generated in triplicate and stored at −80°C prior to HLA extraction. For cell lysis prior to isolation of HLA molecules, cell pellets were resuspended in 5 ml of a mild lysis buffer {0.5% IGEPAL 630 [Sigma], 50 mM Tris pH 8, 150 mM NaCl [Merck-Millipore] and protease inhibitors [Complete Protease Inhibitor Cocktail Tablet (1 tablet per 50 ml solution); Roche Molecular Biochemicals, Switzerland]} and incubated for 45 min at 4°C with slow rolling to mix. Lysates were cleared by centrifugation at 16,000 *g* for 20 min at 4°C in a bench top centrifuge.

Immunoaffinity purification of HLA-peptide complexes from lysates was performed using the pan class I antibody W6/32 (produced in-house from hybridoma) coupled to a protein A affinity resin (Repligen) as described previously (41). Complexes were dissociated using 10% acetic acid (Sigma) and fractionated by reversed-phase high performance liquid chromatography (RP-HPLC) using an ÄKTAmicro™ HPLC system (GE Healthcare) equipped with a monolithic C_{18} RP-HPLC column (4.6 mm i.d. × 50 mm length, Chromolith Speed Rod, Merck-Millipore) and running a mobile phase consisting of buffer A [0.1% trifluoroacetic acid (TFA, Thermo Scientific)] and buffer B [80% acetonitrile (ACN, Fisher Scientific), 0.1% TFA] as described elsewhere (42). UV absorbance at 215 nm monitored the elution of material from the column and the area under the curve for the β_2-microglobulin (β_2m) peak used as a measure of the purified HLA within the sample. Peptide containing fractions were concatenated into three fraction pools, concentrated using a speed vacuum concentration system (LABCONCO) and reconstituted with 30 μl with 0.1% formic acid (FA, Thermo Scientific) prior to LC-mass spectrometry (MS) analysis.

Targeted Mass Spectrometric Detection and Quantitation of HLA Ligands

Liquid chromatography-multiple reaction monitoring (LC-MRM)-MS experiments utilised a Tempo nanoLC (Eksigent) autosampler and cHiPLC nanoflex (Eksigent) paired to a SCIEX QTRAP 5500 mass spectrometer. 10 μl samples were loaded onto a cHiPLC trap column (ChromXP C_{18}-CL column 0.5 mm × 200 μm i.d., 3 μm particle size, nominal pore size 120 Å) at 5 μl/min in 2% ACN, 0.1% FA for 10 min. An analytical cHiPLC column (ChromXP C_{18}-CL 15 cm × 75 μm i.d., 3 μm particle size, nominal pore size 120 Å) was switched in line, and the peptides eluted at 300 nl/min over a gradient of buffer A (0.1% FA) and B (98% ACN, 0.1% FA): 0–1 min 2% B, 1–3 min 2–10% B, 3–40 min 10–35.5% B, 40–45 min 35.5–80% B, 45–50 min hold at 80% B, 50–53 min 80–2% B, re-equilibration at 2% B for 7 min.

The QTRAP 5500 was operated in MRM mode in unit resolution for Q1 and Q3, with any MRM transition exceeding 600 counts triggering an Enhanced Product Ion (EPI) scan. We previously analysed the immunopeptidome of HLA class I from C1R.B*57:01 (untreated or constant 35 μM abacavir treatment) by LC-tandem mass spectrometry (MS/MS) using an SCIEX 5600^+ TripleTOF system (25). LC-MS/MS data were searched against the reviewed human proteome (UniProt/SwissProt accessed April 2016) using ProteinPilot™ software v4.5 considering biological modifications and employing a decoy database for false discovery rate (FDR) analysis. Peptides for quantitation were chosen from these data and MRM parent-product ion transitions were designed from the prominent product ions observed in the experimental spectra of selected peptides. Detection of these transitions overlapping at a particular retention time (RT) was used as an indicator of peptide presence. Peptide identity was validated either through comparison of transition hierarchy and RT to synthetic peptides, or, in the absence of synthetic peptide data, assignment of the fragmentation spectra observed in the linked EPI scan when searched against the list of candidate peptides using Protein Pilot™ software v5.0. Transitions were also designed for the detection of abacavir, a singly charged ion of mass:charge ratio (m/z) +287.2 with fragment ions of 190.9 (Collision energy [CE] 30), 174.0 (CE 45), 164.1 (CE 39), and 150.0 (CE 46).

A relative measure of peptide or abacavir abundance within the immunopeptidome was calculated as the total area under the curve for the detected transitions using Skyline software 64 bit 4.1.0.18169 [MacCoss Laboratory (43)] normalised to the total yield of class I HLA complexes (*i.e.* normalised to the area of the β_2m peak observed on RP-HPLC separation of the immunoaffinity eluate). Mean abundance was calculated from three replicates for each time point and normalised to the maximum mean detection of the

peptide/abacavir. To categorise peptides based on abacavir impact, linear regression was performed over t = 0 (untreated) to t = 16 h abacavir exposure using GraphPad Prism 7.01 (GraphPad Software, San Diego, California, USA). Peptides were defined as abacavir inhibited (slope < −0.02), minimal impact (slope magnitude < 0.02), abacavir facilitated (slope > 0.02, abundance > 0 at t = 0 in at least two of three replicates), abacavir dependent (slope > 0.02, abundance = 0 at t = 0 in at least two of three replicates). Although not matching the slope criteria peptides, KTFTTQETI and KTIETSPSL were classified as abacavir facilitated because the signal observed on constant treatment with abacavir was more than twice that observed in the absence of abacavir treatment. The mass spectrometry proteomics data have been deposited to the ProteomeXchange Consortium *via* the PRIDE (44) partner repository with the dataset identifier PXD024331.

Comparison of the Cellular Proteome Using Label Free Quantitation in LC-MS/MS

Triplicate cultures of C1R.B*57:01 in RF10 +/− 35 μM abacavir were incubated at 37°C, 5% CO_2 for 48 h. Cells were then harvested by centrifugation (500 g, 5 min, room temperature), washed in PBS and pellets of 7×10^6 cells snap frozen on dry ice in Eppendorf® LoBind microcentrifuge tubes and stored at −80°C until time of lysis. Cell pellets were lysed by resuspension in 100 μl 4% Sodium dodecyl sulphate (SDS, Sigma), 0.1 M Tris-HCl pH 7.6 (Merck-Millipore), 0.1 M Dithiothreitol (DTT, Sigma) followed by incubation at 95°C with shaking (1,200 rpm, Eppendorf Thermomixer Comfort). Insoluble material was removed by centrifugation (16,000 *g*, 10 min, RT) and supernatants harvested. Protein concentration was determined using a standard Bradford assay (Expedeon). 15 μl lysate (average 300 μg protein) was subjected to trypsin digestion using a FASP™ Protein Digestion kit (Expedeon) using a 10 kDa cut-off spin filter (Pall Corporation, USA) and proteomics grade trypsin from porcine pancreas (Sigma-Aldrich, USA). 10 μl digested peptides were acidified by addition of FA to a final concentration of 1% and desalted using OMIX C18 tips (Agilent Technologies), eluting in 50% ACN, 0.1% FA. ACN was removed using a speed vacuum concentration system (LABCONCO, USA) and samples resuspended in 15 μl 0.1% FA for mass spectrometry analysis. LC-MS/MS was performed using a Dionex UltiMate 3000 RSLCnano system coupled to a QExactive Plus mass spectrometer (Thermo Scientific). 6 μl of digest samples were loaded onto an Acclaim® PepMap100 20 mm C18 Nano-Trap column (100 μm i.d, 5 μm particle size, 100 Å pore size) at 15 μl/min in 2% ACN, 0.1% FA. Peptides were eluted from the trap column and separated over a 50 cm analytical Acclaim® RSLC PepMap RSLC 50 cm C18 Nano column (75 μm i.d., 2 μm particle size, 100 Å pore size), equilibrated in 97.5% buffer A (0.1% FA)/2.5% buffer B (80% ACN, 0.1% FA) at 250 nl/min using the following gradient conditions: 2.5–7.5% B over 1 min, 7.5–40% B over 120 min, 40–99% B over 5 min, 6 min hold at 99% B, followed by re-equilibration in 2.5% B for 20 min. Peptide detection was performed using a data-dependent acquisition (DDA) strategy in positive mode with a precursor m/z scan range of 375–1,800 (resolution 140,000) triggering fragmentation and MS of the 12 most abundant ions per cycle (m/z scan range 200–2,000, resolution 17,500) and operating with a 15 s dynamic exclusion. Fragmentation was limited to ion charge states of +2 to +5. Spectra were assigned and LFQ intensities calculated across three biological replicates per condition using MaxQuant (45) Version 1.6.1.0 searching against the reviewed human proteome (UniProt/SwissProt accessed April 2016), considering fixed modification carbamidomethyl cysteine, variable modifications of N-terminal acetylation, and methionine oxidation, as well as up to two missed trypsin cleavages. Protein ratios between samples were calculated based on at least two common peptides, including unique and razor peptides. Protein identifications were filtered of decoys, contaminants, and proteins only identified by a modification site. Log2 transformed LFQ intensities for proteins assigned LFQ values in at least three samples were compared between conditions using Perseus Version 1.6.6.0 by a two-sided t-test (46). Missing values were imputed from a normal distribution (default settings). The mass spectrometry proteomics data have been deposited to the ProteomeXchange Consortium *via* the PRIDE (44) partner repository with the dataset identifier PXD024331.

Abacavir-Specific T Cell Culture

To generate abacavir responsive T cells, $2–4 \times 10^6$ *HLA-B*57:01*$^+$ responder PBMCs were resuspended in 1 ml RF10 and placed in a single well of a 24 well tissue culture plate (Greiner Bio-One International AG, Austria). Autologous stimulator *HLA-B*57:01*$^+$ PBMCs were incubated for 4–5 h at 37°C, 5% CO_2 with 35 μM abacavir in 200 μl RF10. Stimulator PBMCs were subsequently added to responder PBMC at a 2:1 responder:stimulator ratio and the final volume of culture made up to 2 ml with RF10. Cells were incubated at 37°C, 5% CO_2 and fed with fresh media as required to sustain cell outgrowth. On day 5 of culture, cell media were supplemented with rhIL-2 (Cetus) at 20 U/ml and maintained at this concentration thereafter. On days 11–14 cultures were tested for antigen specificity by restimulation with abacavir pulsed (incubated with 35 μM abacavir overnight, washed three times in RPMI 1640) C1R.B*57:01 followed by intracellular cytokine staining (ICS).

Intracellular Cytokine Staining Assay

C1R.B*57:01 were incubated with 35 μM abacavir for set time periods (0–30 h) and HLA molecule export abrogated by 1% paraformaldehyde (PFA) fixation (ProSciTech, Australia) in PBS (2 h, room temperature). Cells were washed three times in RPMI 1640 to remove residual PFA, and stored overnight at 4°C in RH10 [RPMI 1640 (Life Technologies) supplemented with 10% human AB serum (HS; Sigma/Merck), 7.5 mM HEPES (MP Biomedicals), 100 U/ml Pen Strep (benzyl–penicillin/streptomycin, Life Technologies), 2 mM L-glutamine (MP Biomedicals), 76 μM β-mercaptoethanolamine (Sigma), and 150 μM non-essential amino acids (Life Technologies)]. C1R.B*57:01 were mixed with 1×10^5 T cells at a 1:2 ratio in a volume of 200 μl fresh RH10. After 2 h at 37°C, 5% CO_2, Brefeldin A (BFA; Sigma-Aldrich) was added to a final concentration of 10 μg/ml and incubated a further 4 h. Cells were stained with anti-CD4-PE [clone RPA-T4, Becton Dickinson (BD) Biosciences, USA] and anti-CD8-PerCP-Cy™5.5 (clone SK1, BD Biosciences, 25 min, 4°C), fixed with 1% PFA/PBS

(20 min, room temperature), washed in PBS, then permeabilised with 0.3% saponin (Sigma-Aldrich) in PBS containing anti-Interferon-γ (IFNγ)-PE-Cy^{TM}7 (clone B27, BD Biosciences) and anti-tumour necrosis factor (TNF)-PE-V450 (clone Mab11, BD Biosciences), and acquired by flow cytometry using an LSR II flow cytometer and BD FACSDIVA^{TM} software (BD). The percentage of CD8$^+$ T cells producing IFNγ and TNF was determined *via* analysis using FlowJo software (BD).

MHC I Pulse-Chase Maturation Assay

In order to assess the ability of abacavir to modulate HLA-B*57:01 maturation kinetics in various cell types, 60 μM abacavir was added to 2×10^7 cells in 50 ml culture medium 20 h before the start of the assay, while 2×10^7 cells were cultured in the absence of abacavir in otherwise identical conditions. Cells were harvested and incubated in 2 ml cysteine/methionine free RPMI (Sigma) containing 10% dialysed foetal bovine serum (Globepharm), 2 mM L-Glutamine (Sigma), and 60 μM abacavir, or no abacavir (as appropriate), for 40 min at 37°C. 3.8 MBq ^{35}S EasyTag (Perkin Elmer) was added for 6 min. The labelling reaction was stopped by adding 20 ml RPMI containing 10% dialysed foetal bovine serum, 2 mM L-Glutamine, and 2 mM Methionine (Sigma). 4 ml samples were taken at time points, and cells were lysed in PBS containing 1% NP-40 (US Biological), 2 mM phenylmethylsulfonyl fluoride (Sigma), and 5 mM iodoacetamide (Sigma) and clarified by centrifugation at 16,060 *g* for 10 min. Supernatants were pre-cleared with protein A sepharose (Sigma) and incubated with W6/32 and Protein A sepharose beads for 1 h. MHC I molecules were eluted from the beads by heating at 95°C for 3 min in 1.5% SDS and 50 mM Tris-HCL pH 6.8. The sample was digested (or mock digested) with 500 U EndoH_f (NEB) using the manufacturer's protocol. Proteins were separated by SDS PAGE, the gels dried, and bands were detected using Personal Molecular Imager FX (BIORAD) and quantified using Image J software. % of EndoH resistant material was calculated as a % of the total Endo H resistant and sensitive material.

Pulse-Chase Thermostability Assay

In order to assess if abacavir stabilised HLA-B*57:01 complexes expressed by various cell types, 60 μM abacavir was added to 2×10^7 cells in 50 ml culture medium 20 h before the start of the assay, while 2×10^7 cells were cultured in the absence of abacavir in otherwise identical conditions. Cells were harvested and incubated in 2 ml cysteine/methionine free RPMI (Sigma) containing 10% dialysed foetal bovine serum (Globepharm), 2 mM L-Glutamine (Sigma), and 60 μM abacavir, or no abacavir (as appropriate), for 40 min at 37°C. 3.8 MBq ^{35}S EasyTag (Perkin Elmer) was added for 6 min. The labelling reaction was stopped by adding 20 ml RPMI containing 10% dialysed foetal bovine serum, 2 mM L-Glutamine, and 2 mM Methionine (Sigma). 5 ml samples were taken at time points, and cells were lysed in PBS containing 1% NP-40 (US Biological), 2 mM phenylmethylsulfonyl fluoride (Sigma), and 5 mM iodoacetamide (Sigma) and clarified by centrifugation at 16,060 *g* for 10 min. Supernatants were pre-cleared with protein A sepharose (Sigma) for 1 h.

Each pre-cleared lysate was split into three tubes and incubated at 50, 37 or 4°C for 12 min then cooled on ice. MHC I molecules were precipitated with W6/32 and Protein A sepharose beads for 1 h. MHC I molecules were eluted from the beads by heating at 95°C for 3 min in 1.5% SDS, 50 mM Tris-HCl pH 6.8, 30% Glycerol, and 2 M 2-Mercaptoethanol. Proteins were separated by SDS PAGE. The gels were dried, and bands were detected using Personal Molecular Imager FX (BIORAD) and quantified using Image J software. Gels were re-hydrated and stained with Coomassie to quantify the IgG heavy chain. % of MHC I recovered after thermal denaturation was calculated by normalising MHC I band intensity against quantity of IgG heavy chain and represented as a proportion of material left compared to 4°C.

Production of Nucleotides Encoding HLA B*57:01fos

DNA encoding the ER luminal domains of HLA-B*57:01 with C-terminal Fos leucine zipper sequence was created by three PCR reactions: nucleotides encoding the ER luminal domains of HLA-B*57:01 were amplified using primers 5′-AGCCATATGGGCT CCCACTCCATGAG-3′ and 5′-ACCGCCGGAACCTCC TGGCTCCCATCTCAG-3′ and HLA-B*57:01 DNA in pET30 plasmid; while nucleotides encoding the Fos leucine zipper were amplified from pET22b HLA-A*02:01fos [described in (47)] using primers 5′-CTGAGATGGGAGCCAGGAGGTTC CGGCGG-3′ and 5′-CGCAAGCTTTTAATGGGCGGCC AGGATGAACT-3′. The purified products from both PCR reactions were used in a third PCR reaction to create HLA-B*57:01fos using primers 5′-AGCCATATGGGCTCCCACT CCATGAG-3′ and 5′-CGCAAGCTTTTAATGGGCGGCC AGGATGAACT-3′. Following agarose gel electrophoresis and digestion of the purified product with restriction enzymes the sequence encoding HLA-B*57:01fos was cloned into pET22b (Novagen).

Production of Monomeric Tapasin-Jun and Conjugated Tapasin-Jun-ERp57 C60A Proteins

Nucleotides encoding human tapasin-jun (47) were modified to allow purification *via* a TwinStrep affinity tag. First, nucleotides encoding a TEV protease cleavage site, TwinStrep affinity tag and stop codon were added to the pMT/BiP/V5-His A plasmid (ThermoFisher) as follows: a plasmid containing a synthetic gene encoding the TEV protease cleavage site, TwinStrep affinity tag and stop codon, flanked by nucleotides constituting 5′ XhoI and 3′ PmeI restriction enzyme sites (XhoI–TEV–TwinStrep–Stop–PmeI) was obtained from GeneArt (ThermoFisher). The nucleotides encoding the TEV–TwinStrep–Stop sequence were excised by digestion with XhoI and PmeI restriction enzymes and ligated into XhoI and PmeI digested pMT/BiP/V5-His A vector that had previously been modified to confer puromycin resistance as described in (47). Second, tapasin-jun was cloned into the pMT-BIP_TEV-TwinStrep (Puro) by one-step sequence and ligation independent cloning (48). Briefly, the vector pMT-BiP TEV-TwinStrep was digested with BglII and XhoI restriction enzymes while the sequence of tapasin-jun was amplified by PCR using the

forward primer (5′- GGCCTCTCGCTCGGGAGATCTGGACCC GCGGTGATCG-3′) and reverse primer (5′- GAAATACAG GTTTTCCTCGAGGTTCATGACTTTCTGTTTAAG-3′). The digested vector and the PCR product were incubated at a molar ratio of 1:4 in the presence of T4 DNA polymerase (NEB) at room temperature for 2 min 30 s, then the reaction was left on ice for 10 min before competent bacteria were transformed.

DNA encoding ERp57, without the signal sequence, but with a C-terminal His_6 tag located before the QEDL ER retrieval sequence was created by PCR using primers 5′-TAA AGATCTTCCGACGTGCTAGAACTCAC-3′ and 5′-GAAG AAGAAGAAGGCACATCACCATCACCATCACCAG GAGGATCTCTAAGAATTCCAC-3′ and human ERp57 DNA in pQE60 plasmid [described in (49)] and ligated to pMT-BiP plasmid modified to confer puromycin resistance following digestion of the purified product with restriction enzymes and agarose gel electrophoresis. The C60A mutation was introduced by PCR using primers 5′-GTGTGGACACGCCAAGAGAC TTG-3′ and 5′-CAAGTCTCTTGGCGTGTCCACAC-3′ and ERp57-His_6-QEDL in pMT-BiP (Puro).

S2 cells were transfected with either the pMT-BiP–Tapasin-Jun–TEV–TwinStrep (Puro) plasmid for the expression of monomeric tapasin-jun protein, or co-transfected with the pMT–BiP–Tapasin-Jun–TEV–TwinStrep (Puro) and pMT–BiP–ERp57 C60A His6 (Puro) plasmids for the expression of ERp57 C60A conjugated tapasin-jun proteins using Fugene6 transfection reagent (Promega) and OptiMEM medium (Fisher Scientific). Stable transfectants were generated by culturing the transfected cells in EX-CELL 420 Serum-Free Medium (Sigma) supplemented with 3 μg/ml puromycin (Melford).

Monomeric tapasin-jun or ERp57 C60A conjugated tapasin-jun proteins were purified from either cell supernatants or from cell pellets. Pooled cell supernatants were concentrated approximately five-fold using a 30 kDa membrane (Amicon). The pH of the concentrated supernatant was adjusted to pH 7–8 by the addition of binding buffer (50 mM Tris-HCl pH 8.0, 150 mM NaCl). BioLock biotin blocking solution (IBA Life Sciences) was added according to the manufacturer's recommendations (to prevent free biotin present in the medium from binding irreversibly to the Strep-Tactin beads) and incubated at room temperature for 5 min, before being passed through a 0.22 μm filter. 10 ml of 50% Strep-Tactin Superflow High Capacity beads (IBA Life Sciences) was washed twice with 50 ml of binding buffer before being mixed with the filtered cell supernatant at 4°C overnight. Following centrifugation at 270 g for 2 min the beads were pooled and washed three times with 50 ml of binding buffer and transferred to a 10 ml column. 5 mM D-desthiobiotin diluted in binding buffer was used to elute the proteins with 1 ml fractions being collected. Protein containing fractions were pooled and concentrated by 30 kDa spin concentrator (ThermoFisher) and dialysed against 20 mM Tris-HCl pH 8.0, 150 mM NaCl at 4°C. The dialysed protein was recovered and concentrated further using a 2 ml 10 kDa spin concentrator. Cell pellets were resuspended in lysis buffer [100 mM Tris-HCl pH 8.0, 150 mM NaCl, 1% NP40, 10 mM MgCl2, Complete EDTA-free protease inhibitors (Roche), and 100 μl/g cell pellet of 2 mg/mL DNAse Sigma)], sonicated on ice, and mixed at 4°C for 30 min. The lysate was clarified by centrifugation at 17,000 *g*, 4°C. The supernatant was passed through a 0.22 μm filter and incubated with Strep-Tactin Superflow High Capacity beads as described for the purification of the proteins from the supernatants.

Synthetic Peptides

For fluorescence polarisation experiments the following HLA-B*57:01 binding peptides were used: the UV-labile conditional peptide ligand LSSPVTKjF [j denotes 3-amino-3-(2-nitro)phenyl-propionic acid], the fluorescent peptides TSLK*SRVTI, LTTK*LTNTNI, ATFK*GIVRAI, NTVELRVK*I, KTFK*DVGNLL, KVFK*LQTSL, VTKK*TYEIW, ITTK*AISRW, RVDPAK*GLFYF (K* denotes TAMRA labelled lysine), non-labelled peptides TSLKSRVTI, LTTKLTNTNI, ATFKGIVRAI, NTVELRVKI, KTFKDVGNLL, KVFKLQTSL, VTKKTYEIW, and RVDPAKGLFYF. TAMRA labelled and unlabelled peptides were synthesised by GL Biochem Ltd (Shanghai, China). The UV labile peptide was synthesised by Peptide Protein Research Ltd (Fareham, UK). Unlabelled peptides used in LC-MRM-MS (**Supplementary Table 1**) were synthesised by GL Biochem Ltd (Shanghai, China).

Production of Peptide-Loaded HLA-B*57:01fos Complexes

Peptide loaded HLA-B*57:01fos complexes were obtained as described (50) by refolding solubilised inclusion bodies of HLA-B*57:01fos heavy chains with human β_2m and UV-labile HLA-B57-conditional peptide ligand.

Fluorescence Polarisation Experiments

Fluorescence polarisation measurements were taken using a SpectraMax i3x Multi-Mode Microplate Reader (Molecular Devices) with rhodamine detection cartridge. All experiments were conducted at 25°C and used PBS supplemented with 0.5 mg/ml bovine-gamma-globulin (Sigma), and a 20 fold molar excess of human β_2m (Fitzgerald) in a volume of 60 μl. Binding of TAMRA-labelled peptides is reported in millipolarisation units (mP) and is obtained from the equation $mP = 1{,}000 \times (S - G \times P)/(S + G \times P)$, where S and P are background subtracted fluorescence count rates (S = polarisation emission filter is parallel to the excitation filter; P = polarisation emission filter is perpendicular to the excitation filter) and G (grating) is an instrument and assay dependent factor.

Association Rate Measurements

Peptide-receptive HLA-B*57:01fos were obtained by exposing HLA-B*57:01fos complexes loaded with UV labile conditional peptide ligand to ~360 nm light for 20 min at 4°C ("UV exposed" hereafter). The binding of fluorescent peptides to UV exposed HLA-B*57:01fos was monitored in the absence or presence of excess (60 μM) abacavir or tapasin-jun or tapasin-jun ERp57 C60A conjugate. Comparable results were obtained with either monomeric tapasin-jun or ERp57 C60A conjugated tapasin-jun proteins. Most experiments used tapasin-jun proteins at a concentration of 0.254 μM, but some experiments used different

preparations of tapasin-jun protein, which required higher concentrations (up to 0.75 μM) to achieve comparable function. Most experiments used 0.55 μM HLA-B*57:01fos molecules, but a minority of experiments involved different preparations of HLA-B*57:01fos which required higher concentrations of HLA-B*57:01fos, up to a maximum of 3.18 μM HLA-B*57:01fos, to achieve equivalent polarisation levels. Comparable results were obtained. Peptide concentrations varied between experiments, but gave comparable results: KTFK*DVGNLL 0.015–0.045 μM, TSLKSRVTI 0.015–0.083 μM, KVFK*LQTSL 0.015–0.1 μM, ATFK*GIVRAI 0.015–0.092 μM, NTVELRVK*I 0.015–0.210 μM, VTKK*TYEIW 0.015–0.106 μM, RVDPAK*GLFYF 0.015–0.087 μM, ITTK*AISRW 0.015–0.353 μM, LTTK*LTNTNI 0.006–0.024 μM.

Dissociation Rate Measurements

HLA-B*57:01fos molecules were UV exposed and then allowed to bind fluorescent peptides overnight at room temperature. Florescence polarisation measurements were taken after the addition of excess non-labelled competitor peptide (otherwise identical to the labelled peptide) in the absence or presence of 60 μM abacavir or conjugated tapasin-jun-ERp57 C60A proteins. Most experiments used tapasin-jun proteins at a concentration of 0.254 μM, but some experiments used different preparations of tapasin-jun protein, which required higher concentrations (up to 0.949 μM) to achieve comparable function. Most experiments used 0.55 μM HLA-B*57:01fos molecules, but some experiments involved different preparations of HLA-B*57:01fos which required higher concentrations of HLA-B*57:01fos, up to a maximum of 1.38 μM HLA-B*57:01fos, to achieve equivalent polarisation levels. Comparable results were obtained. Peptide concentrations varied between experiments, but gave comparable results: KTFK*DVGNLL 0.015–0.045 μM, TSLKSRVTI 0.015–0.034 μM, KVFK*LQTSL 0.015–0.039 μM, ATFK*GIVRAI 0.015–0.063 μM, NTVELRVK*I 0.015–0.165 μM, VTKK*TYEIW 0.015–0.028 μM, RVDPAK*GLFYF 0.015–0.082 μM, ITTK*AISRW 0.015 μM.

RESULTS

Abacavir Induced Changes in the HLA-B*57:01 Immunopeptidome Increase Over Time

We previously characterised the impact of abacavir exposure on the immunopeptidome of HLA-B*57:01 molecules isolated from C1R.B*57:01 cells and determined the sequences of novel drug induced ligands by liquid chromatography-tandem mass spectrometry (LC-MS/MS) (25). This workflow enabled identification of peptides without prior knowledge of sequence but is biased towards those of highest intensity during LC-MS/MS. In contrast, liquid chromatography-multiple reaction monitoring–mass spectrometry (LC-MRM–MS) specifically targets known peptides based on knowledge of their precursor ion mass and sequence specific fragmentation patterns. LC-MRM–MS strategies have been shown to facilitate the detection of both high and low abundance peptides against the complex background of the immunopeptidome and facilitate relative peptide quantitation (42, 51–53). Therefore, to follow the perturbation of the immunopeptidome over time, we designed a LC-MRM–MS based approach to track changes in the relative abundance of a subset of HLA-B*57:01 ligands within the immunopeptidome. Based on this strategy, 58 HLA-B*57:01 ligands were robustly detected; 35 that were originally identified in both treated and untreated cells, 22 that were identified only in treated cells, and one that was previously identified in untreated cells alone (see **Supplementary Table 1** for details). These peptides possessed predominantly canonical HLA-B*57:01 anchor residues at P2 of the peptide (Ser, Thr, Ala, or Val), whilst PΩ residues included both the preferred canonical aromatic PΩ anchors (Trp, Phe, Tyr) and aliphatic residues that increase in representation following exposure to abacavir (Ile, Leu and Val). As C1R.B*57:01 also expresses the HLA class I molecule HLA-C*04:01, five peptides identified as ligands of HLA-C*04:01 in parental C1R cells (54) were also targeted for detection as an internal drug-specificity control.

MHC I molecules were isolated from C1R.B*57:01 cells that had been cultured for 0–16 h, or continuously, in the presence of abacavir. Changes in the immunopeptidome were evident after 2 h of abacavir treatment and became more prominent during the 16 h time course of the experiment. This coincided with the co-purification of increasing amounts of HLA-B*57:01-bound abacavir (**Figure 1** and **Supplementary Figure 1**). The changes in the abundance of peptides in response to abacavir exposure could be categorised into four groups. One group, consisting of six peptides, was abacavir inhibited (decreased in abundance over exposure time, **Figure 1A**). Another group of 20 peptides experienced minimal impact (no marked change in abundance, **Figure 1B**). Eight peptides were observed to be abacavir facilitated (present in the absence of abacavir but increased in abundance with abacavir exposure, **Figure 1C**), and the remaining 24 peptides were abacavir dependent (not robustly detected in the absence of abacavir and increased in abundance during abacavir exposure, **Figure 1D**). Ligands of HLA-C are shown for comparison in **Figure 1E**.

Abacavir Independent Ligands

The majority of the 20 peptides that were minimally impacted by abacavir terminated in canonical PΩ anchor residues for HLA-B*57:01 (25, 55) (**Figure 1B** and **Supplementary Figure 1**, orange symbols and line): 15 peptides terminated in Trp, whilst a further three peptides terminated in less favoured canonical residues, Tyr and Phe. These included LSSPVTKSF for which crystal structures of this peptide in complex with HLA-B*57:01 demonstrate the occupation of the abacavir binding site by P7 Lys and P9 Phe residues (25, 26). Consistent with their conformity to the canonical HLA-B*57:01 peptide binding motif most peptides within this category were predicted to be strong binders of HLA-B*57:01 by NetMHC4.0 (56, 57) (**Supplementary Figure 2**), suggesting these peptides are high affinity ligands, which are not markedly impacted by competition from abacavir and abacavir-induced peptide ligands. The two remaining peptides, ITKTVVENI and LSKPNPPSL, were

predicted to bind B*57:01 with low affinity (**Supplementary Figure 2**, red and green symbols) and, despite their PΩ residues being considered conducive to binding in the presence of abacavir, these peptides appear to be well represented in the constitutive HLA-B57 immunopeptidome.

Abacavir Inhibited Peptides

We observed that six of the peptides in our panel decreased in abundance following the addition of abacavir (**Figure 1A** and **Supplementary Figure 1**, red symbols and line). Three peptides terminated in the canonical Phe residue at PΩ, whilst the remaining three peptides terminated in the combination of Leu at PΩ and Arg at PΩ-2. We have previously observed that Phe at PΩ provides less stability to HLA-B*57:01 complexes than Trp (55) and indeed, two of these peptides were predicted to bind B*57:01 with low affinity (**Supplementary Figure 2** and **Supplementary Table 1**). This suggests that these ligands may be displaced from the repertoire in preference of higher stability HLA-B*57:01-abacavir–peptide complexes. Similarly, whilst Arg at PΩ-2 can act as a secondary anchor for HLA-B*57:01, forming a salt-bridge with Asp114 of the E-pocket and stabilising the peptide within the groove (55), the three peptides with the combination of Leu at PΩ and Arg at PΩ-2 were also predicted to bind with low affinity (**Supplementary Figure 2** and **Supplementary Table 1**). This suggests that these peptides are vulnerable to dissociation due to the interaction between Arg at PΩ-2 and Asp114 being out-competed by the presence of abacavir within the antigen-binding cleft.

Abacavir Enhanced Peptides

We found eight peptides that were detected at relatively low abundance in the immunopeptidome of untreated cells but substantially increased when the cells were grown in abacavir supplemented media (**Figure 1C** and **Supplementary Figure 1**, yellow symbols and line). Seven of these peptides terminated in aliphatic residues (three Ile and four Leu), whilst the remaining peptide, HTIQIRQDW terminated in the preferred canonical Trp residue. Of the eight peptides, HTIQIRQDW possesses the highest predicted binding affinity for HLA-B*57:01 (**Supplementary Figure 2**, blue symbol). Given C-terminal Trp is likely to clash with abacavir binding, the modest enhancement of the HTIQIRQDW peptide may indicate that canonical

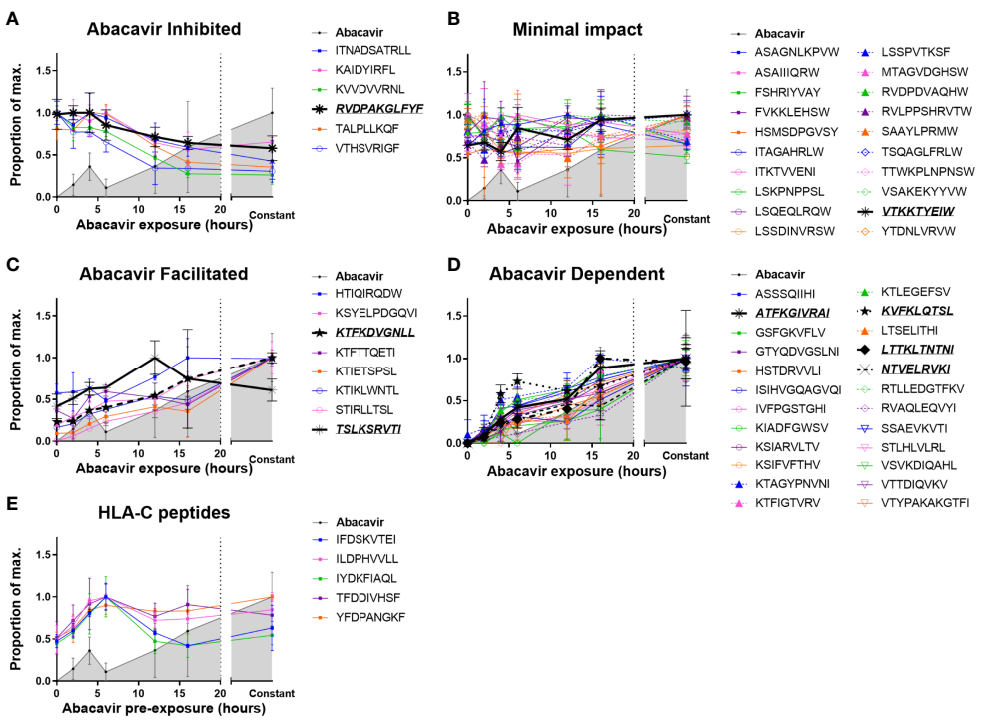

FIGURE 1 | Abacavir perturbs the HLA-B*57:01 immunopeptidome by increasing or decreasing the contribution of distinct subsets of peptides. Analysis of 58 selected HLA-B*57:01 peptide ligands, isolated from 10^8 C1R.B*57:01 cells after 0–16 h, or constant, abacavir treatment using LC-MRM–MS demonstrated four main patterns of impact on contribution to the immunopeptidome; **(A)** inhibition, **(B)** minimal impact, **(C)** facilitated (presented by HLA-B*57:01 of untreated cells but increased in abundance during abacavir treatment) and **(D)** dependent (only presented by HLA-B*57:01 of cells exposed to abacavir). Perturbation of HLA-B*57:01 ligands increased with time, coincident with increased co-purification of abacavir. Perturbations were not mirrored by the HLA-C ligands analysed **(E)**. Peptide and abacavir abundances are shown as a proportion of the maximum normalised peak area detected and are portrayed as the mean of the three biological replicates (mean +/– SD). The decreased recovery of abacavir at the 6 h point is likely to reflect an experimental artefact in the off line fractionation prior to the LC-MS. Importantly there was not a similar decrease in the amount of peptide material eluted at this time point. Peptides that were chosen for *in vitro* peptide binding and dissociation experiments are in italics and underlined.

peptides such as HTIQIRQDW benefit from the altered competition between peptides that follows the addition of abacavir.

Presentation of another 24 peptides appeared entirely dependent on abacavir (**Figure 1D** and **Supplementary Figure 1**, green symbols and line). All of these peptides terminated in aliphatic residues considered characteristic of abacavir-induced peptide ligands: 13 peptides terminated in Ile, three in Leu and eight in Val, whilst only ATFKGIVRAI possessed Arg at PΩ-2. The absence of abacavir dependent peptides from the constitutive immunopeptidome strongly suggests that abacavir is obligatory for these peptides to bind to HLA-B*57:01. Indeed, most peptides within this category were predicted non-binders of HLA-B*57:01 (**Supplementary Figure 2**).

Of note, the abacavir facilitated peptide KTIKLWNTL is derived from Receptor of activated protein C kinase 1 (RACK1), the same source protein as YTDNLVRVW, which was minimally impacted by abacavir. Similarly, the abacavir dependent peptide LTSELITHI and abacavir inhibited peptide KVVDVVRNL are derived from Interferon-induced GTP-binding protein Mx1 (MX1). Thus, it is unlikely that differences in presentation kinetics between these peptide pairs are the result of changes in source protein abundance.

Abacavir Has Minimal Impact on the C1R.B*57:01 Proteome

To further confirm that changes in the abundance of HLA-bound peptides were not due to significant changes in source protein abundance induced by abacavir treatment, we analysed the cellular proteome of C1R.B*57:01 cells that were cultured in the presence or absence of abacavir for 48 h. Cells were lysed before the cellular proteins were isolated and digested and subjected to LC-MS/MS and label free quantitation (LFQ) analysis. A total of 3,077 proteins were identified, of which 2,306 were robustly detected in at least three samples and used for LFQ. This included the source proteins for 37 of the 58 HLA-B*57:01 ligands and three of the five HLA-C*04:01 ligands incorporated in the immunopeptidome analysis. Importantly, no protein showed significant changes in expression following abacavir treatment (**Figure 2**).

Immunogenicity of Abacavir Treated Cells Increases Over Time

To determine if the observed changes in the immunopeptidome occurred over a similar time scale to the acquisition of immunogenicity, C1R.B*57:01 cells were exposed to abacavir for various lengths of time, fixed and assayed for their ability to elicit cytokine production (IFNγand/or TNF) from abacavir responsive $CD8^+$ T cell lines. For the three T cell lines tested, an increase in antigen presenting cell immunogenicity was observed over the first 12 h of abacavir exposure, before levelling out (**Figure 3**).

Intracellular Biogenesis of Stable HLA-B*57:01–Peptide Complexes Is Unchanged by Abacavir Treatment

Polymorphic residues of MHC I allotypes that interact with the C-terminal region of the peptide, including residues 114 and 116, are implicated in determining the dependence upon tapasin for the selection and assembly with high affinity peptides (2, 3, 58). HLA-B*57:01 has been classified as tapasin-dependent because it is poorly expressed at the cell surface in the absence of tapasin (28) (**Supplementary Figure 3**). Given that abacavir binds

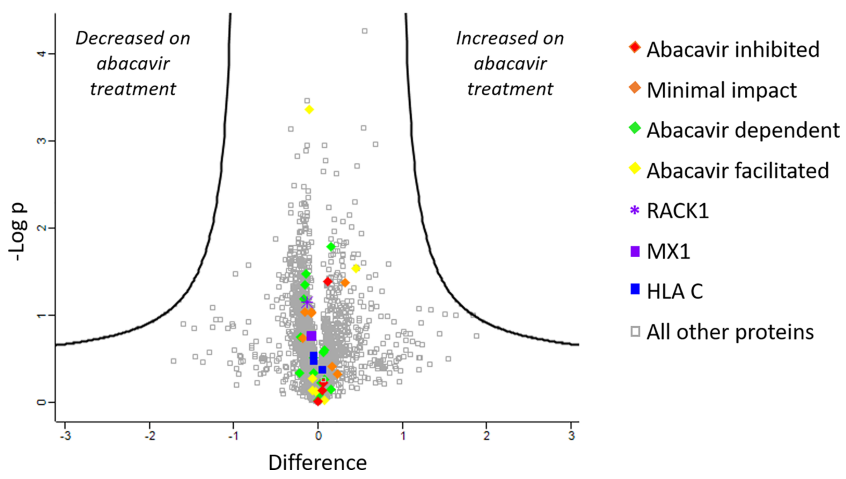

FIGURE 2 | Abacavir does not perturb the proteome of C1R.B*57:01. Comparison of protein abundance between untreated and abacavir treated (48 h, 35 μM) C1R.B*57:01 cells (three replicates per treatment) revealed no major perturbation of the cellular proteome. The volcano plot depicts the difference (log_2FC) *vs* -Logp of 2,306 proteins between untreated and treated conditions. A 5% FDR and a slope of 1 were used as the cut-off for significance (thick black line). No proteins were significantly perturbed by abacavir treatment; furthermore identified source proteins for the HLA ligands analysed clustered close to 0 on the difference axis. Source proteins for HLA ligands from the different subsets analysed are shown as indicated in the key. The purple asterisk shows RACK1, the source protein of peptides KTIKLWNTL (abacavir facilitated), and YTDNLVRVW (minimal impact), and the purple square shows MX1, the source of peptides LTSELITHI (abacavir dependent) and KVVDVVRNL (abacavir inhibited). All other proteins are shown by grey squares.

beneath the C-terminus of the peptide and interacts with residues that influence tapasin dependence (23, 25), we sought to determine whether abacavir i) promotes HLA-B*57:01 maturation independently of, or in conjunction with, tapasin, and/or ii) alters the dependence of HLA-B*57:01 upon tapasin for optimal peptide selection (26, 28). The tapasin-deficient 721.220 cell line (27) and the tapasin reconstituted 721.220.tapasin cell lines have previously been used to measure the rate and extent of intracellular peptide selection by newly synthesised MHC I molecules using pulse chase experiments (3). We therefore utilised this system to explore the maturation and stability of newly generated HLA-B*57:01 complexes in the presence or absence of abacavir. Pulse-chase maturation assays showed impaired acquisition of resistance to digestion with Endoglycosidase-H (Endo-H) by HLA-B*57:01 molecules in the absence of tapasin. Only ~25% of labelled complexes gained Endo-H resistance over the first 60 min of the assay compared to ~85% of HLA-B*57:01 complexes in tapasin expressing cells. This proportion of Endo-H resistant complexes increased to ~44% after 2 h (**Figures 4A, B**). Abacavir did not significantly alter this pattern of biogenesis. The maturation of HLA-B*57:01 molecules was also unaffected by abacavir in tapasin-reconstituted cells (**Figures 4A, B**).

In agreement with the lack of effect on HLA-B*57:01 maturation in tapasin deficient 721.220 cells (**Figures 4A, B**), abacavir had no significant impact on the thermal stability profile of HLA-B*57:01 in the absence of tapasin (**Figure 4C**). As anticipated, tapasin reconstituted cells produced more thermostable complexes (**Figure 4D**). This suggests that abacavir does not compensate for the absence of tapasin to promote the formation of stable HLA-B*57:01 complexes. These data were consistent with measurements of cell-surface expression and stability of HLA-B*57:01 molecules which showed that whilst tapasin increased surface expression as observed previously (28) and prolonged the half-life of HLA-B*57:01 molecules at the cell surface, abacavir did not significantly alter either the expression level or the stability of cell surface HLA-B*57:01 molecules (**Supplementary Figure 3**). This suggests that tapasin, but not abacavir, can increase the proportion of high stability HLA-B*57:01 complexes generated. Collectively, these data confirm that tapasin improves the ability of HLA-B*57:01 molecules to select high quality (ligands that generate complexes stable at 50°C) or medium quality (ligands that generate complexes stable at 37°C but not 50°C) peptide cargo.

Abacavir Enhances the Loading of Specific Peptides From the Immunopeptidome of HLA-B*57:01

We next investigated the mechanism by which abacavir changes the composition of the HLA-B*57:01 immunopeptidome by conducting *in vitro* peptide binding experiments. We first measured the binding of a panel of fluorescently labelled peptides to HLA-B*57:01 in the absence or presence of abacavir, or the MHC I co-factor tapasin or both. This peptide panel included two peptides, KTFK*DVGNLL and TSLK*SRVTI (KTF and TSL hereafter), classified by quantitative mass spectrometry as being abacavir facilitated. Consistent with this observation, HLA-B*57:01fos molecules displayed a limited intrinsic ability to bind either KTF or TSL peptides (**Figures 5A, B**, grey lines), with binding strongly enhanced when either

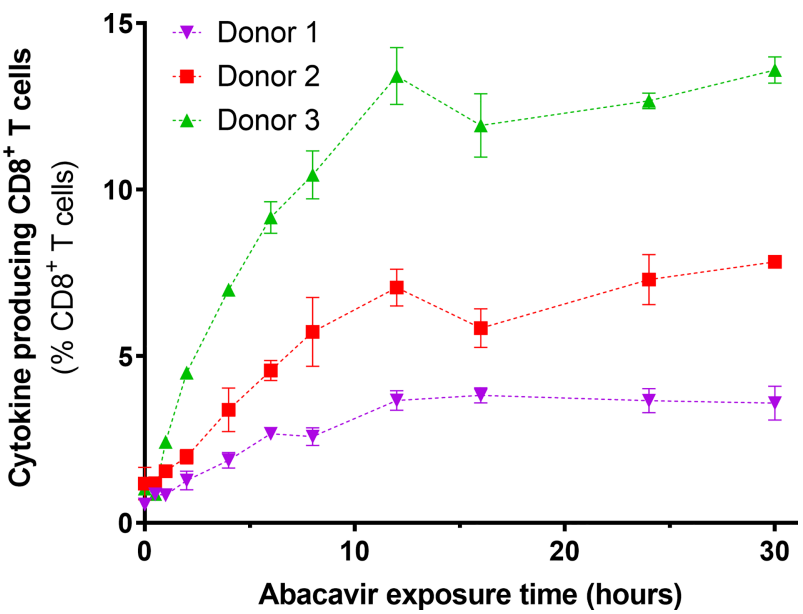

FIGURE 3 | Immunogenicity of HLA-B*57:01+ antigen presenting cells increases with abacavir exposure time. C1R.B*57:01 cells were cultured in 35 μM abacavir for 0–30 h prior to fixation in paraformaldehyde. Immunogenicity was then gauged by their ability to stimulate cytokine (IFNγ and/or TNF) production in $CD8^+$ abacavir responsive T cells during a 6 h stimulation assay, detected *via* intracellular cytokine staining. Responses from T cell lines derived from three different *HLA-B*57:01*$^+$ donors are shown. Donor 1 T cells were assayed in triplicate, whilst donor 2 and 3 T cells were assayed in duplicate in a separate experiment (mean +/– SD).

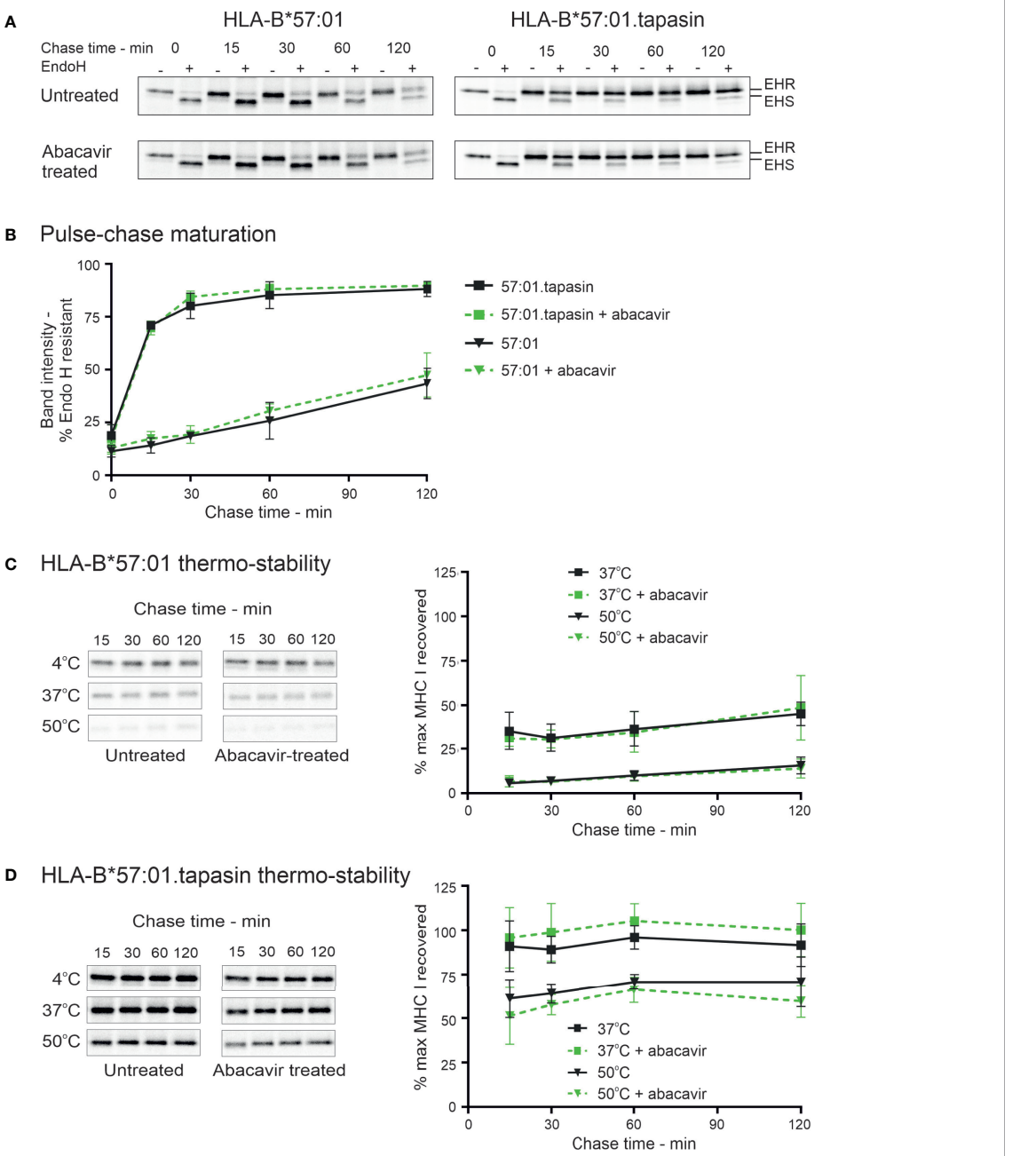

FIGURE 4 | Abacavir does not significantly alter maturation or global stability of HLA-B*57:01. **(A)** and **(B)** Maturation [acquisition of resistance to digestion with endoglycosidase-H (Endo-H)] of HLA-B*57:01 molecules was determined by pulse chase in 721.220.B*57:01 or 721.220.B*57:01.tapasin cells, immunoprecipitation of MHC I molecules, and digestion with endoglycosidase-H. **(A)** depicts representative SDS-PAGE gels for untreated and abacavir treated cells; only the HLA-B*57:01 heavy chain bands are shown. The location of Endo-H resistant (EHR) and Endo-H sensitive (EHS) bands is distinguished by their altered migration pattern. **(B)** The % EHR material was calculated [EHR/(EHR+EHS)] and plotted as the mean (+/– SD) of three or four replicate experiments for abacavir treated and untreated cells respectively excluding time point 15, which was only included in two experiments. Abacavir had no apparent impact on HLA-B*57:01 maturation in either the presence or absence of tapasin. **(C)** and **(D)** Pulse-chase thermostability assays were performed in 721.220.B*57:01 **(C)** and 721.220.B*57:01.tapasin **(D)** cells: lysates were prepared from pulse radio-labelled cells and incubated at either 4, 37, or 50°C before β_2m associated MHC I molecules were immunoprecipitated using W6/32 antibody and resolved by SDS-PAGE. Representative SDS-PAGE gels for untreated and abacavir treated cells depict the HLA-B*57:01 heavy chain bands recovered at each chase time after thermal denaturation. Graphs show the amount of HLA-B*57:01 molecules recovered after thermal denaturation at 37 and 50°C as a percentage of that recovered at 4°C (mean +/– SD of four or five replicate experiments for abacavir treated and untreated cells respectively).

abacavir (blue lines) or tapasin (red lines) was included. When tapasin and abacavir were both added (green lines), binding of both peptides occurred faster than in the presence of tapasin or abacavir alone.

Four peptides within our panel were classified by quantitative mass spectrometry as being dependent on abacavir. There was negligible to very little intrinsic binding of any of these peptides to the B*57:01fos molecules (**Figures 5C–F**, grey lines). Abacavir strongly enhanced binding of all four peptides (blue lines) although enhancement of the binding of the ATF peptide was less pronounced than the other three abacavir dependent peptides, consistent with Arg at PΩ-2 being unfavourable for the binding of abacavir. Tapasin did not affect the binding of the LTT or NTV peptides, and only slightly enhanced binding of the ATF and KVF peptides during the first few hours of the experiment (**Figures 5C–F**, red lines). Notably the binding of all four peptides occurred faster with the combined addition of abacavir and tapasin in comparison to that which was evident in the presence of abacavir or tapasin alone (**Figures 5C–F**, blue, red and green lines).

Our panel also included two canonical HLA-B*57:01 peptides VTKK*TYEIW and ITTK*AISRW (VTK and ITT hereafter) with VTK classified by quantitative mass spectrometry as being minimally affected by abacavir. Both peptides bound to HLA-B*57:01 molecules (**Figures 5G–H**, grey lines), but in contrast to the abacavir dependent peptides, tapasin (red lines) catalysed

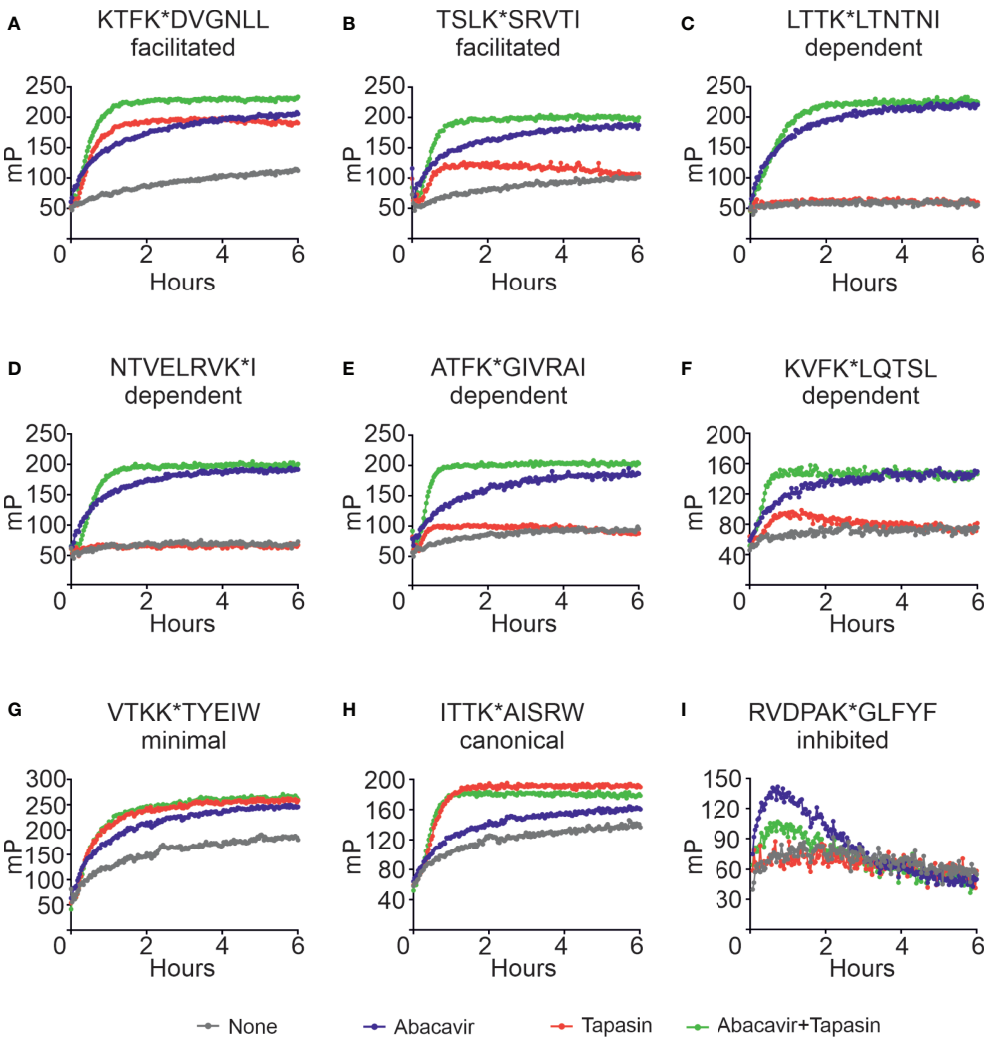

FIGURE 5 | Abacavir diversifies the HLA-B*57:01 peptide repertoire by enhancing the loading of specific peptides. Conditional ligand loaded HLA-B*57:01fos molecules were UV exposed before the binding of the indicated peptide (**A** = KTFK*DVGNLL, **B** = TSLK*SRVTI, **C** = LTTK*LTNTNI, **D** = NTVELRVK*I, **E** = ATFK*GIVRAI, **F** = KVFK*LQTSL, **G** = VTKK*TYEIW, **H** = ITTK*AISRW, **I** = RVDPAK*GLFYF) was followed at 25°C in the presence or absence of excess abacavir and/or monomeric or ERp57 C60A conjugated tapasin-jun. Binding of fluorescent peptide is reported in millipolarisation units (mP). Unbound fluorescent peptide is assumed to have an mP level of 50. Data shown are representative of triplicate or greater experiments. The extent that tapasin, abacavir, or the combination of both enhanced the binding of fluorescent peptides to HLA-B*57:01fos molecules in the replicate experiments is presented in **Figure 6**. Colour coding is as follows: grey—peptide alone, blue—abacavir, red—tapasin, green—abacavir + tapasin.

binding of the VTK and ITT peptides to a greater extent than abacavir (blue lines). The combined addition of tapasin and abacavir did not enhance the binding of the VTK and ITT peptides beyond the enhancement that tapasin afforded (green lines).

The last peptide included in our panel was RVDPAK*GLFYF (RVD hereafter), which quantitative mass spectrometry experiments indicated decreased in the immunopeptidome when cells were cultured in abacavir. Consistent with this peptide being predicted to bind B*57:01 with very low affinity (**Supplementary Figure 2**, blue symbol), we observed poor binding of RVD to B*57:01 molecules (**Figure 5I**, grey line). Surprisingly, binding of RVD was enhanced by abacavir during the first hour of the experiment when tapasin was absent (blue line); but tapasin partially mitigated this effect (green line), providing an example of how some peptides may be "edited out" of the repertoire.

To enable comparison of the effects of abacavir, tapasin, or the combination of abacavir and tapasin on the binding of our panel of peptides, we calculated how much each enhanced the binding of specific peptides (**Figure 6**). **Figure 6A** shows that tapasin enhanced the binding of abacavir-facilitated peptides (KTF and TSL) to a greater extent than abacavir dependent peptides, consistent with peptides belonging to the latter category being absent from, or poorly represented in, the immunopeptidome of untreated cells. **Figure 6B** shows that binding of abacavir-facilitated (KTF and TSL) and abacavir-dependent (LTT, NTV and KVF) peptides increased to a greater extent than those peptides that were minimally affected (VTK and ITT) or decreased in representation within the immunopeptidome (RVD) following the addition of abacavir. The combined addition of tapasin and abacavir produced a similar enhancement hierarchy to that observed for abacavir (**Figure 6C**).

Abacavir Diversifies the HLA-B*57:01 Peptide Repertoire by Decreasing Dissociation of Specific Peptides

We next characterised the effect that abacavir has on peptide dissociation. Conditional ligand loaded HLA-B*57:01fos molecules were UV exposed and then incubated with eight of the labelled peptides from our panel before unlabelled competing peptide, used to block rebinding of the labelled peptide, was added in the presence or absence of abacavir, tapasin, or both. Dissociation of the labelled peptides was measured by fluorescence polarisation. **Figure 7** and **Supplementary Table 2** show that the peptides dissociated from HLA-B*57:01fos molecules at different rates (black lines), ranging from hundreds of hours (*e.g.* VTK, **Figure 7A**) to minutes (*e.g.* RVD, **Figure 7B**). Notably, the fast off-rate of RVD is consistent with the depletion of this peptide from the immunopeptidome upon exposure to abacavir (**Figure 1A**), whilst the slow off-rate of VTK may explain the persistence of this peptide in the immunopeptidome (**Figure 1B**). Tapasin has been shown to enhance the dissociation of peptides from MHC molecules, the extent of this effect being peptide-dependent (31). In accordance, we saw a range of tapasin dependent enhancements of dissociation (red lines), ranging from significant (*e.g.* KTF, **Figure 7F**) to minimal (*e.g.* NTV, **Figure 7D**).

The addition of abacavir together with competing peptide (blue lines) led to a pronounced decrease in the dissociation of the abacavir dependent (KVF, NTV and ATF, **Figures 7C–E**) and abacavir facilitated (KTF and TSL, **Figures 7F–G**) peptides. In contrast, the addition of abacavir and competing peptide had minimal impact on the dissociation of the VTK and ITT peptides (**Figures 7A, H**), consistent with minimal impact of abacavir on the contribution of VTK to the immunopeptidome. Notably, we observed that the fast dissociation rate of the RVD peptide from

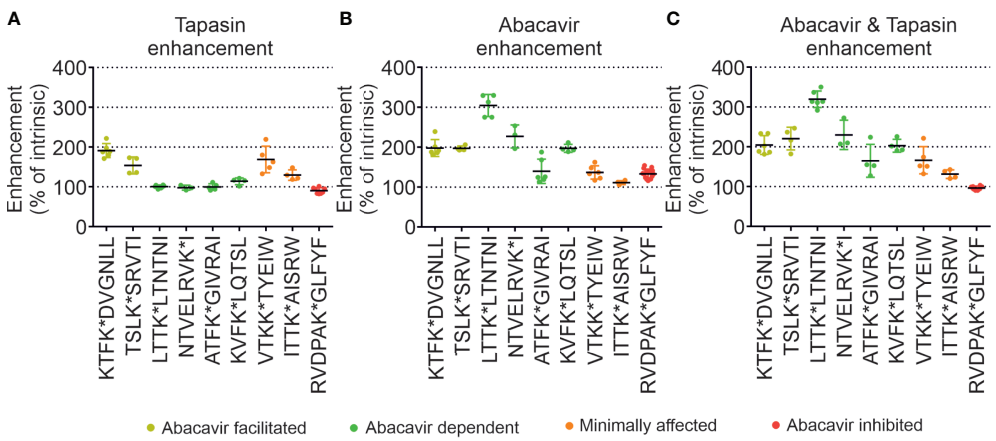

FIGURE 6 | Tapasin and abacavir differentially enhance the binding of fluorescent peptides. The extent that **(A)** tapasin, **(B)** abacavir, or **(C)** the combination of both enhanced the binding of fluorescent peptides to HLA-B*57:01fos molecules was compared over independent experiments. For each polarisation measurement taken in an experiment the enhancement factor was calculated by: dividing polarisation in the presence of tapasin (or abacavir or both) by the intrinsic polarisation level; multiplying by 100 to obtain a percentage; and calculating the mean enhancement for the experiment. The enhancement factors obtained from different experiments are shown as dots, with the mean average shown as a horizontal black bar, and the standard deviation of multiple experiments shown as a coloured vertical line edged with horizontal bars. Peptides are coloured according to their classification by mass spectrometry: abacavir facilitated = yellow, abacavir dependent = green, minimally affected = orange, abacavir inhibited = red.

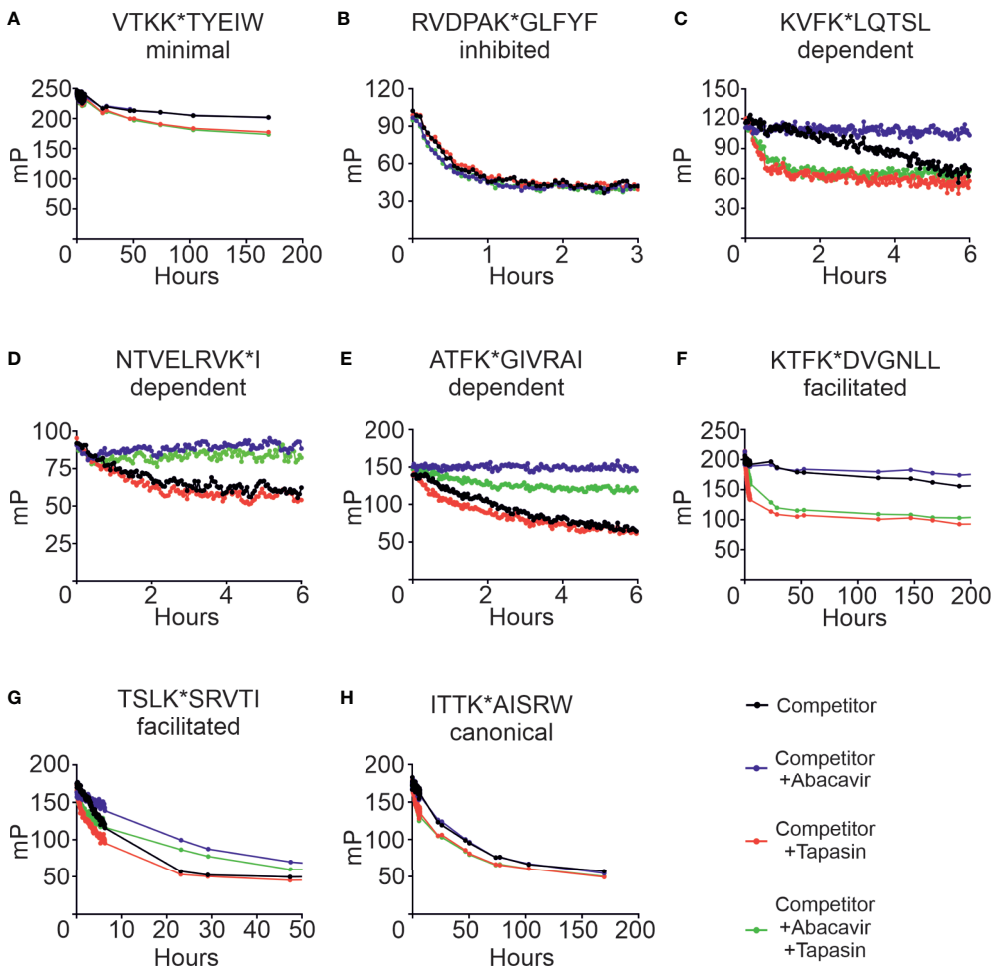

FIGURE 7 | Abacavir diversifies the HLA-B*57:01 peptide repertoire by decreasing dissociation of specific peptides. Conditional ligand loaded HLA-B*57:01fos molecules were UV exposed and incubated with the indicated fluorescent peptide (**A** = VTKK*TYEIW, **B** = RVDPAK*GLFYF, **C** = KVFK*LQTSL, **D** = NTVELRVK*I, **E** = ATFK*GIVRAI, **F** = KTFK*DVGNLL, **G** = TSLK*SRVTI, **H** = ITTK*AISRW). Fluorescence polarisation measurements were taken after the addition of excess unlabelled competing peptide in the absence or presence of abacavir and/or conjugated tapasin-jun-ERp57 C60A proteins. Data shown are representative of triplicate or greater experiments.

B*57:01fos molecules was modestly enhanced by the addition of abacavir and competing peptide (**Figure 7B**), providing insight into why this peptide is depleted from the immunopeptidome following exposure to abacavir. In summary, the combined addition of competing peptide, abacavir and tapasin (green lines) affected the dissociation of the assayed peptides in different ways, which is likely to reflect the variation in the enhancement of peptide dissociation that tapasin mediates (*e.g.* significant for the KVF and KTF peptides, but minimal for the NTV peptide) combined with the variation in the stabilisation that the drug affords to specific HLA-B*57:01–abacavir–peptide complexes.

DISCUSSION

We and others have shown that abacavir exclusively binds within the HLA-B*57:01 antigen binding groove, altering the preference for the C-terminal amino acid residue of the bound peptide, and changing the immunopeptidome in a process dependent on tapasin and the conventional MHC I antigen presentation pathway (23–26). Whilst this perturbation accounts for many of the T cell responses observed against drug treated HLA-B*57:01^{+} cells, the kinetics of abacavir mediated perturbation of the immunopeptidome, and the specific peptide editing function of tapasin has remained largely unexplored. In this study, we found that HLA-B*57:01 expressing cells rapidly acquired the ability to elicit drug-specific responses from drug-responsive T cell lines following the addition of abacavir, and that the magnitude of these responses increased over several hours (**Figure 3**). Importantly the kinetics at which immunogenicity was acquired generally coincided with the rate that newly synthesised thermostable HLA-B*57:01 molecules progress through the secretory pathway (**Figure 4**) and match the rate at which abacavir and abacavir-induced peptides accumulated within the population of HLA-

B*57:01–peptide complexes (**Figure 1**). In addition, abacavir-dependent peptides derive from source proteins occupying similar cellular compartments to those of the constitutive repertoire (**Supplementary Table 1**), consistent with a shared loading pathway. This suggests that immune responses are primarily elicited following the appearance of newly synthesised HLA-B*57:01 complexes at the cell surface, that have selected peptides in the ER and transited the secretory pathway in the presence of abacavir, as opposed to abacavir modifying cell surface HLA-B*57:01–peptide complexes (see model **Figure 8**).

However, the fact that abacavir decreased the dissociation of some "constitutive" relatively stable peptide-loaded B*57:01 complexes (such as KTF and TSL, **Figures 7F, G**) highlights the potential for certain cell surface HLA-B*57:01–peptide complexes to

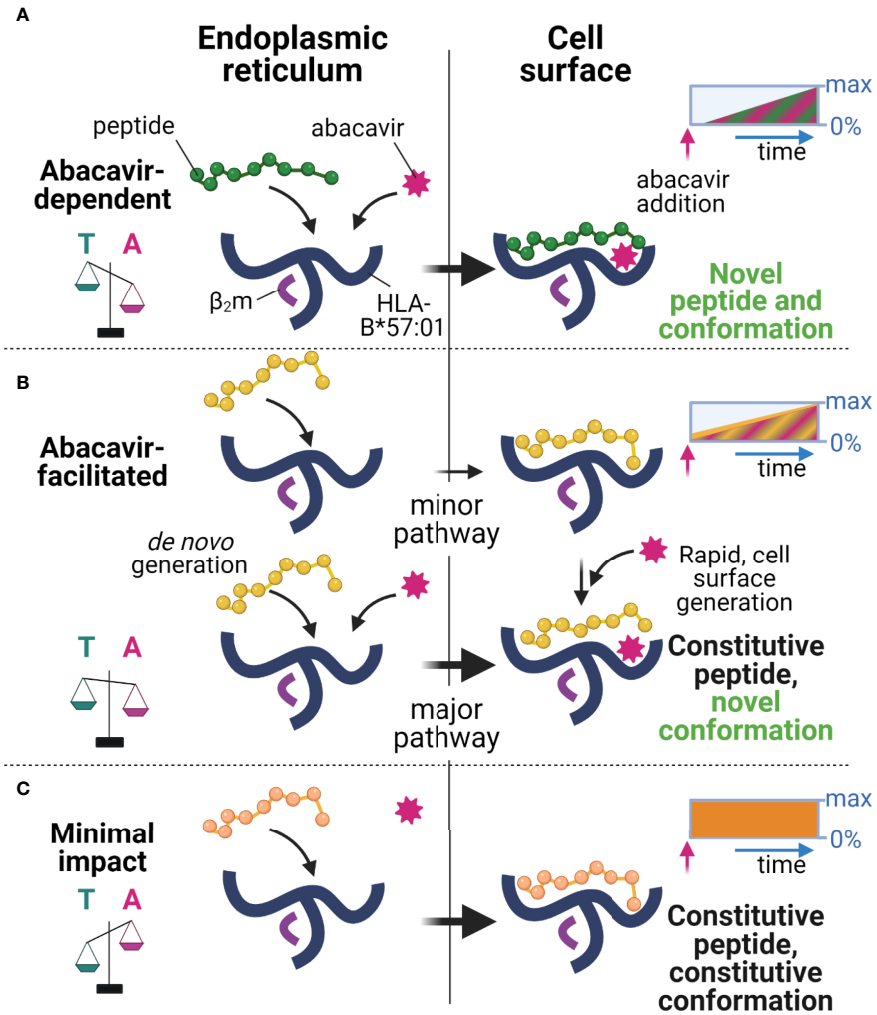

FIGURE 8 | Proposed model of peptide-loading of HLA-B*57:01 in the presence of abacavir. **(A)** When abacavir is present, abacavir-dependent peptides are loaded into HLA-B*57:01 within the endoplasmic reticulum (left). For the abacavir-dependent peptides in our panel, loading was highly dependent on abacavir as compared to tapasin, represented by the scales tipping towards abacavir (magenta, A), as opposed to tapasin (teal, T). After a slight delay consistent with *de novo* complex generation in the ER and progression through the secretory pathway, this generates conformationally novel HLA–abacavir–peptide complexes at the cell surface (right, novel self-peptide and novel conformation). The inset box represents the increasing appearance of cell surface complexes (0%–max) incorporating abacavir-dependent peptides (green) and abacavir (magenta hatching) over time (blue arrow) after abacavir addition (pink arrow), until a maximum is reached (not to scale). **(B)** Abacavir-facilitated peptides are part of the constitutive immunopeptidome (upper panel). For the abacavir-facilitated peptides in our panel, tapasin aids loading in the endoplasmic reticulum in the absence of abacavir, and peptide-loaded HLA traffic to the cell surface. On addition of abacavir, abacavir can load into these HLA-peptide complexes at the cell surface generating novel conformations/stabilising the structure (constitutive peptide, novel conformation), contributing immediately to cellular immunogenicity. In addition, *de novo* generation of HLA-abacavir-peptide complexes occurs within the endoplasmic reticulum, with both abacavir and tapasin promoting peptide binding (lower panel). As such abacavir-facilitated peptides are present in the immunopeptidome prior to abacavir addition (inset box, yellow), with immediate loading of abacavir at the cell surface as well as during *de novo* complex generation, contributing an increasing number of abacavir occupied HLA from the time of abacavir addition (inset box, magenta hatching). **(C)** These changes occur against a background of constitutive peptides which maintain a similar contribution to the immunopeptidome regardless of the presence of abacavir (minimal impact, inset box, orange), whilst a proportion of constitutive peptides are reduced in presentation (inhibited, **Figure 1**, not shown here). This figure was created with BioRender.com.

be abacavir receptive (see model **Figure 8**), as hypothesised by Yun et al. for HLA-B*58:01 and oxypurinol (59). This provides a possible mechanism for the formation of immunogenic cell surface abacavir-loaded HLA–peptide complexes, available to stimulate reported "immediate" responding abacavir-responsive T cell clones (37). The relative abundance of these complexes might be expected to rise in the presence of abacavir as a result of a reduction in their turnover at the cell surface (KTF and TSL increased in abundance in the immunopeptidome with abacavir treatment, **Figure 1C**), in addition to increased loading in the ER. We conceive two potential modes by which such "constitutive" HLA–peptide complexes might elicit T cell responses: 1) incorporation of abacavir within the antigen binding cleft results in a structurally novel immunogenic HLA–abacavir–peptide complex, potentially leading to an immediate immune response, or 2) incorporation of abacavir within the antigen binding cleft decreases the dissociation rate of specific peptide complexes, resulting in their increased accumulation within the immunopeptidome, eventually breaching a quantitative threshold required to trigger self-reactive T cells that would otherwise "ignore" the low level of cognate ligand. Notably, the impact of abacavir on peptide presentation and immunogenicity appears analogous to that of micropolymorphism. The location of abacavir within the antigen binding cleft mirrors that of buried polymorphic residues between HLA-B*57:01, HLA-B*57:03, and HLA-B*58:01, which not only change the range and quantitative contribution of peptides within the immunopeptidome, but influence peptide presentation through altered bound-peptide conformation upon binding of identical peptides (55). These parallels between abacavir induced changes in peptide presentation and allo-HLA presentation align with previous investigations defining the overlap in functional responses to abacavir and alloreactivity towards HLA-B*58:01 (60). Overall, the peptide specific modulation of the HLA-B57 immunopeptidome by abacavir reconciles the biophysical studies of abacavir induced altered self with functional studies demonstrating a spectrum of kinetics and dose dependence for activation of abacavir-reactive T cell clones (37).

Through our multifaceted analysis, we observed heterogeneity in the sequence and nature of abacavir modulated peptides such that no simple predictive rule could be applied to estimate the ability of abacavir to induce or modulate levels of presentation of given peptide ligands. For example, abacavir enhanced the binding of two canonical peptide ligands to HLA-B*57:01 molecules (VTKKTYEIW and ITTKAISRW), despite these peptides having C-terminal amino acid residues considered ill-suited for abacavir binding (**Figures 5**, **6**). Our analysis of the assembly of HLA-B*57:01 molecules shows that abacavir does not significantly change the maturation kinetics, dependence on tapasin, or thermal-stability profile of HLA-B*57:01–peptide complexes at a population level (**Figure 4**). This suggests abacavir does not change the intrinsic conformational plasticity of the HLA-B*57:01 protein, which has been hypothesised to determine the ability of MHC I molecules to select a high affinity peptide cargo (34, 61, 62). In this model, peptides are suggested to bind to an unstable, open, intermediate state that is also a substrate for tapasin. Abacavir may also bind preferentially to this open, intermediate state of HLA-B*57:01 molecules, remodelling the peptide-receptive F-pocket whilst the remainder of the peptide binding groove is either empty or partially occupied by interactions with the N-terminus of the peptide ligand (63).

Overall, our *in vitro* analysis has illustrated that abacavir-induced peptides likely accrue within the immunopeptidome as a result of their improved binding kinetics in the presence of abacavir, which can be further enhanced by tapasin. In conjunction with our quantitative analysis of the contribution of specific peptides to the immunopeptidome, these data suggest that abacavir diversifies the HLA-B*57:01 immunopeptidome by enabling the stable binding of peptides with aliphatic C-terminal anchors that are either low abundance or absent in the constitutive immunopeptidome. These abacavir-induced peptides potentially bind at the expense of rapidly dissociating peptides, such as RVD, whilst peptides that bind with longer half-lives are less effected. Furthermore, a low level of tapasin independent loading of HLA-B*57:01 molecules was observed, which may allow some abacavir-induced (and constitutive) peptides to enter the immunopeptidome in cellular compartments beyond the ER. Such effects could further explain some of the heterogeneity reported for the kinetics of activation of drug specific T cells (37, 64). Although beyond the scope of the current study, dissection of the contribution of peptides exhibiting different loading characteristics to the immune response, using *in vitro* expanded T cells or through the use of HLA-B*57:01 transgenic mouse models of abacavir hypersensitivity (65), is critical to pinpoint their contribution to drug hypersensitivity.

Overall, our data highlight that the majority of the immunopeptidome perturbation occurs during *de novo* loading of complexes. Collectively, these findings highlight the importance of the ER environment in generation of the immunopeptidome, demonstrating the potential for not only chaperones, but small molecule ligands, to differentially impact the binding and dissociation of distinct peptides to and from assembling MHC I molecules, raising the possibility that alterations in the cellular metabolome may also alter peptide presentation.

DATA AVAILABILITY STATEMENT

The datasets presented in this study can be found in online repositories. The names of the repository/repositories and accession number(s) can be found below: ProteomeXchange Consortium via the PRIDE (44) partner repository, https://www.ebi.ac.uk/pride/archive/, PXD024331.

ETHICS STATEMENT

The studies involving human participants were reviewed and approved by Monash University (HREC 4717 & 2297) and the Australian Bone Marrow Donor Registry (2013/04). The patients/participants provided their written informed consent to participate in this study.

AUTHOR CONTRIBUTIONS

PI, AvH, TE, and AP designed the experiments. PI, AvH, RD, NC, NM, and SK performed the experiments. LK, MB, and JM provided the reagents. PI, AvH, RD, NC, NM, SK, TE, and AP analyzed the data. PI, AvH, TE, and AP wrote the manuscript. All authors contributed to the article and approved the submitted version.

FUNDING

This work was funded by the National Health and Medical Research Council Australia (NHMRC) Project grants 1122099 and 1165490 (awarded to AP) and by a Cancer Research UK programme grant C7056A and BBSRC project grant BB/L010402/1 (both awarded to TE). PI was supported by a NHMRC Early Career Fellowship (1072159) and a Monash University Faculty of Medicine, Nursing and Health Sciences Senior Postdoctoral Fellowship. AP acknowledges salary support from a NHMRC Principal Research Fellowship (1137739).

ACKNOWLEDGMENTS

The authors acknowledge the provision of instrumentation, training and technical support by the Monash University Technology Research platforms; the Monash Biomedical Proteomics Facility and FlowCore. Computational resources were supported by the R@CMon/Monash Node of the NeCTAR Research Cloud, an initiative of the Australian Government's Super Science Scheme and the Education Investment Fund. The authors thank Patrick Duriez and Leon Douglas of the Cancer Research UK Protein Production facility, as well as Nasia Kontouli, Hadil Said, Joe Morilla and Hana Ellingham for their help and technical expertise.

SUPPLEMENTARY MATERIAL

The Supplementary Material for this article can be found online at: https://www.frontiersin.org/articles/10.3389/fimmu.2021.672737/full#supplementary-material

REFERENCES

1. Yewdell JW, Anton LC, Bennink JR. Defective Ribosomal Products (DriPs): A Major Source of Antigenic Peptides for MHC Class I Molecules? *J Immunol* (1996) 157(5):1823–6.
2. Zernich D, Purcell AW, Macdonald WA, Kjer-Nielsen L, Ely LK, Laham N, et al. Natural HLA Class I Polymorphism Controls the Pathway of Antigen Presentation and Susceptibility to Viral Evasion. *J Exp Med* (2004) 200(1):13–24. doi: 10.1084/jem.20031680
3. Williams AP, Peh CA, Purcell AW, McCluskey J, Elliott T. Optimization of the MHC Class I Peptide Cargo is Dependent on Tapasin. *Immunity* (2002) 16(4):509–20. doi: 10.1016/S1074-7613(02)00304-7
4. Turnquist HR, Thomas HJ, Prilliman KR, Lutz CT, Hildebrand WH, Solheim JC. HLA-B Polymorphism Affects Interactions With Multiple Endoplasmic Reticulum Proteins. *Eur J Immunol* (2000) 30(10):3021–8. doi: 10.1002/1521-4141(200010)30:10<3021::AID-IMMU3021>3.0.CO;2-U
5. Fang Q, Liu Z, Zhang T. Human Leukocyte Antigen Polymorphisms and Kaposi's Sarcoma-Associated Herpesvirus Infection Outcomes: A Call for Deeper Exploration. *J Med Virol* (2019) 91(4):541–8. doi: 10.1002/jmv.25342
6. Akcay IM, Katrinli S, Ozdil K, Doganay GD, Doganay L. Host Genetic Factors Affecting Hepatitis B Infection Outcomes: Insights From Genome-Wide Association Studies. *World J Gastroenterol* (2018) 24(30):3347–60. doi: 10.3748/wjg.v24.i30.3347
7. Bellamy R, Hill AV. Genetic Susceptibility to Mycobacteria and Other Infectious Pathogens in Humans. *Curr Opin Immunol* (1998) 10(4):483–7. doi: 10.1016/S0952-7915(98)80125-8
8. Lima-Junior Jda C, Pratt-Riccio LR. Major Histocompatibility Complex and Malaria: Focus on Plasmodium Vivax Infection. *Front Immunol* (2016) 7:13. doi: 10.3389/fimmu.2016.00013
9. McLaren PJ, Carrington M. The Impact of Host Genetic Variation on Infection With HIV-1. *Nat Immunol* (2015) 16(6):577–83. doi: 10.1038/ni.3147
10. Tough RH, McLaren PJ. Interaction of the Host and Viral Genome and Their Influence on HIV Disease. *Front Genet* (2018) 9:720. doi: 10.3389/fgene.2018.00720
11. Nyaga DM, Vickers MH, Jefferies C, Perry JK, O'Sullivan JM. The Genetic Architecture of Type 1 Diabetes Mellitus. *Mol Cell Endocrinol* (2018) 477:70–80. doi: 10.1016/j.mce.2018.06.002
12. Siegel RJ, Bridges SLJr, Ahmed S. HLA-C: An Accomplice in Rheumatic Diseases. *ACR Open Rheumatol* (2019) 1(9):571–9. doi: 10.1002/acr2.11065
13. Simone D, Al Mossawi MH, Bowness P. Progress in Our Understanding of the Pathogenesis of Ankylosing Spondylitis. *Rheumatology* (2018) 57(suppl_6): vi4–9. doi: 10.1093/rheumatology/key001
14. Sidney J, Vela JL, Friedrich D, Kolla R, von Herrath M, Wesley JD, et al. Low HLA Binding of Diabetes-Associated CD8+ T-Cell Epitopes is Increased by Post Translational Modifications. *BMC Immunol* (2018) 19(1):12. doi: 10.1186/s12865-018-0250-3
15. McGinty JW, Marre ML, Bajzik V, Piganelli JD, James EA. T Cell Epitopes and Post-Translationally Modified Epitopes in Type 1 Diabetes. *Curr Diabetes Rep* (2015) 15(11):90. doi: 10.1007/s11892-015-0657-7
16. Skowera A, Ellis RJ, Varela-Calvino R, Arif S, Huang GC, Van-Krinks C, et al. CTLs are Targeted to Kill Beta Cells in Patients With Type 1 Diabetes Through Recognition of a Glucose-Regulated Preproinsulin Epitope. *J Clin Invest* (2008) 118(10):3390–402. doi: 10.1172/JCI35449
17. Prinz JC. Human Leukocyte Antigen-Class I Alleles and the Autoreactive T Cell Response in Psoriasis Pathogenesis. *Front Immunol* (2018) 9:954. doi: 10.3389/fimmu.2018.00954
18. Giza M, Koftori D, Chen L, Bowness P. Is Behcet's Disease a 'Class 1-Opathy'? The Role of HLA-B*51 in the Pathogenesis of Behcet's Disease. *Clin Exp Immunol* (2018) 191(1):11–8. doi: 10.1111/cei.13049
19. Illing PT, Vivian JP, Purcell AW, Rossjohn J, McCluskey J. Human Leukocyte Antigen-Associated Drug Hypersensitivity. *Curr Opin Immunol* (2013) 25 (1):81–9. doi: 10.1016/j.coi.2012.10.002
20. Martin AM, Nolan D, Gaudieri S, Almeida CA, Nolan R, James I, et al. Predisposition to Abacavir Hypersensitivity Conferred by HLA-B*5701 and a Haplotypic Hsp70-Hom Variant. *Proc Natl Acad Sci U S A* (2004) 101 (12):4180–5. doi: 10.1073/pnas.0307067101
21. Chung WH, Hung SI, Hong HS, Hsih MS, Yang LC, Ho HC, et al. Medical Genetics: A Marker for Stevens-Johnson Syndrome. *Nature* (2004) 428 (6982):486. doi: 10.1038/428486a
22. Hung SI, Chung WH, Liou LB, Chu CC, Lin M, Huang HP, et al. HLA-B*5801 Allele as a Genetic Marker for Severe Cutaneous Adverse Reactions Caused by Allopurinol. *Proc Natl Acad Sci U S A* (2005) 102(11):4134–9. doi: 10.1073/pnas.0409500102
23. Ostrov DA, Grant BJ, Pompeu YA, Sidney J, Harndahl M, Southwood S, et al. Drug Hypersensitivity Caused by Alteration of the MHC-presented Self-Peptide Repertoire. *Proc Natl Acad Sci U S A* (2012) 109(25):9959–64. doi: 10.1073/pnas.1207934109
24. Norcross MA, Luo S, Lu L, Boyne MT, Gomarteli M, Rennels AD, et al. Abacavir Induces Loading of Novel Self-Peptides Into HLA-B*57: 01: An Autoimmune Model for HLA-associated Drug Hypersensitivity. *Aids* (2012) 26(11):F21–9. doi: 10.1097/QAD.0b013e328355fe8f
25. Illing PT, Vivian JP, Dudek NL, Kostenko L, Chen Z, Bharadwaj M, et al. Immune Self-Reactivity Triggered by Drug-Modified HLA-peptide Repertoire. *Nature* (2012) 486(7404):554–8. doi: 10.1038/nature11147

26. Chessman D, Kostenko L, Lethborg T, Purcell AW, Williamson NA, Chen Z, et al. Human Leukocyte Antigen Class I-restricted Activation of CD8+ T Cells Provides the Immunogenetic Basis of a Systemic Drug Hypersensitivity. *Immunity* (2008) 28(6):822–32. doi: 10.1016/j.immuni.2008.04.020
27. Greenwood R, Shimizu Y, Sekhon GS, DeMars R. Novel Allele-Specific, Post-Translational Reduction in HLA Class I Surface Expression in a Mutant Human B Cell Line. *J Immunol* (1994) 153(12):5525–36.
28. Rizvi SM, Salam N, Geng J, Qi Y, Bream JH, Duggal P, et al. Distinct Assembly Profiles of HLA-B Molecules. *J Immunol* (2014) 192(11):4967–76. doi: 10.4049/jimmunol.1301670
29. Lewis JW, Elliott T. Evidence for Successive Peptide Binding and Quality Control Stages During MHC Class I Assembly. *Curr Biol* (1998) 8(12):717–20. doi: 10.1016/S0960-9822(98)70280-5
30. Garstka MA, Fish A, Celie PH, Joosten RP, Janssen GM, Berlin I, et al. The First Step of Peptide Selection in Antigen Presentation by MHC Class I Molecules. *Proc Natl Acad Sci U S A* (2015) 112(5):1505–10. doi: 10.1073/pnas.1416543112
31. Chen M, Bouvier M. Analysis of Interactions in a Tapasin/Class I Complex Provides a Mechanism for Peptide Selection. *EMBO J* (2007) 26(6):1681–90. doi: 10.1038/sj.emboj.7601624
32. Fleischmann G, Fisette O, Thomas C, Wieneke R, Tumulka F, Schneeweiss C, et al. Mechanistic Basis for Epitope Proofreading in the Peptide-Loading Complex. *J Immunol* (2015) 195(9):4503–13. doi: 10.4049/jimmunol.1501515
33. Fisette O, Wingbermuhle S, Tampe R, Schafer LV. Molecular Mechanism of Peptide Editing in the Tapasin-MHC I Complex. *Sci Rep* (2016) 6:19085. doi: 10.1038/srep19085
34. Bailey A, Dalchau N, Carter R, Emmott S, Phillips A, Werner JM, et al. Selector Function of MHC I Molecules is Determined by Protein Plasticity. *Sci Rep* (2015) 5:14928. doi: 10.1038/srep14928
35. Howarth M, Williams A, Tolstrup AB, Elliott T. Tapasin Enhances MHC Class I Peptide Presentation According to Peptide Half-Life. *Proc Natl Acad Sci U S A* (2004) 101(32):11737–42. doi: 10.1073/pnas.0306294101
36. Wearsch PA, Cresswell P. Selective Loading of High-Affinity Peptides Onto Major Histocompatibility Complex Class I Molecules by the tapasin-ERp57 Heterodimer. *Nat Immunol* (2007) 8(8):873–81. doi: 10.1038/ni1485
37. Adam J, Eriksson KK, Schnyder B, Fontana S, Pichler WJ, Yerly D. Avidity Determines T-cell Reactivity in Abacavir Hypersensitivity. *Eur J Immunol* (2012) 42(7):1706–16. doi: 10.1002/eji.201142159
38. Storkus WJ, Howell DN, Salter RD, Dawson JR, Cresswell P. NK Susceptibility Varies Inversely With Target Cell Class I HLA Antigen Expression. *J Immunol* (1987) 138(6):1657–9.
39. Zemmour J, Little AM, Schendel DJ, Parham P. The HLA-A,B "Negative" Mutant Cell Line C1R Expresses a Novel HLA-B35 Allele, Which Also has a Point Mutation in the Translation Initiation Codon. *J Immunol* (1992) 148(6):1941–8.
40. Kostenko L, Kjer-Nielsen L, Nicholson I, Hudson F, Lucas A, Foley B, et al. Rapid Screening for the Detection of HLA-B57 and HLA-B58 in Prevention of Drug Hypersensitivity. *Tissue Antigens* (2011) 78(1):11–20. doi: 10.1111/j.1399-0039.2011.01649.x
41. Purcell AW, Ramarathinam SH, Ternette N. Mass Spectrometry-Based Identification of MHC-bound Peptides for Immunopeptidomics. *Nat Protoc* (2019) 14(6):1687–707. doi: 10.1038/s41596-019-0133-y
42. Dudek NL, Tan CT, Gorasia DG, Croft NP, Illing PT, Purcell AW. Constitutive and Inflammatory Immunopeptidome of Pancreatic Beta-Cells. *Diabetes* (2012) 61(11):3018–25. doi: 10.2337/db11-1333
43. MacLean B, Tomazela DM, Shulman N, Chambers M, Finney GL, Frewen B, et al. Skyline: An Open Source Document Editor for Creating and Analyzing Targeted Proteomics Experiments. *Bioinformatics* (2010) 26(7):966–8. doi: 10.1093/bioinformatics/btq054
44. Perez-Riverol Y, Csordas A, Bai J, Bernal-Llinares M, Hewapathirana S, Kundu DJ, et al. The PRIDE Database and Related Tools and Resources in 2019: Improving Support for Quantification Data. *Nucleic Acids Res* (2019) 47 (D1):D442–d50. doi: 10.1093/nar/gky1106
45. Cox J, Hein MY, Luber CA, Paron I, Nagaraj N, Mann M. Accurate Proteome-Wide Label-Free Quantification by Delayed Normalization and Maximal Peptide Ratio Extraction, Termed MaxLFQ. *Mol Cell Proteomics* (2014) 13 (9):2513–26. doi: 10.1074/mcp.M113.031591
46. Tyanova S, Temu T, Sinitcyn P, Carlson A, Hein MY, Geiger T, et al. The Perseus Computational Platform for Comprehensive Analysis of (Prote) Omics Data. *Nat Methods* (2016) 13:731. doi: 10.1038/nmeth.3901
47. Hermann C, van Hateren A, Trautwein N, Neerincx A, Duriez PJ, Stevanovic S, et al. TAPBPR Alters MHC Class I Peptide Presentation by Functioning as a Peptide Exchange Catalyst. *eLife* (2015) 4:e09617. doi: 10.7554/eLife.09617
48. Jeong JY, Yim HS, Ryu JY, Lee HS, Lee JH, Seen DS, et al. One-Step Sequence- and Ligation-Independent Cloning as a Rapid and Versatile Cloning Method for Functional Genomics Studies. *Appl Environ Microbiol* (2012) 78(15):5440–3. doi: 10.1128/AEM.00844-12
49. Peaper DR, Wearsch PA, Cresswell P. Tapasin and ERp57 Form a Stable Disulfide-Linked Dimer Within the MHC Class I Peptide-Loading Complex. *EMBO J* (2005) 24(20):3613–23. doi: 10.1038/sj.emboj.7600814
50. Garboczi DN, Hung DT, Wiley DC. HLA-A2-peptide Complexes: Refolding and Crystallization of Molecules Expressed in Escherichia Coli and Complexed With Single Antigenic Peptides. *Proc Natl Acad Sci U S A* (1992) 89(8):3429–33. doi: 10.1073/pnas.89.8.3429
51. Tan CT, Croft NP, Dudek NL, Williamson NA, Purcell AW. Direct Quantitation of MHC-bound Peptide Epitopes by Selected Reaction Monitoring. *Proteomics* (2011) 11(11):2336–40. doi: 10.1002/pmic.201000531
52. Wu T, Guan J, Handel A, Tscharke DC, Sidney J, Sette A, et al. Quantification of Epitope Abundance Reveals the Effect of Direct and Cross-Presentation on Influenza CTL Responses. *Nat Commun* (2019) 10(1):2846. doi: 10.1038/s41467-019-10661-8
53. Croft NP, Smith SA, Pickering J, Sidney J, Peters B, Faridi P, et al. Most Viral Peptides Displayed by Class I MHC on Infected Cells are Immunogenic. *Proc Natl Acad Sci U S A* (2019) 116(8):3112–7. doi: 10.1073/pnas.1815239116
54. Schittenhelm RB, Dudek NL, Croft NP, Ramarathinam SH, Purcell AW. A Comprehensive Analysis of Constitutive Naturally Processed and Presented HLA-C*04:01 (Cw4)-specific Peptides. *Tissue Antigens* (2014) 83(3):174–9. doi: 10.1111/tan.12282
55. Illing PT, Pymm P, Croft NP, Hilton HG, Jojic V, Han AS, et al. HLA-B57 Micropolymorphism Defines the Sequence and Conformational Breadth of the Immunopeptidome. *Nat Commun* (2018) 9(1):4693. doi: 10.1038/s41467-018-07109-w
56. Andreatta M, Nielsen M. Gapped Sequence Alignment Using Artificial Neural Networks: Application to the MHC Class I System. *Bioinformatics* (2016) 32 (4):511–7. doi: 10.1093/bioinformatics/btv639
57. Nielsen M, Lundegaard C, Worning P, Lauemoller SL, Lamberth K, Buus S, et al. Reliable Prediction of T-cell Epitopes Using Neural Networks With Novel Sequence Representations. *Protein Sci* (2003) 12(5):1007–17. doi: 10.1110/ps.0239403
58. Park B, Lee S, Kim E, Ahn K. A Single Polymorphic Residue Within the Peptide-Binding Cleft of MHC Class I Molecules Determines Spectrum of Tapasin Dependence. *J Immunol* (2003) 170:961–8. doi: 10.4049/jimmunol.170.2.961
59. Yun J, Marcaida MJ, Eriksson KK, Jamin H, Fontana S, Pichler WJ, et al. Oxypurinol Directly and Immediately Activates the Drug-Specific T Cells Via the Preferential Use of HLA-B*58:01. *J Immunol* (2014) 197(7):2984–93. doi: 10.4049/jimmunol.1302306
60. Adam J, Wuillemin N, Watkins S, Jamin H, Eriksson KK, Villiger P, et al. Abacavir Induced T Cell Reactivity From Drug Naïve Individuals Shares Features of Allo-Immune Responses. *PLoS One* (2014) 9(4):e95339. doi: 10.1371/journal.pone.0095339
61. van Hateren A, Bailey A, Elliott T. Recent Advances in Major Histocompatibility Complex (MHC) Class I Antigen Presentation: Plastic MHC Molecules and TAPBPR-mediated Quality Control. *F1000Research* (2017) 6(158). doi: 10.12688/f1000research.10474.1
62. van Hateren A, Anderson M, Bailey A, Werner JM, Skipp P, Elliott T. Direct Evidence for Conformational Dynamics in Major Histocompatibility Complex Class I Molecules. *J Biol Chem* (2017) 292(49):20255–69. doi: 10.1074/jbc.M117.809624
63. McShan AC, Natarajan K, Kumirov VK, Flores-Solis D, Jiang J, Badstübner M, et al. Peptide Exchange on MHC-I by TAPBPR is Driven by a Negative Allostery Release Cycle. *Nat Chem Biol* (2018) 14(8):811–20. doi: 10.1038/s41589-018-0096-2
64. Pichler WJ, Adam J, Watkins S, Wuillemin N, Yun J, Yerly D. Drug Hypersensitivity: How Drugs Stimulate T Cells Via Pharmacological Interaction With Immune Receptors. *Int Arch Allergy Immunol* (2015) 168 (1):13–24. doi: 10.1159/000441280
65. Cardone M, Garcia K, Tilahun ME, Boyd LF, Gebreyohannes S, Yano M, et al. A Transgenic Mouse Model for HLA-B*57:01-linked Abacavir Drug Tolerance and Reactivity. *J Clin Invest* (2018) 128(7):2819–32. doi: 10.1172/JCI99321

Conflict of Interest: The authors declare that the research was conducted in the absence of any commercial or financial relationships that could be construed as a potential conflict of interest.

frontiers in Genetics

METHODS
published: 17 June 2021
doi: 10.3389/fgene.2021.642012

Visual Genomics Analysis Studio as a Tool to Analyze Multiomic Data

Rebecca J. Hertzman[1†], Pooja Deshpande[1†], Shay Leary[1†], Yueran Li[1], Ramesh Ram[1], Abha Chopra[1,2], Don Cooper[1], Mark Watson[1], Amy M. Palubinsky[2], Simon Mallal[1,2], Andrew Gibson[1] and Elizabeth J. Phillips[1,2]*

[1] Institute for Immunology and Infectious Diseases, Murdoch University, Murdoch, WA, Australia, [2] Department of Medicine, Vanderbilt University Medical Centre, Nashville, TN, United States

Type B adverse drug reactions (ADRs) are iatrogenic immune-mediated syndromes with mechanistic etiologies that remain incompletely understood. Some of the most severe ADRs, including delayed drug hypersensitivity reactions, are T-cell mediated, restricted by specific human leukocyte antigen risk alleles and sometimes by public or oligoclonal T-cell receptors (TCRs), central to the immunopathogenesis of tissue-damaging response. However, the specific cellular signatures of effector, regulatory, and accessory immune populations that mediate disease, define reaction phenotype, and determine severity have not been defined. Recent development of single-cell platforms bringing together advances in genomics and immunology provides the tools to simultaneously examine the full transcriptome, TCRs, and surface protein markers of highly heterogeneous immune cell populations at the site of the pathological response at a single-cell level. However, the requirement for advanced bioinformatics expertise and computational hardware and software has often limited the ability of investigators with the understanding of diseases and biological models to exploit these new approaches. Here we describe the features and use of a state-of-the-art, fully integrated application for analysis and visualization of multiomic single-cell data called Visual Genomics Analysis Studio (VGAS). This unique user-friendly, Windows-based graphical user interface is specifically designed to enable investigators to interrogate their own data. While VGAS also includes tools for sequence alignment and identification of associations with host or organism genetic polymorphisms, in this review we focus on its application for analysis of single-cell TCR–RNA–Cellular Indexing of Transcriptomes and Epitopes by Sequencing (CITE)-seq, enabling holistic cellular characterization by unbiased transcriptome and select surface proteome. Critically, VGAS does not require user-directed coding or access to high-performance computers, instead incorporating performance-optimized hidden code to provide application-based fast and intuitive tools for data analyses and production of high-resolution publication-ready graphics on standard specification laptops. Specifically, it allows analyses of comprehensive single-cell TCR sequencing (scTCR-seq) data, detailing (i) functional pairings of α–β heterodimer TCRs, (ii) one-click histograms to display entropy and gene rearrangements, and (iii) Circos and Sankey plots to visualize clonality and dominance. For unbiased single-cell RNA sequencing (scRNA-seq) analyses, users extract cell

OPEN ACCESS

Edited by:
Nicole Andrea Mifsud, Monash University, Australia

Reviewed by:
Nick Wong, Monash University, Australia
Martin Hemberg, Wellcome Sanger Institute (WT), United Kingdom

***Correspondence:**
Andrew Gibson
a.gibson@iiid.murdoch.edu.au

† These authors have contributed equally to this work

Specialty section:
This article was submitted to Pharmacogenetics and Pharmacogenomics, a section of the journal Frontiers in Genetics

Received: *15 December 2020*
Accepted: *20 May 2021*
Published: *17 June 2021*

Citation:
Hertzman RJ, Deshpande P, Leary S, Li Y, Ram R, Chopra A, Cooper D, Watson M, Palubinsky AM, Mallal S, Gibson A and Phillips EJ (2021) Visual Genomics Analysis Studio as a Tool to Analyze Multiomic Data. Front. Genet. 12:642012. doi: 10.3389/fgene.2021.642012

transcriptome signatures according to global structure via principal component analysis, t-distributed stochastic neighborhood embedding, or uniform manifold approximation and projection plots, with overlay of scTCR-seq enabling identification and selection of the immunodominant TCR-expressing populations. Further integration with similar sequence-based detection of surface protein markers using oligo-labeled antibodies (CITE-seq) provides comparative understanding of surface protein expression, with differential gene or protein analyses visualized using volcano plot or heatmap functions. These data can be compared to reference cell atlases or suitable controls to reveal discrete disease-specific subsets, from epithelial to tissue-resident memory T-cells, and activation status, from senescence through exhaustion, with more finite transcript expression displayed as violin and box plots. Importantly, guided tutorial videos are available, as are regular application updates based on the latest advances in bioinformatics and user feedback.

Keywords: bioinformatics, heterogeneity, immunogenomics, single-cell TCR sequencing, single-cell RNA sequencing, single-cell CITE-seq

INTRODUCTION TO VISUAL GENOMICS ANALYSIS STUDIO: ANALYSIS AND VISUALIZATION OF MULTIDIMENSIONAL SINGLE-CELL SEQUENCING DATA

Understanding the immunogenic risk factors associated with immune-mediated disease has seen significant progress in recent decades, linked to the rapid and continued development of genomic sequence–based technologies initially at a bulk and more recently at a single-cell level. While progress spans an entire spectrum of immune disease, T-cell–mediated delayed drug hypersensitivity reactions (DHRs) stand out as some of the strongest associations with distinct human leukocyte antigen (HLA) alleles. These HLA associations are specific to reaction phenotype, drug, and patient ethnicity (Chung et al., 2004; Lonjou et al., 2006; Wu et al., 2016; Nakkam et al., 2018; Konvinse et al., 2019). However, for all associations to date, a positive predictive gap remains (Phillips, 2018), limiting the clinical impact of HLA screening for particular drugs and our understanding of reaction mechanisms, driving active research to identify those additional risk parameters imposed on HLA-restricted response. In 2019, a role for specific T-cell receptor (TCR) clonotypes among the expansive human repertoire was reported by Pan et al., who detailed expression of a single, dominant, public TCR in the reacted skin of patients with HLA-B*15:02-restricted carbamazepine Stevens–Johnson syndrome and toxic epidermal necrolysis (SJS/TEN), but which was absent from tolerant controls and healthy donors (Pan et al., 2019). Using genetic engineering to insert a synthetic construct of the dominant TCR into a murine drug-exposure model, they showed that this TCR recognized carbamazepine, functionally validating the risk TCR as a key driver of early drug-specific response in tissue. Aside from inferring critical structural restriction regarding binding of the drug and/or peptide by the HLA and TCR molecules to bridge the immunological synapse, the dominantly expanded TCR may serve as a functional biomarker to identify and characterize the specific effector populations driving disease. Cost-effective genetic screening pipelines for HLA and other polymorphic genes see continued clinical progress toward better genetic risk prediction (Rauch et al., 2006; Chen et al., 2011; Plumpton et al., 2015). However, mechanistic understanding of these reactions has been hampered by limited availability of singular platforms for fully integrated user-friendly analyses by the non-coding-proficient researcher. Techniques including flow cytometry, microscopy, *in situ* hybridization, and more recently mass cytometry have been utilized, yielding insights into the phenotype of cells participating in response, but have not simultaneously characterized the TCRs and transcriptome and surface protein markers at a single-cell level (Chattopadhyay et al., 2014). Comparatively, sequencing-based strategies have delivered unrivaled opportunity as markers are tagged with synthetic DNA barcodes, providing truly limitless sequence combinations for high-dimensional detection of RNA or protein, or indeed distinct pooled ("hashed") samples to enhance cost efficiency per run. These techniques were initially applied to bulk analyses, providing average expression across an entire sample and so potentially hiding response from individual effector populations preventing resolution from total sample expression. Thus, as with all bulk assays, opportunity to detail the true complex cellular heterogeneity of clinical samples was lost, but which is integral to complete understanding of disease as immune interactions are complex and continuously regulated by intercell interactions and secretions. Concurrent with advances in cell sorting and droplet technologies, single-cell sequencing by Smart-Seq2 and 10x platforms, respectively, now provide information for each and every cell (Nguyen et al., 2018; Svensson et al., 2018). With the support of bioinformatics-driven algorithms, the complete transcriptomic signature of each cell provides means to cluster similar cells without user-directed imposition of preconceived expression, which, when aligned to the open-access human cell atlas under continued development, enables verification of subsets identified through unsupervised clustering for user-directed signature analyses.

Already this technology is revealing a spectrum of heterogeneous clusters within previously thought homogeneous populations (Villani et al., 2017), driving immunogenic discovery across the spectrum of immune-mediated diseases. These platforms now present as fully integrated, multifocal pipelines for simultaneous assessment of (i) unbiased transcriptome (single-cell RNA sequencing; scRNA-seq), (ii) select surface proteome (single-cell Cellular Indexing of Transcriptomes and Epitopes by Sequencing; scCITE-seq), and, for T-cells, (iii) functional TCR (single-cell TCR sequencing; scTCR-seq) α–β pairings with VDJ complementarity determining region 3 (CDR3) inference of antigen restriction. Importantly, aside from discovery analyses via differential expression, investigational studies can be performed on interest markers in distinct subpopulations with exquisite specificity. Specific allelic risk variants on interacting cells can also be identified and investigated, which is important given the observation that the level of HLA expression, beyond a simple yes or no presence, impacts effector response (Thananchai et al., 2007). Critically, samples pooled using hashtags within a single analysis for overlaid visual inspection or differential expression provide opportunity to detail similarities or discrepancies between samples with unique clinical metadata such as disease phenotype or mortality. These approaches provide an opportunity to discover disease-specific cell populations and targets for development of diagnostic tools or treatments.

The advent of microfluidics devices to accurately encapsulate single cells in droplet suspension, barcoding, and contemporary sequencing now delivers high-yield single-cell data. Consequently, the needs have moved to data quality assurance, management (informatics), analysis, and visualization, specifically, how to qualify and interpret the immense amount of complex data acquired. This traditionally necessitates specialist bioinformatics support, coding expertise, and access to high-end and robust computing software and servers, imposing a significant cost of implementation to laboratories of all sizes (Lähnemann et al., 2020). While data analysis tools are typically developed at pace with advancements in sequencing technologies, they are mostly limited to command line usage of code, restricting their direct utility to research scientists and clinicians. Moreover, although other platforms exist for similar analyses, many are designed for singular and specific utilities. To navigate, we present Visual Genomics Analysis Studio (VGAS), a Windows-aligned, application-based intuitive graphical user interface with performance-optimized hidden code to drive comprehensive differential analyses, specifically designed to allow basic and clinical researchers to interrogate and dissect their own data and generate publication-ready visuals for presentation on standard specification laptops. It is designed to package existing tools in a single accessible format, otherwise beyond the reach of basic researchers lacking coding proficiencies for a variety of analysis options. Moreover, VGAS, which also incorporates tools for sequence alignment and viral integration site analyses, remains constantly updated to incorporate user-defined features and recently developed tools from this rapidly evolving field. Here, with reference to screenshots and web-accessible tutorial videos, we introduce the investigation capacity offered by single-cell analyses in the context of VGAS. Critically, while our own translation discussed within is tailored to focus on T-cell–mediated DHRs, the functions offered are broadly applicable to single-cell study of diverse samples and diseases. Here we demonstrate the utility of VGAS using a 10x Genomics test dataset (available at: https://support.10xgenomics.com/single-cell-vdj/datasets/5.0.0/sc5p_v2_hs_PBMC_10k_multi_5gex_5fb_b_t) in a VGAS-compatible matrix file (available at https://www.iiid.com.au/software/vgas).

Utility of scTCR-Seq: Diversity and Dominance Define Tissue and Antigen Restriction

Within each individual, there is enormous diversity in TCRα–β heterodimer repertoire, with an estimated 10^{13}–10^{16} unique TCR per person (Robins et al., 2009; Soto et al., 2020). In T-cell–mediated DHRs, where specific HLA alleles expressed on antigen-presenting cells are associated with immunogenic risk, distinct TCRs have recently been reported to similarly restrict response on the corresponding effector T-cells (Pan et al., 2019). Specifically, through use of scTCR-seq, capable of ascertaining α–β TCR pairs, Pan et al. identified a single, public TCRβ CDR3 "ASSLAGELF" paired with TCRα CDR3 "VFDNTDKLI" dominantly expanded in the blister fluid of multiple patients with HLA-B*15:02-restricted carbamazepine-induced SJS/TEN. Importantly, this pairing was absent from healthy and tolerant controls, and while present in peripheral blood mononuclear cells from the same allergic patients, abundance was far lower than detected in blister fluid. Such TCR specificity is similarly identified for other immunodominant T-cell responses in alternate disease settings, including infectious disease, such as inflated HLA-B*44:03-restricted CMV-specific $CD8^+$ T-cell responses to a defined immunodominant immediate-early 2 derived epitope (Attaf et al., 2018). Importantly, TCR specificity may also provide an explanation for the skin-directed targeting of cutaneous DHR by more widely distributed drugs, as the T-cell tissue-resident repertoire is not consistent throughout the body but compartmentalized into enclaves specific to tissue, in part directed by previous antigenic exposures (Kumar et al., 2018). Indeed, large populations of antigen-specific tissue-resident memory (Trm) effector T-cells reside within organs, with those in the skin and mucous membranes, typical microbial entry sites, distributed as such for rapid activation following secondary exposures. These microbially primed Trm cells are retained in the skin but remain motile within, with recently demonstrated capacity to proliferate (Behr et al., 2018). Such tissue-specific locality of viral-specific T-cell effectors with epitope-restricted TCR reactivity is the basis of the heterologous immunity model, whereby drug antigens may cross-react with viral-specific T-cells, driving the tissue-specific targeting of these reactions (Pavlos et al., 2015). To this end, even simple comparative analysis of TCR repertoire between affected and unaffected sample may be informative as divergent expression would be indicative of an active immune infiltrate, or conversely, similarity may point to activation of tissue-retained effectors. These considerations emphasize (a) the importance of collecting clinically relevant tissue samples during early response to

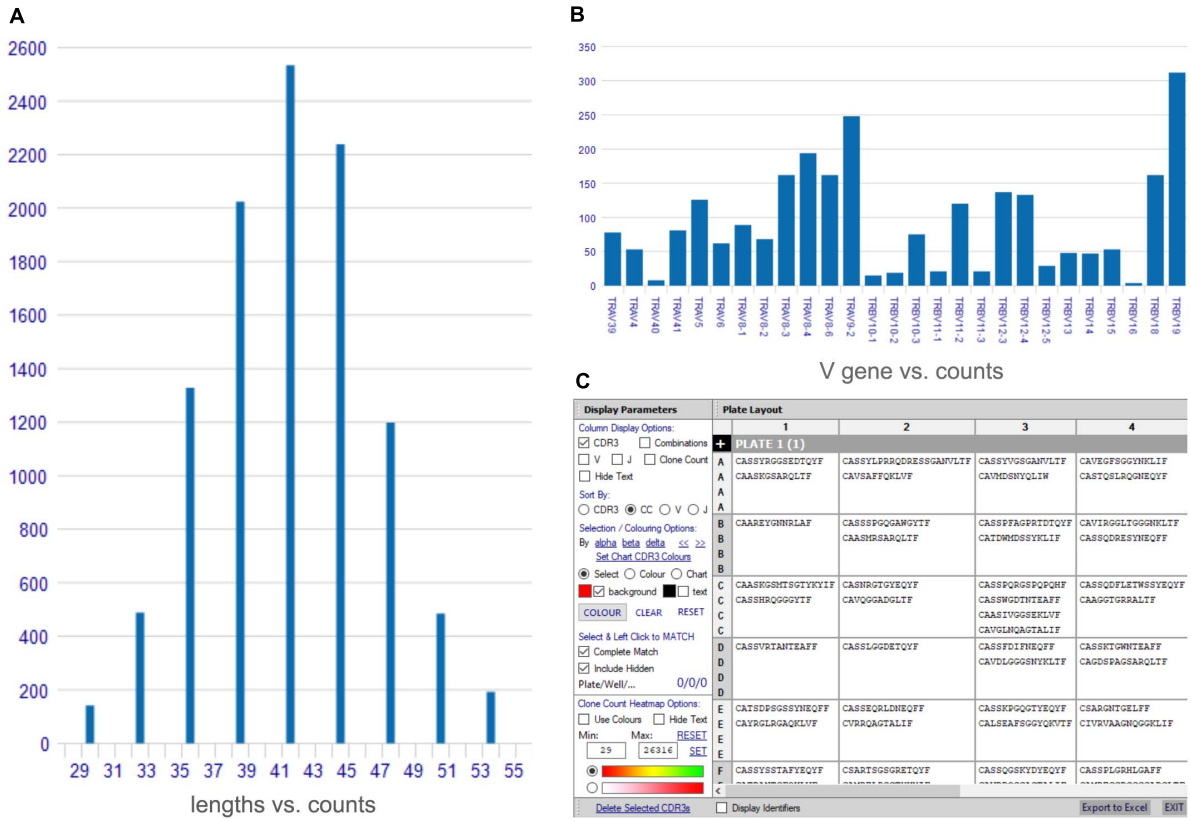

FIGURE 1 | Access tools for analysis of single-cell TCR-seq data. A variety of rapid access tools are available for analyses of single-cell TCR-seq data including **(A)** comparative CDR3 length histogram, **(B)** gene frequency histogram for individual TCR genes (TRV α and β genes shown), **(C)** plate/well layout explorer for plate-based assays listing paired CDR3 chain sequence, with options to show individual genes.

detect drug- and disease-specific dominant TCR expansion and (b) the utility of scTCR-seq to detail such dominance and provide α–β (and J chain) structure of the TCR for further functional studies. Indeed, while traditional TCR analyses have focused on expression of the β chain alone, including CDR3 spectra typing and flow cytometry–based detection kits, the influence of the corresponding TCRα variable (TRAV) chain and associated CDR3 to define antigen specificity is critical (Gras et al., 2008; Rossjohn et al., 2015). Thus, scTCR-seq provides complete human paired TCRα–β sequences enabling synthetic reconstruction for functional validation with culprit antigen and risk HLA as demonstrated by Pan et al. using an engineered murine model (Pan et al., 2019).

VGAS: scTCR Analyses and Visualization Tools

VGAS provides a platform for multidimensional analysis of scTCR-seq with tools to visualize dominance of α–β combinations and respective CDR3 sequences[1] (TCR analysis tutorials). Several one-click functions are available direct from the scTCR-seq home menu screen after file upload, including comparative graphical presentation of CDR3 lengths (see *TCR analysis tutorials: CDR3 length*) (**Figure 1A**), scatterplots to represent TCRs common to samples (see *TCR analysis tutorials: scatterplot*), and VDJ gene frequency histograms (see *TCR analysis tutorials: gene frequency*) (**Figure 1B**) in linear or logarithmic scaling with filters to exclude non-productive TCR containing stop codons or out-of-frame alignments. Further, the "CDR3/well plate explorer" function (**Figure 1C**) provides the full detailed numerical list view of TCR pair representation in each well to link with multimodal or functional data if performing plate-based assays (Smart-Seq2).

More detailed visualization of dominance and holistic α–β TCR pairings to detail clonality within and between samples is possible via the main TCR analysis screen (**Figure 2**). Users can select individual pairings of interest including α and β chains or α and β CDR3 (**Figure 2(1)**). This selection is visualized in the "paired gene frequency" domain (**Figure 2(2)**), where one chain is depicted per pie and the colored edge surrounding indicative of the number and proportion of pairings with alternate corresponding chains. An active cursor hover tool over each pie provides full details of each pairing and comparative percentage expression (**Figure 2(3)**), with full details of all pairings, inclusive of J chains and CDR3 observed in the bottom window (**Figure 2(4)**) from which BLOSUM scoring can ascertain sequence similarity for inference of similar restriction

[1]https://www.iiid.com.au/software/vgas/tcranalysis/

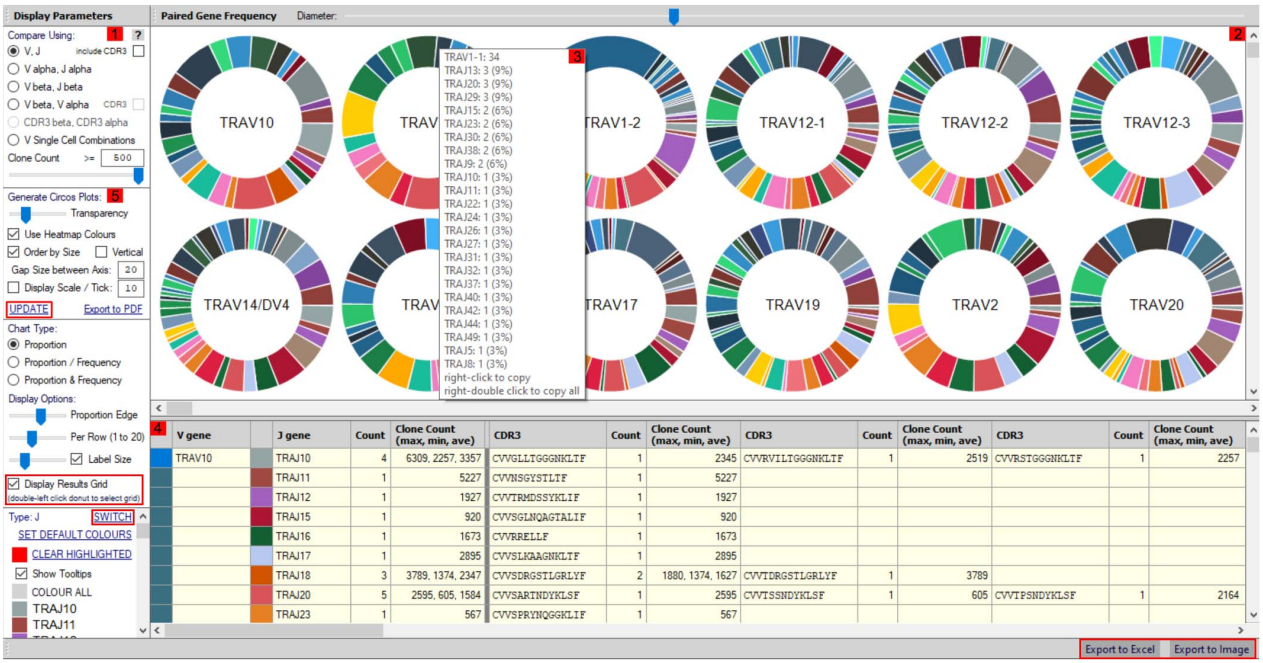

FIGURE 2 | scTCR-seq paired gene/CDR3 frequency window. The scTCR-seq analysis home screen window is divided into key domains to help direct analyses by the user. **(1)** Gene pairings or corresponding CDR3 sequences can be selected for analysis by the user within the "display parameters" domain. **(2)** Representative pie charts display proportion (and frequency) of TCR genes/CDR3 within the selected sample for initial indication of data. Each pie depicts one TCR chain with the colored border representing proportional number of pairings with corresponding chains as selected in domain 1. The central chain can be switched using "Switch" (highlighted red) in the parameters panel for alternate pairing view. **(3)** Hovering over select pies provides an information box with proportional representation (%) of total pairings within. **(4)** Paired genes are displayed in grid format by selecting "display results grid" (highlighted red), which can be exported direct to Excel or Image (highlighted red). **(5)** Circos plots can be generated for selected samples/pairings by clicking "Update" (highlighted red).

between different TCRs. From here, complex TCR visuals can be generated using the "Generate Circos plots" domain, specifically through selection of the "Update" toggle (**Figure 2(5)**). Circos plots, linking one chain at the top to another at the bottom, are best suited for holistic representation of clonality and are auto colored to indicate dominant (red) compared to subdominant (green) TCRs. The extent of a specific pairing between an α and β chain is represented by the width of each connection (**Figure 3A**). The settings for these Circos plots are configurable. For example, plots may be set to visualize the α and β combinations but also α or β and respective J chains, or α and β CDR3 sequences, which ultimately define peptide specificity. For ease of identification, each segment is annotated in the plot, which can be set to display proportion and/or frequency of combinations. Scaled plots may be exported to an image or raw data exported to Excel to produce tables and access numerical representation of TCR within. Sankey plots provide an alternate view for complex pairing interactions between single α chains and multiple β chains or *vice versa* (**Figure 3B**). This is often appropriate for a restricted data set, i.e., top 20 pairings. Each chain can be moved independently up or down the figure such that a TCR of interest can be listed as required. Sankey plots therefore allow visualization of pairings between two α genes or two β genes as are increasingly being detected by single-cell sequencing. A new feature also allows the TCR repertoire for a specific study to be instantly compared to that of previous samples, stored as an active database, which can be adapted for inclusion of external datasets, such that the user can search for similar findings in other studies.

Utility of scRNA-Seq: Unsupervised Holistic Dissection of Signature Transcriptomes

For certain reactions such as abacavir hypersensitivity, TCR responses appear to be polyclonal, suggesting a role for diverse immunogenic antigens, and epitopes in keeping with the altered peptide hypothesis (Redwood et al., 2019). However, as described above for carbamazepine, single dominant TCRs have been identified in patient blister during reaction, providing an antigen-relevant functional marker to identify and characterize the critical effector population driving destructive disease. While output cellular functionality is largely imposed by surface protein, the transcriptome is the vastly more complex precursor, now almost completely measurable by scRNA-seq without bias of preselect markers providing a holistic transcriptomic signature for an individual cell. Algorithms, outlined by Allaoui et al. (2020), then "pull" similar RNA signatures together by k-means clustering, enabling visualized clusters in t-distributed stochastic neighborhood embedding (t-SNE) or uniform manifold approximation and projection (UMAP) plots to be grouped and independently characterized direct from sample suspension.

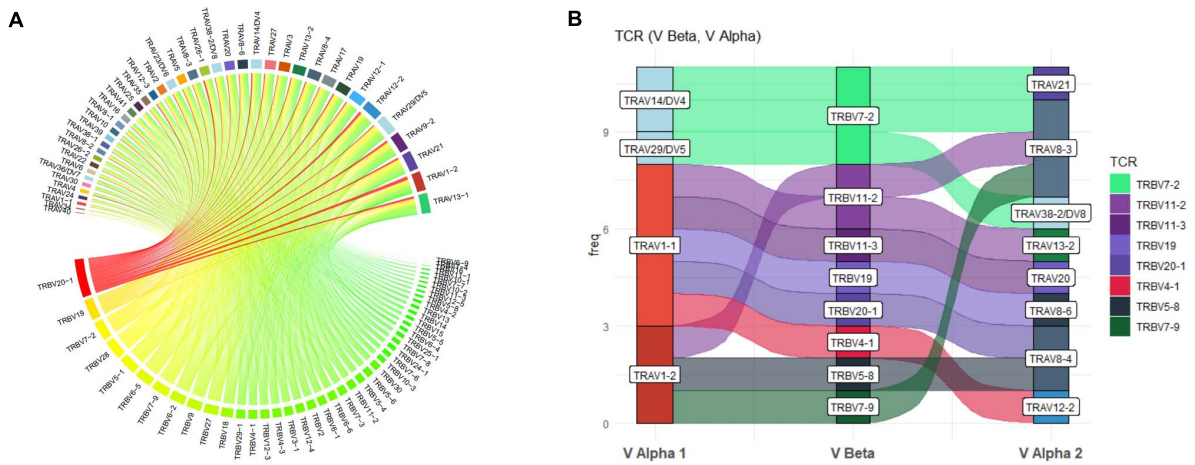

FIGURE 3 | Circos and Sankey plots to display holistic clonality, dominance, and complex pairings. **(A)** Circos plots provide an overview of TCR pairing clonality and dominance within a selected sample as shown for TRAV and TRBV pairings and can also be produced for paired CDR3. Alpha genes are listed at the top and paired to respective β genes at the bottom with width and color (red to green) of each segment proportionate to comparative dominance of total functional TCR pairings. **(B)** Sankey plot illustrating more complex gene interactions identified by sequencing, shown for TRAV-TRBV-TRAV triad, detailing clone frequency on *y*-axis.

Unbiased transcriptome analyses have recently proven utility in defining critical cellular signatures with influence in varied diseases including cancer (Dai et al., 2019; Zhang et al., 2020) and infection (Bossel Ben-Moshe et al., 2019; Yao et al., 2019), driving immunological understanding and identification of disease-relevant biomarkers (Szabo et al., 2019; Cheng et al., 2020). Similar application to DHRs remains limited to a handful of studies, one detailing rechallenge response during HLA-restricted positive patch test (Redwood et al., 2019), and another the effector signature during a single case of treatment-refractory drug reaction with eosinophilia and systemic symptoms (Kim et al., 2020). In this latter study, the merit of unbiased scRNA-seq to directly identify targetable biomarkers of disease was clearly demonstrated when investigators found the JAK-STAT pathway to be enriched in effectors directing the clinical investigators to repurpose tofacitinib and effectively control disease (Chattopadhyay et al., 2014). Application across samples from patients with similar reactions may therefore provide more distinct, reaction-specific biomarkers. However, scRNA-seq captures the transcriptome at unparalleled resolution, posing a challenge for managing, analyzing, and visualizing data. While a range of software has been developed within tools such as R for the analysis of high-dimensional datasets, the user must be proficient in this type of programming and its strict framework, reducing capacity for the researcher to freely explore their data.

VGAS: scRNA Analyses and Visualization Tools

VGAS integrates a number of genomic dataset tools developed for specific scRNA-seq analyses[2] (RNA-seq plot viewer tutorials). These include k-means clustering and UMAP/t-SNE plots, varied differential expression analyses with statistical inference, and plots to compare expression levels of specific transcripts. Although suited to both UMAP and t-SNE, VGAS typically uses UMAP, a well-documented non-linear dimensionality reduction algorithm to convert high-dimensional scRNA-seq data into a visual representation maintaining the global structure of data. Compared to alternative t-SNE algorithms, UMAP presents a faster method of clustering with reproducibility and conservation of subtle differences in cellular populations (Becht et al., 2019). Typically for data generated at our center, a single VGAS plot view (VGAS.pv) file is released to the end-user after bioinformatics quality control, for simple upload to VGAS, first opening the single plot viewer control screen from which all analyses are performed (**Figure 4**). The file is inclusive of all batched samples in a combined UMAP; however, the master normalized gene expression count (.csv) and metadata (.txt) files are additionally provided should the user choose to recapitulate the UMAP modeling. This can be directed through VGAS with automated R plot functions for generation of typical Euclidean, Manhattan, Cosine, Pearson, and Pearson 2 distributions. All distributions may be selected, and plots toggled between as required in the "Plot Viewer."

The control "Plot viewer" screen is split into six key domains: "Genes," "Metadata," "Groupings," "Sample/cell metadata," "Color options," and "TCR clonotypes," respectively, depicted in **Figure 4(1–6)**. All metadata are accessible in the control panel "Metadata" domain, e.g., patient ID, sex, age, etc., dependent on that provided by the investigator, offering flexibility and customizability to analyses (**Figure 4(2)**). The same "Metadata" dropdown menu also holds information acquired during the initial bioinformatics quality assurance and UMAP generation, including cell cycle phase and assigned cell clusters according to individual human cell atlases from which consensus is drawn. This provides the user with an initial overview of the populations present, which can then be highlighted on the UMAP (see *RNA-seq plot viewer tutorials: coloring plots by metadata*) or grouped with ease through one-click selection from the right click control

[2]https://www.iiid.com.au/software/vgas/vgas-rnaseqplotviewer

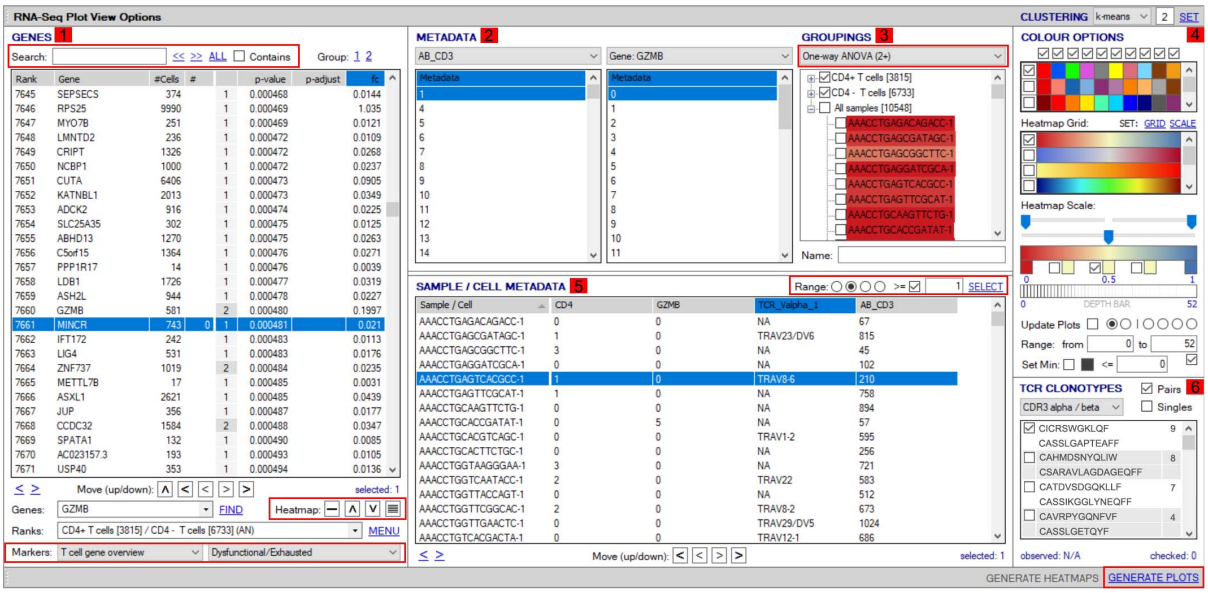

FIGURE 4 | Workflow for analyses of scTCR–RNA-seq data using VGAS plot viewer window. The scTCR–RNA-seq analysis home screen window is divided into key domains to help direct analyses by the user. **(1)** "Genes" panel lists all genes expressed with options to search for specific genes of interest (highlighted red), reorder, and find literature determined groups of interest genes using the "Markers" dropdown tab or heatmap (highlighted red) individual genes on the UMAP for selected sample. **(2)** "Metadata" is displayed with dropdown tabs to select data by sample, clinical metadata, or phenotype groupings defined by indexed flow data or via unsupervised K means clustering on whole sample with consensus calling from reference atlas databases. **(3)** Grouped data/clusters appear in the "Groupings" domain for selection and differential analyses using a range of statistical algorithms contained in the dropdown tab (highlighted red). Differential gene analysis results provide *p*-value, *p*-adjusted, and fold change displayed in "Genes" panel. **(4)** Groups and plots can be fully color-customized in the "Color options" panel and heatmap scales set to user preference. **(5)** Genes of interest, metadata, or groupings can be saved and set as metadata for further interrogation or grouping by several parameters in the "Sample/cell metadata panel." User-defined positive cutoff range for numerical data can be applied to filter samples using "Range" function toggle (highlighted red). **(6)** scTCR-seq defined clonotypes can be set from whole data or distinct RNA-defined groups in the "TCR clonotypes" domain. Circos plots can also be generated from within this panel. The "generate plots" function, bottom right (highlighted red), provides access to associated UMAP.

panel and which then appear in the "Groupings" domain (see *RNA-seq plot viewer tutorials: creating groups*) (**Figure 4(3)**). Of note, each group may be formatted by color, which will translate to all subsequent visuals, through the "Color options" domain (**Figure 4(4)**). More specific groupings according to select gene expression (all genes listed in the left hand "Genes" domain (**Figure 4(1)**) can then be developed through import to the "Sample/cell metadata" domain (**Figure 4(5)**) by selecting either a preselected "Metadata" or individual gene and selecting "Set as metadata." Four metadata columns are available for combined parameter assessment; however, sequential groupings and reapplication as metadata allow limitless combinations to build a single signature. Imported RNA data are numerical, and the user must define cutoffs for positivity/negativity before analysis. This is possible through the single gene expression plot function to graph the spectrum of gene expression from low to high, which, in a manner similar to conventional histogram-based gating in flow cytometry, provides the user guidance of where to set the positive gate and may further identify bimodal or multimodal expression within or between samples for further gating or low, mid, or high expressors (**Figure 5**) (see *RNA-seq plot viewer tutorials: generating gene expression level plots*). When defined, the boundary value above a deemed positive can be input into the "Range" function at the top of the "Sample/cell metadata" domain, stripping those not meeting this inclusion criteria from selection in the sample grid. The TCR repertoire for each group, ascertained using the right-click function to generate the correlating data in the "TCR clonotypes" domain (**Figure 4(6)**), can be used to directly generate Circos plots.

Each group can be renamed and identified using the highlight tool by opening a UMAP plot through the "Generate plots" function, which has fully scalable *x* and *y* axes and formatting functions for coloring, titles, and sizing. Multipanel UMAPs can be generated in the plot viewer for easy comparison between cell populations (**Figure 6(1–5)**). As alternative to groupings defined by metadata (**Figure 6(2–4)**), groups can also be selected directly via the UMAP using the highlight function in the plot viewer to lasso an interest population before highlighting and grouping these cells within the sample grid (**Figure 6(5)**). Such analysis may be particularly useful for subclustering islands that fall within the same cell-type metadata consensus, i.e., $CD8^+$ T-cells that express dominant-TCR versus non-dominant TCR, for authentic signature exploration.

Once two or more groups are created and selected in the "Groupings" domain, the number of cells in each group is shown in brackets, and then two analyses are typically done. First, TCR clonotypes in a particular group can be set via the right-click menu to appear in the bottom right "TCR clonotype" domain if scTCR–RNA-seq was performed, listing combinations of α–β pairs or respective CDR3 pairs in order of dominance

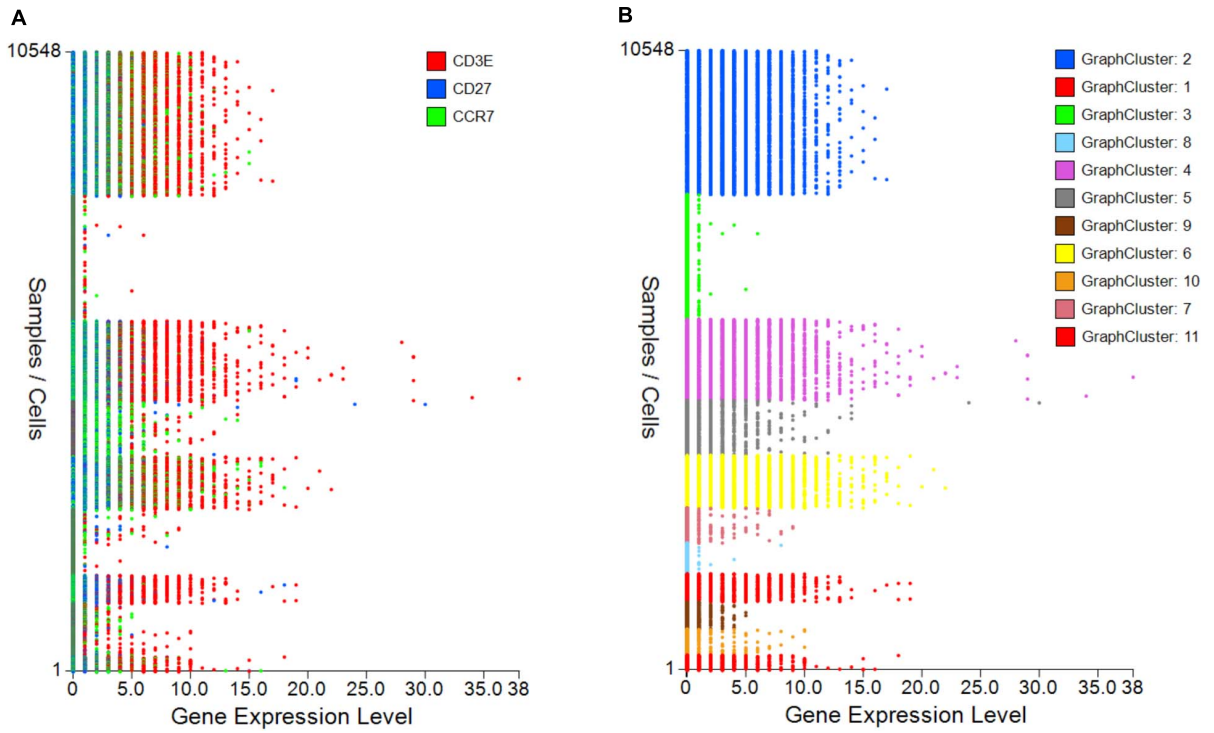

FIGURE 5 | Gene expression plots to provide cutoffs for negative/positive expression or show differences between samples/groups. **(A)** Single or grouped gene expression plots for all cells within a selected sample provides a platform to set cutoff for positivity and identify outlier expression or **(B)** highlight expression differences between samples/plates.

(**Figure 7**). Of note, if scTCR-seq was not performed but a defined interest TCR is known, gene selection for individual TRAV and TRBV within the "Genes" panel will provide an indication of the transcriptome of cells expressing those TRAV or TRBV genes. Selected clonotype pairs (or specific single chains) may be added to a separate group or highlighted on the UMAP to identify the unique effector clusters for comparative scRNA-seq analyses (**Figure 7**). This facilitates the second analysis, differential gene expression, performed with selection of appropriate statistical comparison test using the dropdown menu in the "Groupings" section inclusive of *t*-test, Kruskal–Wallis, one-way analysis of variance (ANOVA), Wilcoxon rank sum test, MAST, Limma, paired *t*-test, paired ANOVA, or mean difference (see *RNA-seq plot viewer tutorials: performing differential gene expression*). The resulting differential analyses appear in a reordered "Genes" section, ordered according to rank and with representation of significance, relevant cell group (i.e., number 1 indicates this gene is more highly expressed in the first grouping), and comparative fold change in expression. More stringent significance can be applied by the user through adjusting *P*-value according to Holm, Hochberg, Hommel, Bonferroni, BH, BY, or false discovery rate, and genes lists reordered according to user preference on fold change or the number of cells expressing each gene (see *RNA-seq plot viewer tutorials: displaying number of cells with expression per gene*). Markers of interest for discovery studies may also be pulled to the top of the "Genes" domain via a simple name search, via the preset subsets tab, which contains predefined groups of markers, or by import from clipboard (see *RNA-seq plot viewer tutorials: genes: sorting, searching and selecting*).

Initial differential gene analyses are best visualized by volcano plots incorporated into the "generate plots" function, separating differential RNA by both statistical inference and fold change (see *RNA-seq plot viewer tutorials: generating volcano plots*) (**Figure 8A**). If groupings have been chosen on select markers, these may be excluded from the plot as to prevent skewed axes and more accurately dissect data. Alternatively, traditional heatmap plots can be created using the "RNAseqHEAT" tool, of particular utility when more than two populations are being comparably assessed, again with user-adjustable heat scaling (**Figure 8B**).

Expression of markers of interest may also be individually displayed as a heatmap directly onto the UMAP by selecting a specific marker in the gene list and accessing the one-click function tab at the bottom of panel labeled "heatmap" (see *RNA-seq plot viewer tutorials: coloring plots using heatmaps*) (**Figure 9**). Given a UMAP is a two-dimensional (2D) image of a 3D projection, respective arrow buttons plot those with highest expression at the front or back of the plot, respectively (see *RNA-seq plot viewer tutorials: setting the draw order of plot points*). Importantly, to aid in the visualization of multidimensional datasets, UMAPs may be aligned side-by-side to assess different zoomed regions of the total UMAP or the same populations from different samples and be similarly displayed as a heatmap with user-defined formatting using the right-hand-side menu.

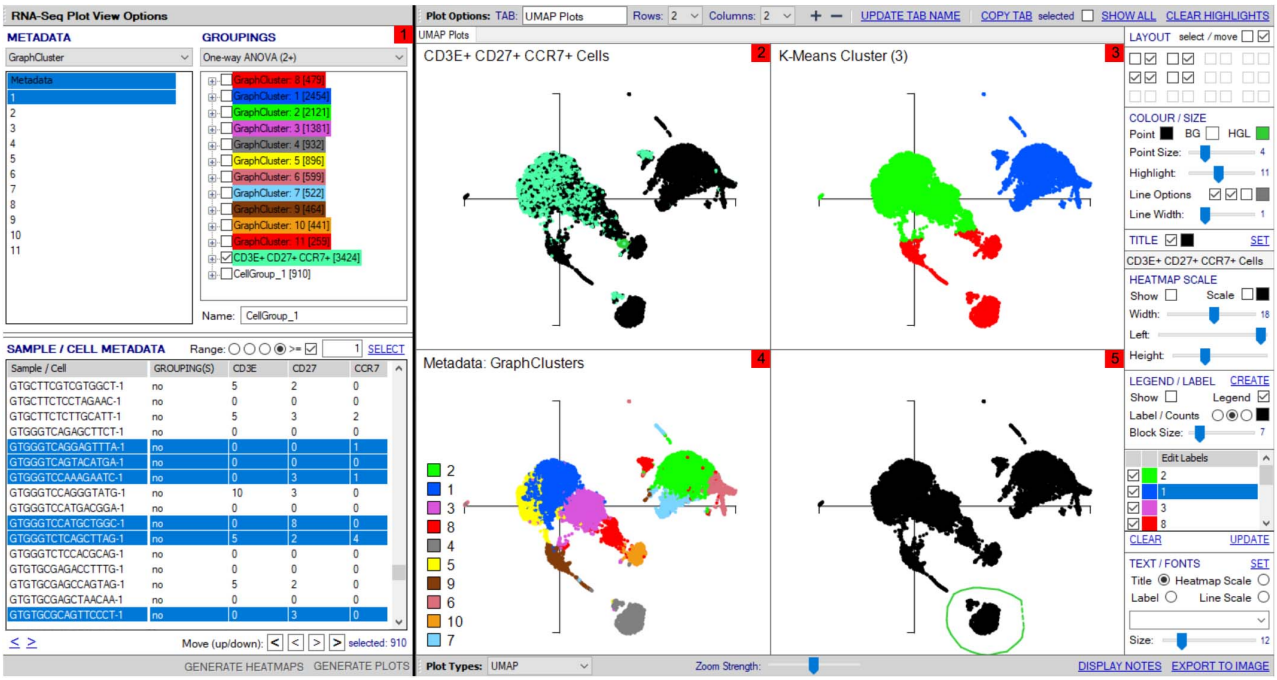

FIGURE 6 | Multipanel UMAP investigation. **(1)** Sample/cell groupings created in "Groupings" panel can be plotted on multipanel UMAPs, with zoomed view possible to focus on different regions of interest (2–5). **(2)** Groupings created from differentially expressed genes and metadata can be highlighted within the total cell population, shown for $CD3E^{+}CD27^{+}CCR7^{+}$ cells group defined in panel 1. **(3)** K-means clustering can be set in the scRNA-seq Plot View Options window and illustrated within UMAP. **(4)** Cell types from unsupervised clustering can be separately colored on a UMAP with legend for visualization. **(5)** Cell clusters can be "lassoed" on the UMAP and highlighted within the "Sample/cell metadata" grid for addition to distinct groups within "Groupings" for further analyses, named "CellGroup_1" in groupings tab.

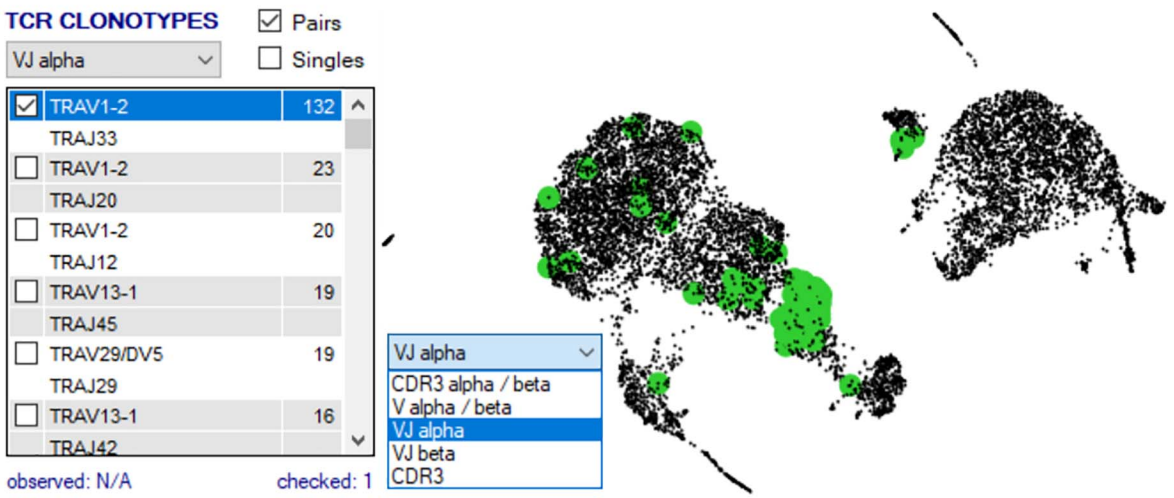

FIGURE 7 | scRNA-defined UMAP overlay of scTCR-seq. Single-cell defined functional TCR clonotypes can be imported for selected populations/samples, displayed in order of dominance within the Plot View Options window, and highlighted on the scRNA-defined UMAP to pinpoint clusters with expression of dominant or interest TCR (highlighted green).

Currently, plots may be compared up to four columns wide and three rows deep on a single screen, but with additional tabs available with rapid toggle function such that unlimited parameters may be compared during a single analysis.

Significant differential expression does not necessarily infer predominant expression in a subset. If more finite expression level plots are required, this is performed in VGAS by simply highlighting the interest genes and selecting "Generate violin/box

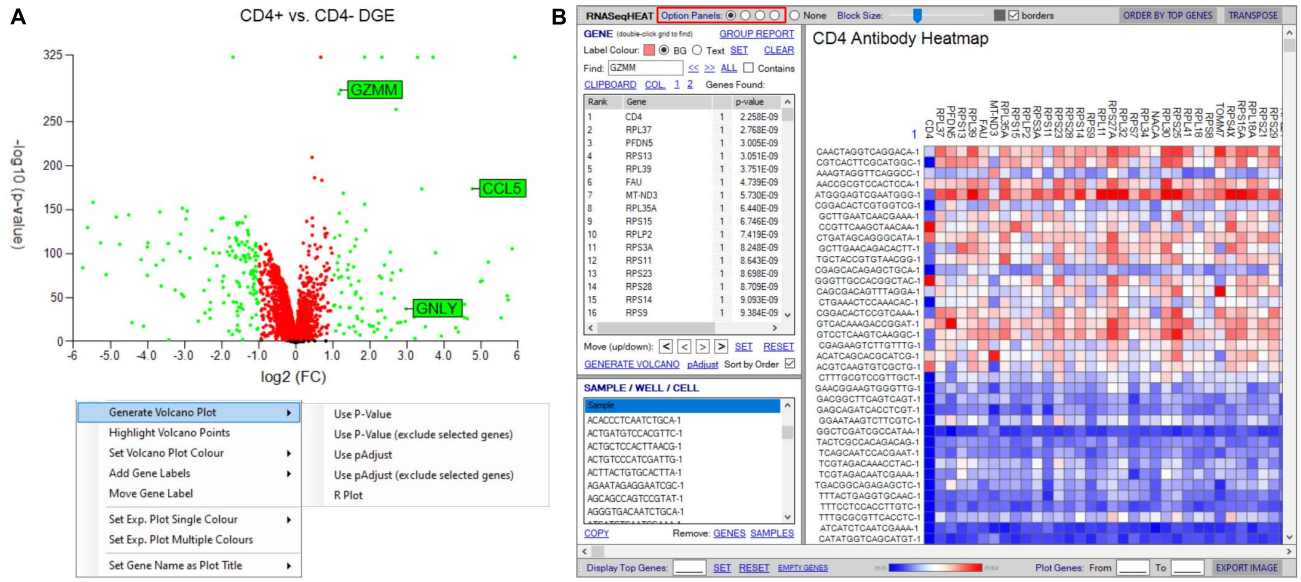

FIGURE 8 | Tools to visualize differential gene expression. **(A)** Volcano plot for differential expression analysis between two groupings/samples. User-defined thresholds can be set for fold change and significance, visualized according to color (red and green represent genes above different preselected fold change (FC) and significance (*p*-value). Right-click menu provides options for addition and formatting of gene labels, plot coloring, and exclusion of selected genes. **(B)** RNASeqHEAT enables generation of a heatmap of selected genes as shown on horizontal axis and with selected samples on vertical axis. Option panel (highlighted in red) allows customization.

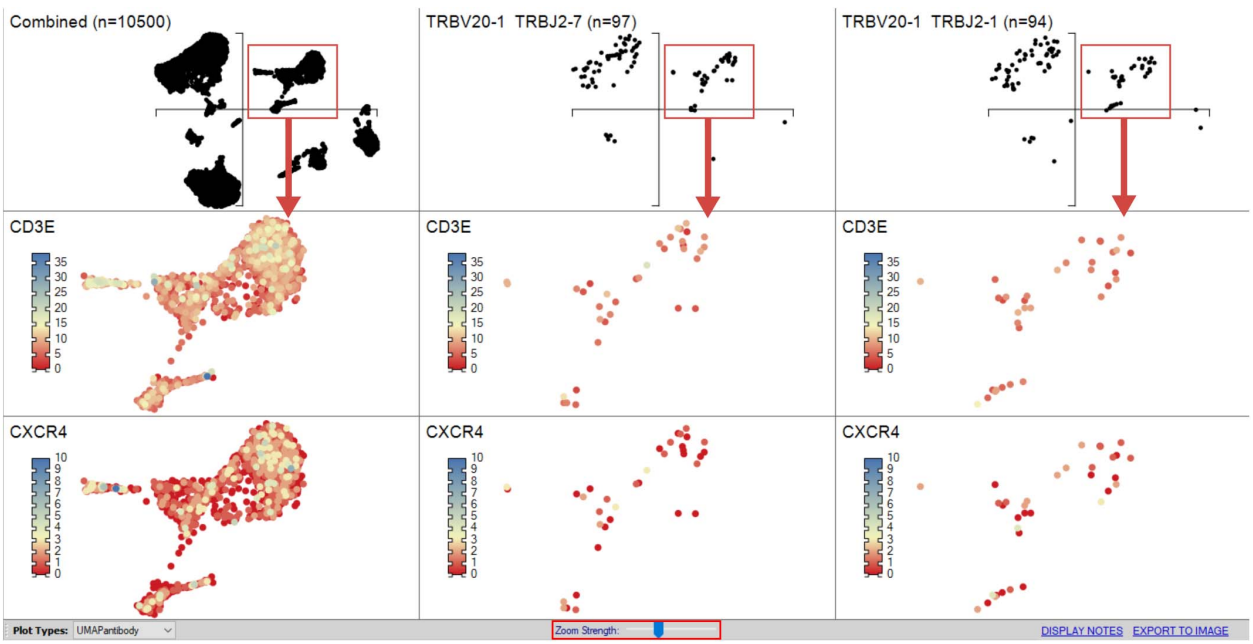

FIGURE 9 | Heatmapping scRNA-seq gene expression on UMAP. Combined sample or subpopulation UMAPs can be compared on a single screen simultaneously providing an overview and more discrete dissection of sample. The "Zoom Strength" slider (highlighted red) enables focus on a particular region of interest directed by grouped analyses for heatmapping gene expression between samples as dictated by interest of prior differential gene expression analyses.

plots by gene(s)" from the right-click drop menu in the "Groupings" tab [see *RNA-seq plot viewer tutorials: generating gene plots* (Violin and Box plots etc.)]. Alternatively, a specific interest gene list in a specific order for presentation can be selected by using the "Select from clipboard" function. An initial window provides an overview of expression for each group showing the minimum, average, and maximum expression, along with the number of positive versus negative expressing cells for

each selected gene (**Figure 10A**). Fully customizable violin or box plots are readily generated with displayed average expression, with added option to include jitters and/or heatmap colors to align directly with other figures [see *RNA-seq plot viewer tutorials: coloring gene plot (jitter) points, coloring gene plot (jitter) points using heatmaps*; **Figures 10B,C**].

Utility of scCITE-Seq: Integrated Single-Cell Delineation of Surface Proteome

Transcriptome analyses provide highly complex cellular signatures of disease, revealing extensive heterogeneity among previously considered homogeneous populations (Bjorklund et al., 2016). However, RNA transcription profiles do not correlate completely with functional protein profiles, a more tangible measure of output functionality and more traditional diagnostic or therapeutic target. This divergence in comparative expression is a product of several processes including posttranscriptional processing, investigational error, and variable protein turnover, but importantly, there remains a direct RNA–protein concentration correlation, reported to be approximately 40% (Vogel and Marcotte, 2012).

Surface protein is traditionally assessed by indexed flow data, but this remains substantially limited by availability and spectral overlap of fluorescent tags and thus provides a far more restricted glimpse into the rich and diverse phenotypic landscape truly expressed on each and every cell. Thus, in recent years, unique tripartite DNA barcodes have been similarly generated and tagged to protein-specific antibodies unique to surface proteins of interest as to similarly sequence select surface protein expression on the same cell as scTCR–RNA-seq. Two separate modalities, CITE-seq and REAP-seq, respectively, were developed by teams at the New York Genome Center (NYGC) and Merck group (Peterson et al., 2017). While both are suitable for analysis in VGAS, we use scCITE-seq, reviewed in detail by the Stockieus laboratory at NYGC (Stoeckius et al., 2017), which is fully integrated with scTCR–RNA-seq. As with flow and mass cytometric methods, there remains a requirement to validate titrations for each antibody combined in a single panel, but we have found it straightforward to develop panels of more than 40 antibodies. We have optimized staining of different human samples, including skin, blood, adipose tissue, and blister fluid, using combinations of more than 45 oligo-tagged antibodies for the investigation of DHR and other diseases. This technology forms an integrated pipeline for holistic dissection of populations by single-cell transcriptomics and comparative surface protein markers and TCR.

VGAS: scCITE-Seq Analyses and Visualization Tools

VGAS can incorporate scCITE-seq data, listing normalized count files for each antibody in the "Metadata" dropdown menu (**Figure 11**). Much of the analysis options described above for scRNA-seq are possible for CITE-seq including differential expression analyses with statistical inferences. Protein values can also be displayed as a heatmap directly onto the same UMAPs as scTCR–RNA-seq to delineate comparative RNA to protein expression (**Figures 12A,B**). If required, protein markers can be similarly explored and combined in the "Sample/cell metadata" columns with specific TCR pairs or RNA interest markers, generating a complete cell signature. Differential protein analyses are possible between groups with inference determined by varied statistical tests and heatmapping directly onto the same UMAPs for comparable expression plots with corresponding RNA (**Figure 12C**). Importantly, numerical positive expression gates must be reset for protein data with different expression ranges between markers. The right-click function allows the user to set coverage depth for a particular antibody detailing the numerical spread of expression, which appears in the depth bar (see *RNA-seq plot viewer tutorials: coloring plots using heatmaps*) (red highlight, **Figure 11**). This bar also provides detail of expression density via a white-to-black scaling, with darker areas representing the most abundant expression. This can be plotted next to the heatmap scale on UMAPs to provide comparative information on whether expression is high, mid, or low or even multimodal. This complements the visual given the 3D nature of the 2D UMAP such that some points may be hidden behind others. Heatmap scaling may then be adjusted by the user such to identify finite comparative expression even between two low-expressing populations. More familiar flow-type histograms are soon to be incorporated as an alternative gating and presentation strategy to dissect multimodal expression given the observed subtlety of variation on UMAP between similar but spatially distinct clusters. Our own analyses to date (data not shown) comparing flow-based and CITE-seq protein expression show distinct overlap with similar population representation, in line with that in the original pilot report from the Stockieus laboratory (Stoeckius et al., 2017).

Brief Technical Overview and Performance Benchmark

The requirements and complexity of "big data" meant loading data files is typically slow, and subsequent analyses cumbersome. Thus, the VGAS development team, critically bridging software developers, bioinformaticians, laboratory scientists, and clinical researchers all with extensive experience of handling genomic data, has a major goal to develop and optimize performance solutions for individual data acquisition functions. Successful in this objective, VGAS incorporates non-standard and interlinked algorithms from different programming languages, most typically C sharp (C#), and provides highly efficient data structure solutions to enable everyday use on standard specification 8- to 16-GB laptops. Enhanced storage efficiency is critical for ease of file sharing and limits expense of long-term cold data storage whereby a 10-GB normalized gene file can be saved in an application specific (.VGASpv) plot view file and zipped to 350 Mb. Furthermore, modular framework of the application allows for inclusion of third-party tools and development of novel analysis modules without affecting functionality. Using R.Net to negate direct coding, VGAS utilizes widely available R-based packages, hidden to the user, adapting such to provide full customization of traditionally static

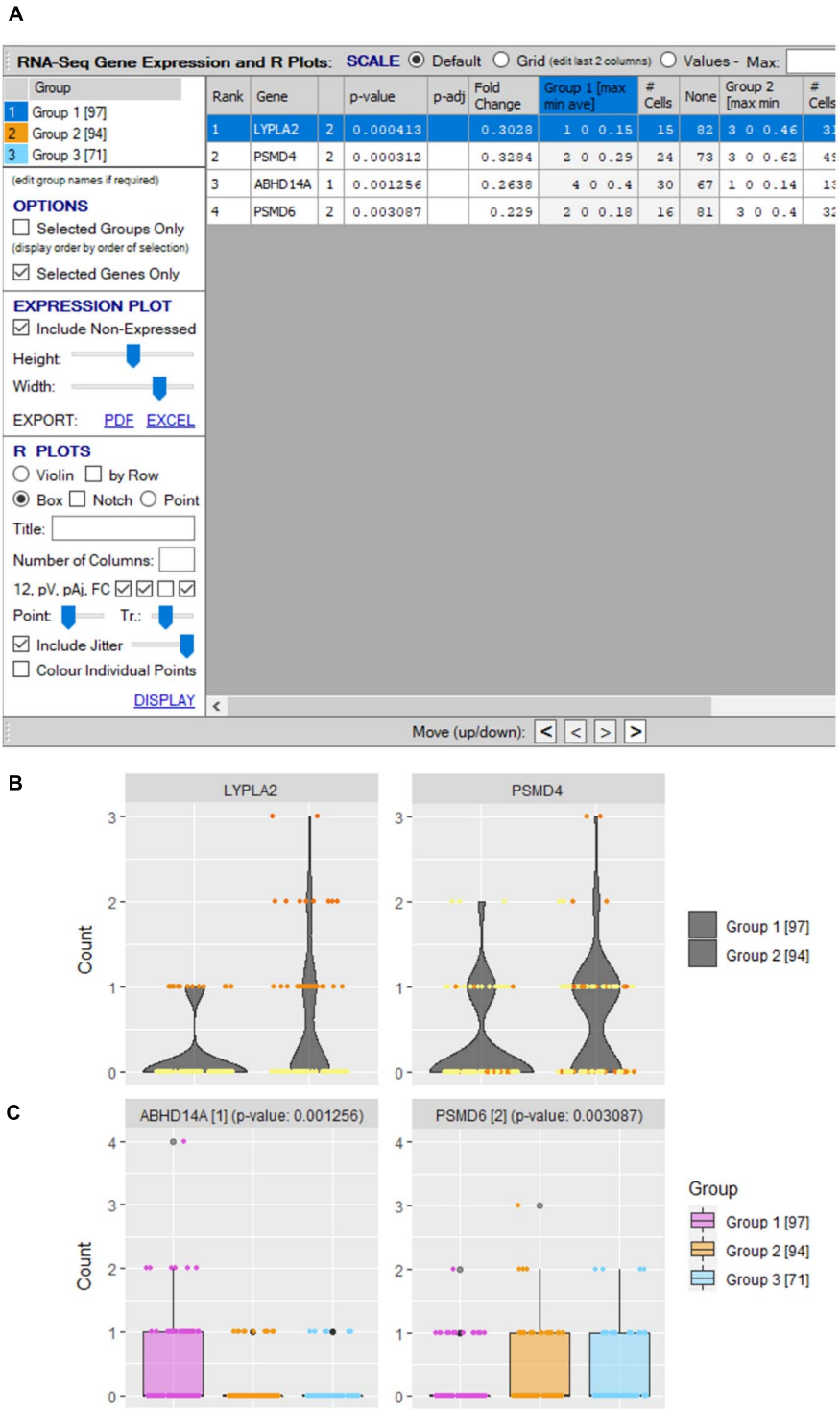

FIGURE 10 | Differential gene expression plots. **(A)** "scRNA-seq gene expression and R plots" window allows user to define genes for inclusion in single/comparative **(B)** violin and **(C)** boxplots with optional inclusion of jitters and defined heatmap coloring of groups.

R plots for scale, color, and resolution for rapid generation of publication-quality images available in all bitmap formats (tiff, png, jpeg) or as vector graphics. Importantly, VGAS has been programmed by an experienced software engineer through the entire software development "life cycle" using an integrated development environment, Microsoft Visual Studio,

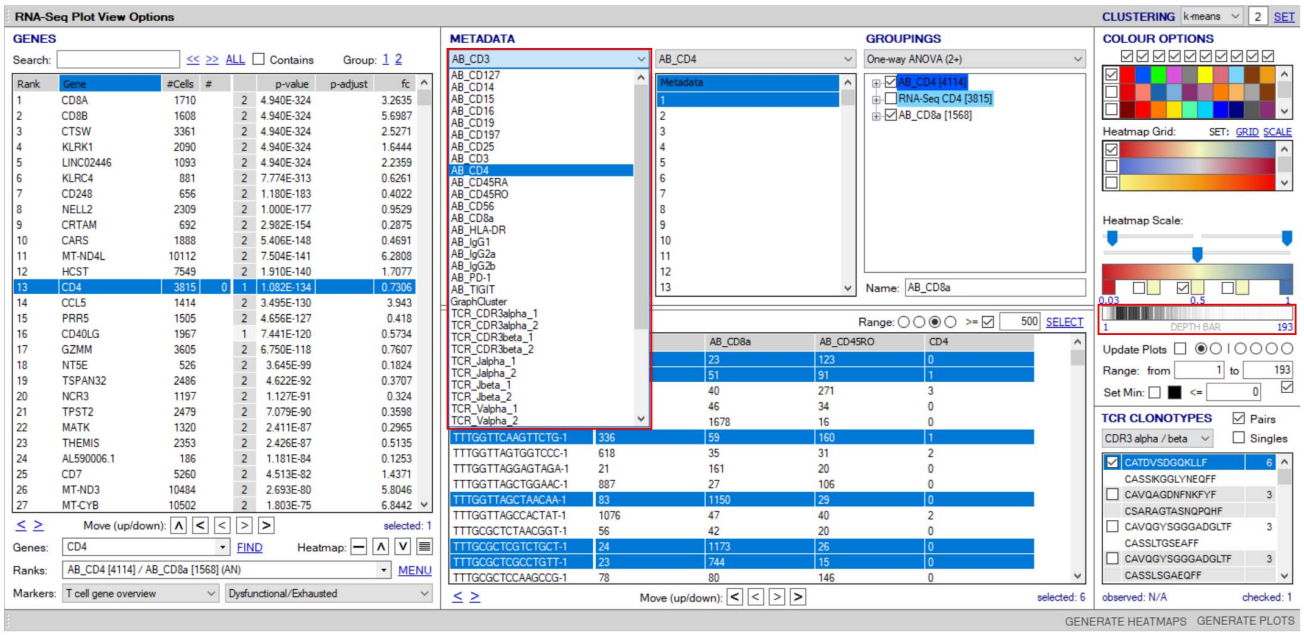

FIGURE 11 | Overlay of surface protein expression (scCITE-seq) onto scTCR–RNA-seq analyses. Within the "RNA-seq plot viewer options" window, normalized CITE-seq data are included in the "Metadata" panel, accessible via the dropdown tab (highlighted red). All applications discussed for scRNA-seq analyses are applicable to protein with differential analyses between groups, selection into groupings or dissection via the "cell/sample metadata/domain. Depth bar (highlighted red) provides detail of protein expression density via a white-to-black scaling with darker areas representing most abundant expression.

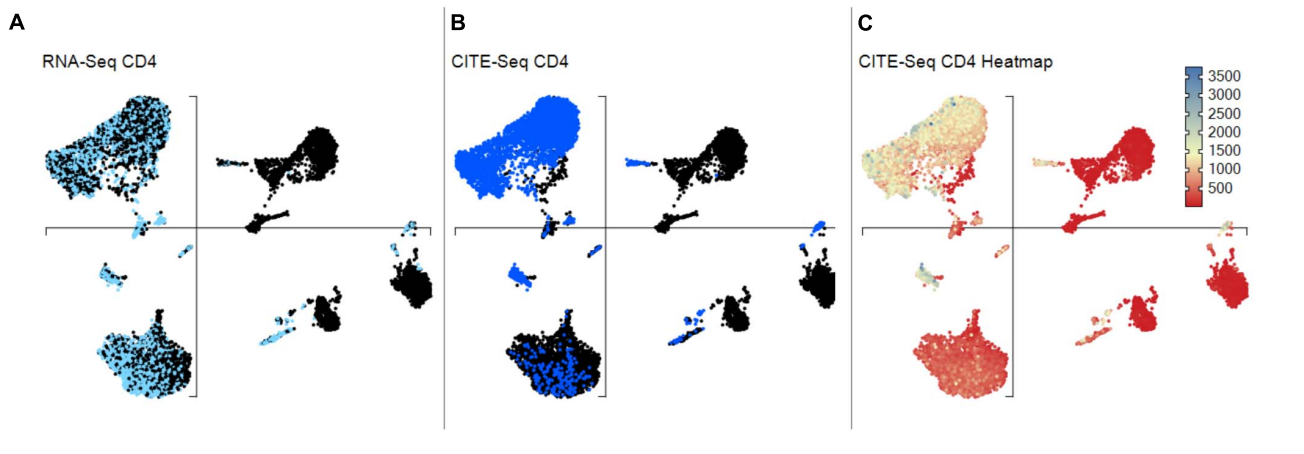

FIGURE 12 | scCITEseq data visualization on scRNA-defined UMAP. Gene and corresponding surface protein expression can be compared across individual cells on the same unsupervised UMAP. **(A)** Cells highlighted with scRNA-seq defined positive CD4 expression. **(B)** Cells highlighted with surface CD4 expression using scCITE-seq antibody. **(C)** CD4 scCITE-seq antibody expression displayed as a heatmap onto scRNA-defined UMAP.

which provides comprehensive testing tools for validation. To provide a performance benchmarks, we utilized a standard eighth-generation i7 Windows-based laptop with m.2 SSD as now typically used in research institutions to load a 3-GB file representing counts for more than 23,000 genes and 120 metadata (integer, numeric, and factor) across 30,000 cells in less than 3 min. Active file upload used 4–5 GB, which was maintained even during subsequent active display of 12, albeit potentially unlimited, comparative UMAP plots. A crude sample split into two groups of 15,000 cells was then used to benchmark performance for differential gene expression analyses by one-way ANOVA, taking less than 3 min. To ensure speed of analyses, we recommend a laptop with 8-GB RAM and i5 processor or equivalent as the minimum hardware specification.

Prior to investigator release, raw sequencing data are run through a standard data normalization and quality-assurance pipeline by our on-site bioinformatician. Importantly, VGAS is independent of this standard pipeline, which uses open-access tools, and may load data processed by any best-practice approach. For droplet-based (10×) assays, Cell Ranger is used to

align data from 10X-5′sc-RNA-TCR-CITE-seq, with processing of antibody-derived reads by Seurat[3] to analyze the multimodal data and cluster cells based on both RNA and protein expression. scRNA-seq measurements are normalized using SCTransform and scale-factor transform method. scCITE-seq measurements are normalized using centered-log ratio transformation in Seurat. Cells with fewer than 200 genes and more than 10% mitochondrial content are typically removed, but alternate cutoffs may be defined by individual investigators. Furthermore, genes with more than 0 counts in fewer than three cells are also typically removed. Initial first-pass analyses are performed using a combination of most current versions of Seurat for unsupervised clustering and SingleR for cell-type prediction. After normalization, data input for VGAS is a comma-separated (.csv) normalized expression file and tab-separated metadata text file (.txt), with the sample identifier as the first column and a second column to display metadata as factor, integer, or numeric value. This easily modifiable format enables additional metadata to be included if not known at time of initial analysis. We also provide a UMAP/t-SNE.csv file to view x, y coordinates; however, data are also released as a merged VGAS plot view (VGAS.pv) master file, which encompasses all three individual files (normalized.csv, UMAP/t-SNE.csv, metadata.txt) for simple one-click file open during software trial. All four test data files are available to view input by download from our website[4] ("VGAS RNA-Seq Plot Viewer files" provides download link to all four VGAS files (metdata.txt, normaliation.csv, UMAP.csv, VGAS.pv).

Summary and Future Development

Single-cell sequencing technologies are revolutionizing our ability to understand complex cellular systems, providing unparalleled ability to dissect the previously undefinable finite cellular discrepancies that delineate disease phenotypes, patient outcomes, and treatments. Moreover, because only 1,000–2,000 cells are thought to be required for sufficient *de novo* population dissection of any heterogeneous sample (Giladi and Amit, 2018), it is feasible to explore even limited clinical samples from relevant reaction sites. Collaborative effort to map the entire human body by cell in the Human Cell Atlas provides a critical reference resource to facilitate interpretation of the results (Regev et al., 2017). For T-cell–mediated disease such as DHRs, the integration of multifocal scTCR–RNA–CITE-seq provides a pipeline to identify actively responding tissue-based effectors driving destructive outcome, first identifying dominantly expanded or newly recruited TCR, before determination of unbiased transcriptome and select proteome signature to delineate disease- and tissue-specific biomarkers. This is possible not only for critical T-cell effectors, but also all accessory populations, enabling more complete understanding of the entire cellular microenvironment. These single-cell technologies require investigators to be able to manage and analyze their own big data. Investigators are at risk of losing the understanding of their own data if they are completely dependent on bioinformatics experts with the coding expertise required for suitable data handling, quantification, and analysis. VGAS is specifically designed to enable researchers to be increasingly self-sufficient. One limitation is that the program has to be administrator-distributed and linked to the highly specialist sequencing pipelines available at a few specialist genomics facilities worldwide. Critically, such sequencing is a core service provided to external laboratories by our center with VGAS made freely available for download to investigators. Access is also provided to researchers who run their own sequencing; however, there is a requirement for VGAS access that initial bioinformatics normalization must be performed in collaboration. However, prospective users can request for a 2-week trial of VGAS by contacting software@iiid.murdoch.edu.au.

VGAS is strategically a non-web-based, Windows-aligned application to minimize the effect of variable download speed, allow analysis on the go, provide highest resolution images for presentation, and, moreover, provide means to secure confidential data to internal servers. Background coding has been meticulously performance-optimized for different functions to provide timely analyses that run on standard laptops without need for high-end hardware and servers. With the fundamental vision to provide researchers with intelligible means to access and interrogate single-cell data and develop publication-ready figures, a key ongoing principle remains user-directed development. Next versions under construction are to include flow-type histogram-based gating for alternative dissection of multimodal RNA and protein expression and trajectory analyses of pseudo time. Pseudo time, or "pseudotemporal reconstruction," an inference of time through the shortest transcriptomic path between all linked populations, provides insight into both the transcriptome-predictive before and after precursors and exhausted counterparts of identified effector populations. This enables conversion of what is a static snapshot of cellular transcriptome in time into a continuum of cellular development given the breadth of developmental stages for each cell type, based on subtle discrepancies in similar gene expression (Haghverdi et al., 2016). Importantly, interest transitions may be verified by transposase-accessible chromatin sequencing (ATAC-seq) to inform upon the plasticity from epigenetic modifications toward a specific signature within a lineage as described by Gury-BenAri for helper-like innate lymphoid cells in healthy mouse intestine (Gury-BenAri et al., 2016). Thus, from a single sample, a longitudinal view of cellular response may be obtained. These additional analyses performed by our bioinformatics team will not alter the input data, but rather extend the existing metadata matrix, for example, by providing pseudotime clustered populations with n = populations set by user. Further information on our dedicated webpage (see text footnote 4) will guide prospective users through the plethora of sequencing technologies and associated analyses provided by VGAS.

DATA AVAILABILITY STATEMENT

The original contributions presented in the study are included in the article/supplementary material, further inquiries can be directed to the corresponding author/s.

[3]https://satijalab.org/seurat/

[4]https://www.iiid.com.au/software/vgas

ETHICS STATEMENT

The studies involving human participants were reviewed and approved by Murdoch HREC. Written informed consent for participation was not required for this study in accordance with the national legislation and the institutional requirements.

AUTHOR CONTRIBUTIONS

SM, EP, SL, AC, and MW conceptualized VGAS. SL, RR, and DC contributed to technical design. RH, PD, and AG contributed to analysis. RH, PD, AG, and RR wrote the manuscript. AC, SL, SM, YL, AP, AG, and EP reviewed the manuscript. All authors have approved the submitted manuscript.

FUNDING

EP reports grants from the National Institutes of Health (P50GM115305, R01HG010863, R01AI152183, R21AI139021, and U01AI154659) and the National Health and Medical Research Council of Australia. Funders played no role in any aspect of this work. Development costs for VGAS have been provided direct by Murdoch University development funds, VGAS is proprietary software owned by Murdoch University.

REFERENCES

Allaoui, M., Kherfi, M. L., and Cheriet, A. (eds) (2020). *Considerably Improving Clustering Algorithms Using UMAP Dimensionality Reduction Technique: A Comparative Study*. Cham: Springer International Publishing.

Attaf, M., Malik, A., Severinsen, M. C., Roider, J., Ogongo, P., Buus, S., et al. (2018). Major TCR repertoire perturbation by immunodominant HLA-B(*)44:03-Restricted CMV-Specific T cells. *Front. Immunol.* 9:2539. doi: 10.3389/fimmu.2018.02539

Becht, E., McInnes, L., Healy, J., Dutertre, C.-A., Kwok, I. W. H., Ng, L. G., et al. (2019). Dimensionality reduction for visualizing single-cell data using UMAP. *Nat. Biotechnol.* 37, 38–44. doi: 10.1038/nbt.4314

Behr, F. M., Chuwonpad, A., Stark, R., and van Gisbergen, K. (2018). Armed and ready: transcriptional regulation of tissue-resident memory CD8 T cells. *Front. Immunol.* 9:1770. doi: 10.3389/fimmu.2018.01770

Bjorklund, A. K., Forkel, M., Picelli, S., Konya, V., Theorell, J., Friberg, D., et al. (2016). The heterogeneity of human CD127(+) innate lymphoid cells revealed by single-cell RNA sequencing. *Nat. Immunol.* 17, 451–460. doi: 10.1038/ni.3368

Bossel Ben-Moshe, N., Hen-Avivi, S., Levitin, N., Yehezkel, D., Oosting, M., Joosten, L. A. B., et al. (2019). Predicting bacterial infection outcomes using single cell RNA-sequencing analysis of human immune cells. *Nat. Commun.* 10:3266. doi: 10.1038/s41467-019-11257-y

Chattopadhyay, P. K., Gierahn, T. M., Roederer, M., and Love, J. C. (2014). Single-cell technologies for monitoring immune systems. *Nat. Immunol.* 15, 128–135. doi: 10.1038/ni.2796

Chen, P., Lin, J.-J., Lu, C.-S., Ong, C.-T., Hsieh, P. F., Yang, C.-C., et al. (2011). Carbamazepine-induced toxic effects and HLA-B*1502 screening in Taiwan. *New England J. Med.* 364, 1126–1133. doi: 10.1056/NEJMoa1009717

Cheng, Q., Li, J., Fan, F., Cao, H., Dai, Z.-Y., Wang, Z.-Y., et al. (2020). Identification and analysis of glioblastoma biomarkers based on single cell sequencing. *Front. Bioeng. Biotechnol.* 8:167. doi: 10.3389/fbioe.2020.00167

Chung, W. H., Hung, S. I., Hong, H. S., Hsih, M. S., Yang, L. C., Ho, H. C., et al. (2004). Medical genetics: a marker for Stevens-Johnson syndrome. *Nature* 428:486. doi: 10.1038/428486a

Dai, W., Zhou, F., Tang, D., Lin, L., Zou, C., Tan, W., et al. (2019). Single-cell transcriptional profiling reveals the heterogenicity in colorectal cancer. *Medicine (Baltimore)* 98:e16916. doi: 10.1097/md.0000000000016916

Giladi, A., and Amit, I. (2018). Single-cell genomics: a stepping stone for future immunology discoveries. *Cell* 172, 14–21. doi: 10.1016/j.cell.2017.11.011

Gras, S., Kjer-Nielsen, L., Burrows, S. R., McCluskey, J., and Rossjohn, J. (2008). T-cell receptor bias and immunity. *Curr. Opin. Immunol.* 20, 119–125. doi: 10.1016/j.coi.2007.12.001

Gury-BenAri, M., Thaiss, C. A., Serafini, N., Winter, D. R., Giladi, A., Lara-Astiaso, D., et al. (2016). The spectrum and regulatory landscape of intestinal innate lymphoid cells are shaped by the microbiome. *Cell* 166, 1231.e13–1246.e13. doi: 10.1016/j.cell.2016.07.043

Haghverdi, L., Büttner, M., Wolf, F. A., Buettner, F., and Theis, F. J. (2016). Diffusion pseudotime robustly reconstructs lineage branching. *Nat. Methods* 13, 845–848. doi: 10.1038/nmeth.3971

Kim, D., Kobayashi, T., Voisin, B., Jo, J.-H., Sakamoto, K., Jin, S.-P., et al. (2020). Targeted therapy guided by single-cell transcriptomic analysis in drug-induced hypersensitivity syndrome: a case report. *Nat. Med.* 26, 236–243. doi: 10.1038/s41591-019-0733-7

Konvinse, K. C., Trubiano, J. A., Pavlos, R., James, I., Shaffer, C. M., Bejan, C. A., et al. (2019). HLA-A*32:01 is strongly associated with vancomycin-induced drug reaction with eosinophilia and systemic symptoms. *J. Allergy Clin. Immunol.* 144, 183–192. doi: 10.1016/j.jaci.2019.01.045

Kumar, B. V., Connors, T. J., and Farber, D. L. (2018). Human T cell development, localization, and function throughout life. *Immunity* 48, 202–213. doi: 10.1016/j.immuni.2018.01.007

Lähnemann, D., Köster, J., Szczurek, E., McCarthy, D. J., Hicks, S. C., Robinson, M. D., et al. (2020). Eleven grand challenges in single-cell data science. *Genome Biol.* 21:31. doi: 10.1186/s13059-020-1926-6

Lonjou, C., Thomas, L., Borot, N., Ledger, N., Toma, C., LeLouet, H., et al. (2006). A marker for Stevens-Johnson syndrome ...: ethnicity matters. *Pharmacogenom. J.* 6, 265–268. doi: 10.1038/sj.tpj.6500356

Nakkam, N., Konyoung, P., Kanjanawart, S., Saksit, N., Kongpan, T., Khaeso, K., et al. (2018). HLA pharmacogenetic markers of drug hypersensitivity in a Thai population. *Front. Genet.* 9:277. doi: 10.3389/fgene.2018.00277

Nguyen, A., Khoo, W. H., Moran, I., Croucher, P. I., and Phan, T. G. (2018). Single cell RNA sequencing of rare immune cell populations. *Front. Immunol.* 9:1553. doi: 10.3389/fimmu.2018.01553

Pan, R. Y., Chu, M. T., Wang, C. W., Lee, Y. S., Lemonnier, F., Michels, A. W., et al. (2019). Identification of drug-specific public TCR driving severe cutaneous adverse reactions. *Nat. Commun.* 10:3569. doi: 10.1038/s41467-019-11396-2

Pavlos, R., Mallal, S., Ostrov, D., Buus, S., Metushi, I., Peters, B., et al. (2015). T cell-mediated hypersensitivity reactions to drugs. *Annu. Rev. Med.* 66, 439–454. doi: 10.1146/annurev-med-050913-022745

Peterson, V. M., Zhang, K. X., Kumar, N., Wong, J., Li, L., Wilson, D. C., et al. (2017). Multiplexed quantification of proteins and transcripts in single cells. *Nat. Biotechnol.* 35, 936–939. doi: 10.1038/nbt.3973

Phillips, E. J. (2018). New strategies to predict and prevent serious immunologically mediated adverse drug reactions. *Trans. Am. Clin. Climatol. Assoc.* 129, 74–87.

Plumpton, C. O., Yip, V. L., Alfirevic, A., Marson, A. G., Pirmohamed, M., and Hughes, D. A. (2015). Cost-effectiveness of screening for HLA-A*31:01 prior to initiation of carbamazepine in epilepsy. *Epilepsia* 56, 556–563. doi: 10.1111/epi.12937

Rauch, A., Nolan, D., Martin, A., McKinnon, E., Almeida, C., and Mallal, S. (2006). Prospective genetic screening decreases the incidence of abacavir hypersensitivity reactions in the Western Australian HIV cohort study. *Clin. Infect. Dis.* 43, 99–102. doi: 10.1086/504874

Redwood, A. J., Rwandamuriye, F., Chopra, A., Leary, S., Ram, R., McDonnell, W., et al. (2019). Single-cell transcriptomics reveal polyclonal memory T-cell responses in skin with positive abacavir patch test results. *J. Allergy Clin. Immunol.* 144, 1413.e7–1416.e7. doi: 10.1016/j.jaci.2019.09.013

Regev, A., Teichmann, S. A., Lander, E. S., Amit, I., Benoist, C., Birney, E., et al. (2017). The human cell atlas. *Elife* 6:e27041. doi: 10.7554/eLife.27041

Robins, H. S., Campregher, P. V., Srivastava, S. K., Wacher, A., Turtle, C. J., Kahsai, O., et al. (2009). Comprehensive assessment of T-cell receptor beta-chain diversity in alphabeta T cells. *Blood* 114, 4099–4107. doi: 10.1182/blood-2009-04-217604

Rossjohn, J., Gras, S., Miles, J. J., Turner, S. J., Godfrey, D. I., and McCluskey, J. (2015). T cell antigen receptor recognition of antigen-presenting molecules. *Annu. Rev. Immunol.* 33, 169–200. doi: 10.1146/annurev-immunol-032414-112334

Soto, C., Bombardi, R. G., Kozhevnikov, M., Sinkovits, R. S., Chen, E. C., Branchizio, A., et al. (2020). High frequency of shared clonotypes in human T cell receptor repertoires. *Cell Rep.* 32:107882. doi: 10.1016/j.celrep.2020.107882

Stoeckius, M., Hafemeister, C., Stephenson, W., Houck-Loomis, B., Chattopadhyay, P. K., Swerdlow, H., et al. (2017). Simultaneous epitope and transcriptome measurement in single cells. *Nat. Methods* 14, 865–868. doi: 10.1038/nmeth.4380

Svensson, V., Vento-Tormo, R., and Teichmann, S. A. (2018). Exponential scaling of single-cell RNA-seq in the past decade. *Nat. Protocols* 13, 599–604. doi: 10.1038/nprot.2017.149

Szabo, P. A., Levitin, H. M., Miron, M., Snyder, M. E., Senda, T., Yuan, J., et al. (2019). Single-cell transcriptomics of human T cells reveals tissue and activation signatures in health and disease. *Nat. Commun.* 10:4706. doi: 10.1038/s41467-019-12464-3

Thananchai, H., Gillespie, G., Martin, M. P., Bashirova, A., Yawata, N., Yawata, M., et al. (2007). Cutting edge: allele-specific and peptide-dependent interactions between KIR3DL1 and HLA-A and HLA-B. *J. Immunol.* 178, 33–37. doi: 10.4049/jimmunol.178.1.33

Villani, A.-C., Satija, R., Reynolds, G., Sarkizova, S., Shekhar, K., Fletcher, J., et al. (2017). Single-cell RNA-seq reveals new types of human blood dendritic cells, monocytes, and progenitors. *Science* 356:eaah4573. doi: 10.1126/science.aah4573

Vogel, C., and Marcotte, E. M. (2012). Insights into the regulation of protein abundance from proteomic and transcriptomic analyses. *Nat. Rev. Genet.* 13, 227–232. doi: 10.1038/nrg3185

Wu, R., Cheng, Y. J., Zhu, L. L., Yu, L., Zhao, X. K., Jia, M., et al. (2016). Impact of HLA-B*58:01 allele and allopurinol-induced cutaneous adverse drug reactions: evidence from 21 pharmacogenetic studies. *Oncotarget* 7, 81870–81879. doi: 10.18632/oncotarget.13250

Yao, C., Sun, H.-W., Lacey, N. E., Ji, Y., Moseman, E. A., Shih, H.-Y., et al. (2019). Single-cell RNA-seq reveals TOX as a key regulator of CD8(+) T cell persistence in chronic infection. *Nat. Immunol.* 20, 890–901. doi: 10.1038/s41590-019-0403-4

Zhang, M., Hu, S., Min, M., Ni, Y., Lu, Z., Sun, X., et al. (2020). Dissecting transcriptional heterogeneity in primary gastric adenocarcinoma by single cell RNA sequencing. *Gut* 70, 464–475. doi: 10.1136/gutjnl-2019-320368

Conflict of Interest: VGAS is proprietary software owned by Murdoch University who employ many of the lead authors.

The authors declare that the research was conducted in the absence of any commercial or financial relationships that could be construed as a potential conflict of interest.

frontiers in Immunology

MINI REVIEW
published: 29 June 2021
doi: 10.3389/fimmu.2021.653102

Drug and Chemical Allergy: A Role for a Specific Naive T-Cell Repertoire?

Rami Bechara[1], *Alexia Feray*[2] *and Marc Pallardy*[2]*

[1] Division of Rheumatology & Clinical Immunology, University of Pittsburgh, Pittsburgh, PA, United States, [2] Inflammation, Microbiome and Immunosurveillance, Université Paris-Saclay, INSERM, Châtenay-Malabry, France

Allergic reactions to drugs and chemicals are mediated by an adaptive immune response involving specific T cells. During thymic selection, T cells that have not yet encountered their cognate antigen are considered naive T cells. Due to the artificial nature of drug/chemical-T-cell epitopes, it is not clear whether thymic selection of drug/chemical-specific T cells is a common phenomenon or remains limited to few donors or simply does not exist, suggesting T-cell receptor (TCR) cross-reactivity with other antigens. Selection of drug/chemical-specific T cells could be a relatively rare event accounting for the low occurrence of drug allergy. On the other hand, a large T-cell repertoire found in multiple donors would underline the potential of a drug/chemical to be recognized by many donors. Recent observations raise the hypothesis that not only the drug/chemical, but also parts of the haptenated protein or peptides may constitute the important structural determinants for antigen recognition by the TCR. These observations may also suggest that in the case of drug/chemical allergy, the T-cell repertoire results from particular properties of certain TCR to recognize hapten-modified peptides without need for previous thymic selection. The aim of this review is to address the existence and the role of a naive T-cell repertoire in drug and chemical allergy. Understanding this role has the potential to reveal efficient strategies not only for allergy diagnosis but also for prediction of the immunogenic potential of new chemicals.

Keywords: naive T cells, drug allergy, hapten, thymic selection, TCR

OPEN ACCESS

Edited by:
Patricia Illing,
Monash University, Australia

Reviewed by:
Wen-Hung Chung,
Chang Gung Memorial Hospital, Taiwan
James Yun,
The University of Sydney, Australia

***Correspondence:**
Marc Pallardy
marc.pallardy@universite-paris-saclay.fr

Specialty section:
This article was submitted to Alloimmunity and Transplantation, a section of the journal Frontiers in Immunology

Received: *13 January 2021*
Accepted: *15 June 2021*
Published: *29 June 2021*

Citation:
Bechara R, Feray A and Pallardy M (2021) Drug and Chemical Allergy: A Role for a Specific Naive T-Cell Repertoire? Front. Immunol. 12:653102. doi: 10.3389/fimmu.2021.653102

INTRODUCTION

Adverse drug reactions (ADRs) are a major public health problem. Up to one third of ADRs are attributable to unpredictable drug hypersensitivity mediated by an adaptive immune response and named drug allergy. The consequences of drug and chemical allergy can be severe, including systemic adverse effects (1–3). T cells are central to allergic reactions. On one hand, drug-specific T cells provide the necessary help for mounting an effective B-cell response observed in immediate-type hypersensitivity reactions. On the other hand, T cells constitute the main pathogenic effector cells in delayed hypersensitivity reactions (4–6). Most studies have focused on the identification of memory T cells that recognize drugs/chemicals and the insights obtained have led to the

development of allergy diagnostic tests (7–21). However, attention has recently turned to the naive T-cell repertoire, since it may largely determine the efficacy of the induced immune response (22).

The aim of this review is to describe the role of the naive T-cell repertoire in drug and chemical allergy. We provide an overview of the data supporting different models of T-cell recognition of drugs and chemicals and discuss speculative models addressing the origin of drug/chemical responsive naive T cells.

NOTION OF NAIVE T CELL REPERTOIRE

The identification of lymphocytes as the main cell type responsible for both cellular and humoral immunity started in the early 1950s with the emergence of cell culture techniques. It is now clear that the ability of T cells to promote an effective immune response depends on a large repertoire of unique T-cell receptors (TCRs) generated and selected in the thymus. Indeed, T-cell precursors randomly and imprecisely rearrange V and J segments of the TCR alpha and V, D, and J segments of the TCR beta chains to create a complete TCR.

Estimation of the TCR repertoire diversity ranges from > 10^{20} (23) to 10^{61} (24, 25). Nevertheless, there are only an estimated 10^{12} T cells in the human body (26). Hence, TCR repertoire estimation vastly outnumbers the actual diversity of a person's TCR repertoire (27). This discrepancy is explained by thymic selection where the fate of T-cell precursors is dependent on the recognition of self-peptides (self-p) presented by MHC molecules on thymic stromal cells (28). The overall outcome of the thymic selection is the maintenance of a T-cell repertoire that has sufficient, but not too strong, affinity for any self-pMHC complex (29). T cells surviving thymic selection have not yet encountered their cognate antigen, and hence are considered naive T cells (25) (**Figure 1**). Typical naive T cells express CD45RA, the co-stimulatory molecule CD27 in addition to lymph node-homing receptors CD62L and CCR7 (30). However, similar to naive T cells, human stem cell-like memory T cells (Tscm) express CD45RA, CD62L and CCR7 (31) (**Figure 1**). In this case, the expression of the death receptor CD95 that is upregulated on Tscm is taken into consideration to distinguish them from naive T cells (31). In general, Tscm constitute around 2-4% of the total T-cell population in the periphery. Due to their self-renewal and long-term persistence, Tscm were studied in autoimmunity, cancer models and HIV-1 infections. However, their implication in drug allergy is less understood (32, 33).

In the periphery, naive T cells constantly circulate between secondary lymphoid organs and blood in pursuit of their specific antigens. During their journey, the fate of naive T cells is dictated by multiple checkpoints that maintain naive T cells in quiescence (34). Upon encountering antigen, naive T cells proliferate and differentiate into activated effector T cells as well as migrate to peripheral tissues (30). A loss of thymus productivity is observed during aging. However, the human naive T-cell repertoire is maintained by peripheral T-cell proliferation driven by homeostatic factors such as IL-7 and tonic TCR signaling mediated by self-pMHC recognition (35, 36).

HOW DO T CELLS RECOGNIZE DRUGS AND CHEMICALS?

Different studies have demonstrated that it is possible to detect drug/chemical-responding T cells in allergic patients (37–42). These T cells are activated following multiple non-mutually exclusive models, illustrating the puzzling features of TCR recognition by drugs/chemicals (43). In general, the mode of T-cell activation depends on the chemical properties of the molecule, the exposure conditions and the genetic background of the patient.

In the hapten model, drugs/chemicals or haptens bind to self-proteins to form a complex of a sufficient size to trigger an immune response. This structure is then processed by antigen-presenting cells (APCs) and the resulting haptenated peptides are presented through MHC class I or class II-dependent pathways to TCRs as *de novo* antigens (43, 44). Indeed, it is now well-accepted that MHC-restricted hapten-specific TCRs in their majority do not react to modified MHC molecules, but to haptenized peptides associated with the MHC peptide-binding groove (**Figure 1B**). Work conducted with synthetic hapten-peptide conjugates showed two major types of hapten-specific TCRs: one reacting to hapten without caring for the chemical composition of the carrier peptide, and the other contacting hapten and peptide by two apparently independent contact sites (44, 45).

In the pharmacologic interaction with immune receptors (p-i) model (**Figure 1C**), the drug binds non-covalently to either the TCR (p-i TCR) or MHC protein (p-i HLA) or to both in a peptide-independent manner to directly activate T cells (4, 46–49). Moreover, in the sulfamethoxazole (SMX) model of p-i TCR, molecular dynamics simulations studies showed that the drug may also bind to TCR at a position that is distant from the site of TCR-pMHC interaction, altering TCR conformation and resulting in higher affinity for self-pMHC (50). Several experimental evidence support the p-i model showing that some drugs can trigger T-cell activation without requiring intracellular antigen processing. This interaction leads to rapid T-cell-mediated reaction, which has features of hypersensitivity, and/or alloimmune and/or autoimmune reactions (4, 46–48).

The hapten hypothesis and the pi-concept did not provide a convincing mechanism explaining how abacavir induces adverse reactions through the activation of CD8+ T cells in a HLA-B*57:01-restricted manner (51). In this case, a new concept emerged: the altered peptide model. This model postulates that a small molecule can bind non-covalently to the MHC-binding cleft directly or in the endoplasmic reticulum (ER) and alter the specificity of peptide binding resulting in the presentation of novel peptide ligands (51–53). Using molecular dynamics simulations, recent studies demonstrated that abacavir may alter the conformational ensemble of these neo-peptides with the consequence of exposing peptide surfaces no longer recognized as self by circulating T cells (54). Peptides presented in this context

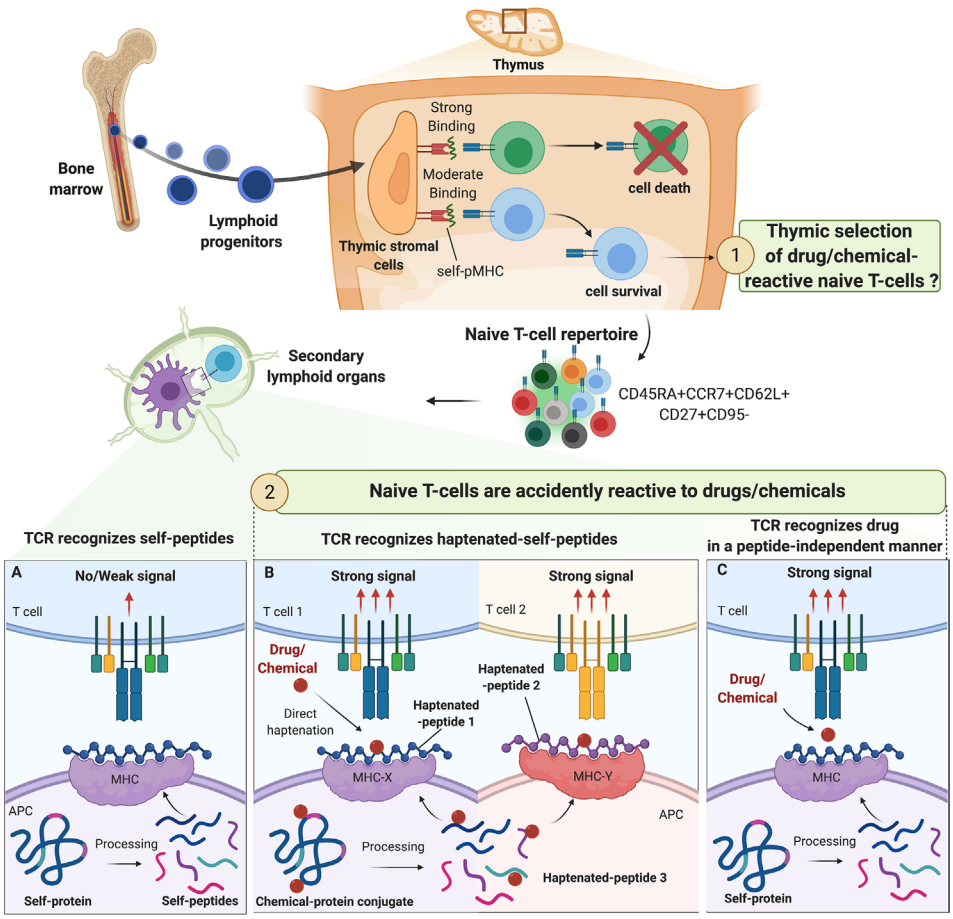

FIGURE 1 | Origin of drug/chemical-reactive naive T-cell repertoire. The fate of naive T-cell precursors is dependent on the recognition of self-peptides (self-p) presented by MHC molecules on thymic stromal cells. In the periphery, naive T cells expressing CD45RA, CD62L and CCR7 constantly circulate between secondary lymphoid organs and blood in pursuit of their specific antigens. The origin of drug/chemical responsive T cells is unclear but thymic selection of drug/chemical-specific naive T cells is unlikely. The process of central selection ensures that TCRs do not bind strongly to any self-pMHC molecules in the periphery, preventing autoimmune reactions **(A)**. Drugs/chemicals may alter self-pMHC complex and haptenated self-pMHC could have a high affinity for their corresponding TCR. Depending on chemical reactivity, multiple haptenated peptides can be generated from one self-protein allowing a diversity of association with different alleles and contributing to the high prevalence of immunization/allergy observed with some drug/chemicals (beta-lactams, skin sensitizers) **(B)**. In some cases, drugs/chemicals bind to MHC proteins in a peptide-independent manner to directly activate naive T cells mimicking the conditions of alloreactivity **(C)**.

are recognized as "foreign" by the immune system and therefore may elicit a T-cell response.

The clinical outcomes of drug or chemical allergic reactions could vary from contact dermatitis, maculopapular rashes to severe cutaneous adverse reactions and anaphylaxis, among others (1, 3, 47, 48, 55). Different T-cell recognition models can explain these multiple clinical outcomes. Contact hypersensitivity and IgE-mediated response are characterized by: 1) hapten-peptide formation, 2) dose-response effect of hapten, 3) recognition of peptide-hapten conjugates by specific TCRs and 4) rare HLA association with some allergens (13, 43, 44, 56, 57). For severe cutaneous adverse drug reactions (SCARs), the (p-i) model with drug binding to either the TCR (p-i TCR) or MHC (p-i HLA) results in T-cell activation (46). For the altered peptide repertoire model and Abacavir Hypersensitivity Syndrome, drugs bind non-covalently to regions of the HLA class I molecules within the antigen-binding cleft altering the repertoire of presented peptides and resulting in a polyclonal T-cell response (4, 52, 53, 58).

EVIDENCE AND CHARACTERIZATION OF A DRUG/CHEMICAL NAIVE T CELL REPERTOIRE

The presence of activated and memory T cells in drug/chemical allergic patients leads to the question of the origin of these drug/chemical-responsive T cells. Since a naive T-cell repertoire is mandatory for the induction of an antigen-specific T-cell response, extensive efforts were taken to characterize drug/

chemical-responsive naive T cells. T-cell priming assays provided valuable tools to detect these drug/chemical-responsive T cells (13, 59–61). Different approaches have been considered with respect to the populations of T cells and APCs used as well as the cell culture protocols and readouts (7–18, 62). Most protocols are relying on T-cell cloning performed by limiting dilutions with repetitive stimulation using APCs. Studies have tested hapten-modified dendritic cells (DCs) (12, 63) or haptenated self-proteins as an antigen source for purified naive T cells (18, 64, 65). In some protocols, regulatory T cells are removed from the co-culture system to increase the detection of weakly immunogenic drugs/chemicals (12, 60, 66). The presence of drug/chemical-responsive T cells is then detected most of the time using proliferation or cytokine production as endpoints. These approaches are not only useful to understand the mechanism of drug recognition but can also provide valuable insights for the replacement of animal testing (67). However, as expected, there are a number of problems associated with the analysis of rare antigen-specific T cells as T-cell priming assays present technical and conceptual limitations. Indeed, the high inter-donor variability limits the reliability and reproducibility of these assays. The choice of a reference protein for haptenization as well as the drug concentration used might govern the spectrum of T-cell responses. Moreover, artificial *in vitro* conditions used in these assays limit their *in vivo* relevance (67, 68).

In the early 1990s, Moulon et al. showed the ability of naive CD4+ T cells to respond to 2,4,6-trinitrobenzene sulfonic acid (TNBS), the water-soluble derivative of the contact allergen 2,4,6-trinitrochlorobenzene (TNCB) (7). These findings were further confirmed by different groups using TNBS or other chemicals (*e.g.*, nickel, Bandrowski's base, the oxidation product of p-phenylenediamine) (11, 16, 42, 61, 63, 69–72) as well as different drugs (*e.g.*, β-lactam antibiotics, SMX, dapsone, telaprevir) (18, 37, 38, 64, 65, 69, 73). Thus, the naive T-cell repertoire from every individual seems to harbor T cells able to recognize drugs and chemicals of different origins and structures. It is worth noting, that despite the presence of drug-responding T-cell repertoire in the large population, only few individuals develop allergic reactions due to additional susceptibility factors, reviewed elsewhere. (*e.g.*, HLA risk alleles, immune regulation, diseases) (55, 74, 75). Moreover, the concomitant presence of chemical-specific regulatory and effector T cells also suggests that for allergy to occur, additional signals need to be provided to break tolerance and to favor effector immune response (76).

The hapten hypothesis with binding of drug/chemical to self-proteins is the most common pathway by which chemicals (TNBS) and drugs (β-lactam and SMX) recognize and activate naive T cells (**Figure 1**). In these settings, T-cell response is dependent on (1) the presence of APCs, (2) MHC molecules, with anti-class I and II Abs blocking their activation and (3) an intact antigen processing mechanism. However, this concept was challenged with the identification of a nickel-responding naive T-cell repertoire (11, 63, 70). Indeed, nickel, like other transitional metal ions, cannot form covalent bonds with proteins. Hence, activation of nickel-specific naive T cells may not require antigen processing as seen with classical haptens (57, 77). Instead, nickel ions form coordination complexes predominantly with nitrogen residues in histidine or arginine (57). These observations suggest that organic chemicals need to bind to MHC-associated peptides to be recognized by TCR, whereas metal ions are recognized after forming non-covalent coordination bonds with MHC molecules, bound peptides and TCR.

Beyond the simple presence of drug/chemical-responding naive T cells, the question of their frequencies in relation with the different chemical classes is also an open question. Determination of antigen specific T-cell frequency relies on different techniques. The diversity of the techniques used such as HLA class II tetramers (78–80), libraries of polyclonal expanded naive T cells followed by antigen priming (81), repeated naive T-cell priming with antigen-loaded APCs or long-term T-cell priming (16, 18, 62, 63, 65, 69, 82–85) contributed to the heterogeneity of the results. Interestingly, a good concordance was found when addressing the frequency of strong immunogens such as keyhole limpet hemocyanin (KLH)-specific T-cells with these different techniques (86). When benzylpenicillin (BP)-specific T-cell frequency was evaluated after repeated stimulation with APCs loaded with BP bioconjugates, an estimated 0.3 to 0.6 pre-existing reactive naive T cells were detected in the blood of healthy donors per million of peripheral blood circulating CD4+ T cells (18, 65, 69). Using the same technique, 0.3 to 0.5 nickel-specific naive T cells were detected per million of circulating naive CD4+ T cells (63). These estimated frequencies can be considered very low as expected for hapten-naive specific T cells in healthy individuals (11). Surprisingly, this frequency of drugs/chemical-specific naive T cells was in the range of the one calculated for foreign antigens such as immunogenic therapeutic Abs (82), ovalbumin (82), and HIV peptide vaccine (87) but below the frequency found for KLH (18, 65, 82).

In addition to the number of naive T cells, the composition of the naive T-cell repertoire can shape immune responses. Advances in high-throughput sequencing technologies have enabled the detailed analysis of naive T-cell spectrum. A private T cell response is identified when the TCR specificity toward a specific epitope is rarely observed in multiple individuals. In contrast, some other antigen-specific TCRs are frequently observed in multiple individuals and generate a public T cell response (88). For instance, nickel or SMX-responding naive T cells were driven by public TCR present in all individuals as well as by T cell Receptor Beta Variable (TRBV) genes specific for each individual (63, 89). Historically, the presence of antigen-specific public TCR was observed in a variety of infectious and autoimmune diseases and turned out to be useful for the development of vaccines and therapeutic intervention (90). Recently, Pan et al. identified a public αβTCR from the cytotoxic T cells of patients with carbamazepine-mediated SCAR and a bias for HLA-B*15:02 was also reported (91). A likely hypothesis is a pi-concept response with a public TCR recognizing a small chemical antigen presented by the preferred HLA molecule from the preexisting memory T cells. However, the cause and the role of TCR sharing within the drug/chemical-reactive naive T-cell pool of multiple individuals is still poorly addressed (**Figure 2**).

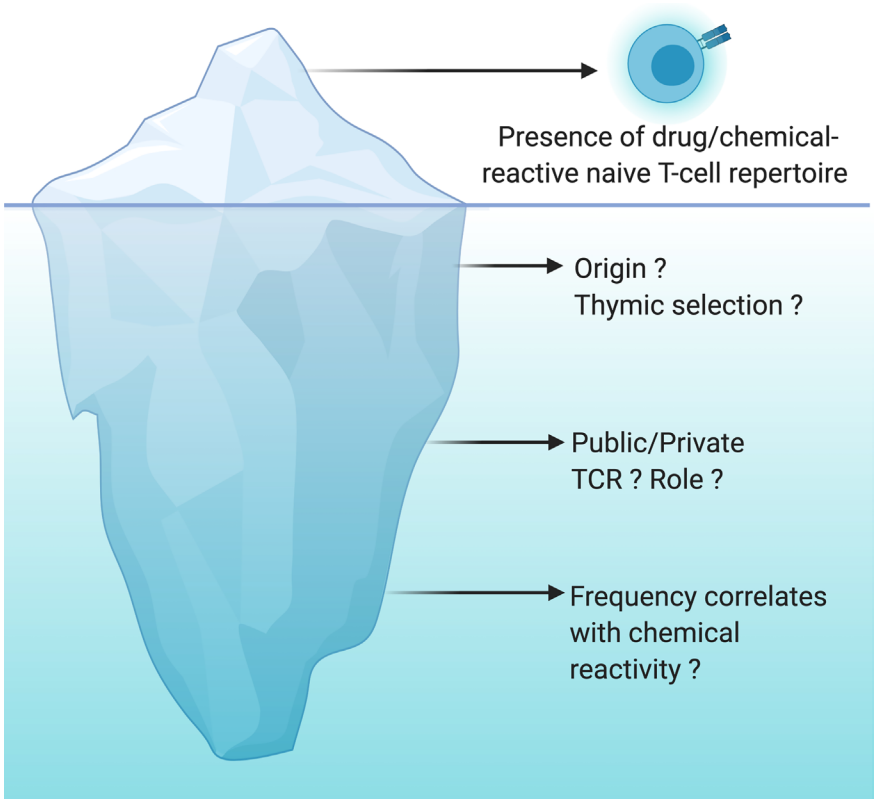

FIGURE 2 | Drug/chemical-reactive naive T-cell repertoire: the tip of the iceberg. The naive T-cell repertoire of every individual harbors T cells able to recognize drugs and chemicals of different origins and structures. This concept is now well recognized and accepted but is only the tip of the iceberg. However, the origin of these T cells, the nature of their TCR (public *vs* private) as well as the correlation between their frequency and their chemical reactivity are still largely unknown. The origin of these cells is not yet clearly determined, cross-reactivity with viral antigens or specific recognition of the chemical moiety bound to a self-peptide are a working hypothesis. Do we have specific TCRs that will be more likely to expand depending on the type of recognition by TCRs (peptide-drug bioconjugates and hapten, pi-concept)? Is the frequency of naïve T cells specific for drugs and chemicals very different between individuals? Is the frequency of these T cells constant with time suggesting a constant thymic selection of T cells capable of expanding upon recognition of a drug or a chemical? All these questions are still open and are the unknown part of the iceberg.

HYPOTHESIS FOR THE ORIGIN OF DRUG/CHEMICAL-RESPONDING NAIVE T-CELL REPERTOIRE

Although based on a limited number of tested drugs and experiments, we can now acknowledge that most, if not all, individuals harbor a naive T-cell repertoire for drugs and chemicals. However, while our understanding of the molecular mechanisms of TCR recognition by drugs/chemicals is expanding, the question of the mechanism driving the existence of drug/chemical-responding naive T-cell repertoire is still a challenge to be solved. Due to the artificial nature of drug-T-cell epitopes, it is unclear whether thymic selection of drug-specific T cells is a common phenomenon, remains limited to few donors, or simply does not exist. Selection of drug/chemical-specific T cells could be a relatively rare event accounting for the low occurrence of drug/chemical allergy. On the other hand, the large T-cell repertoire found in multiple donors underlines the potential of chemical/drug to be recognized by many donors. This latter hypothesis suggests that drugs/chemicals could be accidentally recognized by a TCR specific for another target.

Our immune system must be able to discriminate harmless non-self from dangerous non-self. There is multiple evidence that some chemicals have found very specific ways to activate the immune system by acting as danger signals (55, 64, 68, 92–102). Therefore, our immune system may have evolved to mount a specific defense mechanism avoiding prolonged exposure to reactive drugs/chemicals. Consequently, one can speculate that drug/chemical-reactive T cells are taking advantage of the imperfect central tolerance to reach the periphery and mount a protective immune response (**Figure 1**). However, there is no experimental evidence in favor of this hypothesis. It is more likely that the T-cell clones that are positively selected to recognize foreign antigens are accidently reactive with drugs or chemicals. Drugs/chemicals may alter self-pMHC complexes and haptenated self-pMHC have a high affinity for their corresponding TCR (**Figure 1B**). This concept was first elegantly described with trinitrophenyl (TNP)-reactive T cells in the context of mouse MHC-class I restricted responses (H-2K^b) (45, 56, 72, 103, 104).

This MHC class I typically harbors an octameric sequence with Phe or Tyr in position 5 and hydrophobic aliphatic amino acids in position 8 as anchors (45). As expected, this pMHC complex did not induce a strong cytotoxic T-cell response. Nevertheless, TNP-modification, mainly in position 4 of the peptide sequence, leads to CD8+ T-cell activation (45, 56). Thus, TCR recognized TNP mainly in the form of MHC-associated with haptenated peptides, and the immunodominant TNP epitopes were largely independent of the carriers' amino acid sequence. However, how drugs/chemicals increase the affinity of pMHC to TCR is largely unknown. Haptenation of a specific amino acid could block protease-mediated enzymatic processing and/or modify the peptide-binding affinity to the transporter associated with antigen processing (TAP) (43), thereby creating structurally distinct peptide-HLA complexes. In addition, in contrast to albumin-derived peptides, BP-haptenated peptides, derived from BP-albumin conjugate, can be recognized by multiple T-cell clones and like TNP-peptides, the position of the lysine modified by BP dictates the T-cell response (18, 64). In these settings, many T cells react to haptens in a MHC-restricted but carrier-independent fashion. Thus, drug/chemical protein modification results in a particularly repetitive array of cross-reactive, immunodominant determinants that may explain the unusual strong antigenicity of these compounds (22).

Chemical reactivity may dictate the number of different proteins or residues that are haptenated. High chemical reactivity may increase the number of generated T-cell epitopes and consequently may be translated into an increase in the number of recruited naive T cells bearing different TCRs (22). Consistently, it has been shown that strong contact sensitizers induced a polyclonal T-cell response (105). Similarly, β-lactam antibiotics covalently bind to lysine residues of many proteins (20, 21, 64, 106), generating multiple binding sites on proteins and expanding the number of haptenated peptides to be recognized by T cells (22). Moreover, binding on a specific amino acid such as lysine with BP can generate more than one immunogenic epitope demonstrating that drug conjugates have some TCR specificity (43). The consequence is an augmentation of the size of the repertoire of T cells involved in β-lactam recognition.

The situation for some drugs/chemicals (*e.g.*, carbamazepine, abacavir) may be somehow more restrictive (**Figure 1C**). Indeed a specific HLA, a drug-peptide complex and a unique TCR are the drivers of the T-cell response to certain drugs (51, 107). The most significant example is the association between abacavir hypersensitivity reaction and HLA-B*57:01 (51). Moreover, carbamazepine-specific T cells could be primed from PBMCs of healthy human donors, carriers of both HLA-B*15:02 and a specific TCR Vβ (108). It should be also noted that some drugs (*e.g.*, abacavir) may alter the intracellular processing of self-proteins and generate new antigenic determinants for TCRs that may not be removed from the naive T-cell repertoire during thymic selection. In these settings, naive T-cell activation may be perceived as an accident due to genetic predispositions or specific features of the molecule of concern.

Numerous patients suffering from allergic reactions are concomitantly treated for infections. Specifically, SMX-reactive T cells as well as Bandrowski's base-responding T cells could be primed from the memory pool of healthy donors (16). Thus, one can speculate that chemical or drug naïve T-cell repertoires are mainly pathogen-specific and in some cases, these T cells may have a high propensity to cross-react with drugs or chemicals (109). Indeed, T cells responding to abacavir were also shown to recognize herpes viruses such as HSV1/2 derived-peptides (110). Moreover, carbamazepine, allopurinol, or SMX-induced DRESS can be a result of cutaneous and systemic manifestations of CD8+ T cells directed against herpes virus antigens (109, 111).

In some cases, a nonspecific inflammation, independent of chemical/drug exposure, may be sufficient to bypass the general tolerance feature of naïve T cells, irrespective of their antigen specificity. Similarly, a break in immune tolerance due to co-inhibitory molecule blockade (*e.g.*, PD-1 and CTLA-4) enhanced the priming of naïve T cells to drugs (74, 89). These observations were consistent with clinical studies showing increased incidence of drug hypersensitivity reactions in patients receiving immune checkpoint inhibitor therapy (112, 113). Collectively, in these different situations, the immune system may be fooled by the presence of drugs or chemicals which could lead to immunopathology.

CONCLUDING REMARKS

It has been 30 years since the chemical-responsive naive T-cell repertoire was first described. Since then, multiple examples have been documented and there is no doubt that more will be uncovered. Not surprising anymore that drugs/chemicals, in their majority, seem to be recognized by the same molecular mechanisms as protein antigens. However, whether thymic selection of drug/chemical-specific T cells is a common phenomenon, remains limited to few donors, or simply does not exist is still unclear (**Figure 2**). If the naive T-cell repertoire contributes to drug/chemical allergy, then it is plausible that these reactions stem from *de novo* responses to the drug/chemical, where these specific T cells took advantage of the imperfect central tolerance to reach the periphery and mount a protective immune response. Yet, it is more likely that naive T cells are accidently reactive to a drug or a chemical. Several studies support the theory that chemical modification of self-proteins increases the affinity of self-pMHC to their cognate TCR or results in new antigenic determinants (**Figure 1**). Good progress has also been made in our mechanistic understanding of TCR recognition of drugs and chemicals (13, 43). However, less is known about the origin of these T cells, the nature of their TCR (public *vs* private) as well as the correlation between their frequency and the chemical reactivity (**Figure 2**). Answering these questions can be expected to open up new and exciting avenues for drug/chemical allergy.

AUTHOR CONTRIBUTIONS

RB, AF, and MP wrote the manuscript. All authors contributed to the article and approved the submitted version.

ACKNOWLEDGMENTS

Figures were made on BioRender.com.

REFERENCES

1. Hammond S, Thomson PJ, Ogese MO, Naisbitt DJ. T-Cell Activation by Low Molecular Weight Drugs and Factors That Influence Susceptibility to Drug Hypersensitivity. *Chem Res Toxicol* (2020) 33(1):77–94. doi: 10.1021/acs.chemrestox.9b00327
2. Vocanson M, Naisbitt DJ, Nicolas JF. Current Perspective of the Etiopathogenesis of Delayed-Type, and T-Cell-Mediated Drug-Related Skin Diseases. *J Allergy Clin Immunol* (2020) 145(4):1142–4. doi: 10.1016/j.jaci.2020.01.030
3. Wheatley LM, Plaut M, Schwaninger JM, Banerji A, Castells M, Finkelman FD, et al. Report From the National Institute of Allergy and Infectious Diseases Workshop on Drug Allergy. *J Allergy Clin Immunol* (2015) 136 (2):262–71.e2. doi: 10.1016/j.jaci.2015.05.027
4. Pichler WJ, Naisbitt DJ, Park BK. Immune Pathomechanism of Drug Hypersensitivity Reactions. *J Allergy Clin Immunol* (2011) 127(3 Suppl): S74–81. doi: 10.1016/j.jaci.2010.11.048
5. Amali MO, Sullivan A, Jenkins RE, Farrell J, Meng X, Faulkner L, et al. Detection of Drug-Responsive B Lymphocytes and Antidrug Igg in Patients With Beta-Lactam Hypersensitivity. *Allergy* (2017) 72(6):896–907. doi: 10.1111/all.13087
6. Rozieres A, Vocanson M, Said BB, Nosbaum A, Nicolas JF. Role of T Cells in Nonimmediate Allergic Drug Reactions. *Curr Opin Allergy Clin Immunol* (2009) 9(4):305–10. doi: 10.1097/ACI.0b013e32832d565c
7. Moulon C, Peguet-Navarro J, Courtellemont P, Redziniak G, Schmitt D. *In Vitro* Primary Sensitization and Restimulation of Hapten-Specific T Cells by Fresh and Cultured Human Epidermal Langerhans' Cells. *Immunology* (1993) 80(3):373–9.
8. Krasteva M, Peguet-Navarro J, Moulon C, Courtellemont P, Redziniak G, Schmitt D. *In Vitro* Primary Sensitization of Hapten-Specific T Cells by Cultured Human Epidermal Langerhans Cells–A Screening Predictive Assay for Contact Sensitizers. *Clin Exp Allergy* (1996) 26(5):563–70. doi: 10.1046/j.1365-2222.1996.d01-342.x
9. Dai R, Streilein JW. Naive, Hapten-Specific Human T Lymphocytes Are Primed *In Vitro* With Derivatized Blood Mononuclear Cells. *J Invest Dermatol* (1998) 110(1):29–33. doi: 10.1046/j.1523-1747.1998.00088.x
10. Rougier N, Redziniak G, Schmitt D, Vincent C. Evaluation of the Capacity of Dendritic Cells Derived From Cord Blood CD34+ Precursors to Present Haptens to Unsensitized Autologous T Cells *In Vitro*. *J Invest Dermatol* (1998) 110(4):348–52. doi: 10.1046/j.1523-1747.1998.00150.x
11. Rustemeyer T, De Ligter S, Von Blomberg BM, Frosch PJ, Scheper RJ. Human T Lymphocyte Priming *In Vitro* by Haptenated Autologous Dendritic Cells. *Clin Exp Immunol* (1999) 117(2):209–16. doi: 10.1046/j.1365-2249.1999.00958.x
12. Vocanson M, Cluzel-Tailhardat M, Poyet G, Valeyrie M, Chavagnac C, Levarlet B, et al. Depletion of Human Peripheral Blood Lymphocytes in CD25+ Cells Allows for the Sensitive *In Vitro* Screening of Contact Allergens. *J Invest Dermatol* (2008) 128(8):2119–22. doi: 10.1038/jid.2008.15
13. Martin SF, Esser PR, Schmucker S, Dietz L, Naisbitt DJ, Park BK, et al. T-Cell Recognition of Chemicals, Protein Allergens and Drugs: Towards the Development of *In Vitro* Assays. *Cell Mol Life Sci* (2010) 67(24):4171–84. doi: 10.1007/s00018-010-0495-3
14. El-Ghaiesh S, Monshi MM, Whitaker P, Jenkins R, Meng X, Farrell J, et al. Characterization of the Antigen Specificity of T-Cell Clones From Piperacillin-Hypersensitive Patients With Cystic Fibrosis. *J Pharmacol Exp Ther* (2012) 341(3):597–610. doi: 10.1124/jpet.111.190900
15. Naisbitt DJ, Nattrass RG, Ogese MO. *In Vitro* Diagnosis of Delayed-Type Drug Hypersensitivity: Mechanistic Aspects and Unmet Needs. *Immunol Allergy Clin North Am* (2014) 34(3):691–705. doi: 10.1016/j.iac.2014.04.009
16. Gibson A, Kim SH, Faulkner L, Evely J, Pirmohamed M, Park KB, et al. *In Vitro* Priming of Naive T-Cells With P-Phenylenediamine and Bandrowski's Base. *Chem Res Toxicol* (2015) 28(10):2069–77. doi: 10.1021/acs.chemrestox.5b00294
17. Moed H, von Blomberg M, Bruynzeel DP, Scheper R, Gibbs S, Rustemeyer T. Improved Detection of Allergen-Specific T-Cell Responses in Allergic Contact Dermatitis Through the Addition of 'Cytokine Cocktails'. *Exp Dermatol* (2005) 14(8):634–40. doi: 10.1111/j.0906-6705.2005.00344.x
18. Azoury ME, Fili L, Bechara R, Scornet N, de Chaisemartin L, Weaver RJ, et al. Identification of T-Cell Epitopes From Benzylpenicillin Conjugated to Human Serum Albumin and Implication in Penicillin Allergy. *Allergy* (2018) 73(8):1662–72. doi: 10.1111/all.13418
19. Castrejon JL, Berry N, El-Ghaiesh S, Gerber B, Pichler WJ, Park BK, et al. Stimulation of Human T Cells With Sulfonamides and Sulfonamide Metabolites. *J Allergy Clin Immunol* (2010) 125(2):411–8.e4. doi: 10.1016/j.jaci.2009.10.031
20. Meng X, Al-Attar Z, Yaseen FS, Jenkins R, Earnshaw C, Whitaker P, et al. Definition of the Nature and Hapten Threshold of the Beta-Lactam Antigen Required for T Cell Activation *In Vitro* and in Patients. *J Immunol* (2017) 198(11):4217–27. doi: 10.4049/jimmunol.1700209
21. Whitaker P, Meng X, Lavergne SN, El-Ghaiesh S, Monshi M, Earnshaw C, et al. Mass Spectrometric Characterization of Circulating and Functional Antigens Derived From Piperacillin in Patients With Cystic Fibrosis. *J Immunol* (2011) 187(1):200–11. doi: 10.4049/jimmunol.1100647
22. Esser PR, Kimber I, Martin SF. Correlation of Contact Sensitizer Potency With T Cell Frequency and TCR Repertoire Diversity. *Exp Suppl* (2014) 104:101–14. doi: 10.1007/978-3-0348-0726-5_8
23. Zarnitsyna VI, Evavold BD, Schoettle LN, Blattman JN, Antia R. Estimating the Diversity, Completeness, and Cross-Reactivity of the T Cell Repertoire. *Front Immunol* (2013) 4:485. doi: 10.3389/fimmu.2013.00485
24. Das J, Jayaprakash C. Systems Immunology: An Introduction to Modeling Methods for Scientists. In: *Foundations of Biochemistry and Biophysics*. Boca Raton, FL: CRC Press, Taylor and Francis Group (2019). p. 1.
25. de Greef PC, Oakes T, Gerritsen B, Ismail M, Heather JM, Hermsen R, et al. The Naive T-Cell Receptor Repertoire has an Extremely Broad Distribution of Clone Sizes. *Elife* (2020) 9:e49900. doi: 10.7554/eLife.49900
26. Arstila TP, Casrouge A, Baron V, Even J, Kanellopoulos J, Kourilsky P. A Direct Estimate of the Human Alphabeta T Cell Receptor Diversity. *Science* (1999) 286(5441):958–61. doi: 10.1126/science.286.5441.958
27. Laydon DJ, Bangham CR, Asquith B. Estimating T-Cell Repertoire Diversity: Limitations of Classical Estimators and a New Approach. *Philos Trans R Soc Lond B Biol Sci* (2015) 370(1675):20140291. doi: 10.1098/rstb.2014.0291
28. Klein L, Kyewski B, Allen PM, Hogquist KA. Positive and Negative Selection of the T Cell Repertoire: What Thymocytes See (and Don't See). *Nat Rev Immunol* (2014) 14(6):377–91. doi: 10.1038/nri3667
29. McDonald BD, Bunker JJ, Erickson SA, Oh-Hora M, Bendelac A. Crossreactive Alphabeta T Cell Receptors Are the Predominant Targets of Thymocyte Negative Selection. *Immunity* (2015) 43(5):859–69. doi: 10.1016/j.immuni.2015.09.009
30. van den Broek T, Borghans JAM, van Wijk F. The Full Spectrum of Human Naive T Cells. *Nat Rev Immunol* (2018) 18(6):363–73. doi: 10.1038/s41577-018-0001-y
31. Gattinoni L, Lugli E, Ji Y, Pos Z, Paulos CM, Quigley MF, et al. A Human Memory T Cell Subset With Stem Cell-Like Properties. *Nat Med* (2011) 17 (10):1290–7. doi: 10.1038/nm.2446
32. Flynn JK, Gorry PR. Stem Memory T Cells (TSCM)-Their Role in Cancer and HIV Immunotherapies. *Clin Transl Immunol* (2014) 3(7):e20. doi: 10.1038/cti.2014.16
33. Gattinoni L, Speiser DE, Lichterfeld M, Bonini C. T Memory Stem Cells in Health and Disease. *Nat Med* (2017) 23(1):18–27. doi: 10.1038/nm.4241
34. ElTanbouly MA, Noelle RJ. Rethinking Peripheral T Cell Tolerance: Checkpoints Across a T Cell's Journey. *Nat Rev Immunol* (2020) 21 (4):257–67. doi: 10.1038/s41577-020-00454-2
35. Egorov ES, Kasatskaya SA, Zubov VN, Izraelson M, Nakonechnaya TO, Staroverov DB, et al. The Changing Landscape of Naive T Cell Receptor Repertoire With Human Aging. *Front Immunol* (2018) 9:1618. doi: 10.3389/fimmu.2018.01618
36. Velardi E, Tsai JJ, van den Brink MRM. T Cell Regeneration After Immunological Injury. *Nat Rev Immunol* (2020) 21(5):277–91. doi: 10.1038/s41577-020-00457-z
37. Yaseen FS, Yaseen FS, Saide K, Kim SH, Monshi M, Tailor A, Wood S, et al. Promiscuous T-Cell Responses to Drugs and Drug-Haptens. *J Allergy Clin Immunol* (2015) 136(2):474–6.e8. doi: 10.1016/j.jaci.2015.02.036
38. Zhao Q, Alhilali K, Alzahrani A, Almutairi M, Amjad J, Liu H, et al. Dapsone- and Nitroso Dapsone-Specific Activation of T Cells From

Hypersensitive Patients Expressing the Risk Allele HLA-B*13:01. *Allergy* (2019) 74(8):1533–48. doi: 10.1111/all.13769
39. Sullivan A, Wang E, Farrell J, Whitaker P, Faulkner L, Peckham D, et al. Beta-Lactam Hypersensitivity Involves Expansion of Circulating and Skin-Resident TH22 Cells. *J Allergy Clin Immunol* (2018) 141(1):235–49.e8. doi: 10.1016/j.jaci.2017.01.020
40. Meng X, Earnshaw CJ, Tailor A, Jenkins RE, Waddington JC, Whitaker P, et al. Amoxicillin and Clavulanate Form Chemically and Immunologically Distinct Multiple Haptenic Structures in Patients. *Chem Res Toxicol* (2016) 29(10):1762–72. doi: 10.1021/acs.chemrestox.6b00253
41. Usui T, Whitaker P, Meng X, Watson J, Antoine DJ, French NS, et al. Detection of Drug-Responsive T-Lymphocytes in a Case of Fatal Antituberculosis Drug-Related Liver Injury. *Chem Res Toxicol* (2016) 29 (11):1793–5. doi: 10.1021/acs.chemrestox.6b00393
42. Cavani A, Mei D, Guerra E, Corinti S, Giani M, Pirrotta L, et al. Patients With Allergic Contact Dermatitis to Nickel and Nonallergic Individuals Display Different Nickel-Specific T Cell Responses. Evidence for the Presence of Effector CD8+ and Regulatory CD4+ T Cells. *J Invest Dermatol* (1998) 111(4):621–8. doi: 10.1046/j.1523-1747.1998.00334.x
43. Meng X, Yerly D, Naisbitt DJ. Mechanisms Leading to T-Cell Activation in Drug Hypersensitivity. *Curr Opin Allergy Clin Immunol* (2018) 18(4):317–24. doi: 10.1097/ACI.0000000000000458
44. Earnshaw CJ, Pecaric-Petkovic T, Park BK, Naisbitt DJ. T Cell Responses to Drugs and Drug Metabolites. *Exp Suppl* (2014) 104:137–63. doi: 10.1007/978-3-0348-0726-5_10
45. Weltzien HU, Moulon C, Martin S, Padovan E, Hartmann U, Kohler J. T Cell Immune Responses to Haptens. Structural Models for Allergic and Autoimmune Reactions. *Toxicology* (1996) 107(2):141–51. doi: 10.1016/0300-483X(95)03253-C
46. Pichler WJ, Adam J, Watkins S, Wuillemin N, Yun J, Yerly D. Drug Hypersensitivity: How Drugs Stimulate T Cells *via* Pharmacological Interaction With Immune Receptors. *Int Arch Allergy Immunol* (2015) 168(1):13–24. doi: 10.1159/000441280
47. Pichler WJ, Hausmann O. Classification of Drug Hypersensitivity Into Allergic, P-I, and Pseudo-Allergic Forms. *Int Arch Allergy Immunol* (2016) 171(3-4):166–79. doi: 10.1159/000453265
48. Pichler WJ. Immune Pathomechanism and Classification of Drug Hypersensitivity. *Allergy* (2019) 74(8):1457–71. doi: 10.1111/all.13765
49. Zanni MP, von Greyerz S, Schnyder B, Brander KA, Frutig K, Hari Y, et al. HLA-Restricted, Processing- and Metabolism-Independent Pathway of Drug Recognition by Human Alpha Beta T Lymphocytes. *J Clin Invest* (1998) 102(8):1591–8. doi: 10.1172/JCI3544
50. Watkins S, Pichler WJ. Sulfamethoxazole Induces a Switch Mechanism in T Cell Receptors Containing Tcrvbeta20-1, Altering Phla Recognition. *PLoS One* (2013) 8(10):e76211. doi: 10.1371/journal.pone.0076211
51. Mallal S, Nolan D, Witt C, Masel G, Martin AM, Moore C, et al. Association Between Presence of HLA-B*5701, HLA-DR7, and HLA-DQ3 and Hypersensitivity to HIV-1 Reverse-Transcriptase Inhibitor Abacavir. *Lancet* (2002) 359(9308):727–32. doi: 10.1016/S0140-6736(02)07873-X
52. Illing PT, Vivian JP, Dudek NL, Kostenko L, Chen Z, Bharadwaj M, et al. Immune Self-Reactivity Triggered by Drug-Modified HLA-Peptide Repertoire. *Nature* (2012) 486(7404):554–8. doi: 10.1038/nature11147
53. Ostrov DA, Grant BJ, Pompeu YA, Sidney J, Harndahl M, Southwood S, et al. Drug Hypersensitivity Caused by Alteration of the MHC-Presented Self-Peptide Repertoire. *Proc Natl Acad Sci USA* (2012) 109(25):9959–64. doi: 10.1073/pnas.1207934109
54. Fodor J, Riley BT, Kass I, Buckle AM, Borg NA. The Role of Conformational Dynamics in Abacavir-Induced Hypersensitivity Syndrome. *Sci Rep* (2019) 9 (1):10523. doi: 10.1038/s41598-019-47001-1
55. Pallardy M, Bechara R. Chemical or Drug Hypersensitivity: Is the Immune System Clearing the Danger? *Toxicol Sci* (2017) 158(1):14–22. doi: 10.1093/toxsci/kfx084
56. Martin S, Ortmann B, Pflugfelder U, Birsner U, Weltzien HU. Role of Hapten-Anchoring Peptides in Defining Hapten-Epitopes for MHC-Restricted Cytotoxic T Cells. Cross-Reactive TNP-Determinants on Different Peptides. *J Immunol* (1992) 149(8):2569–75.
57. Weltzien HU, Martin SF, Nicolas JF. T Cell Responses to Contact Allergens. *Exp Suppl* (2014) 104:41–9. doi: 10.1007/978-3-0348-0726-5_4
58. Adam J, Eriksson KK, Schnyder B, Fontana S, Pichler WJ, Yerly D. Avidity Determines T-Cell Reactivity in Abacavir Hypersensitivity. *Eur J Immunol* (2012) 42(7):1706–16. doi: 10.1002/eji.201142159
59. Usui T, Faulkner L, Farrell J, French NS, Alfirevic A, Pirmohamed M, et al. Application of *In Vitro* T Cell Assay Using Human Leukocyte Antigen-Typed Healthy Donors for the Assessment of Drug Immunogenicity. *Chem Res Toxicol* (2018) 31(3):165–7. doi: 10.1021/acs.chemrestox.8b00030
60. Ogese MO, Watkinson J, Lister A, Faulkner L, Gibson A, Hillegas A, et al. Development of an Improved T-Cell Assay to Assess the Intrinsic Immunogenicity of Haptenic Compounds. *Toxicol Sci* (2020) 175(2):266–78. doi: 10.1093/toxsci/kfaa034
61. Dietz L, Esser PR, Schmucker SS, Goette I, Richter A, Schnolzer M, et al. Tracking Human Contact Allergens: From Mass Spectrometric Identification of Peptide-Bound Reactive Small Chemicals to Chemical-Specific Naive Human T-Cell Priming. *Toxicol Sci* (2010) 117(2):336–47. doi: 10.1093/toxsci/kfq209
62. Faulkner L, Gibson A, Sullivan A, Tailor A, Usui T, Alfirevic A, et al. Detection of Primary T Cell Responses to Drugs and Chemicals in HLA-Typed Volunteers: Implications for the Prediction of Drug Immunogenicity. *Toxicol Sci* (2016) 154(2):416–29. doi: 10.1093/toxsci/kfw177
63. Bechara R, Pollastro S, Azoury ME, Szely N, Maillere B, de Vries N, et al. Identification and Characterization of Circulating Naive CD4+ and CD8+ T Cells Recognizing Nickel. *Front Immunol* (2019) 10:1331. doi: 10.3389/fimmu.2019.01331
64. Scornet N, Delarue-Cochin S, Azoury ME, Le Mignon M, Chemelle JA, Nony E, et al. Bioinspired Design and Oriented Synthesis of Immunogenic Site-Specifically Penicilloylated Peptides. *Bioconjug Chem* (2016) 27 (11):2629–45. doi: 10.1021/acs.bioconjchem.6b00393
65. Nhim C, Delluc S, Halgand F, de Chaisemartin L, Weaver RJ, Claude N, et al. Identification and Frequency of Circulating CD4(+) T Lymphocytes Specific to Benzylpenicillin in Healthy Donors. *Allergy* (2013) 68(7):899–905. doi: 10.1111/all.12173
66. Curotto de Lafaille MA, Lafaille JJ. Natural and Adaptive Foxp3+ Regulatory T Cells: More of the Same or a Division of Labor? *Immunity* (2009) 30 (5):626–35. doi: 10.1016/j.immuni.2009.05.002
67. Martin SF, Schmucker SS, Richter A. Tools and Methods for Identification and Analysis of Rare Antigen-Specific T Lymphocytes. *Exp Suppl* (2014) 104:73–88. doi: 10.1007/978-3-0348-0726-5_6
68. van Vliet E, Kuhnl J, Goebel C, Martinozzi-Teissier S, Alepee N, Ashikaga T, et al. State-of-the-Art and New Options to Assess T Cell Activation by Skin Sensitizers: Cosmetics Europe Workshop. *ALTEX* (2018) 35(2):179–92. doi: 10.14573/altex.1709011
69. Bechara R, Maillere B, Joseph D, Weaver RJ, Pallardy M. Identification and Characterization of a Naive CD8+ T Cell Repertoire for Benzylpenicillin. *Clin Exp Allergy* (2019) 49(5):636–43. doi: 10.1111/cea.13338
70. Lisby S, Hansen LH, Menn T, Baadsgaard O. Nickel-Induced Proliferation of Both Memory and Naive T Cells in Patch Test-Negative Individuals. *Clin Exp Immunol* (1999) 117(2):217–22. doi: 10.1046/j.1365-2249.1999.00967.x
71. Cavani A, Nasorri F, Ottaviani C, Sebastiani S, De Pita O, Girolomoni G. Human CD25+ Regulatory T Cells Maintain Immune Tolerance to Nickel in Healthy, Nonallergic Individuals. *J Immunol* (2003) 171(11):5760–8. doi: 10.4049/jimmunol.171.11.5760
72. Moulon C, Vollmer J, Weltzien HU. Characterization of Processing Requirements and Metal Cross-Reactivities in T Cell Clones From Patients With Allergic Contact Dermatitis to Nickel. *Eur J Immunol* (1995) 25(12):3308–15. doi: 10.1002/eji.1830251216
73. Alhilali KA, Al-Attar Z, Gibson A, Tailor A, Meng X, Monshouwer M, et al. Characterization of Healthy Donor-Derived T-Cell Responses Specific to Telaprevir Diastereomers. *Toxicol Sci* (2019) 168(2):597–609. doi: 10.1093/toxsci/kfz007
74. Naisbitt DJ, Olsson-Brown A, Gibson A, Meng X, Ogese MO, Tailor A, et al. Immune Dysregulation Increases the Incidence of Delayed-Type Drug Hypersensitivity Reactions. *Allergy* (2020) 75(4):781–97. doi: 10.1111/all.14127
75. Gibson A, Ogese M, Pirmohamed M. Genetic and Nongenetic Factors That May Predispose Individuals to Allergic Drug Reactions. *Curr Opin Allergy Clin Immunol* (2018) 18(4):325–32. doi: 10.1097/ACI.0000000000000459

76. Cavani A. Breaking Tolerance to Nickel. *Toxicology* (2005) 209(2):119–21. doi: 10.1016/j.tox.2004.12.021
77. Thierse HJ, Gamerdinger K, Junkes C, Guerreiro N, Weltzien HU. T Cell Receptor (TCR) Interaction With Haptens: Metal Ions as Non-Classical Haptens. *Toxicology* (2005) 209(2):101–7. doi: 10.1016/j.tox.2004.12.015
78. Obar JJ, Khanna KM, Lefrancois L. Endogenous Naive CD8+ T Cell Precursor Frequency Regulates Primary and Memory Responses to Infection. *Immunity* (2008) 28(6):859–69. doi: 10.1016/j.immuni.2008.04.010
79. Hataye J, Moon JJ, Khoruts A, Reilly C, Jenkins MK. Naive and Memory CD4+ T Cell Survival Controlled by Clonal Abundance. *Science* (2006) 312 (5770):114–6. doi: 10.1126/science.1124228
80. Moon JJ, Chu HH, Pepper M, McSorley SJ, Jameson SC, Kedl RM, et al. Naive CD4(+) T Cell Frequency Varies for Different Epitopes and Predicts Repertoire Diversity and Response Magnitude. *Immunity* (2007) 27(2):203–13. doi: 10.1016/j.immuni.2007.07.007
81. Geiger R, Duhen T, Lanzavecchia A, Sallusto F. Human Naive and Memory CD4+ T Cell Repertoires Specific for Naturally Processed Antigens Analyzed Using Libraries of Amplified T Cells. *J Exp Med* (2009) 206(7):1525–34. doi: 10.1084/jem.20090504
82. Delluc S, Ravot G, Maillere B. Quantitative Analysis of the CD4 T-Cell Repertoire Specific to Therapeutic Antibodies in Healthy Donors. *FASEB J* (2011) 25(6):2040–8. doi: 10.1096/fj.10-173872
83. Meunier S, Menier C, Marcon E, Lacroix-Desmazes S, Maillere B. CD4 T Cells Specific for Factor VIII Are Present at High Frequency in Healthy Donors and Comprise Naive and Memory Cells. *Blood Adv* (2017) 1 (21):1842–7. doi: 10.1182/bloodadvances.2017008706
84. Azam A, Gallais Y, Mallart S, Illiano S, Duclos O, Prades C, et al. Healthy Donors Exhibit a CD4 T Cell Repertoire Specific to the Immunogenic Human Hormone H2-Relaxin Before Injection. *J Immunol* (2019) 202 (12):3507–13. doi: 10.4049/jimmunol.1800856
85. Meunier S, de Bourayne M, Hamze M, Azam A, Correia E, Menier C, et al. Specificity of the T Cell Response to Protein Biopharmaceuticals. *Front Immunol* (2020) 11:1550. doi: 10.3389/fimmu.2020.01550
86. Maillere B. Comment on "The Role of Naive T Cell Precursor Frequency and Recruitment in Dictating Immune Response Magnitude". *J Immunol* (2013) 190(5):1895. doi: 10.4049/jimmunol.1290079
87. Castelli FA, Szely N, Olivain A, Casartelli N, Grygar C, Schneider A, et al. Hierarchy of CD4 T Cell Epitopes of the ANRS Lipo5 Synthetic Vaccine Relies on the Frequencies of Pre-Existing Peptide-Specific T Cells in Healthy Donors. *J Immunol* (2013) 190(11):5757–63. doi: 10.4049/jimmunol.1300145
88. Venturi V, Price DA, Douek DC, Davenport MP. The Molecular Basis for Public T-Cell Responses? *Nat Rev Immunol* (2008) 8(3):231–8. doi: 10.1038/nri2260
89. Gibson A, Faulkner L, Lichtenfels M, Ogese M, Al-Attar Z, Alfirevic A, et al. The Effect of Inhibitory Signals on the Priming of Drug Hapten-Specific T Cells That Express Distinct Vbeta Receptors. *J Immunol* (2017) 199(4):1223–37. doi: 10.4049/jimmunol.1602029
90. Li H, Ye C, Ji G, Han J. Determinants of Public T Cell Responses. *Cell Res* (2012) 22(1):33–42. doi: 10.1038/cr.2012.1
91. Pan RY, Chu MT, Wang CW, Lee YS, Lemonnier F, Michels AW, et al. Identification of Drug-Specific Public TCR Driving Severe Cutaneous Adverse Reactions. *Nat Commun* (2019) 10(1):3569. doi: 10.1038/s41467-019-11396-2
92. Antonios D, Rousseau P, Larange A, Kerdine-Romer S, Pallardy M. Mechanisms of IL-12 Synthesis by Human Dendritic Cells Treated With the Chemical Sensitizer Niso4. *J Immunol* (2010) 185(1):89–98. doi: 10.4049/jimmunol.0901992
93. Bechara R, Antonios D, Azouri H, Pallardy M. Nickel Sulfate Promotes IL-17A Producing CD4+ T Cells by an IL-23-Dependent Mechanism Regulated by TLR4 and Jak-STAT Pathways. *J Invest Dermatol* (2017) 137(10):2140–8. doi: 10.1016/j.jid.2017.05.025
94. Raffalli C, Clouet E, Kuresepi S, Damiens MH, Lepoittevin JP, Pallardy M, et al. Editor's Highlight: Fragrance Allergens Linalool and Limonene Allylic Hydroperoxides in Skin Allergy: Mechanisms of Action Focusing on Transcription Factor Nrf2. *Toxicol Sci* (2018) 161(1):139–48. doi: 10.1093/toxsci/kfx207
95. Sanderson JP, Naisbitt DJ, Farrell J, Ashby CA, Tucker MJ, Rieder MJ, et al. Sulfamethoxazole and its Metabolite Nitroso Sulfamethoxazole Stimulate Dendritic Cell Costimulatory Signaling. *J Immunol* (2007) 178(9):5533–42. doi: 10.4049/jimmunol.178.9.5533
96. Zhang X, Sharma AM, Uetrecht J. Identification of Danger Signals in Nevirapine-Induced Skin Rash. *Chem Res Toxicol* (2013) 26(9):1378–83. doi: 10.1021/tx400232s
97. Elzagallaai AA, Sultan EA, Bend JR, Abuzgaia AM, Loubani E, Rieder MJ. Role of Oxidative Stress in Hypersensitivity Reactions to Sulfonamides. *J Clin Pharmacol* (2020) 60(3):409–21. doi: 10.1002/jcph.1535
98. Schmidt M, Raghavan B, Muller V, Vogl T, Fejer G, Tchaptchet S, et al. Crucial Role for Human Toll-Like Receptor 4 in the Development of Contact Allergy to Nickel. *Nat Immunol* (2010) 11(9):814–9. doi: 10.1038/ni.1919
99. Rachmawati D, Bontkes HJ, Verstege MI, Muris J, von Blomberg BM, Scheper RJ, et al. Transition Metal Sensing by Toll-Like Receptor-4: Next to Nickel, Cobalt and Palladium Are Potent Human Dendritic Cell Stimulators. *Contact Dermatitis* (2013) 68(6):331–8. doi: 10.1111/cod.12042
100. Lopez S, Gomez E, Torres MJ, Pozo D, Fernandez TD, Ariza A, et al. Betalactam Antibiotics Affect Human Dendritic Cells Maturation Through MAPK/NF-Kb Systems. Role in Allergic Reactions to Drugs. *Toxicol Appl Pharmacol* (2015) 288(3):289–99. doi: 10.1016/j.taap.2015.08.001
101. Martin SF, Dudda JC, Bachtanian E, Lembo A, Liller S, Durr C, et al. Toll-Like Receptor and IL-12 Signaling Control Susceptibility to Contact Hypersensitivity. *J Exp Med* (2008) 205(9):2151–62. doi: 10.1084/jem.20070509
102. Esser PR, Wolfle U, Durr C, von Loewenich FD, Schempp CM, Freudenberg MA, et al. Contact Sensitizers Induce Skin Inflammation *via* ROS Production and Hyaluronic Acid Degradation. *PLoS One* (2012) 7(7):e41340. doi: 10.1371/journal.pone.0041340
103. Martin S, Weltzien HU. T Cell Recognition of Haptens, a Molecular View. *Int Arch Allergy Immunol* (1994) 104(1):10–6. doi: 10.1159/000236703
104. Kohler J, Hartmann U, Grimm R, Pflugfelder U, Weltzien HU. Carrier-Independent Hapten Recognition and Promiscuous MHC Restriction by CD4 T Cells Induced by Trinitrophenylated Peptides. *J Immunol* (1997) 158 (2):591–7.
105. Martin S, Delattre V, Leicht C, Weltzien HU, Simon JC. A High Frequency of Allergen-Specific CD8+ Tc1 Cells Is Associated With the Murine Immune Response to the Contact Sensitizer Trinitrophenyl. *Exp Dermatol* (2003) 12 (1):78–85. doi: 10.1034/j.1600-0625.2003.120110.x
106. Jenkins RE, Meng X, Elliott VL, Kitteringham NR, Pirmohamed M, Park BK. Characterisation of Flucloxacillin and 5-Hydroxymethyl Flucloxacillin Haptenated HSA *In Vitro* and *In Vivo*. *Proteomics Clin Appl* (2009) 3 (6):720–9. doi: 10.1002/prca.200800222
107. Adam J, Wuillemin N, Watkins S, Jamin H, Eriksson KK, Villiger P, et al. Abacavir Induced T Cell Reactivity From Drug Naive Individuals Shares Features of Allo-Immune Responses. *PLoS One* (2014) 9(4):e95339. doi: 10.1371/journal.pone.0095339
108. Ko TM, Chung WH, Wei CY, Shih HY, Chen JK, Lin CH, et al. Shared and Restricted T-Cell Receptor Use is Crucial for Carbamazepine-Induced Stevens-Johnson Syndrome. *J Allergy Clin Immunol* (2011) 128(6):1266–76.e11. doi: 10.1016/j.jaci.2011.08.013
109. White KD, Chung WH, Hung SI, Mallal S, Phillips EJ. Evolving Models of the Immunopathogenesis of T Cell-Mediated Drug Allergy: The Role of Host, Pathogens, and Drug Response. *J Allergy Clin Immunol* (2015) 136 (2):219–34; quiz 235. doi: 10.1016/j.jaci.2015.05.050
110. Yerly D, Pompeu YA, Schutte RJ, Eriksson KK, Strhyn A, Bracey AW, et al. Structural Elements Recognized by Abacavir-Induced T Cells. *Int J Mol Sci* (2017) 18(7):1464. doi: 10.3390/ijms18071464
111. Picard D, Janela B, Descamps V, D'Incan M, Courville P, Jacquot S, et al. Drug Reaction With Eosinophilia and Systemic Symptoms (DRESS): A Multiorgan Antiviral T Cell Response. *Sci Transl Med* (2010) 2(46):46ra62. doi: 10.1126/scitranslmed.3001116
112. Ford M, Sahbudin I, Filer A, Steven N, Fisher BA. High Proportion of Drug Hypersensitivity Reactions to Sulfasalazine Following its Use in Anti-PD-1-Associated Inflammatory Arthritis. *Rheumatol (Oxf)* (2018) 57 (12):2244–6. doi: 10.1093/rheumatology/key234
113. Phillips GS, Wu J, Hellmann MD, Postow MA, Rizvi NA, Freites-Martinez A, et al. Treatment Outcomes of Immune-Related Cutaneous

Adverse Events. *J Clin Oncol* (2019) 37(30):2746–58. doi: 10.1200/JCO.18.02141

Conflict of Interest: The authors declare that the research was conducted in the absence of any commercial or financial relationships that could be construed as a potential conflict of interest.

frontiers in Immunology

REVIEW
published: 06 August 2021
doi: 10.3389/fimmu.2021.676354

MRGPRX2 and Adverse Drug Reactions

Benjamin D. McNeil *

Division of Allergy and Immunology, Feinberg School of Medicine, Northwestern University, Chicago, IL, United States

Many adverse reactions to therapeutic drugs appear to be allergic in nature, and are thought to be triggered by patient-specific Immunoglobulin E (IgE) antibodies that recognize the drug molecules and form complexes with them that activate mast cells. However, in recent years another mechanism has been proposed, in which some drugs closely associated with allergic-type events can bypass the antibody-mediated pathway and trigger mast cell degranulation directly by activating a mast cell-specific receptor called Mas-related G protein-coupled receptor X2 (MRGPRX2). This would result in symptoms similar to IgE-mediated events, but would not require immune priming. This review will cover the frequency, severity, and dose-responsiveness of allergic-type events for several drugs shown to have MRGPRX2 agonist activity. Surprisingly, the analysis shows that mild-to-moderate events are far more common than currently appreciated. A comparison with plasma drug levels suggests that MRGPRX2 mediates many of these mild-to-moderate events. For some of these drugs, then, MRGPRX2 activation may be considered a regular and predictable feature after administration of high doses.

Keywords: MRGPRX2 receptor, anaphylaxis, mast cells, perioperative anaphylaxis, morphine, atracurium, vancomycin, rocuronium

OPEN ACCESS

Edited by:
Jason Trubiano,
University of Melbourne, Australia

Reviewed by:
Tao Zhang,
Xi'an Jiaotong University, China
Jeremy McComish,
Royal Melbourne Hospital, Australia

***Correspondence:**
Benjamin D. McNeil
benjamin.mcneil@northwestern.edu

Specialty section:
This article was submitted to Alloimmunity and Transplantation, a section of the journal Frontiers in Immunology

Received: *05 March 2021*
Accepted: *15 June 2021*
Published: *06 August 2021*

Citation:
McNeil BD (2021) MRGPRX2 and Adverse Drug Reactions. Front. Immunol. 12:676354. doi: 10.3389/fimmu.2021.676354

INTRODUCTION

Acute adverse reactions to therapeutic drugs are those which occur within minutes to hours of drug exposure, and many of these present clinically as allergic episodes (1, 2). Mild-to-moderate symptoms include rash, erythema, pruritus, tachycardia, local tissue swelling, moderate bronchospasm, transient hypotension, and gastrointestinal distress (3, 4). The most extreme of these reactions are classified as "anaphylaxis" and can be life-threatening; these include more severe hypotension, bronchospasm, and tissue swelling, and even collapse of the cardiovascular system (3, 4).

Most of these are assumed to be driven by activation of mast cells by drug-specific Immunoglobulin E (IgE) antibodies, which are called Type I immediate hypersensitivity reactions (1, 2, 5). Prior exposure to the drug, or to a compound with a structurally similar element, stimulates production of antibodies that recognize the drug or a conjugate formed when the drug or a metabolite binds to an endogenous protein. These antibodies then associate with

high-affinity IgE receptors on the surface of mast cells in a manner that leaves their drug-binding sites free. When a drug recognized by the antibodies is administered, it (or the conjugate) binds to multiple antibodies at the same time. This brings the IgE receptors associated with the antibodies into prolonged close contact, triggering activation of the receptors and the release of mediators like histamine that generate the allergic responses (6).

Another cause of acute mast cell activation has been proposed, in which drugs trigger reactions very similar to Type I events – but without the need for antibodies or immune priming – by activating mast cells directly through a receptor called Mas-related G protein-coupled receptor X2 (MRGPRX2). MRGPRX2 is a seven transmembrane G protein-coupled receptor which is expressed almost exclusively by a subset of mast cells that populate connective tissues like the skin (7, 8). It is classified as an orphan receptor (9), meaning that the ligand(s) it is intended to recognize has not been determined. However, multiple screens with hundreds of small molecules, peptides, and proteins have established that it is responsive to a wide range of molecules, and that the overwhelming majority of them carry a net cationic, or positive, charge (8, 10–14). A recent review identified that most also have bulky hydrophobic groups, perhaps to increase affinity for plasma membranes (15). In 2015 a study reported that several therapeutic drugs with cationic groups, all of which induce high rates of allergic-type reactions, are agonists for MRGPRX2 (12). Moreover, activation of a cell line called LAD2, which has properties similar to human mast cells and often is used as a surrogate because primary cells are very difficult to extract, was dependent upon MRGPRX2 (12). Other drugs capable of activating MRGPRX2 have since been found, many of which also trigger allergic-type events. This finding raises the possibility that side effects that appear to be Type I – i.e., allergic and IgE-mediated – may in some cases arise instead from direct activation of mast cells through MRGPRX2. Such events have been called "pseudo-allergic" or "anaphylactoid" to distinguish them from true allergies. All events that present as allergic episodes will be referred to as "allergic-type" in this review, as the etiology is not always clear.

This review will present an analysis of the frequencies of allergic-type events for many drugs/MRGPRX2 agonists that are particularly closely associated with such events. Calculated EC_{50} values for MRGPRX2, compiled from several studies, are presented in **Table 1** (12–14, 16–19). Two specific issues are addressed for each drug: 1.) whether the mild-to-moderate events truly are mast cell-mediated; and 2.) whether MRGRPX2 involvement is supported. The first issue is important because, while anaphylaxis elicits a stereotyped and coordinated set of symptoms with a clear mast cell origin, the milder events only include some of these, and mast cell activation is not the only possible cause of the symptoms. The second issue, of whether MRGPRX2 is involved, is impossible to prove without specific antagonists. However, if events are much more common only when plasma levels are high enough to activate MRGPRX2, it certainly supports a role for this receptor. Therefore, plasma concentrations are provided for each drug. A more detailed discussion on methods of distinguishing IgE from MRGPRX2 or other non-IgE origins is provided in Section II.

The most surprising finding from this analysis is that mild-to-moderate allergic-type events can be very frequent, much more so than generally presumed. These events generally are neglected in favor of anaphylactic episodes, which are much more serious but are extremely rare. In contrast, mild-to-moderate events have been reported to occur in a majority of patients at some drug dosages. These are not trivial and may have serious impacts on health when patients already are highly compromised. Peak drug plasma concentrations support MRGPRX2 involvement in these events for several drugs; this suggests that MRGPRX2 activation might be considered a common, not a rare, feature when these drugs are administered.

TABLE 1 | Calculated EC50 values for selected MRGPRX2 agonists.

Name	EC_{50}	Reference
Vancomycin	~ 60 micrograms/ml	(14)
Atracurium	28.6 micrograms/ml	(12)
Mivacurium	39 micrograms/ml	(16)
Cisatracurium	103 micrograms/ml	(17)
Rocuronium	261 micrograms/ml	(12)
Morphine	4.5 - 7 micromolar (1.3 – 2.0 micrograms/ml)	(13, 18, 19)
Ciprofloxacin	6.8 micrograms/ml	(12)
Levofloxacin	22.7 micrograms/ml	(12)
Moxifloxacin	9.9 micrograms/ml	(12)

DETERMINATION OF IGE- *VS.* MRGPRX2-MEDIATED MAST CELL ACTIVATION

A pressing issue in the field is how to determine whether mast cell activation is mediated by IgE or MRGPRX2 when a patient has suffered an allergic-type event due to a drug that is an MRGPRX2 agonist. These drugs also may be immunogenic, so simply exhibiting MRGPRX2 agonism does not rule out IgE. Technically, distinguishing between these is not yet possible because there are no biomarkers that reliably identify or exclude one or the other mechanism, such as a mediator only released after stimulation of one but not the other receptor. However, specific measurements can be made that support the involvement of each pathway.

MRGPRX2 Involvement

MRGPRX2 should be suspected if an event is *only* observed at concentrations high enough to activate the receptor, and resolves when the concentration drops below this. As described in detail in th next section, the drug concentrations needed to activate MRGPRX2 are very high and only achieved transiently for most drugs. Many allergic-type reactions also are very transient and only occur at very high drug concentrations. In contrast, there is a widespread assumption that IgE-mediated mast cell activation occurs even at very low concentrations of an antigen – for example, food allergies only require miniscule amounts of food- though this is not proven for every allergy. Another factor is that mediator release after IgE-driven mast cell activation persists for much longer than after antibody-independent mast cell stimulation (20), so events that are short-lived are less likely to be IgE-driven,

especially if they only occur at high drug concentrations and disappear when plasma or tissue concentrations drop below EC_{50} values for MRGPRX2.

EC_{50} values for MRGPRX2 can be used to determine whether plasma or tissue drug concentrations are high enough to activate the receptor. However, several additional factors should be considered when evaluating these. First, plasma concentration measurements may not reflect concentrations in some tissues; specific examples are discussed in the fluoroquinolones and neuromuscular blocking drug sections. Second, EC_{50} values must be taken in context, as caveats exist. The values were calculated for the most common MRGPRX2 variant, but dozens of others with slightly different amino acid compositions, due to natural variations in the coding DNA, have been identified (21, 22). These sometimes have altered properties; most of the ones characterized are loss-of-function, but ones with enhanced signaling have also been reported (23, 24). It is quite possible that alleles that respond to much lower drug concentrations are expressed by some patients, and if so, EC_{50} values for those variants should be used instead. Also, MRGPRX2 expression levels vary tremendously between subjects (25), and those with abnormally high expression may also respond to low drug concentrations, even when the canonical receptor variant is expressed. Another consideration is that EC_{50} values usually are calculated in cell lines, not in primary cells. Finally, concurrent illnesses may either enhance or reduce mast cell responsiveness, or how tissues respond to mast cell mediators. An example is provided below in the vancomycin section, in which bacterial infections appear to dramatically reduce systemic mast cell responses. On the other hand, patients with chronic spontaneous urticaria appear to have much stronger responses to MRGPRX2 agonists (26). This is an emerging topic and more research needs to be performed, but it is clear that comorbidities can have a profound influence on allergic-type reactions.

IgE Involvement

IgE-mediated mast cell activation should be suspected when events occur at low drug concentrations, when the events are of long duration, or when drug-specific IgE titers are high. Four tests are recognized by the World Allergy Organization to help determine whether a patient has drug-specific IgE antibodies: a skin prick test, intradermal injection of the drug, plasma or serum IgE quantification, and basophil activation tests (27). Protocols are not standardized, and interpretation of the results can be quite controversial (28, 29). Of these, skin prick and intradermal injection tests are, by far, the most common methods for identifying IgE involvement. The concept behind them is that concentrations are too low to activate MRGPRX2, but are sufficient to trigger IgE reactions. However, concentrations are not standardized and in many cases likely are enough to activate MRGPRX2 – for instance, a commonly-used skin prick test concentration for morphine and atracurium is 1 mg/ml (30), dozens of times higher than their EC_{50} values for MRGPRX2 activation (**Table 1**). Intradermal concentrations generally do not exceed these values, though morphine is recommended at 10 micrograms/ml, over 5 times higher than its EC_{50} value. As mentioned above, MRGPRX2 variants may have greater sensitivity and may trigger signaling at even lower drug concentrations. Even when several tests are used, the results can be equivocal. In one study, all four tests were conducted in each of 140 instances of anaphylaxis after administration of the neuromuscular blocker rocuronium (31). Strikingly, the tests all were in agreement in less than 15% of the cases. This is not meant to imply that IgE tests are not useful, only that they are not yet optimized, and that tests for MRGPRX2 involvement should be conducted, as well.

Unfortunately, the assays described for MRGPRX2 and IgE essentially never are conducted together. Plasma drug concentrations and MRGPRX2 allele analysis are almost exclusively limited to controlled experiments in which mild-to-moderate but not anaphylactic events are observed. Conversely, IgE tests are used as a diagnostic only after anaphylactic episodes. Until they are all performed in tandem, even a perfect IgE test cannot rule out MRGPRX2; likewise, evidence of extraordinarily high drug concentrations cannot rule out IgE. It even seems quite plausible that both can operate together in some cases. It is hoped that future studies with a more comprehensive approach will be undertaken to help clarify this matter, particularly in cases of anaphylaxis.

ALLERGIC-TYPE ADVERSE EVENT FREQUENCIES AND ANALYSIS

This section summarizes and analyzes the available data on allergic-type event frequency for several drugs known to have MRGPRX2 agonist properties. It also discusses evidence for and against a mast cell origin for these events, as well as peak plasma drug concentrations to help evaluate whether MRGPRX2 plays a role when mast cells are involved. Plasma drug concentrations are almost totally unknown in patients who have suffered anaphylactic episodes, so correlations cannot be made for these events.

Vancomycin

Vancomycin is a glycopeptide antibiotic used for difficult-to-treat Gram-positive bacterial infections like methicillin-resistant *Staphylococcus aureus* (32, 33). It is given orally or, more frequently, intravenously as a slow infusion, and is closely associated with allergic-type reactions – often regrettably described as "Red Man Syndrome" – that begin during or shortly after infusion (34).

Allergic-Type Event Frequency and Mast Cell Dependence

Allergic-type reactions are the most common side effects of vancomycin, and are characterized by erythema of the head and neck, hypotension, tachyphylaxis, pruritus, and occasional angioedema (33, 35, 36). These usually are associated with elevated plasma histamine (37–41), and often can be mitigated by antihistamines (42–46), confirming mast cell involvement in these reactions.

The reported frequency of allergic-type reactions is highly variable, with most studies reporting either 5% or less [e.g (47–54)] or over 70% [e.g (38–40, 42, 46, 49, 55–57)]. No systematic differences in dosage exist between the high and low incidence studies, suggesting that other factors were responsible for this

vast disparity. Notably, with very rare exceptions (43, 58), the studies reporting high incidence rates were conducted specifically to examine side effects, while the studies with low rates were designed to assess antibacterial efficacy. It is plausible that the different aims resulted in different thresholds for what constituted a medically relevant side effect.

Another difference between the high and low incidence studies is the makeup of the study populations. The high incidence studies examined healthy subjects or hospital patients without infections, while the low incidence studies were almost all of patients with severe bacterial infections. Mast cells can be activated by bacteria (59), and it is possible that persistent activation during infection leads to mast cell desensitization to further stimuli, and/or systemic desensitization to mast cell mediators. In support of this, one small study compared responses in healthy volunteers to those in infected patients, and found that no infected patients had any reactions, while nearly all of the healthy controls did (49). No definitive conclusion can be drawn yet, but the inverse correlation between infection and mast cell responsiveness appears to be quite strong.

In a massive study of over four million patients given vancomycin, anaphylaxis was reported to occur with a frequency of 0.018%, or approximately 1 in 5000 (54).

Peak Plasma Concentrations and Potential MRGPRX2 Involvement

Vancomycin is a weak agonist, with a calculated EC_{50} of about 60 micrograms/ml (14). Recorded peak plasma levels of vancomycin cluster around the 30-50 micrograms/ml range, which is enough to activate mast cells but not to a large extent. Patients with more severe reactions may have plasma levels on the upper end of this range – indeed, levels exceeding 70 micrograms/ml have been reported (55). Importantly, most measurements were taken after the infusion was complete and they may underreport the actual peak. Small differences in concentration are important when considering MRGPRX2 activation, as the reported dose-response curve in cell lines is very steep (14) and slight changes can have large effects. For example, in one study, reducing the average peak concentration from 65.7 to 40.3 micrograms/ml was sufficient to completely abolish all allergic-type reactions (55). Plasma drug levels and MRGPRX2 allele expression were not recorded in the large study that calculated anaphylaxis rates (54), so no correlations are available.

Atracurium, Cisatracurium, and Mivacurium

These all are non-depolarizing neuromuscular blocking drugs (NMBDs). NMBDs are routinely used during surgical procedures to facilitate tracheal intubation of breathing tubes, and to reduce aberrant muscle activity during the surgeries. They bind to and block acetylcholine receptors expressed by muscles, preventing innervation by nerves (60). High doses of atracurium and mivacurium are associated with allergic-type side effects (61); these are much less frequent after cisatracurium administration (62, 63), which may be due to the fact that relatively low doses are used.

Allergic-Type Event Frequency and Mast Cell Dependence

Non-depolarizing NMBDs are associated with flushing, erythema, and hypotension (61). Preclinical studies suggested that high doses of atracurium would cause hypotension and histamine release in patients (64). This was indeed the case – after rapid injection of 0.5 mg/kg or more, elevated histamine levels in the plasma were recorded (65–69), drops in mean arterial blood pressure (MAP) of at least 20% were observed in most studies, and this could be blocked by pre-treatment with a combination of H1 and H2 histamine receptor antagonists (65–68). Flushing or erythema also were blocked in studies that monitored this AE (66, 69). The choice of antihistamine may be important, as some can counteract their own effects by blocking the enzyme that breaks down histamine, which would elevate histamine levels (65). One study demonstrated that the anesthetic thiopental, commonly used with atracurium, also can cause a drop in MAP, and suggested that this is the primary reason for the drop (69). However, this does not explain the cases where thiopental was not used (68) or was administered well before atracurium (66, 67), nor does it explain why the drop in MAP could be abolished by slowing down the atracurium injection time (65, 66), which would produce a lower peak plasma concentration. Taken together, the data strongly suggest that the immediate drop in MAP and cutaneous allergic-type effects, the primary side effects of atracurium, are caused by mast cell activation.

Mivacurium injection is associated with elevated plasma histamine levels, flushing/erythema, and drops in mean arterial pressure (MAP) of greater than 20%, which all correlate with the speed of injection and drug dose. Elevated histamine levels were frequently observed when measured, sometimes in more than 50% of patients (70–73). Flushing/erythema has been observed in from 6% to 73% of patients (70–72, 74–82). MAP changes also occur at a lesser frequency, from 0% to 50% (70, 72, 73, 77, 80–83). Studies that examined all at once found that MAP changes nearly always were accompanied by flushing and histamine release (70, 73, 78). Antihistamines block all these effects (72, 78). It should be noted that occasional studies only reported average changes in histamine levels and/or mean arterial pressure, which sometimes did not achieve significance as a group (71, 79, 82, 84). This does not mean that zero patients in the group suffered from an AE. The heterogeneity of responses, compared to atracurium, likely stems from the variety of mivacurium doses and speeds of injection.

Cisatracurium is very rarely associated with allergic-type side effects, with incidence rates of 0.5% or less (62, 63), even in patients with existing cardiovascular morbidity (85). Elevated plasma histamine levels, though usually mild, have been recorded after high doses (0.2 mg/kg or more) of cisatracurium in approximately 5-10% of patients, so it is possible that the allergic-type events are indeed mast cell-mediated (86–89).

Recent studies have estimated the incidence of atracurium-induced anaphylaxis at approximately 1 in 20,000-50,000 (90–93). Anaphylactic episodes after cisatracurium administration are exceedingly rare, as low as 1 in 250,000 (92), though data are not common and estimates are not necessarily representative. Anaphylaxis after mivacurium was estimated as occurring in less

than 1 in 1,000,000 administrations in a recent study (90), though, as with cisatracurium, data are relatively sparse, compared to rocuronium and atracurium. Plasma drug levels and MRGPRX2 allele data are not available for these events.

Peak Plasma Concentrations and Potential MRGPRX2 Involvement

Peak recorded plasma concentrations after rapid atracurium injections are usually less than 10 microgram/ml range, even when high concentrations of 0.5 mg/ml or more are administered (94, 95). This is lower than the calculated EC_{50} for MRGPRX2 of 28.6 micrograms/ml (12), and it is not clear from intradermal injection studies that mast cells respond to lower concentrations (96). However, even though measurements were taken 1-2 minutes after injection, there is reason to believe that these are not truly peak plasma or interstitial concentrations. Two studies found that extending injection times from 5-30 seconds to 75 seconds was sufficient to abolish most AEs (65, 66). This suggests that rapid injections produce plasma or interstitial concentrations somewhere in the body that are enough to activate mast cells; these are achieved for only several seconds and a very slight reduction in injection speed is enough to prevent this. These might not be captured in blood samples, even shortly after injection; notably, the cited pharmacokinetic studies did not include information about injection speed.

Peak reported plasma concentrations of the combined isomers of mivacurium cluster in the 3 to 10 micrograms/ml range when measurements are taken within a few minutes of injection (97–101). These also are too low for efficient activation of MRGPRX2, if the recorded EC_{50} of 39.0 micrograms/ml is accurate (16), and skin tests provide little evidence for activation at lower concentrations. Interestingly, 10-15 second injection times produced far more AEs than when administration was 30 seconds or more (70, 77, 80). This suggests that, as with atracurium, the true peak plasma and/or interstitial concentrations may be missed by the recordings.

Data on peak cisatracurium plasma concentrations are relatively scarce, but usually are less than 2 micrograms/ml (102, 103). This is far below the calculated EC_{50} of 103 micrograms/ml (17). These seem to be too far apart to consider any side effects to be MRGPRX2-related. However, skin reactions to intradermal cisatracurium have been observed at 12 micrograms/ml (104, 105), and LAD2 cell activation by cisatracurium is dependent on MRGPRX2 (17), so it is possible that the EC_{50} for primary mast cells may be lower.

Rocuronium

Rocuronium is a member of the aminosteroid group of NMBDs that, like atracurium, acts as a muscle nicotinic receptor antagonist (60). Its onset is only slightly slower than the fastest-acting NMBD, succinylcholine, while its duration is longer (106). One attractive reason to use rocuronium is that its effects can be reversed rapidly by administering sugammadex, which binds to and inactivates rocuronium (107) and allows for precise control over paralysis. Unlike atracurium, very few adverse events related to off-target activity like mast cell degranulation are reported (106, 108–111). Somewhat surprisingly, the incidence of anaphylactic reactions, while still rare, has been estimated in some studies as being higher after administration of rocuronium that of most other NMBDs (91, 93).

Allergic-Type Event Frequency and Mast Cell Dependence

The most commonly-reported acute side effect specifically associated with rocuronium is tachycardia (112). Tachycardia, or increase in heart rate, has been observed with histamine-releasing drugs, but in the case of rocuronium, this is thought to be caused by off-target block of acetycholine receptors that regulate cardiac pacemaker activity (112). In fact, elevated histamine levels are extremely rare (72, 73, 113) and immediate hypersensitivity events are not observed in the vast majority of patients (108–111), though occasional mild skin reactions do occur (72). Estimates of anaphylaxis are highly variable (90, 114, 115) but are as high as 1 in 2500-4000 patients (91, 92, 116).

One plausible mast cell-related AE is an injection site reaction, which occurs in up to 80% of patients given rocuronium (106). However, while intravenous rocuronium can cause a local rash (117), intravenous and intradermal rocuronium injections are associated not with itch – typical of mast cell-driven reactions – but with sharp pain and involuntary limb withdrawal (118, 119). One study in mice suggests that rocuronium directly activates skin C-fibers, which transmit noxious sensations like pain (119). This apparently is pH-dependent, as neutralizing its pH from 3.5 to 7.4 abolished pain sensation in one human study (120). Another study reported that pain was reduced after pretreatment with the antihistamine chlorpheniramine maleate (121). However, it is quite possible that this is due to off-target activity, as the dosage given was 10 times higher than the standard amount and also was given as an intravenous bolus, which results in extremely high plasma concentrations, compared to an equivalent oral dose (122). In sum, mast cells may play a role in injection site reactions, but it seems likely that other mechanisms also contribute.

Peak Plasma Concentrations and Potential MRGPRX2 Involvement

Peak recorded plasma concentrations of rocuronium within a few minutes after rapid injection are between 6-15 micrograms/ml (123–128). The calculated EC_{50} for MRGRPX2 activation is 261 micrograms/ml (12), so even with the caveat that plasma concentration measurements underestimate the peak when taken after infusion, it seems impossible that MRGPRX2 could be systemically activated. This readily explains why histamine-associated AEs are so rare. MRGPRX2 alleles and drug concentrations are generally not available for patients who have suffered anaphylactic episodes. One study identified expression of an allele in one patient (129), though this does not appear to increase receptor sensitivity (130).

Injection site reactions may involve MRGPRX2. Rocuronium is supplied as a 10 mg/ml injection solution, which is much higher than the reported EC_{50} for MRGPRX2 of 261 micrograms/ml (12), and the threshold for evoking wheal and

flare after intradermal injection is as low as 61 micrograms/ml (104). Local leakage of the drug into the area surrounding the injection site may trigger MRGPRX2-mediated mast cell activation.

Morphine

Morphine is a small molecule alkaloid which is used clinically to activate endogenous opioid receptors and relieve pain. It usually is administered orally, intravenously, or spinally as an epidural or intrathecal injection. It has been linked to allergic-type reactions for over 100 years (131).

Allergic-Type Event Frequency and Mast Cell Dependence

Pruritus is one of the most commonly-reported adverse events of any kind associated with morphine (132–134). Frequencies after epidural administration are from 8.5% to over 50% (135–137); 30% - 100% after intrathecal administration (136–138); up to 40% after intravenous administration (139); and generally 2 - 10% after oral delivery (140), though higher rates have been reported (141). Oddly, other mast cell-associated adverse events like rash and hypotension are not nearly as common, and are rarely mentioned in clinical studies that use typical drug dosing regimens (132–134). The unusually specific dominance of pruritus can be explained, at least in part, by the fact that morphine and other opioid receptor agonists can engage a mast cell-independent mechanism to trigger pruritus. The details of this mechanism have not been fully worked out, but some evidence suggests that it is mediated by a subset of opioid receptor-expressing neurons in the spinal cord that specifically mediate itch transmission (142). This may be why epidural and intrathecal administration of morphine still trigger pruritus – in fact, they have the highest incidence rates of all routes of administration – even though they bypass systemic exposure and do not activate skin mast cells at all. This also may explain why the mu opioid receptor agonist fentanyl, which does not activate mast cells (or MRGPRX2) (13, 143), induces pruritus with incidence rates comparable to, though somewhat less than, morphine (144, 145). Thus, it is not clear how much of a role mast cells play in morphine-induced pruritus after normal clinical doses.

High doses of intravenous morphine produce side effects like flushing, changes in mean arterial pressure and lowered vascular resistance (131, 146–150), which almost certainly are mediated by mast cells. Plasma histamine levels usually were highly elevated when measured (146, 147, 150, 151), and in two studies the cardiovascular effects were reduced by pretreatment with H1 and H2 receptor antagonists (147) or the H1 receptor antagonist promethazine (149). Local administration of high doses of morphine into the forearm by skin prick, intradermal injection, or infusion into a local artery produced wheals and blood vessel dilation (often reported as a "flare"), which are common markers of mast cell activation and which could be reduced by antihistamines (152–156), though it is important to note that not all of the drugs used are specific for histamine receptors. Interestingly, an *in vitro* study of rat aortic endothelial cells demonstrated that morphine could influence their behavior directly through opioid receptors (157), suggesting a direct effect of morphine on blood vessels. This may have a minor role in humans, as well, as skin responses could partially be blocked by the opioid receptor antagonist naloxone (154, 156), at least when relatively low morphine doses were used (158). Still, taken together, the studies strongly suggest that most of the vascular changes induced by high doses of morphine are due to mast cell activation.

Anaphylaxis after morphine administration is thought to be exceedingly rare, though exact calculations are lacking. It has been proposed that some deaths from overdoses may involve anaphylaxis, but this is still unclear (159).

Peak Plasma and Tissue Concentrations, and Potential MRGPRX2 Involvement

Injection site reactions after morphine administration likely are due to MRGPRX2, as formulations usually are at 10 mM concentrations or higher and are well above the EC_{50} for MRGPRX2 activation of 4.5 to 7 μM (13, 18, 19). Typical systemic doses of morphine do not achieve plasma concentrations high enough to activate MRGPRX2 to a significant extent. For instance, peak concentrations rarely exceed 14 nM after oral dosing (160) and usually are 2 μM or less, often substantially so, after intravenous administration (161–166). This lends more support to a mast cell-independent origin for morphine-induced pruritus. Higher doses and/or those delivered rapidly are much more likely to result in concentrations that exceed the EC_{50}, though not enough recordings have been made to determine just how high these are. As described above, this is when typical events like rash and swelling are seen. Since human skin mast cells do not express opioid receptors (7), it appears likely that most true mast cell-mediated events are mediated by MRGPRX2.

Fluoroquinolones

Fluoroquinolones are a group of small molecule antibiotics which are structurally similar and are effective against Gram-positive and Gram-negative bacteria (167). Popular members are ciprofloxacin, levofloxacin, and moxifloxacin. They are administered orally or intravenously. Fluoroquinolones are associated with a constellation of mild-to-moderate adverse events, including typical allergic-type effects and others that potentially have a mast cell component. Fluoroquinolones also are linked to extremely serious side effects (168–172), which, while rare, are common enough that the FDA and European Medicines Agency now discourage their use for relatively mild infections, as the risks might outweigh the benefits (173). One of these, anaphylaxis, certainly is related to mast cells; of the others, tendinopathy and tendon rupture have been linked to mast cells in other diseases.

Allergic-Type Event Frequency and Mast Cell Dependence

Fluoroquinolones have a broad side effect profile and are not as clearly linked to mast cell activation as the other drugs in this review. Surprisingly, no systematic human studies have been carried out – for instance, measuring blood histamine or tryptase levels, and pretreating patients with antihistamines – to assess

which of the symptoms are mast cell-driven. However, many frequently reported mild-to-moderate adverse events are highly suggestive of allergic-type reactions. Rash, pruritus, injection site reactions, and hypotension have been reported in 1-4% of patients (174–177), though occasionally frequencies are much higher (178). A relatively generic description of "allergy" occasionally is reported, with frequencies of up to 2% (179). Gastrointestinal symptoms, which could be driven by mast cells (180), occur at frequencies of up to 20% (170). With the exception of anaphylaxis, the severe side effects of fluoroquinolones – tendinitis and tendon rupture, peripheral neuropathy, central nervous system effects, increased risks of damage to the aorta, and decreases in blood sugar (171) – are not typically linked to mast cell activation. Interestingly, mast cells have been proposed to influence tendon healing after injury, perhaps weakening them (181, 182), so it is possible that they are involved in some way in fluoroquinolone-induced tendon inflammation. The risk of tendinopathy or tendon rupture depends dramatically on many other factors, including activity level, age, and use of corticosteroids, but fluoroquinolone use can increase this by several-fold (183). Unfortunately, the link between mast cells and any of the above symptoms remains speculative; an understanding of the full extent of mast cell involvement in fluoroquinolone-induced AEs awaits dedicated studies of the subject.

Anaphylaxis is rare but increasing in frequency; in fact, fluoroquinolones now are the second-most frequent cause of drug-induced anaphylaxis in total cases, behind beta-lactams (172). The calculated frequency of these events is as high as 1 in 20,000 administered doses, though other estimates are lower (184).

Peak Plasma and Tissue Concentrations, and Potential MRGPRX2 Involvement

Reported peak plasma concentrations for fluoroquinolones generally average 2-6 micrograms/ml after a single dose, with intravenous administration often producing higher levels than oral (174, 185–187). As seen in **Table 1**, only ciprofloxacin can activate MRGPRX2 at these levels. However, plasma concentrations can be much higher after multiple high dose administration – for example, plasma levels exceeding 10 micrograms/ml have been recorded for ciprofloxacin (188), and over 20 micrograms/ml for levofloxacin (189–191), even several hours after intravenous infusion (189). Abnormally high plasma concentrations may also occur in patients with renal impairment (192) and poor metabolism (168). Peak concentrations may be even higher, as sampling of blood during infusions usually wasn't measured. Nonetheless, it seems likely that levels required for clinically relevant MRGPRX2 activation are only transiently achieved. This may account for the relative rarity of systemic mast cell-associated reactions, compared to other MRGPRX2 agonists like vancomycin. No measurements of drug concentrations have been made immediately after anaphylactic events that could help determine whether they might also involve MRGPRX2, nor has an analysis of allele expression been conducted.

An unusual property of many fluoroquinolones is that they accumulate in specific tissues at concentrations well above peak plasma concentrations (187, 193, 194), and can exceed those needed to activate MRGPRX2. This is linked to the lipophilicity of the molecule (194), and some are much more likely than others to distribute unevenly. The lung, especially the epithelial lining fluid (ELF), is a site of some of the highest reported concentrations (195) – for instance, levofloxacin concentrations in the ELF have been measured at over 40 micrograms/ml (189), and two hours after a single dose of moxifloxacin, ELF concentrations reached 21 micrograms/ml (196). Limited data, mostly from experimental animal models, suggest that fluoroquinolones also accumulate in cartilage (197). This may have some significance, as fluoroquinolones are associated with arthralgia, myalgia, and joint damage in some studies (198), and mast cell mediators have been shown to weaken tendons (181). In sum, this unusual tissue distribution pattern of fluoroquinolones may result in intense mast cell activation that is both delayed and restricted to certain tissues. This would not be accompanied by the typical signs of degranulation like rash and pruritus, but a closer look at mast cell, and MRGPRX2, involvement in these delayed and long-lived side effects might be justified.

DISCUSSION

A question that is raised repeatedly in the literature is whether MRGPRX2 activation is capable of triggering anaphylaxis. This likely would require a sustained period of high plasma drug levels, and/or expression of a rare MRGRPX2 allele with greatly enhanced sensitivity to the drug or abnormally strong signaling downstream of receptor activation. Tandem testing of MRGPRX2 allele expression, drug concentrations, and IgE titers in patients with anaphylaxis would be extremely informative; unfortunately, these tests are rarely conducted and most MRGPRX2 alleles remain uncharacterized. Ultimately, an MRGPRX2 antagonist is needed to provide direct proof of MRGPRX2 involvement. Development of antagonists is in its infancy and none has made it to clinical trials yet, though several promising candidates have been identified and rapid development on this front is expected (15).

Perhaps the most surprising finding from the analysis is how common the mild-to-moderate events are. These events are not life-threatening like anaphylaxis is, and rightly should be a lesser priority for clinicians. However, they should not be neglected, either. For instance, one allergic-type response classified as moderate is a drop in mean arterial pressure of over 20% - this certainly is not a trivial effect and may have an impact on vascular stability, especially in patients who have serious cardiovascular impairment already. Comparisons with plasma drug levels suggest that MRGPRX2 drives many of these mild-to-moderate events. An MRGPRX2 antagonist is not yet available, but if one enters clinical use, it would be interesting to see if prophylactic administration before surgical procedures lowers overall perioperative patient mortality. In sum, it is clear that there is much still to be learned about MRGPRX2 and its impact on human health.

AUTHOR CONTRIBUTIONS

The author confirms being the sole contributor of this work and has approved it for publication.

FUNDING

This article was written with the support of the Ernest S. Bazley Trust.

REFERENCES

1. Riedl MA, Casillas AM. Adverse Drug Reactions: Types and Treatment Options. *Am Fam Physician* (2003) 68:1781–90.
2. Ebo DG, Clarke RC, Mertes P-M, Platt PR, Sabato V, Sadleir PHM. Molecular Mechanisms and Pathophysiology of Perioperative Hypersensitivity and Anaphylaxis: A Narrative Review. *Br J Anaesthesia* (2019) 123:e38–49. doi: 10.1016/j.bja.2019.01.031
3. Cook TM, Harper NJN, Farmer L, Garcez T, Floss K, Marinho S, et al. Anaesthesia, Surgery, and Life-Threatening Allergic Reactions: Protocol and Methods of the 6th National Audit Project (NAP6) of the Royal College of Anaesthetists. *Br J Anaesthesia* (2018) 121:124–33. doi: 10.1016/j.bja.2018.04.001
4. Savic LC, Garvey LH. Perioperative Anaphylaxis: Diagnostic Challenges and Management. *Curr Opin Anaesthesiol* (2020) 33:448–53. doi: 10.1097/ACO.0000000000000857
5. Dykewicz MS, Lam JK. Drug Hypersensitivity Reactions. *Med Clin North Am* (2020) 104:109–28. doi: 10.1016/j.mcna.2019.09.003
6. Galli SJ, Tsai M. Ige and Mast Cells in Allergic Disease. *Nat Med* (2012) 18:693–704. doi: 10.1038/nm.2755
7. Motakis E, Guhl S, Ishizu Y, Itoh M, Kawaji H, de Hoon M, et al. Redefinition of the Human Mast Cell Transcriptome by Deep-CAGE Sequencing. *Blood* (2014) 123:e58–67. doi: 10.1182/blood-2013-02-483792
8. Tatemoto K, Nozaki Y, Tsuda R, Konno S, Tomura K, Furuno M, et al. Immunoglobulin E-Independent Activation of Mast Cell Is Mediated by Mrg Receptors. *Biochem Biophys Res Commun* (2006) 349:1322–8. doi: 10.1016/j.bbrc.2006.08.177
9. Armstrong JF, Faccenda E, Harding SD, Pawson AJ, Southan C, Sharman JL, et al. The IUPHAR/BPS Guide to PHARMACOLOGY in 2020: Extending Immunopharmacology Content and Introducing the IUPHAR/MMV Guide to MALARIA PHARMACOLOGY. *Nucleic Acids Res* (2019) 48:D1006–21. doi: 10.1093/nar/gkz951
10. Robas N, Mead E, Fidock M. MrgX2 Is a High Potency Cortistatin Receptor Expressed in Dorsal Root Ganglion. *J Biol Chem* (2003) 278:44400–4. doi: 10.1074/jbc.M302456200
11. Kamohara M, Matsuo A, Takasaki J, Kohda M, Matsumoto M, Matsumoto S, et al. Identification of MrgX2 as a Human G-Protein-Coupled Receptor for Proadrenomedullin N-Terminal Peptides. *Biochem Biophys Res Commun* (2005) 330:1146–52. doi: 10.1016/j.bbrc.2005.03.088
12. McNeil BD, Pundir P, Meeker S, Han L, Undem BJ, Kulka M, et al. Identification of a Mast-Cell-Specific Receptor Crucial for Pseudo-Allergic Drug Reactions. *Nature* (2015) 519:237–41. doi: 10.1038/nature14022
13. Lansu K, Karpiak J, Liu J, Huang XP, McCorvy JD, Kroeze WK, et al. In Silico Design of Novel Probes for the Atypical Opioid Receptor MRGPRX2. *Nat Chem Biol* (2017) 13:529–36. doi: 10.1038/nchembio.2334
14. Grimes J, Desai S, Charter NW, Lodge J, Moita Santos R, Isidro-Llobet A, et al. MrgX2 is a Promiscuous Receptor for Basic Peptides Causing Mast Cell Pseudo-Allergic and Anaphylactoid Reactions. *Pharmacol Res Perspect* (2019) 7:e00547. doi: 10.1002/prp2.547
15. McNeil BD. Minireview: Mas-Related G Protein-Coupled Receptor X2 Activation by Therapeutic Drugs. *Neurosci Lett* (2021) 751:135746. doi: 10.1016/j.neulet.2021.135746
16. Che D, Wang J, Ding Y, Liu R, Cao J, Zhang Y, et al. Mivacurium Induce Mast Cell Activation and Pseudo-Allergic Reactions *via* MAS-Related G Protein Coupled Receptor-X2. *Cell Immunol* (2018) 332:121–8. doi: 10.1016/j.cellimm.2018.08.005
17. Che D, Rui L, Cao J, Wang J, Zhang Y, Ding Y, et al. Cisatracurium Induces Mast Cell Activation and Pseudo-Allergic Reactions *via* MRGPRX2. *Int Immunopharmacol* (2018) 62:244–50. doi: 10.1016/j.intimp.2018.07.020
18. Zhang T, Liu R, Che D, Pundir P, Wang N, Han S, et al. A Mast Cell–Specific Receptor Is Critical for Granuloma Induced by Intrathecal Morphine Infusion. *J Immunol* (2019) 203:1701–14. doi: 10.4049/jimmunol.1801423
19. Akuzawa N, Obinata H, Izumi T, Takeda S. Morphine Is an Exogenous Ligand for MrgX2, a G Protein-Coupled Receptor for Cortistatin. *J Cell Anim Biol* (2009) 3:216–21. doi: 10.5897/JCAB.9000111
20. Gaudenzio N, Sibilano R, Marichal T, Starkl P, Reber LL, Cenac N, et al. Different Activation Signals Induce Distinct Mast Cell Degranulation Strategies. *J Clin Invest* (2016) 126:3981–98. doi: 10.1172/JCI85538
21. Porebski G, Kwiecien K, Pawica M, Kwitniewski M. Mas-Related G Protein-Coupled Receptor-X2 (MRGPRX2) in Drug Hypersensitivity Reactions. *Front Immunol* (2018) 9. doi: 10.3389/fimmu.2018.03027
22. Munk C, Isberg V, Mordalski S, Harpsøe K, Rataj K, Hauser AS, et al. Gpcrdb: The G Protein-Coupled Receptor Database - An Introduction. *Br J Pharmacol* (2016) 173:2195–207. doi: 10.1111/bph.13509
23. Alkanfari I, Gupta K, Jahan T, Ali H. Naturally Occurring Missense MRGPRX2 Variants Display Loss of Function Phenotype for Mast Cell Degranulation in Response to Substance P, Hemokinin-1, Human β-Defensin-3, and Icatibant. *J Immunol* (2018) 201:343–9. doi: 10.4049/jimmunol.1701793
24. Chompunud Na Ayudhya C, Roy S, Alkanfari I, Ganguly A, Ali H. Identification of Gain and Loss of Function Missense Variants in MRGPRX2's Transmembrane and Intracellular Domains for Mast Cell Activation by Substance P. *Int J Mol Sci* (2019) 20:5247. doi: 10.3390/ijms20215247
25. Varricchi G, Pecoraro A, Loffredo S, Poto R, Rivellese F, Genovese A, et al. Heterogeneity of Human Mast Cells With Respect to MRGPRX2 Receptor Expression and Function. *Front Cell Neurosci* (2019) 13. doi: 10.3389/fncel.2019.00299
26. Shtessel M, Limjunyawong N, Oliver ET, Chichester K, Gao L, Dong X, et al. MRGPRX2 Activation Causes Increased Skin Reactivity in Patients With Chronic Spontaneous Urticaria. *J Invest Dermatol* (2021) 141:678–81.e672. doi: 10.1016/j.jid.2020.06.030
27. Ansotegui IJ, Melioli G, Canonica GW, Caraballo L, Villa E, Ebisawa M, et al. Ige Allergy Diagnostics and Other Relevant Tests in Allergy, a World Allergy Organization Position Paper. *World Allergy Organ J* (2020) 13:100080. doi: 10.1016/j.waojou.2019.100080
28. Ariza A, Mayorga C, Bogas G, Barrionuevo E, Torres MJ, Doña I, et al. Advances and Novel Developments in Drug Hypersensitivity Diagnosis. *Allergy* (2020) 75:3112–23. doi: 10.1111/all.14603
29. Decuyper II, Mangodt EA, Van Gasse AL, Claesen K, Uyttebroek A, Faber M, et al. *In Vitro* Diagnosis of Immediate Drug Hypersensitivity Anno 2017: Potentials and Limitations. *Drugs R&D* (2017) 17:265–78. doi: 10.1007/s40268-017-0176-x
30. Brockow K, Garvey LH, Aberer W, Atanaskovic-Markovic M, Barbaud A, Bilo MB, et al. Skin Test Concentrations for Systemically Administered Drugs - An ENDA/EAACI Drug Allergy Interest Group Position Paper. *Allergy* (2013) 68:702–12. doi: 10.1111/all.12142
31. Van Gasse AL, Elst J, Bridts CH, Mertens C, Faber M, Hagendorens MM, et al. Rocuronium Hypersensitivity: Does Off-Target Occupation of the MRGPRX2 Receptor Play a Role? *J Allergy Clin Immunol Pract* (2019) 7:998–1003. doi: 10.1016/j.jaip.2018.09.034
32. Liu C, Bayer A, Cosgrove SE, Daum RS, Fridkin SK, Gorwitz RJ, et al. Clinical Practice Guidelines by the Infectious Diseases Society of America for the Treatment of Methicillin-Resistant Staphylococcus Aureus Infections in Adults and Children: Executive Summary. *Clin Infect Dis* (2011) 52:285–92. doi: 10.1093/cid/cir034
33. De Luca JF, Holmes NE, Trubiano JA. Adverse Reactions to Vancomycin and Cross-Reactivity With Other Antibiotics. *Curr Opin Allergy Clin Immunol* (2020) 20:352–61. doi: 10.1097/ACI.0000000000000665
34. Myers AL, Gaedigk A, Dai H, James LP, Jones BL, Neville KA. Defining Risk Factors for Red Man Syndrome in Children and Adults. *Pediatr Infect Dis J* (2012) 31:464–8. doi: 10.1097/INF.0b013e31824e10d7
35. Huang V, Clayton NA, Welker KH. Glycopeptide Hypersensitivity and Adverse Reactions. *Pharmacy* (2020) 8:70. doi: 10.3390/pharmacy8020070

36. Polk RE. Anaphylactoid Reactions to Glycopeptide Antibiotics. *J Antimicrobial Chemotherapy* (1991) 27:17–29. doi: 10.1093/jac/27.suppl_B.17
37. Levy JH, Kettlekamp N, Goertz P, Hermens J, Hirshman CA. Histamine Release by Vancomycin: A Mechanism for Hypotension in Man. *Anesthesiology* (1987) 67:122–5. doi: 10.1097/00000542-198707000-00026
38. Polk RE, Healy DP, Schwartz LB, Rock DT, Garson ML, Roller K. Vancomycin and the Red-Man Syndrome: Pharmacodynamics of Histamine Release. *J Infect Dis* (1988) 157:502–7. doi: 10.1093/infdis/157.3.502
39. Healy DP, Sahai JV, Fuller SH, Polk RE. Vancomycin-Induced Histamine Release and "Red Man Syndrome": Comparison of 1- and 2-Hour Infusions. *Antimicrobial Agents Chemotherapy* (1990) 34:550–4. doi: 10.1128/AAC.34.4.550
40. Sahai J, Healy DP, Shelton MJ, Miller JS, Ruberg SJ, Polk R. Comparison of Vancomycin- and Teicoplanin-Induced Histamine Release and "Red Man Syndrome". *Antimicrob Agents Chemother* (1990) 34:765–9. doi: 10.1128/AAC.34.5.765
41. Renz C, Lynch J, Thurn J, Moss J. Histamine Release During Rapid Vancomycin Administration. *Inflammation Res* (1998) 47:69–70. doi: 10.1007/s000110050279
42. Sahai J, Healy DP, Garris R, Berry A, Polk RE. Influence of Antihistamine Pretreatment on Vancomycin-Induced Red-Man Syndrome. *J Infect Dis* (1989) 160:876–81. doi: 10.1093/infdis/160.5.876
43. Wallace MR, Mascola JR, Oldfield EC. Red Man Syndrome: Incidence, Etiology, and Prophylaxis. *J Infect Dis* (1991) 164:1180–5. doi: 10.1093/infdis/164.6.1180
44. Renz CL, Thurn JD, Finn HA, Lynch JP, Moss J. Oral Antihistamines Reduce the Side Effects From Rapid Vancomycin Infusion. *Anesth Analg* (1998) 87:681–5. doi: 10.1213/00000539-199809000-00036
45. Renz CL, Thurn JD, Finn HA, Lynch JP, Moss J. Antihistamine Prophylaxis Permits Rapid Vancomycin Infusion. *Crit Care Med* (1999) 27:1732–7. doi: 10.1097/00003246-199909000-00006
46. Renz CL, Laroche D, Thurn JD, Finn HA, Lynch JP, Thisted R, et al. Tryptase Levels Are Not Increased During Vancomycin-Induced Anaphylactoid Reactions. *Anesthesiology* (1998) 89:620–5. doi: 10.1097/00000542-199809000-00010
47. Svetitsky S, Leibovici L, Paul M. Comparative Efficacy and Safety of Vancomycin Versus Teicoplanin: Systematic Review and Meta-Analysis. *Antimicrob Agents Chemother* (2009) 53:4069–79. doi: 10.1128/AAC.00341-09
48. Korman TM, Turnidge JD, Grayson ML. Risk Factors for Adverse Cutaneous Reactions Associated With Intravenous Vancomycin. *J Antimicrobial Chemotherapy* (1997) 39:371–81. doi: 10.1093/oxfordjournals.jac.a020861
49. Rybak MJ, Bailey EM, Warbasse LH. Absence of "Red Man Syndrome" in Patients Being Treated With Vancomycin or High-Dose Teicoplanin. *Antimicrob Agents Chemother* (1992) 36:1204–7. doi: 10.1128/AAC.36.6.1204
50. O'Sullivan TL, Ruffing MJ, Lamp KC, Warbasse LH, Rybak MJ. Prospective Evaluation of Red Man Syndrome in Patients Receiving Vancomycin. *J Infect Dis* (1993) 168:773–6. doi: 10.1093/infdis/168.3.773
51. Marinho DS, Huf G, Ferreira BL, Castro H, Rodrigues CR, Sousa VPD, et al. The Study of Vancomycin Use and Its Adverse Reactions Associated to Patients of a Brazilian University Hospital. *BMC Res Notes* (2011) 4:236. doi: 10.1186/1756-0500-4-236
52. Downs NJ. Mild Nephrotoxicity Associated With Vancomycin Use. *Arch Internal Med* (1989) 149:1777. doi: 10.1001/archinte.1989.00390080053013
53. Rubin M, Hathorn JW, Marshall D, Gress J, Steinberg SM, Pizzo PA. Gram-Positive Infections and the Use of Vancomycin in 550 Episodes of Fever and Neutropenia. *Ann Intern Med* (1988) 108:30–5. doi: 10.7326/0003-4819-108-1-30
54. Alvarez-Arango S, Yerneni S, Tang O, Zhou L, Mancini CM, Blackley SV, et al. Vancomycin Hypersensitivity Reactions Documented in Electronic Health Records. *J Allergy Clin Immunol Pract* (2021) 9:906–12. doi: 10.1016/j.jaip.2020.09.027
55. Healy DP, Polk RE, Garson ML, Rock DT, Comstock TJ. Comparison of Steady-State Pharmacokinetics of Two Dosage Regimens of Vancomycin in Normal Volunteers. *Antimicrobial Agents Chemotherapy* (1987) 31:393–7. doi: 10.1128/AAC.31.3.393
56. Polk RE, Israel D, Wang J, Venitz J, Miller J, Stotka J. Vancomycin Skin Tests and Prediction of "Red Man Syndrome" in Healthy Volunteers. *Antimicrobial Agents Chemotherapy* (1993) 37:2139–43. doi: 10.1128/AAC.37.10.2139
57. Boeckh M, Lode H, Borner K, Hoffken G, Wagner J, Koeppe P. Pharmacokinetics and Serum Bactericidal Activity of Vancomycin Alone and in Combination With Ceftazidime in Healthy Volunteers. *Antimicrobial Agents Chemotherapy* (1988) 32:92–5. doi: 10.1128/AAC.32.1.92
58. Odio C. Adverse Reactions to Vancomycin Used as Prophylaxis for CSF Shunt Procedures. *Arch Pediatr Adolesc Med* (1984) 138:17. doi: 10.1001/archpedi.1984.02140390009004
59. Johnzon C-F, Rönnberg E, Pejler G. The Role of Mast Cells in Bacterial Infection. *Am J Pathol* (2016) 186:4–14. doi: 10.1016/j.ajpath.2015.06.024
60. Lee C. Structure, Conformation, and Action of Neuromuscular Blocking Drugs †. *Br J Anaesthesia* (2001) 87:755–69. doi: 10.1093/bja/87.5.755
61. Claudius C, Garvey LH, Viby-Mogensen J. The Undesirable Effects of Neuromuscular Blocking Drugs. *Anaesthesia* (2009) 64:10–21. doi: 10.1111/j.1365-2044.2008.05866.x
62. Bryson HM, Faulds D. Cisatracurium Besilate. *Drugs* (1997) 53:848–66. doi: 10.2165/00003495-199753050-00012
63. Konstadt SN, Reich DL, Stanley TE, Deperio M, Chuey C, Schwartzbach C, et al. A Two-Center Comparison of the Cardiovascular Effects of Cisatracurium (Nimbex Trademmark) and Vecuronium in Patients With Coronary Artery Disease. *Anesthesia Analgesia* (1995) 81:1010–4. doi: 10.1213/00000539-199511000-00020
64. Hughes R, Chapple DJ. The Pharmacology of Atracurium: A New Competitive Neuromuscular Blocking Agent. *Br J Anaesthesia* (1981) 53:31–44. doi: 10.1093/bja/53.1.31
65. Scott RP, Savarese JJ, Basta SJ, Embree P, Ali HH, Sunder N, et al. Clinical Pharmacology of Atracurium Given in High Dose. *Br J Anaesth* (1986) 58:834–8. doi: 10.1093/bja/58.8.834
66. Scott RP, Savarese JJ, Basta SJ, Sunder N, Ali HH, Gargarian M, et al. Atracurium: Clinical Strategies for Preventing Histamine Release and Attenuating the Haemodynamic Response. *Br J Anaesth* (1985) 57:550–3. doi: 10.1093/bja/57.6.550
67. Hosking MP, Lennon RL, Gronert GA. Combined H1 and H2 Receptor Blockade Attenuates the Cardiovascular Effects of High-Dose Atracurium for Rapid Sequence Endotracheal Intubation. *Anesth Analg* (1988) 67:1089–92. doi: 10.1213/00000539-198867110-00012
68. Adt M, Baumert JH, Reimann HJ. The Role of Histamine in the Cardiovascular Effects of Atracurium. *Br J Anaesthesia* (1992) 68:155–60. doi: 10.1093/bja/68.2.155
69. Doenicke A, Moss J, Lorenz W, Hoernecke R, Gottardis M. Are Hypotension and Rash After Atracurium Really Caused by Histamine Release? *Anesthesia Analgesia* (1994) 78:967???972. doi: 10.1213/00000539-199405000-00023
70. Savarese JJ, Ali HH, Basta SJ, Scott RP, Embree PB, Wastila WB, et al. The Cardiovascular Effects of Mivacurium Chloride (BW B1090U) in Patients Receiving Nitrous Oxide-Opiate-Barbiturate Anesthesia. *Anesthesiology* (1989) 70:386–94. doi: 10.1097/00000542-198903000-00003
71. Shorten GD, Crawford MW, St Louis P. The Neuromuscular Effects of Mivacurium Chloride During Propofol Anesthesia in Children. *Anesth Analg* (1996) 82:1170–5. doi: 10.1213/00000539-199606000-00012
72. Xiang Z, Yan-Liang Q, Xiao-Yang S, Yan-Hui Z, Min C, Guo-Shen G, et al. Effects of Promethazine or Dexamethasone Pretreatment on Mivacurium-Induced Histamine Release in Children. *Pediatr Anesthesia* (2014) 24:322–6. doi: 10.1111/pan.12305
73. Naguib M, Samarkandi AH, Bakhamees HS, Magboul MA, El-Bakry AK. Histamine-Release Haemodynamic Changes Produced by Rocuronium, Vecuronium, Mivacurium, Atracurium and Tubocurarine. *Br J Anaesthesia* (1995) 75:588–92. doi: 10.1093/bja/75.5.588
74. Brandom BW, Meretoja OA, Simhi E, Taivainen T, Wolfe SR, Woelfel SK, et al. Age Related Variability in the Effects of Mivacurium in Paediatric Surgical Patients. *Can J Anaesthesia* (1998) 45:410–6. doi: 10.1007/BF03012575
75. Miguel R, Witkowski T, Nagashima H, Fragen R, Bartkowski R, Foldes FF, et al. Evaluation of Neuromuscular and Cardiovascular Effects of Two Doses of Rapacuronium (ORG 9487) Versus Mivacurium and Succinylcholine. *Anesthesiology* (1999) 91:1648–54. doi: 10.1097/00000542-199912000-00016

76. Sarner JB, Brandom BW, Woelfel SK, Dong M-L, Horn MC, Cook RD, et al. Clinical Pharmacology of Mivacurium Chloride (BW B1090U) in Children During Nitrous Oxide-Halothane and Nitrous Oxide-Narcotic Anesthesia. *Anesthesia Analgesia* (1989) 68:116–21. doi: 10.1213/00000539-198902000-00009
77. Ali HH, Lien CA, Witkowski T, Brull SJ, Stout RG, Bartkowski R, et al. Efficacy and Safety of Divided Dose Administration of Mivacurium for a 90-Second Tracheal Intubation. *J Clin Anesthesia* (1996) 8:276–81. doi: 10.1016/0952-8180(96)85617-0
78. Doenicke A, Moss J, Lorenz W, Mayer M, Rau J, Jedrzejewski A, et al. Effect of Oral Antihistamine Premedication on Mivacurium-Induced Histamine Release and Side Effects. *Br J Anaesthesia* (1996) 77:421–3. doi: 10.1093/bja/77.3.421
79. Loan PB, Elliott P, Mirakhur RK, Bunting HF, Bhanumurthy S, McMurray TJ. Comparison of the Haemodynamic Effects of Mivacurium and Atracurium During Fentanyl Anaesthesia. *Br J Anaesthesia* (1995) 74:330–2. doi: 10.1093/bja/74.3.330
80. Plaud B, Marty J, Debaene B, Meistelman C, Pellissier D, LePage JY, et al. The Cardiovascular Effects of Mivacurium in Hypertensive Patients. *Anesth Analg* (2002) 95:379–84. doi: 10.1213/00000539-200208000-00025
81. Miloudi Y, El Harrar N, Bensaid A, Hussein MA. Les Réactions Cutanées Consécutives À L'induction Anesthésique Au Mivacurium. *Annales Françaises d'Anesthésie Réanimation* (2007) 26:717. doi: 10.1016/j.annfar.2007.04.002
82. Stoops CM, Curtis CA, Kovach DA, McCammon RL, Stoelting RK, Warren TM, et al. Hemodynamic Effects of Mivacurium Chloride Administered to Patients During Oxygen-Sufentanil Anesthesia for Coronary Artery Bypass Grafting or Valve Replacement. *Anesth Analg* (1989) 68:333–9. doi: 10.1213/00000539-198903000-00028
83. Hodgson R, Harvey P, Burrows R. Mivacurium Compared With Three Different Doses of Suxamethonium for Nasotracheal Intubation. *Anaesthesia Intensive Care* (1998) 26:521–5. doi: 10.1177/0310057X9802600508
84. Zeng R, Liu X, Zhang J, Yin N, Fei J, Zhong S, et al. The Efficacy and Safety of Mivacurium in Pediatric Patients. *BMC Anesthesiology* (2017) 17:58–65. doi: 10.1186/s12871-017-0350-2
85. Reich DL, Mulier J, Viby-Mogensen J, Konstadt SN, Van Aken HK, Jensen FS, et al. Comparison of the Cardiovascular Effects of Cisatracurium and Vecuronium in Patients With Coronary Artery Disease. *Can J Anaesthesia* (1998) 45:794–7. doi: 10.1007/BF03012152
86. Lepage JY, Malinovsky JM, Malinge M, Lechevalier T, Dupuch C, Cozian A, et al. Pharmacodynamic Dose-Response and Safety Study of Cisatracurium (51W89) in Adult Surgical Patients During N2O-O2-Opioid Anesthesia. *Anesth Analg* (1996) 83:823–9. doi: 10.1097/00000539-199610000-00030
87. Doenicke A, Soukup J, Hoernecke R, Moss J. The Lack of Histamine Release With Cisatracurium: A Double-Blind Comparison With Vecuronium. *Anesth Analg* (1997) 84:623–8. doi: 10.1213/00000539-199703000-00030
88. Doenicke AW, Czeslick E, Moss J, Hoernecke R, time O. Endotracheal Intubating Conditions, and Plasma Histamine After Cisatracurium and Vecuronium Administration. *Anesth Analg* (1998) 87:434–8. doi: 10.1213/00000539-199808000-00038
89. Lien CA, Belmont MR, Abalos A, Eppich L, Quessy S, Abou-Donia MM, et al. The Cardiovascular Effects and Histamine-Releasing Properties of 51W89 in Patients Receiving Nitrous Oxide/Opioid/Barbiturate Anesthesia. *Anesthesiology* (1995) 82:1131–8. doi: 10.1097/00000542-199505000-00007
90. Harper NJN, Cook TM, Garcez T, Farmer L, Floss K, Marinho S, et al. Anaesthesia, Surgery, and Life-Threatening Allergic Reactions: Epidemiology and Clinical Features of Perioperative Anaphylaxis in the 6th National Audit Project (NAP6). *Br J Anaesthesia* (2018) 121:159–71. doi: 10.1016/j.bja.2018.04.014
91. Reddy JI, Cooke PJ, Van Schalkwyk JM, Hannam JA, Fitzharris P, Mitchell SJ. Anaphylaxis is More Common With Rocuronium and Succinylcholine Than With Atracurium. *Anesthesiology* (2015) 122:39–45. doi: 10.1097/ALN.0000000000000512
92. Petitpain N, Argoullon L, Masmoudi K, Fedrizzi S, Cottin J, Latarche C, et al. Neuromuscular Blocking Agents Induced Anaphylaxis: Results and Trends of a French Pharmacovigilance Survey From 2000 to 2012. *Allergy* (2018) 73:2224–33. doi: 10.1111/all.13456
93. Sadleir PHM, Clarke RC, Bunning DL, Platt PR. Anaphylaxis to Neuromuscular Blocking Drugs: Incidence and Cross-Reactivity in Western Australia From 2002 to 2011. *Br J Anaesthesia* (2013) 110:981–7. doi: 10.1093/bja/aes506
94. Kent AP, Parker CJR, Hunter JM. Pharmacokinetics of Atracurium and Laudanosine in the Elderly. *Br J Anaesthesia* (1989) 63:661–6. doi: 10.1093/bja/63.6.661
95. Ward S, Neill EAM, Weatherley BC, Corall IM. Pharmacokinetics of Atracurium Besylate in Healthy Patients (After a Single I.V. Bolus Dose). *Br J Anaesthesia* (1983) 55:113–8. doi: 10.1093/bja/55.2.113
96. Levy JH, Adelson D, Walker B. Wheal and Flare Responses to Muscl Relaxants in Humans. *Agents Actions* (1991) 34:302–8. doi: 10.1007/BF01988720
97. Østergaard D, Viby-Mogensen J, Rasmussen SN, Gätke MR, Varin F. Pharmacokinetics and Pharmacodynamics of Mivacurium in Patients Phenotypically Homozygous for the Atypical Plasma Cholinesterase Variant. *Anesthesiology* (2005) 102:1124–32. doi: 10.1097/00000542-200506000-00011
98. Lacroix M, Donati F, Varin F. Pharmacokinetics of Mivacurium Isomers and Their Metabolites in Healthy Volunteers After Intravenous Bolus Administration. *Anesthesiology* (1997) 86:322–30. doi: 10.1097/00000542-199702000-00008
99. Cook DR, Freeman JA, Lai AA, Kang Y, Stiller RL, Aggarwal S, et al. Pharmacokinetics of Mivacurium N Normal Patients and in Those With Hepatic or Renal Failure. *Br J Anaesthesia* (1992) 69:580–5. doi: 10.1093/bja/69.6.580
100. Lien CA, Schmith VD, Embree PB, Belmont MR, Wargin WA, Savarese JJ. The Phamtacokinetics and Pharmacodynamics of the Stereoisomers of Mivacurium in Patients Receiving Nitrous Oxide/Opioid/Barbiturate Anesthesia. *Anesthesiology* (1994) 80:1296–302. doi: 10.1097/00000542-199406000-00017
101. Østergaard D, Gätke MR, Berg H, Rasmussen SN, Viby-Mogensen J. The Pharmacodynamics and Pharmacokinetics of Mivacurium in Children. *Acta Anaesthesiologica Scandinavica* (2002) 46:512–8. doi: 10.1034/j.1399-6576.2002.460507.x
102. De Wolf AM, Freeman JA, Scott VL, Tullock W, Smith DA, Kisor DF, et al. Pharmacokinetics and Pharmacodynamics of Cisatracurium in Patients With End-Stage Liver Disease Undergoing Liver Transplantation. *Br J Anaesthesia* (1996) 76:624–8. doi: 10.1093/bja/76.5.624
103. Kisor DF, Schmith VD, Wargin WA, Lien CA, Ornstein E, Cook DR. Importance of the Organ-Independent Elimination of Cisatracurium. *Anesth Analg* (1996) 83:1065–71. doi: 10.1213/00000539-199611000-00029
104. Levy JH, Gottge M, Szlam F, Zaffer R, McCall C. Weal and Flare Responses to Intradermal Rocuronium and Cisatracurium in Humans. *Br J Anaesthesia* (2000) 85:844–9. doi: 10.1093/bja/85.6.844
105. Berg CM, Heier T, Wilhelmsen V, Florvaag E. Rocuronium and Cisatracurium-Positive Skin Tests in non-Allergic Volunteers: Determination of Drug Concentration Thresholds Using a Dilution Titration Technique*. *Acta Anaesthesiologica Scandinavica* (2003) 47:576–82. doi: 10.1034/j.1399-6576.2003.00093.x
106. Sparr HJ, Beaufort TM, Fuchs-Buder T. Newer Neuromuscular Blocking Agents. *Drugs* (2001) 61:919–42. doi: 10.2165/00003495-200161070-00003
107. Sorgenfrei IF, Norrild K, Larsen PB, Stensballe J, Østergaard D, Prins ME, et al. Reversal of Rocuronium-Induced Neuromuscular Block by the Selective Relaxant Binding Agent Sugammadex. *Anesthesiology* (2006) 104:667–74. doi: 10.1097/00000542-200604000-00009
108. Booij LHDJ, Knape HTA. The Neuromuscular Blocking Effect of Org 9426. *Anaesthesia* (1991) 46:341–3. doi: 10.1111/j.1365-2044.1991.tb09539.x
109. Hudson ME, Rothfield KP, Tullock WC, Firestone LL. Haemodynamic Effects of Rocuronium Bromide in Adult Cardiac Surgical Patients. *Can J Anaesthesia* (1998) 45:139–43. doi: 10.1007/BF03013252
110. Schramm WM, Strasser K, Bartunek A, Gilly H, Spiss CK. Effects of Rocuronium and Vecuronium on Intracranial Pressure, Mean Arterial Pressure and Heart Rate in Neurosurgical Patients. *Br J Anaesthesia* (1996) 77:607–11. doi: 10.1093/bja/77.5.607
111. McCoy EP, Maddineni VR, Elliott P, Mirakhur RK, Carson IW, Cooper RA. Haemodynamic Effects of Rocuronium During Fentanyl Anaesthesia: Comparison With Vecuronium. *Can J Anaesthesia* (1993) 40:703–8. doi: 10.1007/BF03009764

112. Murray MJ, Deblock H, Erstad B, Gray A, Jacobi J, Jordan C, et al. Clinical Practice Guidelines for Sustained Neuromuscular Blockade in the Adult Critically Ill Patient. *Crit Care Med* (2016) 44:2079–103. doi: 10.1097/CCM.0000000000002027
113. Levy JH, Davis GK, Duggan J, Szlam F. Determination of the Hemodynamics and Histamine Release of Rocuronium (Org 9426) When Administered in Increased Doses Under N2O/O2-Sufentanil Anesthesia. *Anesth Analg* (1994) 78:318–21. doi: 10.1213/00000539-199402000-00020
114. Takazawa T, Mitsuhata H, Mertes PM. Sugammadex and Rocuronium-Induced Anaphylaxis. *J Anesthesia* (2016) 30:290–7. doi: 10.1007/s00540-015-2105-x
115. Hepner DL, Castells MC. Anaphylaxis During the Perioperative Period. *Anesthesia Analgesia* (2003) 97:1381–95. doi: 10.1213/01.ANE.0000082993.84883.7D
116. Neal SM, Manthri PR, Gadiyar V, Wildsmith JA. Histaminoid Reactions Associated With Rocuronium. *Br J Anaesthesia* (2000) 84:108–11. doi: 10.1093/oxfordjournals.bja.a013365
117. Erbabacan E, Koksal GM, Tutuncu CA, Ekici B, Tunali Y, Kaya G, et al. Comparison of the Effect of Different Concentrations of Rocuronium on Injection Pain and Haemodynamics Using Isolated Forearm Technique. *Turkish J Anesthesia Reanimation* (2013) 41:162–6. doi: 10.5152/TJAR.2013.35
118. Borgeat A, Kwiatkowski D. Spontaneous Movements Associated With Rocuronium: Is Pain on Injection the Cause? *Br J Anaesth* (1997) 79:382–3. doi: 10.1093/bja/79.3.382
119. Blunk JA, Seifert F, Schmelz M, Reeh PW, Koppert W. Injection Pain of Rocuronium and Vecuronium is Evoked by Direct Activation of Nociceptive Nerve Endings. *Eur J Anaesthesiol* (2003) 20:245–53. doi: 10.1097/00003643-200303000-00011
120. Han DW, Koo BN, Choi SH, Lee JS, Shin YS, Sharma M, et al. Neutralized Rocuronium (Ph 7.4) Before Administration Prevents Injection Pain in Awake Patients: A Randomized Prospective Trial. *J Clin Anesthesia* (2007) 19:418–23. doi: 10.1016/j.jclinane.2007.02.012
121. Lee HJ, Han SJ, Kim H, Lee IO, Kong MH, Kim NS, et al. Antihistamine Pretreatment to Reduce Incidence of Withdrawal Movement After Rocuronium Injection. *J Korean Med Sci* (2009) 24:879. doi: 10.3346/jkms.2009.24.5.879
122. Huang SM, Athanikar NK, Sridhar K, Huang YC, Chiou WL. Pharmacokinetics of Chlorpheniramine After Intravenous and Oral Administration in Normal Adults. *Eur J Clin Pharmacol* (1982) 22:359–65. doi: 10.1007/BF00548406
123. Wierda JMKH, Kleef UW, Lambalk LM, Kloppenburg WD, Agoston S. The Pharmacodynamics and Pharmacokinetics of Org 9426, A New Non-Depolarizing Neuromuscular Blocking Agent, in Patients Anaesthetized With Nitrous Oxide, Halothane and Fentanyl. *Can J Anaesthesia* (1991) 38:430–5. doi: 10.1007/BF03007578
124. Magorian T, Wood P, Caldwell J, Fisher D, Segredo V, Szenohradszky J, et al. The Pharmacokinetics and Neuromuscular Effects of Rocuronium Bromide in Patients With Liver Disease. *Anesthesia Analgesia* (1995) 80:754–9. doi: 10.1213/00000539-199504000-00018
125. Cooper RA, Maddineni VR, Mirakhur RK, Wierda JM, Brady M, Fitzpatrick KT. Time Course of Neuromuscular Effects and Pharmacokinetics of Rocuronium Bromide (Org 9426) During Isoflurane Anaesthesia in Patients With and Without Renal Failure. *Br J Anaesth* (1993) 71:222–6. doi: 10.1093/bja/71.2.222
126. Van Miert MM, Eastwood NB, Boyd AH, Parker CJR, Hunter JM. The Pharmacokinetics and Pharmacodynamics of Rocuronium in Patients With Hepatic Cirrhosis. *Br J Clin Pharmacol* (1997) 44:139–44. doi: 10.1046/j.1365-2125.1997.00653.x
127. Szenohradszky J, Fisher DM, Segredo V, Caldwell JE, Bragg P, Sharma ML, et al. Pharmacokinetics of Rocuronium Bromide (ORG 9426) in Patients With Normal Renal Function or Patients Undergoing Cadaver Renal Transplantation. *Anesthesiology* (1992) 77:899–904. doi: 10.1097/00000542-199211000-00010
128. Servin FS, Lavaut E, Kleef U, Desmonts JM. Repeated Doses of Rocuronium Bromide Administered to Cirrhotic and Control Patients Receiving Isoflurane. *Anesthesiology* (1996) 84:1092–100. doi: 10.1097/00000542-199605000-00011
129. Suzuki Y, Liu S, Kadoya F, Takasaki Y, Yorozuya T, Mogi M. Association Between Mutated Mas-Related G Protein-Coupled Receptor-X2 and Rocuronium-Induced Intraoperative Anaphylaxis. *Br J Anaesth* (2020) 125:e446–8. doi: 10.1016/j.bja.2020.05.046
130. Chompunud Na Ayudhya C, Amponnawarat A, Roy S, Oskeritzian CA, Ali H. MRGPRX2 Activation by Rocuronium: Insights From Studies With Human Skin Mast Cells and Missense Variants. *Cells* (2021) 10:156. doi: 10.3390/cells10010156
131. Baldo BA, Pham NH. Histamine-Releasing and Allergenic Properties of Opioid Analgesic Drugs: Resolving the Two. *Anaesthesia Intensive Care* (2012) 40:216–35. doi: 10.1177/0310057X1204000204
132. Swegle JM, Logemann C. Management of Common Opioid-Induced Adverse Effects. *Am Fam Physician* (2006) 74:1347–54.
133. Donnelly S, Davis MP, Walsh D, Naughton M. Morphine in Cancer Pain Management: A Practical Guide. *Supportive Care Cancer* (2002) 10:13–35. doi: 10.1007/s005200100274
134. Aronson JK. *Meyler's Side Effects of Drugs. Sixteenth Edition*. JK Aronson, editor. Oxford: Elsevier (2016). p. 1111–27.
135. Du B-X, Song Z-M, Wang K, Zhang H, Xu F-Y, Zou Z, et al. Butorphanol Prevents Morphine-Induced Pruritus Without Increasing Pain and Other Side Effects: A Systematic Review of Randomized Controlled Trials. *Can J Anesthesia/Journal canadien d'anesthésie* (2013) 60:907–17. doi: 10.1007/s12630-013-9989-4
136. Ballantyne JC, Loach AB, Carr DB. Itching After Epidural and Spinal Opiates. *Pain* (1988) 33:149–60. doi: 10.1016/0304-3959(88)90085-1
137. Kjellberg F, Tramèr MR. Pharmacological Control of Opioid-Induced Pruritus: A Quantitative Systematic Review of Randomized Trials. *Eur J Anaesthesiol* (2001) 18:346–57. doi: 10.1097/00003643-200106000-00002
138. Kumar K, Singh SI. Neuraxial Opioid-Induced Pruritus: An Update. *J Anaesthesiol Clin Pharmacol* (2013) 29:303–7. doi: 10.4103/0970-9185.117045
139. Remy C, Marret E, Bonnet F. Effects of Acetaminophen on Morphine Side-Effects and Consumption After Major Surgery: Meta-Analysis of Randomized Controlled Trials † †Presented in Part at the Annual Meeting of the Société Française d'anesthésie-Réanimation, Paris, April 2004. *Br J Anaesthesia* (2005) 94:505–13. doi: 10.1093/bja/aei085
140. Cherny N, Ripamonti C, Pereira J, Davis C, Fallon M, McQuay H, et al. Strategies to Manage the Adverse Effects of Oral Morphine: An Evidence-Based Report. *J Clin Oncol* (2001) 19:2542–54. doi: 10.1200/JCO.2001.19.9.2542
141. Zernikow B, Lindena G. Long-Acting Morphine for Pain Control in Paediatric Oncology. *Med Pediatr Oncol* (2001) 36:451–8. doi: 10.1002/mpo.1109
142. Liu X-Y, Liu Z-C, Sun Y-G, Ross M, Kim S, Tsai F-F, et al. Unidirectional Cross-Activation of GRPR by MOR1D Uncouples Itch and Analgesia Induced by Opioids. *Cell* (2011) 147:447–58. doi: 10.1016/j.cell.2011.08.043
143. Liu R, Wang J, Zhao T, Cao J, Che D, Ma P, et al. Relationship Between MRGPRX2 and Pethidine Hydrochloride- or Fentanyl Citrate-Induced LAD2 Cell Degranulation. *J Pharm Pharmacol* (2018) 70:1596–605. doi: 10.1111/jphp.13009
144. Dinges HC, Otto S, Stay DK, Bäumlein S, Waldmann S, Kranke P, et al. Side Effect Rates of Opioids in Equianalgesic Doses *via* Intravenous Patient-Controlled Analgesia: A Systematic Review and Network Meta-Analysis. *Anesth Analg* (2019) 129:1153–62. doi: 10.1213/ANE.0000000000003887
145. Reich A, Szepietowski JC. Opioid-Induced Pruritus: An Update. *Clin Exp Dermatol* (2010) 35:2–6. doi: 10.1111/j.1365-2230.2009.03463.x
146. Rosow CE, Moss J, Philbin DM, Savarese JJ. Histamine Release During Morphine and Fentanyl Anesthesia. *Anesthesiology* (1982) 56:93–6. doi: 10.1097/00000542-198202000-00003
147. Philbin DM, Moss J, Akins CW, Rosow CE, Kono K, Schneider RC, et al. The Use of H1 and H2 Histamine Antagonists With Morphine Anesthesia: A Double-Blind Study. *Anesthesiology* (1981) 55:292–6. doi: 10.1097/00000542-198109000-00019
148. Wong KC, Wayne WE, Hornbein TF, Everett J. The Cardiovascular Effects of Morphine Sulfate With Oxygen and With Nitrous Oxide in Man. *Anesthesiology* (1973) 38:542–9. doi: 10.1097/00000542-197306000-00007
149. Hsu HO, Hickey RF, Forbes AR. Morphine Decreases Peripheral Vascular Resistance and Increases Capacitance in Man. *Anesthesiology* (1979) 50:98–102. doi: 10.1097/00000542-197902000-00005
150. Fahmy NR, Sunder N, Soter NA. Role of Histamine in the Hemodynamic and Plasma Catecholamine Responses to Morphine. *Clin Pharmacol Ther* (1983) 33:615–20. doi: 10.1038/clpt.1983.83
151. Kaliner M, Shelhamer JH, Ottesen EA. Effects of Infused Histamine: Correlation of Plasma Histamine Levels and Symptoms. *J Allergy Clin Immunol* (1982) 69:283–9. doi: 10.1016/S0091-6749(82)80005-5

152. Afshari R, Maxwell SRJ, Webb DJ, Bateman DN. Morphine Is an Arteriolar Vasodilator in Man. *Br J Clin Pharmacol* (2009) 67:386–93. doi: 10.1111/j.1365-2125.2009.03364.x
153. Long WF, Taylor RJ, Wagner CJ, Leavengood DC, Nelson HS. Skin Test Suppression by Antihistamines and the Development of Subsensitivity. *J Allergy Clin Immunol* (1985) 76:113–7. doi: 10.1016/0091-6749(85)90813-9
154. Levy JH, Brister NW, Shearin A, Ziegler J, Hug CC Jr, Adelson DM, et al. Wheal and Flare Responses to Opioids in Humans. *Anesthesiology* (1989) 70:756–60. doi: 10.1097/00000542-198905000-00008
155. Taylor RJ, Long WF, Nelson HS. The Development of Subsensitivity to Chlorpheniramine. *J Allergy Clin Immunol* (1985) 76:103–7. doi: 10.1016/0091-6749(85)90811-5
156. Casale TB, Bowman S, Kaliner M. Induction of Human Cutaneous Mast Cell Degranulation by Opiates and Endogenous Opioid Peptides: Evidence for Opiate and Nonopiate Receptor Participation. *J Allergy Clin Immunol* (1984) 73:775–81. doi: 10.1016/0091-6749(84)90447-0
157. Stefano GB, Hartman A, Bilfinger TV, Magazine HI, Liu Y, Casares F, et al. Presence of the μ3Opiate Receptor in Endothelial Cells. *J Biol Chem* (1995) 270:30290–3. doi: 10.1074/jbc.270.51.30290
158. Saucedo R, Erill S. Morphine-Induced Skin Wheals: A Possible Model for the Study of Histamine Release. *Clin Pharmacol Ther* (1985) 38:365–70. doi: 10.1038/clpt.1985.189
159. Maurer U, Kager C, Fellinger C, Loader D, Pollesböck A, Spitzer B, et al. Risk of Anaphylaxis in Opioid Dependent Persons: Effects of Heroin Versus Substitution Substance. *Subst Abuse Treatment Prevention Policy* (2014) 9:12. doi: 10.1186/1747-597X-9-12
160. Collins S, Faura C, Moore RA, McQuay H. Peak Plasma Concentrations After Oral Morphine. *J Pain Symptom Manage* (1998) 16:388–402. doi: 10.1016/S0885-3924(98)00094-3
161. Pauli-Magnus C. Pharmacokinetics of Morphine and its Glucuronides Following Intravenous Administration of Morphine in Patients Undergoing Continuous Ambulatory Peritoneal Dialysis. *Nephrol Dialysis Transplant* (1999) 14:903–9. doi: 10.1093/ndt/14.4.903
162. Portenoy RK, Thaler HT, Inturrisi CE, Friedlander-Klar H, Foley KM. The Metabolite Morphine-6-Glucuronide Contributes to the Analgesia Produced by Morphine Infusion in Patients With Pain and Normal Renal Function. *Clin Pharmacol Ther* (1992) 51:422–31. doi: 10.1038/clpt.1992.42
163. Dale O, Thoner J, Nilsen T, Tveita T, Borchgrevink PC, Klepstad P. Serum and Cerebrospinal Fluid Morphine Pharmacokinetics After Single Doses of Intravenous and Intramuscular Morphine After Hip Replacement Surgery. *Eur J Clin Pharmacol* (2007) 63:837–42. doi: 10.1007/s00228-007-0329-x
164. Crews KR, Murthy BP, Hussey EK, Passannante AN, Palmer JL, Maixner W, et al. Lack of Effect of Ondansetron on the Pharmacokinetics and Analgesic Effects of Morphine and Metabolites After Single-Dose Morphine Administration in Healthy Volunteers. *Br J Clin Pharmacol* (2001) 51:309–16. doi: 10.1046/j.1365-2125.2001.01369.x
165. Dershwitz M, Walsh JL, Morishige RJ, Connors PM, Rubsamen RM, Shafer SL, et al. Pharmacokinetics and Pharmacodynamics of Inhaled Versus Intravenous Morphine in Healthy Volunteers. *Anesthesiology* (2000) 93:619–28. doi: 10.1097/00000542-200009000-00009
166. Hand CW, Moore RA, McQuay HJ, Allen MC, Sear JW. Analysis of Morphine and its Major Metabolites by Differential Radioimmunoassay. *Ann Clin Biochem: Int J Lab Med* (1987) 24:153–60. doi: 10.1177/000456328702400205
167. Pham TDM, Ziora ZM, Blaskovich MAT. Quinolone Antibiotics. *MedChemComm* (2019) 10:1719–39. doi: 10.1039/C9MD00120D
168. Marchant J. When Antibiotics Turn Toxic. *Nature* (2018) 555:431–3. doi: 10.1038/d41586-018-03267-5
169. Stahlmann R, Lode H. Toxicity of Quinolones. *Drugs* (1999) 58:37–42. doi: 10.2165/00003495-199958002-00007
170. Owens RC, Ambrose PG. Antimicrobial Safety: Focus on Fluoroquinolones. *Clin Infect Dis* (2005) 41:S144–57. doi: 10.1086/428055
171. F. a. D. Administration. (2018) 2020.
172. McGee EU, Samuel E, Boronea B, Dillard N, Milby MN, Lewis SJ. Quinolone Allergy. *Pharmacy* (2019) 7:97. doi: 10.3390/pharmacy7030097
173. Yarrington ME, Anderson DJ, Dodds Ashley E, Jones T, Davis A, Johnson M, et al. Impact of FDA Black Box Warning on Fluoroquinolone and Alternative Antibiotic Use in Southeastern US Hospitals. *Infection Control Hosp Epidemiol* (2019) 40:1297–300. doi: 10.1017/ice.2019.247
174. Ball P, Stahlmann R, Kubin R, Choudhri S, Owens R. Safety Profile of Oral and Intravenous Moxifloxacin: Cumulative Data From Clinical Trials and Postmarketing Studies. *Clin Ther* (2004) 26:940–50. doi: 10.1016/S0149-2918(04)90170-1
175. Reich A, Ständer S, Szepietowski J. Drug-Induced Pruritus: A Review. *Acta Dermato Venereologica* (2009) 89:236–44. doi: 10.2340/00015555-0650
176. Ren H, Li X, Ni Z-H, Niu J-Y, Cao B, Xu J, et al. Treatment of Complicated Urinary Tract Infection and Acute Pyelonephritis by Short-Course Intravenous Levofloxacin (750 Mg/Day) or Conventional Intravenous/Oral Levofloxacin (500 Mg/Day): Prospective, Open-Label, Randomized, Controlled, Multicenter, non-I. *Int Urol Nephrol* (2017) 49:499–507. doi: 10.1007/s11255-017-1507-0
177. Ball P. Ciprofloxacin: An Overview of Adverse Experiences. *J Antimicrob Chemother* (1986) 18 Suppl D:187–93. doi: 10.1093/jac/18.SD.187
178. Brunner M, Stabeta H, Möller JG, Schrolnberger C, Erovic B, Hollenstein U, et al. Target Site Concentrations of Ciprofloxacin After Single Intravenous and Oral Doses. *Antimicrob Agents Chemother* (2002) 46:3724–30. doi: 10.1128/AAC.46.12.3724-3730.2002
179. Wall GC, Taylor MJ, Smith HL. Prevalence and Characteristics of Hospital Inpatients With Reported Fluoroquinolone Allergy. *Int J Clin Pharm* (2018) 40:890–4. doi: 10.1007/s11096-018-0613-0
180. De Winter BY, van den Wijngaard RM, de Jonge WJ. Intestinal Mast Cells in Gut Inflammation and Motility Disturbances. *Biochim Biophys Acta* (2012) 1822:66–73. doi: 10.1016/j.bbadis.2011.03.016
181. Alim MA, Peterson M, Pejler G. Do Mast Cells Have a Role in Tendon Healing and Inflammation? *Cells* (2020) 9:1134. doi: 10.3390/cells9051134
182. Behzad H, Sharma A, Mousavizadeh R, Lu A, Scott A. Mast Cells Exert Pro-Inflammatory Effects of Relevance to the Pathophyisology of Tendinopathy. *Arthritis Res Ther* (2013) 15:R184. doi: 10.1186/ar4374
183. Alves C, Mendes D, Marques FB. Fluoroquinolones and the Risk of Tendon Injury: A Systematic Review and Meta-Analysis. *Eur J Clin Pharmacol* (2019) 75:1431–43. doi: 10.1007/s00228-019-02713-1
184. Johannes CB, Ziyadeh N, Seeger JD, Tucker E, Reiter C, Faich G. Incidence of Allergic Reactions Associated With Antibacterial Use in a Large, Managed Care Organisation. *Drug Saf* (2007) 30:705–13. doi: 10.2165/00002018-200730080-00007
185. Aminimanizani A, Beringer P, Jelliffe R. Comparative Pharmacokinetics and Pharmacodynamics of the Newer Fluoroquinolone Antibacterials. *Clin Pharmacokinetics* (2001) 40:169–87. doi: 10.2165/00003088-200140030-00003
186. Schlender J-F, Teutonico D, Coboeken K, Schnizler K, Eissing T, Willmann S, et al. A Physiologically-Based Pharmacokinetic Model to Describe Ciprofloxacin Pharmacokinetics Over the Entire Span of Life. *Clin Pharmacokinetics* (2018) 57:1613–34. doi: 10.1007/s40262-018-0661-6
187. Fish DN, Chow AT. The Clinical Pharmacokinetics of Levofloxacin. *Clin Pharmacokinetics* (1997) 32:101–19. doi: 10.2165/00003088-199732020-00002
188. Mertes PM, Voiriot P, Dopff C, Scholl H, Clavey M, Villemot JP, et al. Penetration of Ciprofloxacin Into Heart Valves, Myocardium, Mediastinal Fat, and Sternal Bone Marrow in Humans. *Antimicrobial Agents Chemotherapy* (1990) 34:398–401. doi: 10.1128/AAC.34.3.398
189. Gotfried MH, Danziger LH, Rodvold KA. Steady-State Plasma and Intrapulmonary Concentrations of Levofloxacin and Ciprofloxacin in Healthy Adult Subjects. *Chest* (2001) 119:1114–22. doi: 10.1378/chest.119.4.1114
190. Furlanut M. Pharmacokinetic Aspects of Levofloxacin 500 Mg Once Daily During Sequential Intravenous/Oral Therapy in Patients With Lower Respiratory Tract Infections. *J Antimicrobial Chemotherapy* (2003) 51:101–6. doi: 10.1093/jac/dkg035
191. Chow AT, Fowler C, Williams RR, Morgan N, Kaminski S, Natarajan J. Safety and Pharmacokinetics of Multiple 750-Milligram Doses of Intravenous Levofloxacin in Healthy Volunteers. *Antimicrobial Agents Chemotherapy* (2001) 45:2122–5. doi: 10.1128/AAC.45.7.2122-2125.2001
192. Yan A, Bryant EE. *Statpearls*. Treasure Island (FL: StatPearls PublishingCopyright © 2020, StatPearls Publishing LLC. (2020).
193. Rodvold KA, Neuhauser M. Pharmacokinetics and Pharmacodynamics of Fluoroquinolones. *Pharmacotherapy* (2001) 21:233S–52S. doi: 10.1592/phco.21.16.233S.33992

194. Perletti G, Wagenlehner FME, Naber KG, Magri V. Enhanced Distribution of Fourth-Generation Fluoroquinolones in Prostatic Tissue. *Int J Antimicrobial Agents* (2009) 33:206–10. doi: 10.1016/j.ijantimicag.2008.09.009
195. Kiem S, Schentag JJ. Interpretation of Antibiotic Concentration Ratios Measured in Epithelial Lining Fluid. *Antimicrobial Agents Chemotherapy* (2008) 52:24–36. doi: 10.1128/AAC.00133-06
196. Soman A, Honeybourne D, Andrews J, Jevons G, Wise R. Concentrations of Moxifloxacin in Serum and Pulmonary Compartments Following a Single 400 Mg Oral Dose in Patients Undergoing Fibre-Optic Bronchoscopy. *J Antimicrobial Chemotherapy* (1999) 44:835–8. doi: 10.1093/jac/44.6.835
197. Kato M. Chondrotoxicity of Quinolone Antimicrobial Agents. *J Toxicol Pathol* (2008) 21:123–31. doi: 10.1293/tox.21.123
198. Hall MM, Finnoff JT, Smith J. Musculoskeletal Complications of Fluoroquinolones: Guidelines and Precautions for Usage in the Athletic Population. *PM&R* (2011) 3:132–42. doi: 10.1016/j.pmrj.2010.10.003

Conflict of Interest: The author declares that the research was conducted in the absence of any commercial or financial relationships that could be construed as a potential conflict of interest.

frontiers in Immunology

MINI REVIEW
published: 23 August 2021
doi: 10.3389/fimmu.2021.654190

Skin Resident Memory T Cells May Play Critical Role in Delayed-Type Drug Hypersensitivity Reactions

Elisa Maria Schunkert, Pranali Nitin Shah and Sherrie Jill Divito *

Department of Dermatology, Brigham & Women's Hospital, Harvard Medical School, Boston, MA, United States

Delayed-type drug hypersensitivity reactions (dtDHR) are immune-mediated reactions with skin and visceral manifestations ranging from mild to severe. Clinical care is negatively impacted by a limited understanding of disease pathogenesis. Though T cells are believed to orchestrate disease, the type of T cell and the location and mechanism of T cell activation remain unknown. Resident memory T cells (T_{RM}) are a unique T cell population potentially well situated to act as key mediators in disease pathogenesis, but significant obstacles to defining, identifying, and testing T_{RM} in dtDHR preclude definitive conclusions at this time. Deeper mechanistic interrogation to address these unanswered questions is necessary, as involvement of T_{RM} in disease has significant implications for prediction, diagnosis, and treatment of disease.

Keywords: adverse drug reactions, delayed-type drug hypersensitivity reactions, fixed drug eruption, maculopapular exanthem, drug reaction with eosinophil and systemic symptoms, Stevens-Johnson syndrome, tissue-resident memory T cells, toxic epidermal necrolysis

OPEN ACCESS

Edited by:
Jason Trubiano, University of Melbourne, Australia

Reviewed by:
Philippe Saas, U1098 Interactions Hôte-Greffon-Tumeur & Ingénierie Cellulaire et Génique (INSERM), France
Wen-Hung Chung, Chang Gung Memorial Hospital, Taiwan

***Correspondence:**
Sherrie Jill Divito
sdivito@bwh.harvard.edu

Specialty section:
This article was submitted to Alloimmunity and Transplantation, a section of the journal Frontiers in Immunology

Received: *15 January 2021*
Accepted: *06 August 2021*
Published: *23 August 2021*

Citation:
Schunkert EM, Shah PN and Divito SJ (2021) Skin Resident Memory T Cells May Play Critical Role in Delayed-Type Drug Hypersensitivity Reactions. Front. Immunol. 12:654190. doi: 10.3389/fimmu.2021.654190

INTRODUCTION

Delayed-type drug hypersensitivity reactions (dtDHR) are a significant public health problem with potential for high morbidity and mortality and considerable cost to healthcare systems (1–5). Skin is the most commonly affected organ with severity ranging from a mild exanthem (maculopapular drug eruption, MPE), to life-threatening blistering and sloughing of skin (Stevens-Johnson syndrome/toxic epidermal necrolysis, SJS/TEN), with potential for significant visceral involvement (drug reaction with eosinophilia and systemic symptoms, DRESS). The pathobiology of dtDHR remains poorly understood, impeding prediction and prevention, diagnosis, identification of culprit drug, and effective treatment. DtDHR are immune-mediated adverse drug reactions that typically appear days to weeks after drug exposure (3). The timing of onset combined with epidemiological, histopathological and laboratory data incriminate T cells as primary drivers of disease, however, the type of pathogenic T cell and the location and mechanism of its activation are unknown. Tissue-resident memory T cells (T_{RM}) are an increasingly appreciated unique population of T cells that persist long-term in peripheral tissues including skin (6, 7). Critical roles for skin T_{RM} in cutaneous health and several inflammatory skin diseases have been identified (6, 8), raising the question of whether skin T_{RM} contribute to or cause dtDHR. This mini-review aims to provide the reader with a clearer understanding of these enigmatic cells, evidence supporting skin T_{RM} involvement in dtDHR pathogenesis, and current barriers limiting investigation in this field.

AN OVERVIEW OF SKIN T_{RM} BIOLOGY

T Cell Classification and Identification

T cell classification is increasingly complex due to significant heterogeneity within T cell compartments and lack of consensus on nomenclature. Differences between mouse and human contribute further to confusion. This review therefore focuses on the most salient features required to understand skin T_{RM} in the context of dtDHR.

Mature T cells are broadly classified into naïve, effector, and memory subsets. When a naïve T cell is stimulated with cognate antigen, changes in surface expression of multiple proteins occur that are easily assayed by flow cytometry. In both humans and mice, cell surface expression of CD44 is increased, thereby differentiating naïve T cells ($CD44^{low}$) from effector and memory T cells ($CD44^{high}$) (9, 10). Additionally, activated T cells decrease surface expression of CD62L (L-selectin) and the chemokine receptor CCR7, and transiently up-regulate CD69 (11–14). In addition to these phenotypic changes, T cell proliferation, migration to the site of inflammation, and acquisition of effector function occur, ultimately resulting in resolution of the antigenic insult (14, 15). Once resolved, the effector phase of the response concludes with T cell contraction. However, a small population of antigen-specific memory T cells survive that are capable of responding faster and more robustly upon re-exposure to their cognate antigen (14–16). In humans, different isoforms of CD45 expressed on T cells are generally helpful in distinguishing naïve T cells, $CD45RA^+$, from memory T cells, which are typically $CD45RO^+$ (17).

Memory T cells were previously classified into two major subsets: central (T_{CM}) and effector (T_{EM}) memory T cells (18). T_{CM} reside predominantly in secondary lymphoid organs due to their surface expression of CCR7 and CD62L and carry a high proliferative capacity upon antigen re-exposure, but lack the ability to rapidly produce effector molecules (18). Comparatively, T_{EM} lack CCR7 and have low CD62L expression allowing them to circulate throughout the body during steady-state (18). In keeping with their role as circulating sentinels, they are capable of rapid effector function (18). More recently, T_{RM} have been appreciated as a unique memory T cell population playing key roles in health and disease. T_{RM} persist in robust numbers long-term in peripheral tissues despite absence of inflammation. Barrier sites including skin, gut, liver, lung, and mucosa are the main tissues containing large numbers of T_{RM} (19–24), presumably due to the constant barrage of these tissues with environmental antigens. Phenotypically, T_{RM} have low/absent expression of CD62L and CCR7 (16, 22), which helps prevent migration to secondary lymphoid organs (25, 26), and low expression of the transcription factor KLF2 and the protein S1P1 while maintaining surface expression of CD69, which further facilitates retention in peripheral tissue (27–30).

Skin T_{RM} consist of both $CD4^+$ and $CD8^+$ type T cells, each with variable phenotype and distribution throughout skin. A subset of epidermal $CD4^+$ and $CD8^+$ T_{RM} express CD103, the α_E subunit of $\alpha_E\beta_7$ integrin, which helps anchor T_{RM} to epithelial cells expressing E-cadherin (29–32). The majority of T_{RM} in healthy human skin reside in the dermis and are phenotypically $CD4^+CD103^-$ (29). Skin T_{RM} commonly express on their surface the skin homing molecule cutaneous lymphocyte antigen (CLA) (22) and variably the chemokine receptors CCR4, CCR6, CCR8, CCR10, and CXCR6 (22, 33–37). Taken together, T_{RM} are overall best phenotypically identified in healthy human skin as $CD3^+$, $CD4^+$ or $CD8^+$, $CD45RO^+CD69^+CLA^+CCR7^-CD62L^{low}$ and either $CD103^+$ or $CD103^-$.

T_{RM} Maintain Skin Health

T_{RM} play an important role in immunity. Protective skin T_{RM} can be generated in mice by immunizing with vaccinia virus (38, 39) or HSV (40, 41), and these T_{RM} clear pathogens faster and more effectively than, or even in the absence of, circulating T cells (38–41). Skin T_{RM} in humans likewise appear to effectively prevent cutaneous infection in the absence of circulating T cells, as patients depleted of circulating T cells by alemtuzumab, an anti-CD52 antibody, do not experience increased rates of infection (42). T_{RM} provide surveillance by actively patrolling skin (43, 44) and are capable of rapid and potent pro-inflammatory cytokine release (29), though data suggest that rapid cytotoxicity may be constrained by PD-1 signaling (45). Surface expression of the integrin CD49a reportedly denotes functionality of skin T_{RM}, with $CD8^+CD49a^+$ T_{RM} capable of IFNγ production and cytotoxicity, while $CD8^+CD49a^-$ T_{RM} are polarized toward IL-17 production (46, 47). Notably, localized skin infection generates T_{RM} not only at the site of infection but potentially at distant skin sites as well, particularly in the setting of repeat inoculation (39, 48, 49). Repeated exposure to a diversity of microbes could therefore generate an army of sentinel antigen-specific T cells across the expanse of skin, poised to rapidly defend against infection.

Skin T_{RM} Are Instrumental in Several Inflammatory Skin Diseases

Increasing data support skin T_{RM} as potentially causal or contributory to acute and chronic inflammatory skin conditions. In atopic dermatitis and psoriasis, T Cell Receptor (TCR) sequencing identified that pathogenic T cell clones persisted in skin at the site of resolved lesions supporting their classification as skin T_{RM} (50, 51). T cells remaining in resolved psoriatic lesional skin retained the propensity to produce psoriasis-inducing cytokines, explaining predisposition to disease recurrence at the same skin location after treatment discontinuation (51, 52), and pathogenic T_{RM} residing in non-lesional skin from psoriasis patients are capable of eliciting a psoriasiform reaction when stimulated ex vivo (53).

Moreover, human studies suggest a role for skin T_{RM} in acute graft-versus-host disease (GVHD), as skin T cells were shown to survive robust chemotherapy ± total body irradiation and were present and activated during acute skin GVHD (54). Findings were complemented by a humanized mouse model showing that human skin T_{RM} could mediate a GVHD-like dermatitis in the absence of donor T cells (54). These findings have direct implications for dtDHR, as acute skin GVHD clinically and histologically mirrors MPE in mild form and SJS/TEN in severe form.

Finally, skin T_{RM} have been directly implicated in allergic contact dermatitis (ACD), another form of cutaneous delayed-

type hypersensitivity reaction. In an ACD mouse model, increased allergen dose and number of exposures resulted in increased frequency of epidermal $CD8^+$ T_{RM} and worsened disease (55), and skin T_{RM} were observed to mediate allergic reactions upon allergen re-exposure in the absence of circulating T cells (49, 56). Allergen exposure induced antigen-specific T_{RM} locally and at distant skin sites, and concurrently antigen-specific T_{CM} in draining and distant lymph node, all bearing identical TCR, indicating that the newly generated memory T cells derived from a common clone (49). Interestingly, disease was exacerbated by checkpoint inhibitor antagonists which stimulated T_{RM} effector function, intimating that checkpoint inhibitors do constrain the T_{RM} response (56).

DO T_{RM} MEDIATE DTDHR?

T Cells in dtDHR

Ample evidence implicates T cell mediation of dtDHR. T cell infiltrate and pro-inflammatory molecules commonly attributed to effector T cells are observed within biopsies or blister fluid from affected skin (57, 58). Additionally, drug-specific T cells from peripheral blood have been identified by clonality studies, and in some diseased patients T cells from peripheral blood respond to drug in lymphocyte stimulation tests (59, 60). Moreover, several HLA associations have been identified that predispose patients to specific drug reactions (61–63). Prominent examples include HLA*B57:01 which predisposes patients taking the drug abacavir to DRESS (64), and HLA*B15:02 which predisposes patients to SJS/TEN if administered carbamazepine (65). T cell effector functions in dtDHR are increasingly appreciated, particularly in SJS/TEN, as $CD8^+$ T cell produced cytotoxic granules and soluble granulysin are thought to mediate keratinocyte death (58, 66). Comparatively, MPE is largely considered $CD4^+$ T cell/cytokine driven. Contradictory findings have been observed in DRESS, with some research supporting Th2 polarization, while other studies have observed cytotoxic $CD8^+$ T cells and IFNγ and TNFα signatures (66). Despite significant advancements in the above areas of research, the type of T cell mediating disease (effector, central *vs* effector *vs* resident memory) and the location and mechanism by which T cells are stimulated against drug remains largely unknown.

Evidence Supporting a Role for T_{RM} in dtDHR

Studies directly investigating T_{RM} in dtDHR are sparse, though there is increasing circumstantial evidence suggesting that skin T_{RM} may be critical players in disease. Anecdotally, patients with few circulating lymphocytes secondary to chemotherapy are capable of developing dtDHRs. Iriki et al. reported a case of SJS/TEN in a patient with severe lymphopenia secondary to chemotherapy. They demonstrated by immunofluorescence microscopy of affected skin the presence of $CD45RO^+CD69^+$ $CD4^+$ and $CD8^+$ T cells despite the lack of circulating T cells (67). The presumption is that disease resulted from skin T_{RM} that survived chemotherapy, while naïve and central and effector memory T cells were depleted by the treatment. However, the possibility that a low number of T cells survived chemotherapy in secondary lymphoid organs and were recruited to skin to mediate disease has not been ruled out.

A recent publication by Trubiano et al. investigated skin T_{RM} in patients with MPE and DRESS (68). The study reported increased number of $CD45RO^+CD69^+$ $CD4^+$ and $CD8^+$ T cells in skin after resolution of DRESS in one patient. In addition, the authors performed a localized drug challenge by intradermally injecting culprit drug into skin of patients with history of MPE or DRESS. Skin biopsies performed acutely after challenge during active localized inflammation and again 8 weeks after resolution demonstrated accumulation of $CD45RO^+CD69^+CD103^+$ $CD4^+$ and $CD8^+$ T cells at the 8-week time point. The increased frequency of cells with this phenotype supports that skin T_{RM} are generated by systemic disease and localized drug exposure (68). Similarly, patch testing suspected culprit drug in some cases induces skin inflammation in patients with history of dtDHR, affirming that drug-specific memory T cells are present in skin after disease resolution. For example, patch testing against abacavir has high sensitivity in patients with history of DRESS who express HLA-B*57:01 (69). Comparatively, drug naïve HLA-B*57:01 positive patients were demonstrated to have circulating abacavir-reactive T cells yet patch test negative, reinforcing the idea that drug exposure induces skin T_{RM} (70). Of note though, patch testing reportedly has low sensitivity for dtDHR reactions (71–73), raising the question of whether skin T_{RM} accumulation is dependent on type of dtDHR, culprit drug, and/or presence of specific HLA alleles, or alternatively low sensitivity may be secondary to a technical issue for example suboptimal drug concentration or vehicle applied during testing.

Lastly and perhaps most intriguingly, the idea that T_{RM}-mediated immunity is restrained by immune checkpoint signaling further bolsters the link between skin T_{RM} and dtDHR (56). The coinhibitory molecules CTLA-4 and PD-1 have been linked to hypersensitivity reactions from multiple drugs in both human and animal studies (74). Clinically, immune checkpoint inhibitors (ICI) can induce dtDHR-like reactions, most notably an SJS/TEN-like phenomenon (75, 76). It is currently unknown whether these reactions develop due to ICI-provoked loss of tolerance to a concurrently administered drug or bystander activation in the setting of a robust anti-tumor T cell response. Further investigation of these reactions has substantial potential to illuminate pathobiology of dtDHR.

The Curious Case of Fixed Drug Eruptions

Perhaps the best case for skin T_{RM} mediating at least one form of dtDHR is that of fixed drug eruption (FDE). Remarkably, FDE lesions reappear at the exact same skin site upon re-exposure to causative drug. Studies in resolved FDE lesions in human skin showed that intraepidermal $CD8^+$ T cells constitutively expressed CD69 in the absence of inflammation, and upon drug challenge produced IFNγ (77). Though these findings are consistent with skin T_{RM}, these T cells expressed primarily $CD45RA^+$ rather than $CD45RO^+$ (77). A separate unique subset of memory T cells termed T_{emra} can express CD45RA rather than CD45RO (18, 78, 79), but in this study, the intraepidermal $CD8^+$ T cells lacked CD57, a marker suggestive

of T_{emra}. This peculiar finding is yet to be resolved but highlights the phenotypic heterogeneity of memory T cell populations and a major challenge to accurately identifying T_{RM}.

INSIGHT INTO POTENTIAL MECHANISMS OF DRUG-REACTIVE T CELL STIMULATION

The fact that only a subset of patients expressing a predisposing HLA allele develop dtDHR upon exposure to the associated drug (80) suggests that a second "X" factor is necessary for disease. Evidence supports that viral infection or reactivation, particularly with herpes family viruses (HHV6, HHV7, EBV, CMV), may be this "X" factor (80–83). Presumably, the viral infection provides co-stimulation necessary to break T cell tolerance to drug (**Figure 1A**). In this scenario, drug-reactive naïve T cells could be primed in skin draining lymph nodes by dendritic cells activated by virally induced inflammation, the drug-reactive effector T cells migrate to skin and mediate disease as a primary immune response, then after contraction, a population of drug-reactive T_{RM} remain in skin, capable of mediating a reaction upon drug re-exposure. Though most research has focused on infection/reactivation of herpes family viruses in the context of DRESS, similar observations have been made in MPE, the classic example being ampicillin-induced MPE in the context of EBV mononucleosis (84), and in two publications in SJS/TEN (one reporting HHV6 reactivation and one EBV reactivation) (85, 86). Another potential "X" factor could be increased drug levels secondary to altered drug metabolism or reduced drug clearance. For example, data demonstrate that reduced renal function predisposes to allopurinol-induced severe dtDHR (87, 88).

Alternatively, virus-specific skin T_{RM} generated in response to a previous viral infection could potentially *cross-react* to drug/drug altered peptide repertoire presented by self-MHC expressed on skin antigen presenting cells or keratinocytes (80) (**Figure 1B**). In support of this, activated $CD8^+$ T cells mediating cutaneous and visceral symptoms of DRESS were shown to be EBV reactive (81), and HIV-specific memory T cell clones were demonstrated to react *in vitro* against abacavir-altered peptide repertoire presented in the context of HLA-B*57:01 (89) Whether cross-reactivity is causal to dtDHR other than DRESS remains to be elucidated.

Either scenario may help explain the link between skin T_{RM} and dtDHR with systemic manifestations. Research supports that cutaneous viral infection and ACD can generate clonal T_{RM} and T_{CM} simultaneously in local and distant skin and secondary lymphoid organs (39, 48, 49) and potentially antigen-specific T_{RM} in other tissues as well (90). In support of this concept, identical pathogenic clones were identified in blood, skin, liver, and lung of one patient with DRESS and blood, skin, and liver in a second patient (81).

Moreover, either above scenario could account for development of dtDHR upon first exposure to a drug. Lucas et al. demonstrated that drug naïve, HLA-B*57:01 positive patients contained both naïve and memory T cells in circulation capable of responding to abacavir upon *in vitro* stimulation (91). Presumably, rapid development of DRESS upon first drug exposure reflects mediation by cross-reactive memory T cells, while slower onset points toward priming of a primary drug-specific immune response. Whether this phenomenon occurs in other types of dtDHR remains unknown.

LIMITATIONS TO THE STUDY OF SKIN T_{RM} IN dtDHR

Several barriers impede the study of skin T_{RM} in dtDHR. First, many studies rely on limited phenotypic analysis by flow cytometry or tissue immunostaining to identify skin T_{RM}. Flow cytometry commonly requires digestion and disaggregation of skin by chemical and/or physical measures resulting in loss of spatial information and potential alteration of surface marker expression (92–94). Standard tissue immunostaining overcomes these barriers but is limited to co-staining of maximum 3 antigens, and some antigens are difficult to reliably stain in formalin-fixed tissue. Further, because no single marker or combination of markers defines all skin T_{RM}, cursory phenotypic analysis can be misleading. This is especially true during active inflammation, as CD69 can be expressed by other activated T cell populations, and as alluded to above, $CD45RO^+CD45RA^-$ phenotype is not universal for all memory T cells (18, 78, 79, 95). More perplexing, the definition that T_{RM} remain resident in peripheral tissue without recirculating has been called into question. Klicznik et al. reported that $CD4^+CD69^+CD103^+$ T_{RM} are capable of downregulating the tissue-retention marker CD69 and entering circulation (96). Moreover, elegant work by Buggert et al., transforms the current construct of memory T cell classification with observations that well-differentiated cytolytic memory $CD8^+$ T cells remain in intravascular circulation under steady-state conditions, while less differentiated non-cytolytic non-resident memory $CD8^+$ T cells recirculate between lymphoid and non-lymphoid tissues such as liver and gut (97). Whether these findings apply to skin T_{RM} in steady-state or during dtDHR is unknown, though one can imagine that preferential maintenance of less differentiated non-cytolytic T cells rather than cytolytic T cells in tissue could be a potential means of preventing bystander tissue damage.

A second major barrier is that researchers have limited ability to investigate the immunologic events preceding clinical manifestations of dtDHR due to either lack of predictability or that it may be unsafe to (re)expose a patient to drug in the event that a reaction is predictable. Prospective studies of active disease can be equally challenging particularly for rarer forms of dtDHR and for severe forms that may require rapid initiation of treatment prior to sampling. This type of clinical scenario is where mouse models become essential. Historically, dtDHR research has been hampered by the lack of mouse models that meaningfully recapitulate disease, but recent advances have been achieved by administering drug to mice transgenically expressing predisposing HLA alleles (98, 99). Though generation of, or

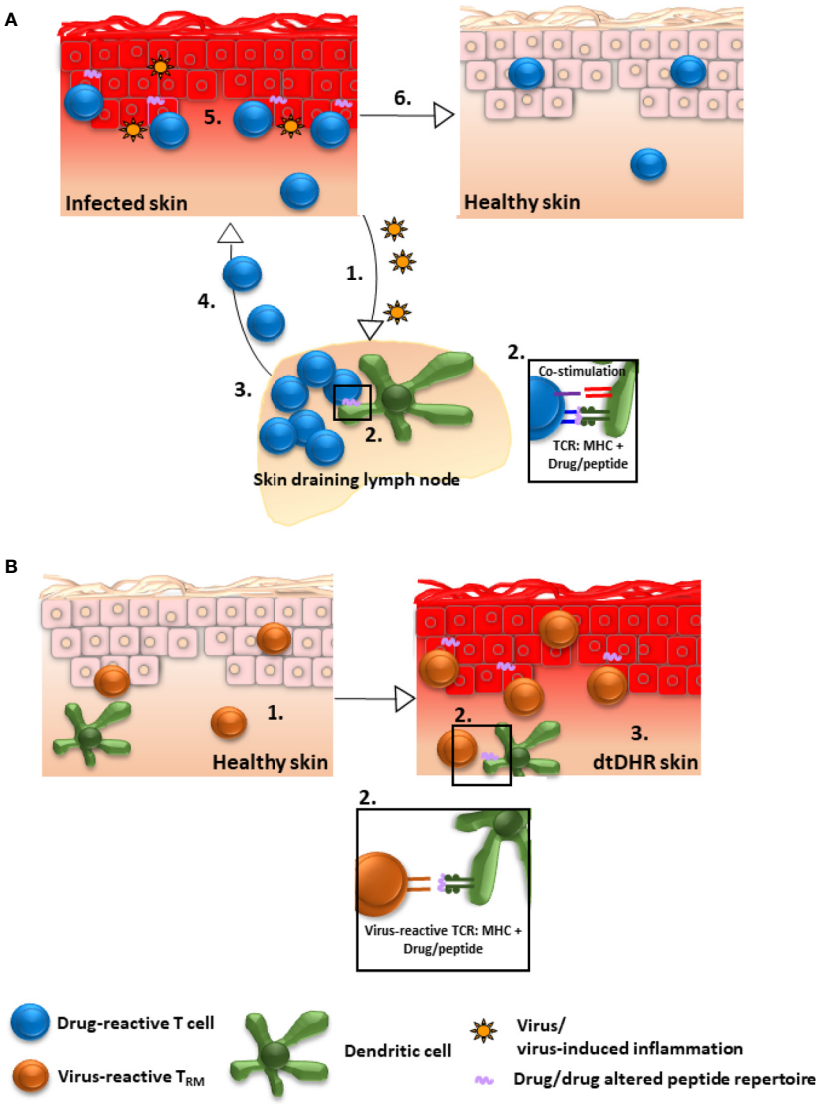

FIGURE 1 | Possible mechanisms by which drug-reactive T_{RM} could be generated in skin. **(A)** Drug/drug altered peptide repertoire is presented to drug-reactive T cells and concurrent viral infection/reactivation provides sufficient co-stimulation to break T cell tolerance to drug: 1. Inflammatory mediators secondary to infection stimulate dendritic cells. 2. Activated dendritic cells in skin draining lymph nodes present drug/drug altered peptide repertoire to naïve drug-reactive T cells and provide ample co-stimulation resulting in T cell priming. 3. Primed T cells proliferate and differentiate into effector cells, 4. migrate to skin, and 5. mediate damage as a primary immune response. 6. Despite resolution of inflammation, drug-reactive T_{RM} remain in skin, poised to mediate repeat dtDHR upon re-exposure to drug. Alternatively, factors other than viral infection, for example altered drug metabolism or reduced clearance, could potentially lead to T cell activation (not shown). **(B)** Drug-reactive T cells are cross-reactive to viral epitopes: 1. Virus-specific T_{RM} accumulate in skin as a consequence of prior infection. 2. These virus-reactive T cells are capable of recognizing (cross-reacting to) drug/drug altered peptide repertoire presented by MHC on the surface of skin dendritic cells, macrophages and/or keratinocytes resulting in T_{RM} stimulation. 3. The stimulated T_{RM} produce pro-inflammatory molecules inducing DRESS, or potentially other dtDHR.

mediation by, skin T_{RM} has not yet been tested in these mice, these models provide for the first time a platform allowing for deeper mechanistic interrogation of T_{RM} in disease.

CONCLUSIONS

A contribution from skin T_{RM} in dtDHR pathogenesis is an intriguing possibility with potential to shed light on a number of unanswered questions in the field. From a basic immunology perspective, it would address not only which T cells mediate disease but would also provide insight into mechanism(s) of T cell activation against drug. From a clinical perspective, it could aid predictability and diagnosis, allow for development of novel strategies to identify culprit drug, and provide insight into alternative approaches to treatment. Despite current obstacles to the study of T_{RM} in dtDHR, there is an increasingly strong framework in place and clearly a clinical need to justify further investigation.

AUTHOR CONTRIBUTIONS

ES prepared the manuscript with assistance from PS. SD supervised the project and oversaw the authoring and revision of the manuscript. All authors contributed to the article and approved the submitted version.

FUNDING

This work was funded by the National Institutes of Health DP5 OD023091 and R21 AI150657 (SD) the German Research Foundation, DFG Project number: 423175926, GZ: SCHU 3377/1-1 (ES) and the Sun Pharma/SID Innovation Research Fellowship (PS).

REFERENCES

1. Hsu DY, Brieva J, Silverberg NB, Silverberg JI. Morbidity and Mortality of Stevens-Johnson Syndrome and Toxic Epidermal Necrolysis in United States Adults. *J Invest Dermatol* (2016) 136(7):1387–97. doi: 10.1016/j.jid.2016.03.023
2. Velasco-Tirado V, Alonso-Sardon M, Cosano-Quero A, Romero-Alegria A, Sanchez-Los Arcos L, Lopez-Bernus A, et al. Life-Threatening Dermatoses: Stevens-Johnson Syndrome and Toxic Epidermal Necrolysis. Impact on the Spanish Public Health System (2010-2015). *PloS One* (2018) 13(6):e0198582. doi: 10.1371/journal.pone.0198582
3. Wheatley LM, Plaut M, Schwaninger JM, Banerji A, Castells M, Finkelman FD, et al. Report From the National Institute of Allergy and Infectious Diseases Workshop on Drug Allergy. *J Allergy Clin Immunol* (2015) 136 (2):262–71.e2. doi: 10.1016/j.jaci.2015.05.027
4. Patel S, John AM, Handler MZ, Schwartz RA. Fixed Drug Eruptions: An Update, Emphasizing the Potentially Lethal Generalized Bullous Fixed Drug Eruption. *Am J Clin Dermatol* (2020) 21(3):393–9. doi: 10.1007/s40257-020-00505-3
5. Lipowicz S, Sekula P, Ingen-Housz-Oro S, Liss Y, Sassolas B, Dunant A, et al. Prognosis of Generalized Bullous Fixed Drug Eruption: Comparison With Stevens-Johnson Syndrome and Toxic Epidermal Necrolysis. *Br J Dermatol* (2013) 168(4):726–32. doi: 10.1111/bjd.12133
6. Clark RA. Resident Memory T Cells in Human Health and Disease. *Sci Transl Med* (2015) 7(269):269rv1. doi: 10.1126/scitranslmed.3010641
7. Schenkel JM, Masopust D. Tissue-Resident Memory T Cells. *Immunity* (2014) 41(6):886–97. doi: 10.1016/j.immuni.2014.12.007
8. Park CO, Kupper TS. The Emerging Role of Resident Memory T Cells in Protective Immunity and Inflammatory Disease. *Nat Med* (2015) 21(7):688–97. doi: 10.1038/nm.3883
9. Budd RC, Cerottini JC, Horvath C, Bron C, Pedrazzini T, Howe RC, et al. Distinction of Virgin and Memory T Lymphocytes. Stable Acquisition of the Pgp-1 Glycoprotein Concomitant With Antigenic Stimulation. *J Immunol* (1987) 138(10):3120–9.
10. Croft M, Duncan DD, Swain SL. Response of Naive Antigen-Specific CD4+ T Cells In Vitro: Characteristics and Antigen-Presenting Cell Requirements. *J Exp Med* (1992) 176(5):1431–7. doi: 10.1084/jem.176.5.1431
11. Cebrian M, Yague E, Rincon M, Lopez-Botet M, de Landazuri MO, Sanchez-Madrid F. Triggering of T Cell Proliferation Through AIM, an Activation Inducer Molecule Expressed on Activated Human Lymphocytes. *J Exp Med* (1988) 168(5):1621–37. doi: 10.1084/jem.168.5.1621
12. Testi R, Phillips JH, Lanier LL. Leu 23 Induction as an Early Marker of Functional CD3/T Cell Antigen Receptor Triggering. Requirement for Receptor Cross-Linking, Prolonged Elevation of Intracellular [Ca++] and Stimulation of Protein Kinase C. *J Immunol* (1989) 142(6):1854–60.
13. Lambrecht BN, Pauwels RA, Fazekas De St Groth B. Induction of Rapid T Cell Activation, Division, and Recirculation by Intratracheal Injection of Dendritic Cells in a TCR Transgenic Model. *J Immunol* (2000) 164(6):2937–46. doi: 10.4049/jimmunol.164.6.2937
14. Nolz JC, Starbeck-Miller GR, Harty JT. Naive, Effector and Memory CD8 T-Cell Trafficking: Parallels and Distinctions. *Immunotherapy* (2011) 3 (10):1223–33. doi: 10.2217/imt.11.100
15. Golubovskaya V, Wu L. Different Subsets of T Cells, Memory, Effector Functions, and CAR-T Immunotherapy. *Cancers (Basel)* (2016) 8(3):36. doi: 10.3390/cancers8030036
16. Martin MD, Badovinac VP. Defining Memory CD8 T Cell. *Front Immunol* (2018) 9:2692. doi: 10.3389/fimmu.2018.02692
17. Akbar AN, Terry L, Timms A, Beverley PC, Janossy G. Loss of CD45R and Gain of UCHL1 Reactivity Is a Feature of Primed T Cells. *J Immunol* (1988) 140(7):2171–8.
18. Sallusto F, Lenig D, Forster R, Lipp M, Lanzavecchia A. Two Subsets of Memory T Lymphocytes With Distinct Homing Potentials and Effector Functions. *Nature* (1999) 401(6754):708–12. doi: 10.1038/44385
19. Clark RA, Chong BF, Mirchandani N, Yamanaka K, Murphy GF, Dowgiert RK, et al. A Novel Method for the Isolation of Skin Resident T Cells From Normal and Diseased Human Skin. *J Invest Dermatol* (2006) 126(5):1059–70. doi: 10.1038/sj.jid.5700199
20. Sathaliyawala T, Kubota M, Yudanin N, Turner D, Camp P, Thome JJ, et al. Distribution and Compartmentalization of Human Circulating and Tissue-Resident Memory T Cell Subsets. *Immunity* (2013) 38(1):187–97. doi: 10.1016/j.immuni.2012.09.020
21. Purwar R, Campbell J, Murphy G, Richards WG, Clark RA, Kupper TS. Resident Memory T Cells (T(RM)) Are Abundant in Human Lung: Diversity, Function, and Antigen Specificity. *PloS One* (2011) 6(1):e16245. doi: 10.1371/journal.pone.0016245
22. Clark RA, Chong B, Mirchandani N, Brinster NK, Yamanaka K, Dowgiert RK, et al. The Vast Majority of CLA+ T Cells Are Resident in Normal Skin. *J Immunol* (2006) 176(7):4431–9. doi: 10.4049/jimmunol.176.7.4431
23. Pallett LJ, Davies J, Colbeck EJ, Robertson F, Hansi N, Easom NJW, et al. IL-2 (High) Tissue-Resident T Cells in the Human Liver: Sentinels for Hepatotropic Infection. *J Exp Med* (2017) 214(6):1567–80. doi: 10.1084/jem.20162115
24. Stelma F, de Niet A, Sinnige MJ, van Dort KA, van Gisbergen K, Verheij J, et al. Human Intrahepatic CD69 + CD8+ T Cells Have a Tissue Resident Memory T Cell Phenotype With Reduced Cytolytic Capacity. *Sci Rep* (2017) 7 (1):6172. doi: 10.1038/s41598-017-06352-3
25. Bromley SK, Thomas SY, Luster AD. Chemokine Receptor CCR7 Guides T Cell Exit From Peripheral Tissues and Entry Into Afferent Lymphatics. *Nat Immunol* (2005) 6(9):895–901. doi: 10.1038/ni1240
26. Bai A, Hu H, Yeung M, Chen J. Kruppel-Like Factor 2 Controls T Cell Trafficking by Activating L-Selectin (CD62L) and Sphingosine-1-Phosphate Receptor 1 Transcription. *J Immunol* (2007) 178(12):7632–9. doi: 10.4049/jimmunol.178.12.7632
27. Skon CN, Lee JY, Anderson KG, Masopust D, Hogquist KA, Jameson SC. Transcriptional Downregulation of S1pr1 Is Required for the Establishment of Resident Memory CD8+ T Cells. *Nat Immunol* (2013) 14(12):1285–93. doi: 10.1038/ni.2745
28. Mackay LK, Braun A, Macleod BL, Collins N, Tebartz C, Bedoui S, et al. Cutting Edge: CD69 Interference With Sphingosine-1-Phosphate Receptor Function Regulates Peripheral T Cell Retention. *J Immunol* (2015) 194 (5):2059–63. doi: 10.4049/jimmunol.1402256
29. Watanabe R, Gehad A, Yang C, Scott LL, Teague JE, Schlapbach C, et al. Human Skin Is Protected by Four Functionally and Phenotypically Discrete Populations of Resident and Recirculating Memory T Cells. *Sci Transl Med* (2015) 7(279):279ra39. doi: 10.1126/scitranslmed.3010302
30. Mackay LK, Rahimpour A, Ma JZ, Collins N, Stock AT, Hafon ML, et al. The Developmental Pathway for CD103(+)CD8+ Tissue-Resident Memory T Cells of Skin. *Nat Immunol* (2013) 14(12):1294–301. doi: 10.1038/ni.2744
31. Zhang N, Bevan MJ. Transforming Growth Factor-Beta Signaling Controls the Formation and Maintenance of Gut-Resident Memory T Cells by Regulating Migration and Retention. *Immunity* (2013) 39(4):687–96. doi: 10.1016/j.immuni.2013.08.019
32. Cepek KL, Shaw SK, Parker CM, Russell GJ, Morrow JS, Rimm DL, et al. Adhesion Between Epithelial Cells and T Lymphocytes Mediated by E-Cadherin and the Alpha E Beta 7 Integrin. *Nature* (1994) 372(6502):190–3. doi: 10.1038/372190a0
33. McCully ML, Ladell K, Andrews R, Jones RE, Miners KL, Roger L, et al. CCR8 Expression Defines Tissue-Resident Memory T Cells in Human Skin. *J Immunol* (2018) 200(5):1639–50. doi: 10.4049/jimmunol.1701377

34. Schaerli P, Ebert L, Willimann K, Blaser A, Roos RS, Loetscher P, et al. A Skin-Selective Homing Mechanism for Human Immune Surveillance T Cells. *J Exp Med* (2004) 199(9):1265–75. doi: 10.1084/jem.20032177
35. McCully ML, Ladell K, Hakobyan S, Mansel RE, Price DA, Moser B. Epidermis Instructs Skin Homing Receptor Expression in Human T Cells. *Blood* (2012) 120(23):4591–8. doi: 10.1182/blood-2012-05-433037
36. Xia M, Hu S, Fu Y, Jin W, Yi Q, Matsui Y, et al. CCR10 Regulates Balanced Maintenance and Function of Resident Regulatory and Effector T Cells to Promote Immune Homeostasis in the Skin. *J Allergy Clin Immunol* (2014) 134 (3):634–44.e10. doi: 10.1016/j.jaci.2014.03.010
37. Zaid A, Hor JL, Christo SN, Groom JR, Heath WR, Mackay LK, et al. Chemokine Receptor-Dependent Control of Skin Tissue-Resident Memory T Cell Formation. *J Immunol* (2017) 199(7):2451–9. doi: 10.4049/jimmunol.1700571
38. Liu L, Zhong Q, Tian T, Dubin K, Athale SK, Kupper TS. Epidermal Injury and Infection During Poxvirus Immunization Is Crucial for the Generation of Highly Protective T Cell-Mediated Immunity. *Nat Med* (2010) 16(2):224–7. doi: 10.1038/nm.2078
39. Jiang X, Clark RA, Liu L, Wagers AJ, Fuhlbrigge RC, Kupper TS. Skin Infection Generates Non-Migratory Memory CD8+ T(RM) Cells Providing Global Skin Immunity. *Nature* (2012) 483(7388):227–31. doi: 10.1038/nature10851
40. Gebhardt T, Wakim LM, Eidsmo L, Reading PC, Heath WR, Carbone FR. Memory T Cells in Nonlymphoid Tissue That Provide Enhanced Local Immunity During Infection With Herpes Simplex Virus. *Nat Immunol* (2009) 10(5):524–30. doi: 10.1038/ni.1718
41. Mackay LK, Stock AT, Ma JZ, Jones CM, Kent SJ, Mueller SN, et al. Long-Lived Epithelial Immunity by Tissue-Resident Memory T (TRM) Cells in the Absence of Persisting Local Antigen Presentation. *Proc Natl Acad Sci USA* (2012) 109(18):7037–42. doi: 10.1073/pnas.1202288109
42. Clark RA, Watanabe R, Teague JE, Schlapbach C, Tawa MC, Adams N, et al. Skin Effector Memory T Cells do Not Recirculate and Provide Immune Protection in Alemtuzumab-Treated CTCL Patients. *Sci Trans Med* (2012) 4 (117):117ra7. doi: 10.1126/scitranslmed.3003008
43. Dijkgraaf FE, Matos TR, Hoogenboezem M, Toebes M, Vredevoogd DW, Mertz M, et al. Tissue Patrol by Resident Memory CD8(+) T Cells in Human Skin. *Nat Immunol* (2019) 20(6):756–64. doi: 10.1038/s41590-019-0404-3
44. Ariotti S, Beltman JB, Chodaczek G, Hoekstra ME, van Beek AE, Gomez-Eerland R, et al. Tissue-Resident Memory CD8+ T Cells Continuously Patrol Skin Epithelia to Quickly Recognize Local Antigen. *Proc Natl Acad Sci USA* (2012) 109(48):19739–44. doi: 10.1073/pnas.1208927109
45. Seidel JA, Vukmanovic-Stejic M, Muller-Durovic B, Patel N, Fuentes-Duculan J, Henson SM, et al. Skin Resident Memory CD8(+) T Cells Are Phenotypically and Functionally Distinct From Circulating Populations and Lack Immediate Cytotoxic Function. *Clin Exp Immunol* (2018) 194(1):79–92. doi: 10.1111/cei.13189
46. Cheuk S, Schlums H, Gallais Serezal I, Martini E, Chiang SC, Marquardt N, et al. CD49a Expression Defines Tissue-Resident CD8(+) T Cells Poised for Cytotoxic Function in Human Skin. *Immunity* (2017) 46(2):287–300. doi: 10.1016/j.immuni.2017.01.009
47. Bromley SK, Akbaba H, Mani V, Mora-Buch R, Chasse AY, Sama A, et al. CD49a Regulates Cutaneous Resident Memory CD8(+) T Cell Persistence and Response. *Cell Rep* (2020) 32(9):108085. doi: 10.1016/j.celrep.2020.108085
48. Davies B, Prier JE, Jones CM, Gebhardt T, Carbone FR, Mackay LK. Cutting Edge: Tissue-Resident Memory T Cells Generated by Multiple Immunizations or Localized Deposition Provide Enhanced Immunity. *J Immunol* (2017) 198 (6):2233–7. doi: 10.4049/jimmunol.1601367
49. Gaide O, Emerson RO, Jiang X, Gulati N, Nizza S, Desmarais C, et al. Common Clonal Origin of Central and Resident Memory T Cells Following Skin Immunization. *Nat Med* (2015) 21(6):647–53. doi: 10.1038/nm.3860
50. Brunner PM, Emerson RO, Tipton C, Garcet S, Khattri S, Coats I, et al. Nonlesional Atopic Dermatitis Skin Shares Similar T-Cell Clones With Lesional Tissues. *Allergy* (2017) 72(12):2017–25. doi: 10.1111/all.13223
51. Matos TR, O'Malley JT, Lowry EL, Hamm D, Kirsch IR, Robins HS, et al. Clinically Resolved Psoriatic Lesions Contain Psoriasis-Specific IL-17-Producing Alphabeta T Cell Clones. *J Clin Invest* (2017) 127(11):4031–41. doi: 10.1172/JCI93396
52. Gallais Serezal I, Classon C, Cheuk S, Barrientos-Somarribas M, Wadman E, Martini E, et al. Resident T Cells in Resolved Psoriasis Steer Tissue Responses That Stratify Clinical Outcome. *J Invest Dermatol* (2018) 138(8):1754–63. doi: 10.1016/j.jid.2018.02.030
53. Gallais Serezal I, Hoffer E, Ignatov B, Martini E, Zitti B, Ehrstrom M, et al. A Skewed Pool of Resident T Cells Triggers Psoriasis-Associated Tissue Responses in Never-Lesional Skin From Patients With Psoriasis. *J Allergy Clin Immunol* (2019) 143(4):1444–54. doi: 10.1016/j.jaci.2018.08.048
54. Divito SJ, Aasebo AT, Matos TR, Hsieh PC, Collin M, Elco CP, et al. Peripheral Host T Cells Survive Hematopoietic Stem Cell Transplantation and Promote Graft-Versus-Host Disease. *J Clin Invest* (2020) 130(9):4624–36. doi: 10.1172/JCI129965
55. Gadsboll AO, Jee MH, Funch AB, Alhede M, Mraz V, Weber JF, et al. Pathogenic CD8(+) Epidermis-Resident Memory T Cells Displace Dendritic Epidermal T Cells in Allergic Dermatitis. *J Invest Dermatol* (2020) 140 (4):806–15.e5. doi: 10.1016/j.jid.2019.07.722
56. Gamradt P, Laoubi L, Nosbaum A, Mutez V, Lenief V, Grande S, et al. Inhibitory Checkpoint Receptors Control CD8(+) Resident Memory T Cells to Prevent Skin Allergy. *J Allergy Clin Immunol* (2019) 143(6):2147–57.e9. doi: 10.1016/j.jaci.2018.11.048
57. Posadas SJ, Padial A, Torres MJ, Mayorga C, Leyva L, Sanchez E, et al. Delayed Reactions to Drugs Show Levels of Perforin, Granzyme B, and Fas-L to be Related to Disease Severity. *J Allergy Clin Immunol* (2002) 109(1):155–61. doi: 10.1067/mai.2002.120563
58. Chung WH, Hung SI, Yang JY, Su SC, Huang SP, Wei CY, et al. Granulysin Is a Key Mediator for Disseminated Keratinocyte Death in Stevens-Johnson Syndrome and Toxic Epidermal Necrolysis. *Nat Med* (2008) 14(12):1343–50. doi: 10.1038/nm.1884
59. Ko TM, Chung WH, Wei CY, Shih HY, Chen JK, Lin CH, et al. Shared and Restricted T-Cell Receptor Use Is Crucial for Carbamazepine-Induced Stevens-Johnson Syndrome. *J Allergy Clin Immunol* (2011) 128(6):1266–76.e11. doi: 10.1016/j.jaci.2011.08.013
60. Keane NM, Pavlos RK, McKinnon E, Lucas A, Rive C, Blyth CC, et al. HLA Class I Restricted CD8+ and Class II Restricted CD4+ T Cells Are Implicated in the Pathogenesis of Nevirapine Hypersensitivity. *AIDS* (2014) 28(13):1891–901. doi: 10.1097/QAD.0000000000000345
61. Sousa-Pinto B, Correia C, Gomes L, Gil-Mata S, Araujo L, Correia O, et al. HLA and Delayed Drug-Induced Hypersensitivity. *Int Arch Allergy Immunol* (2016) 170(3):163–79. doi: 10.1159/000448217
62. Sukasem C, Katsila T, Tempark T, Patrinos GP, Chantratita W. Drug-Induced Stevens-Johnson Syndrome and Toxic Epidermal Necrolysis Call for Optimum Patient Stratification and Theranostics via Pharmacogenomics. *Annu Rev Genomics Hum Genet* (2018) 19:329–53. doi: 10.1146/annurev-genom-083115-022324
63. Cheng CY, Su SC, Chen CH, Chen WL, Deng ST, Chung WH. HLA Associations and Clinical Implications in T-Cell Mediated Drug Hypersensitivity Reactions: An Updated Review. *J Immunol Res* (2014) 2014:565320. doi: 10.1155/2014/565320
64. Mallal S, Nolan D, Witt C, Masel G, Martin AM, Moore C, et al. Association Between Presence of HLA-B*5701, HLA-DR7, and HLA-DQ3 and Hypersensitivity to HIV-1 Reverse-Transcriptase Inhibitor Abacavir. *Lancet* (2002) 359(9308):727–32. doi: 10.1016/S0140-6736(02)07873-X
65. Chung WH, Hung SI, Hong HS, Hsih MS, Yang LC, Ho HC, et al. Medical Genetics: A Marker for Stevens-Johnson Syndrome. *Nature* (2004) 428(6982):486. doi: 10.1038/428486a
66. Bellon T. Mechanisms of Severe Cutaneous Adverse Reactions: Recent Advances. *Drug Saf* (2019) 42(8):973–92. doi: 10.1007/s40264-019-00825-2
67. Iriki H, Adachi T, Mori M, Tanese K, Funakoshi T, Karigane D, et al. Toxic Epidermal Necrolysis in the Absence of Circulating T Cells: A Possible Role for Resident Memory T Cells. *J Am Acad Dermatol* (2014) 71(5):e214–6. doi: 10.1016/j.jaad.2014.07.013
68. Trubiano JA, Gordon CL, Castellucci C, Christo SN, Park SL, Mouhtouris E, et al. Analysis of Skin-Resident Memory T Cells Following Drug Hypersensitivity Reactions. *J Invest Dermatol* (2019) 140(7):1442–5.e4. doi: 10.1016/j.jid.2019.11.020
69. Mallal S, Phillips E, Carosi G, Molina JM, Workman C, Tomazic J, et al. HLA-B*5701 Screening for Hypersensitivity to Abacavir. *N Engl J Med* (2008) 358 (6):568–79. doi: 10.1056/NEJMoa0706135
70. Schnyder B, Adam J, Rauch A, Thurnheer MC, Pichler WJ. HLA-B*57:01(+) Abacavir-Naive Individuals Have Specific T Cells But No Patch Test Reactivity. *J Allergy Clin Immunol* (2013) 132(3):756–8. doi: 10.1016/j.jaci.2013.04.013

71. Hassoun-Kheir N, Bergman R, Weltfriend S. The Use of Patch Tests in the Diagnosis of Delayed Hypersensitivity Drug Eruptions. *Int J Dermatol* (2016) 55(11):1219–24. doi: 10.1111/ijd.13306
72. Barbaud A, Reichert-Penetrat S, Trechot P, Jacquin-Petit MA, Ehlinger A, Noirez V, et al. The Use of Skin Testing in the Investigation of Cutaneous Adverse Drug Reactions. *Br J Dermatol* (1998) 139(1):49–58. doi: 10.1046/j.1365-2133.1998.02313.x
73. Osawa J, Naito S, Aihara M, Kitamura K, Ikezawa Z, Nakajima H. Evaluation of Skin Test Reactions in Patients With Non-Immediate Type Drug Eruptions. *J Dermatol* (1990) 17(4):235–9. doi: 10.1111/j.1346-8138.1990.tb01631.x
74. Hsu YO, Lu KL, Fu Y, Wang CW, Lu CW, Lin YF, et al. The Roles of Immunoregulatory Networks in Severe Drug Hypersensitivity. *Front Immunol* (2021) 12:597761. doi: 10.3389/fimmu.2021.597761
75. Goldinger SM, Stieger P, Meier B, Micaletto S, Contassot E, French LE, et al. Cytotoxic Cutaneous Adverse Drug Reactions During Anti-PD-1 Therapy. *Clin Cancer Res* (2016) 22(16):4023–9. doi: 10.1158/1078-0432.CCR-15-2872
76. Raschi E, Antonazzo IC, La Placa M, Ardizzoni A, Poluzzi E, De Ponti F. Serious Cutaneous Toxicities With Immune Checkpoint Inhibitors in the U.S. Food and Drug Administration Adverse Event Reporting System. *Oncologist* (2019) 24(11):e1228–31. doi: 10.1634/theoncologist.2019-0250
77. Mizukawa Y, Yamazaki Y, Teraki Y, Hayakawa J, Hayakawa K, Nuriya H, et al. Direct Evidence for Interferon-Gamma Production by Effector-Memory-Type Intraepidermal T Cells Residing at an Effector Site of Immunopathology in Fixed Drug Eruption. *Am J Pathol* (2002) 161(4):1337–47. doi: 10.1016/S0002-9440(10)64410-0
78. Sallusto F, Geginat J, Lanzavecchia A. Central Memory and Effector Memory T Cell Subsets: Function, Generation, and Maintenance. *Annu Rev Immunol* (2004) 22:745–63. doi: 10.1146/annurev.immunol.22.012703.104702
79. Tian Y, Babor M, Lane J, Schulten V, Patil VS, Seumois G, et al. Unique Phenotypes and Clonal Expansions of Human CD4 Effector Memory T Cells Re-Expressing CD45RA. *Nat Commun* (2017) 8(1):1473. doi: 10.1038/s41467-017-01728-5
80. Pavlos R, White KD, Wanjalla C, Mallal SA, Phillips EJ. Severe Delayed Drug Reactions: Role of Genetics and Viral Infections. *Immunol Allergy Clin North Am* (2017) 37(4):785–815. doi: 10.1016/j.iac.2017.07.007
81. Picard D, Janela B, Descamps V, D'Incan M, Courville P, Jacquot S, et al. Drug Reaction With Eosinophilia and Systemic Symptoms (DRESS): A Multiorgan Antiviral T Cell Response. *Sci Transl Med* (2010) 2(46):46ra62. doi: 10.1126/scitranslmed.3001116
82. Ushigome Y, Kano Y, Ishida T, Hirahara K, Shiohara T. Short- and Long-Term Outcomes of 34 Patients With Drug-Induced Hypersensitivity Syndrome in a Single Institution. *J Am Acad Dermatol* (2013) 68(5):721–8. doi: 10.1016/j.jaad.2012.10.017
83. Seishima M, Yamanaka S, Fujisawa T, Tohyama M, Hashimoto K. Reactivation of Human Herpesvirus (HHV) Family Members Other Than HHV-6 in Drug-Induced Hypersensitivity Syndrome. *Br J Dermatol* (2006) 155(2):344–9. doi: 10.1111/j.1365-2133.2006.07332.x
84. Onodi-Nagy K, Kinyo A, Meszes A, Garaczi E, Kemeny L, Bata-Csorgo Z. Amoxicillin Rash in Patients With Infectious Mononucleosis: Evidence of True Drug Sensitization. *Allergy Asthma Clin Immunol* (2015) 11(1):1. doi: 10.1186/1710-1492-11-1
85. Teraki Y, Murota H, Izaki S. Toxic Epidermal Necrolysis Due to Zonisamide Associated With Reactivation of Human Herpesvirus 6. *Arch Dermatol* (2008) 144(2):232–5. doi: 10.1001/archdermatol.2007.48
86. Ishida T, Kano Y, Mizukawa Y, Shiohara T. The Dynamics of Herpesvirus Reactivations During and After Severe Drug Eruptions: Their Relation to the Clinical Phenotype and Therapeutic Outcome. *Allergy* (2014) 69(6):798–805. doi: 10.1111/all.12410
87. Chung WH, Chang WC, Stocker SL, Juo CG, Graham GG, Lee MH, et al. Insights Into the Poor Prognosis of Allopurinol-Induced Severe Cutaneous Adverse Reactions: The Impact of Renal Insufficiency, High Plasma Levels of Oxypurinol and Granulysin. *Ann Rheum Dis* (2015) 74(12):2157–64. doi: 10.1136/annrheumdis-2014-205577
88. Ng CY, Yeh YT, Wang CW, Hung SI, Yang CH, Chang YC, et al. Impact of the HLA-B(*)58:01 Allele and Renal Impairment on Allopurinol-Induced Cutaneous Adverse Reactions. *J Invest Dermatol* (2016) 136(7):1373–81. doi: 10.1016/j.jid.2016.02.808
89. Almeida CA, van Miert P, O'Driscoll K, Zoet YM, Chopra A, Witt C, et al. Virus-Specific T-Cell Clonotypes Might Contribute to Drug Hypersensitivity Reactions Through Heterologous Immunity. *J Allergy Clin Immunol* (2019) 144(2):608–11.e4. doi: 10.1016/j.jaci.2019.05.009
90. Pan Y, Liu L, Tian T, Zhao J, Park CO, Lofftus SY, et al. Epicutaneous Immunization With Modified Vaccinia Ankara Viral Vectors Generates Superior T Cell Immunity Against a Respiratory Viral Challenge. *NPJ Vaccines* (2021) 6(1):1. doi: 10.1038/s41541-020-00265-5
91. Lucas A, Lucas M, Strhyn A, Keane NM, McKinnon E, Pavlos R, et al. Abacavir-Reactive Memory T Cells Are Present in Drug Naive Individuals. *PloS One* (2015) 10(2):e0117160. doi: 10.1371/journal.pone.0117160
92. Abuzakouk M, Feighery C, O'Farrelly C. Collagenase and Dispase Enzymes Disrupt Lymphocyte Surface Molecules. *J Immunol Methods* (1996) 194(2):211–6. doi: 10.1016/0022-1759(96)00038-5
93. Autengruber A, Gereke M, Hansen G, Hennig C, Bruder D. Impact of Enzymatic Tissue Disintegration on the Level of Surface Molecule Expression and Immune Cell Function. *Eur J Microbiol Immunol (Bp)* (2012) 2(2):112–20. doi: 10.1556/EuJMI.2.2012.2.3
94. Botting RA, Bertram KM, Baharlou H, Sandgren KJ, Fletcher J, Rhodes JW, et al. Phenotypic and Functional Consequences of Different Isolation Protocols on Skin Mononuclear Phagocytes. *J Leukoc Biol* (2017) 101(6):1393–403. doi: 10.1189/jlb.4A1116-496R
95. Gattinoni L, Lugli E, Ji Y, Pos Z, Paulos CM, Quigley MF, et al. A Human Memory T Cell Subset With Stem Cell-Like Properties. *Nat Med* (2011) 17(10):1290–7. doi: 10.1038/nm.2446
96. Klicznik MM, Morawski PA, Hollbacher B, Varkhande SR, Motley SJ, Kuri-Cervantes L, et al. Human CD4(+)CD103(+) Cutaneous Resident Memory T Cells Are Found in the Circulation of Healthy Individuals. *Sci Immunol* (2019) 4(37):eaav8995. doi: 10.1126/sciimmunol.aav8995
97. Buggert M, Vella LA, Nguyen S, Wu VH, Chen Z, Sekine T, et al. The Identity of Human Tissue-Emigrant CD8(+) T Cells. *Cell* (2020) 183(7):1946–61.e15. doi: 10.1101/2020.08.11.236372
98. Cardone M, Garcia K, Tilahun ME, Boyd LF, Gebreyohannes S, Yano M, et al. A Transgenic Mouse Model for HLA-B*57:01-Linked Abacavir Drug Tolerance and Reactivity. *J Clin Invest* (2018) 128(7):2819–32. doi: 10.1172/JCI99321
99. Pan RY, Chu MT, Wang CW, Lee YS, Lemonnier F, Michels AW, et al. Identification of Drug-Specific Public TCR Driving Severe Cutaneous Adverse Reactions. *Nat Commun* (2019) 10(1):3569. doi: 10.1038/s41467-019-11396-2

Conflict of Interest: The authors declare that the research was conducted in the absence of any commercial or financial relationships that could be construed as a potential conflict of interest.

frontiers in Immunology

MINI REVIEW
published: 19 November 2021
doi: 10.3389/fimmu.2021.688930

Antibody or Anybody? Considering the Role of MRGPRX2 in Acute Drug-Induced Anaphylaxis and as a Therapeutic Target

Graham A. Mackay[1]*, *Nithya A. Fernandopulle*[1], *Jie Ding*[1], *Jeremy McComish*[2] *and Paul F. Soeding*[1,3]

[1] Department of Biochemistry and Pharmacology, The University of Melbourne, Parkville, VIC, Australia, [2] Department of Clinical Immunology and Allergy, The Royal Melbourne Hospital, Parkville, VIC, Australia, [3] Department of Anaesthesia and Pain Medicine, The Royal Melbourne Hospital, Parkville, VIC, Australia

Acute anaphylaxis to small molecule drugs is largely considered to be antibody-mediated with immunogloblin E (IgE) and mast cell activation being key. More recently, a role for drug-reactive immunoglobulin G (IgG) with neutrophil activation has also been suggested, at least in reactions to neuromuscular blocking agents (NMBAs). However, the mast cell receptor MRGPRX2 has also been highlighted as a possible triggering mechanism in acute anaphylaxis to many clinically used drugs. Significantly, MRGPRX2 activation is not dependent upon the presence of drug-recognising antibody. Given the reasonable assumption that MRGPRX2 is expressed in all individuals, the corollary of this is that in theory, anybody could respond detrimentally to triggering drugs (recently suggested to be around 20% of a drug-like compound library). But this clearly is not the case, as the incidence of acute drug-induced anaphylaxis is very low. In this mini-review we consider antibody-dependent and -independent mechanisms of mast cell activation by small molecule drugs with a focus on the MRGPRX2 pathway. Moreover, as a juxtaposition to these adverse drug actions, we consider how increased understanding of the role of MRGPRX2 in anaphylaxis is important for future drug development and can complement exploration of this receptor as a drug target in broader clinical settings.

Keywords: anaphylaxis, mast cells, drug hypersensitivity, MRGPRX2, IgE (immunoglobulin E)

OPEN ACCESS

Edited by:
Patricia Illing,
Monash University, Australia

Reviewed by:
Didier G. Ebo,
University of Antwerp, Belgium
Hydar Ali,
University of Pennsylvania, United States

***Correspondence:**
Graham A. Mackay
gmackay@unimelb.edu.au

Specialty section:
This article was submitted to Alloimmunity and Transplantation, a section of the journal Frontiers in Immunology

Received: *31 March 2021*
Accepted: *03 November 2021*
Published: *19 November 2021*

Citation:
Mackay GA, Fernandopulle NA, Ding J, McComish J and Soeding PF (2021) Antibody or Anybody? Considering the Role of MRGPRX2 in Acute Drug-Induced Anaphylaxis and as a Therapeutic Target. Front. Immunol. 12:688930. doi: 10.3389/fimmu.2021.688930

INTRODUCTION, OVERVIEW AND SIGNIFICANCE

The risk of adverse drug reactions such as anaphylaxis, whilst rare, remains a serious concern. In susceptible individuals, specific drug exposure may trigger a sudden life-threatening reaction, and unless a history of previous hypersensitivity exists, this response is mostly unpredictable. Even within the perioperative setting, where facilities for resuscitation are optimal, drug-induced anaphylaxis still causes a significant incidence of patient injury and mortality (1–3). Here we examine recent mechanistic advances in the understanding of drug-induced anaphylaxis in humans, with a focus on the critical role played by mast cell activation and the role of the Mas-related G protein-coupled receptor X2 (MRGPRX2). It is noteworthy that there have been several recent

excellent and comprehensive reviews of drug hypersensitivity and MRGPRX2 involvement in human disease that complement the present article (4–7).

Commonly, mechanisms of drug-induced acute anaphylaxis are classified as either being 'antibody (IgE)-dependent' or 'other' depending upon the clinical diagnostic workup. With the identification of MRGPRX2, the activation of this receptor has emerged as a viable explanation to classify these previously mechanistically uncertain cases (reported to be around 30% of events). Studies in mice clearly support the involvement of MrgprB2 (the murine homologue of MRGPRX2) in drug-induced anaphylaxis to polybasic compounds such as NMBAs (8). However, unsurprisingly, this is more challenging to prove in humans. Whilst skin injection site reactions are observed very commonly to certain known MRGPRX2 activators (e.g. icatibant), consistent with the high expression of MRGPRX2 in mast cells in this location (discussed later), systemic anaphylactic responses to such compounds have not been reported (9, 10). To date, there is no means of unambiguously attributing a clinical event of drug-induced acute anaphylaxis to MRGPRX2 activation.

From a patient perspective, defining the role of MRGPRX2 is important as if confirmed, it may provide predictive, preventative and therapeutic strategies for drug-induced anaphylaxis. Moreover, the pharmaceutical industry is increasingly examining drug agonism at MRGPRX2 in their pre-clinical drug candidate evaluations (11, 12). In one such study, around 20% of a drug-screening chemical library was shown to be MRGPRX2-activating (11). Presumably, such pre-clinical screening could be used to discard, or at least de-prioritise, drug candidates/leads. Whilst this might be seen as improving drug safety, using icatibant as an example, it may result in future life-saving therapeutics being discarded unnecessarily. As such, defining the true clinical role of MRGPRX2 in drug-induced anaphylaxis has wide-sweeping importance.

Lost in Translation: Discriminating Antibody-Dependent and MRGPRX2-Dependent Drug-Induced Anaphylaxis

Conclusive evidence that MRGPRX2 activation is a primary mechanism in drug-induced anaphylaxis continues to be a clinical challenge. Here we largely compare IgE-dependent with MRGPRX2-dependent reactions although we acknowledge that this is oversimplistic and IgE and mast cell-centric. For instance, IgG-dependent reactions involving neutrophils have been reported, initially in mice, but more recently suggested to be important to drug-induced anaphylaxis in humans, at least with NMBAs (4, 13, 14). Involvement of the mast cell activating complement anaphylatoxins (C3a/C5a) in immune-mediated anaphylaxis has also been reported (13, 15).

Whilst it is well established that IgE is responsible for the majority of drug-induced acute anaphylaxis, new information on this pathway is also arising. A recent study has shown a role for a subset of T follicular helper cells in the production of high-affinity IgE to allergens (16). Whilst it is unclear if this extends to small molecule drugs acting as haptens, it nonetheless suggests that 'quality over quantity' might be important for IgE-dependent anaphylaxis, which has implications for the identification of culprit pathways. For instance, it is possible that the inability to attribute drug anaphylaxis to IgE is a result of an inability to detect it rather than the lack of its presence. Drug-'specific' serum IgE testing is however commonly incorporated into diagnostic algorithms. For this, prototypic drugs that display chemical structural features of common culprit agents (e.g. morphine, penicilloyl conjugates) are often used in testing. This approach not only lacks sensitivity (17) but also specificity as it might ignore IgE that recognises diverse drug epitopes. Whilst some clinical centres use a wider range of potential culprit drugs in screening, this is relatively uncommon and thus assays to detect true drug-specific IgE (or indeed IgG) are needed.

Whilst it was originally thought that changes to serum levels of tryptase could be used to discriminate between IgE and MRGPRX2-dependent reactions, recent work has suggested against this (18, 19) which supports *in vitro* studies that report non-IgE-dependent secretion of tryptase (20, 21).

The use of the skin prick and intra-dermal tests are common in clinical investigations to identify culprit anaphylaxis-inducing drugs. Indeed, morphine/codeine have such predictable general reactivity in intradermal testing that they are often used as a positive control stimuli. This approach is thus clearly not a discriminatory tool between IgE- and MRGPRX2-dependent pathways as both could be active in skin mast cells.

More recently, addition of the basophil activation test (BAT) has been suggested as a discriminatory assay in mechanistic attribution of drug-induced anaphylaxis (22). The discriminatory utility of this *ex vivo* assay is based on the observation that basophils, in general, are not thought to have functional expression of MRGPRX2. Basophil activation by NMBAs therefore would strongly suggest an IgE-dependent mechanism. However, a recent study has suggested functional expression of MRGPRX2 on basophils (23), although this has been suggested to relate to basal activation of the cells and consequent expression of a normally intracellular pool of receptor (24). A broader discussion of the potential utility of the BAT approach in identifying non-IgE-dependent pathways in drug-induced anaphylaxis has been recently published (22).

The possibility of using the known differences in the FcεRI and MRGPRX2 signaling pathways (25) also has potential to resolve the IgE *vs* MRGPRX2 conundrum. Bruton's tyrosine kinase (Btk) inhibitors, clinically used to treat leukemia, have been shown to be powerful inhibitors of IgE-dependent human mast cell activation (26). Importantly, based on the receptor's signalling cascade, these approved drugs would not be predicted to affect the MRGPRX2 pathway. In theory, Btk inhibitors could be used locally during skin challenge testing, and thereby provide mechanistic evidence for the pathway underpinning anaphylaxis. The feasibility and safety of this approach has already been partially established using the Btk-inhibitor ibrutinib (27). Other approved compounds such as fostamatinib, a spleen tyrosine kinase (Syk) inhibitor, could be used in a similar way. Whilst speculative, such extension of skin-prick testing is clinically feasible although, from an ethical and safety perspective, would be easier to incorporate into existing *ex vivo* approaches such as in BAT analysis and/or in studies using skin biopsies.

Accurate clinical differentiation of a likely MRGPRX2-dependent subgroup of patients at risk of severe reactions to a given medication would enhance prospects of developing predictive biomarkers (**Figure 1**). What such a biomarker might be remains elusive, but we consider some of the possibilities and gaps in understanding below.

Elevated and/or Expanded Expression or Function of MRGPRX2 in Mast Cells

Mast cells mature into their characteristic highly granular form within tissues. However, variation in the type and levels of soluble factors and extracellular matrix proteins results in differential mast cell gene expression patterns and consequent functional heterogeneity to drug stimulation (28–30). More recently, antibody tools and transcriptomic and proteomic approaches have characterised this heterogeneity more comprehensively at the molecular level and provided alternative approaches for quantifying mast cells and MRGPRX2 expression in tissues (31–33). However, responses to compounds/agents now known to be direct activators of MRGPRX2 (e.g. compound 48/80) can also be used as a surrogate marker of the functional expression of MRGPRX2. Using these combined approaches, MRGPRX2 expression is particularly pronounced and consistently found in primary human mast cells isolated from the skin and fat with more variable expression in the gut and lung (32) that reflects the well-reported heterogeneity of mast cells in the latter organs (29). There is also evidence of MRGPRX2 functional expression in the heart and synovial tissue (20, 34). Thus, while skin mast cells are undoubtedly a focal point, as observed with the common injection reactions seen to some MRGPRX2 activating drugs, mast cells in other locations also have the potential to be triggered by the same compounds and may therefore contribute to systemic adverse responses to drugs.

Given the strong expression of MRGPRX2 in skin mast cells, it might be expected that cutaneous symptoms would be overt in putative MRGPRX2-dependent anaphylaxis. However, this has to our knowledge not been formally reported and might be complicated by core hypotension and the rapid administration of a variety of life-sustaining drugs upon signs of anaphylaxis.

It is possible that an elevated or more diverse tissue expression of MRGPRX2, perhaps associated with disease, may enhance an individual's susceptibility to drug-induced anaphylaxis. To our knowledge there are no published studies that examine mast cell MRGPRX2 expression in the context of acute drug-induced anaphylaxis. These studies are challenging as given the highly selective expression of MRGPRX2 to mature, tissue-resident mast cells, blood cell transcriptomics approaches will likely not be optimal. Skin biopsies would be much more useful in this regard especially with the increasing use of single cell genomic approaches. Furthermore, whilst transcriptomic approaches would seem the best approach to resolve this, studies have shown that MRGPRX2 mRNA levels are not a good measure of surface expression of the receptor (24, 35). This suggests non-transcriptional factors may also dynamically regulate MRGPRX2 surface levels, although the regulators of this process are unclear.

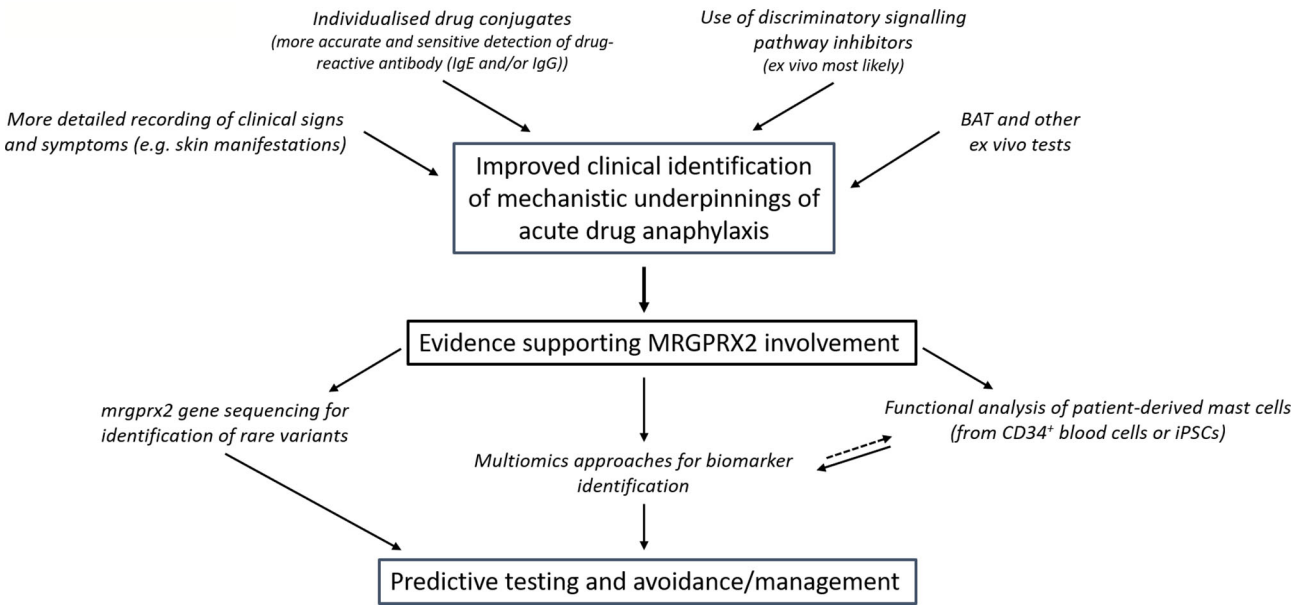

FIGURE 1 | Proposed approaches to overcome the current deficiencies in clinical discrimination of patients who suffer MRGPRX2-dependent anaphylaxis and their prospective value. Better defining patients who likely suffered MRGPRX2 dependent anaphylaxis enables more focused, powerful and feasible research that can be used prospectively in predictive testing. The acute and commonly severe nature of drug-induced anaphylaxis means that discrimination between the pathways would likely have little consequence to the present-day management of patient symptoms. However, further comparative insights might highlight approaches that could perhaps provide more discrete benefit. (BAT- basophil activation test).

Regulators of MRGPRX2 expression, at the transcriptional and/or post-transcription levels remain unclear. Chronic IL-6 treatment during the generation of blood-derived mast cells only modestly enhanced MRGPRX2 surface levels and function (36). Thymic stromal lymphopoetin (TSLP) was recently shown to selectively enhance MRGPRX2-mediated degranulation of skin mast cells (37). This effect was mediated at the functional level which again emphasises the possibility of MRGPRX2 pathway enhancement beyond simple receptor expression level. Echoing the importance of the microenvironment to mast cell differentiation and functional responses, the culture of normally unresponsive mast cells in fibronectin or with fibroblasts has been shown to induce sensitivity to polybasic stimuli (38). Development of complex, yet more physiologically relevant mast cell culture systems (39), as well as proteomic (32) and transcriptomic (31, 33) characterisation from patient tissue samples will assist with better understanding the regulation of mast cell MRGPRX2 expression *in vivo*.

There is evidence in some disease states, including severe chronic urticaria (CSU) (35) and asthma (40), that MRGPRX2 levels on mast cells are elevated. A recent study has also provided functional evidence for enhanced MRGPRX2 activation in lesional biopsies taken from patients with ulcerative colitis compared to matched non-lesional controls (41). However, these conditions are not known to be strongly associated with increased susceptibility to drug-induced anaphylaxis.

A clearer understanding of patients with diagnosed mast cell disorders might also help clarify mechanisms leading to drug-induced, IgE-independent anaphylaxis. Whilst mastocytosis has been identified as a risk factor for a largely IgE-dependent anaphylaxis to *Hymenoptera* stings (42), evidence for enhanced drug-induced sensitivity is not as clear. A systematic review of reactions to invasive procedures in patients with mastocytosis, did indeed find an increased rate of reaction to drug exposure. Compared to the general population this varied from 5% in some studies, to 1% in larger studies (43), but significantly this rate was lower than anticipated for this population. However, in the surgical setting, patients with mast cells disorders are routinely given prophylactic drugs, including antihistamines and glucocorticoids, to protect from presumed reactions. This may then account for the relatively low incidence of drug-induced anaphylaxis recorded. Intriguingly, Deepak et al. have recently demonstrated enhanced MRGPRX2 expression in patients with maculopapular cutaneous mastocytosis (44). However, another study has shown that a lower burden of skin mast cells is a risk factor for anaphylaxis in systemic mastocytosis (45). This again reinforces the lack of clarity in the role that MRGPRX2 expression plays clinically in drug-induced anaphylaxis even in mast cell disease.

Mast cell models derived from patients who suffered acute drug-induced anaphylaxis would be a highly valuable tool to identify if elevated MRGPRX2 expression or function underpin the drug hypersensitivity. In such studies, $CD34^+$ blood progenitor cells could be cultured into mature mast cells. Numerous methods exist, and these have been recently compared (36). A recent study has compared blood-derived mast cells from patients who had likely IgE-dependent with a possible MRGPRX2-dependent drug-induced anaphylaxis (46). Whilst the study was small in terms of patient numbers, interestingly, they could show no difference in reactivity to MRGPPRX2 agonists between the cohorts. Further work is needed to extend and confirm these findings. Whilst blood volumes might be a limitation to this targeted, patient-specific approach, single cell analytical methods, including analysis of mast cell function (47), increasingly make such limitations less challenging.

Recently, a new approach has been described where mast cells derived from human induced pluripotent stem cells (iPSCs) exhibit responsiveness to MRGPRX2 agonists (48). Previous studies using iPSC-derived mast cells have been reported, but these did not examine MRGPRX2 activation (49, 50). Whilst these studies used existing iPSC lines, they support the generation of patient-specific mast cells from those who experienced possible MRGPRX2-dependent, acute-drug-induced anaphylaxis. The extensive time and costs associated with this approach, again highlights the need to accurately characterize drug-responsive patients to ensure the utility of this endeavor.

Polymorphisms in MRGPRX2 and/or Other Pathways That Might Heighten Mast Cell Responses to Drugs

Perhaps the most straightforward explanation behind the rare, proposed heightened sensitivity of some individuals to MRGPRX2-dependent anaphylaxis is receptor polymorphism. Given the incidence of drug-induced anaphylaxis, this polymorphism would have likely low penetrance. The GPCR database (GPCRdb.org) identifies numerous natural missense mutations in the MRGPRX2 protein coding region with predicted disruptive effects. Several studies have investigated these polymorphisms on MRGPRX2 activity. One study, examining some of the most common variants, revealed that all had neutral activity or demonstrated a loss of function to MRGPRX2 agonists (51). Importantly, the authors examined a range of agonists as studies have demonstrated evidence for biased agonism in MRGPRX2 activation (52, 53). Further studies have examined MRGPRX2 mutants where indeed some gain-of-function polymorphisms in the receptor C-terminal region were identified with modest enhancement of degranulation (54, 55). The clinical significance of these variants is however as yet unclear.

It is also possible that gene variants in mast cell signaling pathways underpin heightened sensitivity to MRGPRX2 agonists, increasing susceptibility to anaphylaxis. A precedent for this possibility is a rare PLCG2 variant that is associated with cold-induced mast cell activation and urticaria (56). Moreover, a recent study has identified diminished levels of PGE_2 as a contributing factor to anaphylaxis (57). Whilst this study focused exclusively on clinical samples from likely IgE-dependent *Hymenoptera* sting-induced anaphylaxis, a deficiency in PGE2 levels would also be predicted to potentiate MRGPRX2 agonist-induced mast cell activation.

Clearly, more expansive genetic analyses are needed to correlate MRGPRX2 receptor or pathway polymorphism with clinical episodes of drug-induced acute anaphylaxis. Again, this connection will be greatly facilitated by improved clinical classification of presenting patients, and if shown, could be extraordinarily beneficial, given the potential rapid translation to predictive testing.

Targeting MRGPRX2 for Therapeutic Benefit: Iterative Learning From Drug-Induced Anaphylaxis

To this point, we have focused attention towards considering if and how MRGPRX2 contributes to drug-induced acute anaphylaxis. As proposed in **Figure 1**, further research is needed to establish this connection to an extent where it has clinically predictive value. This improved understanding will importantly also help inform the actual clinical risk of MRGPRX2 activation by novel drug candidates across the therapeutic spectrum and more clearly direct the proposed modulation of MRGPRX2 in a number of clinical settings. Whilst based on the discussion above, MRGPRX2 antagonists would seem of most clinical utility, the potential value of agonist drugs has also been examined. This makes clarification of the role of MRGPRX2 in drug-induced anaphylaxis of particular importance. Below, we summarise a number of current approaches to regulating MRGPRX2 activity (**Figure 2**), which has also been reviewed recently by others (5).

Chemical antagonism of NMBAs such as rocuronium by the reversal agent sugammadex has been proposed as a means of managing acute drug-induced anaphylaxis, although a consensus statement recommends against it (58). A recent study by our group has however shown inhibitory activity of sugammadex on some, but not all, endogenous activators of MRGPRX2 (59). Whilst speculative, this raises the possibility of using sugammadex, outside of the drugs conventional rocuronium-reversal role, to selectively modulate MRGPRX2 activation by endogenous agonists in certain disease states.

The selective expression of MRGPRX2 on mast cells has been recently harnessed for mast cell ablation. Utilising an anti-MRGPRX2 antibody conjugated to the compound IR700DX, which is activated by near infrared light exposure, Plum et al. demonstrated the depletion of dermal mast cells in a human skin explant model (32). This work exemplifies the innovative research that targets MRGPRX2 which could lead to new therapeutic approaches for mast cell-mediated disease.

A number of small molecule MRGPRX2 antagonists have been proposed/identified with many having relatively low potency and uncertain mechanism of antagonism (60–62). Recent compound screening efforts have identified some more potent and diverse agents however (63–65). As evidence continues to be established on the role of MRGPRX2 in inflammatory diseases of the skin and airways, it is likely that further momentum in this area will lead to compounds that could be envisaged to enter clinical development. Assuming an

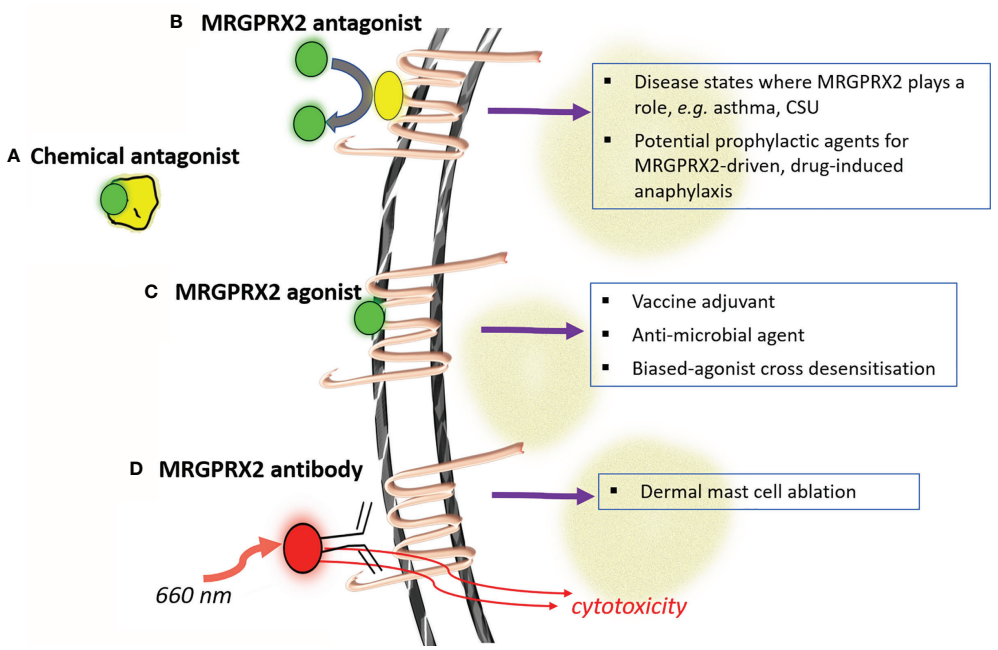

FIGURE 2 | Modulating MRGPRX2 for putative therapeutic benefit. Four major strategies have been advanced for modulating the activity of mast cells through MRGPRX2 (labeled a-d). Antagonism at MRGPRX2 can be harnessed at both the ligand **(A)** and receptor **(B)** levels whilst complete or signaling-biased MRGPRX2 agonists **(C)** could be used in a number of settings to modulate immunity. Considerations around the safety of this later approach would be clarified through better understanding if/how MRGPRX2 contributes to acute drug-induced anaphylaxis. The relatively unique and high-expression levels of MRGPRX2 in skin mast cells has also been proposed as a strategy for antibody-targeted selective mast cell ablation **(D)**. (CSU- chronic spontaneous urticaria).

appropriate evidence-base, and predictive test, such compounds could in theory also serve as prophylactic agents to minimize MRGPRX2-dependent anaphylaxis risk, particularly in the perioperative setting.

MRGPRX2 agonists have shown potential as both vaccine adjuvants (66) and anti-microbial agents, both directly and through enhancing adaptive immunity (67, 68). Several new humanized mast cell mouse models have been developed that will better facilitate the predictive value of such studies to the human system (26, 69). Desensitisation of MRGPRX2 by agonists biased towards receptor internalization has also been proposed as a therapeutic option, particularly in cutaneous disorders where mast cells can be targeted topically (53). The broad safety of such an approach would benefit from a much clearer appreciation of MRGPRX2 gained through investigation of drug-induced anaphylaxis. It is plausible, for instance, that polymorphisms in MRGPRX2 and/or its downstream signaling might skew the nature of the biased agonism rendering this approach inappropriate at least in some.

Summary and Conclusions

The number of clinically used drugs now known to act as MRGPRX2 agonists, at least in a laboratory setting, continues to expand. This reinforces the necessity of better understanding the role of MRGPRX2 in drug-induced anaphylaxis to determine if this receptor plausibly explains events where a clear connection to IgE sensitization cannot be made. In this review, we have discussed potential patient-specific factors that might account for rare and detrimental sensitivity. Throughout, the key value in developing better clinical stratification of patients experiencing drug-induced anaphylaxis, to highlight those likely to have a MRGPRX2 basis, has also been emphasised. This improved stratification, accompanied by more comprehensive cell, genomic and proteomic approaches are needed to firstly establish and secondly understand the basis of heightened patient MRGPRX2 responses. This knowledge could be key to predicting and hence avoiding these potentially devasting anaphylactic reactions. This insight will moreover better inform new drug development, establishing the real-world implications of MRGPRX2 agonism and moreover assisting in realising the full therapeutic potential of MRGPRX2 as a drug target.

AUTHOR CONTRIBUTIONS

All authors contributed to the writing, review, editing and final presentation of this manuscript.

FUNDING

This work was in part supported by a research grant from the Australian and New Zealand College of Anaesthetists (ANZCA).

REFERENCES

1. Harper NJN, Cook TM, Garcez T, Lucas DN, Thomas M, Kemp H, et al. Anaesthesia, Surgery, and Life-Threatening Allergic Reactions: Management and Outcomes in the 6th National Audit Project (NAP6). *Br J Anaesth* (2018) 121:172–88. doi: 10.1016/j.bja.2018.04.015
2. Reitter M, Petitpain N, Latarche C, Cottin J, Massy N, Demoly P, et al. Fatal Anaphylaxis With Neuromuscular Blocking Agents: A Risk Factor and Management Analysis. *Allergy* (2014) 69:954–9. doi: 10.1111/all.12426
3. Ebo DG, Clarke RC, Mertes PM, Platt PR, Sabato V, Sadleir PHM. Molecular Mechanisms and Pathophysiology of Perioperative Hypersensitivity and Anaphylaxis: A Narrative Review. *Br J Anaesth* (2019) 123:e38–49. doi: 10.1016/j.bja.2019.01.031
4. Bruhns P, Chollet-Martin S. Mechanisms of Human Drug-Induced Anaphylaxis. *J Allergy Clin Immunol* (2021) 147:1133–42. doi: 10.1016/j.jaci.2021.02.013
5. Roy S, Chompunud Na Ayudhya C, Thapaliya M, Deepak V, Ali H. Multifaceted MRGPRX2: New Insight Into the Role of Mast Cells in Health and Disease. *J Allergy Clin Immunol* (2021) 148:293–308. doi: 10.1016/j.jaci.2021.03.049
6. Kühn H, Kolkhir P, Babina M, Düll M, Frischbutter S, Fok JS, et al. Mas-Related G Protein-Coupled Receptor X2 and Its Activators in Dermatologic Allergies. *J Allergy Clin Immunol* (2021) 147:456–69. doi: 10.1016/j.jaci.2020.08.027
7. Thapaliya M, Chompunud Na Ayudhya C, Amponnawarat A, Roy S, Ali H. Mast Cell-Specific MRGPRX2: A Key Modulator of Neuro-Immune Interaction in Allergic Diseases. *Curr Allergy Asthma Rep* (2021) 21:3. doi: 10.1007/s11882-020-00979-5
8. McNeil BD, Pundir P, Meeker S, Han L, Undem BJ, Kulka M, et al. Identification of a Mast-Cell-Specific Receptor Crucial for Pseudo-Allergic Drug Reactions. *Nature* (2015) 519:237–41. doi: 10.1038/nature14022
9. Sinert R, Levy P, Bernstein JA, Body R, Sivilotti MLA, Moellman J, et al. Randomized Trial of Icatibant for Angiotensin-Converting Enzyme Inhibitor-Induced Upper Airway Angioedema. *J Allergy Clin Immunol Pract* (2017) 5:1402–9. doi: 10.1016/j.jaip.2017.03.003
10. Baş M, Greve J, Stelter K, Havel M, Strassen U, Rotter N, et al. A Randomized Trial of Icatibant in ACE-Inhibitor-Induced Angioedema. *N Engl J Med* (2015) 372:418–25. doi: 10.1056/NEJMoa1312524
11. Grimes J, Desai S, Charter NW, Lodge J, Moita Santos R, Isidro-Llobet A, et al. Mrgx2 is a Promiscuous Receptor for Basic Peptides Causing Mast Cell Pseudo-Allergic and Anaphylactoid Reactions. *Pharmacol Res Perspect* (2019) 7:e00547. doi: 10.1002/prp2.547
12. John LM, Dalsgaard CM, Jeppesen CB, Conde-Frieboes KW, Baumann K, Knudsen NPH, et al. *In Vitro* Prediction of *In Vivo* Pseudo-Allergenic Response *via* MRGPRX2. *J Immunotoxicol* (2021) 18:30–6. doi: 10.1080/1547691X.2021.1877375
13. Finkelman FD, Khodoun MV, Strait R. Human IgE-Independent Systemic Anaphylaxis. *J Allergy Clin Immunol* (2016) 137:1674–80. doi: 10.1016/j.jaci.2016.02.015
14. Jönsson F, de Chaisemartin L, Granger V, Gouel-Chéron A, Gillis CM, Zhu Q, et al. An Igg-Induced Neutrophil Activation Pathway Contributes to Human Drug-Induced Anaphylaxis. *Sci Transl Med* (2019) 11:eaat1479s. doi: 10.1126/scitranslmed.aat1479
15. Reber LL, Hernandez JD, Galli SJ. The Pathophysiology of Anaphylaxis. *J Allergy Clin Immunol* (2017) 140:335–48. doi: 10.1016/j.jaci.2017.06.003
16. Gowthaman U, Chen JS, Zhang B, Flynn WF, Lu Y, Song W, et al. Identification of a T Follicular Helper Cell Subset That Drives Anaphylactic IgE. *Science* (2019) 365:eaaw6433. doi: 10.1126/science.aaw6433
17. *Drug Allergy: Diagnosis and Management. National Institute for Health and Care Excellence (NICE), Clinical Guideline [CG183]*. Available at: https://www.nice.org.uk/guidance/cg183.
18. Ebo DG, van der Poorten ML, Elst J, Van Gasse AL, Mertens C, Bridts C, et al. Immunoglobulin E Cross-Linking or MRGPRX2 Activation: Clinical Insights From Rocuronium Hypersensitivity. *Br J Anaesth* (2021) 126:e27–9. doi: 10.1016/j.bja.2020.10.006

19. Noguchi S, Takekawa D, Saito J, Hashiba E, Hirota K. Serum Tryptase Cannot Differentiate Vancomycin-Induced Anaphylaxis From Red Man Syndrome. *J Clin Immunol* (2019) 39:855–6. doi: 10.1007/s10875-019-00707-3
20. Varricchi G, Pecoraro A, Loffredo S, Poto R, Rivellese F, Genovese A, et al. Heterogeneity of Human Mast Cells With Respect to MRGPRX2 Receptor Expression and Function. *Front Cell Neurosci* (2019) 13:299. doi: 10.3389/fncel.2019.00299
21. Veien M, Szlam F, Holden JT, Yamaguchi K, Denson DD, Levy JH. Mechanisms of Nonimmunological Histamine and Tryptase Release From Human Cutaneous Mast Cells. *Anesthesiology* (2000) 92:1074–81. doi: 10.1097/00000542-200004000-00026
22. Ebo DG, Bridts CH, Mertens CH, Sabato V. Principles, Potential, and Limitations of *Ex Vivo* Basophil Activation by Flow Cytometry in Allergology: A Narrative Review. *J Allergy Clin Immunol* (2021) 147:1143–53. doi: 10.1016/j.jaci.2020.10.027
23. Wedi B, Gehring M, Kapp A. The Pseudoallergen Receptor MRGPRX2 on Peripheral Blood Basophils and Eosinophils: Expression and Function. *Allergy* (2020) 75:2229–42. doi: 10.1111/all.14213
24. Sabato V, Elst J, Van Houdt M, Bridts C, Mertens C, Ebo DG. Surface Expression of MRGPRX2 on Resting Basophils: An Area of Controversy. *Allergy* (2020) 75:2421–2. doi: 10.1111/all.14252
25. Gaudenzio N, Sibilano R, Marichal T, Starkl P, Reber LL, Cenac N, et al. Different Activation Signals Induce Distinct Mast Cell Degranulation Strategies. *J Clin Invest* (2016) 126:3981–98. doi: 10.1172/JCI85538
26. Dispenza MC, Krier-Burris RA, Chhiba KD, Undem BJ, Robida PA, Bochner BS. Bruton's Tyrosine Kinase Inhibition Effectively Protects Against Human IgE-Mediated Anaphylaxis. *J Clin Invest* (2020) 130:4759–70. doi: 10.1172/JCI138448
27. Dispenza MC, Pongracic JA, Singh AM, Bochner BS. Short-Term Ibrutinib Therapy Suppresses Skin Test Responses and Eliminates IgE-Mediated Basophil Activation in Adults With Peanut or Tree Nut Allergy. *J Allergy Clin Immunol* (2018) 141:1914–6. doi: 10.1016/j.jaci.2017.12.987
28. Bradding P, Arthur G. Mast Cells in Asthma–State of the Art. *Clin Exp Allergy* (2016) 46:194–263. doi: 10.1111/cea.12675
29. Metcalfe DD, Baram D, Mekori YA. Mast Cells. *Physiol Rev* (1997) 77:1033–79. doi: 10.1152/physrev.1997.77.4.1033
30. Valent P, Akin C, Hartmann K, Nilsson G, Reiter A, Hermine O, et al. Mast Cells as a Unique Hematopoietic Lineage and Cell System: From Paul Ehrlich's Visions to Precision Medicine Concepts. *Theranostics* (2020) 10:10743–68. doi: 10.7150/thno.46719
31. Dwyer DF, Barrett NA, Austen KF. Immunological Genome Project Consortium. Expression Profiling of Constitutive Mast Cells Reveals a Unique Identity Within the Immune System. *Nat Immunol* (2016) 17:878–87. doi: 10.1038/ni.3445
32. Plum T, Wang X, Rettel M, Krijgsveld J, Feyerabend TB, Rodewald HR. Human Mast Cell Proteome Reveals Unique Lineage, Putative Functions, and Structural Basis for Cell Ablation. *Immunity* (2020) 52:404–16. doi: 10.1016/j.immuni.2020.01.012
33. Jiang J, Faiz A, Berg M, Carpaij OA, Vermeulen CJ, Brouwer S, et al. Gene Signatures From Scrna-Seq Accurately Quantify Mast Cells in Biopsies in Asthma. *Clin Exp Allergy* (2020) 50:1428–31. doi: 10.1111/cea.13732
34. Patella V, Marinò I, Lampärter B, Arbustini E, Adt M, Marone G. Human Heart Mast Cells. Isolation, Purification, Ultrastructure, and Immunologic Characterization. *J Immunol* (1995) 154:2855–65.
35. Fujisawa D, Kashiwakura J, Kita H, Kikukawa Y, Fujitani Y, Sasaki-Sakamoto T, et al. Expression of Mas-Related Gene X2 on Mast Cells Is Upregulated in the Skin of Patients With Severe Chronic Urticaria. *J Allergy Clin Immunol* (2014) 134:622–33. doi: 10.1016/j.jaci.2014.05.004
36. Elst J, Sabato V, van der Poorten MM, Faber M, Van Gasse AL, De Puysseleyr LP, et al. Peripheral Blood Cultured Mast Cells: Phenotypic and Functional Outcomes of Different Culture Protocols. *J Immunol Methods* (2021) 492:113003. doi: 10.1016/j.jim.2021.113003
37. Babina M, Wang Z, Franke K, Zuberbier T. Thymic Stromal Lymphopoietin Promotes MRGPRX2-Triggered Degranulation of Skin Mast Cells in a STAT5-Dependent Manner With Further Support From JNK. *Cells* (2021) 10:102. doi: 10.3390/cells10010102
38. Swieter M, Hamawy MM, Siraganian RP, Mergenhagen SE. Mast Cells and Their Microenvironment: The Influence of Fibronectin and Fibroblasts on the Functional Repertoire of Rat Basophilic Leukemia Cells. *J Periodontol* (1993) 64:492–6.
39. Ozpinar EW, Frey AL, Arthur GK, Mora-Navarro C, Biehl A, Snider DB, et al. Dermal Extracellular Matrix-Derived Hydrogels as an *In Vitro* Substrate to Study Mast Cell Maturation. *Tissue Eng Part A* (2020) 27:1008–22. doi: 10.1089/ten.TEA.2020.0142
40. Manorak W, Idahosa C, Gupta K, Roy S, Panettieri RJr, Ali H. Upregulation of Mas-Related G Protein Coupled Receptor X2 in Asthmatic Lung Mast Cells and its Activation by the Novel Neuropeptide Hemokinin-1. *Respir Res* (2018) 19(1):1. doi: 10.1186/s12931-017-0698-3
41. Chen E, Chuang LS, Giri M, Villaverde N, Hsu NY, Sabic K, et al. Inflamed Ulcerative Colitis Regions Associated With MRGPRX2-Mediated Mast Cell Degranulation and Cell Activation Modules, Defining a New Therapeutic Target. *Gastroenterology* (2021) 160:1709–24. doi: 10.1053/j.gastro.2020.12.076
42. Gülen T, Oude Elberink JNG, Brockow K. Anaphylaxis in Mastocytosis (Chapter 9). In: Akin C, editor. *Mastocytosis: A Comprehensive Guide*. Cham: Springer (2020).
43. Hermans MAW, Arends NJT, Gerth van Wijk R, van Hagen PM, Kluin-Nelemans HC, Oude Elberink HNG, et al. Management Around Invasive Procedures in Mastocytosis. *Ann Allergy Asthma Immunol* (2017) 199:304–9. doi: 10.1016/j.anai.2017.07.022
44. Deepak V, Komarow HD, Alblaihess AA, Carter MC, Metcalfe DD, Ali H. Expression of MRGPRX2 in Skin Mast Cells of Patients With Maculopapular Cutaneous Mastocytosis. *J Allergy Clin Immunol Pract* (2021) 9:3841–3.e1. doi: 10.1016/j.jaip.2021.05.042
45. Gülen T, Ljung C, Nilsson G, Akin C. Risk Factor Analysis of Anaphylactic Reactions in Patients With Systemic Mastocytosis. *J Allergy Clin Immunol Pract* (2017) 5:1248–55. doi: 10.1016/j.jaip.2017.02.008
46. Elst J, Maurer M, Sabato V, Faber MA, Bridts CH, Mertens C, et al. Novel Insights on MRGPRX2-Mediated Hypersensitivity to Neuromuscular Blocking Agents and Fluoroquinolones. *Front Immunol* (2021) 12:668962. doi: 10.3389/fimmu.2021.668962
47. Folkerts J, Gaudenzio N, Maurer M, Hendriks RW, Stadhouders R, Tam SY, et al. Rapid Identification of Human Mast Cell Degranulation Regulators Using Functional Genomics Coupled to High-Resolution Confocal Microscopy. *Nat Protoc* (2020) 15:1285–310. doi: 10.1038/s41596-019-0288-6
48. Luo Y, Vallone VF, He J, Frischbutter S, Kolkhir P, Moñino-Romero S, et al. A Novel Approach for Studying Mast Cell-Driven Disorders: Mast Cells Derived From Induced Pluripotent Stem Cells. *J Allergy Clin Immunol* (2021) 6:S0091–6749(21)01201-X. doi: 10.1016/j.jaci.2021.07.027
49. Igarashi A, Ebihara Y, Kumagai T, Hirai H, Nagata K, Tsuji K. Mast Cells Derived From Human Induced Pluripotent Stem Cells are Useful for Allergen Tests. *Allergol Int* (2018) 67(2):234–42. doi: 10.1016/j.alit.2017.08.008
50. Ikuno T, Ito S, Inoue T. Human Induced Pluripotent Stem Cell-Derived Mast Cells Useful for *In Vitro* Mast Cell Activation Assay Exhibiting Phenotypes and Morphological Characteristics of Human Mast Cells. *J Toxicol Sci* (2019) 44(11):789–97. doi: 10.2131/jts.44.789
51. Alkanfari I, Gupta K, Jahan T, Ali H. Naturally Occurring Missense MRGPRX2 Variants Display Loss of Function Phenotype for Mast Cell Degranulation in Response to Substance P, Hemokinin-1, Human Beta-Defensin-3, and Icatibant. *J Immunol* (2018) 201:343–9. doi: 10.4049/jimmunol.1701793
52. Roy S, Ganguly A, Haque M, Ali H. Angiogenic Host Defense Peptide AG-30/5C and Bradykinin B_2 Receptor Antagonist Icatibant Are G Protein Biased Agonists for MRGPRX2 in Mast Cells. *J Immunol* (2019) 202:1229–38. doi: 10.4049/jimmunol.1801227
53. Babina M, Wang Z, Roy S, Guhl S, Franke K, Artuc M, et al. MRGPRX2 is the Codeine Receptor of Human Skin Mast Cells: Desensitization Through Beta-Arrestin and Lack of Correlation With the FcεRI Pathway. *J Invest Dermatol* (2020) 141:1286–96.e4. doi: 10.1016/j.jid.2020.09.017
54. Chompunud Na Ayudhya C, Roy S, Alkanfari I, Ganguly A, Ali H. Identification of Gain and Loss of Function Missense Variants in MRGPRX2's Transmembrane and Intracellular Domains for Mast Cell Activation by Substance P. *Int J Mol Sci* (2019) 20(21). doi: 10.3390/ijms20215247
55. Chompunud Na Ayudhya C, Amponnawarat A, Roy S, Oskeritzian CA, Ali H. MRGPRX2 Activation by Rocuronium: Insights From Studies With Human

Skin Mast Cells and Missense Variants. *Cells* (2021) 10:156. doi: 10.3390/cells10010156
56. Ombrello MJ, Remmers EF, Sun G, Freeman AF, Datta S, Torabi-Parizi P, et al. Cold Urticaria, Immunodeficiency, and Autoimmunity Related to PLCG2 Deletions. *N Engl J Med* (2012) 366:330–8. doi: 10.1056/NEJMoa1102140
57. Rastogi S, Willmes DM, Nassiri M, Babina M, Worm M. PGE_2 Deficiency Predisposes to Anaphylaxis by Causing Mast Cell Hyperresponsiveness. *J Allergy Clin Immunol* (2020) 146:1387–96. doi: 10.1016/j.jaci.2020.03.046
58. Garvey LH, Dewachter P, Hepner DL, Mertes PM, Voltolini S, Clarke R, et al. Management of Suspected Immediate Perioperative Allergic Reactions: An International Overview and Consensus Recommendations. *Br J Anaesth* (2019) 123:e50–64. doi: 10.1016/j.bja.2019.04.044
59. Fernandopulle NA, Zhang SS, Soeding PF, Mackay GA. MRGPRX2 Activation in Mast Cells by Neuromuscular Blocking Agents and Other Agonists: Modulation by Sugammadex. *Clin Exp Allergy* (2020) 51:685–95. doi: 10.1111/cea.13801
60. Ding Y, Che D, Li C, Cao J, Wang J, Ma P, et al. Quercetin Inhibits Mrgprx2-Induced Pseudo-Allergic Reaction *via* Plcγ-IP3R Related Ca^{2+} Fluctuations. *Int Immunopharmacol* (2019) 66:185–97. doi: 10.1016/j.intimp.2018.11.025
61. Callahan BN, Kammala AK, Syed M, Yang C, Occhiuto CJ, Nellutla R, et al. Osthole, a Natural Plant Derivative Inhibits MRGPRX2 Induced Mast Cell Responses. *Front Immunol* (2020) 11:703. doi: 10.3389/fimmu.2020.00703
62. Kumar M, Singh K, Duraisamy K, Allam A A, Ajarem J, Kwok Chong Chow B. Protective Effect of Genistein Against Compound 48/80 Induced Anaphylactoid Shock *via* Inhibiting MAS Related G Protein-Coupled Receptor X2 (MRGPRX2). *Molecules* (2020) 25:1028. doi: 10.3390/molecules25051028
63. Suzuki Y, Liu S, Ogasawara T, Sawasaki T, Takasaki Y, Yorozuya T, et al. A Novel MRGPRX2-Targeting Antagonistic DNA Aptamer Inhibits Histamine Release and Prevents Mast Cell-Mediated Anaphylaxis. *Eur J Pharmacol* (2020) 878:173104. doi: 10.1016/j.ejphar.2020.173104
64. Ogasawara H, Furuno M, Edamura K, Noguchi M. Novel MRGPRX2 Antagonists Inhibit Ige-Independent Activation of Human Umbilical Cord Blood-Derived Mast Cells. *J Leukoc Biol* (2019) 106:1069–77. doi: 10.1002/JLB.2AB1018-405R
65. Dondalska A, Rönnberg E, Ma H, Pålsson SA, Magnusdottir E, Gao T, et al. Amelioration of Compound 48/80-Mediated Itch and LL-37-Induced Inflammation by a Single-Stranded Oligonucleotide. *Front Immunol* (2020) 11:559589. doi: 10.3389/fimmu.2020.559589
66. Johnson-Weaver B, Choi HW, Abraham SN, Staats HF. Mast Cell Activators as Novel Immune Regulators. *Curr Opin Pharmacol* (2018) 41:89–95. doi: 10.1016/j.coph.2018.05.004
67. Pundir P, Liu R, Vasavda C, Serhan N, Limjunyawong N, Yee R, et al. A Connective Tissue Mast-Cell-Specific Receptor Detects Bacterial Quorum-Sensing Molecules and Mediates Antibacterial Immunity. *Cell Host Microbe* (2019) 26:114–22. doi: 10.1016/j.chom.2019.06.003
68. Arifuzzaman M, Mobley YR, Choi HW, Bist P, Salinas CA, Brown ZD, et al. MRGPR-Mediated Activation of Local Mast Cells Clears Cutaneous Bacterial Infection and Protects Against Reinfection. *Sci Adv* (2019) 5:eaav0216. doi: 10.1126/sciadv.aav0216
69. Mencarelli A, Gunawan M, Yong KSM, Bist P, Tan WWS, Tan SY, et al. A Humanized Mouse Model to Study Mast Cells Mediated Cutaneous Adverse Drug Reactions. *J Leukoc Biol* (2020) 107:797–807. doi: 10.1002/JLB.3MA1219-210RR

Conflict of Interest: The authors declare that the research was conducted in the absence of any commercial or financial relationships that could be construed as a potential conflict of interest.

Publisher's Note: All claims expressed in this article are solely those of the authors and do not necessarily represent those of their affiliated organizations, or those of the publisher, the editors and the reviewers. Any product that may be evaluated in this article, or claim that may be made by its manufacturer, is not guaranteed or endorsed by the publisher.

Advantages of publishing in Frontiers

OPEN ACCESS
Articles are free to read for greatest visibility and readership

FAST PUBLICATION
Around 90 days from submission to decision

HIGH QUALITY PEER-REVIEW
Rigorous, collaborative, and constructive peer-review

TRANSPARENT PEER-REVIEW
Editors and reviewers acknowledged by name on published articles

Frontiers
Avenue du Tribunal-Fédéral 34
1005 Lausanne | Switzerland

Visit us: www.frontiersin.org
Contact us: frontiersin.org/about/contact

REPRODUCIBILITY OF RESEARCH
Support open data and methods to enhance research reproducibility

DIGITAL PUBLISHING
Articles designed for optimal readership across devices

FOLLOW US
@frontiersin

IMPACT METRICS
Advanced article metrics track visibility across digital media

EXTENSIVE PROMOTION
Marketing and promotion of impactful research

LOOP RESEARCH NETWORK
Our network increases your article's readership